THÈSE POUR OBTENIR LE GRADE DE DOCTEUR DE MONTPELLIER SUPAGRO

en Sciences de l'Eau

École doctorale GAIA – Biodiversité, Agriculture, Alimentation, Environnement, Terre, Eau

portée par

l'Unité Mixte de Recherche : Laboratoire d'Etude des Interactions entre Sol-Agrosystème-Hydrosystème

A Framework for Flood Modeling in Data-Sparse Regions Based on a New Cost-Performance Grid, Application on the Awali Basin in Lebanon

présentée par Rouya HDEIB

soutenue le 08 mars 2019

sous la direction de Roger MOUSSA, Directeur de Recherche, INRA, Montpellier
et Chadi ABDALLAH, Chercheur Associé, CNRS, Liban

Devant le jury composé de

Christophe CUDENNEC	Professeur, Agrocampus Ouest, Rennes	**Rapporteur**
Rabi MOHTAR	Professeur et Doyen, FAFS, AUB, Liban TEES research professor, Texas A&M University, Etats-Unis	**Rapporteur**
Marie-George TOURNOUD	Professeur, Université de Montpellier, Montpellier	**Président**
Patrick ARNAUD	Ingénieur de Recherche, IRSTEA, Aix-en-Provence	**Examinateur**
Luca BROCCA	Chercheur, National Research Council, Perugia, Italie	**Invité**
François COLIN	Professeur, Montpellier SupAgro, Montpellier	**Invité**

UNIVERSITÉ DE MONTPELLIER

Montpellier SupAgro

Dedicated to
my beloved parents,
my lovely husband,
and little son.

ACKNOWLEGMENT

My sincere thanks go to the Authorities of the Lebanese National Council for Scientific Research represented by the Secretary General ***Dr. Mouin Hamzé****, and to the Remote Sensing Center represented by its director* ***Dr. Ghaleb Faour*** *who have supported my scholarship.*

At this moment of accomplishment, I am greatly indebted to my research guide ***Dr. Chadi Abdallah****, for accepting me as his PhD student and offering me his mentorship, without whom this PhD could not have been launched, for his continuous encouragement, support and valuable guidance through my dissertation and all other works.*

My earnest thanks to ***Dr. Roger Moussa****, for supporting and guiding this PhD. I am grateful for his valuable advice, constructive criticism, positive appreciation and counsel which led to the successful completion of the research work.*

Thanks, extend to all the staff of the Lebanese National Centre for Remote Sensing, and especially for my friends and colleagues ***Eng. Samar Hijazi*** *and* ***Eng. Samah Termos****, for their help and for the wonderful times we shared together all the years that passed.*

I am thankful to ***Dr. François Colin*** *for his tremendous help and contribution and for his comments that were of great value to this work. Thanks also extend to all the staff of the* ***LISAH*** *research unit in Montpellier for supporting and hosting me in France.*

Thanks also for ***Dr. Luca Brocca*** *for his help and contribution to this thesis and to the Italian CNR project for their financial support of the field work.*

Many thanks go to ***Dr. Rabi Mohtar*** *and* ***Dr. Christophe Cudennec*** *for accepting reviewing this work; and for* ***Dr. Marie-George Tournoud*** *and* ***Dr. Arnaud Patrick*** *for their participation in the jury.*

I owe thanks to a very special person, my husband ***Eng. Mohamed Alsayegh*** *for his continued and unfailing love, support and understanding that made the completion of the thesis possible. You were always around at times I thought that it is impossible to continue, you helped me to keep things in perspective. I appreciate my son, my little boy* ***Ali*** *for whom I'm so grateful for being a blessing in my life. Words would never say how grateful I am to both of you.*

Finally, I acknowledge the people who mean a lot to me, my parents; ***Bassem*** *and* ***Nada****, for showing faith in me. I salute you both for the selfless love, care, pain and sacrifice you did to shape my life. I would never be able to pay back the love and affection showered upon by my parents. My deep gratitude goes to my sisters* ***Rayan, Aya,*** *and* ***Razan*** *for being such great and caring sisters.*

Thanks also extends to my parents in-law ***Salman*** *and* ***Fakhriya****, and sisters in-law* ***Bushra*** *and* ***Yousra*** *for their support during the past three years and to my friends* ***Bayan Al Mutaghwi, Sara Abdul Aal, Marwa kamaleddine, Sara Kawrani,*** *and* ***Eng. Hajar Saikouk*** *for their encouragement and support during the hard times.*

Résumé

Les inondations touchent un grand nombre de personnes et sont susceptibles de causer des dommages. La mise au point d'outils de modélisation des inondations pour mieux comprendre et atténuer leurs ampleurs est un défi pour la recherche. De nombreux modèles de niveaux de complexités différents sont maintenant disponibles afin de comprendre les processus de propagation des crues et des inondations. Choisir un modèle efficace et économique n'est pas un exercice facile. Dans les régions où uniquement des données éparses sont disponibles, la modélisation des inondations est une tâche ardue en raison du manque de données permettant de caler et de valider les modèles hydrologiques et hydrauliques. La question se pose alors de savoir s'il est possible de modéliser les inondations à partir de modèles hydrologiques et hydrauliques utilisant des données rares et si cette approche reste rentable compte tenu de la grande complexité du modèle et de la disponibilité limitée des données. Ce travail vise à développer un cadre pour la modélisation des inondations dans les régions avec des données éparses en développant une approche coût-performance. Une application sur le bassin du Awali au Liban. Le mémoire est structuré en trois parties: (i) un recueil des inondations au Liban émanant des journaux et analyse de leurs fréquences d'occurrence spatiale, (ii) mise au point d'une nouvelle approche coût-performance permettant de comparer différentes approches de modélisation, (iii) un cadre pour le choix du modèle adéquat des inondations en utilisant des données éparses.

Dans la première partie, une analyse intensive des archives des journaux nous a permis d'extraire 711 événements d'inondation au Liban. La variabilité spatiale des inondations a été reliée aux caractéristiques morphologiques, hydrologiques et de vulnérabilité. La carte d'occurrence des inondations peut être traitée comme une carte de risque d'inondation. Les informations extraites des journaux étaient prometteuses mais restent descriptives, et ne peuvent donc pas remplacer le besoin d'une modélisation détaillée.

Dans la deuxième partie, nous proposons une nouvelle grille coût-performance pour évaluer les approches de modélisation des crues et des inondations. La grille repose sur la définition de métriques permettant d'évaluer la disponibilité des données, la complexité du modèle et les performances de la modélisation. Pour les applications, 10 études sont choisies et ont été évaluées et représentées dans un diagramme coût-performance. Les approches couplées hydrologie-hydraulique sont les plus complexes et coûteuses alors que les approches empiriques sont les moins coûteuses et les moins performantes.

Dans la troisième partie, nous avons utilisé un modèle couplé hydrologique-hydraulique (HEC-HMS et HEC-RAS) contraint par les données des événements passés et les mesures post-événement. L'approche est testée sur le bassin de l'Awali au Liban. Le modèle hydrologique a été étalonné avec 12 événements Pluie/Débit visant à définir des plages de paramètres hydrologiques. L'incertitude des paramètres du modèle a été évaluée en effectuant une simulation Monte Carlo pour les plages des paramètres estimés. L'incertitude sur les variables simulées est réduite. Les informations des médias sociaux constituaient une valeur ajoutée pour contraindre les simulations de modèles hydrologiques. Les mesures post-événement étaient prometteuses pour valider la carte des inondations.

Basé sur la grille coût-performance, le cadre proposé révèle un bon niveau coût-performance. L’approche de modélisation est en position intermédiaire entre les approches complexes et simples. La démarche peut être étendue et appliquée dans d’autres zones avec des données éparses. La grille coût-performance est un outil utile pour la comparaison, la classification et la sélection d'approches adéquates de modélisation.

Mots-clefs : hydrologie ; hydraulique ; inondation ; bassins peu jaugés ; données éparses ; cartes d'inondation ; mesures post-événement ; incertitude ; Liban, Méditerranée ; coût-performance ; disponibilité des données ; complexité du modèle.

Résumé substantiel

Chapitre 1 : Introduction

1.1 Le problème des inondations dans le monde

Les inondations continuent de causer des pertes de vies humaines et des dégâts graves dans le monde entier. De toutes les catastrophes naturelles, les inondations touchent le plus grand nombre de personnes et sont les plus susceptibles de causer des dégâts (UNISDR, 2002). L'ampleur des catastrophes a ravivé la controverse récurrente sur l'impact du développement humain, alors que les sociétés contemporaines s'enrichissent, mais deviennent de plus en plus vulnérables aux catastrophes naturelles, notamment en termes de dégâts matériels causés aux infrastructures. Cette vulnérabilité est également le résultat de l'installation des activités humaines sur des zones fortement exposées (Brázdil et al., 2006). De plus, avec l'apparition du phénomène de réchauffement global planétaire et la croissance démographique, le nombre de personnes exposées à des inondations catastrophiques augmentent à un rythme alarmant.

Dans la région méditerranéenne, de nombreuses inondations catastrophiques survenues au cours des dernières décennies ont provoqué des pertes de vies humaines considérables. Le nombre de morts et de pertes économiques a augmenté dans les régions de l'est et du sud du fait de la fréquence et de l'intensité croissantes des fortes tempêtes hivernales et des inondations dans la région (Brauch, 2015). Les inondations dans la seule région méditerranéenne de 1990 à 2006 ont causé la mort de plus de 4 500 personnes (Llasat et al., 2010), les dégâts estimés à plus de 29 milliards d'euros, l'Italie étant le pays enregistrant les pertes les plus importantes, suivie par la France, la Roumanie, la Turquie, l'Espagne (Kömüşcü et Çelik, 2013). Enfin, les risques météorologiques devraient être croissants en raison du changement climatique prévu qui devrait s'accompagner d'une augmentation à la fois de la fréquence et de l'intensité des phénomènes météorologiques extrêmes (Dankers et Feyen, 2009).

1.2 Le problème des inondations au Liban

Le Liban (10 452 km²) est un petit pays montagneux situé sur la côte orientale de la mer Méditerranée. Il a un climat typiquement méditerranéen avec des variations locales importantes en raison de son relief complexe. C'est un pays très urbanisé avec plus de 88% de la population vivant sur une bande côtière étroite (World Bank, 2010). Ce dernier est traversé par un grand nombre de cours d'eau intermittents et environ 15 rivières pérennes susceptibles d'occasionner des inondations chaque année. Pendant les inondations, les rivières débordent provoquant des dégâts aux bâtiments et aux terres agricoles. Les raisons directes des inondations sont évidemment les fortes précipitations en plus de la nature topographique des lits des rivières. Mais de nombreux autres facteurs anthropiques augmentent les risques d'inondation, jouant sur l'intensité de l'aléa et la gravité des dégâts.

Plusieurs inondations ont touché le Liban au cours du siècle dernier. Parmi elles, l'inondation de la rivière Abou Ali, qui a touché les Caza de Tripoli et de Zgharta en 1955, est la plus importante : plus de 400 personnes sont décédées, 2000 familles se sont retrouvées sans maison, des milliers d'hectares de plantations d'agrumes ont été détruites, et 4 ponts de la ville se sont effondrés (Beydoun, 1976; Khawlie, 1994). En mars 2003, les inondations ont duré 10 jours et ont endommagé de vastes zones du territoire libanais, provoquant de nombreux effondrements d'ouvrages et de nombreuses pannes (Kabout, 2011). Les zones semi-arides de Baalbeck El Hermel

ont également été touchées par plusieurs crues soudaines, notamment en 1994, 1999, 2001, 2003, 2007, 2010, 2013 et 2018 (Abdallah et al., 2013). Les conséquences de tels événements sont très graves : pertes en vies humaines (5 morts par an), pertes financières annuelles (15 millions de dollars), destruction de maisons et de terres agricoles, perte de bovins, immenses dommages aux structures, services publics (électricité, communications, etc.) et d'énormes glissements de terrain (Abdallah et Hdeib, 2015).

Les études scientifiques sur les inondations au Liban sont assez rares. Sene et al. (1999) ont étudié les variations spatiales et temporelles des flux dans cinq bassins versants du Liban. Plus tard, Sene et al. (2001) ont mis au point une analyse préliminaire de la fréquence des inondations en analysant la distribution régionale des débits instantanés maximaux au Liban et ont proposé un schéma régional. Abdallah et al. (2013) ont élaboré des cartes des risques d'inondation pour le Liban pour différentes périodes de retour à une échelle de 1/20 000 sur la base de la modélisation hydrologique / hydraulique. Abdallah et Hdeib (2015) ont ensuite développé une évaluation des risques d'inondation, sur la base de vastes enquêtes de terrain et des évaluations de la vulnérabilité et des dommages. Il existe également des rapports techniques réalisés par le ministère de l'Énergie et de l'Eau, décrivant la situation des cours d'eau et proposant plusieurs suggestions pour réduire les risques d'inondation.

Les structures de surveillance sont très rares. Elles se limitent à des limnimètres traditionnels qui mesurent les fluctuations du niveau de l'eau sur très peu de points des rivières libanaises affiliées à « Litani River Authority » (LRA) et au réseau national de stations de mesure météorologique affiliés au Service météorologique national libanais (LNMS). Ce sont les seules sources de données permettant de surveiller les événements pluvieux et leurs relations avec les inondations. De plus, les cours d'eau secs généralement exposés aux crues soudaines ne disposent pas de stations de jaugeage et le volume d'eau en cas d'inondation n'est pas mesuré ; cela constitue un facteur très limitant pour les stratégies de prévention des inondations. Il convient également de mentionner que la guerre civile libanaise (1975-1990) a engendré un important déficit de données sur une période de plus de 20 ans : la plupart des stations de surveillance ayant été détruites ou non entretenues, elles ont donc interrompu leurs enregistrements. Un nouveau réseau est en construction depuis 1990. Cependant, les données mesurées restent très incertaines et manquent de fiabilité pour effectuer des études détaillées sur les inondations et des analyses à long terme (Merheb et al., 2016).

1.3 Le problème et les défis de la modélisation des inondations

Face au nombre important d'inondations signalées qui augmente à un rythme alarmant, la mise au point et l'application de modélisation des inondations sont devenues un défi majeur pour les recherches hydrologiques et hydrauliques au cours des dernières années. La littérature scientifique compte désormais de nombreux modèles hydrologiques et hydrauliques dont la complexité varie, allant de simples modèles empiriques (black box) comportant peu de paramètres, à des modèles complexes, distribués, à base physique, comportant de nombreux paramètres. Ces modèles diffèrent fortement en matière de type de données d'entrée requises, nature de calculs, de nature des variables de sortie, de résolutions spatio-temporelles et de précision. Bien que les modèles distribués à base physique soient de plus en plus utilisés pour mieux représenter les processus physiques au sein du bassin versant, leur application pratique induit des problèmes spécifiques liés à la forte exigence en matière de calcul, de nombre de paramètres à évaluer et de compétences requises pour les mettre en œuvre (Bathurst et O'Connell, 1992). Par conséquent, la réflexion

sur le choix judicieux de l'approche de modélisation, qui recherche un équilibre entre objectifs de simulation, complexité du modèle et disponibilité des données, est un sujet d'intérêt scientifique croissant (Bergström et al., 2002; Grayson et Blöschl, 2001; Neal et al., 2012b). Pour les applications pratiques, le principal défi du modélisateur est le choix d'une approche de modélisation des inondations efficace, à faible coût, adaptée aux objectifs et aux données disponibles. Jusqu'à présent, il n'existe pas de cadre commun pour comparer différentes approches de modélisation basées sur une quantification de la complexité du modèle, de la disponibilité des données et des performances. De nombreuses études ont comparé et référencé différents modèles et algorithmes, mais la plupart étaient basées sur la comparaison de leur structure ou de leur représentation des processus. En outre, les modélisateurs ont comparé leurs modèles à un ou plusieurs autres modèles très utilisés et considérés comme référence dans la littérature (Singh et Woolhiser, 2002). Grayson et Blöschl (2001) ont décrit la notion de compromis entre la complexité et les performances de prévision du modèle pour des conditions données de disponibilité des données (voir la figure 1.2 dans le texte principal). Ces auteurs montrent que pour une disponibilité des données fixée, il existe une complexité optimale de modèle au-delà de laquelle une complexité supplémentaire induit des problèmes d'identification des paramètres qui réduit les performances. L'explicitation de cette relation conceptuelle entre données, modèles et performances peut donc servir de base à l'évaluation ou à la comparaison de différentes approches de modélisation de complexité variable. Afin d'alimenter cette relation, il est nécessaire de développer des métriques permettant de quantifier ces trois composantes du problème de modélisation. L'objectif est d'aider à évaluer le rapport coût-performance de l'approche de modélisation choisie, en particulier pour les inondations.

1.4 Modélisation des inondations dans les régions avec des données éparses

Pour la plupart des bassins dans le monde, et en particulier dans les pays en développement, les données, ou les informations, fiables sur les caractéristiques spatiales et temporelles en relation aux inondations extrêmes sont rares ou inexistantes (voir par exemple Wilby et Yu, 2013 ; Jarihani et al., 2015; Komi et al., 2017). Dans les régions où des données éparses existent, le problème posé est celui de la compatibilité de leur résolution, dans le temps et dans l'espace avec les exigences des modèles hydrologiques et hydrauliques. Les données sont qualifiées d'éparses en référence à des mesures disponibles à des résolutions spatio-temporelles limitées, des mesures ponctuelles, des séries avec lacunes, ou des paramètres qui n'ont pas été collectés au cours de périodes simultanées (Samaniego et al., 2011; Mascaro et al., 2013). En raison de la rareté des données, la modélisation des inondations est devenue une tâche ardue, en particulier dans les régions caractérisées par des inondations d'une durée de quelques heures, offrant peu de possibilités d'enregistrement en temps réel sur les réseaux pluviométriques traditionnels, la télédétection ou l'imagerie par satellite. En conséquence, les approches de modélisation dans les régions avec des données éparses se limitent en majorité à des estimations incertaines des précipitations et des débits des crues fondées sur des données empiriques (i.e. Koutroulis et Tsanis, 2010), statistiques (i.e. Castellarin, 2007; Castellarin et al., 2009), ou des approches géomorphologiques (i.e. Manfreda et al., 2014). De telles applications sont utiles pour l'analyse des inondations régionales, à des résolutions grossières, mais ne sont pas adaptées aux bassins de taille petite à moyenne (<1000 km^2). En règle générale, pour les applications à l'échelle de tels bassin, nécessitant une compréhension plus détaillée d'une inondation, il est nécessaire de recourir à une modélisation hydrologique / hydraulique. Dans ce contexte, et lorsque les données sont incertaines et trop rares pour répondre aux

exigences du modèle, deux questions se posent alors : (i) est-il possible de contraindre le modèle hydrologique et hydraulique avec des données éparses afin de simuler des inondations extrêmes et d'établir des niveaux d'eau utiles pour l'évaluation des inondations ?, et (ii) quel est le rapport coût-performance de cette approche de modélisation, compte tenu de la grande complexité du modèle et de la disponibilité limitée des donnée ?.

1.5 Objectifs de la thèse

Ce travail vise à développer un cadre pour la modélisation des inondations dans des régions avec des données éparses, en analysant différentes approches de modélisation des inondations selon une approche coût-performance. L'étude est appliquée au Liban, un pays de la Méditerranée orientale. Nous analysons d'abord les rares données disponibles sur les inondations dans le pays, puis examinons et évaluons les inondations historiques extraites des archives de journaux pour en tirer des conclusions sur l'intensité et la fréquence des inondations au Liban. Nous discutons des opportunités et des limites de telles sources de données pour l'application d'une approche de modélisation hydrologique / hydraulique à un site d'étude sélectionné. Comme première étape vers la sélection d'une approche de modélisation appropriée, nous développons une nouvelle grille coût-performance permettant d'évaluer différentes approches de modélisation des crues disponibles dans la littérature. La grille est basée sur la définition de métriques permettant d'évaluer les trois axes d'un problème de modélisation: la disponibilité des données, la complexité du modèle et les performances de la modélisation. La dernière étape consiste à élaborer un cadre de modélisation des inondations à partir d'un modèle couplé hydrologique-hydraulique contraint par des observations post-crue et des mesures hydrologiques issues d'événements passés. La thèse est structurée en trois parties principales et neuf chapitres avec quatre annexes.

Chapitre 2 : Etat de l'art

Ce chapitre présente l'étude bibliographique pour le travail de thèse

Partie I: Analyse des inondations historiques à l'échelle régionale

Cette première partie de la thèse est composée de trois chapitres (chapitres 3, 4 et 5) qui présentent les jeux de données disponibles afin d'analyser les caractéristiques géographiques, hydrologiques et climatiques du Liban. Le site d'étude sélectionné pour une analyse détaillée est celui du bassin de la rivière Awali. 711 enregistrements d'inondations au Liban extraits d'archives de journaux et de rapports des archives sont ensuite examinés. Une analyse de l'intensité et de l'occurrence spatiale des événements est réalisée afin de tirer certaines conclusions sur le problème des inondations au Liban. Cette partie se termine par une discussion sur les opportunités et les limites de telles sources de données.

Chapitre 3 : Liban: description du site d'étude et analyse des données

Dans ce chapitre, nous décrivons les principales caractéristiques géographiques, hydrologiques et climatiques du Liban. La topographie du Liban est principalement montagneuse, composée de deux chaînes de montagnes à tendance NNE-SSO, séparées par une plaine étroite, la fertile plaine de la Bekaa. Une étroite bande de terre côtière borde la mer Méditerranée. Le point culminant est Qornet Es-Saouda qui culmine à 3 088 m. La géologie sous-jacente du pays est constituée principalement de roches carbonatées (calcaire et dolomie) datant principalement du Jurassique et du Crétacé. La séquence stratigraphique affleurante au Liban expose des formations rocheuses allant du Jurassique moyen au Quaternaire récent (Abdallah et al., 2005).

Les types de sol prédominants sont : sols rouges, sols bruns, sols montagneux jaunâtres, sols noirs, sols griséris, sols de châtaigniers, sols sableux, sols alluviaux, sols jaunâtres sub-désertiques, Rendzine et Sols Mixtes. Les caractéristiques de l'occupation des sols sont également présentées. Elles peuvent être divisées en sept catégories: zones artificielles, zones agricoles, terres boisées, terres herbeuses, zones humides, zones non productives et plans d'eau.

Le climat du Liban est méditerranéen. Les précipitations moyennes annuelles sont très variables et vont de 500 mm dans la zone intérieure d'Assi, une zone semi-aride au nord-est du pays, à plus de 1 200 mm dans les hautes montagnes du Mont-Liban. Les données sur les précipitations sont disponibles pour la période 2001-2012 à partir d'un réseau pluviométrique traditionnel d'environ 37 stations enregistrant des mesures de précipitations quotidiennes et parfois mensuelles. Un grand déficit de données correspond à la période de guerre civile (1975-1990), où la plupart des stations ont cessé leurs activités. Le Liban compte 17 cours d'eau pérennes et environ 23 cours d'eau saisonniers. Le réseau de surveillance des rivières est limité aux limnimètres traditionnels qui enregistrent les mesures horaires du niveau de l'eau sur un très petit nombre de points car plusieurs rivières n'ont pas de sections correctement définies. La plupart de ces stations ne sont pas fonctionnelles lors des inondations.

Chapitre 4 : Le bassin du Awali, description du site d'étude et analyse des données

Dans ce chapitre, nous présentons une description du site d'étude choisi pour effectuer l'analyse détaillée de la modélisation hydrologique-hydraulique, les résultats des enquêtes sur le terrain et l'analyse des données disponibles. Le bassin de la rivière Awali est l'un des bassins versants côtiers de la Méditerranée orientale, situé au sud du Liban. Le fleuve est l'un des principaux fleuves pérennes du pays et subit des inondations environ tous les deux ans. Ce site d'étude a été choisi parce que nous avons eu l'occasion d'enquêter sur l'inondation extrême de début janvier 2013, considérée comme l'un des plus importants événements des trois dernières décennies. Des enquêtes de terrain détaillées, réalisées un mois après l'inondation, ont permis de relever 57 mesures de laisses de hautes eaux, correspondant aux débits de crue maximum, à plusieurs endroits le long de la rivière. La géométrie du lit des rivières et des plaines d'inondations a été extraite d'un MNT à haute résolution (10 cm) généré par plusieurs clichés de drones UAV. Les mesures journalières des précipitations ont été obtenues pour sept stations météorologiques exploitées par le LNMS après la guerre civile (2000-2016). Deux stations limnimétriques effectuent des mesures horaires des niveaux d'eau. Le volume écoulé annuel moyen du bassin est d'environ 347 Mm^3 et le débit journalier moyen est de 11m^3/s. Ces données ont été analysées pour sélectionner les 12 événements de crue passés d'intensités variables et pour lesquels il existait des mesures simultanées des précipitations et des débits.

Chapitre 5 : Analyse d'événements d'inondation historiques – Liban

Dans ce chapitre, nous présentons les résultats d'une analyse approfondie des archives de journaux et de rapports pour extraire des informations sur les inondations survenues dans le pays. Nous avons pu extraire 196 événements s'étendant de 1293 à 2013, parmi lesquels nous avons pu distinguer 711 inondations dans 86 villages du Liban. La fréquence mensuelle d'occurrence a été analysée et l'occurrence spatiale de ces événements a été cartographiée à l'échelle du district (caza) sur cinq niveaux. Les principales caractéristiques morphologiques et hydrologiques des bassins versants concernés ont été extraites et leur vulnérabilité aux inondations en matière de d'utilisation des sols a été déterminée. Nous avons tenté d'analyser les raisons des

occurrences d'inondations. Pour cela, nous avons cherché les relations entre la fréquence des événements et les caractéristiques des bassins versants prises une à une ou combinées.

Les cinq bassins versants de la côte nord, el Kabir, Ostouane, Arka, Bared et Abu Ali (partie principale basse à Tripoli), montrent le plus grand nombre d'événements avec les bassins versants centraux du fleuve Beyrouth et de la ville de Beyrouth. Les bassins versants d'Assi, de Litani, d'Hasbani, d'Awali et de Damour viennent en deuxième position. La variation spatiale du nombre d'occurrences d'inondations dans les bassins versants étudiés ne peut pas être liée à un seul facteur, mais à une combinaison de facteurs morphologiques, hydrologiques et de facteur lié à leur vulnérabilité. Par conséquent, la carte développée est une combinaison de l'aléa climatique et de la vulnérabilité et est équivalente à une carte des risques d'inondation.

En l'absence de mesures, les événements extraits des journaux et des rapports constituent une preuve qui permet d'extraire des informations sur les inondations de la période pré-instrumentée. Ces informations permettent pour la première fois d'analyser la fréquence et l'occurrence spatiale d'inondations dans tout le pays. Lorsqu'elle est superposée à la carte de vulnérabilité, la carte permet de mettre en évidence les zones à fort aléa et peut être considérée comme une carte de risque d'inondation en l'absence d'autres études détaillées. Les résultats peuvent ne pas être clairs, mais ouvrent des perspectives pour comprendre les inondations et les changements dans leurs régimes., Ces informations restent cependant descriptives et se montrent plus les dommages de l'événement que sur ses caractéristiques. La carte est développée à grande échelle (échelle de district), ce qui ne permet pas l'analyse détaillée des débits des crues, des niveaux d'eau et de l'étendue du champ d'inondation. Or ces informations sont indispensables dans tout projet détaillé d'atténuation des inondations ou de système de prévision des inondations. Par conséquent, la carte développée ne peut pas remplacer une modélisation hydraulique du bassin versant. Nous avons donc choisi le bassin de la rivière Awali comme site d'étude afin d'effectuer une analyse et une modélisation détaillées.

Partie II: Une grille d'analyse coût-performance pour la modélisation des crues

La deuxième partie de la thèse est constituée de deux chapitres (chapitres 6 et 7), dans lesquels nous développons une nouvelle grille coût-performance. L'objectif est de proposer une démarche pour analyser différentes approches de modélisation des inondations présentées dans la littérature afin de tirer des conclusions sur la manière de sélectionner celle appropriée pour une étude donnée en équilibrant la complexité du modèle et la disponibilité des données.

Chapitre 6 : La grille coût-performance proposée

Dans ce chapitre, nous présentons la structure d'une grille d'analyse coût-performance proposée pour la modélisation des crues. Dans cette approche, nous émettons l'hypothèse que le «coût de modélisation» est une fonction (i) de la «disponibilité des données», c'est-à-dire la quantité et la qualité des données utilisées pour la simulation, le calage et la validation des modèles, et (ii) de la «complexité des modèles», en lien avec le niveau de détails associé aux processus représentés. À cet égard, nous avons classé les données et les modèles en catégories et sous-catégories. Le coût de chaque sous-catégorie est calculé en fonction de critères d'évaluation. Chaque critère d'évaluation se voit attribuer une note basée sur cinq niveaux (variant de «VL» (Very Low ou très bas) à «VH» (Very High ou très haut)) et un poids (faible, moyen ou élevé). Le coût d'une sous-catégorie est calculé suivant une somme pondérée. Des pondérations globales sont attribuées à chaque sous-catégorie pour souligner son

influence par rapport aux autres sous-catégories, et le coût total est la somme pondérée des coûts de toutes les sous-catégories. Les performances de la modélisation sont calculées sur la base de six critères d'évaluation reflétant le type de sortie obtenu, les fonctions critères utilisées pour évaluer le modèle et les valeurs des fonctions d'erreur correspondant aux quatre types de sortie (débit et hydrogramme de crue, niveau d'eau, et étendue des inondations). Afin de collecter des données sur différentes approches de modélisation dans la littérature et de générer une base de données bien organisée, une enquête coût-performance sous forme d'un formulaire à remplir a été mise au point et disponible en ligne. Cette enquête doit permettre de collecter des informations sur le retour d'expérience de différents utilisateurs de différentes approches de modélisation, de manière cohérente et sur la base de la grille coût-performance proposée.

Chapitre 7 : Application de la grille coût-performance

Dans ce chapitre, nous présentons une application de la grille d'analyse coût-performance proposée. Dix études ont été choisies et évaluées. Le niveau de coût total moyen était de 0,36 (sans dimension, 1 indiquant le coût maximal) et le niveau de performance moyen était de 0,59 (sans dimension, 1 indiquant les performances maximales). Les coûts de modélisation les plus bas étaient associés à des approches empiriques et à des performances inférieures. Les approches de modélisation basées sur des données *Open Source* ont été associées à des coûts moindres et des performances élevées, en particulier dans les applications à de bassins bien jaugés. Tracer les cas d'étude sur le diagramme coût-performance nous permet de mettre en évidence 4 zones de modélisation correspondant à 4 catégories de modélisation (empirique, hydraulique, hydrologique et couplée). Les zones correspondant aux modèles couplés sont associées à de bonnes performances et se situent au-dessus de la courbe coût-performance. La zone de modélisation hydraulique est associée à des coûts moindres. Les zones des approches empirique et hydrologique sont situées en dessous de la courbe de performance de coût et sont associées à des niveaux de performance inférieurs, car les résultats de ces approches ne répondent pas à l'objectif de cartographie des inondations.

Une analyse de sensibilité de la grille aux scores et aux pondérations montre que la grille est très sensible à l'échelle des scores sélectionnés mais moins sensible à la sélection des pondérations. Une échelle linéaire de scores sur cinq niveaux donne de meilleurs résultats par rapport à un niveau d'échelle logarithmique. La grille est également sensible au point de vue de l'auteur; les niveaux de coûts sont principalement sensibles à l'année et au pays d'application et les niveaux de performance sont principalement sensibles à l'objectif de l'approche de modélisation.

Partie III: Un cadre pour la modélisation des inondations dans les régions à données rares

La troisième partie de la thèse est composée de deux chapitres (chapitres 8 et 9) comprenant un article publié en août 2018 dans *Journal of Hydrology*.

Dans cette partie, nous évaluons s'il est possible de contraindre les modèles hydrologiques et hydrauliques à l'aide de données limitées pour simuler des inondations extrêmes et établir des niveaux d'eau utiles pour la cartographie des inondations et donc adaptée aux applications à l'échelle des bassins. Le défi consistait à développer une approche de modélisation rentable qui équilibre la complexité du modèle avec la condition de disponibilité limitée des données. À cette fin, nous proposons un cadre de modélisation basé sur un modèle couplé hydrologique-hydraulique contraint par données éparse, c'est-à-dire, dans notre cas, relatives à des

événements de crues passés et des mesures post-crue. La partie se termine par une discussion sur les opportunités et les limites du cadre proposé, ainsi que sur le coût-performance de l'approche appliquée.

Chapitre 8 : Présentation du cadre proposé

Dans ce chapitre, nous avons proposé un cadre pour la modélisation des inondations dans les régions avec des données éparses. Le cadre repose sur le couplage d'un modèle hydrologique conceptuel semi-distribué (HEC-HMS) avec un modèle hydraulique 1D (HEC-RAS). Le modèle hydrologique est calibré et évalué avec les événements de crues mesurés dans le passé afin de définir des plages de valeurs des paramètres. Une simulation Monte Carlo est réalisée pour ces plages de paramètres. Les simulations du modèle hydraulique, basé sur un MNT à résolution fine, sont effectuées à l'aide des sorties du modèle hydrologique et validées par des mesures post-crue.

Chapitre 9 : Application du cadre proposé

L'approche est appliquée sur le site d'étude du bassin de la rivière Awali (301 km^2), au Liban, pour simuler l'inondation extrême ayant fait l'objet d'une caractérisation de terrain début janvier 2013. Le modèle hydrologique a été calibré à partir de 12 événements de crue afin de définir des plages de paramètres. Les incertitudes associées aux paramètres du modèle ont été évaluées en effectuant la technique Monte Carlo. On observe que l'incertitude sur les valeurs de sortie peut être réduite par rapport aux simulations basées sur des plages de paramètres larges choisies arbitrairement. Les informations issues des médias sociaux sur les caractéristiques des événements, en particulier sur la durée des précipitations maximales, ont constitué une valeur ajoutée pour contraindre les simulations du modèle hydrologique. Les mesures post-événement des laisses de crue ont permis de valider la représentation spatiale de l'inondation. Les résultats montrent que de bonnes mesures spatiales d'un événement, même de très courtes durées, jouent un rôle important dans la modélisation hydrologique/hydraulique. Ces données spatiales éparses, à une date donnée, peuvent être utilisées en l'absence de données temporelles classiques acquises à des stations de mesure sur le cours d'eau. Sur la base de la grille coût-performance, la comparaison de cette approche avec d'autres approches de modélisation de crue, en particulier les approches de couplage des modèles, révèle un bon compromis. Le MNT à résolution fine a légèrement augmenté les coûts de modélisation, mais a également considérablement amélioré les performances de modélisation.

Conclusion générale

Dans les régions avec des données éparses, les événements de crue et d'inondation extraits des journaux et des rapports d'archives sont prometteurs pour cartographier l'occurrence spatiale d'inondations et mettre en évidence les zones à haut risque. Cependant, ces informations restent descriptives et globales et ne permettent pas une compréhension détaillée des phénomènes d'inondation. De même, les approches géomorphologiques, récemment appliquées dans les régions avec des données éparses, se sont également révélées efficaces pour la cartographie des inondations, principalement pour des applications sur de grandes étendues spatiales. Les cartes résultantes peuvent être principalement utilisées pour des études régionales sur le risque d'inondation et ne sont pas suffisantes pour des applications à petite échelle. Par conséquent, lorsque des informations détaillées sur les débits des crues et les niveaux d'eau sont nécessaires dans les applications à petite échelle, l'utilisation de modèles hydrologiques et hydrauliques est inévitable.

Une difficulté majeure associée à ce type de modélisation provient du manque de données d'observation suffisantes pour le calage et validation. Mieux exploiter les données et les modèles disponibles est une opportunité pour réduire les coûts de modélisation et améliorer les performances. La grille coût-performance proposée constitue un outil permettant de faciliter la comparaison, la classification et la sélection de modélisation. Sur la base de la grille, la modélisation couplée des crues proposée s'est révélée une approche rentable. Cette application constitue une position intermédiaire entre les approches complexes et simples. En effet, plusieurs simplifications en matière de représentation du processus ont été opérées pour réduire les exigences du modèle et le nombre de paramètres. La complexité du modèle dépend de la manière dont nous le définissons, du site d'application et du moment de l'application. Ce qui était considéré comme complexe il y a plusieurs années est maintenant plus simple avec l'évolution rapide de la puissance de calcul, le développement de MNT à très haute résolution et la généralisation des systèmes d'information géographique (SIG). Malgré la légère augmentation des coûts des données, la recherche d'une précision plus élevée dans certains types de mesure, tels que l'obtention de MNT à haute résolution, peut aider à améliorer les performances de modélisation et est donc recommandée dans un cadre de modélisation hydrologique-hydraulique dans les régions à données éparses.

Enfin, le travail de thèse ouvre des perspectives pour plusieurs applications. À des fins opérationnelles, le cadre proposé ne se limite pas au site d'étude sélectionné, il peut être appliqué aux autres bassins versants libanais et aux autres régions confrontées aux mêmes problèmes pour modéliser les inondations. Dans ce sens, il peut faire partie d'un système national de prévision des inondations. L'avantage évident de l'approche proposée est qu'il s'agit d'une approche sur mesure, adaptée aux applications à l'échelle des bassins dans des régions des données éparse, qui utilise le maximum de données disponibles et vise à produire des cartes d'inondation plus performantes que les cartes régionales. La méthode permet de modéliser avec une incertitude réduite des inondations particulières en termes d'estimation des hydrogrammes, des niveaux d'eau et de la cartographie de la zone inondée. Elle présente un potentiel pour l'intégration d'informations issues de « crowdsourcing » : estimations spatiales post-crue extraites de publications sur les réseaux sociaux, de témoins locaux, ainsi que d'images et de vidéos. Ce type d'information, potentiellement de masse, gagne maintenant en popularité et pourraient compenser les faiblesses des réseaux de mesure traditionnels. Par ailleurs, la méthode peut potentiellement inclure des MNT à haute résolution qui évoluent à un rythme élevé. La grille coût-performance permet de comparer différentes approches de modélisation des crues sur une échelle unifiée, de les classer en fonction des niveaux de coût et de performance et de choisir les meilleures pour les applications futures en fonction d'objectifs définis, de données et de modèles disponibles. Cette grille introduit la notion de rentabilité des approches de modélisation. D'un point de vue philosophique, la grille permet l'étude de l'évolution de la recherche. Elle permet également d'étudier l'évolution historique des coûts et des performances des modélisations. La grille est flexible et peut être ajustée pour s'adapter à différents objectifs de modélisation et peut être mise à jour périodiquement pour suivre les progrès récents en matière de données disponibles et de capacités de modélisation.

A framework for flood modelling in data-sparse regions based on a new cost-performance grid, application on the Awali Basin in Lebanon

Abstract

Floods affect the greatest number of people worldwide and have the greatest potential to cause damage. Developing flood modelling tools to better understand and mitigate floods has become a global endeavor. Numerous models of variable complexity are now available aiming at understanding the flood processes. Therefore, the choice of selection of an effective and economic model is not an easy exercise. In data-sparse regions, flood modeling is a challenging task because of the shortage in observational data to calibrate and validate the hydrological-hydraulic models and the question arises to whether there is opportunity to model floods based on hydrological-hydraulic models using sparse data, and whether such approach remains cost-effective given the high model complexity and limited data availability. Consequently, this work aims to develop a framework for flood modeling in data-sparse regions based on analyzing different flood modeling approaches in a cost-performance approach. It is structured into three parts: (i) a collection of flood events in Lebanon from newspapers to analyze the spatial occurrence of events, (ii) a new cost-performance gird to compare different modeling approaches, (iii) a cost-effective framework for flood modelling using sparse data.

In part I an intensive history scan of newspaper archives allows us to extract 711 flood events (1293-2013) in Lebanon. The spatial occurrence of these events was mapped and analyzed to extract the reasons behind such variability. The spatial variability of flood events in the studied catchments was linked to a combination of morphological, hydrological, and vulnerability characteristics and the developed spatial flood occurrence map can be treated as a flood risk map. The extracted events from newspapers were promising in retrieving information on previous flood events, but these records remain descriptive and hence cannot replace the need for a detailed hydrological-hydraulic modeling.

In part II we propose a new cost-performance grid to evaluate flood modeling approaches. The grid is based on defining metrics to evaluate the three axes of a modeling problem: data availability, model complexity, and modeling performance. As an application, 10 arbitrability selected study cases were evaluated and plotted on a cost-performance diagram. Hydraulic and coupling approaches are associated with good performances and are located above the cost-performance curve, whereas, empirical and hydrological approaches are located below and are associated with less performance levels.

In part III we develop a framework for flood modeling in data-sparse regions, based on a coupled hydrological-hydraulic model (HEC-HMS - HEC-RAS) constrained by past storm events and post-event measurements. The approach is tested to the Awali river basin (301 km^2), in Lebanon, particularly to simulate the investigated early January 2013 extreme flood event. The hydrological model was calibrated with 12 past storm events aiming at defining narrow hydrological parameter ranges. The uncertainty in the model parameters was assessed by performing Monte Carlo simulation for the estimated parameter ranges. The uncertainty in the resulting outflow values is reduced

when compared to simulations based on arbitrarily chosen wide parameter ranges. Social media information was an added value to constrain the hydrological model simulations. Post-event measurements of high-water marks were promising in validating the flood map in space.

Based on the cost-performance grid, the proposed framework reveals a good cost-performance level. The modeling approach falls in an intermediate position between complex and simple approaches. The framework can be extended to other data-sparse regions facing the same problems and can be part of a national flood forecasting system. The cost-performance grid can be a tool to support the comparison, classification, and future selection of cost-effective modeling approaches.

Keywords hydrology, hydraulics, floods, poorly gauged basins, sparse data; flood model; post-event measurements; uncertainty; Lebanon, Mediterranean; Cost-performance; data availability; model complexity.

Foreword

Financial support

The thesis was funded by the National Council for Scientific Research-Lebanon (CNRS-L) under the PhD scholarship program 2015. Part of the work was partially funded by the Italian National Research Council (CNR) project (Third Call for Proposals for joint research projects 2015-2016 CNR- CNRS-L) entitled “Hydrological modelling optimization in poorly gauged and small sized basins – Lebanon as a case study”.

Hosting laboratories

The hosting laboratories for the following thesis are the Remote Sensing Center of the National Council for Scientific Research-Lebanon and the Laboratory for the study of Soil-Agrosystem- Hydrosystem interactions at the French National Institute for Agricultural Research (INRA-LISAH).

Publications

The thesis gives rise to three publications in peer reviewed journals, one published online and the other two are in process of submission. In addition to one oral presentation in an international conference.

Publications in peer reviewed journals:

- Hdeib R., Abdallah C., Colin F., Brocca L., Moussa R., 2018. Constraining coupled hydrological-hydraulic flood model by past storm events and post-event measurements in data-sparse regions. Journal of Hydrology, October 2018, Volume 565, pages:160-176, doi: 10.1016/j.jhydrol.2018.08.008

- Hdeib R. et al., 2019. A cost-performance grid to compare different flood modelling approaches. Manuscript expected to be submitted May 2019.

- Hdeib R. et al., 2019. Evaluating historical flood events from newspapers, Application in Lebanon. Manuscript under preparation based on chapter 5.

Conferences:

- Hdeib R., Abdallah C., Moussa R., Hijazi S., 2016. Flood Hazard Mapping Assessment for El-Awali River Catchment-Lebanon General Assembly (EGU), 19/4/2015, Vienna, Austria. Geophysical Research Abstracts; Vol. 18, EGU2016-17305-1, 2016

- Hdeib R., Abdallah C., Colin F., Moussa R., Brocca L., 2018. Flood inundation maps with the associated uncertainty using sparse data in the Mediterranean region. EGU General Assembly 2018 (08-13 April) in Vienna, Austria on 12th of April 2018. Geophysical Research Abstracts; Vol 18, EGU2018-1768-2.

Table of Contents

Part I: Analysis of historical flood events on a regional scale

List of Figures

List of Tables

List of Acronyms

Ac	Catchment area, km^2
Agr	Agricultural areas, %
C_D	Cost of data, unit of score
$C_{D\ [1]}$	Cost of data, dimensionless
C_k	Cost of category *k,* unit of score
$C_{k\ [1]}$	Cost of category *k,* dimensionless
C_M	Cost of models, unit of score
$C_{M\ [1]}$	Cost of models, dimensionless
CN	Curve number
CNRS	National Council for Scientific Research-Lebanon
C_T	Total cost of a modelling approach, unit of score
$C_{T\ [1]}$	Total cost of a modelling approach, dimensionless
D	Event duration, h
Dd	Drainage density, (km/km^2)
DEM	Digital elevation model, 10 m and 10 cm resolution
f_i	Score of evaluation criteria *i*, $1 \leq f \leq 5$; f=0, if criteria is not applied
Grass	Grass land, %
gw_j	Global weight of sub-category j, $1 \leq gw \leq 3$
HSG	Hydrological soil groups
i	Cost evaluation criteria
Ia	Initial abstraction, mm
j	A sub-category for data or models
k	A main category for modelling (hydrological/hydraulic models or data)
Lat.	Latitude (GPS), decimal degrees
LARI	Lebanese Agricultural Research Institute
Lflow	Longest flow path, km
LNMS	Lebanese National Meteorological Service
Long.	Longitude (GPS), decimal degrees
LRA	Litani River Authority
MAE	Mean absolute error, m^3/s
Max Zc	Maximum elevation, m

Min Zc	Minimum elevation, m
n	Manning's coefficient
N	Number of observations
Ne	Number of flood events, level 1 to 5
NSE	Nash-Sutcliffe efficiency
P_{av}	Average rainfall depth over the whole basin
PE	Phase error, h
PFE	Peak flow error, %
P_M	Performance of the modelling approach, dimensionless
P_T	Rainfall depth of return period T, mm
Q_{obs}	Observed peak flow, m^3/s
Q_{peak}	Peak flow, m^3/s
Q_{sim}	Simulated peak flow, m^3/s
Q_T	Discharge of return period T, m^3/s
r	Coefficient of correlation
RMSE	Root mean square error, m^3/s or m
RSC	Remote Sensing Center
Sc	Slope along longest flow path, %
S_j	Cost of sub-category *j*
T	Return period, years (T= 10, 50, or 100 years)
T_{lag}	Lag time, min
Uc	Artificial/Urban areas, %
Unpr	Unproductive areas, %
VE	Volume error, %
V_{obs}	Observed total runoff volume for a storm event, mm
V_{sim}	Simulated total runoff volume for a storm event, mm
Wd	Wooded land, %
w_i	Weight of evaluation criteria *i*, $1 \leq w \leq 3$
Zc	Mean elevation, m

1 GENERAL INTRODUCTION

1.1 The flood problem worldwide

Flood continue to cause loss of life and serious damage worldwide. Of all natural disasters, floods affect the greatest number of people worldwide and have the greatest potential to cause damage (UNISDR, 2002). In fact, floods are responsible for over one third of people affected by natural disasters. Since 1995, floods have accounted for 47% of all weather- related disasters, affecting 2.3 billion people in more than 90 countries exposed to catastrophic floods every year. Floods caused damages of 662 billion US dollars and left behind around 157000 deaths. The number of floods per year rose to an average of 171 in the period 2005-2014, up from an annual average of 127 in the previous decade (UNISDR and CRED, 2015) (Figure 1.1). The scale of the disaster has revived the recurring controversy over the impact of human development as contemporary societies become wealthier, but ever more vulnerable and susceptible to natural disasters, in terms of material damage to complex infrastructures. This is also a result of human encroachment into unsafe areas (Brázdil et al., 2006). Moreover, with the emerging global warming phenomenon, via the enhanced greenhouse effect, the number of people exposed to catastrophic floods and the economic damages resulting from flooding are on the rise at an alarming rate.

In meteorological terms, flooding is usually defined as a localized hazard that is generally the result of excessive and localized precipitation in a short time period over a given location. Around 10 different types of floods are identified by the World Meteorological Organization based on the seasonality, location, meteorological conditions, and resulting impacts (WMO, 2011). Among them, flash floods and single-event floods are the most common (Kömüşcü and Çelik, 2013).

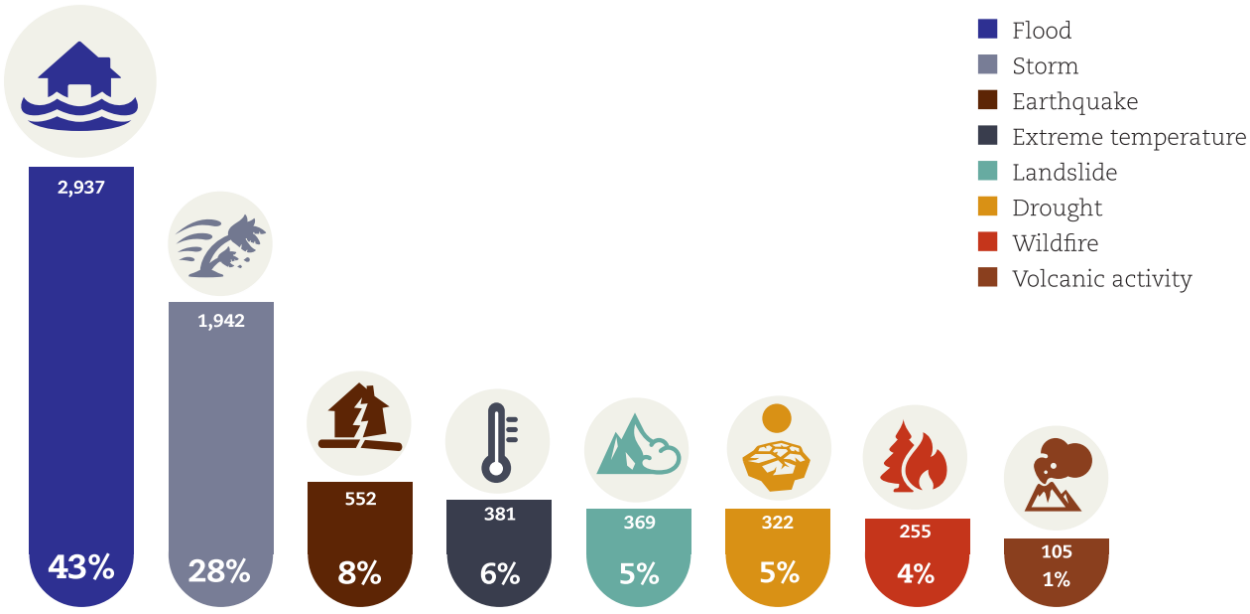

Figure 1.1 Share of occurrence of natural disasters by disaster type, number of events by sub-group (1994-2013) in 10 most disaster-affected countries (CRED, 2015).

In Europe, between 1998 and 2002, over 100 major damaging floods including the catastrophic floods along the Danube and Elbe rivers (2002) were recorded (Barredo, 2007). Since 1998, those floods caused the displacement of almost half a million people and caused around 700 fatalities and at least 25 billion Euros in insured economic losses across Europe.

In the Mediterranean region, many catastrophic floods that occurred in the recent decades, have caused considerable loss of life. The number of fatalities and economic losses has been rising in the eastern and the southern regions as a result of the increased frequency and intensity of severe winter storms and floods being felt in the region (Brauch, 2015). Floods in the Mediterranean region alone from 1990–2006 caused the death of over 4,500 people (Llasat et al., 2010), estimated damages exceeded 29 billion Euros, Italy being the country with the greatest losses followed by France, Romania, Turkey, and Spain (Kömüşcü and Çelik, 2013). The Emergency Events Database (EM-DAT) of the Centre for Research on the Epidemiology of Disasters (CRED) show that generally the Southern and Eastern Mediterranean regions record the highest number of deaths resulting from floods mainly caused by anthropogenic effects in flood prone areas. The Northern Mediterranean countries record the highest economic losses from floods caused mainly by land use change and hitting vulnerable touristic coastal towns. However, more devastating weather-related hazards are expected to occur in the Mediterranean region as a result of the anticipated global climate change that is projected to be accompanied by increases in both the frequency and the intensity of extreme weather events (Dankers and Feyen, 2009).

1.2 **The flood problem in Lebanon**

Lebanon is a small mountainous country located on the eastern shores of the Mediterranean Sea. It has a typical Mediterranean climate with important local variations because of its complex relief. It is a heavily urbanized country with more than 88 % of the population living on a narrow coastal stretch (World Bank, 2010). This includes the western flank of Mount Lebanon from 0 to 800 m of altitude, and the large spaces in the North and the South of the country. The littoral is the most important and the most vulnerable zone in the country. The latter is dissected by a large number of seasonal streams and about 15 perennial rives that are at risk of flooding every year. Floods normally occur during the wet season, generally after a strong storm or at the beginning of the spring with the melting of the snow. During floods, rivers burst their bank causing floods and damages to buildings and agricultural land. The direct reasons of floods are evidently the strong storms with heavy rains in addition to the topographic nature of the river channel. But many other anthropogenic factors increase the chance of inundation, the intensity of the floods and the severity of damages.

Several floods stroked Lebanon in the last century with perhaps the Abou Ali River Flood that hit Caza Tripoli and Zgharta in 1955, being the largest ever impacting an area approximately 400 km^2. More than 400 people died, 2000 families found themselves without houses, thousands of acres of citrus plantations were destroyed, 4 bridges of the city collapsed, as well as several events of failure of surficial cover (Beydoun, 1976; Khawlie, 1994). In March 2003, the floods lasted for 10 days damaging large areas of the Lebanese territory with many slides and mass failure at

various locations. The areas damaged covered vast regions in Akkar plane "North Lebanon"; Litani basin "Bekaa", the coastal stretch from El Abde to Naqoura, in addition to several villages juxtaposing river banks in the mountains (Kabout, 2011). The semi-arid areas in Baalbeck El Hermel also witness several flash floods especially in 1994, 1999, 2001, 2003, 2007, 2010, 2013, and 2018 causing a huge loss in properties, destroying bridges and disrupting the Baalbeck-Syria highway at several occasions and for several hours (Abdallah et al., 2013; Abdallah and Hdeib, 2015). With the global climate change, urbanization growth and land use change the severity of flooding in Lebanon is expected to increase. The consequences of such events are tragic including annual financial losses (15 million dollars), casualties (5 persons dead per year), destruction of houses and agricultural lands, loss of cattle, tremendous damage to structures, utilities and public services (electricity, communications, etc.), and huge landslides.

Flood events studies in Lebanon are almost lacking. Sene et al. (1999) studied the spatial and temporal variations in flows for five catchments in Lebanon. Later, Sene et al. (2001) development a preliminary flood frequency analysis by analysing the regional distribution of maximum instantaneous flows in Lebanon; they found a certain regional pattern. Hreiche (2003) developed a daily lumped conceptual rainfall-runoff model (MEDOR) for the Mediterranean climate. He applied and validated the model on six Lebanese and French catchments. Bernier et al. (2003) used remote sensing techniques (RADARSAT-1 images) to estimate snow water equivalent and improve the hydrological modelling of catchments of Mont Lebanon using the HYDROTEL model. Abdallah et al. (2013) developed flood hazard maps for Lebanon for different return periods at a scale of 1/20,000 based on hydrological/hydraulic modelling and later Abdallah and Hdeib (2015) developed a flood risk assessment for flood prone areas based on extensive field investigations along with vulnerability and damage assessments. There are also some technical reports, realized by the Ministry of Energy and Water, describe the situation on the river channels and propose several suggestions to reduce the probability of flooding.

Flood monitoring structures are very few; they are limited to traditional river stage gauges that measure water level fluctuations on very few points along the Lebanese rivers affiliated to the Litani River National Authority (LRA) and the national network of weather gauging station affiliated to the Lebanese National Meteorological Services (LNMS), Directory of Civil Aviation of the Ministry of Transport and Public Affairs. These are the only sources for data to monitor storm events and their relations to floods. Moreover, dry channels generally exposed to flash floods do not have gauging stations and the volume of water during flood events are not measured and could not be accurately determined: a very limiting factor for flood prevention strategies. One must also mention that the Lebanese civil war (1975-1990) left behind a big data gap of more than 20 years, since most of the monitoring stations were either destroyed or unmaintained and consequently ceased operation. A new network is being constructed since 1990’s, however, data measurements are still highly uncertain and lack adequate reliability to perform detailed flood studies and long-term analysis especially with an increase of anthropogenic pressure on water resources (Merheb et al., 2016).

1.3 The flood modelling problem and challenges

Since 1970's, advances in watershed mathematical modelling occurred at an unprecedented pace and were triggered by the digital revolution in both fields of numerical and statistical analysis (Singh and Woolhiser, 2002). Following the rapid growth in computational power, systematic efforts within the research community have largely improved the capability of mathematical models and paved the way to their use in most water resources and engineering applications, also, more specifically in flood modelling applications (Teng et al., 2017).

In response to the significant number of reported flood events that is increasing at an alarming rate, development and application of flood inundation models has become a major challenge in hydrologic and hydraulic studies over the last years. Flood inundation models have become a prerequisite for various applications, these include but not limited to, real-time flood forecasting (e.g. Liu et al., 2005; Schumann et al., 2013), flood damage assessment and risk mapping (Abdallah and Hdeib, 2015; Apel et al., 2006; Merz et al., 2008, 2010), flood hazard mapping (Aronica et al., 2012; Kvočka et al., 2016), along with other applications related to catchment hydrology, river bank erosion, sediment transport, and contaminant transport.

The scientific literature is now replete with various hydrologic and hydraulic models that vary in complexity from simple empirical or black box models with few parameters to complex physically based, distributed models with many parameters. These models largely differ in terms of type of input data required, computational efficiency and the nature of output variables, their resolution and accuracy. Although physically based distributed models are gaining favour to better represent the physical processes within the catchment, their practical application depends on addressing their specific weaknesses, which include heavy computational requirements, large number of parameters to evaluate, and lengthy training periods (Bathurst and O'Connell, 1992). Hence, the discussion on the wise selection of the modelling approach which balances modelling objectives with model complexity and data availability has become a topic of an increasing scientific interest (Bergstrm et al., 2002; Grayson and Blöschl, 2001; Neal et al., 2012b). For practical applications, the major challenge that awaits the modeler is the proper selection of an efficient low-cost flood modelling approach based on defined modelling objective and available data.

Till now there is no common base for comparing different modelling approaches based on measuring or quantifying model complexity, data availability and performance. Many studies compared and benchmarked various models and algorithms, but most were based on comparing models based on their structure or their representation of processes. Also, developers compared their models with one or few other popular models in literature (Singh and Woolhiser, 2002). Grayson and Blöschl (2001) described the trade-off between model complexity and the prediction performance for given conditions of data availability (Figure 1.2). The authors show that for a given condition of data availability there is an optimum model complexity that corresponds to the highest model performance beyond which additional complexity induces identifiability problems and reduces the performance. In this case complex models require much more data to reach adequate reliability.

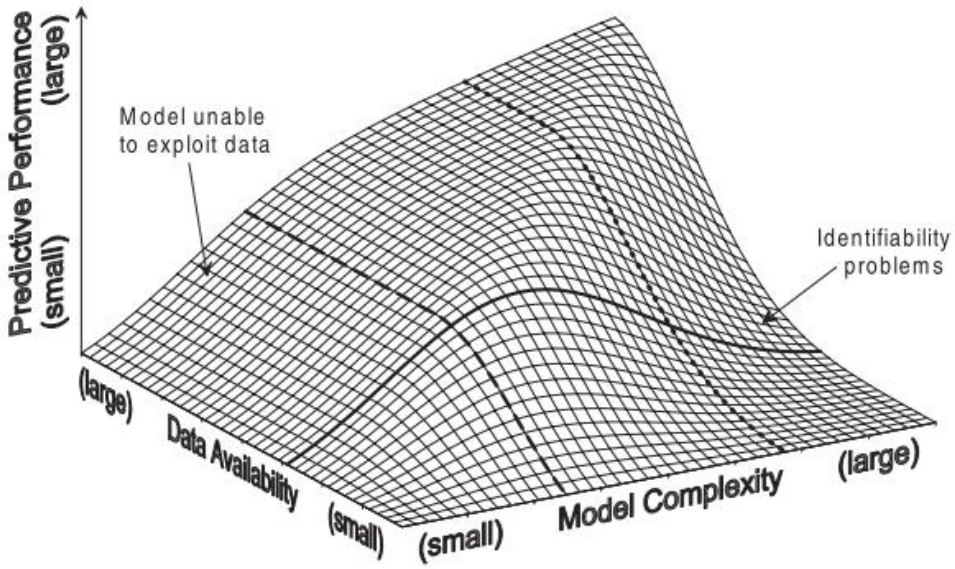

Figure 1.2 The conceptual relationship between model complexity, data availability and predictive performance (Grayson and Blöschl, 2001).

Perhaps, these illustrated conceptual relations between data, models, and performance can form the basis for assessing or comparing different modelling approaches of variable complexities, however, there arises a need to develop metrics that are able to quantify these three components of the modelling problem. In this thesis we develop a cost-performance analysis grid by defining metrics to characterize and quantify the three axes: data availability, model complexity and prediction performance. Quantifying the three axis allows assessing the cost-effectiveness of the flood modelling approach.

1.4 Flood modelling in data-sparse regions

In data-sparse regions, the flood modelling problem is exacerbated by sparse data that is not always compatible with the resolution, in both space and time, of the hydrological and hydraulic models. As a result of such data sparseness, flood modelling has become a challenging task especially in regions characterized by floods of typical duration times of a few hours which offer little opportunity for real-time recording by traditional rain-gauge networks, remote sensing or satellite imaging. Accordingly, modelling approaches in data-sparse regions were always limited to uncertain probabilistic estimates of rainfall, flood flows and water levels based on empirical (e.g. Koutroulis and Tsanis, 2010), statistical (e.g. Castellarin, 2007; Castellarin et al., 2009) or geomorphic approaches (e.g. Manfreda et al., 2014). Such applications are useful for regional flood analysis such as national hazard maps that are mainly of coarse resolution and are not adapted for small to medium size basins (<1000 km^2). Generally, for basin scale applications and when more detailed understanding of a particular flood event is required and when the study area is relatively small, such regional maps cannot do the favor especially when detailed estimates of flows and water levels is required and hence cannot replace the hydrological/hydraulic modelling.

Worldwide, the majority of river basins are either ungauged or poorly gauged and is some cases facing deterioration of the available measurement networks (Sivapalan et al., 2003; Efstratiadis et al., 2014). In a broader classification, most of the basins in the world and especially in developing countries, are denoted as data-sparse basins where reliable information on the characteristics and on the spatial and temporal coverage of extreme flood events are rare or inexistent (see for example Wilby and Yu, 2013; Jarihani et al., 2015; Komi et al., 2017). Classical and sparse data are differentiated in Table 1.1. Data sparseness is often referred to measurements of limited spatiotemporal resolution; point measurements of coarse time step, and series with gaps, or parameters that have not been collected during simultaneous periods (Samaniego et al., 2011; Mascaro et al., 2013). Some also add that such data may not be available in the period of interest, or are of poor quality or unknown accuracy, and the hydro-meteorological network is of very low density that makes interpolation procedures or filling methods impossible (Satyanarayana and Srinivas, 2011; Switzman et al., 2015). In addition, others point out to when detailed channel bed and topography information are coarse or unavailable (Neal et al., 2012a).

Table 1.1 Classical data versus sparse data.

Type	Sparse Data	Classical Data
Hydrology	Series with gaps	Long term series
	Coarse time step	Fine time step
	Point measurements	Spatial measurements (ex: radar rainfall)
	Water levels with pour rating curves	Advanced flow measurement techniques
Hydraulics	Post-event measurements	Time series of water level variation

In the Mediterranean region, data requirement is particularly acute because most floods occur on a short duration, typically a portion of the day, and are mainly generated by high-intensity, short duration, localized rainfall events (Moussa and Chahinian, 2009). These floods, characterized by response times often less than 2h and typically occurring in catchments of drainage area not exceeding 1000 km^2 (Borga et al., 2008), can difficultly be captured even by the traditional rain gauge networks (Norbiato et al., 2007; Lumbroso and Gaume, 2012). In addition, impossible direct current meter measurements of the flood peak discharge (Fukami et al., 2008), coarse time step of measurements often skipping the peak conditions, common failure of river stage gauge, flood water exceeding the gauge measurement level resulting in underestimation of the peak discharge (Koutroulis and Tsanis, 2010) are common weaknesses that lead to poorly defined rating curves during floods. Maybe more than in other regions, the specific rainfall and discharge data requirements result in classifying the Mediterranean region as “data-sparse region”.

In this context, and when data are uncertain and too sparse to meet model requirements, the two questions arise to whether there is opportunity to constrain the hydrological-hydraulic model to simulate extreme floods and establish water levels that can be useful for flood assessment and mitigation and whether this detailed modeling

approach remains cost-effective given the high model complexity with limited data availability.

1.5 **Thesis objectives**

This work aims to develop a framework for flood modeling in data-sparse regions based on analyzing different flood modeling approaches in a cost-performance approach. The study is applied in Lebanon, a data-sparse country of the Eastern Mediterranean. We first analyze available sparse data on flood events in the country and then review and evaluate historical flood events extracted from newspaper archives to draw out conclusions on the intensity and spatial occurrence of floods in Lebanon. We discuss the opportunities and limitations of such data sources and then extend to perform a hydrological/hydraulic modeling approach to a selected study site. As a first step towards the selection of a suitable modeling approach, we develop a new cost-performance grid to evaluate different flood modeling approaches available in literature by comparing their modeling costs and performances. The grid is based on defining metrics to evaluate the three axes of a modeling problem: data availability, model complexity, and modeling performance. Later our approach further extends to assess whether there is an opportunity to constrain the hydrological-hydraulic models by sparse data, in a cost-effective approach, to simulate extreme floods and establish water levels that can be useful for flood assessment and mitigation. The last step involves developing a flood modelling framework from a coupled hydrological-hydraulic model constrained by past storm events and post-event measurements.

The objective of this thesis articulates on three axes:

- Evaluate the flood problem in Lebanon based on available sparse data and assess whether there is opportunity to understand the intensity and spatial occurrence of flood events on a regional scale based on collecting historical flood events from newspapers.

- Develop a cost-performance analysis gird to compare and analyze different flood modelling approaches in literature and discuss its opportunities and limitations.

- Develop a cost-effective framework for flood modelling using sparse data based on constraining a coupled hydrological-hydraulic flood model by past storm events and post-event measurements in space.

1.6 **Thesis structure**

This thesis is structured in three main parts, nine chapters and four annexes:

Chapter 1 Is the general introduction of the thesis, it defines the thesis problems and the main objectives of the work.

Chapter 2 Is the state of the art. It presents different flood modelling approaches, discuss the modelling problems and basic data requirements, presents the models, the basic equations and assumptions.

Part I "Analysis of historical flood events on a regional scale" is formed of three chapters (chapters 3, 4, and 5). This part presents all datasets available and

analyses the geographical, hydrological and climatic characteristics of Lebanon and the selected study site for detailed analysis (Awali River Catchment). Then follows a review of 173 records of historical flood events in Lebanon extracted from newspaper archives and previous reports. An analysis of the intensity and spatial occurrence of such events is performed to draw out some conclusions on the flood problem in Lebanon. This part ends with a discussion on the opportunities and limitations of such data sources.

Chapter 3 analyses the geographical, hydrological and climatic characteristics of Lebanon and presents datasets available.

Chapter 4 analyses the geographical, hydrological and climatic characteristics of the selected study site for detailed analysis; the Awali River Catchment and presents the outcomes of the field investigations and data analysis.

Chapter 5 reviews around 200 records of historical flood events extracted from newspaper archives and previous reports aiming at understanding the intensity and special occurrence of such events over the country. The opportunities and limitations of such data sources are also discussed.

Part II "A Cost-Performance analysis grid for flood modelling" is formed of two chapters (chapters 6 and 7). This part forms an article that will be submitted shortly. In this part we develop a new cost-performance grid to analyze different flood modelling approaches presented in literature to draw out some conclusions on how to select the proper flood modelling approach for our study by balancing model complexity and data availability. We define metrics to quantify the three axes of any modelling problem: data availability, model complexity, and modelling performance. The part ends with a discussion on the opportunities and limitation of the proposed grid.

Chapter 6 presents a proposed cost-performance grid for flood modelling evaluation.

Chapter 7 is an application on the grid, it analyses different flood modelling approaches, and discusses the opportunities and limitation of this grid.

Part III "A framework for flood modelling in data-sparse regions" comprises two chapters (chapters 8 and 9). This part forms an article published online in August 2018 by the Journal of Hydrology. In this part we investigate whether there is opportunity to constrain hydrological/hydraulic models based on sparse data to establish flood flows and water levels that are useful for detailed flood studies. In this part we discuss the different sources of uncertainty in data and models and develop a framework to constrain the hydrological-hydraulic model and reduce the uncertainty in the results. The part ends with a discussion on the opportunities and limitations of the proposed framework.

Chapter 8 presents a framework for flood modelling based on constraining a coupled hydrological-hydraulic model by past storm events and post-event measurements in space.

Chapter 9 is an application of the framework on a selected study site; Awali River Basin.

The thesis ends with a general conclusion that summarizes the main findings and limitations of this work and identifies key questions that need to be addressed for flood modelling in data-sparse regions and more particularity in Lebanon.

Annexes

Annex A: Articles

Annex B: Extracted historical flood events

Annex C: Sample of the developed online survey

Annex D: Results of the cost-performance analysis

2 STATE OF THE ART

2.1 Introduction

2.2 Flood modelling approaches

Reliable information on the flood peak discharge (Gaume et al., 2009), water levels (Saleh et al., 2013; Domeneghetti, 2016) and the flood inundation extent (Merwade et al., 2008), are among the major parameters required in any flood problem and flood modelling represents a way to obtain such information (Bates, 2004; Moussa and Bocquillon, 2009). Recent years, an important effort has been applied to develop flood inundation models. The challenges for such models are directly linked to the representation of flow processes, to the formulation of theoretical physical laws and to practical considerations (Moussa and Cheviron, 2015a) such as data availability. Table 2.1 summarizes the main flood modelling problems (objectives) and the minimum model requirements to meet the objective of modelling.

The scientific literature is replete with various modelling approaches applied for flood inundation modelling that vary in complexity and in concept these include:

1. Application of different empirical methods such as measurements, surveys and remote sensing or statistical approaches (Gaume and Borga, 2008; Horritt et al., 2001; Schumann et al., 2009).

2. Single application of a hydraulic model to simulate flood propagation by solving physical equations of flow dynamics of variable complexity, i.e. in a one-dimensional (1D), two-dimensional (2D) or three-dimensional (3D) approach (Dimitriadis et al., 2016; Neal et al., 2012a).

3. Application of simplified conceptual models that do not solve the physical equations of flow dynamics but are based on simplified hydraulic concepts (Lhomme et al., 2009). An overview of the first three approaches is provided by Teng et al. (2017).

4. Applications limited to hydrologic models, mostly rainfall-runoff, to estimate rainfall excess, overland flows and river flood discharges (Coustau et al., 2012; Dutta et al., 2000; Khan et al., 2009; Sharif et al., 2010), these models vary in complexity from empirical and lumped conceptual models to fully distributed physically based models that simulate surface, sub-surface and groundwater flow processes.

5. Applications that involve coupling hydrologic and hydraulic models , that is mainly applied to estimate flood flows in different locations specially when information on the flood characteristics are lacking (Bonnifait et al., 2009; Hdeib et al., 2018; Lerat et al., 2012), or as part of a flood forecast system where rainfall-runoff models are fed by rainfall forecasts to obtain different realizations of runoff (Pappenberger et al., 2005).

6. Applications based on geomorphic approaches to delineate flood prone areas by using simplified methods that rely on basin geomorphologic feature characterization (Manfreda et al., 2014; Samela et al., 2017), such applications were found to be successful in large-scale applications of data-sparse regions.

These applications largely differ in terms of type of input data required, computational efficiency and the nature of output variables, their resolution and accuracy.

Table 2.1 Flood modeling problems (objectives) and the minimum model requirements.

Flood modeling problem (objective)	Minimum model requirements
Peak flood discharge	Empirical methods Manning's equation Lumped hydrological models
Flood flow hydrograph	Semi-distributed models Fully distributed models
Flood water levels	1D hydraulic models
Flood inundation map (levels and extent)	2D hydraulic models 1D hydraulic models + post-processing (interpolation of water levels with high resolution DEM)

2.2.1 ***Model coupling***

It most cases, flood inundation modeling demand solutions that use output from more than one simulation model especially when information on the flood characteristics are lacking or when upstream flows and lateral inflows are to be estimated through hydrological modelling. In such cases, model coupling is usually applied, it classically requires a coupling between a hydrologic model to simulate the rainfall-runoff transformation along hill shades and estimate peak flood flows, and a hydraulic model to simulate the propagation of flood wave along the river channel and establish the corresponding water levels, along with terrain analysis to extract the flood inundation area.

Coupling rainfall-runoff models and fully dynamic hydraulic models have been applied by several authors in literature on relatively well gauged basins (Knebl et al., 2005; Laganier et al., 2014). Three types of coupling of numerical models are discussed in literature, these are full coupling (Morita and Yen, 2002), internal coupling (Kim et al., 2012) and external coupling (Whiteaker et al., 2006). External coupling (also denoted as unidirectional coupling) is the simplest strategy of coupling, and the most frequently used (Lerat, 2009). Simulations are performed by each model separately and information is exchanged in one direction; results from the hydrological model are used as input information in the hydraulic model. Although model coupling has been applied several times in literature, finding connections between hydrologic models and physically based hydraulic models is always required for the advancement of hydrological modeling (Robinson and Sivapalan, 1995). Table 2.2 presents a summary (authors, study area and models) on some model coupling approaches presented in literature.

Table 2.2 Examples on some model coupling approaches in literature.

Author	Study Area	Hydrological model	Hydraulic model
(Lian et al., 2007)	Illinois River basin, US	HSPF	UNET
(Knebl et al., 2005)	San Antonio River basin, US	HEC-HMS	HEC-RAS
(Whiteaker et al., 2006)	Rosillo Creek, US	HEC-HMS	HEC-RAS
(Montanari et al., 2009)	Alzette River, Luxembourg	Nash IUH	HEC-RAS
(Biancamaria et al., 2009)	Ob River, Siberia	ISBA	LISFLOOD-FP
(Bonnifait et al., 2009)	Gardon river basin, France	n-TOPMODELs	CARIMA
(Mejia and Reed, 2011)	Blue and Illinois River basins, US	HL-RDHM	HEC-RAS
(Lerat et al., 2012)	Illinois River basin, US	GR4J lumped rainfall–runoff model	linearized diffusive wave propagation model
(Laganier et al., 2014)	Gardon river basin, France	SCS-LR	MASCARET
(Fuentes-Andino et al., 2017)	Floodplain of Tegucigalpa, Honduras	TOPMODEL + Muskingum–Cunge–Todini	Sub-Grid LISFLOOD-FP

2.3 Simple vs complex flood modelling approaches

Recent decades the digital revolution in the field of mathematical modeling supported the rapid development of hydrological and hydraulic models. This digital revolution also triggered the revolution of the numerical and statistical simulation that were a great aid to the field of mathematical modeling. This was followed by a rapid increase in the power of computers and as a result, advances in watershed hydrology have occurred at an unprecedented pace (Singh and Woolhiser, 2002). Nowadays, a plethora of hydrological and hydraulic models are now available that vary in complexity from simple empirical (or black box) models with very few parameters to complex distributed physically based models of many parameters. These models largely differ in terms of type of input data required, computational efficiency and the nature of output variables, their resolution and accuracy. In typical modeling applications, modelers usually pay attention to the type of output variables of predictive interest and their time and space scales, the level of accuracy required, and computational efficiency demands (Teng et al., 2017). However, the major challenge that awaits the modeler is the proper selection of the most efficient low-cost modelling approach that balances the data available with model complexity based on defined modelling objective.

2.3.1 Hydrological models

Hydrological modeling could be defined as a simple representation of hydrological processes at a certain scale, generally at catchment scale. Hydrological modeling may simulate continuous hydrological processes at the catchment scale, or simulate

hydrological processes induces by a single event, such as a storm. We differentiate three main approaches for hydrological modeling: (1) physically based models that are based on the understanding of physical processes and their mathematical description, such models required a large set of data (Grayson et al., 1992). Physically-based models represent the component hydrological processes such as evapotranspiration, infiltration, overflow, and saturated and unsaturated zone flow using the governing equations of motion (e.g. Todini and Ciarapica, 2002). (2) conceptual models that are based on the conceptualization of physical processes. Generally, the structure of these models is specified prior to any modeling being undertaken, and not all of the model parameters have a direct physical interpretation and have to be estimated through calibration against observed data. (3) empirical models based on statistical analysis of observed data, and they are usually applicable only to the same conditions under which the observations were made (e.g. SCS, 1972). The simplicity of such models has allowed them to be applied relatively easily to ungauged catchments by regional analysis, relating model properties to physical and climatic descriptors of the catchment.

Much widely used hydrological modeling software are based on one or more of these models, e.g. Morel-Seytoux model which is a simplification of the famous Green and Ampt equation (Chahinian et al., 2005) is used among others in WEPP (Raclot and Albergel, 2006) and KINEROS (Woolhiser et al., 1990); Horton's model is used by example in MARINE (Roux et al., 2011), SCS is used among other in SWAT (Arnold et al., 1998) and HEC-HMS (Feldman, 2000).

Hydrologic models vary in complexity from simple empirical equation of hydrology, to conceptual lumped hydrologic models, and to semi-distributed and fully distributed physically based models. Based on the degree of model spatial representativeness, one can dedifferentiate lumped model and spatially distributed model. Lumped models are simple model that represent the whole basin as one entity, thus, does not account for spatial variability inside the catchment and for small-scales processes. On the contrary, distributed hydrological models are more complex models that take into account catchment subdivisions, and the variability of catchment physical characteristics from one subdivision to another. The major input and output data, advantages and disadvantages of simple and complex hydrological models are differentiated in Figure 2.1.

Empirical models based on statistical analysis of observed data are limited to the fact that they can only be used in the same conditions under which observations were made; otherwise, the model parameters will need intense calibration to fit in for the new environment were the model is applied. Moreover, one should mention, that the fact that these models are based on statistical analysis is a limitation, since statistical analysis are always liable for a certain degree of subjectivity. Furthermore, statistical techniques have their own limitations, sampling procedure, overweighting (sometimes the representativeness of a sample could be altered by the presence of extreme, very rare events), etc.

Physically-based models are highly demanding in term of data. Although these models describe the physical processes inside a catchment, it can only be applied on a very small scale; otherwise, one will need an immense data gathering networks. Such

models are usually used in experimental catchment were data measurements are available. Moreover, such models most be applied on short time-steps to account for the continuous variation of physical parameters in the study area.

The limitations of a conceptual model lie in the reality that these models are a simplification of very complex natural process which is reduced to a mathematical formula. Conceptual models also required an immense parameterization.

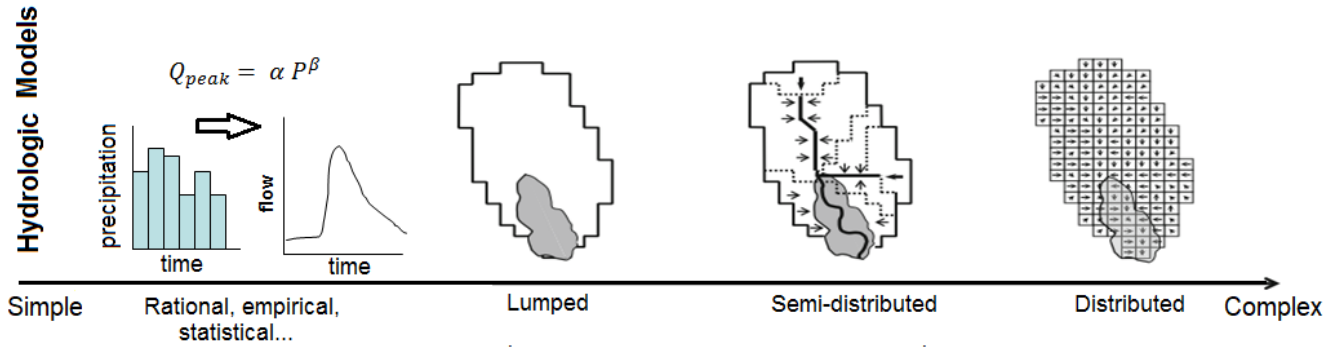

Hydrologic model type	Rational, empirical, statistical…	Lumped	Semi-distributed	Distributed
Input	Easily available data	Mean rainfall/runoff	Spatial rainfall	Specially distributed data (rainfall, LUC, soil, ET, DEM…)
Output	Peak flood discharge	One flow hydrograph at outlet	Flow hydrograph on some points	Flow hydrograph at each cell
Advantage	Simple and fast	Few parameters, easy calibrate, fast in set-up and computational times, few data requirements	Fast in set-up and computational times, modest in terms of data requirements, better understanding hydrology, wide application	Based on theories of small scale processes, detailed understanding of all hydrological processes, wide application
Disadvantage	One rough estimation, very few applications	Point information, limited applications, lack of physical basis	Arbitrary or inappropriate model structures, lack of physical basis, difficulties with calibration	Large data and computer requirements, large set-up and computational times big number of parameters, difficult to calibrate

Figure 2.1 Simple vs Complex hydrological models.

2.3.2 *Hydraulic models*

Hydraulic models vary in complexity from simple application of the manning's equation to a fully dynamic 2D hydraulic model.

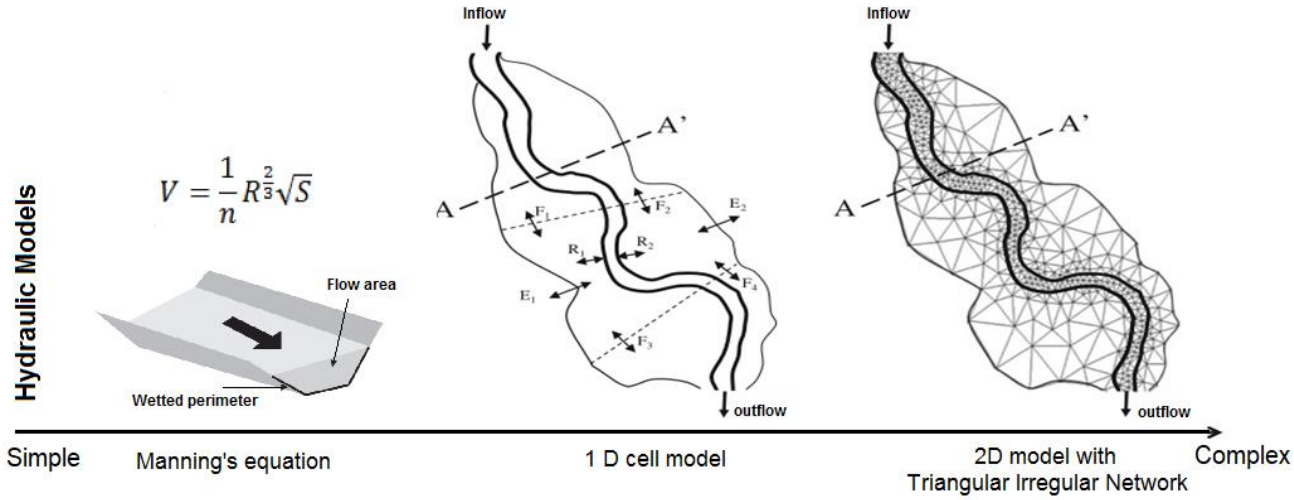

Hydraulic model type	Manning's equation	1D cell model	2D model with triangular irregular network
Input	Flow area/perimeter, manning's, slope	River cross section geometry, Roughness, flow hydrographs at boundary conditions	High resolution DEM, spatial data, Flow hydrographs at boundary conditions
Output	Peak flow value	Water levels at cross sections	Water level at each cell
Advantage	Parsimonious, no numerical or instability problems	Understanding the flow dynamics along the river, wide applicability	Full understanding of the hydraulic processes, wide applicability
Disadvantage	One rough estimation	numerical and instability problems	Expensive data, big number of parameters, difficult to calibrate, numerical and instability problems

Figure 2.2 Simple vs Complex hydraulic models.

Many hydraulic modeling approaches for free surface flows (on the slopes and through the river system) based on solving the equations of Saint-Venant (or simplifications of Saint-Venant) have been developed and applied on gauged basins (see a summary in Cheviron and Moussa, 2015). However, many difficulties lie in the transposition of such methodology to poorly gauged sites.

2.3.3 ***Cost-performance analysis***

One possible method for comparing different modelling approaches is a cost analysis approach. This approach is a form of economic analysis that compares the relative costs and outcomes of different courses of action and help decide if an application is worth the costs by understanding the benefits or effects of pursuing it. One common form of such approaches is the “cost-effectiveness analysis”. The concept is used in many fields, such as pharmacoeconomics and energy efficiency investments, and refers to analyses that examine the ratio of the cost of a particular intervention to a chosen unit of effectiveness of non-monetary value (Zilberberg and Shorr, 2010). Unlike cost-benefit analysis where costs and outcomes are presented in monetary values (Bleichrodt and Quiggin, 1999).

2.4 **Data requirements for flood modelling**

Data requirements for flood inundation modeling have been summarized and discussed several times in literature (Bates, 2004; Mason et al., 2010; Smith et al., 2006), these can be divided into four major sub-categories: topographic data to construct the model grid, time series of bulk flow rates and stage data to provide model inflow and outflow boundary conditions, roughness coefficients of channel and floodplain, and data for model calibration, validation, and assimilation.

2.4.1 ***Topographic data***

The data contained in a DTM of the floodplain and channel form the primary data requirement for the parameterization of a flood inundation model. Several methods exist for the generation of DTMs suitable for flood modelling, these include: cartography, ground surveys, digital aerial photogrammetry, Interferometric synthetic aperture radar (InSAR), light detection and ranging (LIDAR), and sonar bathymetry. Smith et al. (2006) have provided an excellent review of these, together with their advantages and disadvantages for flood inundation modelling, and this is summarized below. The choice of a suitable model in any given situation will depend upon a number of factors, including the vertical accuracy, spatial resolution and spatial extent required, the modelling objectives and any cost limitations. Many air and space-borne sensors generate a Digital Surface Model (DSM), a representation of a surface including features above ground level such as vegetation and buildings. A DTM (also called a Digital Elevation Model (DEM)) is normally created by stripping off above-ground features in the DSM to produce a ‘bald-earth’ model.

2.4.2 ***Time series of bulk flow rate and stage data***

Flood inundation models also require discharge and stage data to provide model boundary conditions. The data are usually acquired from gauging stations spaced 10–60km apart on the river network, which provide input to flood warning systems. Modelers ideally require gauged flow rates to be accurate to 5% for all flow rates, with all significant tributaries in a catchment gauged. However, problems with the rating curve extrapolation to high flows and gauge bypassing might mean that discharge measurement errors can be much higher than this acceptable value during floods. At such times gauged flow rates are likely only to be accurate to 10% at best, and at many

sites errors of 20% will be much more common. At a few sites where the gauge installation is significantly bypassed at high flow, errors may even be as large as 50%.

2.4.3 ***Roughness coefficients of channel and floodplain***

Roughness coefficients were classically estimated based on standard tables. A standard method is to use two separate global static coefficients, one for the channel and the other for the floodplain, and to calibrate these by minimizing the difference between the observed and predicted flood extents. Remotely sensed data may be used to generate spatially distributed floodplain friction coefficients for use in 2-D inundation modelling. The remote-sensing approach has the advantage that it makes unnecessary the non-physical fitting of a global floodplain friction coefficient. For example, Land-sat Thematic Mapper (TM) imagery can be used to estimate friction coefficients from floodplain land cover classification. Data from LIDAR may also be used for friction measurement. Most LIDAR DSM vegetation removal software ignores short vegetation less than 1m or so high. However, even in an urban floodplain, a significant proportion of the land surface may be covered with this type of vegetation, and for floodplains experiencing relatively shallow inundation the resistance due to vegetation may dominate the boundary friction term.

2.4.4 ***Data for model calibration, validation, assimilation***

Data for model calibration and validation constitute information on the flood extent and water levels. Several methods can be applied to obtain such information, those include post-event measurements high water marks and detailed ground surveys using GPS to delineate the flood extent. Field witnesses, videos, and pictures can also support the flood extent mapping and the water level estimation. Nowadays, early launches of satellites and the availability of aerial photography allowed investigation of the potential to support flood monitoring from space. There have been notable studies on integrating data from these instruments with flood modelling since the late 1990s. A more recent consensus among space agencies to strengthen the support that satellites can offer has stimulated more research in this area, and significant progress has been achieved in recent years in fostering our understanding of the ways in which remote sensing can support or even advance flood modelling.

Flood extent mapping

Given the very high spatial resolution of the imagery, flood extent is derived from color or panchromatic aerial photography by digitizing the boundaries at the contrasting land–water interface. The accuracy of the derived shoreline may vary from 10 to 100m, depending largely on the skills of the photo interpreter, of which the georectification error is generally 5m with 10% chance of exceeding that error (Hughes et al., 2006). In recent years, however, mapping flood area and extent from satellite images has clearly gained in popularity, mostly owing to their relatively low post-launch acquisition cost. Flood mapping with optical and thermal imagery has met with some success but the systematic application of such techniques is hampered by persistent cloud cover during floods, particularly in small to medium-sized catchments where floods often recede before weather conditions improve. Also, the inability to map flooding beneath vegetation canopies with radar imagery, limits the applicability of these sensors. Given

these limitations for acquiring flood information routinely, flood detection and monitoring seems realistically only feasible with microwave (i.e. radar) remote sensing, as microwaves penetrate cloud cover and are reflected away from the sensor by smooth open water bodies. Imagery from (active) SAR seems at present to be the only reliable source of information for monitoring floods on rivers <1km in width. Although the operational use of SAR images for flood data retrieval is currently still limited by restricted temporal coverage (up to 35 days for some sensors), recent efforts on satellite constellations (e.g. COSMO-SkyMed) seem promising and should make space-borne SAR an indispensable tool for hydrological/hydraulic studies in future.

2.5 **Flood modelling in data-sparse regions**

Flood modelling applications in data-sparse regions were always limited to uncertain probabilistic estimates of rainfall, flood flows and water levels based on empirical (e.g. Koutroulis and Tsanis, 2010), statistical (e.g. Castellarin, 2007; Castellarin et al., 2009) or geomorphic approaches (e.g. Manfreda et al., 2014). Such applications are useful for regional flood analysis such as national hazard maps that are mainly of coarse resolution and are not adapted for small to medium size basins (<1000 km^2). Generally, for basin scale applications and when more detailed understanding of a particular flood event is required and when the study area is relatively small, such regional maps cannot do the favor especially when detailed estimates of flows and water levels is required and hence cannot replace the hydrological/hydraulic modelling.

When information on the flood event characteristics, catchment hydrological characteristics and river channel characteristics are sparse or lacking, interesting information can be inferred from recorded past storm events, post-event field investigations, newspapers and social media reports, and from crowdsourcing of information from local citizens on flood events characteristics whenever available.

Table 2.3 Induced flood modeling problem by sparse and uncertain data.

Induced flood modeling problem	**Opportunity/ approach**
Model parametrization	Calibration with past-storm events
Absence of measurements during extreme events	Post-events measurements in space
Uncertainty	Monte Carlo simulation, GLUE…

2.5.1 ***Past storm events***

From the hydrological modelling perspective, past storm events can be extracted from the available simultaneous rainfall and flow data measurements. These are often used in literature to estimate and calibrate the unknown model parameters (see for example Sangati et al., 2009; Massari et al., 2014). However, when past storm events data used for calibration are uncertain or does not meet model requirements, bias and uncertainty arise in model predictions (Pappenberger et al., 2008). Additionally, the calibration procedure may induce equifinality when input data and calibration equally fit the sparse

validation data. The latter can be raised through analyzing the uncertainty propagation (Aronica et al., 2002). A good understanding of the uncertainty associated with various parameters inherent in modelling is a critical requirement (Merwade et al., 2008). Accordingly, when all relevant uncertainties are taken into consideration, optimal decisions are to be expected (Apel et al., 2008; Domeneghetti et al., 2013).

2.5.2 ***Post event measurements***

From the hydraulic modelling perspective, detailed post-event surveys in space, based on traces left by water and sediments, provide a good opportunity when systematic water level and flow measurements are lacking (Horritt and Bates, 2002; Borga et al., 2008). Surveyed channel cross sections and flood marks can be used in estimating the peak flood discharge (Gaume, 2006). Pictures and videos taken by witnesses during the flood event are interesting in highlighting affected areas and in understanding the events characteristics such as the flood duration, flow type and velocity at the time of capturing (Le Boursicaud et al., 2016; Fuentes-Andino et al., 2017). Field surveys and witnesses interviews can provide additional information such as the time of peak, water levels, and flood extent (Gaume and Borga, 2008). Post-event measurements have been used to validate the results of the hydraulic models several times in literature (see for example Hervouet, 2000; Romanowicz and Beven, 2003; Horritt et al., 2010).

2.5.3 ***Social media information***

Newspaper and social media information on storm events and floods is an interesting well available data source providing an opportunity to understand some of the events' characteristics. Such information has been used several times in literature to search for historical flood events (Barredo, 2007), develop a flood database and inventories (Barnolas and Llasat, 2007; Llasat et al., 2009), understand the flood regime changes (Hall et al., 2014), support the hydrologic and hydraulic modelling of the flood events (Papaioannou et al., 2016), evaluate flood risk (Llasat et al., 2010; Abdallah and Hdeib, 2015), and understand the socio-economic impacts of floods (Lastoria et al., 2006). Moreover, crowdsourced information from local citizens on flood events is now gaining favour and is facilitated by the wide spread of low-cost monitoring technology and communication systems (Lowry and Fienen, 2013; Montanari et al., 2013; Mazzoleni et al., 2017). All these data sources can give information on the flood characteristics such as the affected areas, the rainfall event characteristics (depth, intensity, and duration), timing of the flood event (duration and time of peak), possible flood depth and inundation area extent, severity, and recorded damages.

2.6 **Key challenges**

In attempting to achieve the objectives of flood modelling in data-sparse regions, several challenges are encountered. These could be divided into three categories: challenges related to application, challenges related to data, and challenges related to modelling procedures.

- Challenges related to application: these are related to the Cost-Performance analysis of the selected flood modelling approaches, aiming at balancing model complexity with data availability, and at the same time obtaining good performance.

- Challenges related to data: include the reliable spatiotemporal estimation of flood flow hydrograph and flood depths

- Challenges relative to modelling: involve the calibration and validation of the hydrological model, the validation of the hydraulic model, and understanding the propagation of uncertainty.

2.7 **Models**

In our work we choose to use the Hydrologic Modelling System (HEC-HMS) (USACE, 2016b) and the River Analysis System (HEC-RAS) (USACE, 2016a) developed by the Hydrologic Engineering Centre (HEC) of the US Army Corps of Engineers (USACE). Both modeling systems are a freeware that is being updated and advanced regularly. Both software has been widely applied and validated by several authors in literature (e.g. Halwatura and Najim, 2013; Horritt and Bates, 2002; Oleyiblo and Li, 2010; Vozinaki et al., 2016) and were found to be efficient. These are mostly coupled together and have structures that permit the easy exchange of information between them. The HEC-HMS software allows the selection of different loss and transform models and the HEC-RAS software allows the simulation of steady and unsteady flow regimes. Details on the selected models will be presented in the coming paragraphs.

2.7.1 ***Hydrological model: HEC-HMS***

Rainfall-runoff processes are modelled using the Hydrologic Engineering Centre's Hydrologic Modelling System (HEC-HMS), version 4.2, developed by the US Army Corps of Engineers. The model is designed to simulate the rainfall–runoff processes of dendritic watershed systems and allows the modeler to choose between numerous infiltration loss parameterizations (USACE, 2016b). The processes represented, and the required model input parameters are summarized in Table 2.4

Table 2.4 Represented processes and required input model parameters.

Model	**Method**	**Parameters**
Loss	SCS curve number	Initial abstraction (mm), Curve Number, imperviousness (%)
Transform	SCS unit hydrograph	Standard Graph Type, Lag time (min)
Routing	Muskingum-Cunge	Length (m), Slope, Manning's "n" & Section

Loss model: SCS curve number

The largely applied curve number loss method was originally developed by the Soil Conservation Service (SCS) in the 1950's. The simplicity of the method is because it allows the estimation of direct surface runoff volume for given rainstorms based on a single parameter, curve number (CN). The CN is a dimensionless number that ranges from 0 to 100 and depends on the land cover, land use and soil types available in a basin and represents its infiltration storage (D'Asaro and Grillone, 2010). Background for this is found in the National Engineering Handbook, Section 4, "Hydrology", or "NEH-4" (SCS, 1972). The infiltration loss method is derived from a set of empirical equations that define the partitioning of rainfall into infiltration and runoff. The general runoff equations can be represented in Eqs. 2.1 to 2.3.

$$Q = \frac{(P - I_a)^2}{((P - I_a) + S)} \quad (2.1)$$

$$I_a = \lambda S \quad (2.2)$$

$$S = \frac{1000}{CN} - 10 \quad (2.3)$$

Where:
Q is the storm runoff in inches
P is the storm rainfall in inches
S is the potential maximum retention
Ia is the initial abstraction
λ is the initial abstraction ratio
CN is the runoff curve number

Initial abstraction is a variable parameter that takes into account losses prior to the start of runoff such as interception and depression storage. The SCS-CN method assumes that the initial abstraction (Ia) is proportional to the potential maximum retention (S) of the basin. One of the major steps is the assumption of the initial abstraction ratio λ=Ia/S which is a variable parameter from storm to storm and watershed to watershed. Originally, Ia was assumed to be equal to 0.2S as developed by the SCS.

$$I_a = 0.2S \quad (2.4)$$

Substituting Eq. 2.4 into Eq. 2.1 Gives:

$$Q = \frac{(P - 0.2S)^2}{P + 0.8S} \quad (2.5)$$

Recently model fitting methods based on large rainfall-runoff data from hundreds of watersheds were applied to determine the ratio of Ia to S. In the model fitting done by Hawkins et al. (2002) (Woodward et al., 2003) which was applied on rainfall-runoff events from US basins, it was found that the assumption of λ=0.2 is usually high and the use of ratio of 0.05 would seem more appropriate. However, this remains debatable and site dependent. Having to mention that it requires a sufficient number of rainfall-runoff data.

In this study, the estimation of the ratio λ was not possible given the sparse information on rainfall-runoff events in the country and hence should be calibrated instead. In favor of parsimony and to reduce the number of parameters to be calibrated, we choose to fix the value of λ to its classical value of 0.2.

The dimensionless curve number parameter is derived based on a developed classification that combines the land use/treatment classes with the hydrological soil groups (HSG). The effect of the surface conditions is evaluated by means of land use and treatment classes and the soil's parametric information is built based on soil profiles.

In this study, the HSG are established by building a weight-rate model that classifies soils following to their infiltration capacity (Table 2.5). The soil map prepared by the National Council for Scientific Researches of Lebanon (Darwish et al, 2006) at a scale of 1: 50 000 have been used to determine the soil groups. The criterion used to classify the soil was by evaluating the soil parameters that have the most infiltration impact and these are: Soil Depth, Soil texture, stoniness, and organic matter percentage. The parametric information is built according to soil profiles and associated within the soil database. Thereof, the original soil type map can be converted to a map of hydrologic soil groups using the model conversions through weight-rate GIS operation. Considering the distribution of the scores over the map, the resulting HSG were assigned their scores (Table 2.6).

The land use map prepared by the Remote Sensing Center is used to define the required land use categories based on the level of detail required for the study. The Standard SCS-CN's are then assigned for each possible soil group combination for average soil moisture conditions (AMCII) for typical winter days in Lebanon (CN values ranging between 0 and 97) (Table 2.7).

Table 2.5 Weight-rate model developed to establish soil's infiltration capacity.

Parameter	Weight	Class	Rate
1. Soil Depth	25%	a. <10 cm	1
		b. 10- 50 cm	2
		c. 50 - 100 cm	3
		d. 100 - 150 cm	4
		e. > 150 cm	5
2. Soil Texture	35%	a. Clay to Clay loam	1
		b. Silt Clay to Silt loam	2
		c. Loam to loam sand	3
		d. Sandy clay to Sandy loam	4
		e. Sandy soils	5
3. Stoniness*	20%	a. N, V	1
		b. F	2
		c. C	3
		d. M	4
		e. A, D	5
4. Organic Matter %	20%	a. < 1	1
		b. 1-2	2
		c. 2-4	3
		d. 4-6	4
		e. > 6	5

*N = None; V= Very few; F= Few; C = Common; M= many; D= Dominant; A= Abundant

Table 2.6 Hydrological soil groups per scores of the weight-rate model.

Hydrological Soil Group	Score
A	> 3.89 - Highest infiltration capacity
B	3.33 < Score < 3.89
C	2.86 < Score < 3.33
D	< 2.86 - Lowest infiltration capacity

To calculate the curve number for model sub-basins an ArcGIS extension “Computing Composite Curve Number (CCCN)” is utilized. The program proceeds by clipping the soils and land use shapefiles with the drainage basin boundaries. The soil types are converted to hydrologic soil groups by joining the soil group look-up table to the clipped soil shapefile. The shapefile is then joined to twice, first to the drainage basin shapefile, second to the land use shapefile. This creates a number of smaller polygons inside the drainage boundaries. The curve number look-up table is joined to this compiled shapefile, and a curve number is assigned to each polygon based on the combination of its soil group and land use records. At this point, all the data necessary to determine an area-weighted curve number is now available in one shapefile. Each polygon contains a record for the drainage basin name, soil group, land use, and curve number. The Curve Number Generator applies the curve number equation to all polygons that have identical drainage sub-basin names, and an area-weighted curve number is determined for each drainage sub-basin.

Table 2.7 Curve number evaluated based on the landuse and hydrological soil groups.

Land use-treatment classes	Hydrological Soil Group							
	Curve numbers (λ=0.2)				Curve numbers (λ=0.05)			
	A	B	C	D	A	B	C	D
Urban areas, high density	74	80	87	90	63	72	82	86
Urban areas, medium density	72	78	85	88	61	69	79	84
Urban areas, low density	70	76	83	86	58	66	76	81
Commercial and business areas	89	92	94	95	85	89	92	94
Streets, roads paved with curbs and storm sewers	98	98	98	98	97	97	97	97
Streets and roads, gravels	76	85	89	91	66	79	85	88
Open spaces, good condition	39	61	74	80	24	47	63	72
Open spaces, fair condition	49	69	79	84	33	57	70	78
Fallow lands	77	86	91	93	68	81	88	91
Row crops contoured and terraced, poor condition	66	74	80	82	53	63	72	75
Row crops contoured and terraced, good condition	62	71	78	81	48	59	69	73
Cultivated land with conservation treatment	62	71	78	81	48	59	69	73
Wood land, poor cover	45	66	77	83	29	53	68	76
Wood land, good cover	25	55	70	77	13	40	58	68
Meadows, good condition	30	58	71	78	16	43	59	69
Shrubs	27	44	60	66	14	28	45	53
Swamps	0.5	0.5	0.5	0.5	0	0	0	0
Water courses	0.5	0.5	0.5	0.5	0	0	0	0
Paved parking lots	0.5	0.5	0.5	0.5	0	0	0	0
Road, hard surface	74	84	90	92	63	78	86	89

2.7.2 ***Hydrological model calibration***

Two main categories of evaluation indices were applied for model calibration. The first category of indices is used to evaluate the model for the entire rainfall event:

Peak flow error (%): $$\mathrm{PFE} = \frac{Q_{obs_{peak}} - Q_{sim_{peak}}}{Q_{obs_{peak}}} \times 100 \quad (2.6)$$

Phase error (hr): $$\mathrm{PE} = \tau_{obs} - \tau_{sim} \quad (2.7)$$

Volume error (%): $$\mathrm{VE} = \frac{|V_{obs} - V_{sim}|}{V_{obs}} \times 100 \quad (2.8)$$

Where $Q_{obs_{peak}}$ and $Q_{sim_{peak}}$ are, the peak observed and simulated flow values for each rainfall-runoff event, τ_{obs} and τ_{sim} are the peak times for the observed and simulated event, V_{obs} and V_{sim} are the total runoff volume for the observed and simulated event, respectively.

The second category is related to the evaluation of the time series of the rainfall-runoff simulation. Most research projects involving watershed modelling utilize some type of predefined model evaluation techniques to compare simulated output with observed data. A combination of graphical techniques, dimensionless, and error index statistics is used for model evaluation (Moriasi et al., 2007):

Coefficient of correlation (standard regression):

$$r = \frac{\sum_{i=1}^{n}[(Q_{obs(i)} - \overline{Q_{obs}})(Q_{sim(i)} - \overline{Q_{sim}})]}{\sqrt{\sum_{i=1}^{n}(Q_{obs(i)} - \overline{Q_{obs}})^2}\sqrt{\sum_{i=1}^{n}(Q_{sim(i)} - \overline{Q_{sim}})^2}} \quad (2.9)$$

Nash-Sutcliffe efficiency (Nash and Sutcliffe, 1970):

$$\mathrm{NSE} = 1 - \frac{\sum_{i=1}^{n}(Q_{obs(i)} - Q_{sim(i)})^2}{\sum_{i=1}^{n}(Q_{obs(i)} - \overline{Q_{obs}})^2} \quad (2.10)$$

Error Index; Root mean square error:

$$\mathrm{RMSE} = \sqrt{\frac{\sum_{i=1}^{n}(Q_{obs(i)} - Q_{sim(i)})^2}{N}} \quad (2.11)$$

Error Index; Mean absolute error:

$$\mathrm{MAE} = \frac{\sum_{i=1}^{n}|Q_{obs(i)} - Q_{sim(i)}|}{N} \quad (2.12)$$

Where $Q_{obs(i)}$ and $Q_{sim(i)}$ are, the observed and simulated flow values for time step *i*, $\overline{Q_{obs}}$ and $\overline{Q_{sim}}$ are the mean observed and simulated flow values for each event and N is the number of observations.

2.7.3 ***Hydraulic model: HEC-RAS***

The hydraulic model is based on the HEC's River Analysis System (HEC-RAS), version 5.0, of the US Army Corps of Engineers (USACE, 2016a). The 1D HEC-RAS model calculates water-surface profiles and energy grade lines in 1-D, steady-state, gradually-varied flow analysis. It is assumed that the dominant velocity is in the flow direction; hydraulic characteristics of flow remain constant for the time interval under consideration; and streamlines are practically parallel and, therefore, hydrostatic pressure distribution prevails over channel section (Chow, 1959). The model solves the full 1D St Venant equations for unsteady open channel flow:

$$\frac{\partial A}{\partial t} + \frac{\partial \phi Q}{\partial x_c} + \frac{\partial (1-\phi) Q}{\partial x_f} = 0$$

$$\frac{\partial Q}{\partial t} + \frac{\partial}{\partial x_c}\left(\frac{\phi^2 Q^2}{A_c}\right) + \frac{\partial}{\partial x_f}\left(\frac{(1-\phi)^2 Q^2}{A_f}\right) + gA_c\left(\frac{\partial z}{\partial x_c} + S_c\right) + gA_f\left(\frac{\partial z}{\partial x_f} + S_f\right) = 0$$

$$\phi = \frac{K_c}{K_c + K_f}, \qquad \text{where } K = \frac{A^{5/3}}{nP^{2/3}}$$

$$S_c = \frac{\phi^2 Q^2 n_c^2}{R_c^{4/3} A_c^2}, \qquad S_f = \frac{(1-\phi)^2 Q^2 n_f^2}{R_f^{4/3} A_f^2}$$

Q is the total flow down the reach, A (A_c, A_f) the cross sectional area of the flow (in channel, floodplain), x_c and x_f are distances along the channel and floodplain (these may differ between cross sections to allow for channel sinuosity), P the wetted perimeter, R the hydraulic radius (A/P), n the Manning's roughness value and S the friction slope. f determines how flow is partitioned between the floodplain and channel, according to the conveyances K_c and K_f. These equations are discretized using the finite difference method and solved using a four point implicit (box) method.

2.7.4 *Hydraulic model evaluation*

The simulated maximum water level bounds are matched with the observed water levels. The root mean square error (RMSE) objective function is used to evaluate the fit between the simulated uncertainty bounds of the water levels and the observed ones at the post-event measurement locations:

$$\mathrm{RMSE} = \sqrt{\frac{\sum_{i=1}^{n}\left(H_{max_{obs}} - H_{max_{sim}}\right)^2}{N'}} \qquad (2.13)$$

$H_{max_{obs}}$ and $H_{max_{sim}}$ are the maximum observed and simulated water levels respectively, and N' is the number of post-event maximum water level measurement points. The RMSE is zero if the observed and simulated water levels fit perfectly; higher RMSE error reflects more divergent values.

2.7.5 *Uncertainty Analysis*

Uncertainty analysis techniques are usually applied to account for possible errors that may be involved in the modelling process, such as errors involved in the estimation of the model parameters and in the input data measurements because of the poor knowledge of their true values or their spatial-variability, or because of the limited knowledge in the behavior of the real system. Say for example the epistemic uncertainty discussed by Beven (2016). Several authors agreed that the predictive uncertainty that is associated with the model parameters and its implication on the model output has to be recognized and evaluated in any modeling procedure (e.g. Apel et al., 2008; Beven and Binley, 1992; Dogulu et al., 2015; Ewen and Parkin, 1996). For example Beven and Binley (1992) developed a generalized likelihood uncertainty estimation (GLUE) framework for representing model parameter and prediction uncertainty within the context of a Monte Carlo analysis (Liu et al., 2005).

In our proposed approach, the uncertainty propagation in the model coupling approach is understood by analyzing the uncertainty on the hydrological model parameters based on two approaches. The first approach involves a sensitivity analysis for the hydrological model to select the key parameters mainly controlling and forcing the model results. The second approach involves a fuzzy combination based on Monte Carlo simulation for the selected parameters (Robert and Casella, 2004). The selected parameters for analysis are statistically sampled based on a uniformly distributed probability density function. Uniform distributions are considered to avoid any prior assumption on the parameters' distribution other than their feasible ranges as discussed by Freer *et al.*, (1996). Random numbers are generated using the Well19937c generator within HEC-HMS (Panneton et al., 2006).

PART I.

ANALYSIS OF HISTORICAL FLOOD EVENTS ON A REGIONAL SCALE

Obtaining information on previous flood events and their characteristics is a first step towards analyzing and evaluating the flood problem in a country. In Lebanon information on floods and their characteristics are almost lacking. There was no authority taking the responsibility of recording information on past flood events and performing the required measurements. Which makes the status of the flood problem (flood intensity and risk) in Lebanon still unclear.

Hence, in an attempt to evaluate the flood problem in Lebanon, this part reviews 711 flood event occurred in Lebanon and extracted from newspapers archives and previous reports. An analysis of the intensity and spatial occurrence of such events is performed, and cross checked with the basin's morphological characteristics, their rainfall and flow occurrence probabilities and their vulnerable areas to draw out some conclusions on the flood problem in Lebanon. This part ends with a discussion on the opportunities and limitations of such data sources. Moreover, this part presents all datasets available and analyses the geographical, hydrological and climatic characteristics of Lebanon and the selected study site for detailed analysis (Awali River Catchment). This part is formed of three chapters:

Chapter 3 presents the geographical, hydrological and climatic characteristics of Lebanon along with all datasets available.

Chapter 4 presents the geographical, hydrological and climatic characteristics of the selected study site for detailed analysis; the Awali River Catchment, along with all datasets available.

Chapter 5 reviews records of previous flood events extracted from newspaper archives and previous reports aiming at understanding the intensity and special occurrence of such events over the country. The opportunities and limitations of such data sources are also discussed

3 LEBANON: STUDY SITE DESCRIPTION AND DATA ANALYSIS

3.1 **Introduction**

Lebanon is part of the North East, located at approximately 34˚N, 35˚E. Stretching along the eastern shore of the Mediterranean Sea, its length almost three times its width. As it stretches from north to south, the width of its terrain becomes narrower. The country extends over an area of 10,452 km^2, it is roughly rectangular in shape, becoming narrower toward the south and the farthest north. Its widest point is 88 km, and its narrowest is 32 km; with an average width about 56 km.

Despite its small surface it presents a complex physiography with many well-defined geomorphological units. The four fundamental divisions of Lebanon are (Abu Al Anin, 1973; El-Fadel et al., 2000; Du Vaumas, 1954):

- The narrow coastal plain
- The Western Mount Lebanon rising to 3088m, (Qornet Es-Saouda).
- The Central Bekaa Valley
- The Eastern Jebel Lubnan al Sharqi or Anti-Lebanon Range with Mount Hermon at 2814 m.

The coastal plain together with Mount Lebanon constitute the occidental segment of Lebanon which makes up 50% of the total area of the country and accommodate 70% of the Lebanese population. The oriental eastern segment is made up of the depression of the Bekaa valley (14%) and Anti-Lebanon ranges (36%).

This country is divided into six governorates; Beirut, Mount Lebanon, North, Bekaa, South and Nabatiye, which are further subdivided into twenty-five districts or caza. Major cities are: Beirut, Tripoli, Jounieh, Saida, Tyre, Zahle, Baalbek and Nabatiye, with the first four cities being coastal cities. It is a highly urbanized country with most population concentrated in the main coastal cities. The Lebanon's resident population in 2007 was estimated at 3.7 million in addition to 425,000 palestinian refugees (CDR, 2004). Beirut is the capital and mostly urbanized area with a population exceeding 1.5 million living in an area of about 253 km^2 (City of Beirut and its suburbs) (Yamout and El-Fadel, 2005)

The climate of Lebanon is typically Mediterranean, humid to sub-humid in the wet season to semi-arid in the dry season. The wet season coincides with winter period, which lasts from October till May. In winter, the atmospheric pressure perturbations originating from South Europe cause abundant rainfall at the coast and on the mountains parallel to it. The dry season coincides with the summer period, which lasts from June till September. During this period, no rain is recorded, and a state of high pressure dominates the whole country.

The objective of this chapter is to describe the geographical, hydrological, and climatic characteristics and datasets of Lebanon and present the major data analysis required for further analysis in the coming chapters (chapters 5, 8 and 9).

3.2 **Geographical dataset**

3.2.1 ***Topography***

Lebanon is a mostly mountainous country, of two NNE-SSW trending mountain chains, separated by a narrow plain, the fertile Bekaa plain. A narrow coastal strip of land fronts the Mediterranean Sea. Most of these topographic features have been mainly shaped by the tectonic activities along the Dead Sea Transform Fault (DSTF), a tectonic plate boundary. The Mount Lebanon chain is central to the West, while the Anti-Lebanon Mountains stretch across its eastern border with Syria. The highest point of Lebanon is Qornet Es-Saouda which peaks at 3,088 m.

These mountain ranges have two antagonistic roles: climatic barriers on the coast, forming by their mass a screen against the access of humidity towards the interior; and climatic barriers in the hinterland, opposing by their massive-reservoirs to evaporation. As a result of this duality in the hydrological mechanism all living conditions of the country reside (Abd-el-Al, 1996).

The Bekaa is almost everywhere above 850m in altitude and that is as high as some of the highest mountains of many countries. The continental shelf of Lebanon is very narrow, it has a maximum width of ten kilometers, and drops down abruptly to water depths of 1500m. We know very little about what lies off the coast of Lebanon and the area has not been mapped in detail. Beyond this shelf break, which is cut by deep canyons, lies what must be ancient ocean crust (Walley, 1998).

The Digital Elevation Model (DEM) of Lebanon of 15m planimetric and altimetric resolution was used to analyze the morphometric characteristics of the country. This DEM was built from 10 m interval contour of elevation maps plotted on 121 topographic sheets at a scale of 1/20 000 and available in a digital form at the CNRS (Figure 3.1).

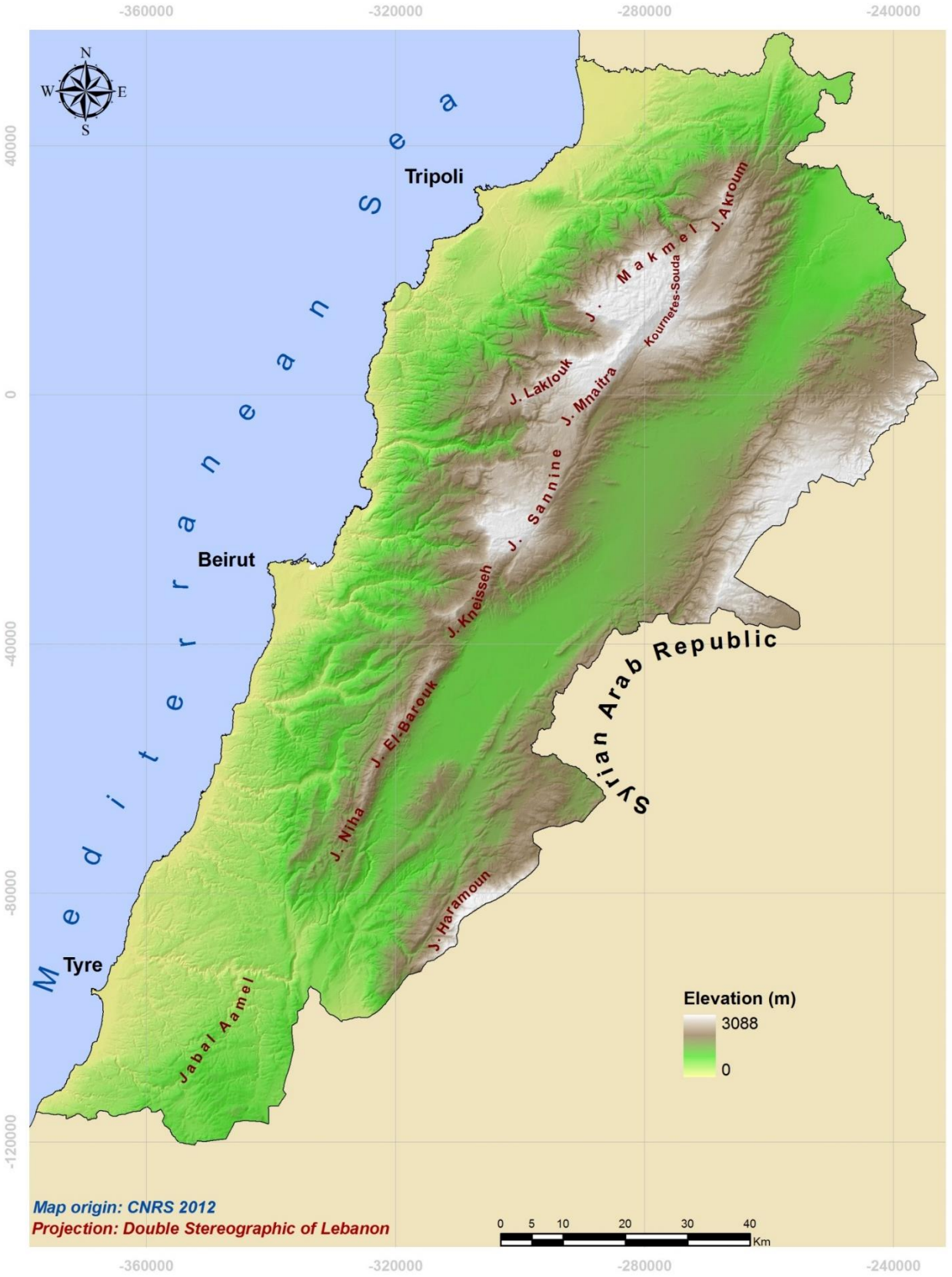

Figure 3.1 Digital Elevation Model for Lebanon.

3.2.2 *Geology*

The geology of Lebanon is well documented in (Beydoun, 1976; Dubertret, 1945; El-Qareh, 1967; Ghattas, 1975; Hakim, 1985; Walley, 1998). The underlining geology of the country is made mainly of carbonate rocks, limestone and dolomite mostly from the Jurassic and the Cretaceous. The outcropping stratigraphic sequence in Lebanon exposes rock formations ranging in age from the Middle Jurassic to the recent Quaternary (Abdallah et al., 2005). These are sediments of the Mesozoic (Jurassic and Cretaceous) and Cenozoic and eruptive rocks (basalts). The entire exposed stratigraphy sequence of Lebanon has an estimated total thickness of 4,000 to 5,700m, depending on the area. Large areas of Eocene limestone also crop out in southern Lebanon. Middle Miocene strata occur occasionally in patches along the coast. Pliocene basalt fills the old valley of the upper Jordan River and a part of Akkar in the northernmost part of the country. Alluvium deposits from the quaternary fills the Bekaa valley, and part of the narrow coastal plain. The dominant formation in Lebanon is the Cenomanian (C4) forming around 35 % of the total area of the country. It is formed by a chert-bearing massive thinly bedded, highly fractured and jointed, well karstified limestone and dolomitic limestone. The Middle to upper Jurassic (J4-7) is another important formation that covers about 13 % of the country, and characterized by massive, thick bedded, highly fissured, jointed and well karstified dolomite, limestone, and dolomitic limestone. Figure 3.2 presents a schematic East-West cross section across Northern Lebanon. The Geological formations of Lebanon are covered by 27 sheets at a scale of 1: 50 000. These maps are present in a digital form at the RSC (Figure 3.3).

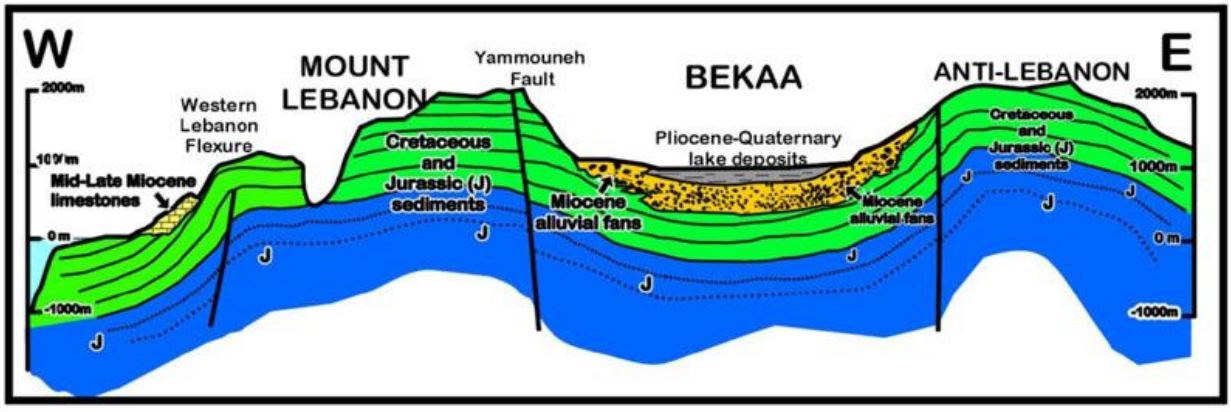

Figure 3.2 Schematic east-west cross section across Northern Lebanon (Walley, 2009).

The geology of the country encompasses highly aquiferous formations that can store and yield considerable volumes of fresh water (Metni et al., 2004). A total of five hydro-stratigraphic units are categorized as aquifers in Lebanon. Two of which are considered the main aquifers of the country: the Kesrouane aquifer (J4 aquifer) and the Sannine-Maameltein aquifer (C4-C5 aquifer). The three remaining aquifers are the Eocene aquifer (e2b aquifer), the Miocene aquifer (mL aquifer) and the Neogene-Quaternary aquifer (ncg-Qcg aquifer) (UNDP, 2014).

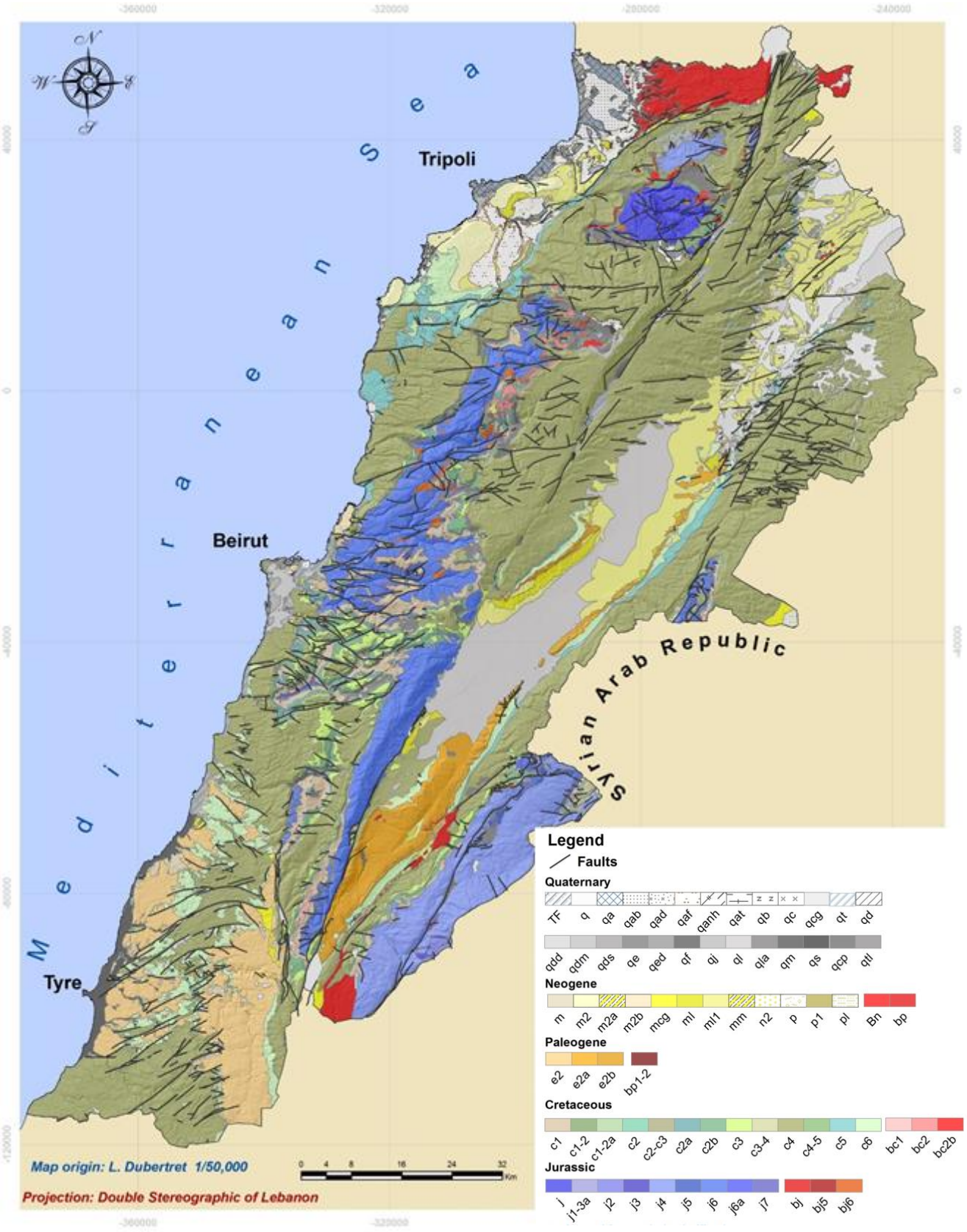

Figure 3.3 Geological map of Lebanon, (map source: Abdallah et al., 2013).

3.2.3 ***Soil***

The National Council for Scientific Research of Lebanon (CNRS) released in 2006 the new soil maps of Lebanon at a scale of 1/50,000 classified according to the modern international systems and based mainly on SOTER (Soil and Terrain) database (Darwish et al., 2006). At a scale of 1/50 000, 106 soil units were identified in Lebanon. Soils occupying small areas relative to the 1/50,000 scale were associated to the dominant soils in the area. These soils are typically Mediterranean in character, the predominant soil types are: Red soils, Brown soils, Yellowish mountainous soils, Black soils, Grayey soils, Chestnuts soils, Sandy soils, Alluvial soil, Sub-desertic yellowish soils, Rendzine and Mixed soils. The Lebanese soils are young, fragile and subject to erosion, especially in the mountains and hills. Topography, rain intensity and surface runoff are major factors increasing erosion caused by the precipitations, especially where the protective green cover has disappeared. The erosion intensity is proved by the stratification of alluvial loam terraces of the coastal rivers (Figure 3.4).

3.2.4 ***Land cover/use***

The Land cover/use map of Lebanon was built from high resolution (1m) satellite images IKONOS established at the RSC-CNRS 2010. The classification was based on the European CORINE (Coordination des Informations sur l'Environnement) classification adapted for Lebanon, level 4 of discrepancies (Figure 3.5). Areas occupying different land cover use can be summarized in Table 3.1.

The period of the Lebanese civil war (1975-1990) has resulted in a low density and fragmented urban sprawl. When the war was ended, nearly after 1990, a major reconstruction and reforms have taken place. This peaceful atmosphere launched a massive construction of roads and buildings, water and sanitation facilities, and energy and transport systems, which transformed eternally land cover and cities of Lebanon (Faour, 2015). However, migration, informal settlements, lack of urban planning, political corruption, as well as internal conflicts have resulted in an uncontrolled urban sprawl. Evaluating the urbanization growth from 1963 till 2005 based on processing and interpreting topographical maps and satellite images acquired by different space platforms, showed that urbanized area in the major Lebanese cities doubled between 1963 and 1994 and between 1994 and 2005 reaching up to 750km^2 (Faour and Mhawej, 2014). A recent study to follow the evolution of urbanization in Lebanon revealed that an uncontrolled urbanization of over 80% have occurred in the country in the last 20 years (reference CNRS,2015) (Figure 3.6).

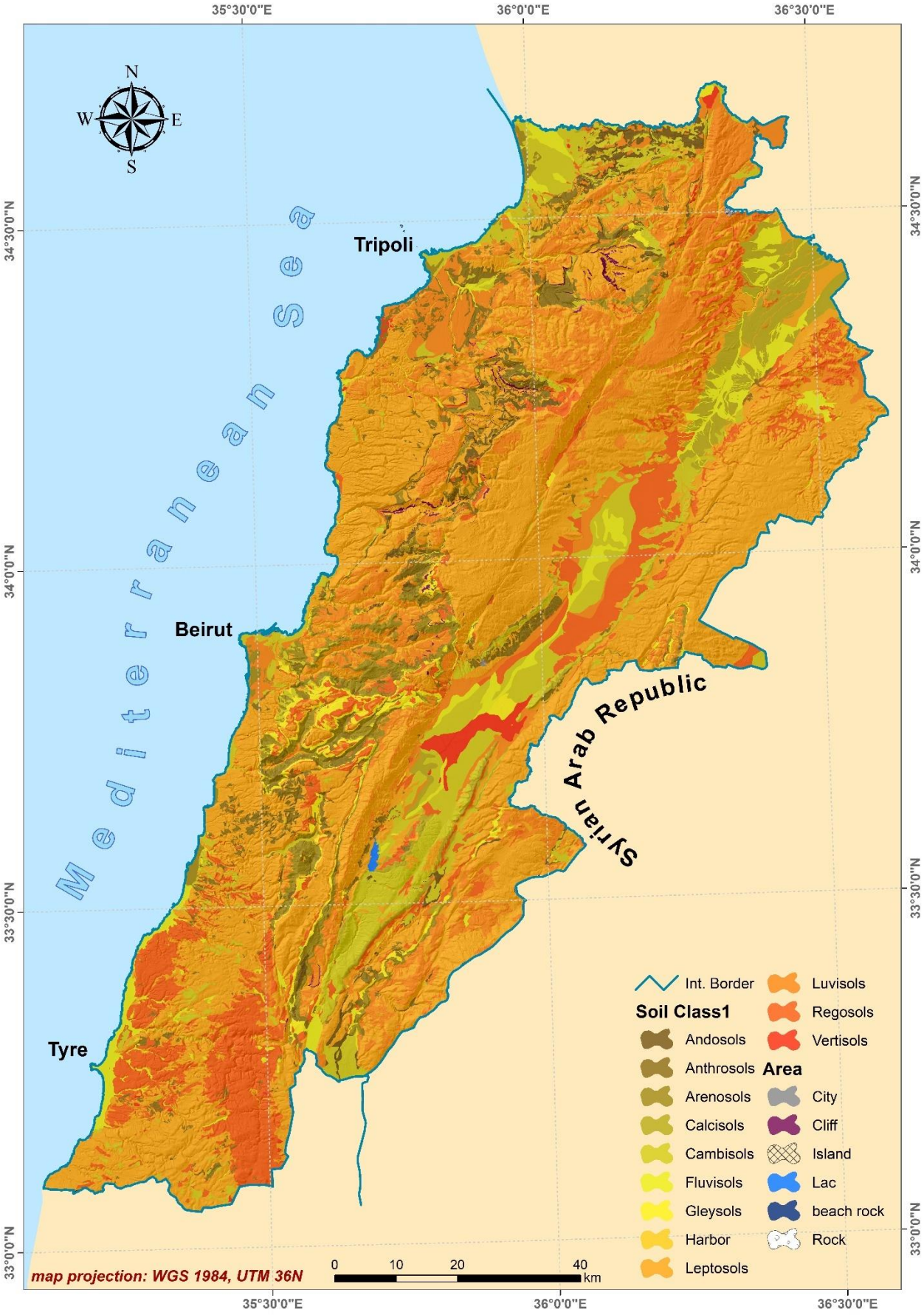

Figure 3.4 Soil map of Lebanon (Darwish et al., 2006).

Table 3.1 Land Cover use description and corresponding areas in Lebanon.

Code	Description	Area [Km^2]	Code	Description	Area [Km^2]
111a	Dense urban fabric	74.22	**242**	Poultry farms	4.04
111b	Dense informal urban fabric	9.67	**310/112c**	Urban sprawl on dense wooded land	7.76
112a	Medium density urban fabric	137.76	**311a**	Dense Pines	136.65
112b	Medium density informal urban fabric	0.92	**311b**	Dense Cedars	14.96
112c	Low-density urban fabric	226.81	**311d**	Dense Fir	27.53
112d	Low-density informal urban fabric	2.34	**311e**	Dense Cypress	38.84
112e	Tourist resort	8.35	**312a**	Dense Oaks	433.73
112f	Diverse equipment	0.60	**312b**	Dense - other types of broadleaved trees	5.95
112g	Archeological site	8.22	**313**	Dense mixed wooded land	134.87
121	Industrial or commercial area	18.58	**320/112c**	Urban sprawl on clear wooded land	8.52
122	Port area	5.02	**321a**	Clear Pines	146.11
123	Airport	12.57	**321b**	Clear Cedars	4.36
124	Railway station	0.09	**321c**	Clear Juniper	260.95
125	Wetland or saltmarsh (including salt)	1.01	**321d**	Clear Fir	1.43
131	Mineral extraction sites	51.28	**321e**	Clear Cypress	23.87
132	Dumpsites	0.25	**322a**	Clear Oaks	643.39
133	Landfill site	0.30	**322b**	Clear - other types of broadleaved trees	30.25
134	Urban extension and/or construction site	7.40	**323**	Clear mixed wooded land	231.94
135	Urban vacant land	3.92	**330/112c**	Urban sprawl on scrubland	3.40
141	Green urban area	2.02	**331**	Scrubland	205.73
142	Sport and leisure facilities	3.00	**332**	Scrubland with some dispersed bigger trees	702.79
210/112c	Urban sprawl on field crops	35.97	**340**	Burnt wooded land	3.01
211	Field crops in medium to large fields	828.86	**410**	Dense grassland	1073.68
212	Field crops in small fields/terraces	720.94	**510**	Inland and Marine wetland	2.99
213	Soils	79.88	**610**	Bare rocks	139.65
220/112c	Urban sprawl on permanent crops	32.82	**620**	Bare soils	77.14
221	Olives	532.47	**630r**	Rock beaches	2.23
222	Vineyards	70.00	**630s**	Sand beaches	3.56
223	Fruit trees	503.49	**650**	Rocky Mountains	2285.08
224	Citrus fruit trees	129.56	**660**	Islands	0.06
225	Banana	32.74	**711**	Lake	8.66
230/112c	Urban sprawl on intensive agriculture	0.20	**712**	Hill lake	4.25
231	Open horticulture	18.90	**722**	Port basin	3.59
232	Protected agriculture	23.37	**R1**	Auto route	7.37
241	Agricultural equipment	3.51	**I**	Streams	11.50

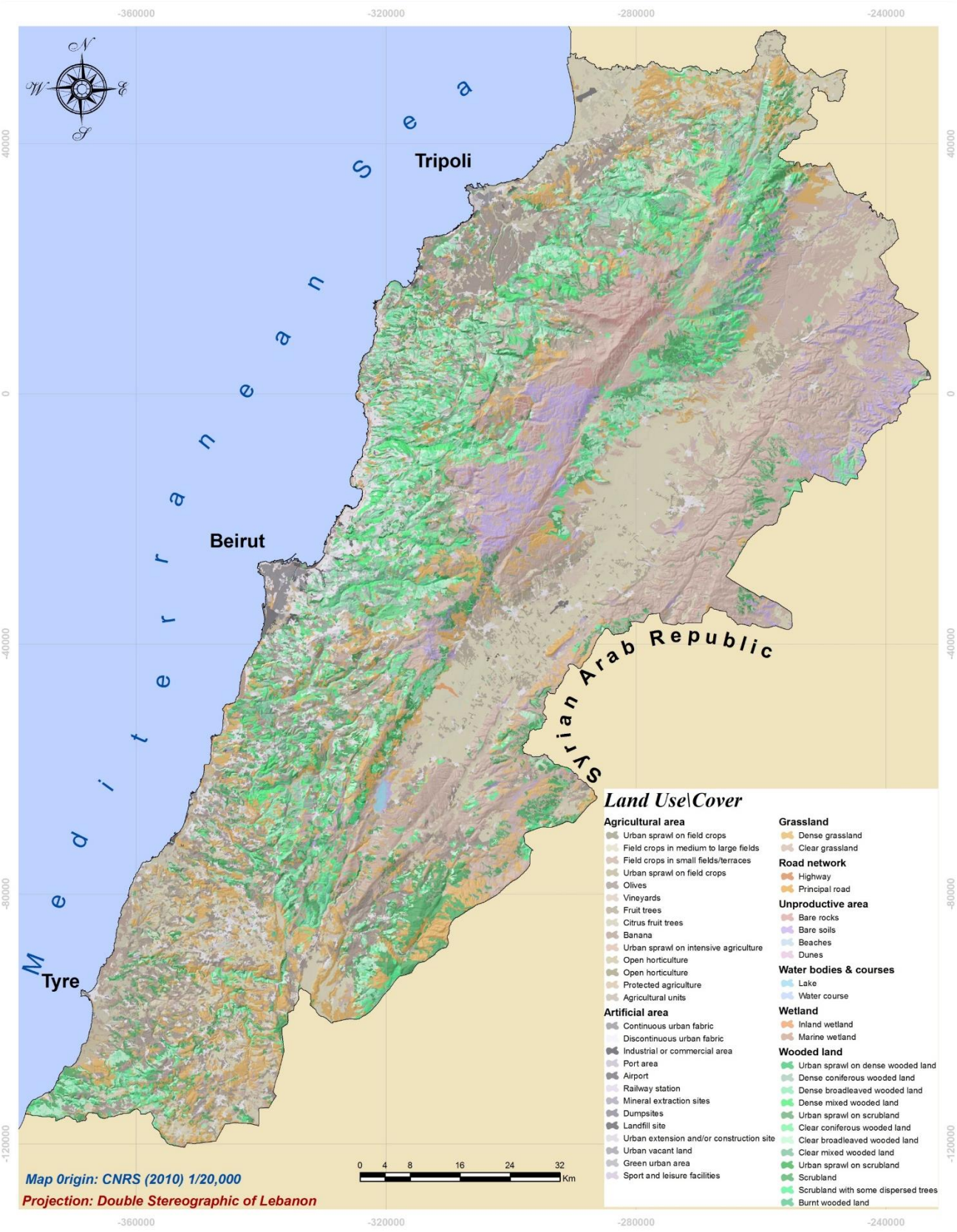

Figure 3.5 Land Cover/Use map of Lebanon (LNCSR-LMoA, 2010).

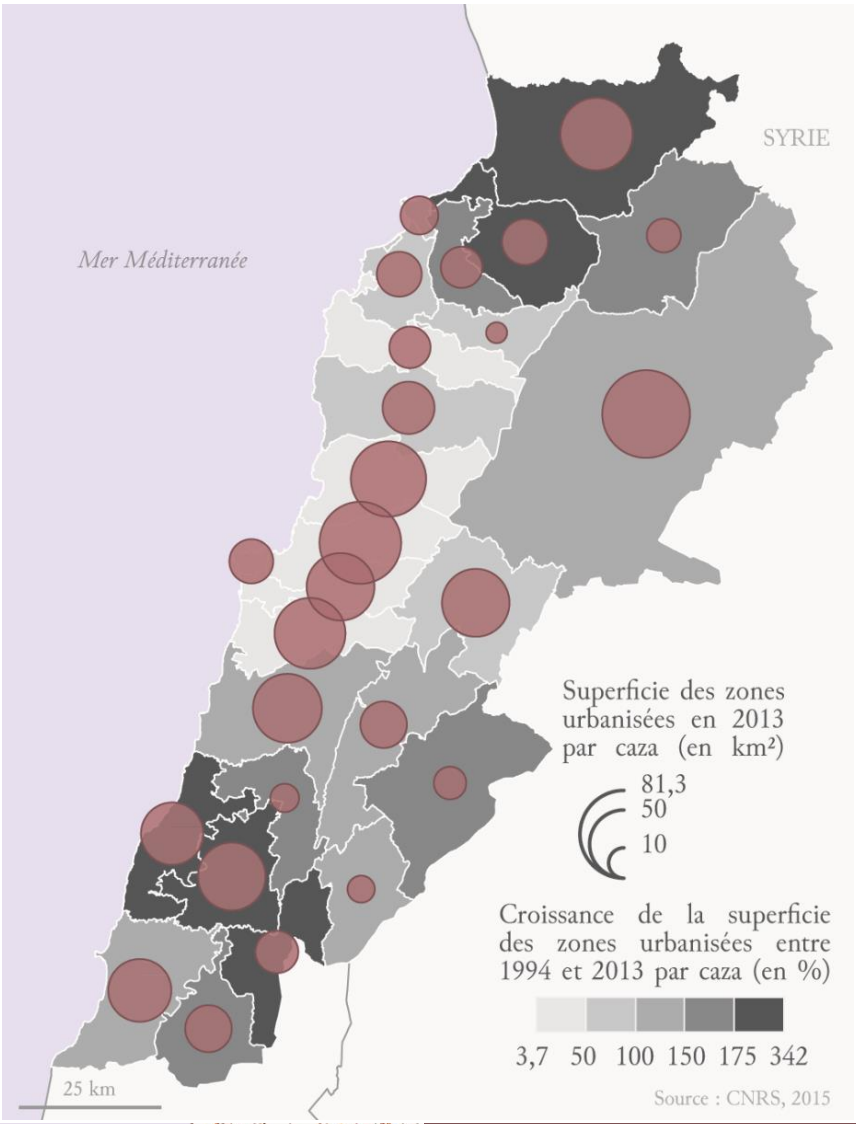

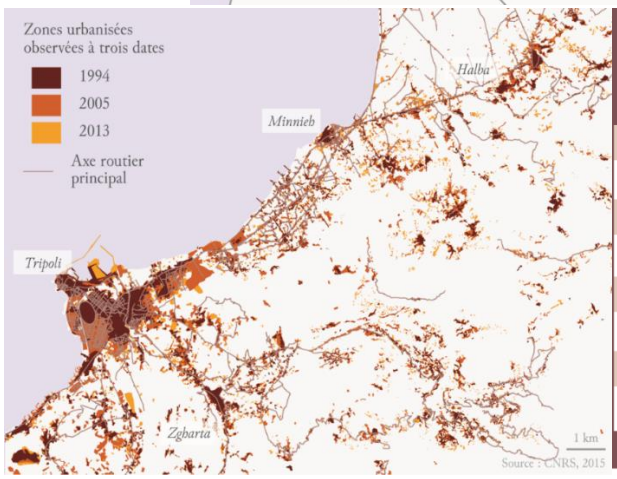

Muhafazat	Superficie totale en km²	Surperficie urbanisée en km² et en pourcentage de la superficie totale					
		1994		2005		2013	
Akkar	790	20	3%	44	6%	55	7%
Baalbek-Hermel	2853	45	2%	73	3%	94	3%
Beyrouth	21	20	95%	21	98%	21	98%
Békaa	1413	46	3%	67	5%	83	6%
Mont Liban	1973	226	11%	281	14%	312	16%
Nabatiyé	1100	30	3%	76	7%	99	9%
Nord	1187	49	4%	89	7%	101	9%
Sud	924	35	4%	68	7%	92	10%
LIBAN	10262	472	5%	719	7%	858	8%

Figure 3.6 (a) map showing the percentage of urbanization growth in Lebanon per Caza, (b) close up view to the city of Tripoli showing the urban evolution between 1994 and 2013, (c) table showing the growth in the percentage of urban areas per districts between 1994 and 2013 in Lebanon (Source CNRS, 2015).

3.3 **Hydrological dataset**

3.3.1 ***Watersheds and rivers***

Lebanon has 17 perennial streams and about 23 seasonal ones. Their combined length is approximately 730 km. In addition, 26 isolated watersheds are drained seasonally through a diffused drainage system and most of them flow to the sea. While most river flows peak during March and April, some may reach maximum flow later during the year, such as the Aasi/Oronte River which peaks in July. Minimum flows are typically recorded in the months of September and October.

The rivers of Lebanon can be divided into two groups. The first group consists of 13 East-West rivers, mostly cut into steep gorges, which drain Mount Lebanon. These are the Ostouane, Arka, Bared, Abou Ali, Jouz, Ibrahim, Kelb, Beirut, Damour, Awali, Sainik, Zahrani, Abou El Assouad; along with the Kebir River that flows west and traces the northern border of Lebanon with Syria. The second group consists of three rivers; the two large rivers of the Bekaa; the Litani River, which drains the southern Bekaa plain, crosses the southern periphery of the Mount-Lebanon range and discharges into the sea north of Tyre and the Assi River which drains the northern Bekaa valley and flows northwards into Syria. And the Hasbani River which crosses the southern border and forms one of the tributaries of the River Jordan (Figure 3.7). The basins names and their corresponding areas are presented in Table 3.2.

3.3.2 ***Rainfall***

The climate of Lebanon is typically Mediterranean, the wet season coincides with winter period, which lasts from October till May. The dry season coincides with the summer period, which lasts from June till September. In winter, the atmospheric pressure perturbations originating from South Europe cause abundant rainfall at the coast and on the mountains parallel to it. In summer, no rain is recorded, and a state of high pressure dominates the whole country. A typical average transects crossing the country consists of: a subtropical coastal climate, a semi-arid continental climate in the Bekaa Valley, and a typical Continental Mediterranean climate in the Northern range of Anti-Lebanon Mountains. The National Meteorological Service defined eight eco-climatic zones (presented in Figure 3.9). The principal criterion for the zonation is rainfall. According to their geographical situation, the eco-climatic zones are distributed as follow:

i. The coastal strip, including northern, central and southern coastal zones;

ii. The mountains, or the Mount-Lebanon, which are divided into two zones; northern and central

iii. The inland divided into three zones: northern, central and southern Bekaa Valley.

While the coastal and mountainous areas are characterized by abundant rainfall distributed over the winter season, the Bekaa Valley has a semi-arid to continental climate with unpredictable rainfall and recurrent drought (Abdallah, 2010). The average annual precipitation is highly variable, it ranges from 500 mm in the interior Assi zone, a north-east semi-arid zone of the country, to over 1200 mm over the upper mountains of Mont Lebanon (Plassard, 1972).

Table 3.2 Lebanese basins and sub-basin names and their corresponding areas.

Name	Area Km^2	Name	Area Km^2	Name	Area Km^2
Jdaide	17.1	Damour	318.6	Marjayoun	33.2
Hasbani	671.6	Ibrahim	309.6	West Hasbani	6.4
Saida	94.3	Jounieh	29.2	Zahrani	155.8
Beirut urban part	44.3	Tbarja	18.9	Barsa	19.7
Abou Ali	490.7	El Kalb	290.9	West Barsa	25.4
Bachta	43.0	Litani	2049.5	Wadi Minieh	31.8
Fidar	50.3	El jouz	193.0	Wadi Barsa	67.2
Ham Maaraboun	57	Maameltein	13.4	Mouhnane	51.5
Ghazir	25.0	Akroum	14.2	Naame	19.6
Awik	39.3	Amshit	4.8	North Abou Ali	13.0
El Dekouane	12.7	Antelias	24.0	North Asfour	19.0
El Kharub	89.2	Arka	171.5	North Bared	22.6
El Madfoun	65.7	Asfour	89.7	North El jouz	8.3
Ostouane	164.0	Abou El Assouad	151.9	Sainik	111.6
South El Madfoun	15.1	Awali	301	South Antelias	3.4
Zouk Mousbeh	5.7	Bared	282.0	South Asfour	5.9
MarjHin	202.9	Beirut	225.3	South Awali	26.0
Yammoune	126.9	Bissariye	43.2	South Fidar	5.7
Between Litani- El Aasi	385.9	Blat	17.7	South El Kalb	10.5
South Litani	514.6	Bshemoun	40.5	Ghadir	36.9
Mansiyye	91.2	El Kabir	297.4	Harissa	6.4
El Aasi	1343.2	Fisan	25.9	Henaidar	15.6
Tfail	18.9				

Figure 3.7 Drainage networks and their corresponding basins.

Several public, academic and private establishments have collected meteorological data in Lebanon, each one operated/ing one or more stations. The American University of Beirut (AUB) was the first to take rainfall measurements (1876), followed by the Jesuits in Ksara (Bekaa) in 1931. These two stations have operated continuously until 1975. On the other hand, the Lebanese National Meteorological Service (LNMS); established in 1921 during the French mandate, operated six stations in September 1928 and reached to 163 stations in 1970, out of which 137 stations were considered reliable from which Plassard published his rainfall map for Lebanon in 1972 (Plassard, 1972). The map represented the annual cumulative rainfall over the country. Since then this map was never updated and is still considered as the most accurate one. The spatial coverage of the pre-war stations is presented in Figure 3.9 and their details are presented in Table 3.3.

By the end of the Lebanese civil war, six stations were only operating (Tripoli-IPC, Beirut International Airport, Al-Arz, Rayak, and AUB) the rest were either destroyed or ceased operation because they were unmaintained. The AUB station was replaced by a simple station managed by the Faculty of Agriculture and relocated near its building.

In the mid 90's, the National Meteorological Service started rebuilding the national meteorological network and managed to establish (to-date) 37 stations, most of them started operating since 2000. Figure 3.8 shows the growth of the meteorological network in Lebanon since 1928 along with its decay during the civil war. Around 20 stations were established almost in their exact location during the pre-war period, these stations are presented in bold in Table 3.3. However, with 37 stations only, the spatial coverage of this network is far from the one of the pre-war network and the quality of measurements is questioned. Likewise, the Lebanese Agriculture Research Institute (LARI) working under the umbrella of the Ministry of Agriculture (MoA) started since 2006 to build up its own agro-meteorological stations. Most of these stations started operating in 2009. To date the number of installed stations is "50". The spatial coverage of the post-war stations is presented in Figure 3.10 and their details are presented in Table 3.4.

These meteorological stations are equipped with traditional rain gauges that record daily rainfall measurements. Some stations (such as Baysour, Beirut Golf, Abde, Qartaba, and Hermel) record hourly rainfall measurements, but till now these measurements possess many gaps and are still considered unreliable compared to daily rainfall records and cannot replace the need for a rainfall radar. Data from the LNMS and LARI are found at the disposal of the CNRS up till 2012. Official letters were sent to both LARI and LNMS- directorate of civil aviation to provide us with the missing data up till 2016. But these data are not free of charge and would cost us a fortune; we were only capable to obtain data for six stations (Baysour, Deir el Kamar, El Meshref, Jezzin, Lebaa, and Saida) covering the Awali Basin, which was the selected study area for detailed analysis and modeling. The directorate of the civil aviation allowed us to sort through their data to select the appropriate dates to be purchased for modeling, afterwards, the data were examined to look for outliers, gaps and shift in the records.

Later, the observed annual rainfall maxima were extracted for each station and fitted to a generalized extreme value function. The rainfall depths corresponding to different return periods (10, 50, and 100 years) were then evaluated based on the known Gumbel method (Gumbel, 1961). These values are then utilized in chapter 5 to evaluate the rainfall probability of occurrence for each basin and then were crossed checked with the catchments' characteristics and the number of historical flood events in each basin extracted from previous reports and newspapers.

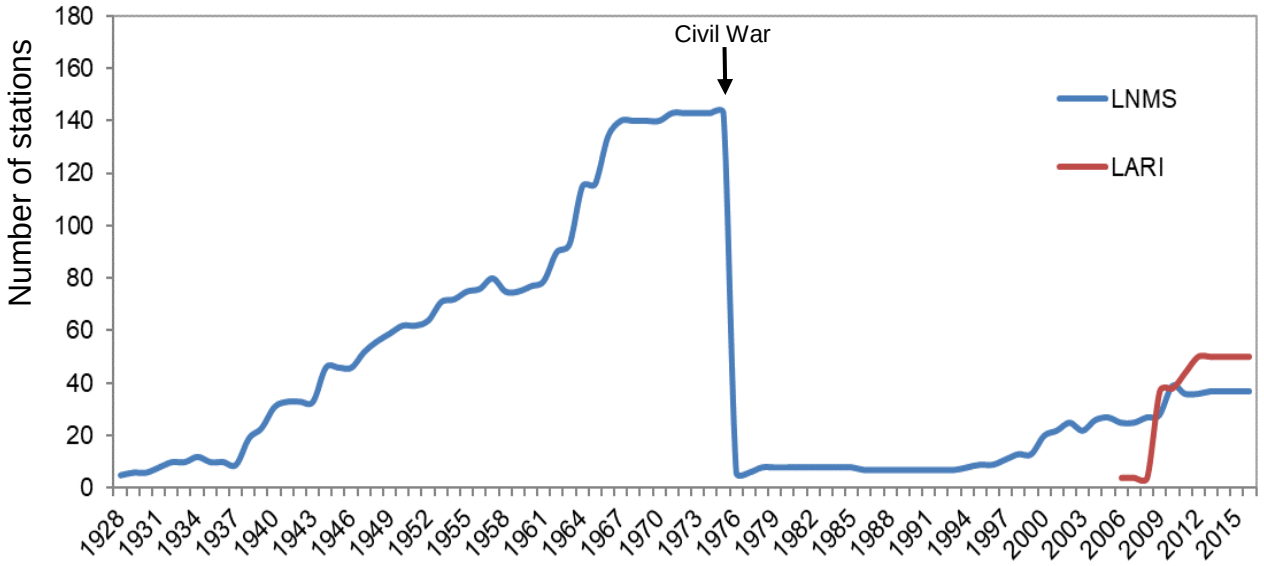

Figure 3.8 Graph showing the growth of the meteorological network since 1928 in Lebanon, its decay during the civil war (1975-1990) and its reconstruction until 2016.

3.3.3 ***Discharge***

Since 1930 water levels and discharges in rivers have been measured in Lebanon. In 1954 the Litani River Authority (LRA) was assigned to take under its responsibility to first measure and then manage 87 gauging stations detailed of which 75 hydrological stations were installed and operated prior to the civil war in addition to several flow measurement sites at springs and canals. During the civil war measurements on gauging stations stopped and were resumed in mid-1990 with the rehabilitation of 20 stations to reach 58 stations in 1998. These were distributed over major watersheds mainly on the river outlets, and tributary connections, canals, and some of the springs. Moreover, LRA conduct also point flow measurements at various sites mainly emergences of some main spring discharging into the rivers (Figure 3.11).

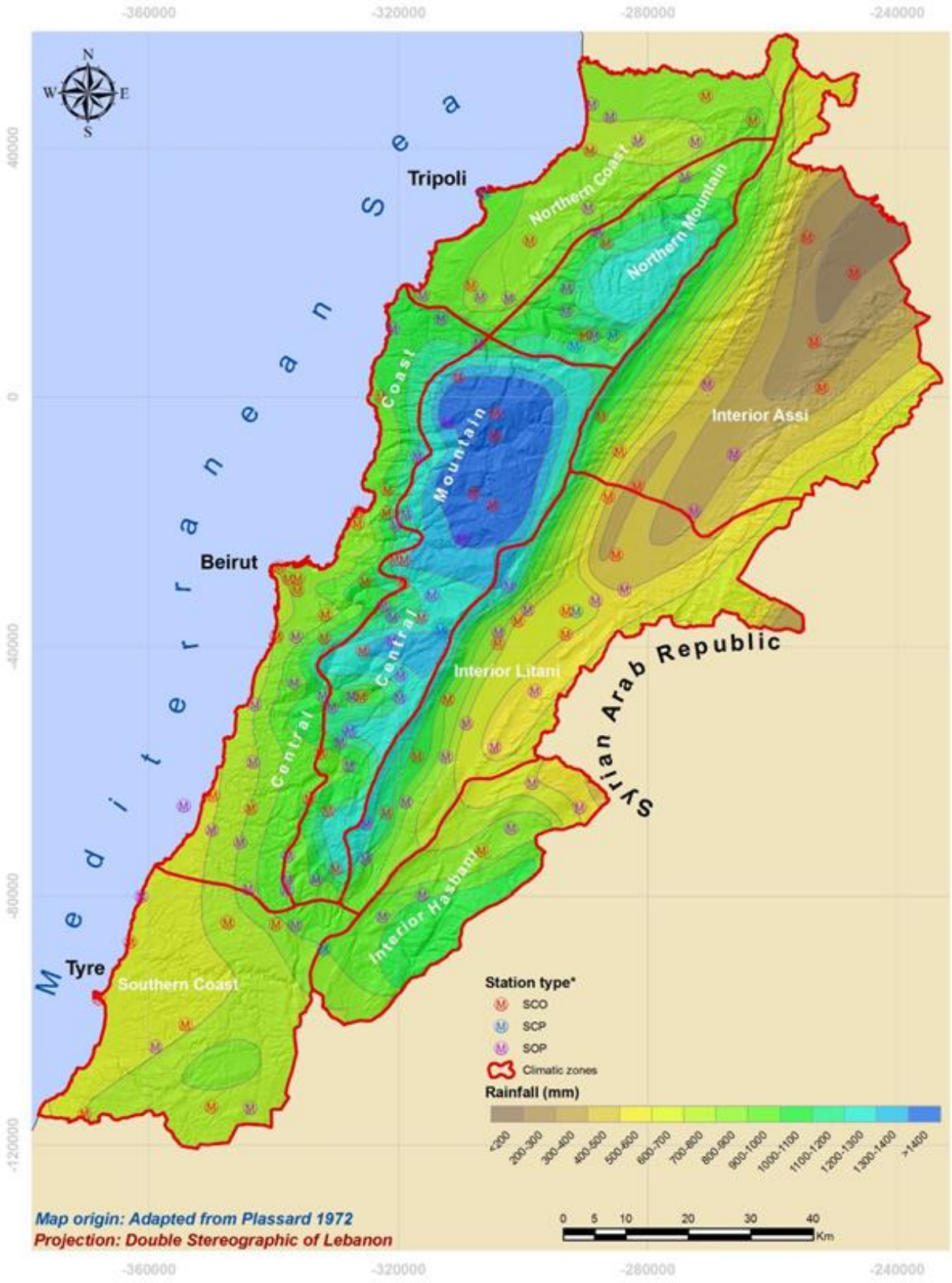

Figure 3.9 Meteorological stations operated by LNMS before the civil war.
**SOP: Station d'observations Pluviométriques, SCP: Station Climatologique Principal, SCO: Station Climatologique Ordinaire.*

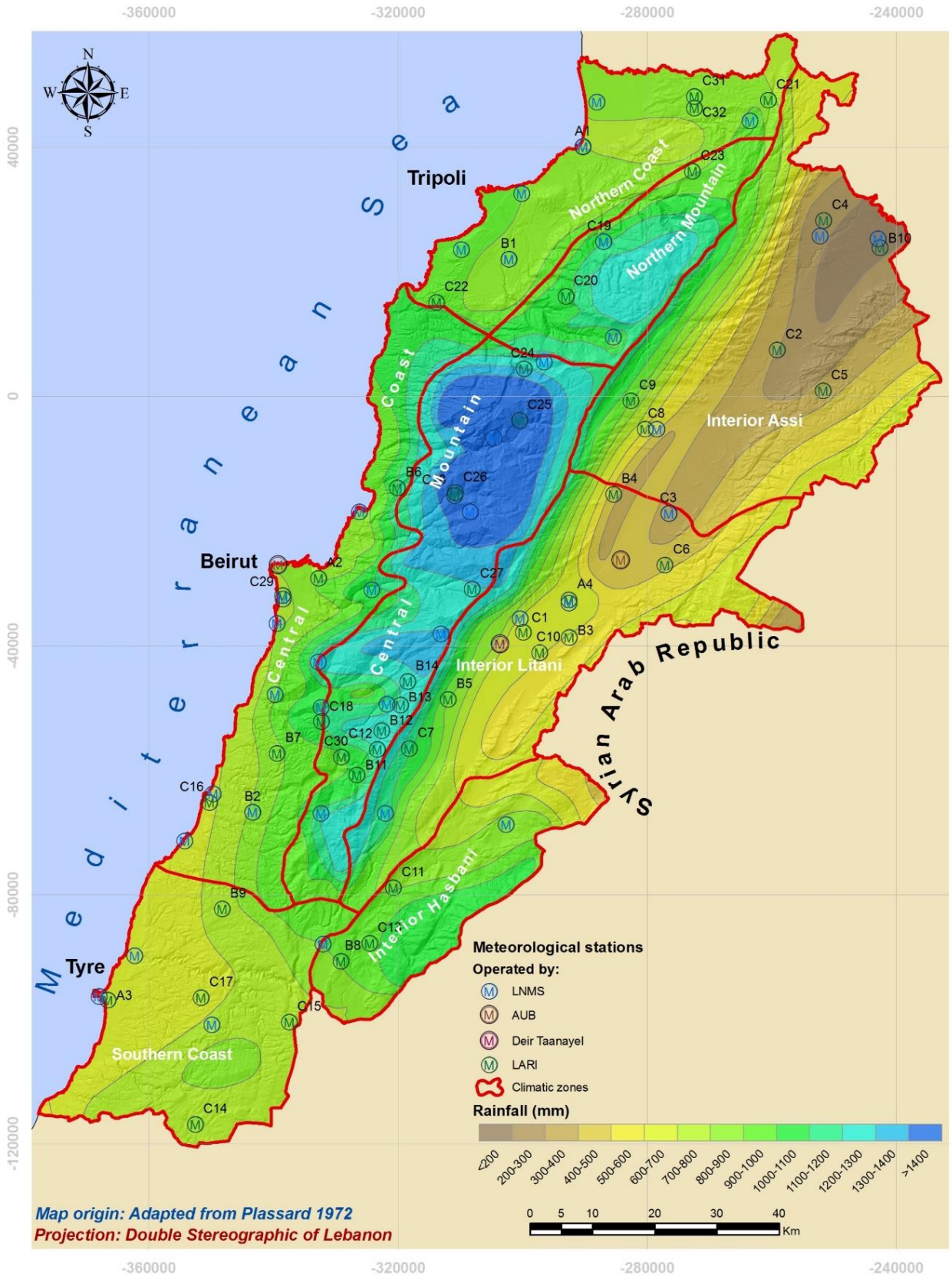

Figure 3.10 Meteorological stations operating in Lebanon after the civil war.

Table 3.3 List of LNMS Climate Stations before Civil War (pre-war network). Stations established in their exact location after the civil war are presented in bold.

Micro Climatic Zone	Stations	Type*	Lat.	Long.	Altitude (m) (ASL)	Starting date
Littoral North	Kouachra	SCO	34.6	36.2	400	1962
	Qlaiaat	**SOP**	**34.5833**	**36**	**5**	**1931**
	Qaabrin	SOP	34.5666	36.0333	25	1966
	Qoubayat	SCO	34.5666	36.2833	540	1962
	Beino	SOP	34.5333	36.1833	510	1966
	Halba (R)	SOP	34.5333	36.0833	160	1938
	El-Abde (R)	**SCO**	**34.5166**	**36**	**40**	**1954**
	Tripoli-Mina (R)	SCP	34.45	35.8166	20	1960
	Bared-Moussa	SOP	34.4333	36	250	1955
	Bakhaoun	SOP	34.4	36.0166	630	1966
	Zgharta	SCO	34.3833	35.9	110	1966
	Bechmezzin	SCO	34.3166	35.8	275	1966
	Chekka (R)	SOP	34.3	35.7166	15	1951
	Abou-Ali (R)	SOP	34.3	35.866	250	1938
	Amioun (R)	SOP	34.3	35.8166	300	1945
Central Littoral	Kaftoun	SOP	34.2666	35.75	215	1951
	Batroun (R)	SOP	34.25	35.6666	20	1939
	Kafar-Halda (R)	SOP	34.2333	35.8166	580	1940
	Amchit	SCO	34.15	35.65	135	1966
	Fanar	SCO	33.8833	35.6333	255	1969
	Ghazir (R)	SCO	34.0166	35.6666	390	1950
	Ghosta	SCO	33.9833	35.6666	650	1950
	Zouq-Mikayel (R)	SCO	33.9666	35.6166	70	1944
	Un.Americaine (Bey)	SCO	33.9	35.4833	35	1891
	Un.Saint-Joseph (Bey)	SCO	33.8833	35.5	45	1933
	Nazareth (Bey) (R)	SCO	33.8833	33.5166	90	1928
	Ins.de Geographic (Bey)	SCO	33.8666	35.5166	55	1933
	Aeroport (Bey) (R)	**SCO**	**33.8**	**35.4833**	**15**	**1933**
	qornet-Chehwan	SCO	33.9166	35.7	605	1948
	Arbaniye-jisr	SCO	33.8833	35.7	510	1960
	Jamhour (R)	SCO	33.8333	35.5666	410	1955
	Choueiffat (R)	SOP	33.8	35.5166	100	1956
	Souq-el-Ghareb (R)	SCO	33.8	35.5666	700	1948
	Abey	SOP	33.7333	35.5166	730	1966
	Dmit	SOP	33.7	35.45	350	1946
	Gharife	SCO	33.6333	35.5666	680	1965
	Katermaya	SOP	33.6166	35.45	380	1964
	Saida	**SCO**	**33.5666**	**35.3833**	**5**	**1962**
	Sfarai	SOP	33.55	35.3333	570	1962

	Maghdouche	SOP	33.5166	35.3833	230	1964
	Anqoun	SOP	33.5	35.4333	380	1965
	deir-el-zahrani	SOP	33.4333	35.45	450	1964
	Arab-salim	SOP	33.4333	35.5166	580	1964
	Jisr-el-Qadi	SOP	33.7166	35.5666	260	1948
Littoral South	Insariye	SOP	33.4166	35.2666	160	1964
	Douair	SCO	33.3833	35.4166	380	1962
	Jarmaq	SOP	33.3833	35.5333	400	1964
	Nabatiye	SCO	33.3833	35.5	410	1964
	El-Qasmiye (R)	**SCO**	**33.35**	**35.25**	**30**	**1951**
	tyr	**SCO**	**33.2666**	**35.2**	**5**	**1955**
	Jouaya	SCO	33.2333	35.35	300	1964
	Qana	SOP	33.2	35.3	300	1964
	lebaa	SCO	33.55	35.45	360	1969
	Aitaroun (R)	SOP	33.1166	35.4666	680	1939
	Ain-Ebel (R)	SCO	33.1166	35.4	765	1960
	Alma-Chaab (R)	SCO	33.1	34.1833	385	1960
Mountain North	Michmich	SOP	34.4833	36.1666	1080	1964
	Syr-ed-Denniye (R)	**SCO**	**34.3833**	**36.0333**	**915**	**1940**
	Bouhairet-Toula	SOP	34.3166	35.9666	1135	1966
	Kafar-Sghab	SOP	342833	35.9666	1310	1964
	Bcharre-ville	SCO	34.25	36	1460	1938
	Bcharre-Usine (R)	SOP	34.25	35.0166	1400	1966
	Les Cedres (R)	**SCP**	**34.25**	**35.05**	**1925**	**1937**
	Hasroun	SCP	34.2333	35.9833	1375	1963
Mountain Central	Maifouq	SCO	34.1833	35.783	875	1966
	Laqlouq	SCO	34.1333	35.85	1700	1940
	Tourzaya (R)	SOP	34.1166	35.7666	880	1940
	Qartaba	SCO	34.1	35.85	1140	1939
	Ghebale	SOP	34.0666	35.7166	970	1944
	Faraya-village	SCO	34.0166	35.8166	1320	1962
	Faraya-Mzar	SCO	34	35.85	1840	1965
	Rayfoun	SOP	33.9833	35.7	1050	1949
	Qlaiaat (R)	SOP	33.9666	35.6833	1050	1939
	Beskinta	SOP	33.95	35.8	1220	1966
	Bikfaya (R)	SCO	33.9166	35.6833	900	1949
	Jouar-el-haouz	SOP	33.8666	35.75	1290	1966
	Arsoun	SOP	33.8333	35.6833	750	1945
	Ras-el-Maten	SOP	33.85	35.6666	920	1944
	Falouga	SCO	33.8333	35.7333	1250	1966
	El-Qraye	SOP	33.8	35.6833	1010	1928
	Dahr-el-Baidar (R)	**SCP**	**33.8166**	**35.7666**	**1510**	**1952**
	Bhamdoun (R)	SCO	33.7833	35.6333	1090	1946
	Ain-Zhalta	SOP	33.75	35.7	1080	1940

	Majdel-Maouch	SOP	33.7166	35.6166	810	1946
	Fraidis	**SOP**	**33.7166**	**35.7**	**1250**	**1966**
	Kafar-Nabrakh	SCO	33.7166	35.6333	1020	1944
	Beit-ed-din (R)	SOP	33.7	35.5833	880	1940
	Jdeidet-ech-chouf	SOP	33.6666	35.6166	770	1944
	Moukhtara (R)	SOP	33.65	35.6	810	1940
	Jbaa-ech-chouf	SOP	33.6166	35.6166	1130	1964
	Jezzin (R)	**SCO**	**33.55**	**35.5833**	**945**	**1928**
	Beit-eddine-loqch	SCO	33.5666	35.55	835	1965
	Jbaa-halawi	SOP	33.4833	35.5166	800	1964
	Dahr-Darje	SCO	33.4666	35.6	1150	1964
	Jarjouaa	SOP	33.45	35.5166	850	1964
	Rihan	SOP	33.45	35.5666	1090	1965
Interior Assi	**Hermel (R)**	**SCO**	**34.4**	**36.3833**	**700**	**1932**
	El-qaa	**SCO**	**34.35**	**36.4666**	**650**	**1966**
	Fakche	SCO	34.25	36.4	1060	1970
	Nabha	SOP	34.1833	36.2166	1100	1966
	Arsal	SCO	34.1833	36.4166	1400	1961
	Yammoune (R)	SCO	34.1333	36.0333	1370	1939
	Chlifa-Flawi	SCO	34.0833	36.0666	1120	1944
	Younin	SOP	34.0833	36.2666	1200	1966
	Haouch-Dahab (R)	SCO	34.0333	36.1	1010	1960
	Baalbek (R)	SOP	34	36.2	1150	1931
Interior Litani	Kafar-dan	SCO	34.0166	36.05	1080	1966
	Haouch-snaid (R)	SCO	33.9333	36.0666	995	1958
	Qaa-el-rim (R)	SOP	33.8833	35.8833	1320	1940
	Sarain (R)	SOP	33.8833	36.0833	1000	1946
	Haouch-el-Ghanam	SOP	33.8666	36.0333	955	1951
	Tell-Amara	SCO	33.85	35.9833	905	1953
	Rayak (R)	**SCP**	**33.85**	**36**	**920**	**1928**
	Zahle (R)	**SOP**	**33.85**	**35.9166**	**990**	**1950**
	Ksara (R)	SCO	33.8333	35.9	920	1928
	Chtaura (R)	SOP	33.8166	35.8666	920	1953
	Terbol	SCO	33.8166	35.9833	890	1954
	Taanayel	SCO	33.8	35.8666	880	1958
	Anjar	SOP	33.7333	35.9333	925	1951
	Ammiq	SCO	33.7166	35.7833	870	1962
	Mansoura (R)	SOP	33.6833	35.8166	860	1939
	Soultan-Yaaqoub	SOP	33.65	35.8666	1400	1965
	Kherbe-Qanafer (R)	SCO	33.6333	35.7333	950	1955
	Joub-Janin	SOP	33.6333	35.7833	920	1948
	Qaraoun-village	SOP	33.5666	35.7166	950	1953
	Qaraoun-Barrage	**SCO**	**33.55**	**35.6833**		**1963**
	Machghara (R)	SOP	33.5333	35.65	1070	1939

	Markabe	SOP	33.4833	35.65	670	1964
Interior Hasbani	Yanta	SOP	33.6	35.9333	1500	1961
	Deir-el-Achayer	SOP	33.5666	36.0166	1280	1965
	Kafar-Qouq	**SOP**	**33.5333**	**35.9**	**1210**	**1961**
	Rachaya (R)	**SCO**	**33.5**	**35.85**	**1235**	**1933**
	Kfair-ez-Zait (R)	SOP	33.4333	35.75	940	1944
	Hasbaya (R)	SOP	33.4	35.6833	750	1944
	Marjayoun (R)	**SCP**	**33.35**	**35.5833**	**760**	**1944**

**SOP: Station d'observations Pluviométriques, SCP: Station Climatologique Principal, SCO: Station Climatologique Ordinaire, R: Reference*

Table 3.4 List of LNMS Climate Stations operating after the civil war (post-war network).

Micro Climatic Zone	Station name	Lat.	Long.	Altitude (m)	Daily Rainfall Record
Littoral north	El Qlaiat-Akkar	34.5859	36.0096	5	Mar 2003 - Dec 2011
	El Qoubayat	34.5656	36.2790	497	Jan 2001 - Dec 2011
	El Abde	34.5210	35.9879	37	Jan 2001 - Dec 2011
	Tripoli-IPC	34.4500	35.8833	5	Aug 1940 - Dec 2010
	Balamand	34.3661	35.7816	359	Jan 2001 - Jan 2012
	Kafar Chakhna	34.3549	35.8650	260	Apr 2003 - Mar 2012
Central Littoral	Kaslik Jounieh	33.9820	35.6195	41	Aug 2001 - Dec 2011
	El Qoussaibah	33.8699	35.6453	584	Jan 2001 - Dec 2011
	Beyrouth-Golf	33.8521	35.4919	14	Feb 1999 - May 2012
	Beirut International Airport	33.8167	35.4833	12	Jul 1932 - Dec 2009
	El Meshref	33.7137	35.4844	395	Jun 2003 - Dec 2016
	Deir El Kamar	33.6976	35.5646	794	Jan 2001 - Dec 2015
	Saida	33.5824	35.3903	14	Jan 2001 - Jul 2014
	Lebaa	33.5423	35.4529	331	Jan 2001 - May 2015
	Zahrani	33.5069	35.3408	10	Jan 2001 - Feb 2012
Littoral south	El Qasmiye	33.3284	35.2589	9	Jan 2001 - Feb 2012
	Sour	33.2628	35.2155	4	Jan 2001 - Sep 2011
	Kafar Dounine	33.2327	35.3957	560	Sep 2004 - Feb 2012
Mountain north	Al Arz-Les Cedres	34.2467	36.0509	1891	Jan 1982 - Apr 2011
	Syr-Ed-Denniye	34.3844	36.0292	926	Feb 2001 - Aug 2012
Mountain central	Tannourine	34.2078	35.9316	1838	Jan 2001 - Dec 2011
	Qartaba	34.0956	35.8486	1222	Jan 2001 - Dec 2011
	Faqra	33.9874	35.8117	1655	Jan 2001 - Dec 2011
	Dahr El Baidar	33.8094	35.7679	1516	Jan 2001 - Dec 2011
	Bayssour	33.7633	35.5567	940	Jan 2001 - Dec 2016
	Barouk Fraidis	33.7053	35.6785	1114	May 2000 - Jan 2009
	Jezzin	33.5440	35.5711	1070	Aug 2001 - Apr 2016
Interior Assi	El Hermel	34.4015	36.4067	605	Jan 2011 - Dec 2011
	El Qaa	34.3996	36.5080	513	Jan 2004 - Dec 2009
	Deir El Ahmar	34.1158	36.1318	943	Jan 2001 - Dec 2011
Interior Litani	Douris	33.9939	36.1569	1009	May 2003 - May 2006
	Rayak-Amara	33.8602	35.9882	852	Feb 1932 - Feb 2010
	Houch El Oumara-Zahle	33.8354	35.9042	926	Jul 1998 - Dec 2011
	El Qaraoun	33.5475	35.6821	843	Mar 2001 - Mar 2012
Interior Hasbani	Kafar qouq/Rachaya	33.5367	35.8914	1205	-
	Marjeyoun	33.3553	35.5823	827	Aug 2009 - Mar 2012

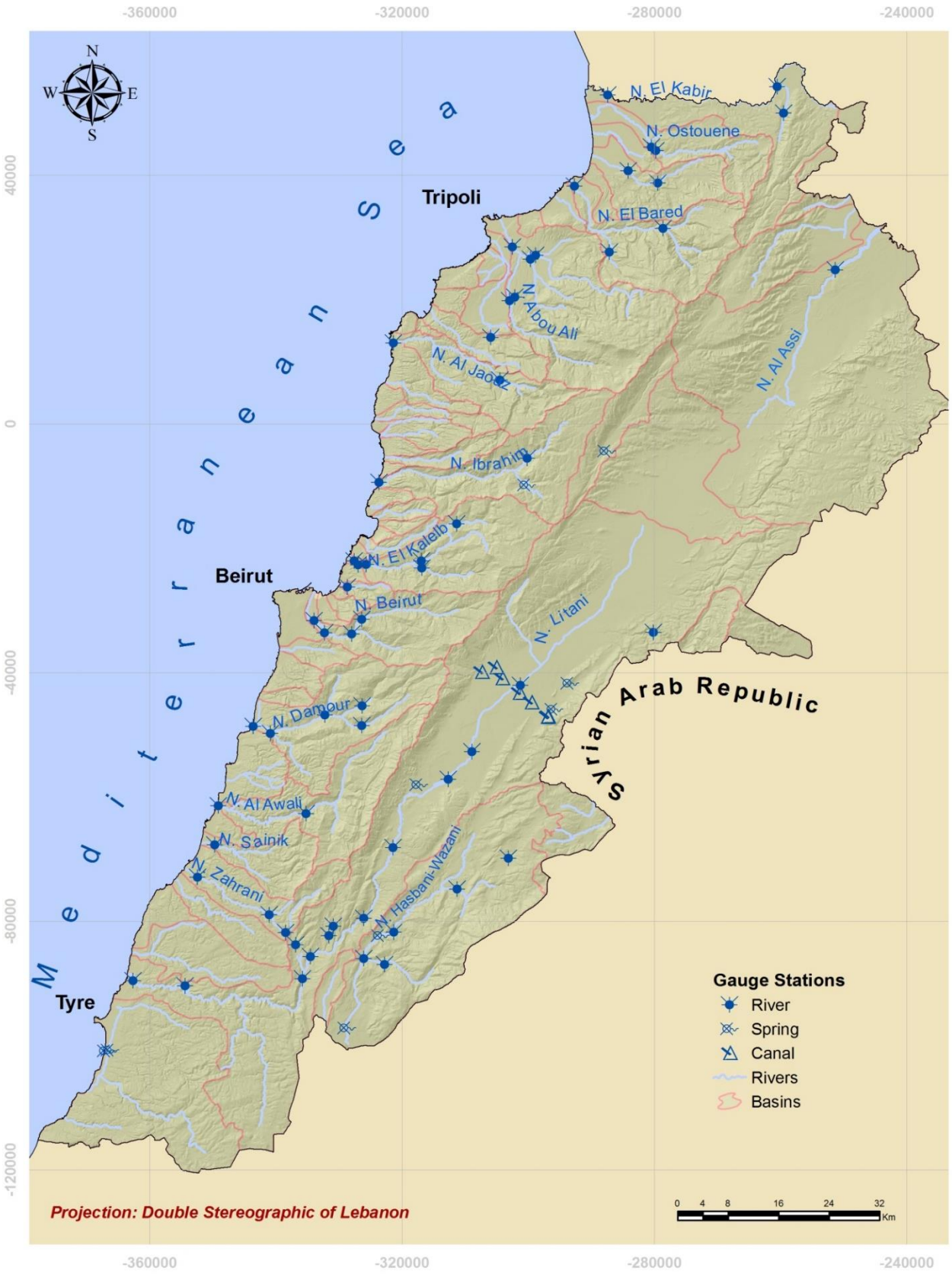

Figure 3.11 Gauging stations network currently operated by the LRA.

Data provided from permanent gauging stations are limited to hourly water levels, average daily flow values, and monthly runoff values. The most intensive period of measurement was between 1968 and 1972 (before 1964 and after 1972, less than half of the network was operating), and the period extending from 1998 to date. Hourly water level and daily flow data up till 2012 are available at the RSC and were previously retrieved from the LRA authorities. The authority of the LRA was officially contacted to obtain the missing gauge measurements up till 2016 for two gauge stations (Awali at Saida 475 and Marj Bisri 473) located on the Awali river which was selected for detailed analysis and modeling. But the LRA stated that no more daily flow measurements are being issued at these two stations and hence the obtained data was in the form of monthly flow measurements only.

Similarly, available discharge data was examined to look for outliers, gaps and shift in the records. Among the available gauge stations 21 stations (preferably at sea mouth location) on 17 major rivers in different regions of the country were selected for analysis. Details on the selected basins, gauge stations and the available records are presented in Table 3.5. The observed annual discharge maxima were extracted for each station and fitted to a generalized extreme value function. The discharges corresponding to different return periods (10, 50, and 100 years) were then evaluated based on the known Gumbel method (Gumbel, 1961). Our main interest was to analyze the discharge values at the outlet of each selected basin (outlets are mainly at sea mouth except for the middle Litani, Assi, and Hasbani rivers). For some basins (Ostouene, El Jouz, El Asfour, Damour, Awali, Zahrani, and Saitaniq) discharge records were not available at the outlet or were not sufficient to apply the Gumbel methods, in this case the Gumbel method was performed on an upstream station of better records and then the discharge at the outlet was estimated through a rapid hydrological modeling (HEC-HMS model) performed during a previous study by the CNRS and funded by the UNDP to develop flood hazard maps for Lebanon (Abdallah et al., 2013). The results of this analysis are then presented in chapter 5 to evaluate the discharge probability of occurrence for each river and then were crossed checked with the catchments' characteristics and the number of historical flood events in each basin extracted from previous reports and newspapers.

Table 3.5 Selected river gauge stations for analysis along with their characteristics and available records.

Region	Station number	Basin	River	Station name	Elv (asl)	Lat.	Long.	Available daily discharge and water level
North	**104**	Kebir	El Kebir	Sea Mouth	0	34.63083	36.02694	2000-2011
	106	Ostouene	Ostouene	Halba Bridge	89	34.56389	36.09333	2002-2012
	121	Ostouene	Ostouene	Sea Mouth	10	34.60238	35.98997	2002-2012
	108	Arka	Arka	Hakour	77	34.52972	36.04444	1967-1974 and 2002-2012
	111	Bared	Bared	Sea Mouth	29	34.30333	35.96333	1967-1974 and 2000-2012
	117	Abou Ali	Abou Ali	Abou Samra	28/64	34.41875	35.85627	1967-1974 and 2000-2012
	120	El jouz	El Jouz	Sea Mouth	9	34.10083	35.66139	2000-2012
	118	El Asfour	El Asfour	Bziza Bridge	320	34.28027	35.81861	2008-2010
Mount Lebanon	**223**	Ibrahim	Ibrahim	Sea Mouth	6	34.06278	35.64528	1967-1974 and 2000-2012
	228	Kelb	El Kelb	Sea Mouth	12	33.95056	35.60611	1967-1974 and 2000-2012
	234	Beirut	Beirut	Jiser El Bacha	22	33.86194	35.54111	1967-1974 and 1990-2012
	238	Damour	Damour	El Qadi Valley	254	33.72694	35.56500	1967-1974, 1992-1996 & 2000-2012
	240	Damour	Damour	Sea mouth	9	33.70528	35.44611	1992-2012
South	**473**	Awali	Awali	Marj Bisri or Bisri yard	398	33.58056	35.39500	2001-2012
	475	Awali	Awali	Saida	7	33.58778	35.39333	1998-2012
	479	Zahrani	Zahrani	Deir El Zahrani	301	33.43750	35.47028	2008-2009
	480	Zahrani	Zahrani	Sea Mouth	3	33.48167	35.35333	2002-2011
	476	Saitaniq	Saitaniq	el Lemon Valley	202	33.52417	35.47361	2008-2010
Bekaa	**345**	Assi/Oronte	Assi/Oronte	Hermel	590	34.39167	36.41556	1967-1974 and 1991-2012
	363	Litani	Joub Janine	Joub Janine Bridge	860	33.63917	35.78000	1998-2012
South	**499**	Hasbani	Hasbani	After Wazzani Spring	281	33.27361	35.61917	2002-2012

3.4 **Conclusion**

In this chapter we presented the major geographical and hydrological characteristics of Lebanon, along with the data sets available. All presented information and data form the base for the upcoming analysis in chapters 5, 8 and 9. The DEM is used to extract the drainage patterns, delineate sub-basins and extract their geometrical and morphological characteristics. The land use, geology and soil maps are used to extract the major basin characteristics. The rainfall and discharge data are used to extract the hydrological characteristics and to evaluate their probability of occurrence in the selected river basins. These values are then then cross checked with the number of flood events extracted from previous reports and newspapers on a regional scale. All information is gathered and standardized in a geographic information system data base (Arc-GIS). The latter is used to perform all the spatial analysis and generate the required maps.

4 THE AWALI CATCHMENT: STUDY SITE DESCRIPTION AND DATA ANALYSIS

4.1 **Introduction**

In this chapter we present a detailed description of the study site chosen to perform the detailed analysis based on hydrological-hydraulic modeling. The Awali River Basin is one of the coastal Eastern Mediterranean catchments, located in Southern Lebanon. The river is one of the major Lebanese perennial rivers witnessing floods every other year. This study site was selected because we had the opportunity to investigate the early January 2013 extreme flood event, which is considered one of the largest events in the last three decades. Detailed field investigations one month after the flood event allowed to take measurements of the high-water marks and peak flood discharge on several locations along the river.

The chapter begins with a description of the basic geographical characteristics of the study site, then details the available hydrological datasets, and presents the results of the field investigations. The chapter ends with summarizing the major sparse datasets available to perform our analysis.

4.2 **Geographical Dataset**

The Awali River basin is one of the coastal Eastern Mediterranean catchments, located in Southern Lebanon covering an area of 301 km^2. The basin is drained by a dendritic drainage system fed by surface runoff as well as by resurgences of some major springs including Barouk, and Azibeh. The river, anciently called Asclepius River, is 48 km long originating from the Barouk mountain at an altitude reaching 1,492 m, and eventually flowing through the western face of Mount Lebanon and into the Mediterranean Sea. Two main tributaries supplement Awali River called the Barouk and the Aaray Rivers. Both tributaries converge to form Bisri river; In its lower section, the river is known as Awali River where it follows a sinuous course meandering with a sandy bed, cutting through old floodplain and deposits (Figure 4.1).

For the purpose of hydrological modelling, the whole basin was divided into four main sub-catchments and five minor sub-catchments (a total of 9 sub-catchments). The four major sub-catchments are: the Barouk River sub-catchment (B_1, 141 km^2), Aaray River sub-catchment (B_2, 51 km^2), Abu Liess valley sub-catchment (B_3, 31 km^2), and Bou Hachem valley sub-catchment (B_4, 11 km^2). The four sub-catchments constitute an area about 234 km^2 that contribute to the major amount of runoff over the catchment. Sub-catchments B_5 and B_8 were delineated at the location of the gauge stations Saida (475) and Marj Bisri (473) respectively, B_9 was delineated at the river's outlet on the Mediterranean Sea, whereas B_6 and B_7 were delineated at the locations of two hydropower plants established on the river.

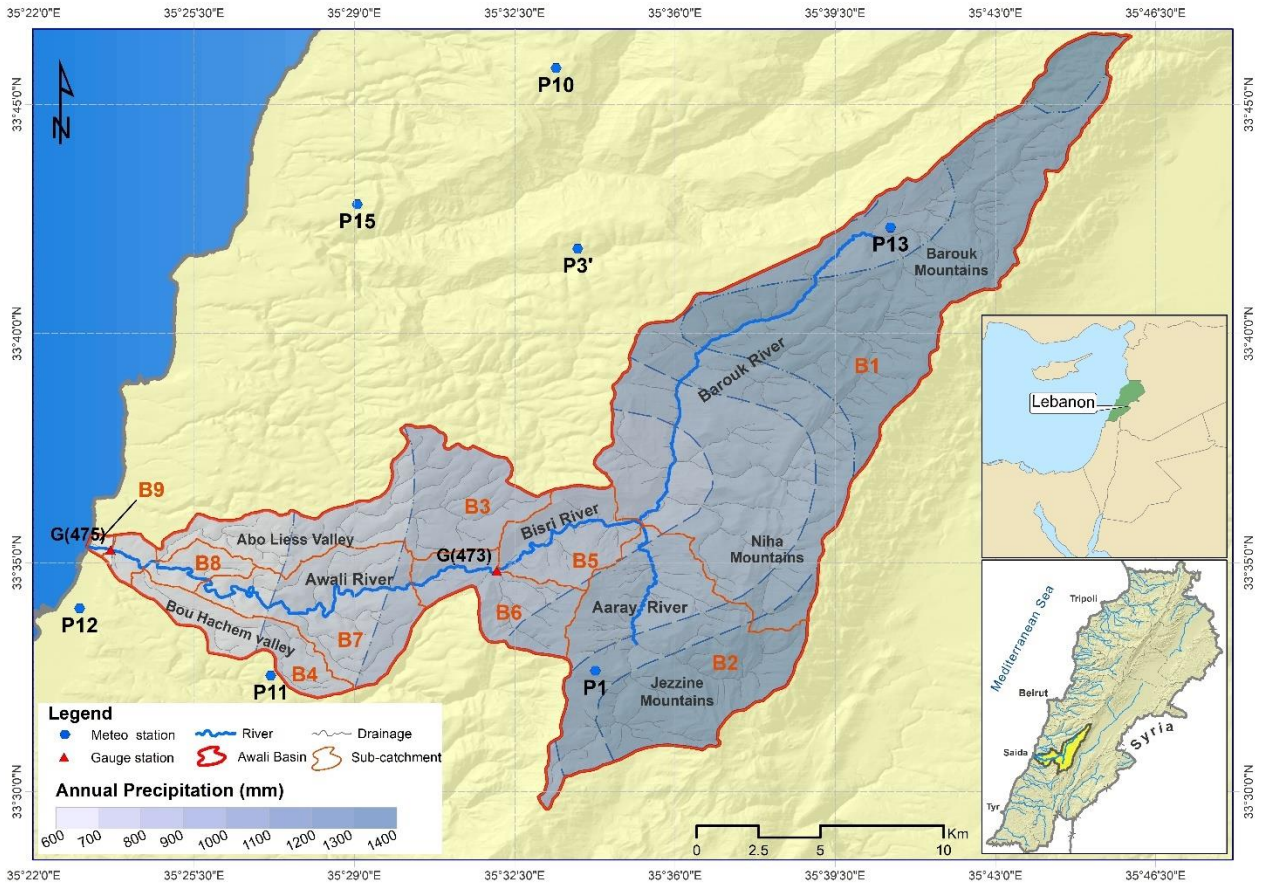

Figure 4.1 The Awali River Catchment; site location, available hydrometeorological stations, and the delineated sub-catchments for the hydrological model.

*4.2.1 **Topography***

The catchment has a rapidly varied topography ranging from elevated areas of Mount Lebanon (1950 m asl), running parallel to the coast and characterized by a continuous snow cover during winter, to flat plains along the low coastal area primarily utilized for agricultural purposes. It is characterized by steep slopes, which converge towards a valley where the Awali River flows (Figure 4.2).

The topography of the entire basin was available from a 10-m digital elevation model (DEM) developed by the Lebanese National Center for Remote Sensing (CNRS-RS). The latter was used to delineate the boundaries of the Awali basin, extract the corresponding stream network, delineate the sub-catchments, and estimate the basin's hydrological characteristics for the hydrological modelling part. The average basin slope in the B1, B2, B3 and B4 sub-catchments is 33.6, 33.3, 29.9, 29.3 % respectively.

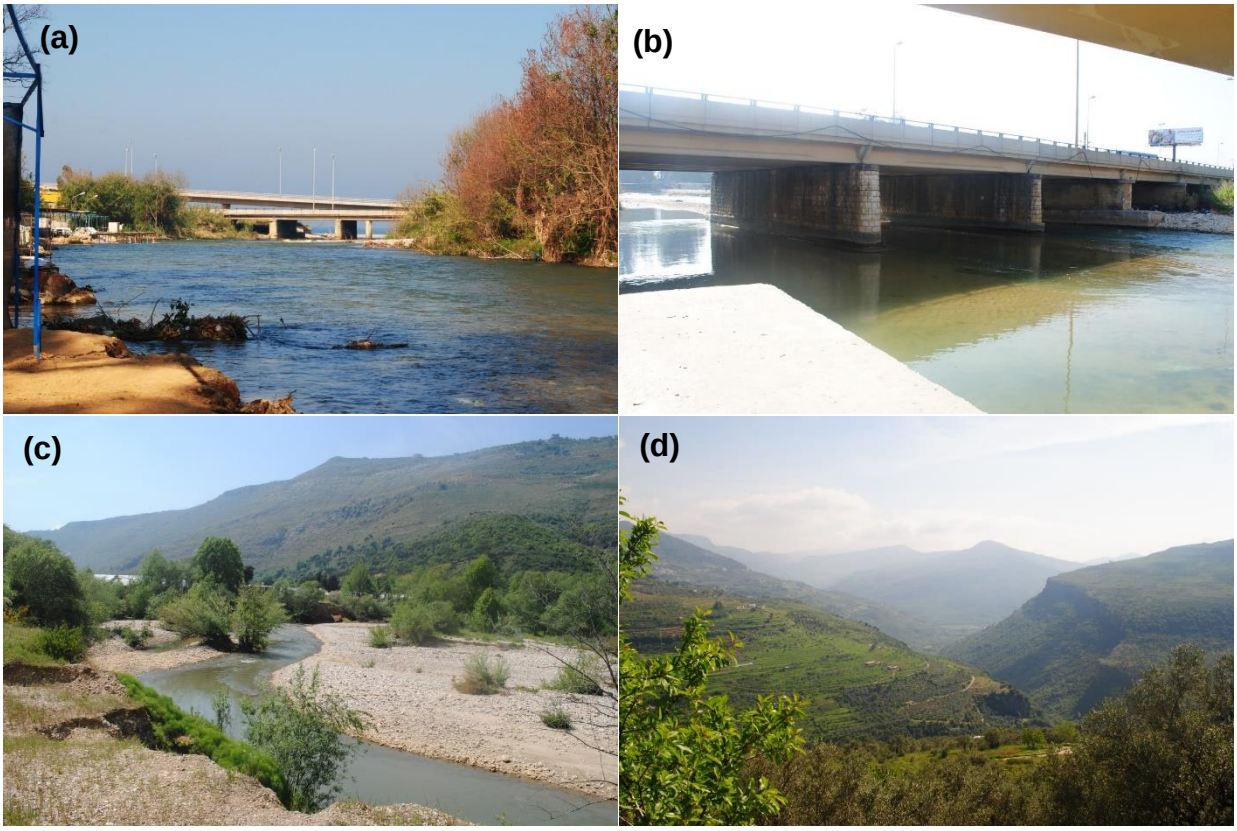

Figure 4.2 Pictures for the study site showing the major morphological units. (a) & (b) Sea mouth, (c) middle zone, (d) mountainous area.

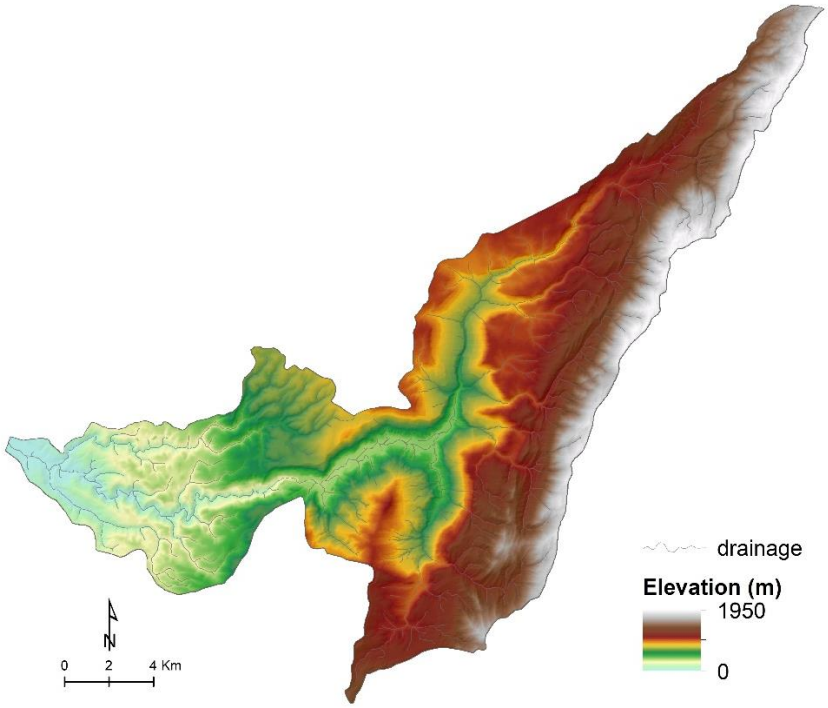

Figure 4.3 Elevation map of the Awali Catchment based on the available 10m DEM.

4.2.2 ***Geology***

The lithology of the catchment covers a sequence from the middle Jurassic rocks to the recent quaternary deposits. The surface is mainly composed of the Cenomanian Sannine limestone formation (C4) which consists of well stratified, fractured, interbedded limestones, dolomites and marls (Dubertret, 1945). The watershed underlies several aquifer formations including the High Central Lebanon Cretaceous, the Kesrouan Jurassic and the Batroun-Jounieh Cretaceous. These aquifers are separated by unproductive formations (Figure 4.6).

4.2.3 ***Land use***

The catchment has a varied land use; wooded lands and grass lands are the dominant, covering 46.5 and 26.8% of the total area respectively. The forests provide firewood and cover non-cultivated hills and mountains. Agricultural areas and artificial/urban areas cover 18.2 and 7.2% respectively, whereas water bodies and greenhouses do not cover more than 1% of the basin each (Figure 4.6). The latest Land cover/use information for the study site was obtained from the land cover use map of Lebanon developed by the CNRS in 2010 and updated 2013 based on CORINE classification adapted for Lebanon at level 1 of discrepancy (LNCSR-LMoA, 2010).

To evaluate the landuse development in the area and assess whether there was a major land use change, landuse patterns were evaluated between 1998 and 2016 based on different satellite images acquired for the area. Five land use maps were generated corresponding to the years 1998, 2005, 2008, 2013, and 2016. Details on the satellite images and their respective resolutions are presented in Table 4.1. Different artificial and natural areas were then analyzed for the selected consecutive years and their percentages of distribution were evaluated. For the artificial areas, results show that there is a little growth in urban areas of around 2% between 1998 and 2016. Results of the land use change evaluation are presented in Figure 4.4. No major growth was noticed in both activity and non-agricultural vegetated areas. Whereas, for the natural areas field crops increased by 5 % and permanent crops decreased by 3%, shrub lands and grass lands decreased by 10% and 15 %, clear wooded lands increased by 5% and dense wooded lands decreased by around 7%. However, taking into consideration the little variation in the urban areas and wooded lands we can say that the Awali basin is not under serious urbanization, or desertification stress for the moment.

Table 4.1 Details on the satellite images used to evaluate the land use change in the Awali River basin.

Satellite	Resolution	Date of acquisition
RAPIDEYE	10 m	2016
GEOEYE	0.46 m	2013
QUICKBIRD	2.4 m	2008
IKONOS	4 m	2005
IRS-LANDSAT	30 m	1998

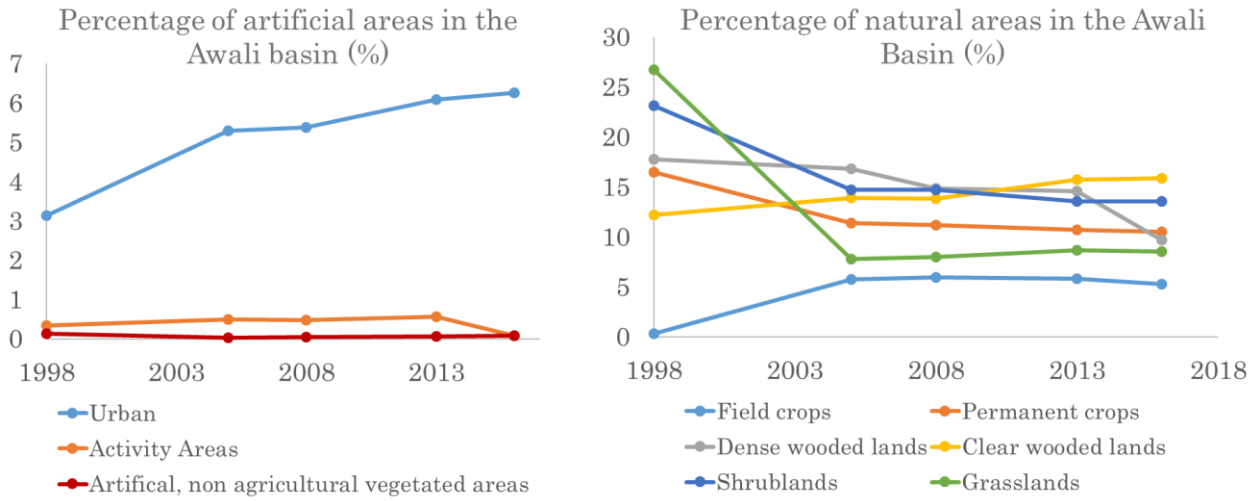

Figure 4.4 Graphs showing the results of the landuse change evaluation in the Awali River basin between 1998 and 2016 based on different satellite images of the area.

4.2.4 ***Soil***

Resulting from the transformation of rocks under the combined influence of weather, vegetation cover, and slope of the terrain, soils are typically Mediterranean. Most soils are calcareous, apart from sandy gravelly soils formed on the cretaceous strata. Leptosols is the dominant soil class in the catchment covering almost 64% of the total area. The most expanded soil types are Terra Rossa and Rendzina. Like all Lebanon's soils, the basin's soils are young, fragile and subject to erosion, especially in the mountains and hills (Der Sarkissian, 2015) (Figure 4.6).

Soil information was available from the recent soil map of Lebanon classified per the FAO-UNESCO legend, World Reference Base for Soil Resources and the American Soil Taxonomy (Darwish et al., 2006).

4.2.5 ***Hydrological Soil Groups (HSG)***

The HSG map was developed following the criteria described in chapter two. The dimensionless curve number parameter was then derived for each sub-catchment based on a developed classification that combines the land use/treatment classes with the hydrological soil groups (HSG). The effect of the surface conditions was evaluated by means of land use and treatment classes and the soil's parametric information was built based on soil profiles (Figure 4.6). Soils B are C are the dominant soil groups in the area accounting for 31% of the total area each. Soil group A accounts for 29% and soil group D accounts for 9% only (Figure 4.5).

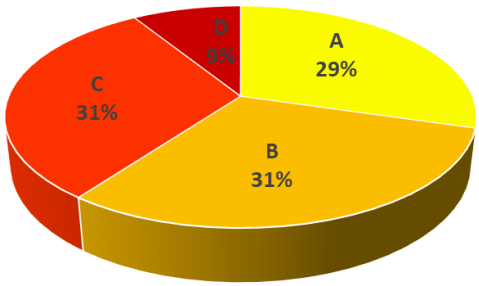

Figure 4.5 Percentages of occupation of different HSG's in the Awali Basin.

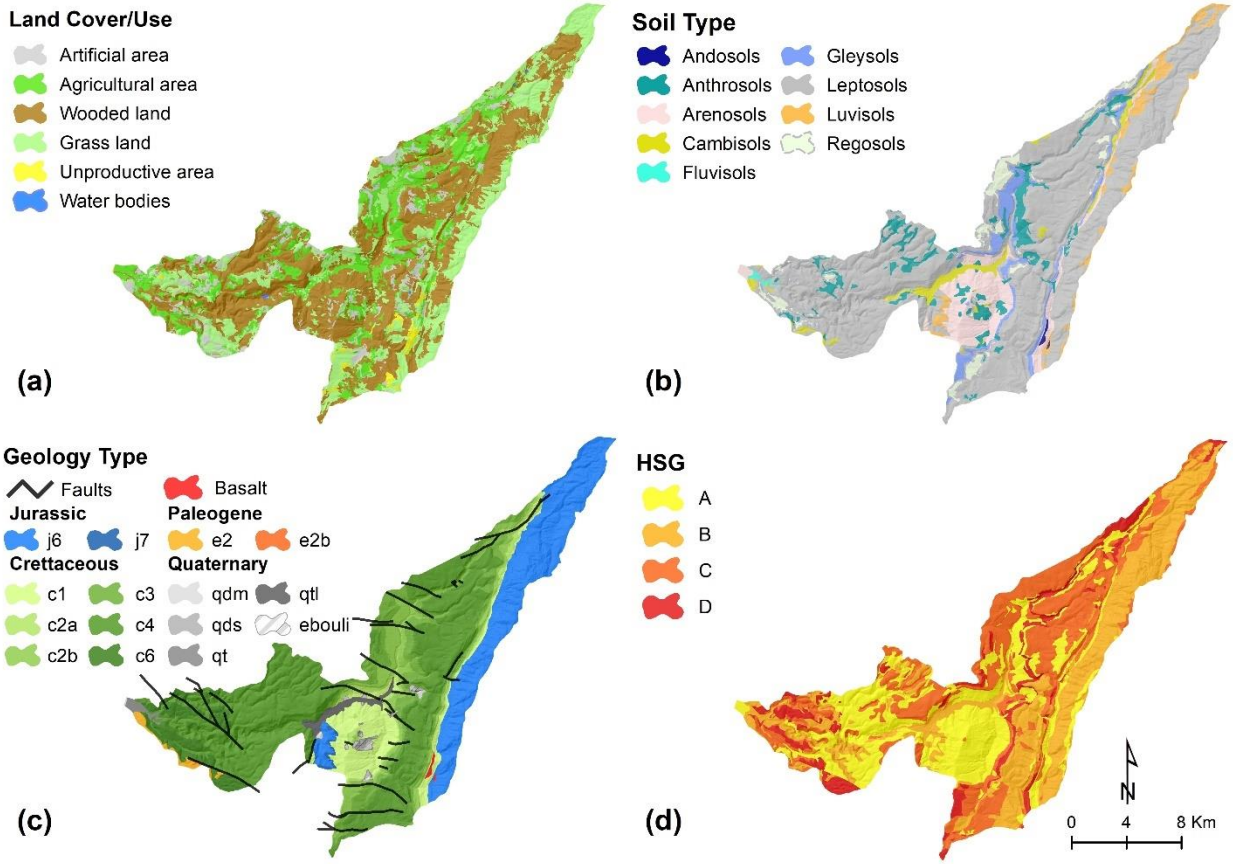

Figure 4.6 Study site cartographic data. (a) Land use map (LNCSR-LMoA, 2010), (b) Soil map (Darwish et al., 2006), (c) Geology map (Dubertret, 1945), (d) developed HSG map.

4.3 **Hydrological dataset**

4.3.1 ***Rainfall***

The catchment has a Mediterranean climate; it receives its majority of mean annual rainfall of 1067 mm during the wet fall-winter period extending from November to April, with little or no rain between June and August. The mean annual precipitation ranges between 600-700 mm along the coast and 1300-1400 mm over the mountains (Plassard, 1972).

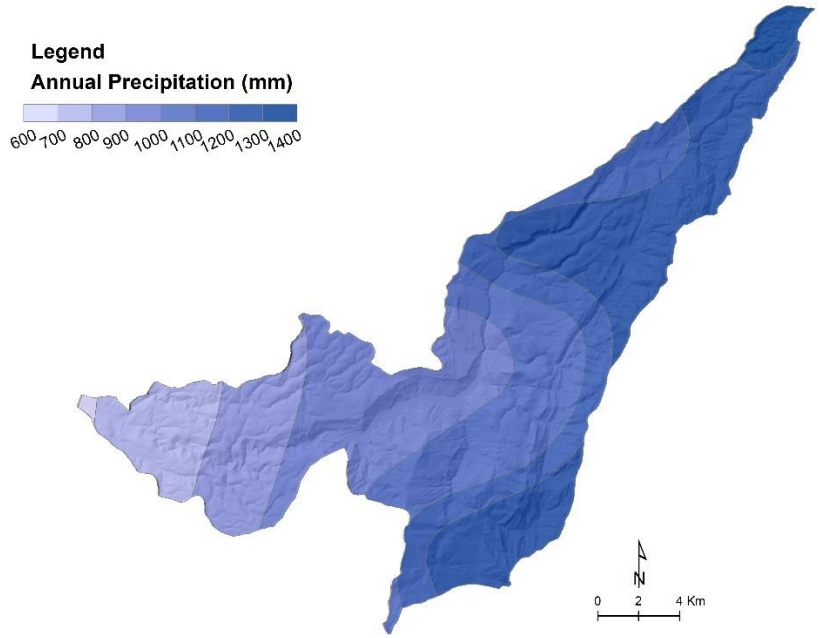

Figure 4.7 Rainfall isohyets maps for the Awali Catchment based on Plassard (1972).

Daily rainfall measurements were obtained from seven meteorological stations operated by the Lebanese National Meteorological Services (LNMS). These stations were recently established after the Lebanese civil war (1975-1990), during which most of the stations ceased their operation, and have however started recording since 1996. The number and distribution of rainfall stations of density around 130 km2 per rain gauge is considered satisfactory for the basin area following the WMO requirements of recommended minimum densities of stations. As previously mentioned in chapter 3, some hourly rainfall measurements can be obtained from Baysour meteorological station (P10), particularly, records of the early January flood event. For simplification these stations were given new ID's. Details on the selected rainfall stations are presented in Table 4.2 and their spatial distribution over the study site is presented in Figure 4.1.

Table 4.2 Meteorological stations covering the study site.

Station	Operator	Station Name	Altitude [m]	Data Series	Mean Annual Rainfall [mm]
P1	LNMS	Jezzine	1070	2001-2016	1102
P3’	LNMS	Deir el Kamar	794	2005-2015	1052
P12	LNMS	Saida	14	2001-2014	692
P10	LNMS	Bayssour	940	2000-2016	1201
P11	LNMS	Lebaa	331	2000-2015	870
P15	LNMS	el Meshref	395	2002-2016	890
P13	LNMS	Barouk Fraidis	1114	2000-2011	Not available

*4.3.2 **Discharge***

Two permanent limnigraphic gauge stations (Figure 4.8), operated by the Lebanese Litani River Authority (LRA), take continuous hourly (or 15 min) measurements of surface water levels. The Marj Bisri gauge station G(473) monitors the flow upstream along the Bisri River and the Saida gauge G(475) monitors the flow at 800 m upstream of the catchment’s outlet on the Mediterranean Sea (see Figure 4.1). The average annual yield for the basin, at G(475), is approximately 347 Mm^3, out of which 85% occurring during the winter (Figure 4.9). Stream flow is normally highest in February and lowest in September with an average daily flow of 11 m^3/s. Flow data are also obtained through periodical field point flow measurements that are used to obtain a rough estimate of the monthly river flow volumes and calibrate the river rating curves. Due to the limited resources of the LRA, the shortage in the frequency of the direct field measurement leads to mis-calibration of the rating curves. Details on gauge stations and the available records are presented in Table 4.3.

Table 4.3 Characteristics of the permanent gauge stations along the Awali River.

Gauge Station	Name	Altitude [m]	Gauged area [km^2]	Data type	Time step	Period of Record	Average annual flow [m^3/s]	Average annual yield [$M.m^3$]
G (475)	Awali at Saida	6	300	water level & discharge	hour	98-99 till 08-09	11	347
				water level & discharge	15 min	09-10 till 11-12		
G (473)	Awali at Marj Bisri	398	222	water level & discharge	hour	01-02 till 08-09	4	131
				water level & discharge	15 min	09-10 till 11-12		

Figure 4.8 Permanent limnigraphic gauge station used to measure the hourly water level.

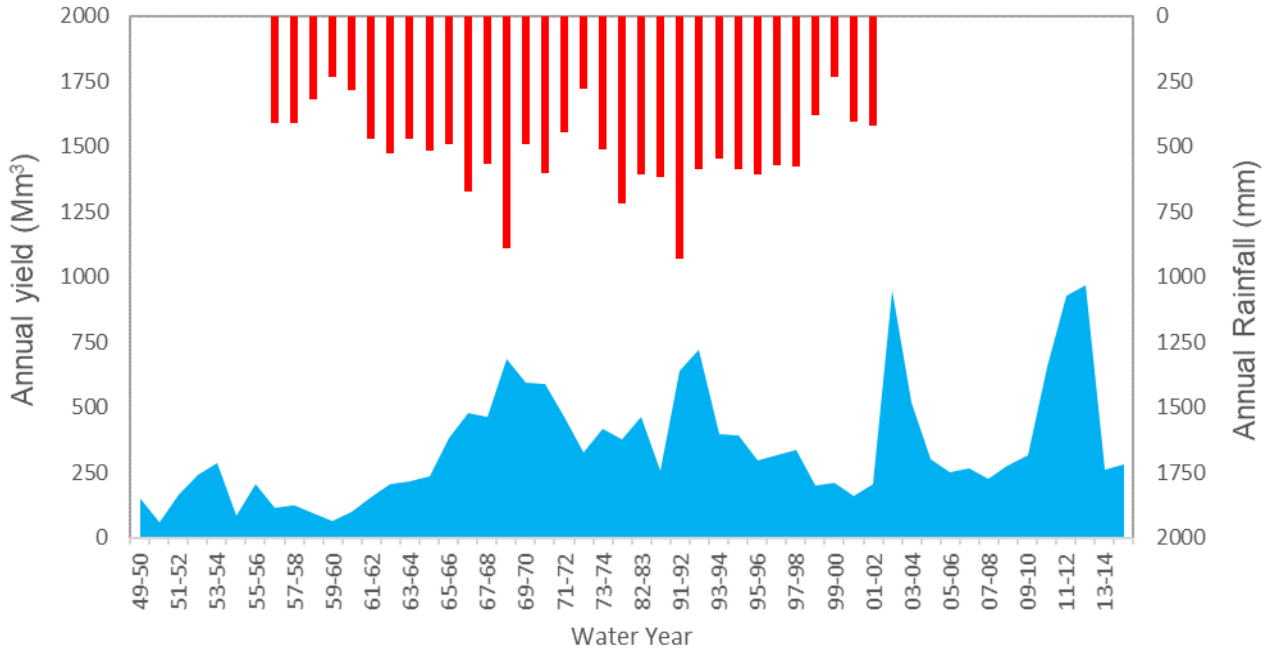

Figure 4.9 Variation of the average annual yield of the basin at Saida gauge G(475).

4.3.3 ***Past storm events***

Twelve past-storm events, occurring before the Jan 2013 flood event, of simultaneous daily rainfall measurements and hourly water levels are used for model calibration. Hourly (or 15 min) water level records were transferred into flow hydrographs for the selected storm events based on the established rating curves. Among the selected events three have information on both gauges in Saida and Marj Bisri, and the rest nine events have only information on downstream Saida gauge. These events were derived from the period extending from 2000 till 2012 in which we consider no major changes on the characteristic of the river have occurred and the hydrometeorological network is the same one operating at the time of the flood. These events vary in intensity of daily rainfall varying between 24 and 199 mm, peak flow varying between 15 and 247 m^3/s, and duration varying between 1 and 7 days. The selected events are the only clearly gauged and consistent for simulation events (Table 4.4 and Figure 4.10).

4.4 **The January 2013 flood dataset**

Early January 2013 a harsh winter storm lashed the eastern Mediterranean coast with snow, high winds, and heavy rains. Flooding caused by torrential rains was recorded in several parts of the region including Turkey, Syria, Lebanon and Jordan (NOAA, 2013). In Lebanon, the storm lasted for 6 days (5th-10th January) and 277 mm total rainfall of 50 years return period was recorded, leaving behind one of the largest floods in the last 25 years. Hourly rainfall records for the Jan2013 storm are available from Baysour meteorological station (P_{10}).

The event of 07 January 2013 is one of the largest floods occurring in the last 25 years. The post-event measurements, pictures, videos, and local witnesses makes this event interesting to assess the robustness of the proposed framework in reproducing flood events of no hydrometric measurements. The presence of both hourly and daily rainfall measurements in addition to social media information on the duration of the storm event is also an added value.

Table 4.4 Summary of selected past storm events at the Awali watershed. Three highest rain depths and three highest flows at Saida G(475) are indicated by *.

Event number	Strom event	Duration	Average Rain depth	Gauge	Average flow	Peak flow	Time of peak flow	Observed Stage	Total Runoff volume
		[h]	[mm]		[m^3/s]	[m^3/s]		[m]	[mm]
1	19-24 Jan 2000	144	199*	475	82.0*	145.7	19 Jan 2000, 04:00; & 20 Jan 00, 14:00	2.27	117.6
2	15 Dec 2001	24	24	475	7.2	17.4	15 Dec 2001, 08:00	0.83	4.8
				473	2.9	15.3	15 Dec 2001, 01:00	0.36	5.5
3	19-20 Dec 2001	48	43	475	13.9	19.1	20 Dec 2001, 09:00	0.89	13.4
				473	6.4	54.1	20 Dec 2001, 01:00	0.56	15.6
4	6-11 Jan 2002	144	79	475	18.4	28.9	07 Jan 2002, 10:00	1.10	32.0
5	20-22 Jan 2002	72	66	475	29.0	68.0	22 Jan 2002, 24:00	2.21	35.1
6	18-21 Dec 2002	55	120	475	51*	163.0	20 Dec 2002, 17:00	2.84	51.6
7	3-7 Jan 2007	96	81	475	18.7	22.6	07 Jan 2007, 03:00	1.10	25.0
8	19-20 Jan 2007	24	59	475	17.7	27.3	21 Jan 2007, 10:00	1.21	13.7
9	1-7 Feb 2007	144	150*	475	35.0	85.9	06 Feb 2007, 15:00	2.06	65.5
10	24-26 Feb 2007	48	75	475	38.3	69.9	26 Feb 2007, 17:00	1.88	41.7
11	14-19 Feb 2012	120	120	475	84.8*	118.7	18 Feb 2012, 08:15	1.60	108.3
				473	22.6	246.5	17 Feb 2012, 22:30	1.27	66.0
12	28 Feb-3 Mar 2012	168	125*	473	17.8, 22.4	69.0	28 Feb 2012, 22:45 & 3 Mar 2012, 17:00	0.81, 0.76	57.2

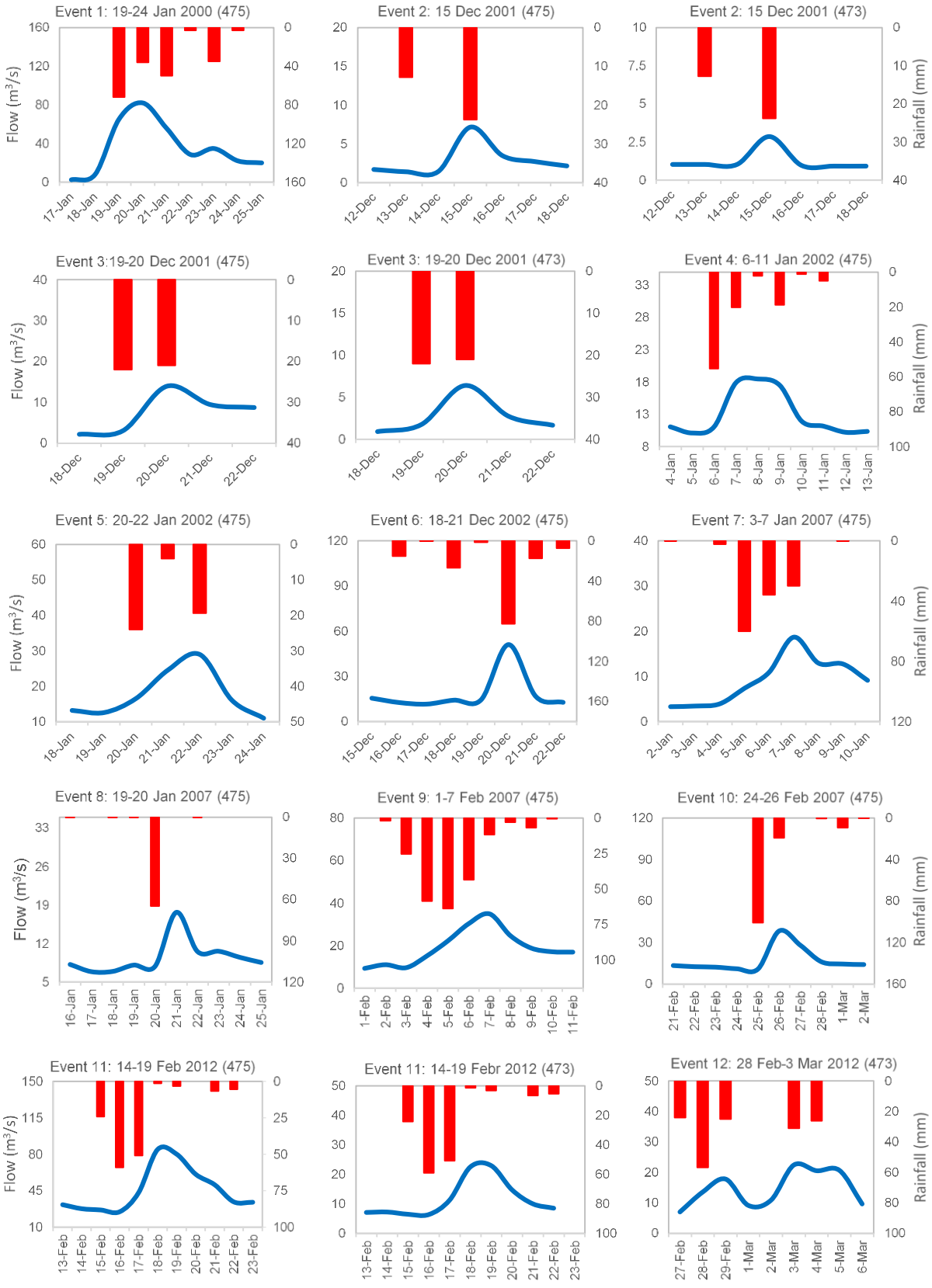

Figure 4.10 Observed flow hydrographs and hyetographs for the selected storm events.

4.4.1 ***The flood magnitude***

On 6th of January 2013 at around 13:00, the intensity of light precipitation that lasted for several hours on the previous day, started to increase reaching a maximum of 17.3 mm/hr at around 20:00. On the second day, 7th of January, at around 05:00 to 06:00 the Awali river level rose and flooded in several locations along the coastal plains and in the middle Marj Bisri plain. The downstream river gauge G(475) was subjected to failure by flood waters. The flood left behind great damages to agricultural lands and green houses. Several cars and roadside walls were damaged causing massive traffic jams (Figure 4.11). Schools were obliged to close for three days (8th-10th January), (Abdallah et al., 2013).

4.4.2 ***Post-event measurements***

Field investigations of the Jan2013 flood marks were performed two months after the flood event, after which newspaper information, local witnesses' declarations and social media reports were analyzed at the time of the flood. The post-event field surveys were carried out to collect ground control and survey river cross sections, measure water level traces that were still identified and estimate the peak discharge values, identify hotspots and measure extent of floodplains, interview locals who have witnessed the flood event and could support the authors not only by information but in many instances by photos and recorded videos. Collected photos and videos enabled to highlight some flood prone areas that were further investigated through field surveys to measure water levels (Figure 4.12).

A total of 57 post-event points scattered in space were surveyed out of which 27 are measurements of high water marks. These measurements were used to evaluate a hydraulic model developed in chapter 9. Figure 4.13 shows the hydraulic model study site along with the locations of the post-event measurements.

4.4.3 ***UAV Drone survey***

Several drone photography surveys covering the whole floodplain (Figure 4.14) were performed to capture around 5000 raw images acquired in strips with adjacent photographs having an overlap of 80% in the flight direction and 70% between parallel flight tracks. These images were then processed using the Pix4DMapper software to generate a point cloud for the area which can be converted to a high- resolution DEM based on the criteria described by the American Society of Photogrammetry and Remote Sensing (ASPRS, 2004). The criteria involved identifying and filtering all above ground features in the DEM to remove false blockages to flow such as bridges. Critical features influencing the flow of water such as walls and building were retained. The established DEM was used to extract the detailed river and floodplain geometry. A screenshot for the developed point cloud of the low main part of the river and its outlet on the Mediterranean Sea is shown in Figure 4.15.

Figure 4.11 Some pictures for the early January 2013 flood event in Lebanon.

Figure 4.12 Post-event field investigations for the Jan2013 flood event. (a) Saida gauge G(475) damaged by flood water, (b) Orange trees swept away by flood water in agricultural fields of the low coastal area, (c) high water level marks traced during the post-event field campaigns, (d) Floodplain evolved in Marj Bisri upstream the river stage gauge G(473).

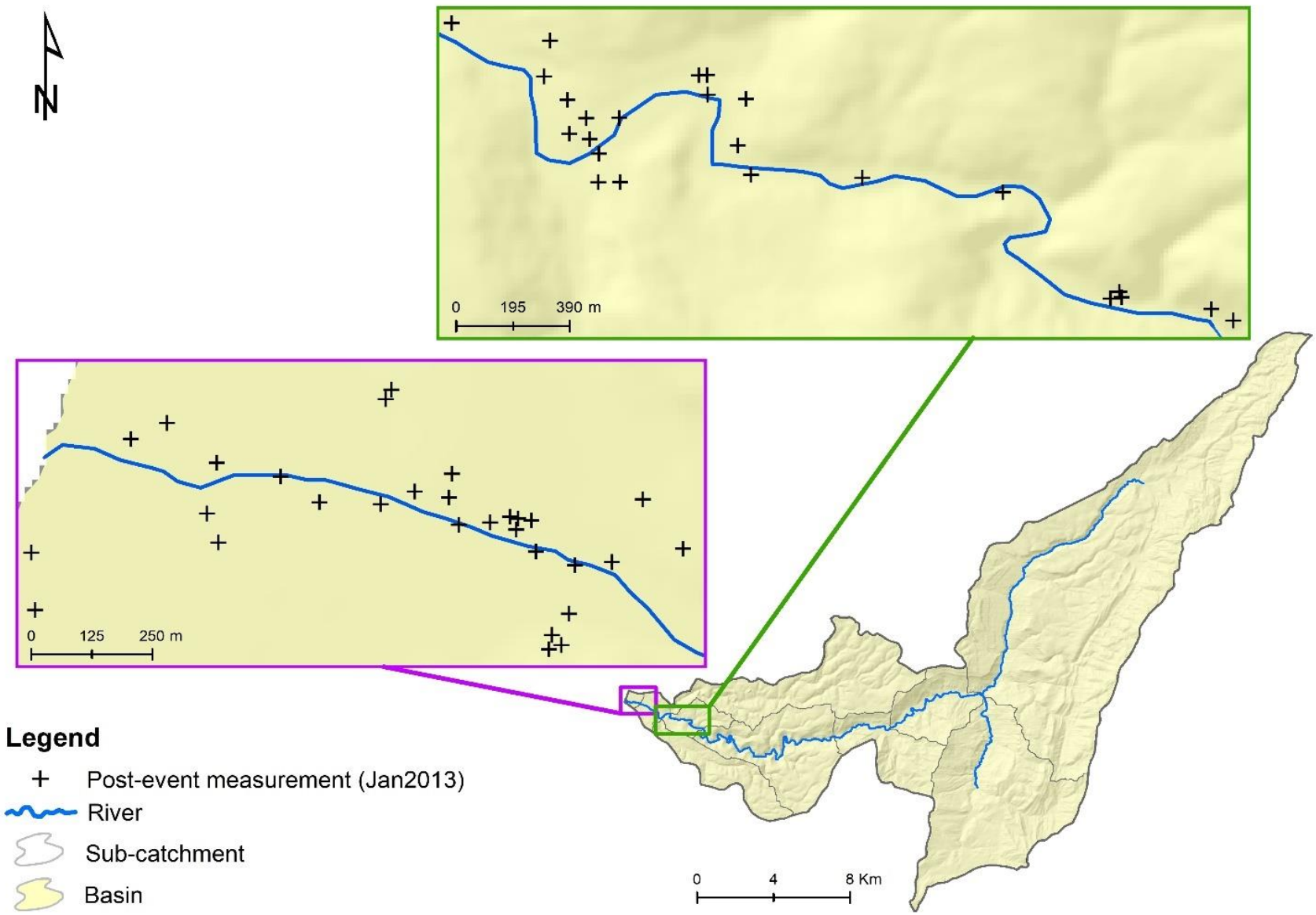

Figure 4.13 Hydraulic model study site and post-event measurement locations.

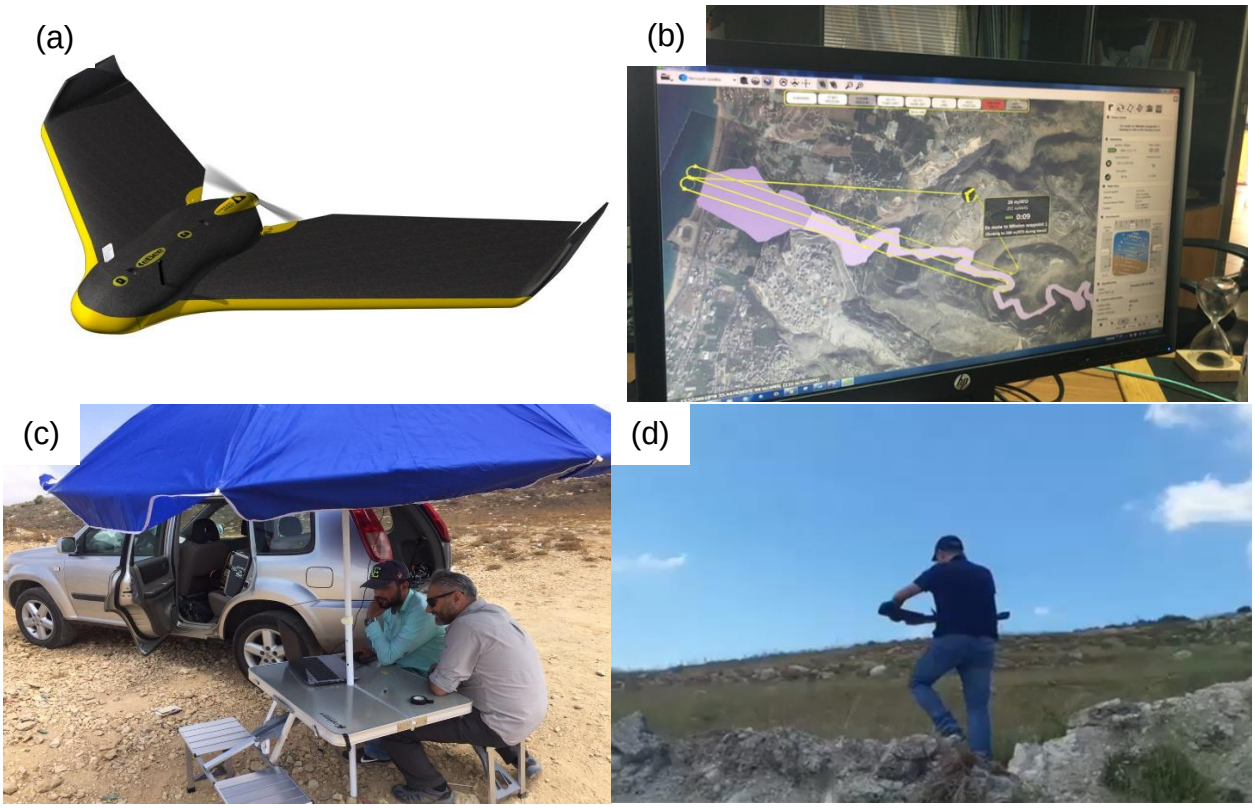

Figure 4.14 Pictures for the UAV drone survey established to develop high resolution DEM for the river channel; (a) the UAV EBEE drone, (b) virtual flight simulations in office, (c) & (d) field drone surveys.

Figure 4.15 Screenshot for the developed point cloud for the Awali basin study site based on several UAV drone surveys, showing the low main part of the river and its outlet on the Mediterranean Sea.

4.5 **The sparse dataset**

In conclusion, our data-sparse area is characterized by data summarized in Table 4.5 in the following form:

1. Past recorded storm events of daily rainfall measurements from ground rainfall gauges incapable of reflecting the rainfall intensity and spatial variability during the storm event, hourly (or 15 min) water level measurements by two traditional river stage gauges mostly non-functional during flood events, and hourly (or 15 min) flow hydrographs extracted based on poorly defined rating curves.

2. Descriptive social media information on the past storm events related to the duration and spatial variability of the rainfall during the storm.

3. A recent extreme flood event but destructed river stage gauge with daily and hourly rainfall measurements in one nearby rainfall station and post-event measurements of peak flood discharge and maximum water level marks.

4. Descriptive information from newspapers, social media, and field investigations on the extreme flood event related to the inundated areas, time of flood peak, duration of the storm and its spatial variability.

Table 4.5 Summary of the observational data types available for the Awali river study site.

Event	Rainfall Data	Flow Data
n past storm events	- daily rainfall data - social media information on the duration of the rain event	- hourly and 15 min water level measurements - hourly and 15 min flow hydrograph extracted based on established rating curves
1 extreme event	- daily and hourly rainfall data	- post-event maximum water marks measurements and peak flood discharge estimation - social media information and local witnesses on the time of peak flow and flood inundation depth and area

4.6 **Conclusion**

In this chapter we have presented the available data for the Awali River Catchment, analyzed the major geographical and hydrological characteristics, described the outcome of the field investigations and the UAV drone surveys, and summarized all the sparse dataset available for later detailed analysis and modeling. All presented information and data form the base for the upcoming analysis in chapters 8 and 9. The DEM form the base for hydrological modeling of the whole catchment area, it is used to extract the drainage patterns, delineate sub-basins and extract their geometrical and morphological characteristics. The fine resolution DEM is used for hydraulic modeling of the downstream channel of the Awali river and for post-processing the results and delineating the inundation area. The land use, geology and soil maps are used to extract the Hydrological Soil Groups and estimate the hydrological modeling parameters. All information is gathered and standardized in a geographic information system data base (Arc-GIS). The latter is used to perform all the analysis, establish the model parametric files, and generate the required maps.

5 ANALYSIS OF HISTORICAL FLOOD EVENTS-LEBANON

5.1 **Introduction**

The Lebanese coastal zone is dissected by a large number of seasonal streams and about 15 perennial rives. Many of these streams and rivers are susceptible to flooding. Wadi Khaled plain and Akkar plain in the North, the coastal plain of Tyr, Qasmiyeh, Sidon, Damour, the littoral of Batroun, Chekka and Khaldeh, are particularly susceptible. The internal parts of the country susceptible to river floods include the Central Bekaa, Assi plain and the North- Eastern part of the Bekaa plain.

Floods normally occur during the wet season, generally after a strong storm or at the beginning of the spring with the melting of the snow. During floods, rivers burst their bank causing floods and damages to buildings and agricultural land. The direct reasons of floods are evidently the strong storms with heavy rains in addition to the topographic nature of the river channel. But many other anthropogenic factors, including urban expansion into floodplains, increase the chance of inundation, the intensity of the floods and the severity of damages.

The flood monitoring network in Lebanon is very traditional; It is limited to the river gauging stations (that measure the river water levels) on one or two locations along main rivers affiliated to the Litani River Authority (LRA), and the national network of weather gauging stations that record daily rainfall measurements and affiliated to the Directory of Civil Aviation of the Ministry of Transport and Public Affairs (LNMS). These are the only sources for data to monitor storm events and their relations to floods. One must also mention that dry channels generally exposed to flash floods do not have gauging stations and the volume of water during flood events is not measured and could not be accurately determined: a very limiting factor for flood prevention strategies.

In Lebanon, studies of river floods and information about historical floods is rare and almost lacking. To our knowledge, there is no clear database, and no one have been systematically collecting and recording information on floods during the last decades, as part of more general information about weather and natural disasters. Perhaps this is one of the major works that should have been done before in the country as a first step towards understanding the flood regime and risk in Lebanon, highlighting risk areas and evaluating its vulnerability. In this regard, there arises the need to develop a flood database for the country by utilizing available resources and through updating it on a regular basis.

In this chapter we present the results of an intensive history scan through archives of newspapers and previous reports to extract records on historical flood events in Lebanon with the objective to reconstruct the temporal and spatial patterns of flood events in the country and to investigate the vulnerability of the Lebanese societies and economies to floods.

5.2 **Literature review**

In Lebanon, studies of river floods are almost absent; there are some technical reports, realized by the Ministry of Energy and Water, that describe the situation on the river channels and propose several suggestions to reduce the probability of flooding.

The report of the Ministry of Energy and Water, on floods and the situation of river channels, highlights the regions that are constantly exposed to flooding events being: the surrounding areas of Al-Kabir River and Oustouane River in the plain of Akkar, the region from Tyr to Naqoura, the estuary of Nahr El-Kalb and Nahr Ibrahim, areas in Central Bekaa near the Litani River. The regions in the North-Eastern part of the country, such as El-Qaa, Aarsal, Fekeheh, Ras Baalbeck, are often exposed to flash floods (Kabout, 2011).

For Instance, Beirut River was transformed from a riparian river to a concrete canal in 1968. In 1970, extensive work was done along the river bank to protect the eastern suburb of Bourj Hammoud from floods. In 1974, ETEC Consulting Engineers were hired to design a flood control system that included a channel 32 meters wide, with capacity of 800 m3/sec. Environmentalists warned in 2003 that some construction companies were dumping illegally in the river that prompted the passing of Law 148 which stipulated that all construction projects should be located at least 500 meters away from the main rivers in Lebanon. In 2005, storms caused flood damage in the suburbs of Bourj Hammoud and Karantina, and a bridge adjacent to the Port of Beiurt collapsed due to water pressure. In 2005, the City of Bourj Hammoud in conjunction with CETE Méditerranée with logistical support from the City of Marseille, initiated a risks diagnosis that revealed seismic, flood and technological risks for the suburb.

In 2008, the UNDP lead a project for “Flood Risk Management and Prevention in Baalbeck-Hermel”, another project for flood risk management was realized in 2008 by ACSAD and GTZ in El-Qaa watershed and has led to the establishment of many water harvesting structures to reduce runoff velocity, thus increasing the time for water to infiltrate to the soil (GTZ/ACSAD, 2008). In 2010, a study was conducted by ELARD-UNDP on flood risk management and prevention in Baalbeck-Hermel area (ELARD, 2010). The study utilized remote sensing and GIS techniques along with dedicated hydrological software (HECRAS) for proper engineering structures to reduce runoff velocity during severe rainfall events in Ras Baalbeck watershed (Abdallah, 2012).

Several floods stroked Lebanon in the last century with perhaps the Abou Ali River Flood that hit Caza Tripoli and Zgharta in 1955, being the largest ever impacting an area approximately 400 km^2. Direct damages occurred first in the rural inner areas (Zgharta, Koura), destroying houses, bridges, killing 10-15 persons and over 2000 head of cattle. In the Tripoli coastal area (the second largest city in Lebanon), where the influence of several branches of the river lie, damages covered about 100 km^2, more than 400 people died, 2000 families found themselves without houses, thousands of acres of citrus plantations were destroyed, 4 bridges of the city collapsed, as well as several events of failure of surficial cover (Khawlie, 1994). After the flood subsided, 1.5 m thick sediments

and debris accumulated in many souks or in the residences, with a 200000 m^3 of sediments being added to the river mouth forming a delta (Beydoun, 1976).

In March 2003, the floods lasted for 10 days damaging large areas of the Lebanese territory with many slides and mass failure at various locations. The areas damaged covered vast regions in Akkar plane “North Lebanon”; Litani basin “Bekaa”, the coastal stretch from El Abde to Naqoura, in addition to several villages juxtaposing river banks in the mountains (Kabout, 2011). Water and mud covered roads, houses, agricultural land and ruined crops specifically in the Akkar plane and Bekaa valley, several villages were cut off (road, electricity, telephone landlines) from the outside world. These damages were manifested in flooding of winter storm water channels and rivers in the water shed area of Naher El Kabir EL Janubi, Oustouane, Arqa in Akar plane and on the banks of Litani Rivers and its tributaries between Dalhamieh-Zahle bridge till Joub Jannine Kefraya.

The semi-arid areas in Baalbeck El Hermel also witness several flash floods especially in 1994, 1999, 2001, 2003, 2007, 2010, 2013, and 2018 causing a huge loss in properties, destroying bridges and disrupting the Baalbeck-Syria highway at several occasions and for several hours (Abdallah and Hdeib, 2018).

Early January 2013, a severe storm hit Lebanon. The harsh winter storm, which began late Saturday (5th of Jan. 2013), left behind a big mess in the country. Almost all rivers were flooded, six people were killed, and landslides were triggered. The daily star wrote” A landslide turned the main road of Nahr al-Mot, north of Beirut, into a muddy swamp, that left drivers stuck for hours. In nearby Antelias, the first floor of a building was flooded after the Antelias River water level rose. Many roadside walls have collapsed due to the storm, including a concrete wall along the Champville College, a private French-language school in Metn. No one was hurt. Several cars were damaged when a concrete wall collapsed in the northeastern Beirut suburb of Hazmieh, causing massive traffic jams. Further up, in Mansourieh, the main road was cut as the floods continued to rise. Rain caused disruption throughout the country as pools of water closed many roads, mainly Shweifat-Aramoun and Beiteddine-Baakline roads in Mount Lebanon. Floods also impeded traffic in east Lebanon, resulting in cars breaking down on the Ablah-Riaq, Ferzol-Zahle and Bar Elias-Masnaa roads. On the Chtaura highway that links Beirut with Damascus, members of the Internal Security Forces prevented motorists from crossing toward Dahr al-Baidar if their cars were not equipped with snow chains. In the north of the country, the picture was similar with floods forcing road closures, particularly the road linking Koura with Tripoli and that leading to Akkar. Public and private schools, including vocational and technical colleges, were ordered to close for three days the 8th, 9th and the 10th of January 2013.

5.3 **Materials and methods**

In this work, the severity and frequency of historical flood events in different Lebanese rivers are analyzed using documentary evidence. The occurrence of floods in the past is analyzed by linking the selected events to the basic topographical, hydrological, and vulnerability characteristics of the river basins investigated, as well as the climatological causes of their flooding during the instrumental period. The work included scanning archived microfilms of the "An-Nahar" (reporting since 1933) and "As-Safir" newspapers that are available in a digital format at the Jafet Library of the American University in Beirut (AUB), in addition to old documents and reports available at the CNRS and requested from relevant authorities. These two newspapers were chosen for scanning because these are the eldest newspapers in the country and their archives are available at the American University in Beirut. "As-Safir" newspaper has been in circulation from March 1974 until December 2016. The last issue of the paper was published on 31 December 2016. "An-Nahar" newspaper has been in circulation since 1933 and is still publishing to date. In newspapers, information on flood events can be found in a specified weather section and sometimes major and harsh events would occupy the cover page.

Figure 5.1 presents an example of the form of recorded flood events in newspapers. This event was recorded in "An-Nahar" newspaper on 21st of February 2003. The events title was as follows: "***Torrents and river floods in both middle and west Bekaa and in Akkar, isolated villages, trapped tenth of houses, and inundated hectares of agricultural lands***".

On that day and as described in the newspaper: *"the damages resulting from the severe storm event hitting Lebanon were exacerbated in all Lebanese territories, especially in the middle and western Bekaa where torrents and river floods trapped tens of houses. Similarly, in Akkar plain the flood water inundated hectares of agricultural lands and isolated several villages. Historical and archaeological monuments were also affected by the storm; a landslide in Diman area caused severe damages to the heritage road between the summer residence of the Maronite Patriarchate and the Qanoubin village. Moreover, a landslide in Barih village threatens the lives of citizens and the situation is worsening since the rescue services are not able to handle it because of the heavily flowing water".* Later several reporters from different regions of the country describe the detailed situation in each area/district. For example, a reporter from Zahle district adds: *"the tragedy of the Bekaa which was sinking in water for the last two weeks, has reached its peak yesterday after additional huge torrents flooded several agricultural fields, houses, shops, nurseries and farms. Many birds and cattle were deceased, and residents were displaced from their houses. The water trapped, according to an unofficial census, around 400 residential units in eights villages and cut several*

main roads. Unfortunately, no official census was conducted to estimate the damages and this catastrophe has revealed the fragility of state's capabilities…"

Another reporter concludes that the economic damages by these floods are estimated at one billion Lebanese pounds (1 billion LBP).

By scanning events recorded in newspapers and previous reports we could mainly identify the source of the information (newspaper, report…), date of the event (year and month), description of the event (flood, torrential or heavy rainfall, avalanche, torrents…), location or area affected, and event's detailed description and estimated damages.

On the other hand, 17 basins (presented in Table 3.5) were selected to extract and analyze their major morphometric characteristics, hydrological characteristics (rainfall and discharge probabilities of occurrence), and vulnerability characteristics (percentage of distribution of different land uses over the basin). The selected catchments characteristics with their notations and units are presented in Table 5.1. The number of occurrences of flood events over the country is then compared with the characteristics of each basin to analyze the reasons behind the occurrence of such events. The morphometric characteristics are obtained after performing a drainage processing based on the available 15 m DEM for Lebanon. Rainfall and Discharge values are calculated based on the known Gumbel method, as described in chapter 3. The vulnerability characteristics are evaluated based on the available land use map for Lebanon. All analysis is performed in a GIS database.

Table 5.1 The chosen catchments characteristics for flood evaluation with their notations and units.

Type	Catchment Descriptors	Notation and units
Morphometry	Catchment area	Ac (km^2)
	Minimum Elevation	Min Zc (m)
	Mean Elevation	Zc (m)
	Maximum Elevation	Max Zc (m)
	Drainage Density	Dd (km/km^2)
	Longest flow path	Lflow (km)
	Slope along Lflow	Sc (%)
Rainfall	10 years rainfall depth	P_{10} (mm)
	50 years rainfall depth	P_{50} (mm)
	100 years rainfall depth	P_{100} (mm)
Discharge	10 years discharge	Q_{10} (m^3/s)
	50 years discharge	Q_{50} (m^3/s)
	100 years discharge	Q_{100} (m^3/s)
Vulnerability	Artificial/Urban areas	Uc (%)
	Agricultural areas	Agr (%)
	Wooded land	Wd (%)
	Grassland	Grass (%)
	Unproductive areas	Unpr (%)
Floods	Number of flood events	Ne (level 1 to 5)

Figure 5.1 Sample of recorded flood events in newspapers. "An-Nahar", 21 February 2003.

5.4 **Dataset**

After an intensive history scan that lasted for more than two months, we could extract 196 records extending between 1293 and 2013. We were also able to find some newspaper reports that document information on historical flood events after interviews with several historians in the country and thus we could extract records even before the 1930's. However, for the eldest records, particularly those before the 1990, fewer information could be obtained about the flood events. However, those records were the most severe ones because they are still in memories of older people and historians. Table 5.2 presents some examples of the extracted events. A complete list of the extracted events can be found in Annex B. These scanned events were transformed to a GIS database and allocated to equivalent district/Caza and Municipality levels.

Most extracted flood events occurred in agricultural areas such as the Akkar and the Litani plain and highly urbanized areas such as Beirut and Tripoli, both are major cities. Most damages occurred to agricultural fields and livestock (poultry, fish breeding, cattle…), residential and urban areas (isolated villages), and floods mainly affected the infrastructural facilities such as roads, telecommunication lines, and electricity lines.

Moreover, most records of flood events were a result of heavy rainfall events (or snow melt) and hence flood records could not be separated from records of heavy storm events. Thus, extracted records were not only limited to flood events, but a combination of heavy or torrential rainfall events and torrents, avalanches and floods (e.g. example events 6 and 7). Similarly, each record is not necessarily related to one event on one river, most the time, records report events in more than one village and river (e.g. example events 8 and 10). As we have mentioned, for most records we could only extract information related to the type of the weather event, time of occurrence (year/ month), location or area affected, and description of the damages and economic losses that occurred. Sometimes, we were able to extract rounded estimates of the economic losses in monetary value, but these estimates were mostly limited to severe and intense events.

Table 5.2 Example of the extracted historical flood events from newspapers and previous reports. Six event characteristics were extracted; source (newspaper, report…), year, month, type of weather extreme (flood, heavy rainfall, torrents…), location or area affected, and damage (estimated losses). A full list of the extracted events is presented in Annex B.

Event	Source	Year	Month	Weather Extreme	Location or Area Affected	Damage (estimated losses; million $)
Example event 1	An-Nahar	1293	Jun	Flood	Baalbek	100,000 people deceased
Example event 2	An-Nahar	1317	May	Flood	Baalbek	500 houses ruined,131 stores,17 bakery, 11 mills, 1 school,40 corn field, 140 or more people deceased
Example event 3	An-Nahar	1503	Summer	Assi, Litani, Fraidis, El-Safa, Kalb, Rivers flood	All Lebanon	Damages in houses, bridges, roads, agricultural lands
Example event 4	An-Nahar	1507	6 Jul	Flood	El Chouf	Agricultural land around Nahr El Safa flooded
Example event 5	(Khawlie, 1994)	1955	-	Abu Ali River Flood	Tripoli	440 people died, 2000 families displaced, thousands of acres of citrus plantations destroyed, 4 bridges collapsed, landslides…
Example event 6	An-Nahar	1975	3 Feb	torrents, floods, tempest, avalanche	Beirut, Zahle, Faraya	structural failure, ships, damage, water pollution, electricity and phones out, agriculture-4 people deceased
Example event 7	An-Nahar	1978	8 Mar	hailstorms, floods	Bhamdoun, Aley, Akkar, Zghorta, Koura, Batroun	huge soil erosion
Example event 8	An-Nahar	1979	9 Jan	ditto; floods in: Al-Kabir river, El-Mot river, sea storm	Cheikh Zennad, Machta Hassan & Machta Hammoud, Bekai'a, Beirut, Tripoli	ditto
Example event 9	An-Nahar	1980	11 Feb	flood in Antelias river	Antelias	agricultural destruction, cattle
Example event 10	An-Nahar	1983	15 Mar	torrents and floods in rivers: Kfarchima, Hauch Harimi (Litani), EL Awali, Barghouth, sea storm, hail storm & avalanches	South Lebanon, Hasbaya, Chouf, Beqaa, Akkar, Broummana, Bar Elias, Niha, EL-Ballout, EL-Kharroub, Rihan, Choueifat, Bcharri, Sir, Fakra, O'iun siman, Ainata, Cedars, all coastal cities	landslides, bridges, canals, roads, houses, ships, agriculture, forest, 90 people deceased, 3000 cattle heads.

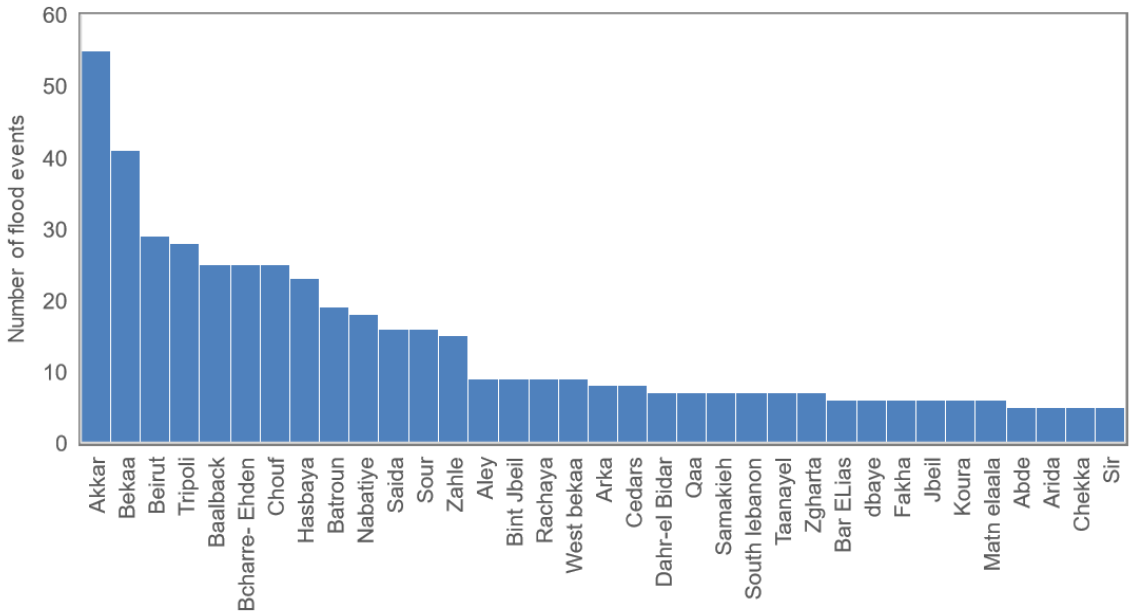

Figure 5.2 Number of occurrences of flood events in top 35 Lebanese villages, based on 711 records of flood events extracted from newspapers and previous reports.

5.5 **Results and discussions**

Analyzing the extracted events, allows us to distinguish 711 records of flood events in 86 villages in Lebanon. Akkar, Bekaa, Beirut and Tripoli being the cities/villages recording the highest number of flood events reaching up to 55, 41, 29, and 28 respectively. Figure 5.2 presents the number of occurrences of flood events in the top 35 villages in Lebanon.

Extracted records of flood events were not only limited to riverine floods but also included torrents, floods by surface runoff and urban floods. However, most records of floods events were limited to mentioning the village or district/caza in which floods occurred instead of mentioning the type of flood or precising the flooded rivers. Filtering all the extracted records (711 flood records) allows us to distinguish 161 riverine floods. Figure 5.4 shows the percentages of occurrence of floods per each river. El Kabir, Hasbani, Ostouane, Litani (and Berdawni), Arka, Abu Ali, Bared, Awali, Zahrani and Assi rivers were the top 10 rivers recording flood events. These records involved major river floods as well as small, seasonal, and river tributaries. For example, the Berdawni river is a tributary of the Litani river and Bisri river is a name given to the Awali river in its upstream part in Marj Bisri. Some river tributaries have common names given by locals which we could not distinguish directly, so it took us some time to relate the tributary to its main river.

5.5.1 ***Monthly frequency of occurrence of floods***

Most floods occurred during the winter period extending from November to March. The monthly frequency of occurrence of flood events is shown in Figure 5.3. The months January and February record the highest frequency of occurrence of flood events with 20% and 19% respectively. This supports our understanding that most floods in Lebanon occur during the winter after heavy and torrential rainfall events and hence burst their banks towards the neighboring areas.

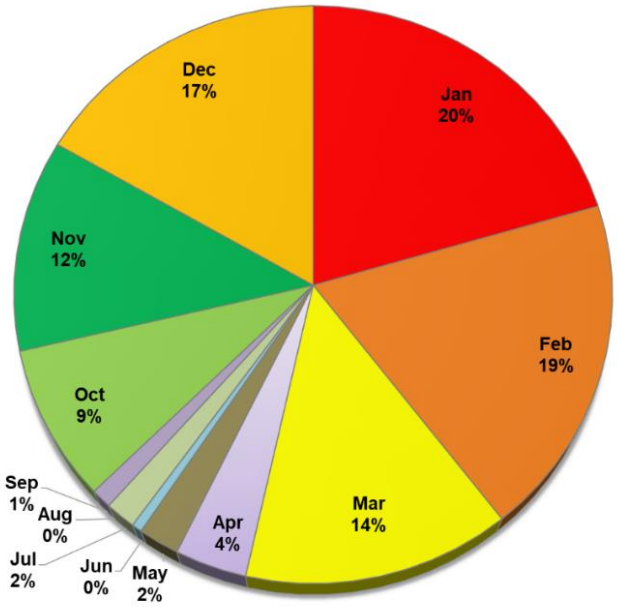

Figure 5.3 Monthly frequency of occurrence of flood events in Lebanon.

5.5.2 ***Spatial flood frequency of occurrence***

After analyzing the monthly frequency of occurrence of flood events, the second step involves analyzing the spatial occurrence of these events over Lebanon. The obstacle was to find a common base/scale to evaluate the flood events in terms of spatial occurrence. Some events were assigned to their respective villages, other events were assigned to the respective district/caza, and some were assigned to their respective rivers. This gives us three scale options (caza, basin, or village). Mapping the spatial occurrence on a small scale (village scale) is not possible because not all events are assigned their respective villages; many events are only assigned to their respective caza. The perfect option would be mapping the spatial occurrence on a basin scale, but however this was not possible, because some districts intersect more than one basin and it was not possible to relate an event in a caza to its respective basin. Whereas the opposite can be done. In this case, it was found that analyzing the spatial occurrence of floods based on a caza (district) scale is the best option, because all other events can be assigned their respective caza. Hence, flood event records assigned to villages and rivers are then assigned to their respective caza. Accordingly, the spatial frequency of occurrence of the flood events can be mapped as shown in Figure 5.5. Basin boundaries and rivers are also presented on the same map.

The spatial frequency of occurrence is mapped in five levels over twenty-five districts. These levels vary from low frequency of occurrence (level 1: 2 to 5 events/caza, and level 2: 6 to 10 events/caza), medium frequency of occurrence (11 to 19 events/caza; level 3), to high frequency of occurrence (level 4: 20 to 25 events/caza, and level 5: 26 to 55 events/caza). The northern districts Akkar (intersecting el Kabir, Ostouane, Arka and Bared river basins) and Tripoli (intersecting Abu Ali river basin), along with the central districts (Beirut and Baabda; intersecting Beirut river basin and urban Beirut catchment) record the highest frequency of occurrence (level 5). The internal Bekaa district, along with Bcharre, Chouf, and Hasbaya also record relatively high frequency of occurrence of level 4. The Bekaa district intersect the Assi and Litani river basins, the Bcharre district intersect the Abu Ali and Asfour river basins, the Chouf district intersect the Awali and Damour river basins, and the Hasbaya district intersect the Hasbani river basin.

*5.5.3 **Linking flood occurrence to catchment characteristics***

After mapping the spatial occurrence of flood events, the question arises to whether there is a relation between the occurrence of these events (as recorded in newspapers and previous reports) and the catchments characteristics. In another example; are these events linked to the morphological characteristics of the basins, or the hydrological characteristics, or are these events an indication of the vulnerability of the catchments to flooding (based on land use characteristics)? Or are these events linked to a combination of all of these characteristics?

The results of the evaluation of the major catchments' characteristics for the selected river basins are presented in Table 5.3. The evaluated characteristics are then overlaid over the spatial flood occurrence map through a GIS operation. The resultant map is shown in an A3 format in Figure 5.6. Main facilities such as airports, hospitals and big factories and power plants are also presented on the map.

The five northern coastal catchments; el Kabir, Ostouane, Arka, Bared, and Abu Ali (in its low main part in Tripoli), record the highest number of events along with the central catchments of Beirut river and urban Beirut.

The low main part of the northern catchments coincides with the Akkar plain which is one of the main agricultural plains of Lebanon (coming in the second place after the Bekaa agricultural plain) of variable agricultural activities and forming the widest coastal area of around 10 km inland. Among all the studied catchments, the northern catchments Ostouane and Arka record the highest percentage of agricultural areas reaching up to 55% and the urban areas do not exceed the 5%; these are mainly agricultural catchments in nature. The Bared and Abu Ali catchments are dominated by wooded lands and agricultural areas. The agricultural areas form 30% and 28.5% of the catchments' area respectively and are concentrated on the lower coastal part. The wooded lands form around 49% and 30% respectively and are concentrated on the upper hills. Whereas the urban areas are no more than 4.5 %. Perhaps these catchments (being located in an important agricultural area) have been under the intention of press, because any flood event, no matter how strong it was, would cause major losses in the agricultural fields and result in great economic losses to farmers.

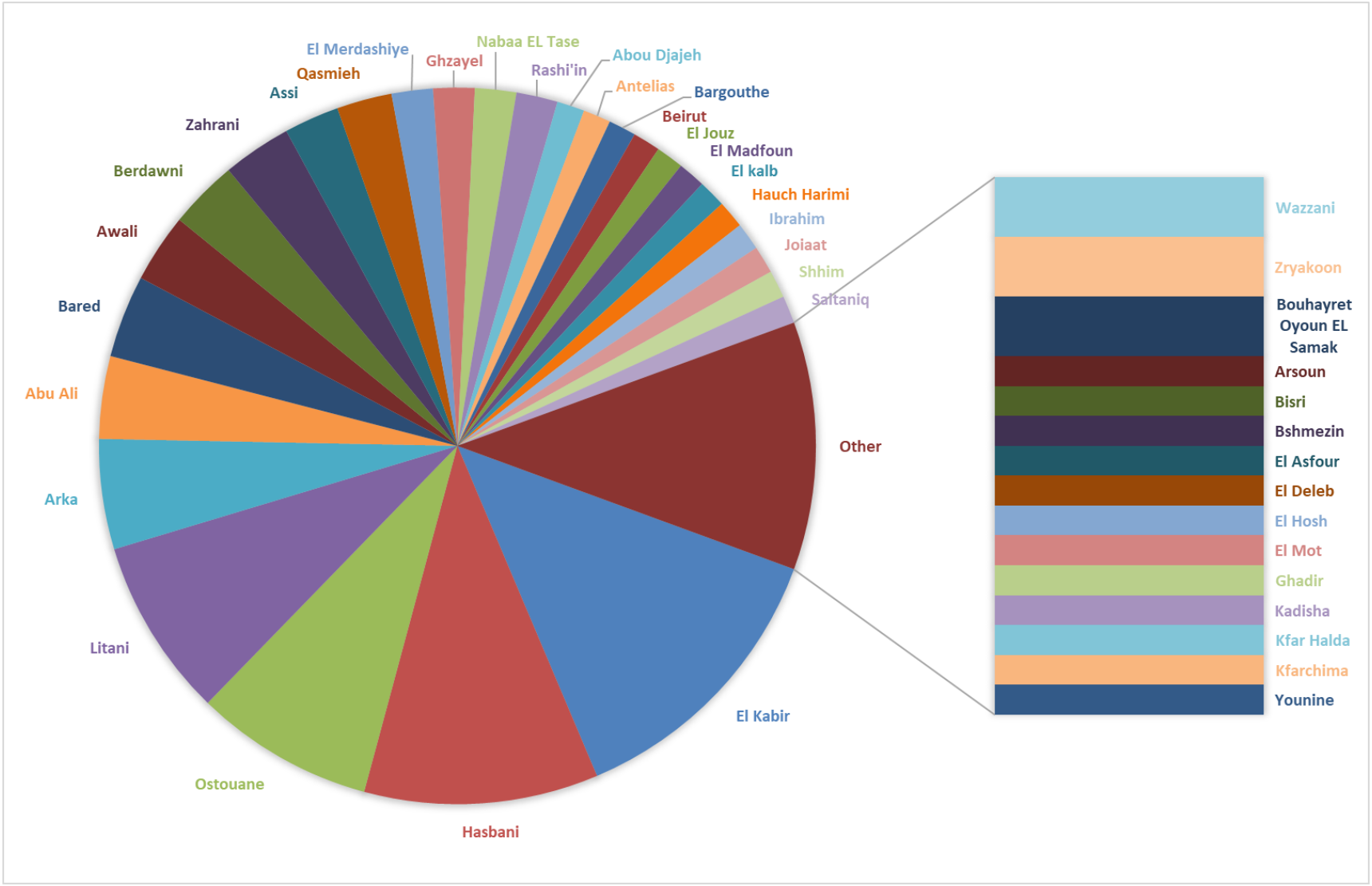

Figure 5.4 Percentage of occurrence of flood events for different rivers and tributaries in Lebanon with el Kabir, Hasbani, Ostouane, Litani (and Berdawni), Arka, Abu Ali, Bared, Awali, Zahrani and Assi rivers being the top 10 rivers recording flood events.

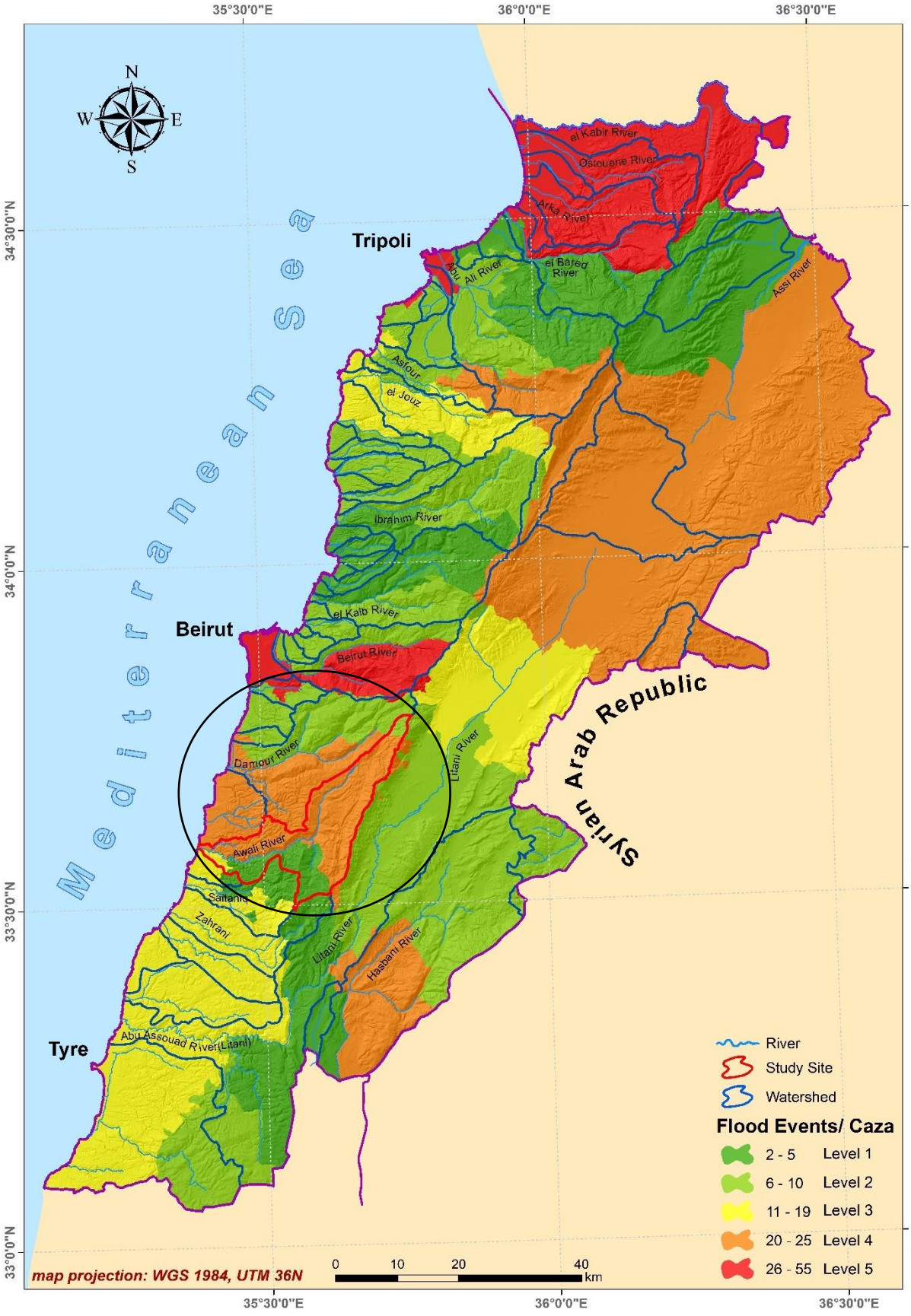

Figure 5.5 Spatial occurrence of extracted flood events per Caza, along with the selected study site for detailed analysis (Awali River Basin).

Table 5.3 Results of the evaluation of the major morphological, hydrological and vulnerability characteristics, along with the number of occurrences of flood events (on a scale of five levels) for the selected catchments. For catchments marked with (*), the discharge values at outlet (sea mouth) are obtained through hydrological modeling of the river basin based on discharge values obtained from an upstream river gauge. For the Assi basin, records were not enough to evaluate the discharge probabilities of occurrence. (refer to Table 5.1 for variable description).

St	Catchments	Physical Characteristics							Rainfall			Discharge			Vulnerability					Floods
		Ac	Zc	Min Zc	Max Zc	Dd	Lflow	Sc	P_{10}	P_{50}	P_{100}	Q_{10}	Q_{50}	Q_{100}	Uc	Agr	Wd	Grass	Unpr	Ne
121	***Ostouane at sea mouth**	151	516	10	1923	3	19	10	107	142	156	97	146	172	3.4	53	25	18.5	0.1	Level 5
108	**Arka at Hakour**	102	737	77	1951	3.8	16.2	11	92	115	125	30	47	54	5	55	30	9.5	0.4	Level 5
111	**Bared at sea mouth**	281	1278	29	2878	4	42	6.7	104	133	145	53	79	90	2	30	49	17	1.7	Level 5/1
117	**Abu Ali at Abou samra**	466	1328	46	3081	3.4	35	8.6	113	144	158	63	80	99	4.5	28.5	30	28	9	Level 5/4
120	***Jouz at sea mouth**	189	1032	9	2342	4.8	29	4.6	129	176	195	118	144	166	12	30	36	20	1.7	Level 3
118	***Asfour at sea mouth**	89.7	670	3	1850	1.4	28.8	5.4	99	126	137	30	37	38	7.5	26.5	49	15	1.5	Level 2
223	**Ibrahim at sea mouth**	326	1541	3	2658	2.4	36.7	7.2	128	169	186	318	498	575	4	8.5	30	36	21.5	Level 2
228	**Kelb at sea mouth**	257	1733	12	2622	3	28.3	9.2	130	176	196	124	180	204	10	13	31	24	21	Level 1/2
234	**Beirut at Jiser El Bacha**	217	1003	22	2086	3.3	27	7.6	90	108	116	170	267	308	12.5	15	51.5	19	1.6	Level 5
238	***Damour at sea mouth**	293	802	9	1941	3.7	56.7	3.4	119	155	170	285	397	426	12	30	36	20	1.7	Level 2/4
475	***Awali at Saida**	301	944	7	1949	4.5	54.3	2.8	105	132	143	292	425	506	7.2	18.2	46.5	26.8	1.4	Level 4
480	***Zahrani at sea mouth**	152	534	3	1670	1.6	15	9	96.5	123	134	51	76	88	9.6	41	31	17	1	Level 3
476	**Saitaniq at el lemon valley**	111	525	2	1411	1.2	23.3	3.9	84	105	114	28	41	46	13.3	25.3	45	16	0.23	Level 1/3
345	**Assi at Hermel**	1241	1393	590	3081	2.9	39	6.3	46.5	62.5	69	-	-	-	1.8	23	18	51	6	Level 4
363	**Litani at Joub jannine**	1433	1223	860	2551	2.5	65.6	2.5	86	110	121	114	169	192	4.7	48	5.4	32	2.7	Level 4/3
499	**Hasbani at wazzani**	566	1198	281	2810	2.1	47.5	5.3	90.5	113	123	110	177	205	1.7	25	28.5	44	0.6	Level 4

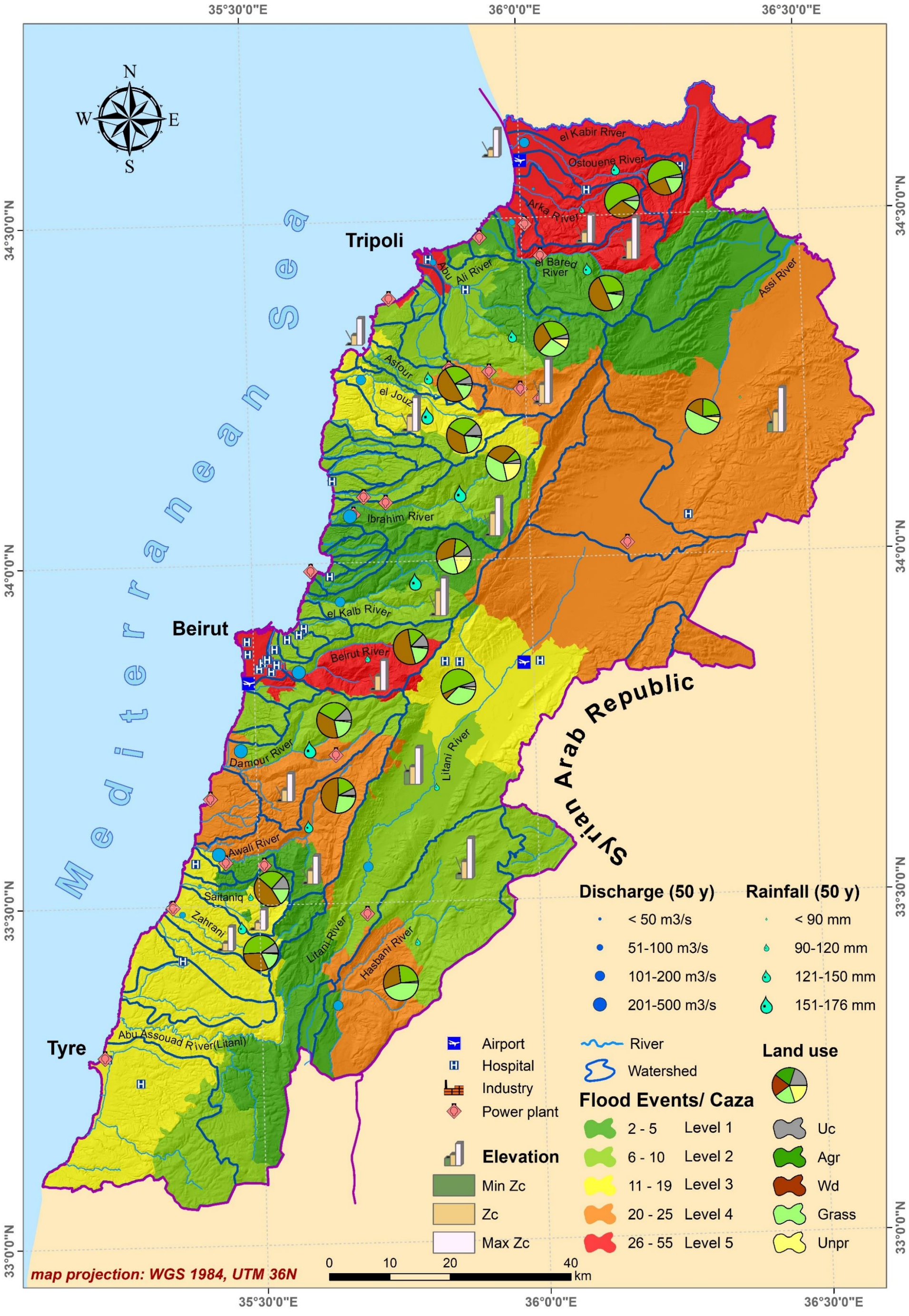

Figure 5.6 Resultant flood frequency of occurrence map.

The northern catchments have variable morphologic characteristics, with area ranging between 102 and 466 km^2, average elevation ranging from the north to the south between 516 and 1328m, and an average slope along the longest flow path ranging between 6.7 and 11%. Compared to other catchments, the average slope is slightly higher, but the low main part is very flat, perhaps this increases the probability of flooding in the plain areas. The Abu Ali river basin is located on a major city (Tripoli), it has a big area (466 km^2) and extends to an elevation reaching 3081m which is the highest elevation compared to other catchments, hence the catchment has a potential to bring big amounts of runoff towards its low main part especially from the very high mountains after heavy rainfall events and after the melting of the snow.

Moreover, those northern catchments belong to the northern coast and northern mountain climatic zones, they receive a 10 years rainfall ranging between 92 mm and 113 mm and yield a 10 years discharge ranging between 30 m^3/s and 97 m^3/s (except for el Kabir catchment which is not selected for analysis because it's a transboundary catchment extending into Syria). However, compared to other catchments of the central coast and the central mountain climatic zones, such as the Ibrahim, el Kalb, el Damour, and Awali river basins, those catchments receive a slightly higher amount of rainfall (10 years rainfall ranging between 105 and 130 mm), but yield much higher amounts of discharge (10 years discharge ranging between 124 and 318 m^3/s). So, the elevated number of flood events cannot be directly related to the hydrological characteristics of the basins, except for the Abu Ali basin where historical records indicate that it produced the largest floods in the history of Lebanon (the peak flood discharge may have exceeded the 500 m^3/s but was not recorded by the traditional stage gauge network).

For the central catchments (urban Beirut and Beirut river catchments), the elevated number of events in the urban Beirut catchment would be an indication of urban flooding. The catchment is mainly urban in nature as it presents the capital of Lebanon were most population is concentrated, this makes it vulnerable to urban flooding, each year, and perhaps puts it under the attention of press because it contains the main governmental, economic and social activities. Now concerning the Beirut river catchment, it has an area of 217 km^2 and average elevation of 1003m. The longest flow path is 27 km and its average slope is 7.6%. Compared to other catchments, Beirut river catchment does not have a remarkable morphological characteristic. The catchment receives a 10 years rainfall of 90 mm and yields a 10 years discharge of 127 m^3/s. the catchment is mainly wooded in the upper hills (wooded lands 51.5 %), slightly agricultural and formed of grass lands in its middle part (agricultural areas 15% and grass lands 19%) and mainly urban in its low main part of urban areas reaching 12.5 % which is a high percentage compared to other catchments. In its lower part houses and neighborhoods are built directly on the edge of the river (such as Bourj Hammoud and Karantina) as part of the wide urban expansion that happened in the city of Beirut in the previous decades. The river used to flood the neighboring houses very frequently, until it was converted into a concrete channel in 1968; which largely reduced flooding. Perhaps the vulnerability of the city of Beirut to floods is an indication of the elevated number of flood events recorded in press.

The Assi, Litani, Hasbani, Awali and Damour catchments come in the second position with level 4 frequency of occurrence of flood events. The Assi catchment extends over an area of 1241 km^2, it has an average elevation of 1393m. Its longest flow path is 39 km and its average slope is 6.3%. The river forms a tributary of the Orontes River that flows northward through Syria and Turkey before entering the Mediterranean Sea. The catchment is mainly formed of bare lands, the agricultural areas and the urban areas do not exceed the 23% and the 1.8% respectively. The catchment is characterized by a semi-arid climate it receives a 10 years rainfall of 46.5 mm. However, available records of river flow possess a lot of gaps and were found insufficient to estimate the river discharge based on different probabilities of occurrence. Floods in the basin mostly occur in the form of flash floods generated after a sudden heavy hail fall or rainfall over the upper semi-arid mountains which yields huge amount of runoff over the bare lands. Those torrents flow in the wadis and strike the lower small villages located in the low land areas along the flood path, such as the villages of Ras Baalbeck and Fekeha. Hence, the elevated amount of flood events in the Assi basin can be related to a combination of the morphological, hydrological and vulnerability characteristics of the basin.

The Litani river is the longest river in Lebanon, it first flows south wise through the Bakaa plain, the primary agricultural plain in Lebanon, and then crosses the country west wise towards the Mediterranean Sea. The morphology of the catchment is complex, it varies from elevated mountains to wide plain areas. The average area of the Litani catchment at Job Jannine (in its middle part, in the Bekaa plain) is around 1433 km^2 and its average elevation is 1223 m. The longest flow path is 66 km and its average slope is 2.5%. The catchment is primarily agricultural; agricultural areas and grass lands form 48% and 32% respectively. The catchment receives a 10 years rainfall of 86 mm and yields a 10 years discharge of 114 m^3/s. Floods mainly occur in the Bekaa plain, where the river branches into several tributaries, because of the low slope gradients, some of which are formed of very small channels that flood after rainfall events. Moreover, farmers also dig channels for irrigation purposes. Those channels are of small capacities and thus induce floods toward the agricultural fields during winter. In parallel, the importance of the Bekaa plain (being the primary agricultural plain in the country), makes it highly vulnerable to flood events that usually leave great damages to the agricultural fields and causes main economic losses to farmers, thus the farmers' suffering and yelling after flood event has brought the intention of press to the area. Therefore, flooding in the catchment is not a result of one characteristic but can be linked to a combination of morphological, vulnerability and hydrological characteristics.

Similarly, the Hasbani river catchment yields runoff from the upper hills of mount Haramon and flows south through the Marjeyoun plain crossing the boarders into the occupied Palestine. The catchment's area at Wazzani is around 566 km^2 and the average elevation is 1198 m. The longest flow path is 47.5 km and the average slope is 5.3%. The catchment is dominated by grass lands forming around 44% of the area of the basin, followed by wooded lands and agricultural areas each forming 28.5% and 25% of the basin's area respectively. The urban areas are limited forming no more than 1.7% of the basin's area. The basin receives a 10 years rainfall of 90.5 mm and yields a 10 years

discharge of 110 m^3/s. There are some agricultural fields and recreations developed along the river that are mainly vulnerable to flooding. The river is shallow in many locations and mainly floods in the low plain areas after heavy rainfall events inundating some roads and fields. Hence, the elevated number of flood events can be mostly linked to the morphology and the hydrology of the basin.

The Awali and the Damour river basins have similar morphological and hydrological characteristics, they extend over an area of 301 km^2 and 293 km^2 and have an average elevation of 944 m and 802 m respectively. The basins receive a 10 years rainfall of 105 mm and 119 mm and yield a 10 years discharge of 292 m^3/s and 285 m^3/s respectively. The Awali basin is located on a major city (Saida), it is mainly dominated by wooded lands that form 46.5% of the basin's area and located up hills, grass lands and agricultural areas form 26.8% and 18.2% of the basin's area respectively. Floods mainly occur after heavy rainfall events where the river bursts its banks in the plain areas; in the middle in Marj Bisri area inundating some agricultural fields, and at the sea mouth inundating some recreations created on the river. Given the morphology of the catchment and the elevated rainfall and discharge values, the elevated number of flood events may be mainly related to the morphology and the hydrology of the catchment. The Damour basin is dominated by wooded lands and agricultural areas. In its low main part, it coincides with the Damour agricultural plain which is an important agricultural area (agricultural areas form 30% of the basin's area) making it more vulnerable to floods. The wooded lands are spread up hills and form 38% of the basin's area. Flooding mainly occur after heavy rainfall events inundating the agricultural fields at the sea mouth causing great losses to farmers. Similarly, the floods in the Damour basin may be related to a combination of morphology, hydrology and vulnerability characteristics.

5.5.4 ***Flood hazard, vulnerability or flood risk?***

In the previous parts we have mapped the spatial occurrence of flood events, analyzed the catchment's major morphological, hydrological characteristics and studied the vulnerability of the catchments to flooding in terms of landuse characteristics. We have analyzed the reasons behind the occurrence of flood events, and we tried to link the frequency of occurrence of these events to one of the catchments' characteristics or to a combination of them. The question now arises about the actual representation of the developed flood occurrence map (shown in Figure 5.6). In another example; is this map equivalent to a flood hazard map? Or is it equivalent to a vulnerability map? Or is it a combination of both and hence equivalent to a flood risk map?

Based on our previous analysis, the elevated number of occurrences of flood events in the northern catchments (Ostouane, Arka, and Bared) can be related to the morphology of the catchments and to the high vulnerability of the catchments to flood events. The elevated number of flood events in the Abu Ali river basin (particularly in Tripoli) and the Litani river basin (at Job Jannine) is related to the morphology and hydrology of the catchment and to its vulnerability to flood events. The flooding in the Assi, Hasbani and Awali basins can be mainly related to the hydrology and morphology of the catchments.

The elevated number of flood events in Beirut river basin along with urban Beirut is a result to its high vulnerability to floods. The flooding in the Damour river basin is a combination of the three characteristics.

The morphological and hydrological characteristics are generally an indication of the flood hazard in the basin. The main land use occupation in the catchment is an indication of the vulnerability of the catchment to flooding. A combination of all these characteristics would be an indication of the flood risk. For the analyzed basins, the morphology plays a big role in the river flooding. Because most of the Lebanese catchments have complex morphology, it varies from elevated mountains and deep valleys in the upper hills to small or wide plain areas at the outlet (mostly at sea mouth), or in the middle (Litani, Assi, and Hasbani catchments). Moreover, one should mention that most rivers are in the form of small channels (average width do not exceed the 15 m), this combination (complex morphology and small channels) is the first reason behind the occurrence of floods especially after heavy rainfall events when the runoff water exceeds the channel's capacity and hence flood over the plain areas.

In this regard, flood hazard could not be neglected in the map of occurrence of flood events, but, at the same time, the map could not be equivalent to a flood hazard map. This is because the level 5 basins recording the highest number of flood events (such as the northern basins (such as el Kabir, Arka, and Ostouane) have lower flood hazard compared to the rivers of Ibrahim, kalb and Awali, that receive higher amounts of rainfall and yield higher flood discharges, but they are rated at lower levels (2, 3 and 4).

Moreover, the basins recording the highest number of flood events are the basins mostly vulnerable to flood events, and one would suggest that the developed map is a flood vulnerability map not more. But this is not the case, because the flood occurrence in those basins was also linked to the morphological and hydrological characteristics of the basins. Hence, the developed map is a combination of flood hazard and vulnerability and would be equivalent to a flood risk map. This interprets, for example, why Awali is given a level 4 rate and Ostouane is given a level 5 rate. Although Awali basin is higher in terms of flood hazard, but the Ostouane basin is more vulnerable to flooding, which puts him at a higher flood risk.

*5.5.5 **Opportunities and limitations***

The extracted events from newspapers and previous reports form a documentary evidence which is promising in retrieving information on previous flood events in the pre-instrumental period and in the absence of data measurements, even during the instrumental period. Such type of information constitutes a data basis for so-called historical hydrology and has the opportunity to understand the flood occurrence and the changes in their regime. Understanding the historical occurrence of flood event is a prerequisite to predict its future projections. Despite the intensive work required to scan newspaper archives, this data source remain a cheap data source available and accessible in most countries worldwide.

The extracted events allow for the first time analyzing the frequency of occurrence of flood events along with mapping their spatial occurrence over the whole country. Such map when overlaid over the vulnerability map is helpful in highlighting high risk areas and can be treated as a flood risk map, especially in the absence of detailed studies on flood risk in the country. The map can be used for general planning purposes and to prioritize areas to be part of future flood mitigation plans and projects.

However, such records remain descriptive focusing on the event's damages more than its characteristics. In most cases, it was not possible to extract information related to the estimated flood peak discharge, water levels, inundated areas, and rainfall amounts; which are indispensable information for flood modeling and detailed analysis. Moreover, the events' locations are not clear or precisely described, most event locations are associated with their respective districts/caza; a large scale that cannot support the detailed analysis. Highly urbanized areas (such as the capital and main cities) and main agricultural fields are gaining more press attention than rural areas. It is possible that several other events occurred in parallel in other locations but were not reported in press because such locations were less vulnerable to floods and did not gain the press attention, or there was no one available to report the event to press. In case of big storm events that cover almost all the country, event's description and damage evaluation is limited to main rivers, districts and cities, ignoring minor tributaries or villages and hence skipping other flood events of minor importance.

The extracted events have become a part of a flood data base generated at the CNRS-Remote Sensing Center. This data base is being updated on a daily basis, and information is being retrieved from different social media sources. Moreover, the RSC is building its capacity to obtain real time crowed sourced information from different agents and partners on field, the center is also developing mobile applications for rapid communication and easy data exchange. All these data sources will serve in supporting the early warning system (SUNAR) developed and operated by the remote sensing center.

*5.5.6 **Selection of a study site for detailed analysis; the Awali River Basin***

As we have mentioned in the previous paragraph, the resultant spatial flood occurrence map is developed on a large scale (district scale), which does not allow the detailed analysis to obtain information on the flood flows, water levels and extent. Such information is indispensable in any detailed flood mitigation project or flood forecasting system. Hence, the developed map cannot replace the need for a detailed hydrological-hydraulic modeling of the river catchment to establish flood flows and water levels.

In this regard, we had to select a study site for detailed analysis and modeling. The northern catchments and the Assi catchment were not selected because of the security situation at the time of performing the study. These catchments are located near the Syrian boarders that was facing terrorist attacks from time to time. The Beirut catchment was not selected because it's a highly urbanized catchment subject to many urban floods and the river was completely transformed to a concrete channel. Hence, we had to move to select a level 4 catchment, so we selected the Awali River catchment (highlighted in

Figure 5.5), primarily because we could perform post-event measurements of an extreme event occurred early January 2013, which was helpful in assisting the detailed flood modeling, and secondly because flooding in this catchment is mainly a result of its morphological and hydrological characteristics which insures that the reason behind the occurrence of floods in the basin is natural with no human intervention; a favorable case for hydrological-hydraulic modeling.

The major geographical, hydrological and climatic characteristics of the study site were previously presented in chapter 4 as part of presenting and analyzing all datasets available for the thesis work.

5.6 **Conclusion**

In this chapter we have presented the results of an intensive scanning of newspaper archives and previous reports to extract records on previous flood events in the country. We were able to extract 196 records extending between 1293 and 2013 out of which we could distinguish 711 flood events in 86 villages in Lebanon. The monthly frequency of occurrence was analyzed, and the spatial occurrence of these events was mapped on a district (caza) scale in five levels.

The major morphological and hydrological characteristics for selected catchments was extracted, along with its vulnerability to flooding in terms of landuse characteristics. We have analyzed the reasons behind the occurrence of flood events, and we tried to link the frequency of occurrence of these events to one of the catchments' characteristics or to a combination of them.

The five northern coastal catchments; el Kabir, Ostouane, Arka, Bared, and Abu Ali (in its low main part in Tripoli), record the highest number of events along with the central catchments of Beirut river and urban Beirut, all at level 5 frequency of occurrence. The Assi, Litani, Hasbani, Awali and Damour catchments come in the second position with level 4 frequency of occurrence of flood events.

The elevated number of occurrences of flood events in the northern catchments (Ostouane, Arka, and Bared) can be related to the morphology of the catchments and to the high vulnerability of the catchments to flood events. The elevated number of flood events in the Abu Ali river basin (particularly in Tripoli) and the Litani river basin (at Job Jannine) is related to the morphology and hydrology of the catchment and to its vulnerability to flood events. The flooding in the Assi, Hasbani and Awali basins can be mainly related to the hydrology and morphology of the catchments. The elevated number of flood events in Beirut river basin along with urban Beirut is a result to its high vulnerability to floods. The flooding in the Damour river basin is a combination of the three characteristics. Hence, the developed spatial flood occurrence map is a combination of the flood hazard and the vulnerability to flooding and would be equivalent to a flood risk map.

The extracted events from newspapers and previous reports form a documentary evidence which is promising in retrieving information on previous flood events in the pre-instrumental period and in the absence of data measurements. Such information allows for the first time analyzing the frequency of occurrence of flood events along with mapping their spatial occurrence over the whole country. The map when overlaid over the vulnerability map is helpful in highlighting high risk areas and can be treated as a flood risk map in the absence of detailed studies. Results may not be clear but there is an opportunity to understand the floods and the changes in their regimes.

However, these records remain descriptive focusing on the event's damages more than its characteristics. The map is developed on a large scale (district scale), which does not allow the detailed analysis to obtain information on the flood flows, water levels and extent. Such information is indispensable in any detailed flood mitigation project or flood forecasting system. Hence, the developed map cannot replace the need for a detailed hydrological-hydraulic modeling of the river catchment to establish flood flows and water levels. In this regard, we selected the Awali River Basin, a study site to perform detailed analysis and modeling.

The selected detailed modeling approach should balance data availability in Lebanon (being a data sparse country) with model complexity, and the question arises on the choice of this cost-effective modeling approach. Hence, there remains a need to develop a cost-performance grid to evaluate flood modeling approaches.

The second part of the thesis (chapters 6 and 7) presents the developed cost-performance grid for flood modeling evaluation and the third part (chapters 8 and 9) presents the selected detailed flood modeling framework in data-sparse regions and its application on the selected study site (Awali Basin).

PART II.

A COST-PERFORMANCE ANALYSIS GRID FOR FLOOD MODELING

In Part I, we have shown that although extracted events from newspapers and previous reports are promising in retrieving information on previous flood events, the developed spatial flood occurrence map cannot replace the need for a detailed hydrological-hydraulic modeling of the river catchment to establish flood flows and water levels suitable for detailed flood mitigation and forecasting projects. The selected detailed modeling approach should balance data availability in Lebanon (being a data sparse country) with model complexity, and the question arises on the choice of this cost-effective modeling approach. Hence, there remains a need to develop a cost-performance grid to evaluate flood modeling approaches.

In this part we develop a new cost-performance grid to analyze different flood modelling approaches presented in literature to draw out some conclusions on how to select the proper flood modelling approach for our study by balancing model complexity and data availability. We define metrics to quantify the three axes of any modelling problem: data availability, model complexity, and modelling performance. The developed grid is applied on ten study cases of flood modeling presented in literature, including our study case (presented later in chapters 8 and 9). The part ends with a discussion on the opportunities and limitation of the proposed grid. This part forms an article that will be submitted shortly.

Chapter 6 presents a proposed cost-performance grid for flood modelling evaluation.

Chapter 7 is an application on the grid, it analyses different flood modelling approaches, and discusses the opportunities and limitations of this grid.

6 THE PROPOSED COST-PERFORMANCE GRID

6.1 **Introduction**

The choice of the modeling approach is largely governed by three main factors: the nature of the prototype system or study site, the objective of modeling, and the nature of input and output data. The adequate definition of the problem, modelling objective, is the primary step towards the successful application of the modeling approach (Dooge, 1981). Once the modelling objective is defined, numerous combinations of data, models and performance criteria are possible.

The choice of selection of a flood modelling approach is affected by many factors these include the type and quality of available observational data, objective of modelling (hazard maps, damage and risk assessment, flood forecast, etc..), country of application, modeler capabilities and experience, type of the flood event (low or extreme event), size/scale of the study site, year of application, etc.

Based on the wide variety of models available, many model configurations are possible. In this chapter we present the structure of a proposed cost-performance analysis grid to evaluate and compare flood modelling approaches, we define several categories and scales for defining the modelling costs and assessing their performance.

6.2 **Methodology**

We define a “simple model” by the model that is able to meet the objective of modeling by reproducing the system behavior efficiently with minimal level of complexity; i.e. based on a low cost and giving high performance. The choice of selection of this “simple model” depends on balancing the modeling costs with the modeling performance.

The “modelling cost” is a measure of the “data availability” which is the amount and quality of the data used for model simulation, calibration, and validation, and the “model complexity” which is the detail of process representation by the model. In this regard, we hypothesize that the “cost of data” is directly proportional to data availability, and the “cost of models” is directly proportional to model complexity. The more data is available in terms of quantity and quality, the higher is the cost of data. Similarly, the more complex the model is the higher is the cost of the model. The total cost of a modeling approach is therefore a function of the cost of data and the cost of models. The general relationship can be illustrated as follows in Eq. 6.1 to 6.3:

$$\text{Cost of data} \propto \text{Data availability} \tag{6.1}$$

$$\text{Cost of models} \propto \text{Model complexity} \tag{6.2}$$

$$\text{Cost of modeling} = f(\text{cost of data, cost of models}) \tag{6.3}$$

In economics, the total cost of any project or plan is the summation of all costs paid in every stage of the project; the total cost you pay to realize a project is the sum of every penny you pay during the project. The addition of costs here is associative and commutative; the order of paying money in every stage does not change the total cost you pay. In this regard, we suggest that the total cost of a modeling approach is a sum function; it is the direct sum of the cost of data and the cost of models.

We define the measure of data availability as "cost of data", denoted as C_D, and the measure of model complexity as "cost of model", denoted as C_M. The modeling cost denoted as C_T is the sum of the cost of data and cost of models and is a measure of the overall complexity of the modeling approach. The more data is required and the more complex the model is, the higher is the modeling cost. The general relation between the cost of data and cost of models is presented in Eq. 6.4.

$$C_T = C_D + C_M \qquad (6.4)$$

The "modelling performance", denoted as P_M, is a measure of how well the model is able to reproduce the system behavior, and how much the modeling outcomes fit to observations and satisfy our understanding of the hydrological processes under study.

Figure 6.1 illustrates the conceptual relationship between the three components of a modelling problem: data availability (X-axis), model complexity (Y-axis) and the prediction performance (Z-axis). Figures 6.1a and 6.1b are the projections of Figure 1.2 in the (X-Z) plane and (Y-Z) plane respectively.

In the (X-Z) plane (Fig. 6.1a), and for a given model complexity, adding more data increases the model predictive performance up to a level where additional data does not improve the performance of the model because the model is no more able to exploit all the information in the data. This is the best performance a model can give based on its complexity level, adding more complexity to the model can exploit more information in the data and improve performance.

Similarly, in the (Y-Z) plane (Fig. 6.1b), and for a given condition of data availability, additional model complexities lead to better model performance reaching an optimum complexity beyond which identifiability problems arise and reduce the model performance. This is because the more complex model has many parameters but not enough data to be verified and tested for reliability. Perhaps this is the most common problem in modelling exercises where too complex models are being used with limited data availability. Either such too complex models should be avoided and replaced with simpler ones or an increasing number of data is required to reach adequate reliability (Grayson and Blöschl, 2001).

Figure 6.2 illustrates our suggestion of the conceptual relationship between modeling costs and modeling performance. The performance of the modelling approach increases with the cost of modelling up to a point where the ratio of the performance to costs, performance-cost ratio denoted as PC, is the highest (Eq. 6.5). Beyond this point adding modelling cost increases the performance at lower rates, up to a level where higher

modelling costs does not add any considerable performance and may reduce the prediction performance. In practical applications there is a minimum mandatory cost that should be paid which represents the basic data required to run the model and the minimal model complexity at which a representative model can be developed.

$$PC = \frac{P_M}{C_T} \qquad (6.5)$$

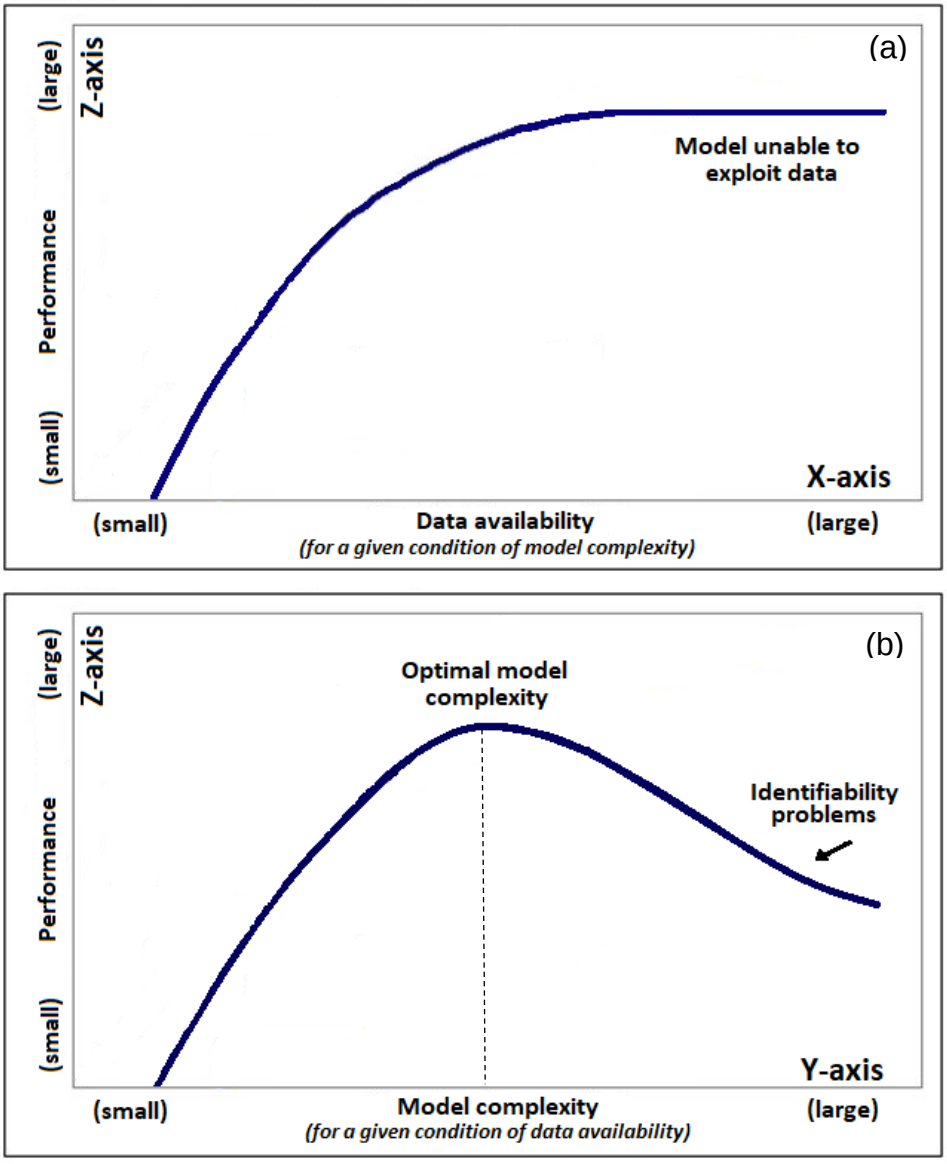

Figure 6.1 (a) The conceptual relationship between data availability and model performance for a given condition of model complexity (X-Z plane), (b) the conceptual relationship between model complexity and prediction performance for a given condition of data availability (Y-Z plane).

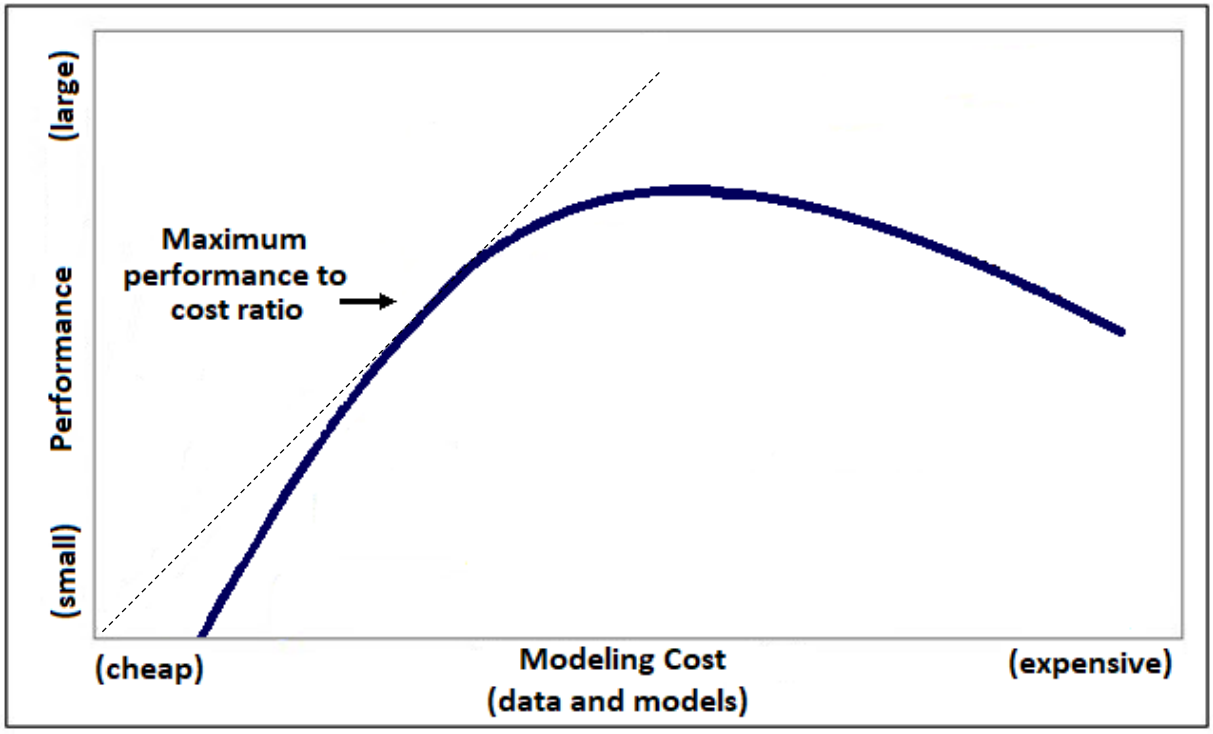

Figure 6.2 The conceptual relationship between modelling cost and modelling performance.

*6.2.1 **The modelling cost***

We define the cost of modeling as the relative cost that encompasses all data utilized (in terms of amount and quality) and resources/models expended (in terms of complexity) to perform the modeling approach. One should distinguish between the relative cost defined here and the actual cost defined in economy as the net amount of money paid to perform the approach. The actual cost (value) is highly variable from one case to another depending on the country of application, availability of data, expertise, and models. It may also differ from one application to another; for example, research centers tend to use their own models that they are familiar with which might be more complex but cheaper if compared to purchasing new modeling software of lower complexity. Whereas, the relative cost is a qualitative measure of the modeling approach that depends on the type, amount and significance of data used and on the complexity of model applied despite the real amount of money paid.

To evaluate the total cost of modeling, we define certain metrics to evaluate the cost of data and cost of models. Figure 6.3 presents a schematic diagram developed to evaluate such values.

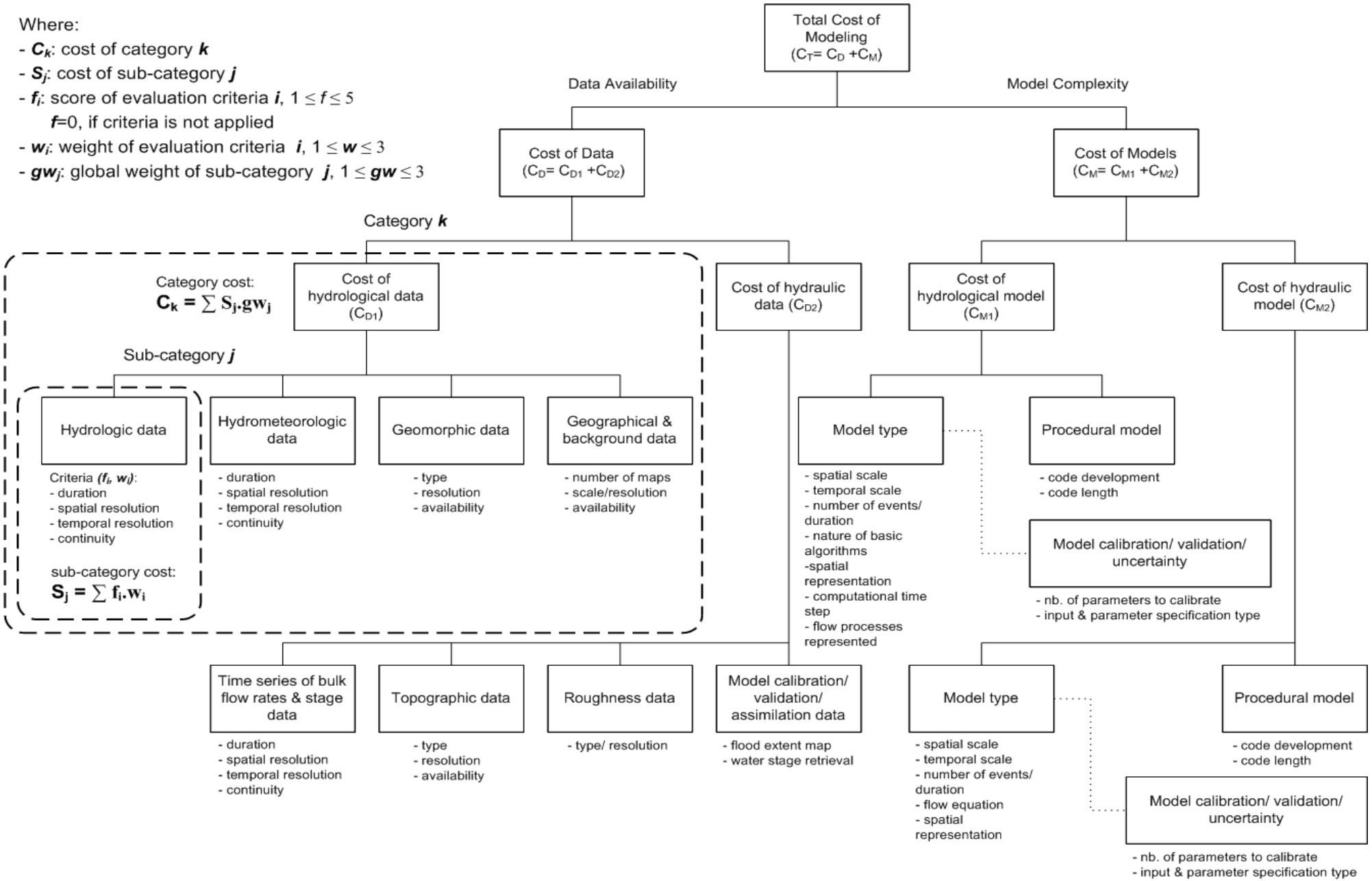

Figure 6.3 Schematic diagram presenting the cost evaluation criteria for data and models.

Data and models are categorized into main categories and subcategories based on data types and model representations. Quantitative or qualitative evaluation criteria are defined for each subcategory to calculate its cost. For the cost evaluation we suggest incorporating a “weighted sum model”. The weighted sum model is the best known and simplest multi-criteria decision model often used for multicriteria decision making projects. i.e. for evaluating a number of alternatives in terms of a number of decision criteria that may influence the choice or decision. The reason for selecting this model is primarily because the total cost is a sum function, as demonstrated before, and secondly to give some elements more "weight" or influence on the result than other elements in the same category or subcategory. This is because some evaluation criteria are more significant than the others and are thought to more impact the quality of data or complexity of models. Say for example, for an event-based flood modeling approach, the spatial or temporal scale of the hydrometeorological data are more significant than the duration of data available, and hence those evaluation criteria (spatial and temporal scale) should be associated with higher weights compared to the other evaluation criterion (duration).

For this reason and to emphasize on the significance of some evaluation criteria with respect to the others, weights, denoted as ***w***, are given to each evaluation criteria. Higher weights imply more significant evaluation criteria. Similarly, within the same category, some subcategories are more significant than the others, and accordingly global weights, denoted as ***gw***, are given to each subcategory.

Indeed, the cost of modeling cannot be presented in monetary values, because some of the cost evaluation criteria are qualitative measures that cannot be compared or summed up together. For this reason, we choose to calculate the cost of each evaluation criteria based on a scoring system, i.e. the cost of the evaluation criteria is defined on a scale of scores, denoted as ***f***, higher score refers to a more expensive measure which is mostly a more complex measure. This is similar to the grading system used in universities and schools to evaluate the total mark of a student. In a subject exam (here a sub-category), each question (here evaluation criterion) is given a certain grade (here score), and the total mark in an exam (here cost of sub-category) is the sum of grades of all questions. Also, the total mark of a student (here total cost of modeling) is the weighted sum of all grades given for each subject. The weighted sum is applied to emphasize on the importance of one subject with respect to the others.

Moreover, one should mention that the grading system is variable from one country to another or from an institution to another. This is because each country has its own grading strategy. Say for example the French system suggests a 20-point grading scale. With a grade from 16 to 20 is given an honor “very good” (très bien: TB), and a grade from 0 to 9.9 is considered a “fail” (insuffisant). The American grading system suggests a numerical grading scale from 0 to 100 which is broken down into a letter grade of five levels as well (A, B, C, D and F), with A considered the highest grade and F considered a fail grade.

In our approach several scoring scales would be suggested to evaluate the cost of an evaluation criterion. We propose to calculate the score ***f*** of an evaluation criterion based on a scale of five levels, an approach similar to the US 5 levels grading system. The values

of ***f*** range from “Very Low” (VL) indicating the lowest score which corresponds to the lowest cost/quality/quantity to “Very High” (VH) indicating the highest score which corresponds to the highest cost/quality/quantity. “Low” (L) indicates a low score, “Medium” (M) indicates a medium score, and “High” (H) indicates a high score. Similarly, and for simplification, the weights are evaluated in three influence levels: low influence (L), medium influence (M), and high influence (H).

Let ***S*** denote the total cost of a sub-category ***j***, hence the cost S_j of a sub-category ***j*** can be evaluated following Eq. (6.6):

$$S_j = \sum f_i . w_i \qquad (6.6)$$

For a given sub-category ***j***, f_i is the score of evaluation criterion ***i*** rated on a scale of five levels {(VL), (L), (M), (H), and (VH)}, ***f*** is zero if the criterion is not applied. w_i is the weight of evaluation criterion ***i*** of value (L), (M), or (H).

Let ***C*** denote the total cost of a category, hence the total cost C_k of a category ***k*** can then be evaluated following Eq. (6.7):

$$C_k = \sum S_j . gw_j \qquad (6.7)$$

For a given category ***k***, gw_j is the global weight of sub-category ***j*** of value (L), (M), or (H).

In typical flood modeling approaches we distinguish four main categories, the first category corresponds to the cost of data for hydrological model (C_{D1}), the second category corresponds to the cost of data for hydraulic model (C_{D2}), the third category corresponds to the cost of the hydrological model (C_{M1}), and the fourth category corresponds to the cost of the hydraulic model (C_{M2}). Flood modeling approaches do not necessarily cover the four categories but may for example cover the C_{D1} and C_{M1} categories if the application is solely a hydrological modeling approach. In this case, the cost of the other categories (C_{D2} and C_{M2}) will be zero. In what follows the hydrological and hydraulic models will be denoted as model 1 and model 2 respectively.

6.2.2 ***The cost of data***

The choice of selection of the models is dictated by the nature and quality of data available and data requirements for modeling. Hydrological and hydraulic models differ largely in terms of data requirements.

In flood inundation modeling approaches that involve a hydrological model, either alone or coupled with a hydraulic model, the most common practice is the application of a rainfall-runoff model to simulate flood producing rainfall events and estimate the flood discharge. Overland flow and channel flow are the major processes simulated by these models. Classically, rainfall is the major input data and runoff is the basic observational data for calibrating and validating the model. With the advance of physically based distributed models, more processes are being represented such as evapotranspiration, sub-surface flow, and ground water flow that require extensive data such as high-resolution digital elevation models, discretization into saturated and unsaturated zones, vegetation cover, soil profiles, etc. The more processes are represented by the model the more are their data requirements.

Data requirements for watershed hydrology modeling were distinguished by Singh and Woolhiser (2002) in six categories: hydrologic data, hydrometeorologic data, geomorphologic data, agricultural data, pedologic data, and geologic data. Hydrologic data includes all hydrological variables such as flow depth, discharge, and base flow. Hydrometeorologic data includes all meteorological variables such as rainfall, snow, humidity and temperature. Geomorphic data represents the topography of the study site in the form of topographic maps or digital elevation models (DEM's). Agricultural (land use and vegetation cover), pedologic (soil information), and geologic (stratigraphy and lithology) data can be grouped in one category named "geographical and background data".

The first two subcategories, hydrologic and hydrometeorologic data, are evaluated following Table 6.1. Four evaluation criteria are assigned to these two subcategories those include: duration of the dataset, spatial resolution of the data (point gauge data versus spatial measurement), temporal resolution of the data (monthly and daily time step of measurement versus hourly or less time steps), and the completeness or continuity of the dataset (gaped data versus time series).

In the presented evaluation table, we present our suggestion on how to evaluate the scores for each evaluation criteria. For example, for the temporal resolution evaluation criterion, higher scores are associated with finer time steps; a score of (VL) is given for a temporal resolution equal or exceeding a monthly time step, a score of (M) is given to daily time steps, and a score of (VH) is given to hourly time steps or less. We suggested the daily time step to be in the middle (score "M") because this is a common case in most countries. Nowadays, daily rainfall measurements are typically recorded by using simple traditional rain gauges and are often available in most countries equipped with monitoring networks.

Moreover, the tables also present our suggestion of the weights associated with each evaluation criterion. For simplification, we choose to present the weights in three levels low (L), medium (M), and high (H). These weights can be understood as the relative influence of each evaluation criterion on the cost with respect to other evaluation criteria in the same sub-category. i.e. evaluation criteria that are thought to have more influence on the cost of a sub-category are given higher weights with respect to the others.

Geomorphic data are evaluated following Table 6.2. For this sub-category three evaluation criteria were assigned those include: the type of the geomorphic information obtained (topographical maps versus gridded elevation data such as DEM's), the scale or resolution of the data (coarse resolution in the order of hundreds of meters versus fine resolution in the order of 10 meters), and the availability of the data (whether available, developed, or purchased). The resolution of geomorphic data is associated with the highest weight and the availability of such data is associated with the lowest.

Geographical and background data are evaluated following Table 6.3. For this sub-category three evaluation criteria were assigned those include: the number of maps required to build the model (land use map, soil map, geology map, vegetation cover map, etc.), the scale or resolution of the data (large scale versus small scale), and the availability of the data (whether available, developed, or purchased).

Table 6.1 evaluation criteria for hydrologic and hydrometeorologic data of the hydrological model.

Hydrologic and Hydrometeorologic data	**Scores**					**Weight**
Evaluation criteria	**VL**	**L**	**M**	**H**	**VH**	
Duration	≤ 1 M	1Y	10 Y	50 Y	≥ 100 Y	M
Spatial resolution	point data/ ground gauge		remote sensing		spatial measurement	H
Temporal resolution	≥ monthly		daily		≤ hourly	H
Continuity/ completeness	many gaps		some gaps		time series	L

Table 6.2 evaluation criteria for geomorphic data of the hydrological model.

Geomorphic data	**Scores**					**Weight**
Evaluation criteria	**VL**	**L**	**M**	**H**	**VH**	
Type	cartographic	Remote sensing (ex: SRTM)	aerial photogrammetry, LIDAR	+ sonar bathymetry	Ground surveying	M
Scale/resolution	low resolution ≥100 m	90 m	60 m	30 m	high resolution ≤ 10 m	H
Availability	Open source/ available		developed		purchased	L

Table 6.3 evaluation criteria for geographical and background data of the hydrological model.

Geographical and background data	**Scores**					**Weight**
Evaluation criteria	**VL**	**L**	**M**	**H**	**VH**	
Number of maps	1	2 maps	3 maps	4 maps	≥ 5 maps	H
Scale/resolution	large scale				small scale	M
Availability	Open source/ available		developed		purchased	L

From a hydraulic modeling perspective, data requirements for flood inundation modeling have been summarized and discussed several times in literature (Bates, 2004; Mason et al., 2010; Smith et al., 2006), these can be divided into four major sub-categories: topographic data to construct the model grid, time series of bulk flow rates and stage data to provide model inflow and outflow boundary conditions, roughness coefficients of channel and floodplain, and data for model calibration, validation, and assimilation.

Topographic data are evaluated following Table 6.4. High accuracy digital elevation models are the major topographic data requirement by hydraulic models to represent the ground surface and overland flow controlling structures. Classically topographic data was obtained either through expensive and time-consuming field surveys in the form of cross sections perpendicular to the channel or by using the available national topographic maps which are often of low accuracy and poor spatial resolution. Nowadays, with the evolution of the remote sensing techniques digital elevation models are obtained for wider areas with higher accuracy compared to national topographic maps.

Topographic data is evaluated based on three criteria: the type of topographic data, the scale or resolution of the data, and the availability of the data. This similar to the geomorphic data of the hydrological model, the only difference is that higher scores are given to the resolution of the data, because hydraulic models require more accurate topographic data than hydrologic models. Hydraulic modeling in rural areas require a DEM accuracy of at least 10 m (Mason et al., 2010), whereas modeling in urban areas require a spatial resolution of 0.5 m to resolve gaps between buildings (Smith et al., 2006).

Roughness data are evaluated following Table 6.5. In general, roughness values are preliminarily assigned based on expert knowledge using two separate global coefficients, one for the channel and the other for the floodplain and then it is usually estimated by calibration. However, such calibration results in a compensation for model structural and input flow errors and it is often difficult to disentangle the contribution due to friction from that attributable to compensation (Mason et al., 2010) . Ideally roughness data has to be calculated based on the physical and biological variables of the channel and the floodplain and should reflect the actual spatial variability of friction.

Information on the flood extent and the water levels are important for the calibration and validation of the hydraulic models. Traditionally, mapping the flood extent was done through intensive field surveys directly after the flood event. However, these surveys remain very time consuming and relatively expensive especially for large inundation areas. Nowadays, with the advancement of the remote sensing techniques, flood extent mapping can be obtained from relevant satellite images or through drone/aerial photography surveys, both thought to be cheaper than heavy ground surveys. Classically information on water levels was obtained from stage gauge records or through post-events measurements. Both measurements do not allow to study the spatial variability of water levels and hence may impact the efficiency of the model in reproducing the flood event and flood plains. Today, spatial measurements of water stage can be obtained from satellite images or altimeters. (refer to Table 6.6).

Table 6.4 evaluation criteria for topographic data of the hydraulic model.

Topographic data	**Scores**					**Weight**
Evaluation criteria	**VL**	**L**	**M**	**H**	**VH**	
Type	cartographic	Remote sensing (ex: SRTM)	aerial photogrammetry , LIDAR	+ sonar bathymetry	Ground surveying	M
Scale/ resolution	low resolution ≥100 m	50 m	10 m	5 m	high resolution ≤ 1 m	H
Availability	Open source/ available		developed		purchased	L

Table 6.5 evaluation criteria for roughness data of the hydraulic model.

Roughness data	**Scores**					**Weight**
Evaluation criteria	**VL**	**L**	**M**	**H**	**VH**	
Type/resolution	static global coefficients				spatial based on LUC, measurement, etc..	1

Table 6.6 evaluation criteria for calibration and validation data of the hydraulic model.

Data for model calibration/ validation/ assimilation	**Scores**					**Weight**
Evaluation criteria	**VL**	**L**	**M**	**H**	**VH**	
Flood extent mapping	descriptive, pictures /witnesses		Remotely sensed: satellite images	aerial / drone photography	field surveys	1
Water stage retrieval	@ gauge station	post-event measurements of maximum marks	Indirect: aerial photography or satellite imagery on Topo maps	Direct: SRTM/ SWOT/ InSAR	Direct: Altimeter on board of satellite emits radar wave	1

6.2.3 *The cost of models*

The scientific literature agreed on the difficulty of providing a common classification scheme for hydrologic models. Several authors proposed different model classification schemes (Dooge, 1981; Kampf and Burges, 2007; Refsgaard, 1996; Singh and Woolhiser, 2002). Dooge (1981) proposed several classification criteria for mathematical models for 34 papers presented at a previous symposium, Singh and Woolhiser (2002) provided a comprehensive compendium of available catchment models and discussed some data and modeling requirements. Kampf and Burges (2007) reviewed and compared different spatially distributed models and proposed criteria for model comparison based on the model representation of flow processes in time and space. The latter is among the best classification schemes proposed for hydrological models. We therefore suggest to develop our cost evaluation criteria following the classification proposed by Kampf and Burges (2007) with minor modifications and eliminations for simplification.

Our methodology for cost evaluation of the hydrological model is suggested as follows: The cost is evaluated based on two main sub-categories; model type and model code (procedural model). The model calibration, and uncertainty analysis methods are also thought to impact the complexity of the modeling approach. Although the latter maybe considered as part of the model type, we suggest keeping it in a separate sub-category.

The hydrological model type subcategory is evaluated based on the model representation of water flow pathways in space and time in seven evaluation criteria: spatial scale (single hillslopes versus continental scale), temporal scale (event-based or continuous), number of events (if event-based) or duration (if continuous), nature of basic algorithm (empirical, conceptual, or physically based), spatial representation (lumped, semi-distributed, or distributed), computational time step (time step of model runs, monthly, daily or hourly…), and flow processes represented (overland flow, channel flow, subsurface flow, other processes…). Indeed, several other evaluation criteria may exist such as those related the model parametrization and computational schemes, the user interfaces and the sensitivity analysis packages, but these model features remain peripheral to the core structure configuration. Also having to mention, that for typical flood modeling approaches, hydrological models are mainly meant to reproduce the rainfall-runoff processes and hence do not requires extra complexity. Perhaps these are the major evaluation criteria that may impact the model type and its complexity (Refer to Table 6.7).

There are several studies in literature that compare and benchmark different hydraulic models of variable complexities aiming at the selection of the best model structure for flood inundation modeling (Chatterjee et al., 2008; Dimitriadis et al., 2016; Horritt and Bates, 2002; Liu et al., 2018; Neal et al., 2012b). most studies agree that the nature of flow equations and the spatial representation of the hydraulic model are the basic characteristics that impact the complexity of a hydraulic model. In what follows, the cost/complexity evaluation of the hydraulic model type is based on five evaluation criteria: spatial scale (global versus reach scale), temporal scale (event-based or continuous), number of events (if event-based) or duration (if continuous), flow equations (empirical vs

complete Saint-Venant equation), and the model spatial representation (1D, 2D, Quasi 2D, or 3D), with the last two criteria being the key evaluation criteria and hence given the highest weights. Table 6.8 presents the evaluation criteria for the hydraulic model type.

Another factor that can impact the model cost and complexity is the model code. For instance, building a new model code is much expensive (in terms of time consumed and expertise employed) than using available and developed model codes. Moreover, purchasing a new modeling software rather than using available freeware would also add costs to the modeling approach. Similarly, the code length may also be an indication of the model complexity. Models of short codes are generally less complex than models of very long codes and algorithms. Hence, the code development and the code length are the two evaluation criteria suggested for the evaluation of the model code for both hydrologic and hydraulic models. Refer to Table 6.9 for the representation of the evaluation criteria and corresponding scores of cost evaluation.

The model calibration and uncertainty evaluation strategy can also impact the modeling cost and complexity. Although these may be indirectly related to the model type, but we choose to keep them in a separate sub-category because the calibration and uncertainty evaluation strategy can highly influence the model performance. Many authors in literature have pointed at the importance of model calibration and uncertainty evaluation in the model predictions (Aronica et al., 2002; Papaioannou et al., 2017). For simplification, we choose to evaluate the cost of calibration based on the “number of parameters to calibrate”; the more parameters selected for calibration the higher is the modeling cost. For instance, applying an uncalibrated model may be cheaper than applying a simpler model with many parameters and rounds of calibration. Similarly, we choose to reflect the uncertainty evaluation criteria by the “type of input and parameter specification”. Models that do not involve uncertainty evaluation are said to be deterministic models. Some applications involve a stochastic input, others involve stochastic parameters, some are more complex and involve both stochastic input and parameters, and few approaches are performed in an uncertainty evaluation framework. Table 6.10 presents the evaluation criteria suggested for calculating the calibration and uncertainty analysis costs.

Table 6.7 evaluation criteria for hydrological model type.

Hydrological model type			**Scores**			**Weight**
Evaluation criteria	**VL**	**L**	**M**	**H**	**VH**	
Spatial scale	global	continental	regional	basin	parcel	L
Temporal scale	event-based				continuous	M
Number of events (if event-based)	1	5	10	15	≥ 20	L
Duration (if continuous)	≤ 1 M	1Y	10 Y	50 Y	≥ 100 Y	L
Nature of basic algorithm	empirical/ black box	regression	conceptual		physically based	H
Spatial representation	lumped		semi-distributed		distributed	H
Computational time step	coarse fixed time step (> day)				fine adaptive time step (< hour)	L
Flow processes presented	overland flow		+channel flow	+sub-surface flow	+other processes	L

Table 6.8 evaluation criteria for hydraulic model type.

Hydraulic model type			**Scores**			**Weight**
Evaluation criteria	**VL**	**L**	**M**	**H**	**VH**	
Spatial scale	global		regional		reach scale	L
Temporal scale	event-based				continuous	M
Number of events (if event-based)	1	5	10	15	≥ 20	L
Duration (if continuous)	≤ 1 M	1Y	10 Y	50 Y	≥ 100 Y	L
Flow equations	empirical/ black box	uniform flow formula	Kinematic wave	Diffusive wave	Complete SV	H
Spatial representation	1D		2D	Quasi 2D/ subgrid	3D	H

Table 6.9 evaluation criteria for the model code.

Procedural model			**Scores**			**Weight**
Evaluation criteria	**VL**	**L**	**M**	**H**	**VH**	
Code development	"Ready-to-wear"		Modify existing code		"Tailor-made"	M
Code length	Simple code				Complex code	L

Table 6.10 evaluation criteria for the model calibration, validation and uncertainty analysis.

Model calibration/ validation/ uncertainty evaluation			**Scores**			**Weight**
Evaluation criteria	**VL**	**L**	**M**	**H**	**VH**	
Number of parameters to calibrate	1		5		> 10	1
Type of input & parameter specification	deterministic		stochastic input	stochastic parameters	stochastic parameters & input	1

6.2.4 ***The modeling performance***

The value and reliability of models affect their performance and efficiency. This is dependent on different factors including the parameter identifiability (uncertainty), the physical process description, and the applicability domain (Brocca et al., 2011). Moreover, the number and type of criteria functions used to evaluate the model are an indication of the performance of the model. Many efforts have been made to compare model outputs with another but model structures differ a lot so that it's difficult to predict the reason for difference in model performance (Kampf and Burges, 2007).

For model performance evaluation, we suggest that the best model performance is understood in how well the model is able to meet the modeling objective with minimal level of error. i.e. how well the model outputs answer the model problem and fit the real or observed values.

In a typical flood modeling approach, we are concerned in four levels of output: the peak flood discharge value, the flood flow hydrograph, the flood water stages, and the flood inundation extent. The model's performance is measured in what type of output it gives and how efficient is the model in predicting the flows, water levels and extent with minimum error levels. For instance, and when the objective of the modeling is flood inundation mapping, models that can only predict flood peak discharge and hydrographs are considered unsatisfactory and hence are rated less in terms of efficiency. Moreover, in any modeling approach the more the criteria functions utilized to evaluate and validate the model the better are the expected results.

In this approach we choose to evaluate the modeling performance based on a fixed objective; flood inundation map. Hence, the modelling performance can be evaluated following Table 6.11 based on six evaluation criteria: the type of output obtained, criteria functions used, and the error value for each level of output. i.e. value of the criteria functions to evaluate the peek flow and volume error, hydrograph error, water level error, and flood extent error. The highest weight is given to the type of output, because this plays a big role in assessing the suitability of the applied modeling approach. The method of evaluation of the modeling performance (criteria functions used) is given a moderate weight, and the error levels are given a low weight compared to the previous two evaluation criteria.

Table 6.11 evaluation criteria for model performance.

Performance	**Scores**					**Weight**
Evaluation criteria	**VL**	**L**	**M**	**H**	**VH**	
Type of output	Peak flood discharge/ flood volume	Flood flow hydrograph at outlet	Flood flow hydrograph at different locations	Flood water levels	Flood inundation map	H
Criteria function	single variable/ single criteria				Multi-variable/ multi-criteria/ multi-site	M
Peak flow and volume error (% error)	≤ 50%	30%	10%	5%	0%	L
Hydrograph error (ex: Nash)	≤ 0.5	0.6	0.7	0.8	1	L
water level error (ex: RMSE)	> 200 cm	150 cm	100 cm	50 cm	≤ 10cm	L
flood extent error (ex: skill of mapping)	0	0.4	0.6	0.8	1	L

6.3 **The cost-performance survey**

In the previous sections of chapter 6, we have presented the whole structure a cost-performance analysis grid. The second step involves collecting information on different flood modeling approaches in literature to test the grid, evaluate the results and give an illustration on how to use the proposed grid. However, the presented grid makes use of a big amount of information relevant to each study case, and it will not be an easy exercise to group and arrange the information in a clear and well-organized database.

Furthermore, although the selection of the evaluation criteria and their corresponding scores and weights has been performed based on our expert knowledge in flood modeling procedures, these selections only reflect our own point of view. Hence, there is a need to collect information and feedback from several colleagues and experts in the field of flood modeling and evaluate their scoring and weighting point of view. For this reason, an online survey has been launched to collect information on different study cases in different countries. The survey allows categorizing all data and models for each study case based on the proposed grid. Participants have the right to select the relevant score based on their understanding of their own approach.

The structure of the developed survey along with a sample response are presented in Annex C. The survey is available online on the following link: https://www.surveymonkey.com/r/RHDEIB082018. It is structured in four parts; Section A is “General Information”, Section B is “Data Availability”, Section C is “Model Complexity”, Section D is “Modeling Performance” and Section E is a “Summary”. There are two categories of questions in the survey: objective questions that involve collecting real data about the study case (data, models...) and subjective questions, marked by (*), that represent the author's point of view, and the author is free to answer or disregard. The survey takes around 23 minutes and it is specified for each study case\report.

6.4 **Conclusion**

In this chapter we have presented the structure of a proposed cost-performance analysis grid for flood modeling. In this approach we hypothesize that the “modelling cost” is a measure of the “data availability” which is the amount and quality of the data used for model simulation, calibration, and validation, and “model complexity” which is the detail of process representation by the model. The “cost of data” is directly proportional to data availability, and the “cost of models” is directly proportional to model complexity.

In this regard we categorized data and models into main categories and sub-categories. The cost of each sub-category is calculated based on defined evaluation criteria. Each evaluation criterion is assigned a score based on five levels (varying from “VL” to “VH”) and a weight (Low, medium, or high) based on its influence on the results compared to other evaluation criteria within the same sub-category. The cost of a sub-category is calculated based on a Weighted Sum Model. Global weights are assigned to

each sub-category to emphasize on its influence compared to other sub-categories, and the total cost is the weighted sum of the costs of all sub-categories.

The modeling performance is calculated based on six evaluation criteria that reflect the type of output obtained, the criteria functions used to evaluate the model, and the values of the error functions corresponding to four levels of output (flood discharge, flood hydrograph, water level, and flood extent).

To collect data on different modeling approaches in literature and to generate a well-organized database, a cost-performance survey has been developed and made available online. The survey allows collecting information on different modeling approaches in a coherent way and based on the proposed cost-performance grid.

In the chapter that follows (chapter 7) we present an application on the proposed cost-performance grid based on ten selected study cases in literature, to demonstrate the methodology employed to calculate the different sections of the grid and to test the efficiency of the proposed grid.

7 APPLICATION ON THE COST-PERFORMANCE GRID

7.1 **Introduction**

In the previous chapter (chapter 6) we have presented the structure of a proposed cost-performance analysis grid for flood modeling. We have defined our main hypotheses in the work, and described the methodology applied for the calculation of the modelling cost and the modeling performance.

In this chapter we present an application on the proposed cost-performance grid based on ten selected study cases in literature, to demonstrate the methodology employed to calculate the different sections of the grid and to test the efficiency of the proposed grid. In this application we do not intend to evaluate or assess the validity of any modeling approach, we basically aim to demonstrate an application on the proposed grid only.

Furthermore, throughout this chapter we suggest some domains of application of the grid and discuss its opportunities and limitations.

7.2 **Methodology**

We recall the discretizing we suggested in chapter 2 for the different flood modeling approaches into six categories:

- Category 1: application of different empirical methods such as measurements, surveys and remote sensing or statistical approaches.
- Category 2: single application of a hydraulic model to simulate flood propagation by solving physical equations of flow dynamics of variable complexity, i.e. in a one-dimensional (1D), two-dimensional (2D) or three-dimensional (3D) approach.
- Category 3: application of simplified conceptual models that do not solve the physical equations of flow dynamics but are based on simplified hydraulic concepts.
- Category 4: applications limited to hydrologic models, mostly rainfall-runoff, to estimate rainfall excess, overland flows and river flood discharges.
- Category 5: applications that involve coupling hydrologic and hydraulic models.
- Category 6: applications based on geomorphic approaches to delineate flood prone areas by using simplified methods that rely on basin geomorphologic feature characterization.

These applications largely differ in terms of type of input data required, computational efficiency and the nature of output variables, their resolution and accuracy.

Our approach involved arbitrarily selecting different flood modeling approaches presented in literature. These approaches were analyzed to extract all the data sets used, models applied, and performance levels evaluated. These data and models were then evaluated based on the evaluation criteria presented in chapter 6 and the corresponding scores and weights were calculated based on tables 6.1 to 6.11.

All scores and rates relative to each selected study case were assigned based on our own understanding of the approach, and thus reflect our own point of view and not the main authors' point of view. In our approach several scoring scales would be suggested to evaluate the cost of an evaluation criterion. We propose to calculate the score ***f*** of an evaluation criterion based on a linear scale of five levels, varying from 1 to 5. 1 indicates the lowest cost/quality/quantity (VL) and 5 indicates the highest cost/quality/quantity (VH). (L) is 2, (M) is 3, and (H) is 4. Similarly, and for simplification, we propose to assign weights and global weights values ranging from 1 to 3. 1 indicates low influence (L), 2 indicates medium influence (M), and 3 indicates highest influence (H).

For each evaluation criterion we also calculate the maximum cost which corresponds to the highest possible score **f(max)**. The maximum possible cost for each sub-category denoted as $\mathbf{C_k(max)}$ is then the weighted sum of all maximum costs of evaluation criteria. A dimensionless cost denoted as $\mathbf{C_{k[1]}}$ can then be evaluated following Eq. 7.1.

$$C_{k[1]} = \frac{C_k}{C_k(\max)}, \qquad 0 < C_{k[1]} \leq 1 \qquad (7.1)$$

Similarly, the dimensionless cost of data $\mathbf{C_{D[1]}}$, models $\mathbf{C_{M[1]}}$ and the total dimensionless cost $\mathbf{C_{T[1]}}$ can be calculated following Eq. 7.2 to 7.4.

$$C_{D[1]} = \frac{C_D}{C_D(\max)}, \qquad 0 < C_{D[1]} \leq 1 \qquad (7.2)$$

$$C_{M[1]} = \frac{C_M}{C_M(\max)}, \qquad 0 < C_{M[1]} \leq 1 \qquad (7.3)$$

$$C_{T[1]} = \frac{C_T}{C_T(\max)}, \qquad 0 < C_{T[1]} \leq 1 \qquad (7.4)$$

Where $\mathbf{C_D(max)}$, $\mathbf{C_M(max)}$, and $\mathbf{C_T(max)}$ are the maximum costs of data, models, and the total maximum cost of modeling.

A maximum performance value, denoted as $\mathbf{P_M(max)}$, is also calculated by assigning the maximum possible score for each evaluation criterion. And the dimensionless performance value, denoted as $\mathbf{P_{M[1]}}$ can be calculated following Eq. 7.5.

$$P_{M[1]} = \frac{P_M}{P_M(\max)}, \qquad 0 < P_{M[1]} \leq 1 \qquad (7.5)$$

The reason behind evaluating these dimensionless values, is to simplify the comparison between different study cases and to interpret the cost levels and performance values obtained.

7.3 **Datasets**

Different flood modelling approaches of variable complexity presented in literature were arbitrarily selected and analyzed to provide guidance on the implementation of the

proposed grid. These studies were part of the bibliographic review performed during the thesis work. Selected cases belong to the flood modeling categories 1, 2, 4 and 5. There is no main reason for this selection but because our first intention was to choose flood modeling categories that apply models similar to our approach suggested in chapters 8 and 9. The study is primarily limited to 10 study cases to test the applicability of the proposed grid. However, an online survey is designed and shared with colleagues working in the same field aiming at collecting information on their modelling approaches. The survey is just launched and will remain open to obtain a sufficient number of study cases for future assessments.

The selected study cases for analysis are presented in Table 7.1. Five study cases are model coupling approaches (study cases 1, 3, 7, 8, and 9) that belong to category 5. Three are hydrological modeling approaches that belong to category 4 (study cases 5, 6, and 10), one is hydraulic modeling approach that belong to category 2 (study case 4), and the last is an empirical approach that belong to category 1 (study case 2).

Among these study cases three are our own studies (Study case 1, 2, and 5) and hence we are familiar with all the data and models employed. Study case 1 (Hdeib et al., 2018) is presented in details in chapters 8 and 9. The approach involves developing a framework for modeling in data-sparse regions. The Study is applied on the Awali river basin in Lebanon (301 km^2), it involves a coupling between a semi-distributed conceptual hydrological model (HEC-HMS) and a 1D hydraulic model (HEC-RAS) to model extreme flood events (category 5). The hydrological model is constrained by 12 past storm events and the hydraulic model is simulated based on different realizations of flood flow hydrographs established based on Monte Carlo uncertainty analysis for the hydrological part. The basic data available are daily rainfall at seven ground gauges, hourly water level measurements at two river gauges, and a fine resolution DEM (10 cm) for the river channel and flood plain based on UAV drone surveys.

Study case 2 (Abdallah et al., 2013) is also applied in the Awali River basin in Lebanon, it involves an empirical approach (category 1) to estimate the flood discharge based on Fuller empirical formula (Salajegheh and Dastorani, 2006) and a 1D hydraulic model (HEC-RAS) to estimate water levels. The approach is deterministic, and the basic available data are daily flow values and post-event measurements at gauge location.

Study case 5 (Moussa, 1991) is a hydrological modeling approach (category 4) applied on the Gardon River in France (542 km^2). It involves developing a new distributed event-based hydrological model based on simplified physical concepts to simulate river flow and establish flow hydrographs. The approach is deterministic, and the model is calibrated based on 30 past storm events. Basic data available are hourly rainfall at seven ground gauges and hourly discharge measurements at two river gauges.

Study case 3 (Knebl et al., 2005) is a flood modeling approach applied on the San Antonio River Basin in Central Texas (10,000 km^2). It involves coupling (category 5) an event-based distributed conceptual hydrological model (HEC-HMS, SCS-CN +Modclark) with a 1D hydraulic model (HEC-RAS) to establish flood inundation maps. The approach

is deterministic, and watershed parameters are calibrated manually to produce a good simulation of discharge at 12 sub-basins. The basic data available are NEXRAD Level III radar rainfall (4x4km), hourly stream flow and water level measurements at 12 USGS river gauges, and Landsat TM images for flood extent evaluation.

Study case 4 (Neal et al., 2012a) is a hydraulic modeling approach (category 2) for simulating the spatially distributed dynamics of water surface elevation, wave speed, and inundation extent over large data sparse domains. The approach is applied on the Niger River in Mali (210,389 km^2). The numerical scheme is based on an extension of the distributed hydraulic model LISFLOOD-FP to include a subgrid-scale representation of channelized flows (2D/1D model), which allows river channels with any width below that of the grid resolution to be simulated. The approach is deterministic, and the model is continuous simulated for 8 years. Basic data available are an SRTM 90m DEM modified to a 905 m DEM and daily discharge values for 8 years. The model is calibrated based on open source 24 Landsat TM5 images for flood extent mapping, and 127 observations of water level from ICESat laser altimeter at 18 locations.

Study case 6 (Coustau et al., 2012) is a hydrological modeling approach (category 4) to establish flood flow hydrographs applied on the Lez River catchment in Montpellier, France (114 km^2). It involves applying an event-based distributed conceptual hydrological model available within the ATHYS modeling platform (modified SCS + linear lag and route). The approach is deterministic, and the model is calibrated based on 21 past-storm events and water levels from 12 piezometers at hourly time step (2000,2008). The basic data available are hourly radar rainfall (1 km^2).

Study case 7 (Koutroulis and Tsanis, 2010) is a flood modeling approach for poorly gauged basins applied on the Giofiros basin in Greece (158 km^2). The approach involves coupling an event-based semi-distributed conceptual hydrological model (HEC-HMS) and a 1D hydraulic model (HEC-RAS) to model flood events (category 5). The hydrological model is calibrated based on 8 past storm events and uncertainty analysis was performed on the input rainfall and on the hydrologic parameters by adding a percent of variation +/- 10%. The hydraulic model is simulated based on different realizations of the flow hydrograph obtained from the hydrological model. The basic data available are daily rainfall measurements from 4 ground gauges, hourly flow measurements at one river stage, available DTM (1/10,000), and post-event field measurements at river gauge location.

Study case 8 (Fuentes-Andino et al., 2017) is a flood modeling approach for ungauged basins with uncertainty analysis within a GLUE framework applied on the floodplain of Tegucigalpa in Honduras (811 km^2). The approach involves coupling (category 5) an event-based distributed physically based hydrological model (TOPMODEL + Muskingum–Cunge–Todini routing) with a 2D/1D hydraulic model (LISFLOOD-FP with subgrid scale). The basic data available are hourly rainfall records for two days from two ground gauges assumed uniformly distributed over the whole area, a LIDAR DTM (15 cm), and around 100 post-event measurements of high water marks along the river channel at 100m spacing.

Table 7.1 Description of the ten arbitrarily selected flood modeling study cases for cost-performance analysis.

Study case ID	Study case	Study Site/ Country	Area [km^2]	Modeling approach	Objective function
Study Case 1	Hdeib et al. (2018)	Awali River Basin, Lebanon	301	(5) Coupling	Flood inundation map
Study Case 2	Abdallah et al. (2013)	Awali River Basin, Lebanon	301	(1) Empirical	Flood inundation map
Study Case 3	Knebl et al. (2005)	San Antonio River Basin, Central Texas, USA	10,000	(5) Coupling	Flood inundation map
Study Case 4	Neal et al. (2012a)	Niger river, Mali.	210,389	(2) Hydraulic 1D/2D	Flood inundation map
Study Case 5	Moussa (1991)	Gardon Basin, France	542	(4) Hydrologic	Flow hydrograph
Study Case 6	Coustau et al. (2012)	Lez catchment, France	114	(4) Hydrologic	Flow hydrograph
Study Case 7	Koutroulis and Tsanis (2010)	Giofiros basin, Greece	158	(5) Coupling	Flow hydrograph
Study Case 8	Fuentes-Andino et al. (2017)	Floodplain of Tegucigalpa, Honduras	811	(5) Coupling	Flood inundation map
Study Case 9	Montanari et al. (2009)	Alzette River (Grand Duchy of Luxembourg)	356	(5) Coupling	Flood inundation, estimation of antecedent moisture condition from volume of runoff
Study Case 10	Liu et al. (2005)	Upper Xixian catchment in Huaihe River, China	10,000	(4) Hydrologic	Flood forecasting

Study case 9 (Montanari et al., 2009) is a model coupling approach for flood modeling (category 5) basically performed for the objective of estimation of antecedent moisture condition from volume of runoff, applied on the Alzette River in the Grand Duchy of Luxembourg (356 km^2). The approach involves coupling an event-based lumped conceptual hydrological model Nash IUH (model developed by Nash (1960); n linear reservoirs of K storage + IUH routing) with a 1D hydraulic model (HEC-RAS). Basic data available are water level values (15 min time step) from 6 stream gauges, rainfall records (15 min time step) from one ground gauge, a LIDAR DEM (2m) with 200 bathymetric cross sections. Model calibration was performed based on Monte Carlo sampling of parameters within intervals of plausible values. The results are evaluated with 84 flood extent marks by GPS, maximum water level measurements at 7 points using a theodolite, and two SAR images (ERS-2 & ENVISAT).

Study case 10 (Liu et al., 2005) is a hydrological modeling approach (category 4) for the purpose of flood forecasting applied to Upper Xixian catchment in Huaihe River, China (10,000 km^2). The approach involves applying a new version of a continuous fully distributed physically based hydrological model (TOPKAPI) that evaluates the runoff depth in each model cell. The approach is deterministic, and the basic data available are rainfall and evapotranspiration records for 1.5 years from 24 rain gauges and 1 evaporation station (6 hr. time step), open source USGS DEM (GTOPO30, 1000m), open source soil texture data (global soils dataset of Reynolds et al. (1999), 10km), and landuse (UMD land cover map of the world, 1 km). the model has around 27 parameters to calibrate, calibration was performed for the first six months period and was chiefly based upon moderate variations of parameter values from those estimated on physical grounds, as in common traditional calibration. The author later assesses four parameter uncertainties by estimating a posterior parameter probability density via Bayesian inference. But here we only choose the first approach for our analysis because we find it more significant.

7.4 **Results**

All costs of data and models and performance levels corresponding to the different study cases were evaluated. Detailed results of the cost-performance analysis for the selected study cases are presented in Table 7.2. Performance levels ranged between 0.33 and 0.82 (dimensionless, 1 indicates maximum possible performance) with study case 9 recording the highest performance level and study case 2 recording the lowest. The total cost of modelling levels ranged between 0.19 and 0.46 (similarly dimensionless, 1 indicates the maximum possible cost) with study case 3 recording the highest modeling cost and study case 2 recording the lowest. The performance-cost ratio ranged between 0.9 and 3.01 with study case 5 recording the lowest performance-cost ratio and study case 4 recording the highest. For the selected ten events, the average total cost of modeling was 0.36 and the average performance level was 0.59. The average cost of data was around 0.23 and the average cost of models was 0.47.

Table 7.2 Results of the cost-performance calculation for ten selected study cases in literature based on the proposed cost-performance grid in chapter 6. Scores are evaluated based on a scale of five levels from 1 to 5. Weights and global weights are evaluated based on three levels 1, 2, and 3. The different parameters are calculated following equations 6.4 to 6.7 and equations 7.2 to 7.5. Refer to Annex D for detailed calculation results, and to the table of abbreviations for parameter description.

Study case ID	**C_D (max)**	**C_M (max)**	**C_T (max)**	**C_D**	**$C_{D\,[1]}$**	**C_M**	**$C_{M\,[1]}$**	**C_T**	**$C_{T\,[1]}$**	**P_M (max)**	**P_M**	**$P_{M\,[1]}$**	**PC = $P_{M\,[1]}$/ $C_{T\,[1]}$**
Study Case 1	460	180	640	183	**0.29**	92	**0.51**	275	**0.43**	45.00	29.00	**0.64**	**1.50**
Study Case 2	460	180	640	69	**0.11**	55	**0.31**	124	**0.19**	45.00	15.00	**0.33**	**1.72**
Study Case 3	460	180	640	210	**0.33**	83	**0.46**	293	**0.46**	45.00	27.00	**0.60**	**1.31**
Study Case 4	460	180	640	115	**0.18**	55	**0.31**	170	**0.27**	45.00	36.00	**0.80**	**3.01**
Study Case 5	460	180	640	155	**0.24**	113	**0.63**	268	**0.42**	45.00	17.00	**0.38**	**0.90**
Study Case 6	460	180	640	150	**0.23**	61	**0.34**	211	**0.33**	45.00	23.00	**0.51**	**1.55**
Study Case 7	460	180	640	139	**0.22**	99	**0.55**	238	**0.37**	45.00	31.00	**0.69**	**1.85**
Study Case 8	460	180	640	154	**0.24**	124	**0.69**	278	**0.43**	45.00	29.00	**0.64**	**1.48**
Study Case 9	460	180	640	151	**0.24**	85	**0.47**	236	**0.37**	45.00	37.00	**0.82**	**2.23**
Study Case 10	460	180	640	120	**0.19**	79	**0.44**	199	**0.31**	45.00	22.00	**0.49**	**1.58**

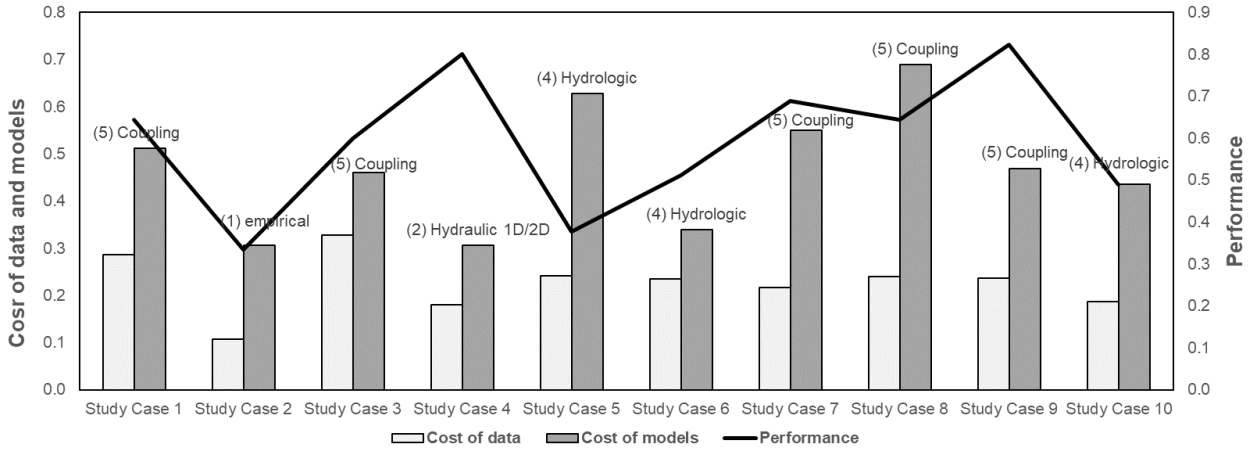

Figure 7.1 Results of the costs and performance evaluation for different study cases.

Figure 7.1 presents the distribution of costs of data and models and the corresponding performances for different categories of modeling. Study case 2 which is an empirical approach is associated with the lowest cost of modelling and the lowest performance ($C_{T[1]}$ and $P_{M[1]}$ are 0.19 and 0.33 respectively), this is not surprising because this is an empirical approach and the only data required are average flow values, estimation of global manning's coefficients, and simple post-event measurements at the river gauge location for validation which minimizes the costs of data and models. Similarly, the low performance value is because the approach only allows the estimation of the flood discharge and water levels at one location (river gauge) and do not allow the spatial validation of the flood inundation.

Study case 8 which is a model coupling approach is associated with the highest cost of models ($C_{M[1]}$ is 0.69), this is because the approach couples two relatively complex models; a distributed physically based hydrological model and a 2D/1D hydraulic model. The whole modeling approach is performed in an uncertainty analysis framework which increases the computational costs. The uncertainty analysis was performed to compensate the lack of observational data to calibrate and validate the models.

Generally, the model coupling approaches (study cases 1, 3, 7, 8 and 9) record the highest cost of models, this is not surprising because compared to other approaches, the model coupling uses two models instead of one, which elevates the model cost. However, study case 5 which is a hydrologic modeling approach also record a high cost of models, this is because the approach uses a new tailor-made hydrological model which elevates the cost of models compared to using available open source models.

The results of the cost-performance analysis are further presented on the graphs below. The total cost of modelling ($\mathbf{C_{T[1]}}$) versus the performance of the modelling approach ($\mathbf{P_{M[1]}}$) is plotted in Figure 7.2, the cost of data ($\mathbf{C_{D[1]}}$) versus the performance of modelling ($\mathbf{P_{M[1]}}$) is plotted in Figure 7.3, the cost of models ($\mathbf{C_{M[1]}}$) versus the performance of modelling ($\mathbf{P_{M[1]}}$) is plotted in Figure 7.4, the cost of models ($\mathbf{C_{M[1]}}$) versus the cost of data ($\mathbf{C_{D[1]}}$) is plotted in Figure 7.5.

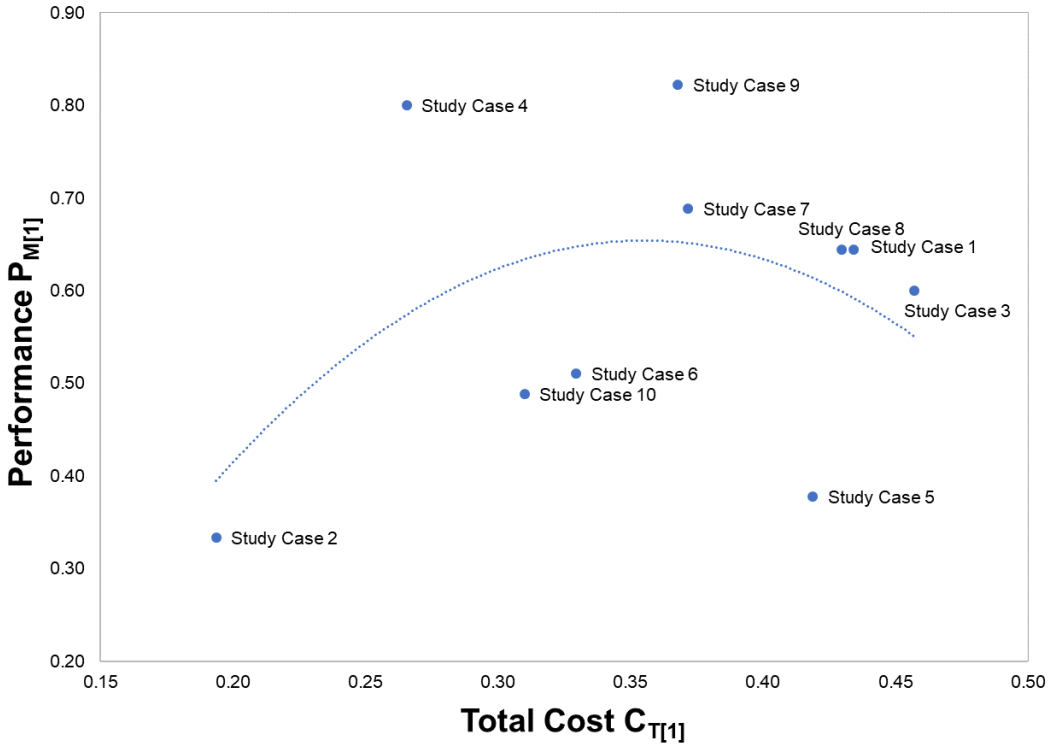

Figure 7.2 Results of the cost-performance analysis for ten selected study cases, the total cost of modelling versus the performance of the modelling approach.

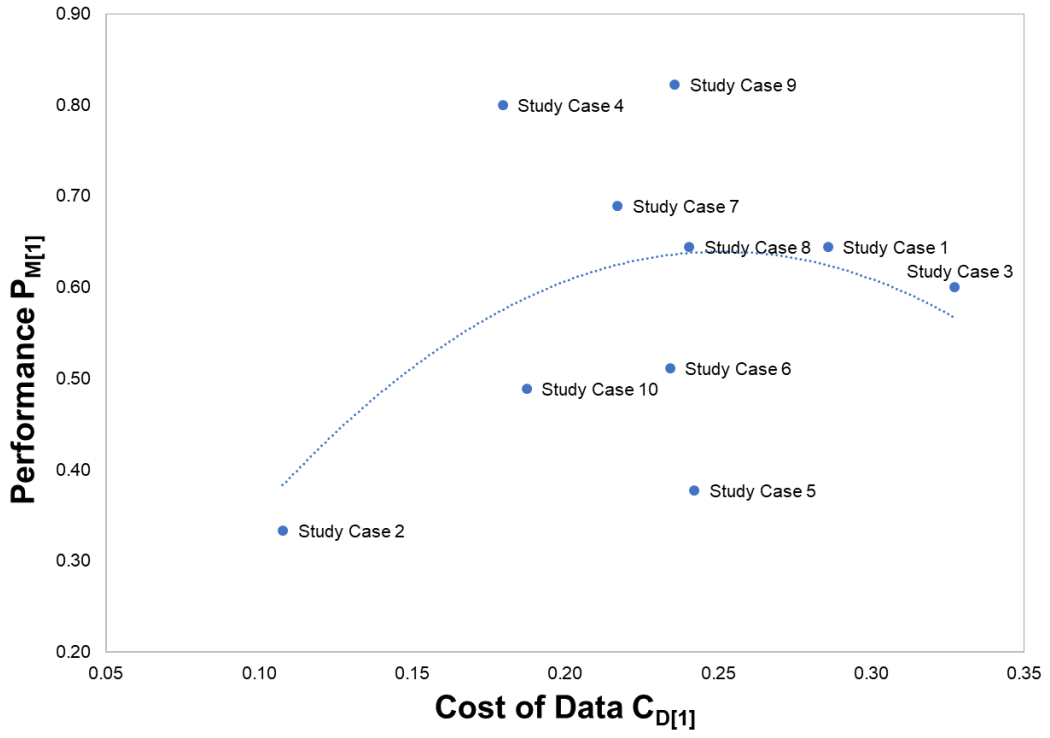

Figure 7.3 Results of the cost-performance analysis for ten selected study cases, the cost of data versus the performance of the modelling approach.

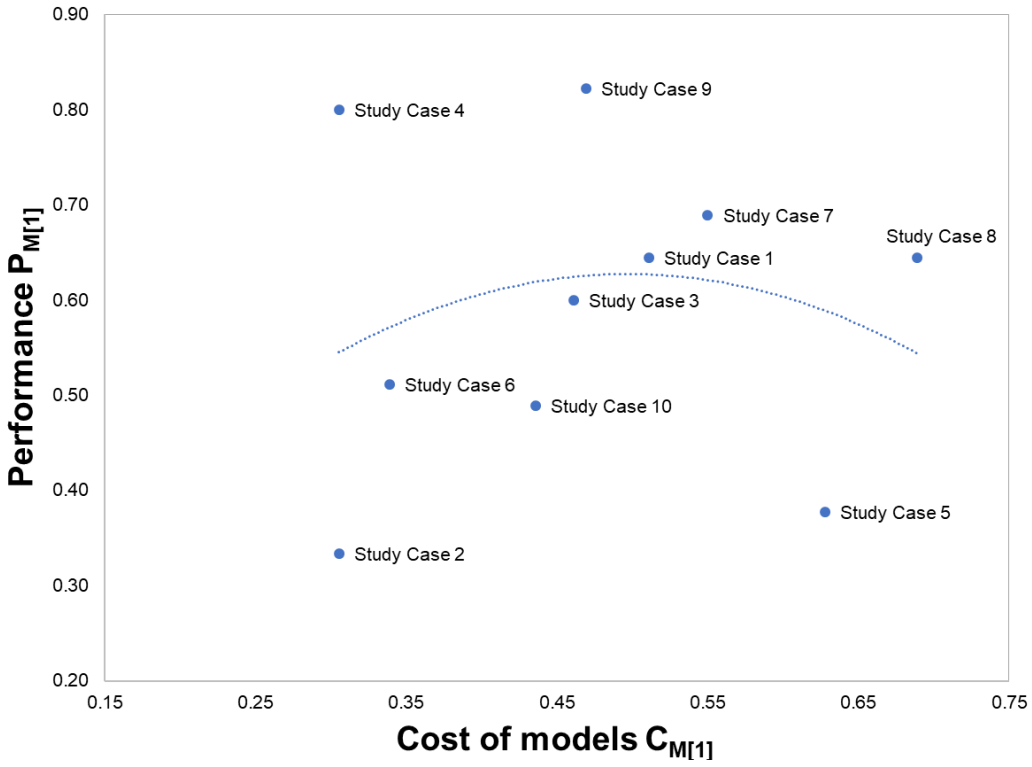

Figure 7.4 Results of the cost-performance analysis for ten selected study cases, the cost of models versus the performance of the modelling approach.

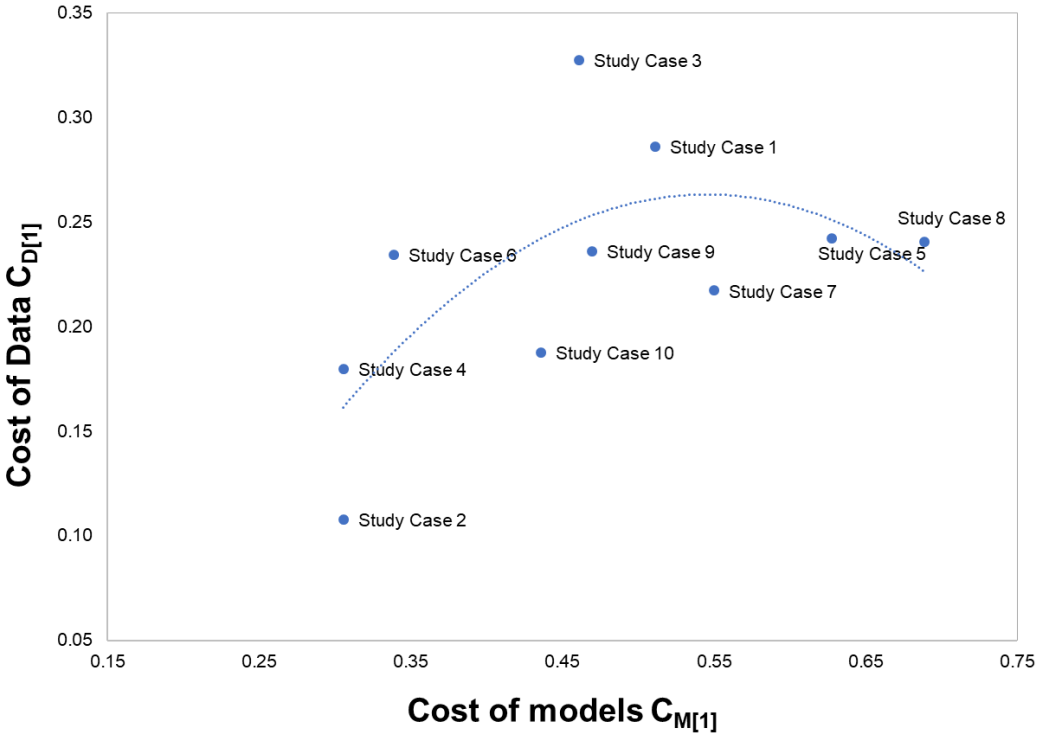

Figure 7.5 Results of the cost-performance analysis for ten selected study cases, the cost of models versus the cost of data.

The graph of Figure 7.2 presents the general relation between the modeling costs and the modeling performance. The general trend of the presented study cases (dotted blue line), in what follows is called cost-performance curve, is consistent with the suggested conceptual relationship between modelling cost and modelling performance presented in Figure 6.2. Six study cases are situated above the cost-performance curve with performance levels ranging between 0.6 and 0.82, and modeling cost levels ranging between 0.27 and 0.46. These correspond to the five model coupling approaches and to the hydraulic (2D/1D) modeling approach. The rest four study cases are hydrologic modeling approaches and empirical approaches, these are situated below the trend line with performance levels ranging between 0.33 and 0.51, and cost levels ranging between 0.19 and 0.42.

The general plot of the modeling costs versus the modeling performance for the selected events allows us to distinguish four major zones presented in Figure 7.6. these are a preliminary proposition for the localization of different modeling approaches on the cost-performance diagram based on the evaluated study cases.

The first zone comprises the model coupling approaches (category 5) and located on the top right corner of the cost-performance diagram. The zone is located above the falling lump of the cost-performance curve. For this zone modeling cost levels approximately range between 0.35 and 0.5, and modeling performance levels approximately range between 0.55 and 0.85. Higher performance levels are associated with lower modeling costs and vice-versa.

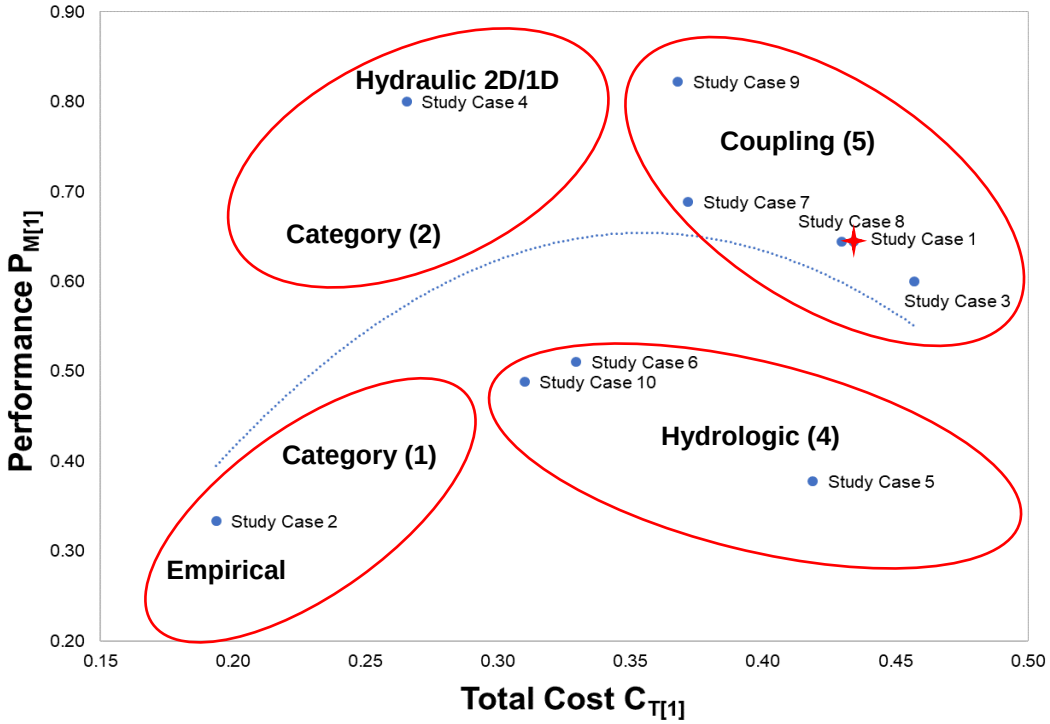

Figure 7.6 Proposed zoning of four modelling categories (empirical (1), hydraulic (2), hydrologic (4), and coupling (5)) based on the cost-performance grid. Study case 1 marked by a red cross is presented in detail in chapters 8 and 9.

The second zone comprises the hydrologic modeling approaches (category 4) and located on the lower right corner of the cost-performance diagram. The zone is located below the falling lump of the cost-performance curve. For this zone modeling cost levels approximately range between 0.3 and 0.5, and modeling performance levels approximately range between 0.3 and 0.55. Higher performance levels are associated with lower modeling costs and vice-versa.

The third zone comprises the hydraulic modeling approaches (category 2) and located on the upper left corner of the cost-performance diagram. The zone is located above the rising lump of the cost-performance curve. For this zone modeling cost levels approximately range between 0.2 and 0.35, and modeling performance levels approximately range between 0.6 and 0.85. Higher performance levels are associated with higher modeling costs and vice-versa.

The fourth zone comprises the empirical or statistical modeling approaches (category 1) and located on the lower left corner of the cost-performance diagram. The zone is located below the rising lump of the cost-performance curve. For this zone modeling cost levels approximately range between 0.17 and 0.3, and modeling performance levels approximately range between 0.2 and 0.5. Higher performance levels are associated with higher modeling costs and vice-versa.

The proposed zones are not fixed and may be modified based on further analysis based on additional study cases. These are preliminarily marked based on the selected

study cases but are thought to be beneficial in highlighting the general localization of different modeling approaches.

Our own proposed modeling approach (study case 1, marked by a red cross in Figure 7.6) falls within the model coupling zone and have cost and performance levels similar to other coupling approaches. Being on the same level with other model coupling approaches indicates the proper selection of the approach, and the applicability of the proposed modeling procedure. Details on the proposed modeling approach (study case 1) are presented in chapters 8 and 9.

7.4.1 ***Sensitivity of the grid to the selection of weights***

In chapter 6 we have proposed the weight levels for different evaluation criteria and for different sub-categories based on three influence levels (high, medium and low). However, these weights are assigned based on our own expert knowledge and may be variable from one author to another based on his point of view and his own understanding of the approach.

In this part we present a sensitivity analysis on the proposed weights and global weights for the cost-performance analysis. In this application we suppose that no weights are associated with the different evaluation criteria and subcategories, and hence all evaluation criteria and subcategories have the same weights or influence levels. i.e. all weights and global weights are considered 1.

The results of the cost-performance application are presented in Table 7.3. The total cost of modeling varies from 0.23 to 0.48, and the performance varies from 0.2 to 0.77. the major observation is that the cost and performance levels are now much closer to each other, but the cost and performance level distribution is still proportional. i.e. study cases recording highest performance did not change, similarly those recording highest cost, lowest cost and lowest performance did not change as well.

The total cost of modeling $C_{T[1]}$ is plotted versus the performance of the modeling $P_{M[1]}$ are plotted in Figure 7.7. The study cases distribution over the cost-performance diagram is still similar to the previous diagram of Figure 7.6 with slight modification in the cost and performance levels. The cost-performance curve is more convex, i.e. the slope of the rising and falling lumps is higher. The same four zoning can be delineated; the right two zones corresponding to the coupling and hydrologic approaches are slightly more inclined, whereas the left two zones corresponding to hydraulic and empirical approaches are still maintained. Study case 3 is now localized below the cost-performance curve whereas it was above before.

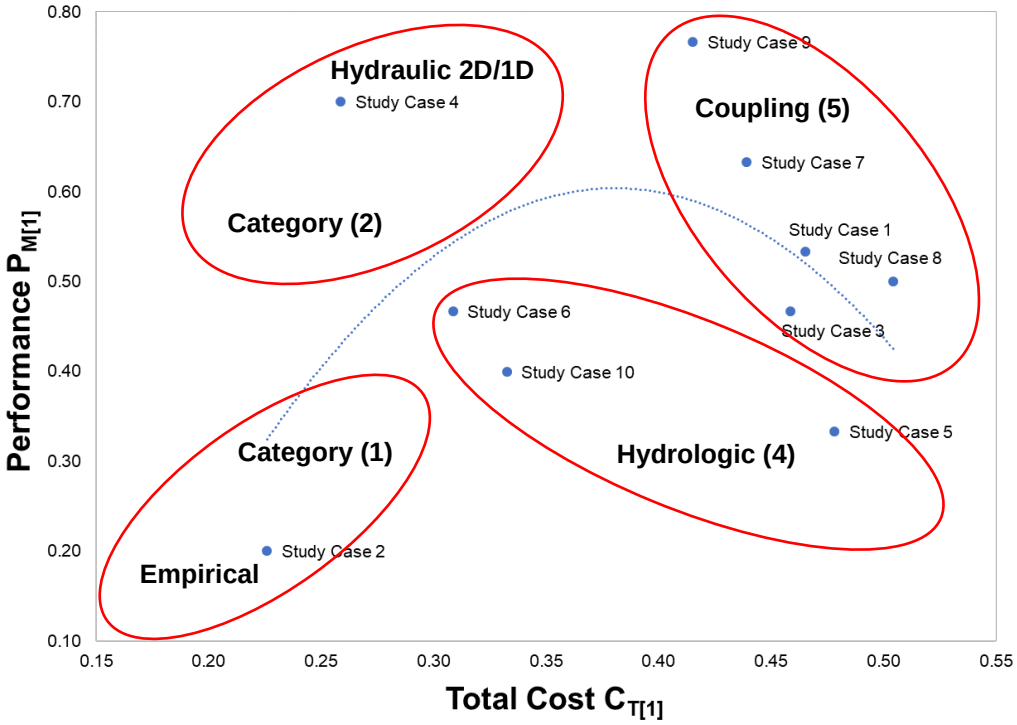

Figure 7.7 Results of the sensitivity analysis on the weights of the cost-performance grid; all weights are considered 1. The total cost of modelling versus the performance of the modelling approach. The proposed zoning of the four modelling categories (empirical (1), hydraulic (2), hydrologic (4), and coupling (5)) are presented in red.

Table 7.3 Results of the cost-performance calculation for ten selected study cases in literature based on sensitivity analysis on the weights of the proposed cost-performance grid in chapter 6. Scores are evaluated based on a scale of five levels from 1 to 5. All weights and global weights are considered 1. The different parameters are calculated following equations 6.4 to 6.7 and equations 7.2 to 7.5. Refer to the table of abbreviations for parameter description.

Study case ID	**C_D (max)**	**C_M (max)**	**C_T (max)**	**C_D**	**$C_{D\,[1]}$**	**C_M**	**$C_{M\,[1]}$**	**C_T**	**$C_{T\,[1]}$**	**P_M (max)**	**P_M**	**$P_{M\,[1]}$**	**PC = $P_{M\,[1]}$/ $C_{T\,[1]}$**
Study Case 1	120	110	230	50	**0.22**	57	**0.52**	107	**0.47**	30	16	**0.53**	1.15
Study Case 2	120	110	230	18	**0.08**	34	**0.31**	52	**0.23**	30	6	**0.20**	0.88
Study Case 3	120	110	230	61	**0.26**	45	**0.41**	106	**0.46**	30	14	**0.47**	1.02
Study Case 4	120	110	230	28	**0.12**	32	**0.29**	60	**0.26**	30	21	**0.70**	2.71
Study Case 5	120	110	230	42	**0.18**	68	**0.62**	110	**0.48**	30	10	**0.33**	0.70
Study Case 6	120	110	230	36	**0.16**	35	**0.32**	71	**0.31**	30	14	**0.47**	1.51
Study Case 7	120	110	230	41	**0.18**	60	**0.55**	101	**0.44**	30	19	**0.63**	1.44
Study Case 8	120	110	230	41	**0.18**	75	**0.68**	116	**0.50**	30	15	**0.50**	0.99
Study Case 9	120	110	230	40	**0.17**	56	**0.50**	96	**0.42**	30	23	**0.77**	1.85
Study Case 10	120	110	230	32	**0.14**	45	**0.40**	77	**0.33**	30	12	**0.40**	1.20

7.4.2 ***Sensitivity of the grid to the selection of scores***

In this application we propose to calculate the score ***f*** of an evaluation criterion based on a linear scale of five levels, varying from 1 to 5. 1 indicates the lowest cost/quality/quantity (VL) and 5 indicates the highest cost/quality/quantity (VH). However, different scoring scales might be proposed. To analyze the sensitivity of the cost-performance grid to the selection of the scoring scale, we perform a sensitivity analysis by proposing a logarithmic scale (non-linear scale) based on five levels ranging from 1 to 10,000 (***f*** values are 1, 10, 100, 1000, and 10,000). 1 indicates the lowest cost/quality/quantity (VL) and 10,000 indicates the highest cost/quality/quantity (VH).

The results of the sensitivity analysis are presented in Table 7.4. The total cost of modeling varies from 0.23 to 0.48, and the performance varies from 0.2 to 0.77. The major observation here is that the cost and performance levels are now much dispersed, i.e. study cases recording highest and lowest performance levels are now very far from other study cases. What was high is now much higher, what was low is now much lower, and everything else is in the middle. The cost-performance curve is not well defined, looking flat a little bit. Zoning cannot be performed because most of the study cases are in the middle. Moreover, the selection of the scores was not flexible, i.e. a score between 100 and 1000 (which is considered 3.5 in the linear scale application) was not easily assigned.

Generally, the logarithmic scale level of scores is not applicable in the cost-performance analysis, because it gives more importance to study cases recording higher scores, and neglects those of lower scores. Which does not allow the proper comparison between study cases. The linear scale is more representative.

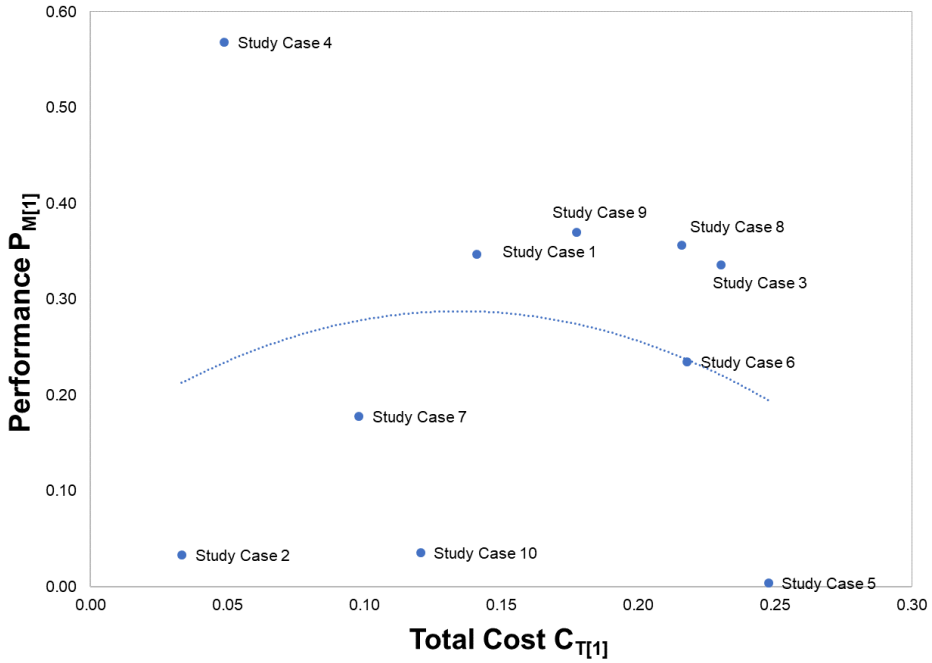

Figure 7.8 Results of the sensitivity analysis on the scores of the cost-performance grid; scores are evaluated based on a log scale of five levels from 1 to 10,000.

Table 7.4 Results of the cost-performance calculation for ten selected study cases in literature based on sensitivity analysis on the scores of the proposed cost-performance grid in chapter 6. Scores are evaluated based on a log scale of five levels from 1 to 10,000. Weights and global weights are evaluated based on three levels 1, 2, and 3. The different parameters are calculated following equations 6.4 to 6.7 and equations 7.2 to 7.5. Refer to the table of abbreviations for parameter description.

Study case ID	**C_D (max)**	**C_M (max)**	**C_T (max)**	**C_D**	**$C_{D\,[1]}$**	**C_M**	**$C_{M\,[1]}$**	**C_T**	**$C_{T\,[1]}$**	**P_M (max)**	**P_M**	**$P_{M\,[1]}$**	**PC = $P_{M\,[1]}$/ $C_{T\,[1]}$**
Study Case 1	920000	360000	1280000	125624	**0.10**	55134	**0.15**	180758	**0.14**	90000	31220	**0.35**	2.46
Study Case 2	920000	360000	1280000	1718	**0.00**	41128	**0.11**	42846	**0.03**	90000	3003	**0.03**	1.00
Study Case 3	920000	360000	1280000	231246	**0.18**	63720	**0.18**	294966	**0.23**	90000	30230	**0.34**	1.46
Study Case 4	920000	360000	1280000	35198	**0.03**	27422	**0.08**	62620	**0.05**	90000	51120	**0.57**	11.61
Study Case 5	920000	360000	1280000	161796	**0.13**	155311	**0.43**	317107	**0.25**	90000	340	**0.00**	0.02
Study Case 6	920000	360000	1280000	224606	**0.18**	54505	**0.15**	279111	**0.22**	90000	21130	**0.23**	1.08
Study Case 7	920000	360000	1280000	65852	**0.05**	59814	**0.17**	125666	**0.10**	90000	16010	**0.18**	1.81
Study Case 8	920000	360000	1280000	144236	**0.11**	132210	**0.37**	276446	**0.22**	90000	32111	**0.36**	1.65
Study Case 9	920000	360000	1280000	156017	**0.12**	71547	**0.20**	227564	**0.18**	90000	33300	**0.37**	2.08
Study Case 10	920000	360000	1280000	52148	**0.04**	102312	**0.28**	154460	**0.12**	90000	3220	**0.04**	0.30

7.5 **Discussion**

7.5.1 ***Sensitivity of the grid to the point of view of the author***

In the previous section we have presented the results of an application on the proposed cost-performance analysis grid. The approach is based on assigning certain scores for defined evaluation criteria based on the cost/quality/quantity of the datasets available and the cost/complexity of models employed.

Regardless of the scoring scale applied, although we propose to be a linear 5 levels scale, variable scores maybe assigned to the same datasets or models based on the user's/author's point of view. In the presented application we assign scores based on our understanding of the approach and on our personal point of view, however, the study cases may be evaluated differently by the original authors. This is because several factors may affect the scoring process; these may include the year of application, country of application, size/scale of the study site, level of expertise employed, and type of the flood event (low vs extreme event or flash flood vs overbank flooding).

For example, in developing countries where the monitoring networks are still limited to traditional rain gauges and river stages, the "daily" measurement time step is the most common measurement time step and would be given a moderate score ("M", here 3). In more developed countries where the monitoring networks are based on the recent advances of technology (e.g. radar measurements), the "hourly" measurement time step is very common and would be given a moderate score ("M", here 3) whereas the "daily" time step would be given a low or very low score ("VL", here 1). For this reason, in our approach we choose an intermediate scoring level that can fit industrialized countries as well as the very developing countries. In general, this does not contradict with the freedom to adjust the scoring if the grid is to be applied for example solely in an industrialized country.

The same applies for the year of application; modeling approaches that were performed in the 80's and 90's would be associated with low data costs but in fact they would have had higher data costs, because the spatio-temporal scale of data measurements was coarser in the past. For example, data measurements of "daily" time step would have been given higher scores in the past compared to the current application. Similarly models that were considered complex in the past would be now considered less complex. For example, semi-distributed models would have been given higher scores in the past when compared to current application. For this purpose, we consider the grid applicable based on the current conditions of data availability and current model complexities. Therefore, the grid should be updated in future to incorporate new advances in data measurements and model capabilities and hence scores are updated accordingly.

The size or scale of the study site plays a role in the score selection. For example, a DEM of 100 m resolution would be scored higher when applied in a large study area (say

for example 10,000 km^2) than in a small study area (say for example 100 km^2). In the proposed grid the scoring of the DEM resolution is selected based on the average required DEM resolution for hydrological modeling and hydraulic modeling separately regardless of the scale of the study site.

The approach is also sensitive to the level of expertise of the modeler himself. A modeler expert in a certain model would consider it less complex even when compared with a really less complex model but of no experience with. The proposed grid evaluates the cost of models (model complexity) regardless of the level of expertise of the modeler but based on the basic model features (spatial representation, temporal representation, flow equations…). Perhaps, the availability of the model (open source vs developed or purchased) would be the most sensitive evaluation criterion.

The selection of scores may differ based on the type of the flood event. For example, in flash flood events finer spatio-temporal scales are required. Hence an “hourly” time step of measurement in flash flood modeling may be assigned less score if compared to an overbank flood event where higher scores are assigned to hourly time step of measurement. In general, scores are assigned in a way acceptable for different types of flood events, but the score values can be tuned to fit the type of flood event under study.

7.5.2 ***Sensitivity of the grid to the objective of the modeling approach***

The objective of the modeling approach highly impacts the categorization of data and models, and accordingly impacts the selection of the criteria functions for cost and performance evaluation. Similarly, the objective of modeling also impacts the selection of the scores and weights for cost and performance evaluation.

For the proposed grid, data and models are categorized based on the flood modeling objective. If the grid is to be applied for other modeling objectives (say for example water budget evaluation) the data and model categorization would differ. The cost of data for hydraulic modeling would be eliminated, similarly the hydraulic model evaluation will also be eliminated. More attention will be paid to the hydrological model evaluation, probably hydrological and hydrometeorological data will be further subdivided (evaporation, snow melt, infiltration, ground water…). Similarly, more evaluation criteria will be added to the hydrological model costing (e.g. number of model layers, the simulation of the water movement through the subsurface, etc.).

For the purpose of flood modeling, the modeling objective may also differ. Some approaches intend to estimate the peak flood discharge only, others intend to estimate the flood flow hydrograph, others are performed for the objective of estimation of water levels, and some are performed for the objective of full flood inundation mapping. The performance evaluation is highly sensitive to the above mentioned objectives. If the objective is the flood flow hydrograph simulation, several study cases would have obtained higher performance levels, particularly the hydrological modeling approaches (study cases 5, 6, and 10). Having to mention that these objectives are nested; if a modeling approach evaluates the flood flow hydrograph it definitely evaluates the peak

flood discharge. Therefore, the smaller the objective of the modeling (say for example estimation of the peak flood discharge) the more study cases obtain high performance levels. For this application, the ten study cases would obtain good performance levels. In the proposed cost-performance grid we choose to fix the objective of modelling to mapping the flood inundation area. This is because mapping the inundation area is the most complicated objective among the other objectives and it's the current goal of most flood modeling approaches. However, the grid is flexible to be adjusted for another modeling objectives, this can be done simply by adjusting the scores of the modeling outcomes and the error levels.

The objective of modeling may also change with time and hence performance levels would also differ. Modeling approaches that were performed in the past, for example in the 80's and 90's, would be associated with higher performance levels if the grid was applied in the past. For example, if the grid was applied in the 90's, study case 5 would have obtained higher performance level compared to the current application. In the past obtaining a flood flow hydrograph with good performance level was considered satisfactory in flood modeling applications, whereas nowadays models are expected to efficiently delineate the whole floodplain extent. Similarly, with the advances of the flood modeling techniques more modeling objectives would be possible and hence the grid should be adjusted to cover any new objective.

*7.5.3 **The use of the grid from an operational point of view***

After presenting the cost-performance methodology and after giving an application to illustrate the methodology employed to apply the grid. The question arises on the real benefit of applying such grid from an operational point of view. i.e. what is the scientific use of this grid and what is the interest behind applying such methodology?

The proposed grid is a new tailor-made cost-performance grid. We are not aware of any similar grid before. The grid allows for the same time plotting different flood modeling approaches on one graph based on a unified scale. It also allows for the first time comparing different modeling approaches in terms of modeling costs and modeling performance. Evaluating the relative position of different modeling approaches on the cost-performance diagram allows us to classify the approaches into categories based on their cost and performance levels. Perhaps comparing and classifying modeling approaches is the first step towards the proper selection of the best modeling methodology for a defined modeling objective and based on available data and models. Hence, the proposed grid can be a tool that supports the future selection of modeling approaches.

Moreover, plotting any new modeling approach on the cost-performance diagram gives an insight on the relative position of this approach with respect to the others, and may improve our understanding in the applicability or the validity of the proposed approach. Also comparing the relative position of the modeling approaches on the cost-performance diagram allows us to extract any outlier approach (say for example approach of very high cost or very high performance and vice-versa) and analyze the reasons behind this difference in position.

7.5.4 ***The use of the grid from a philosophical point of view***

From a philosophical point of view, the grid has many applications. The grid supports research evolution studies. It allows studying the historical evolution of flood modeling procedures and study the corresponding evolution of the modeling costs in terms of data costs and model complexities. It also supports statistical studies that aim to evaluate the major types of data utilized for modeling, the average model complexities, and the mostly applied modeling procedures, etc.

The grid is flexible and can be tuned to adapt with different modeling objectives. The grid can be updated with time to follow the recent advances in data measurements and model capabilities. The grid is preliminarily customized to fit to flood modeling approaches, but the same methodology can be employed in many other modeling fields. Hence, the research is still open, and many other applications are expected to be presented in the future. Moreover, additional study cases are expected to be employed to help in the enhancement of the grid.

7.6 **Conclusion**

In this chapter we have presented an application on the proposed cost-performance analysis grid. Ten arbitrability selected study cases were evaluated and plotted on a cost-performance diagram. The average total cost level was 0.36 and the average performance level was 0.59. The average data cost was 0.23 and the average model cost was 0.47. Lowest modeling costs were associated with empirical approaches but however associated with lower performances. Modelling approaches based on open source data were associated with lower costs but high performances especially in well-gauged basins applications. Plotting the study cases on the cost-performance diagram allows us to highlight 4 modeling zones corresponding to 4 modeling categories (empirical (1), hydraulic (2), hydrological (4), and coupling (5)). The zones of the hydraulic modeling and coupling are associated with good performances and are located above the cost-performance curve. The hydraulic modeling zone is associated with lower costs. The zones of the empirical and the hydrological approaches are located below the cost performance curve and are associated with less performance levels because the outcomes of these approaches do not fulfil the objective of flood inundation mapping.

Our proposed modeling approach (study case 1) falls within the model coupling zone and have cost and performance levels similar to other coupling approaches which indicates the proper selection and the applicability of the approach. Details on this proposed modeling approach are presented in chapters 8 and 9.

A sensitivity analysis of the grid to the scores and weights shows that the grid is very sensitive to the selected scores scale but less sensitive to the weights' selection. A linear scale of scores of five levels gives better results compared to a logarithmic scale level of scores. The grid is also sensitive to the point of view of the author; the cost levels are mostly sensitive to the year and country of application and the performance levels are mostly sensitive to the objective of the modeling approach.

From an operational point of view, the grid allows to compare different approaches on a unified scale , classify approaches based on cost and performance levels, and choose the best flood modeling approaches for future applications based on defined objectives and available data and models. From a philosophical point of view the grid supports research evolution studies. It allows to study the historical evolution of modeling costs and modeling performances. The grid is flexible and can be tuned to adapt with different modeling objectives and can be periodically updated to follow the recent advances in data measurements and model capabilities. The research is still open, and many other applications are expected to be presented in the future.

PART III.

A FRAMEWORK FOR FLOOD MODELLING IN DATA-SPARSE REGIONS

In part II we have presented a new cost-performance grid to evaluate flood modeling approaches in terms of modeling costs and modeling performances. The idea was to support the selection of the best modeling approach (simple model) that fulfils the modeling objectives and fits the conditions of data availability with minimal model complexity. In data-sparse regions data availability is acute and most hydrometeorological measurements are of coarse resolution and present many gaps. Therefore, flood modeling becomes a challenging task because of the shortage in the observational data to constrain and validate the hydrological-hydraulic modeling. The question arises here to whether these modeling approaches remain cost-effective based on the poor conditions of data availability.

In this part we investigate whether there is opportunity to constrain hydrological/hydraulic models based on sparse data in a cost-effective approach to establish flood flows and water levels that are useful for detailed flood studies. In this part we discuss the different sources of uncertainty in data and models and develop a framework to constrain the hydrological-hydraulic model and reduce the uncertainty in the results. The part ends with a discussion on the opportunities and limitations of the proposed framework, along with a discussion on the cost-performance of the applied approach. This part forms an article published online by the journal of hydrology.

Chapter 8 presents a framework for flood modelling based on constraining a coupled hydrological-hydraulic model by past storm events and post-event measurements in space.

Chapter 9 is an application of the framework on a selected study site; Awali River Basin.

Paper published: Hdeib R., Abdallah C., Colin F., Brocca L., Moussa R., 2018. Constraining coupled hydrological-hydraulic flood model by past storm events and post-event measurements in data-sparse regions. Journal of Hydrology, October 2018, Volume 565, pages:160-176, doi: 10.1016/j.jhydrol.2018.08.008

Abstract

Flood modelling in data-sparse regions have been always limited to empirical, statistical and geomorphic approaches that are suitable to produce regional hazard maps. Such coarse resolution maps are not adapted for basin scale applications, small to medium sized basins (<1000 km^2), especially when detailed estimates of flows and water levels of a particular event is required and hence cannot replace the hydrological/hydraulic modelling. The latter is a challenging task in data-sparse regions characterized by floods of typical duration times of a few hours which offer little opportunity for real-time recording by traditional rain-gauge networks, remote sensing or satellite imaging. Such data sparseness is not always compatible with the resolution, in both space and time, of the hydrological and hydraulic models. We propose a framework for flood modelling using sparse data from a coupled hydrological-hydraulic model constrained by past storm events and post-event measurements in space. The approach is applied to the Awali river basin (301 km^2), in Lebanon, particularly to simulate the investigated early January 2013 extreme flood event, which is considered one of the largest events in the last three decades. The hydrological model was calibrated and evaluated with 12 past storm events aiming at defining narrow parameter ranges and uncertainty was performed with Monte Carlo simulations for these parameter ranges. The hydraulic model, based on a fine resolution DEM, was simulated using hydrological outflows and validated with 27 post-event measurements in space of high-water marks. The resulting outflow values were satisfactory, and uncertainty was reduced when compared with arbitrarily wide parameter ranges. The hydrological model performance was highly variable but for the hydraulic model, 93% of the observed water levels fall within the simulated uncertainty bounds with an RMSE error of 0.26 m. The proposed framework allows mapping the possible inundation and can be compared to other approaches dealing with model complexity and associated performances.

Keywords: Sparse data; Flood maps; Post-event measurements; Uncertainty; Lebanon; Mediterranean

8 THE PROPOSED FRAMEWORK USING SPARSE DATA

8.1 **Introduction**

Flood modelling in data-sparse regions have been always limited to empirical, statistical and geomorphic approaches that are suitable to produce regional hazard maps. Such coarse resolution maps are not adapted for basin scale applications, small to medium sized basins (<1000 km^2), especially when detailed estimates of flows and water levels of a particular event is required and hence cannot replace the hydrological/hydraulic modelling. The latter is a challenging task in data-sparse regions characterized by floods of typical duration times of a few hours which offer little opportunity for real-time recording by traditional rain-gauge networks, remote sensing or satellite imaging. Such data sparseness is not always compatible with the resolution, in both space and time, of the hydrological and hydraulic models and cannot meet all model requirements. Therefore, the question arises to whether there is an opportunity to apply such hydrological-hydraulic modeling approaches in a cost-effective approach, based on the current sparse data condition, to simulate flood flows and water levels that are useful for detailed flood studies

In this chapter we hypothesize that there is an opportunity to model flood events based on constraining a hydrological-hydraulic model with sparse data, discontinuous in space and time. The focal point is the proposed modelling framework that involves the hydrologic model HEC-HMS (USACE, 2000), combined with the 1-D hydraulic model HEC-RAS (USACE, 2016a) , along with models' calibration and evaluation with past storm events, and flood post-event measurements, including uncertainty calculation based on Monte Carlo simulation. Furthermore, in this chapter we present the parameterization strategy and the corresponding evaluation procedures. An application on the proposed framework on a selected study (Awali River Basin) is presented in chapter 9.

8.2 **The sparse dataset**

Sparse data are often characterized by measurements of limited spatiotemporal resolution; point measurements of coarse time step, and series with gaps, or parameters that have not been collected during simultaneous periods. This is a common problem in many countries worldwide and particularly in Lebanon. However, when information on the flood event characteristics, catchment hydrological characteristics and river channel characteristics are sparse or lacking, interesting information can be inferred from recorded past storm events, post-event field investigations, newspapers and social media reports, and from crowdsourcing of information from local citizens on flood events characteristics whenever available.

In this part we recall a summary of the major sparse data set available in Lebanon (also might be available in other data-sparse countries) for our analysis that can be summarized as follows Table 8.1:

1. Past recorded storm events of daily rainfall measurements from ground rainfall gauges incapable of reflecting the rainfall intensity and spatial variability during the storm event, hourly (or 15 min) water level measurements by two traditional river stage gauges mostly

non-functional during flood events, and hourly (or 15 min) flow hydrographs extracted based on poorly defined rating curves.

2. Descriptive social media information on the past storm events related to the duration and spatial variability of the rainfall during the storm.

3. A recent extreme flood event but destructed river stage gauge with daily and hourly rainfall measurements in one nearby rainfall station and post-event measurements of peak flood discharge and maximum water level marks.

4. Descriptive information from newspapers, social media, and field investigations on the extreme flood event related to the inundated areas, time of flood peak, duration of the storm and its spatial variability.

Table 8.1 Summary of the observational data types available for our analysis.

Event	Rainfall Data	Flow Data
n past storm events	- daily rainfall data - social media information on the duration of the rain event	- hourly and 15 min water level measurements - hourly and 15 min flow hydrograph extracted based on established rating curves
1 extreme event	- daily and hourly rainfall data	- post-event maximum water marks measurements and peak flood discharge estimation - social media information and local witnesses on the time of peak flow and flood inundation depth and area

8.3 **The modelling framework**

8.3.1 ***Hydrological model***

Hydrological rainfall-runoff models vary in their complexity from simple lumped models to semi-distributed and fully distributed models. Regardless that fully distributed models are capable of better representing the hydrological processes, several difficulties arise when applying them in data-sparse regions because of their complexity, data requirements and parameter identifiability which may limit their efficiency and adequacy. However, when sparse data is available semi-distributed rainfall-runoff models are still efficient alternatives. Thereof, a semi-distributed model based on the SCS-CN method for computing losses, along with Muskingum-Cunge and SCS-unit hydrograph methods for routing flow along channels and hillslopes are respectively selected. The model is integrated within the HEC-HMS software. The simple SCS curve number loss model (SCS, 1972) was applied because it allows the estimation of direct surface runoff volume for given rainstorms based on a single parameter, curve number which represents the basin's infiltration storage (D'Asaro and Grillone, 2010), which reduces the number of parameters to calibrate.

8.3.2 ***Hydraulic model***

The 1D HEC-RAS model is used to establish the water-surface profiles. This model is selected because it is a well-known open software widely applied for hydraulic modelling, it is usually combined with the HEC-HMS and known for its low computational costs. The hydraulic model is applied to the low main part of the river mostly subjected to flooding. Cross sections are performed at main locations such as gauge locations, at locations of considerable changes in flow, morphology, slope, geometry, and roughness, and at representative locations such as sub-basins' outlet of the hydrological model that serve as boundary conditions for the hydraulic model.

The centerline can be traced together with the river banks based on high-resolution UAV drone images captured through field surveys of the study site under interest. The geometry of the river and flood plain can also be extracted from a fine resolution DEM generated based on the UAV drone images. The results of the hydrological model are to be imported into the hydraulic model. Roughness values can be initially estimated based on expert knowledge of channel properties. These values are later manually calibrated by a trial and error approach to maximize the fit between the simulated water levels and the observed ones at arbitrary selected post-event locations on the river channel.

8.3.3 ***Modelling Framework***

The modelling framework is divided into three major steps (Figure 8.1):

- Step (1) involves performing the rainfall-runoff modelling through the hydrological model (here HEC-HMs model is selected) for selected past storm events. Parameters to be calibrated are to be selected based on the model sensitivity analysis. Model calibration and evaluation is performed aiming at defining a narrow range of model parameters, which is taken equal to the estimated range from the calibration.

- Step (2) involves an uncertainty analysis based on the Monte Carlo Sampling of model parameters within the narrow ranges estimated in step (1). The hydrological model is then run to simulate the hydrograph set of the extreme event flood event under study.

- Step (3) involves the hydraulic model simulation (here HEC-RAS model is selected) for the flood event under study based on the hydrograph set obtained in step (2) to generate the respective water surface profiles. This step is followed by post processing and terrain analysis to interpolate the water levels and extract the inundation area. The resultant flood inundation map is validated by the by the post-event measurements in different locations in space.

These steps are preceded by preliminary analysis to delineate the catchment and sub-catchments, extract their characteristics and parameters, and define rough initial values of model parameters based on the modeler's knowledge on the basin's characteristics.

Hydrological model calibration and evaluation

Unlike classical calibration approaches that end up in a deterministic set of model parameters, the calibration procedure herein is applied aiming at defining a narrow range of model parameters for uncertainty sampling, this range is taken equal to the estimated range from the calibration. The estimated parameter ranges are quite narrower than the wide feasible parameter ranges often defined in classical uncertainty analysis studies (e.g. Freer et al., 1996; Huang and Liang, 2006) which are often chosen, arbitrarily or on a basis of physical argument, to be wider than those expected for the catchment under study.

Available and simultaneous rainfall and water level measurements can be analyzed to extract past storm events of reliable information. It is preferable to select storm events of variable intensity and duration and occurring in different time of the year. Daily rainfall measurements are discretized uniformly into hourly measurements; however, this is mostly applicable for floods of long duration and not flash floods. Indeed, several other possible rainfall distributions can be applied and analyzed and may yield more accurate estimates of hourly rainfall depths. In this study we choose the simplest approach (uniform rainfall) as a preliminary analysis. In some cases, additional information can be obtained from social media reports and newspapers on the time period of occurrence of the maximum rainfall which is mainly a portion of the day. In these cases, recorded rainfall

measurements at that day are discretized into hourly measurements uniformly over the period of occurrence of the maximum rainfall; e.g. if we found information that the storm event was localized within the first quarter of the day; daily rainfall is discretized over the first six hours of the day only. This is mainly because there might not be any rain at all for several hours of the day and discretizing over the whole day may show values even for non-rainy hours.

The calibration involves a combination of both manual and automated calibrations. The manual calibration precedes the optimization to ensure that a physically-meaningful set of initial parameters is used in the model based on initial conditions and on expert knowledge of the basin's physical properties. The automated optimization is then applied to optimize the model parameters. The resulting minimum and maximum values of each optimized parameter define an interval of narrow parameter ranges. Perhaps the more past events evaluated the better results are expected. However, there should be certain number of events that insures convergence in the calibration. The convergence in calibration is obtained when calibrating on additional past events do not considerably change the estimated parameter ranges. The major evaluation indices applied for model calibration were detailed in chapter 2, Eqs.2.6 to 2.12.

Uncertainty in the hydrological modelling

The uncertainty propagation in this approach can be understood by analyzing the uncertainty on the hydrological model parameters based on two approaches. The first approach involves a sensitivity analysis for the hydrological model to select the key parameters mainly controlling and forcing the model results. The second approach involves a fuzzy combination based on Monte Carlo simulation for the selected parameters (Robert and Casella, 2004). The selected parameters of minimized ranges in the previous step (1) are statistically sampled based on a uniformly distributed probability density function. Uniform distributions are considered to avoid any prior assumption on the parameters' distribution other than their feasible ranges as discussed by Freer *et al.*, (1996). Random numbers can be generated using the Well19937c generator within HEC-HMS (Panneton et al., 2006).

Hydraulic model validation

Hydraulic models have been typically validated using water level or discharge values obtained from the hydrometric network available on the river. However, this is a major challenge when hydrometric measurements are lacking and when remote sensing products are not able to capture the flood event. In this approach we choose to validate the model with the post-event measurements of high water marks. This step is preceded by a terrain analysis to extract the inundation area using the high-resolution terrain model. The simulated maximum water level bounds are matched with the observed water levels. The root mean square error (RMSE) objective function presented in Eq.2.13 is used to evaluate the fit between the simulated uncertainty bounds of the water levels and the observed ones at the post-event measurement locations.

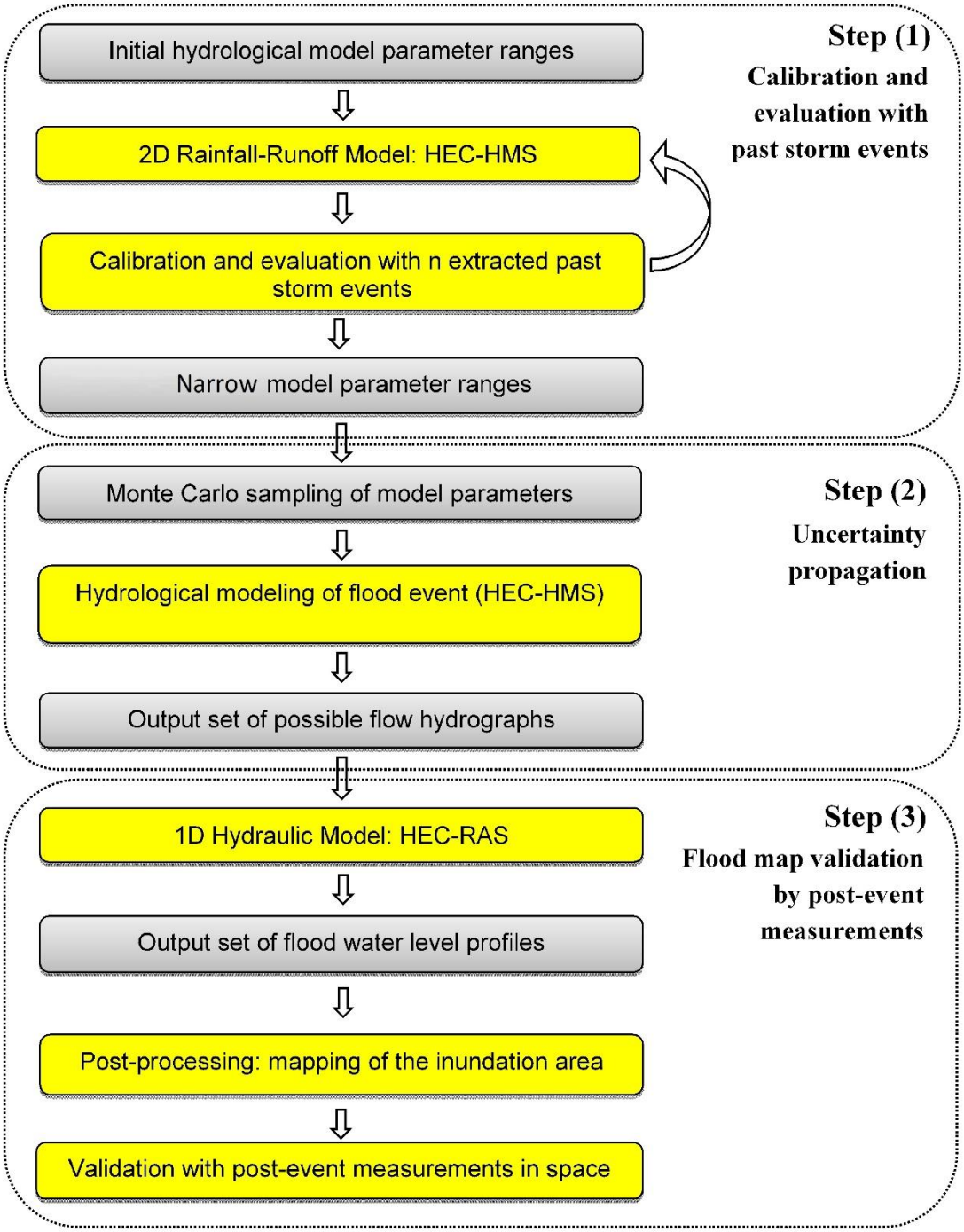

Figure 8.1 Detailed scheme of the proposed modelling framework used to produce flood maps using sparse data and a coupled hydrological-hydraulic model constrained by past storm events and post-event measurements in space. Blocks in yellow present the major computational parts of the modelling framework, whereas, blocks in grey present the input/output of the computational parts.

8.4 **Conclusion**

In this chapter we have proposed a framework for flood modeling in data sparse-regions. The framework is based on coupling a semi-distributed conceptual hydrological model (HEC-HMS) with a 1D hydraulic model (HEC-RAS). The coupled hydrological-hydraulic model is constrained by past storm events and post-event measurements in space. The hydrological model is calibrated and evaluated with past storm events aiming at defining narrow parameter ranges and uncertainty is performed with Monte Carlo simulations for these parameter ranges. The hydraulic model, based on a fine resolution DEM, is simulated using hydrological outflows and validated with post-event measurements in space of high-water marks.

The proposed framework is tested in chapter 9 on the challenging site of the Awali River Basin in Lebanon.

9 APPLICATION OF THE PROPOSED FRAMEWORK USING SPARSE DATA

9.1 Introduction

In this chapter the proposed framework for flood modeling in data-sparse regions is tested and discussed through its application on a challenging study site of the Eastern Mediterranean; “Awali catchment” in Lebanon. This application demonstrates the methodology employed to apply the proposed framework including the parameterization strategy and the corresponding evaluation procedures. The major results of the models’ processing and calibration are given and discussed through several challenges including the model coupling approach, the reliability of the observational data and uncertainty propagation, the post-event measurements and their use in constraining the model, and the cost-performance of the applied approach .

9.2 Study site and data

The study site for this analysis was the Awali River Catchment in Lebanon. Detailed description of the site’s geographical and hydrological characteristics, along with the major data sets available were presented in chapter 4.

In chapter 5 we have discussed the reason behind choosing this study site for detailed analysis and modeling. The study site is one of the major Lebanese catchments facing flood recording a level 4 frequency of occurrence of flood events. Available post-event measurements for an extreme event in the Awali Basin along with the high frequency of occurrence of flood events were among the major reasons for the selection of this study site.

The study area of the hydrological model was the whole catchment area, divided into nine sub-catchments. Whereas, it was the lower main course of the river, approximately 5 km of river length, for the hydraulic model which is experiencing flooding after heavy rainfall events

9.3 Methodology

A semi-distributed model based on the SCS-CN method for computing losses, along with Muskingum-Cunge and SCS-unit hydrograph methods for routing flow along channels and hillslopes are respectively selected. The model is integrated within the HEC-HMS software. The modelling time step is equal to 30 minutes, smaller than the sub-basins’ estimated time of concentration, to ensure that the flood peak is well captured by the model. Evapotranspiration losses are neglected based on the assumption that the evapotranspiration volume generated during a winter storm event is negligible compared to the runoff volume generated, as demonstrated by Knebl et al., (2005). The baseflow in the model is estimated from the available water level records, the induced flow by the hydropower production plants is estimated based on collected schedules of average monthly water flow in the facilities (1994-2015). Rainfall–runoff simulation of several events is then conducted for the whole catchment (301 km^2) in a semi-distributed approach over sub-catchment units.

Initial, rough CN ranges are assigned for each sub-catchment based on the knowledge of the land use and HSG combinations extracted from available information. Rainfall amounts calculated 5 days before each storm event reflect moderate soil moisture conditions of typical winter days in Lebanon. Accordingly, CN values fall within the average soil moisture conditions (AMCII). The hydraulic model is applied to the low main part of the river, approximately 5 km of river length, mostly subjected to flooding

9.4 **Results**

9.4.1 ***Step (1): Hydrological model calibration and evaluation by past storm events***

In what follows please refer to chapter 4 for detailed site and data description, for catchment and sub-catchments delineation, for past storm events description and for post-event measurements locations.

Sensitivity analysis

The sensitivity of the model was first assessed based on the 14-19 February 2012 storm event (event 11), the event was selected because it is the closest to the Jan2013 flood event. The sensitivity analysis was performed at the river stage Saida (475) and was based on the variation of the curve number parameter, Initial abstraction parameter, percent impervious parameter and the lag time. The reference parameter values are 50.4 for the CN, 12.7 mm for the Ia, 7.7 hr for the lag time, and 0.75 % for the percent impervious. The results of the sensitivity analysis are presented in Table 9.1, based on evaluating the total runoff volume, the peak flow, and the time of peak discharge at Saida (475) gauge. The curve number parameter was found to be the parameter that could mostly affect the calculation results. The initial abstraction affects the runoff volume and peak flow, whereas, the impervious percent mainly affects the runoff volume. The lag time mainly affects the time of peak runoff.

Table 9.1 Step (1): Sensitivity analysis results on the 14-19 February 2012 rainfall-runoff event with average total rainfall of 120 mm.

Parameter	Curve number	% impervious	Initial abstraction [mm]	Lag time [h]
Range	[10; 90]	[0; 10]	[0; 50]	[0.5; 30]
Volume error [%]	[-16; 41]	[3; 7]	[1; 22]	[1; 9]
Peak flow error [%]	[-37; 56]	[-6; 0]	[-9; 24]	[-67; 8]
Phase error [h]	[-1; 3]	[-1; 0]	[-4; 2]	[-4; 9]

Calibration by past storm events to estimate parameter ranges

Following the sensitivity analysis, the selected key parameters for calibration are, the Curve number, the initial abstraction, the lag time, and the Manning's coefficient. Model calibration and evaluation were carried out at two points corresponding to the positions of the gauge stations Saida (475) and Marj Bisri (473). Model calibration was performed on three steps; the number of events is increased in each step and the parameter ranges are compared to the preceding ones, allowing to search for the suitable number of events that insures a convergence in the calibration. The first step involves calibrating the model with 3 events arbitrarily chosen (events 2, 4, and 12), the second step involves calibrating with 6 events (events 2, 4, 5, 6, 8, and 12), and the last step involves calibrating with the whole 12 events. The parameter ranges for the different sub-basin are taken equal to those obtained by the calibration in each step. Calibration with 3 events resulted in parameter ranges quite narrower than those obtained by calibrating with 6 events. Whereas, calibrating with 6 and 12 events resulted in similar parameter ranges, which means that our approach works well with 12 events. Calibrating with 3 events was not sufficient, because analyzing additional storm events further increases the parameter ranges, this is because the additional events are more variable in terms of intensity allowing to obtain a wider parameter range. In our case, the similar parameter ranges obtained by 6 and 12 events indicates a convergence in calibration and allows us to say that we are stabilized with 12 events. Indeed, this approach should be further assessed in additional applications because the selected number of past storm events impacts the resulting parameter ranges. The different sub-basin characteristics, their arbitrarily estimated wide parameter ranges, and the estimated ranges by calibrating with 12 events are presented in Table 9.2. The calibration with 12 events resulted in the estimation of narrow ranges of the characteristic parameters of the different sub-basins, these ranges are narrower than the arbitrarily chosen wide parameter ranges.

The model was relatively more sensitive to the characteristic parameters of sub-basin B1 and B2 which form around 60% of the total area and together contribute to over 31% of the total runoff. For the selected storm events, the CN of sub-basin B1 found to vary from 50 to 62, the lag time varies from 232 to 248 min, and the initial abstraction varies from 7 to 21 mm. Table 9.3 summarizes the model performance for the selected storm events in terms of the parameters described in chapter 2, Eqs. (2.6) to (2.12).

The simulation of the 12 events resulted in an average volume error of 10.7%, average peak flow error of 26.3 %, and an average phase error of -3.6 hrs. The performance of the model was highly variable among the storm events, the evaluation analysis resulted in an NSE ranging between 0.84 and 0.06, R ranging between 0.93 and 0.58, RMSE ranging between 1.46 and 19.7 m^3/s, and MAE ranging between 0.62 and 8.7 m^3/s. The low NSE values for events 2, 3, 9, and 10 are mainly because the observed water levels at Saida gauge (475) presented large fluctuations that may not be related to the runoff generated by rainfall events, but maybe related to the sensitivity of the river stage gauge to any perturbation in the water flow that for example may be resulting from the floating objects carried by the river. The low NSE value for event 3 and 11 at Marj Bisri gauge (473) is mainly because the observed hydrograph presented a relatively high peek discharge

which might be overestimated by the rating curve. The good NSE value for event 6 is related to discretizing rainfall over the storm period of occurrence (first quarter of the day) which reduced the error in the time series and gave better peak flow value.

Table 9.2 Step (1): Sub-basins' characteristics, the arbitrarily estimated wide parameter ranges, and the estimated narrower parameter ranges for different sub-basins obtained from the maximization of the Nash-Sutcliffe efficiency of the 12 selected past storm events.

Element	Area (km^2)	Av. Slope (m/m)	Watershed length (km)	Parameter	Wide feasible parameter ranges	Estimated parameter ranges based on 12 events
Sub-basin B1	141	0.0492	27.80	CN	[20; 80]	[50; 62]
				Ia	[1; 100]	[7; 21]
				T_{lag}	[100; 600]	[232; 248]
Sub-basin B2	51	0.0677	14.46	CN	[20; 80]	[45; 49]
				Ia	[1; 100]	[3; 27]
				T_{lag}	[100; 600]	[111; 167]
Sub-basin B3	31	0.0472	18.01	CN	[20; 80]	[49; 58]
				Ia	[1; 100]	[6; 47]
				T_{lag}	[100; 600]	[129; 299]
Sub-basin B4	11	0.0444	11.23	CN	[20; 80]	[34; 66]
				Ia	[1; 100]	[11; 19]
				T_{lag}	[10; 300]	[76; 174]
Sub-basin B5	13	0.0684	7.62	CN	[20; 80]	[37; 57]
				Ia	[1; 100]	[18; 46]
				T_{lag}	[10; 300]	[120; 123]
Sub-basin B6	13	0.0976	8.67	CN	[20; 80]	[36; 58]
				Ia	[1; 100]	[13; 31]
				T_{lag}	[10; 300]	[133; 202]
Sub-basin B7	24	0.0399	13.66	CN	[20; 80]	[34; 38]
				Ia	[1; 100]	[12; 42]
				T_{lag}	[10; 300]	[57; 194]
Sub-basin B8	6	0.0583	6.52	CN	[20; 80]	[57; 69]
				Ia	[1; 100]	[13; 30]
				T_{lag}	[10; 300]	[70; 74]
All model reaches				n	[0.01;0.1]	[0.03; 0.07]

Table 9.3 Step (1): Results of the hydrological model evaluation for the 12 selected past storm events in terms of the parameters presented in equations Eq.2.6 till Eq. 2.12. at locations: Saida gauge (475) and Marj Bisri gauge (473). Q_{peak} refers to observed peak flow estimated from the measured stage with the established rating curves. Refer to the table of acronyms for abbreviations description.

Event	Storm Event	D	P_{av}	Gauge	Q_{peak}	V_{obs}	Q_{sim}	V_{sim}	PFE	VE	PE	r	NSE	RMSE	MAE
		[h]	[mm]		[m^3/s]	[mm]	[m^3/s]	[mm]	[%]	[%]	[h]			[m^3/s]	[m^3/s]
1	19-24 Jan 2000	144	199	475	145.7	117.6	99.6	100.8	31.6	14.3	-11	-	-	-	-
2	15 Dec 2001	24	24	475	17.4	4.8	15.4	5.5	11.5	7.2	-0.5	0.68	0.19	2.66	1.78
				473	15.3	5.9	13.6	6.0	11.1	-2.4	-5	0.92	0.84	1.46	0.62
3	19-20 Dec2001	48	43	475	19.1	13.4	20.1	12.4	-5.2	7.2	-0.5	0.58	0.09	4.26	2.51
				473	54.1	15.6	18.6	11.2	65.6	33.5	-5	0.73	0.45	6.89	4.08
4	6-11 Jan 2002	144	79	475	28.9	32.0	24.7	30.7	14.5	3.9	0.5	-	-	-	-
5	20-22 Jan 2002	72	66	475	68.0	35.1	40.7	31.3	40.1	11.1	-2	0.83	0.66	6.03	3.75
6	18-21 Dec 2002	55	120	475	163.0	51.6	164.9	52.3	-1.2	-1.5	-2	0.93	0.80	12.19	6.69
7	3-7 Jan 2007	96	81	475	22.6	25.0	29.4	19.8	-30.1	20.9	0	-	-	-	-
8	19-20 Jan 2007	24	59	475	27.3	13.7	35.4	13.0	-29.7	5.6	-1	0.84	0.56	3.85	1.90
9	1-7 Feb 2007	144	150	475	85.9	65.5	84.7	69.2	1.4	-5.5	7	0.73	0.06	13.61	8.60
10	24-26 Feb 2007	48	75	475	69.9	41.7	58.3	33.4	16.6	19.9	7.5	0.58	0.12	10.83	7.02
11	14-19 Feb 2012	120	120	475	118.7	108.3	117.2	128.6	1.3	-18.7	1	-	-	-	-
				473	246.5	66.0	79.4	66.4	67.8	5.5	-5	0.70	0.40	19.7	8.70
12	28 Feb-3 Mar 2012	168	125	473	69.0	57.2	29.5	57.3	57.2	-0.3	-6	0.65	0.39	7.25	4.59
							Average values		**26.3**	**10.7**	**-3.6**	**0.74**	**0.53**	**7.87**	**4.67**

9.4.2 ***Step (2): Uncertainty propagation; flood event of 07 January 2013***

The Jan2013 storm event rainfall amounts recorded at the time of flood by the daily rainfall stations P_1, P_3, P_{11}, P_{12}, and P_{15}, and the hourly rainfall station P_{10} are analogous with slight lower values along the coastal area, indicating no major spatial variation in rainfall. The little difference in rainfall among stations is considered by assigning its relative weight preserving the same hyetograph distribution.

The uncertainty analysis involved the hydrological model parameters CN, Ia, Lag time, and the Manning's roughness. Based on the criteria illustrated by Dimitriadis et al. (2016), testing several parameter samples ranging from 100 to 5,000 showed that the convergence in the resulting mean discharge and volume was achieved for sample size starting from 1000 parameters and that increasing the number of samples does not result in a noticeable change in the computed mean discharge and volume. We choose to perform 2000 simulations which is equivalent to more than twelve values per model parameters for an adequate quantitative analysis of acceptable computational cost. The parameters are statistically sampled following a uniformly distributed probability density function within their estimated ranges in step (1). To study the implication of the estimated parameter ranges on the model results, four model simulations were performed, these correspond to the wide parameter ranges defined in Table 9.2 and the estimated parameter ranges by calibrating on 3, 6 and 12 events. The model simulated hydrographs at all sub-catchments' outlets. The results of the four model simulations are presented in Figure 9.1 at Saida G(475) gauge. Simulation based on the wide parameter ranges resulted in numerous possible model realizations of peak flow value ranging between 100 m^3/s and 550 m^3/s with a mean value of 260 m^3/s. In this case the results of the hydrological modelling are no more representative and may be replaced by empirical or lumped modelling approaches. Simulation based on the estimated parameter ranges by 3 events resulted in few model realizations of peak flow value ranging between 276 m^3/s and 364 m^3/s with a mean value of 339 m^3/s. As expected, this simulation ("3-events") is thought to be underestimating the possible peak flow values because it was based on unstable calibration. Simulations based on estimated parameter ranges by 6 and 12 events resulted in similar model realizations of peak flow values ranging between 324 m^3/s and 429 m^3/s with a mean value of 377 m^3/s observed at 05:00 of 07 January 2013, given that the maximum rainfall intensity of 17.3 mm/hr was observed at 20:00 the day before. For these two simulations ("6-events" and "12-events") the simulated total water volume ranges between 67.44 Mm^3 and 75.05 Mm^3 with a mean value of 71.49 Mm^3. The last two simulations reduce uncertainty in the peak flow values and seem to be satisfactory because of the stable model calibration.

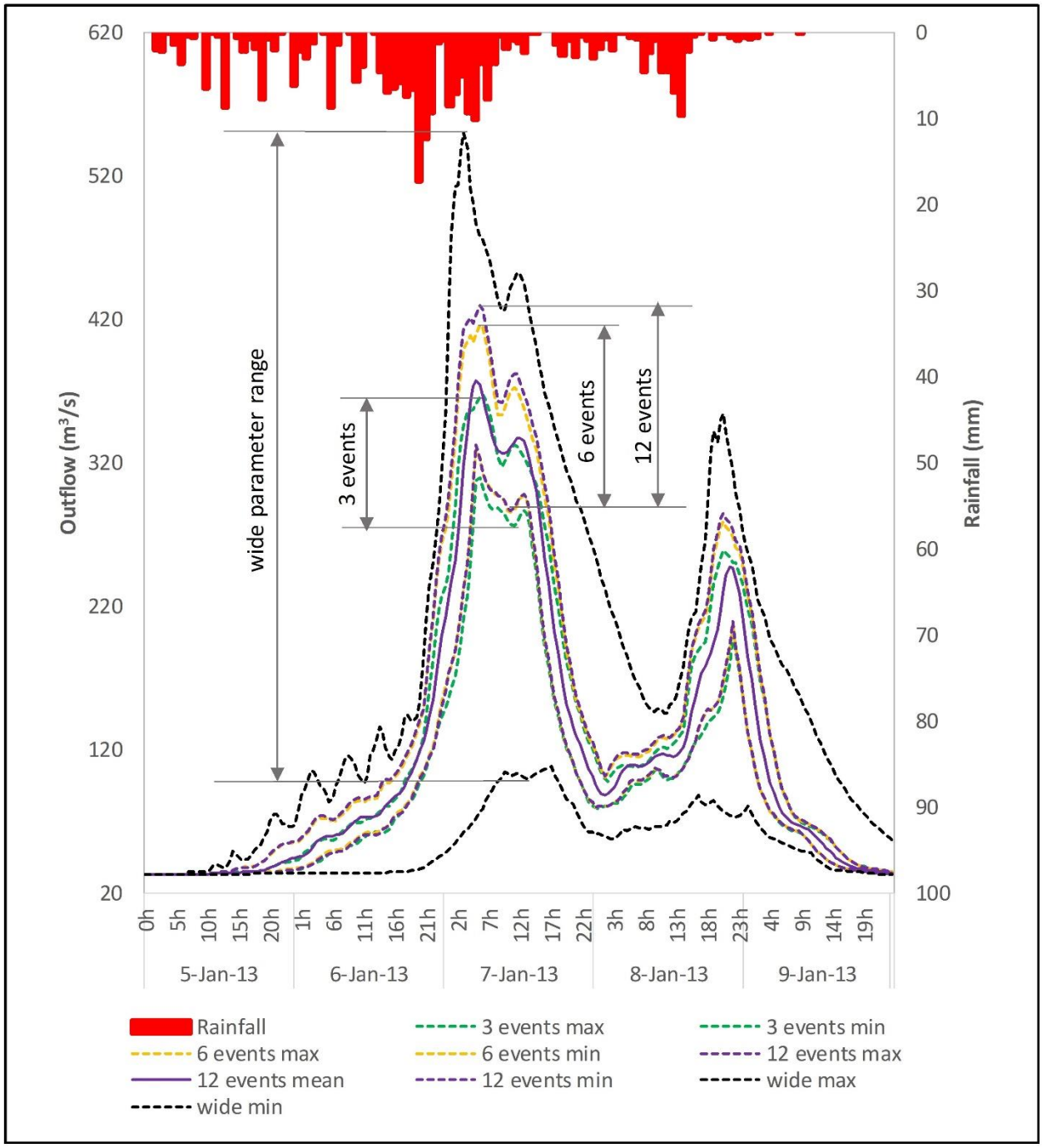

Figure 9.1 Step (2): Simulation of the early January 2013 flood hydrograph at Saida gauge (475) location by HEC-HMS with the corresponding uncertainty boundaries based on the arbitrary wide parameter ranges (in black), ranges obtained by the “3-events” calibration (in green), ranges obtained by the “6-events” calibration (in orange), and ranges obtained by the “12-events” calibration (in purple).

9.4.3 ***Step (3): Hydraulic modelling & flood map validation by post-event measurements***

The HEC-RAS model was applied to the low coastal area that correspond to the channel running in sub-basins B8 and B9, the channel is bounded upstream by Joun hydropower plant and downstream by the gauge station G(475) and the sea mouth. The resulting hydrographs of the hydrological model corresponding to the "12-events" simulation were then assigned as upstream and downstream boundary conditions and input lateral inflows at junctions for the hydraulic model. The propagation of uncertainty through the hydraulic model was examined using the previously established bounds; maximum, mean, and minimum flow hydrographs providing three realizations of the flood extent. The hydraulic model results are presented in Figure 9.2. The resultant flood map is presented in Figure 9.3. 93% of the observed water levels fell within the simulated uncertainty bounds and found to be closer to the mean with RMSE error of 0.26 m. The RMSE error, calculated based on Eq.2.13, was found to be 0.7 m and 0.6 m for the maximum and minimum uncertainty bounds respectively. With an RMSE error in the range of the DEM resolution (10 cm), the results of the hydraulic modelling are found to be very promising.

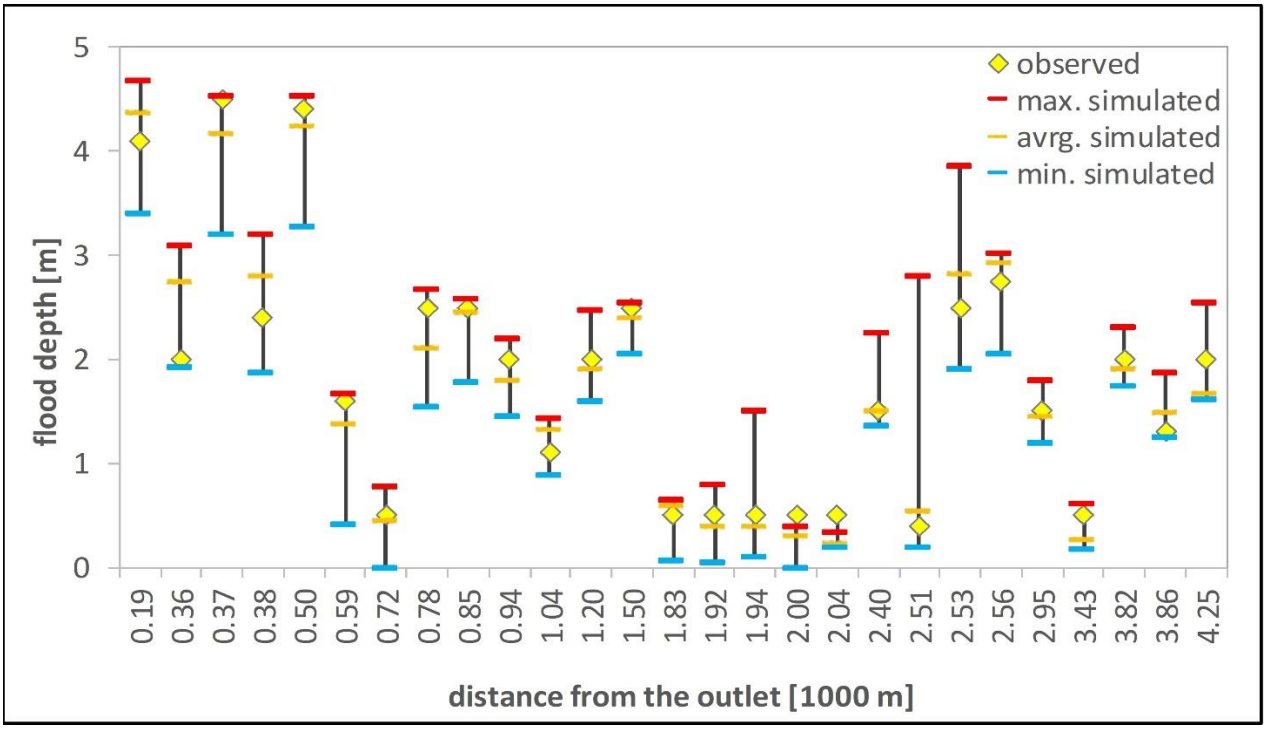

Figure 9.2 Step (3): observed post-event maximum water levels versus simulated maximum water levels by the hydraulic model for three selected bounding scenarios, maximum, minimum and average flood flow hydrographs for the early January 2013 extreme event.

Figure 9.3 Resultant maximum flood inundation extent for the Jan2013 flood event.

9.5 **Discussions**

9.5.1 ***Opportunities in the model coupling approach***

A wide range of hydrological and hydraulic models is nowadays available, out of which many are open software and easy to use by the scientific community. The coupling between these models have been also widely discussed in literature. The HEC-HMS and the HEC-RAS models are among these models. These “open software” have been successfully used in many case studies. Examples include the HEC-HMS model on the Llobregat River in Catalonia (Amengual et al., 2007), the Misai and Wan’an Catchments in China (Oleyiblo and Li, 2010), Sixteen sub-catchments in Johor, Malaysia (Shamsudin et al., 2011), and the Balijore Nala watershed in India (Choudhari et al., 2014). Examples on the HEC-RAS model include the Severn River in UK (Horritt and Bates, 2002), the Eno River Strouds Creek in North Carolina and Brazos river in Texas (Cook and Merwade, 2009), the Po River in Italy (Di Baldassarre and Montanari, 2009), and the Xerias river in Greece (Papaioannou et al., 2017). The HEC-HMS and the HEC-RAS models have been successfully coupled in different study cases, examples include the San Antonio River basin in Texas (Knebl et al., 2005) and the Giofiros basin in Greece (Koutroulis and Tsanis, 2010).Sufficient discussions have been presented in literature to assess the use of many of these models and evaluate their coupling performance. These models have been tested against classical data in well gauged basins and found to be successful. In this project we do not aim to assess the performance of the model structure; the performance of the model structure can be tested with classical data, to be valid for application with sparse data. Based on what we have mentioned before that most of the river basins are data-sparse basins, we aim to discuss the opportunity of applying these hydrological-hydraulic models using sparse-data.

Unlike classical approaches that involve calibrating the model with one past storm event, the robustness of the applied approach is related to the evaluation of the model with several past storm events of variable intensities. The proper number of past events is selected when calibration based on additional past events do not considerably change the estimated parameter ranges. However, this is not straight forward, this number may vary from one application to another depending on the variability of the events in terms of intensity, period of occurrence of the events; how close are the events to the particular event under study and whether there was evolution in the landuse or modification to the river channel, and number of parameters to evaluate. Perhaps the proper number of past events necessary for the hydrological/hydraulic modelling have always been an open question in hydrology, Koutroulis and Tsanis (2010) calibrated their model based on 8 events, Garambois et al.(2013) evaluated their study based on 10 events, and Massari et al.(2014) calibrated and validated their model based on 16 events. Given the scarcity of data about floods in the area, 12 events of variable intensity is an acceptable number in hydrology and was found to be sufficient to insure convergence in the calibration; this is clear from the results of calibration of the model by 6 and 12 events where the parameter ranges do not change considerably and the model is quite stable around this parameter range.

The selected events are of variable intensities, involving low flow as well as high flow events allowing to obtain sufficient ranges of variation of the hydrological parameters. Out of the 12 events, 5 are considered low flow events (events 2, 3, 4 7, and 8; peak flow ranging between 17 and 29 m^3/s), 4 are moderate flow events (events 5, 9, 10, and 12; peak flow ranging between 68 and 86 m^3/s), and 3 are high flow events (events 1, 6, and 11; peak flow ranging between 119 and 163 m^3/s). The events were selected for the period between January 2000 and March 2012. For the studied period no major changes to the landuse and the river network was observed, and the same hydrometeorological network was operating. Moreover, the study is limited to evaluating only 3 parameters that are thought to mostly impact the results of modelling.

The parameter ranges obtained after evaluating the model with the past events can define narrower parameter ranges for uncertainty evaluation. Perhaps the more past events evaluated the better results are expected. The approach is not suitable for evaluating big number of parameters, because it is economically unfeasible to evaluate large number of past events that might not be available in data-sparse regions. The approach might not be suitable when considerable changes in the flow regime or in the basin's characteristics are noticed.

With an NSE ranging from 0.06 to 0.84, the model performance is highly variable. Low NSE values are obtained for minor as well as major events. Therefore, model performance cannot be clearly related with the event type. However, low NSE when modelling flood events doesn't mean necessary a bad simulation. It can be due to a simple translation of the hyetograph (Moussa, 2010) or data quality issues. For high magnitude events (events 1 and 12), the model tends to underestimate the peak flow, mainly because the discretization of the daily rainfall measurements into hourly rainfall measurements does not reflect the actual rainfall intensity, which is expected to be higher. Moreover, the low reliability of the estimated rating curves might produce higher observed peak flow values for events exceeding the maximum stage by the rating curve, see for example event 11; the peak flow estimated by the upstream gauge G(473) by 246.5 m^3/s far exceeds the peak flow estimated by the downstream gauge G(475) by 118.7 m^3/s. In some cases (events 2, 3, 9, and 10), the flow hydrographs exhibited large fluctuations that affected the performance of the model. These fluctuations are not linked to precipitation patterns, because the majority are observed when no rainfall is recorded. The mismatch between the precipitations and observed water levels can be linked to either an error in rainfall measurement, or to a malfunctioning of the river stage gauge that is highly sensitive to any disturbance induced into the river flow. At this stage and considering the low reliability of the rating curves and the lack of hourly rainfall estimates, these should be considered satisfactory results.

9.5.2 ***Uncertainty propagation***

The uncertainty in the model results is a propagation of several uncertainties inherent mainly in the input data, model parameters, and model structure. In data sparse regions, the uncertainty inherent in the hydrological model input and model parameters may be the

major sources of uncertainty compared to the hydrological model structure. This is because the selected hydrological model structure is widely accepted and have been verified before on several properly gauged basins worldwide and the uncertainties inherent in its structure are negligible compared to the poor uncertain data available. This might be a difference between hydrological and hydraulic models in which the uncertainty inherent in the hydraulic model structure might outperform the one emerged from the hydraulic model parameters as demonstrated by Dimitriadis et al. (2016). However, additional hydrological model structures, through other software, should be tested in future research to further test this statement. The lack of sufficient observational data necessary to parameterize the model is the major source of uncertainty in the model parameters which is propagated to the output variables. Classical hydrological modelling techniques in well gauged basins involves calibrating the model with a set of past observation data. The result is a defined set of parameters capable to a certain extent of well reproducing the hydrological rainfall-runoff transformations within the basins in a deterministic way. On the other side, if no model calibration is performed, analyzing the uncertainty propagation through modelling based on a wide range of feasible parameter ranges will result in numerous possible model realizations. Sometimes, when the uncertainty bounds are too wide, the results of the modelling are no more representative and can be substituted by other empirical or simplified methods. Based on what have been discussed, the calibration approach applied in this study aims to define the hydrological model parameters ranges to reduce uncertainty in the output flows. The “12-events” model simulation resulted in a peak flow difference of around 105 m^3/s between the maximum and minimum uncertainty bounds. This is much better than solely performing the uncertainty analysis based on the arbitrarily chosen wide parameter ranges that resulted in a peak flow difference of around 450 m^3/s. The future work involves testing this approach on other study sites to assess the effect of variable number of past storm events chosen for calibration.

Rainfall is the major input data to the model of major uncertainty inherent in the time step of measurement, especially in regions characterized by flash floods of response times in the order of hours. Discretizing the daily rainfall measurements into hourly measurements over the period of occurrence of maximum rainfall was found to be encouraging. This interprets the relatively good NSE value obtained for event 6 for which rainfall was discretized over the first quarter of the day only; the time period of occurrence of maximum rainfall. Further analysis is to be performed to compare different rainfall discretization methods, to analyze the uncertainty induced by the time step of measurement, especially when no information on the time of occurrence of the rain event is available. Other sources of rainfall data uncertainties are inherent in its spatial variability and measurement method. Such uncertainties can be ignored compared to the uncertainties inherent in the time step of measurement because the Jan2013 storm event was widely spread over the whole country with no major spatial variation in the rainfall intensity observed over the relatively small basin’s area. The analogous records of six daily rainfall stations, well distributed over the area, also support our observation and reduces the uncertainty inherent in the spatial variability of rainfall and in its measured values.

9.5.3 *Opportunities in post-event measurements*

The spatial water level measurements based on high water marks such as fragments in trees, traces left by water along the river section and floodplain, and water lines on building walls were acknowledged by several scientists in literature (e.g. Horritt and Bates, 2002; Borga et al., 2008; Fuentes-Andino et al., 2017). Indeed, these measurements are biased by river modification over time and a greater uncertainty is associated with rapid flow conditions. Despite this uncertainty, those measurements may represent the best available evidence for flood events. The uncertainty in measurements can be assessed by the field surveyors themselves considering the conditions that formed the high-water marks. In rapid flow conditions and if good care was taken when measuring the water peaks, uncertainty in measurements may not exceed the 0.15m as suggested by the USGS (Koenig et al., 2016).

In this study, no major modification to the river channel was observed. Maximum water level measurements were carefully chosen with proper awareness. Unreliable or confusing points with variable or unclear high-water marks were avoided, allowing to keep only the clear and best quality points. This evaluation criteria limited the number of post-event measurements to 27 measurements. In some cases, an average of two or three water marks was estimated to improve confidence in the measurement. Sometimes, viewing the complete set of points of a water line on one side of the bank and comparing it to the opposite bank allows estimating the best water line. Moreover, information on water levels obtained from local witnesses was considered reliable because the field survey was performed in two months after the flood event and the local witnesses' memory about the event was still fresh.

In this study and based on our observation, the uncertainty in the post-event measurements may not exceed the 0.5 m. Despite this uncertainty most of the observed water levels fall within the uncertainty bounds and are very close to the mean simulation of the hydraulic model. In the lack of hydrometric measurements, the results indicate the robustness of the applied approach in modelling flood levels and the capability of validating the results on different locations scattered in space.

The resolution of the topographic data is a key element in the accuracy of the hydraulic model (Casas et al., 2006; Cook and Merwade, 2009). Several studies in literature have pointed out to the sensitivity of the hydraulic models to the resolution of digital elevation models (Tsubaki and Fujita, 2010; Papaioannou et al., 2016; Savage et al., 2016). Many have acknowledged the use of high resolution DEM's for hydraulic modelling and flood mapping specially with basins of rapidly varied topography and steep river slopes (Schumann et al., 2009; Bates, 2012; Brandt, 2016).

In this approach, validation of the hydraulic model with post-event measurements in space is encouraging when based on a fine resolution DEM. A prior simulation for the hydraulic model was performed based on the available 10 m resolution DEM. The hydraulic model experienced a lot of numerical instabilities. The resulting water levels were far beyond the real observed water levels, and in some locations, were more than

triple the observed ones. This is primarily because the geometry and slopes of the river channel and the floodplain are not well represented in the coarse DEM; i.e. a river channel of width in the order of 5 to 10 m and a flood plain in the order of 30 to 50 m are unrealistically presented by 3 to 5 cells only in the coarse DEM. In hydraulic models, errors induced by poor terrain and slopes representation are much higher than those induced by poor estimation of the Manning's coefficient (see for example Jaber and Mohtar, 2003). With the advancement of the remote sensing and drone photography techniques, fine resolution DEM's are expected to be widely spread in the future. These techniques, mainly the drone photography, are being favorable because of their ease of use, high accuracy, and wide applicability (McCabe et al., 2017; Leitão and de Sousa, 2018). Accordingly, the availability of the fine resolutions DEM's should not be an issue in data-sparse regions in the coming years.

9.5.4 What if sparse spatial data are better than classical temporal data?

Calibration and evaluation of the hydrological model with several past storm events increased the results robustness. Unlike classical uncertainty analysis techniques in ungauged basins involving wide parameter ranges, the results robustness is obtained by evaluating the model with several storm events of variable intensities that allowed the estimation of possible parameter ranges of the hydrological model that are narrow enough to reduce the uncertainty in the model predictions. Moreover, the presented results must be compared with the classical calibration approach that results in a set of deterministic model parameters and do not allow easily for the uncertainty propagation through the model.

Classically, hydraulic models are calibrated and validated based on "classical temporal data at one point", these are measured water levels or flow values at the gauge stations. However, several potential errors arise when using this type of observational data related to the accuracy of measurement and its spatial resolution. For large flood events and when river stage gauges are not damaged by the flood, water level measurements may exceed the maximum gauge measurement levels or exceed the maximum value used in the derivation of the rating curves that are unable to reflect the hydraulic behaviour of the rated section (Horritt et al., 2010). Even though the river stage accurately measures the water levels that are within the range of the rating curves, it is still required to obtain information on other cross sections based on field investigation of flood marks. Those levels often exceed the range of stage-discharge relationships that may exist on site (Gaume and Borga, 2008). Despite the narrow temporal sampling of the water levels at the river stage, there is lack of spatial data that do not allow the verification of the distributed model predictions, whereas, the use of finer resolution DEM increases the confidence in the distributed model predictions (Moussa and Cheviron, 2015b). The use of "sparse spatial data at one date" in the form of post-event measurements of water levels scattered in space alone supports the spatial validation of the flood inundation model. Such spatial sparse information of non-binary nature may be used in the lack of short time step temporal hydrograph on a given point, especially in time periods of approximately steady flow conditions. Whereas, the "classical temporal data at one point" of too sparse

spatial resolution should always be accompanied with other diverse sources such as the aerial photos, remote sensing or post-event measurements of flood marks to allow the spatial validation of the model predictions. On the other hand, the broader distribution and the greater number of post-event measurements, the better validation is achieved, because this type of data is subjected to several limitations (Hunter et al., 2005). For example, in the case of unsteady flow conditions the flood inundation could behave differently in the upstream and downstream areas and the post-event measurements might not reflect the flood dynamics.

*9.5.5 **Model complexity vs performance for a given condition of data availability***

The more complex the flood model is, the greater is the risk of the uncertainty inherent in the required input data, model parameters, and in the model structure. Applying complex models in a data-sparse basin cannot be easy verified.

Several studies on DEM-based Geomorphic approaches have been performed in literature to delineate flood prone areas. These simplified methods that rely on basin geomorphologic feature characterization revealed to be an efficient low-cost strategy (e.g. Moussa, 1997; Noman et al., 2001; Manfreda et al., 2014; Samela et al., 2017). The geomorphic approaches allow highlighting preliminarily the locations of flooded areas and give rough estimation on the extent and depth of flood inundation. Such approaches proved to be efficient in large scale applications (Samela et al., 2017) and the outcomes are relatively sufficient to inform decision makers on the range of variability of the flood hazard for general planning purposes. However, general geomorphic approaches may not be very efficient when detailed information on the inundation levels and extent is required especially in small scale applications and therefore cannot easily replace the hydrological-hydraulic approaches (Manfreda et al., 2014).

Moreover, most geomorphic approaches require probabilistic information on rainfall (e.g. design rainfalls of 50 years, 100 years, etc..) obtained from statistical analysis of rainfall series and make use of the hydraulic scaling functions based on contributing areas to estimate water levels. These estimations based on probabilistic input do not always allow the detailed understanding of particular events of unknown severity level, such as the Jan2013 flood event. Working with particular event is not like working with statistical approaches.

Although complex models require an increasing number of data to reach adequate reliability and it is preferable to be avoided. But for practical problems the use of complex models is inevitable (Grayson and Blöschl, 2001). It is of a challenge to better use the available information and to seek additional information to increase the confidence in model simulations. Model complexity depends on how we define it, on the site of application and on the time of application; what was considered complex several years ago is now simpler with the rapid evolution of computational power, development of very high resolution DEM’s, and the widespread of geographic information systems (GIS).

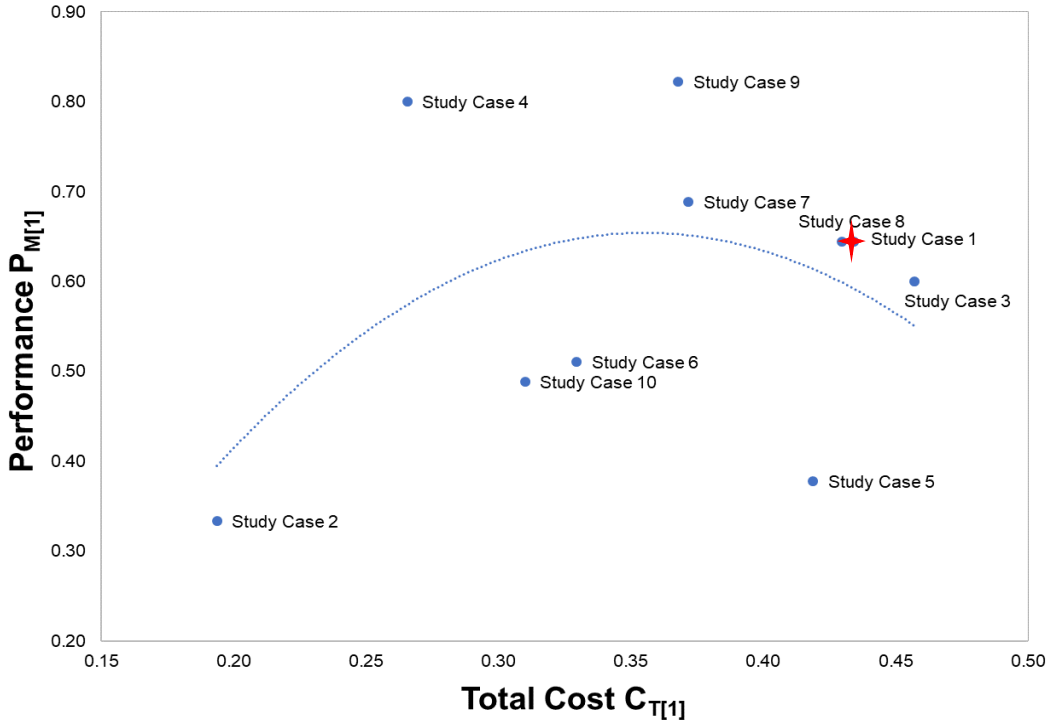

Figure 9.4 The location (highlighted in red cross) of the applied approach on the Awali Basin (study case 1), based on the proposed framework, on the cost-performance diagram developed in chapter 7.

The presented application was compared to other applications of flood modeling presented in chapter 7. The relative location of our application (Study Case 1) is highlighted in red cross on the cost-performance diagram in Figure 9.4. Our application is located above the cost-performance curve and falls within the model coupling zone. The total cost of modeling is 0.43 and the modeling performance is 0.64. Compared to the average total cost of modeling and the average modeling performance for the evaluated ten events (average $C_{T[1]}$ and $P_{M[1]}$ values are 0.36 and 0.59 respectively), the application records slightly higher modeling cost level but at the same time records higher performance level. The slightly higher cost of modeling can be interpreted by the use of high resolution DEM extracted based on detailed UAV Drone surveys which shifted up the cost of data a little from the average. Despite that adding this data type slightly increases the cost of modeling, it highly improved the modeling performance and shifted it above its average level. Whereas without this fine resolution DEM, the hydraulic modeling would been impossible.

Moreover, our own proposed modeling approach falls within the model coupling zone and have cost and performance levels similar to other coupling approaches (study cases 3, 8, 7 and 9). Being on the same level with other model coupling approaches indicates the proper selection of the approach, and the applicability of the proposed modeling procedure.

The presented application is not much complicated but rather an intermediate position between complex and simple approaches. Indeed, several simplifications of the process's representation were applied to reduce model requirements and number of parameters. This can be illustrated for example by using the SCS Curve Number approach for runoff computation, which is empirical in origin, along with the SCS-unit hydrograph routing method. 1D HEC-RAS model can be considered as simple by comparison to 2D or 3D hydraulic models.

Added value information from social media, post-event surveys and past storm events helped constrain the model and improve the quality of results. The availability of a high-resolution DEM encouraged the application of the 1D hydraulic model (HEC-RAS) which proved to give reasonably promising results. The error in the simulated water levels is in the order of 20 to 30 cm which might not be achieved when applying simplified geomorphic approaches. However, this doesn't prove our approach will be efficient in all circumstances, but at least it strengthens our confidence in its value.

9.6 **Conclusions**

The objective of this chapter was to assess whether there is opportunity to constrain hydrological-hydraulic models with sparse data to simulate extreme floods and establish water levels that can be useful for flood maps adapted for basin scale applications. The challenge was to develop a cost-effective modeling approach that balances model complexity with the limited data availability condition. For this purpose, we develop a framework based on a coupled hydrological-hydraulic model constrained by past storm events and post-event measurements. The approach is applied to the Awali river basin (301 km^2), in Lebanon, particularly to simulate the investigated early January 2013 extreme flood event. The hydrological model was calibrated with 12 past storm events aiming at defining narrow hydrological parameter ranges. The uncertainty in the model parameters was assessed by performing Monte Carlo simulation for the estimated parameter ranges. The uncertainty simulation gave satisfactory results. It was found that the uncertainty in the resulting outflow values is reduced when compared with running simulations based on arbitrarily chosen wide parameter ranges. Social media information on the event characteristics especially on the duration of maximum rainfall was an added value to constrain the hydrological model simulations. Post-event measurements of high-water marks were promising in validating the flood map in space.

The results show the potentials and the limitations of applying hydrological-hydraulic models using sparse data and the challenge of producing flood maps that can replace the coarse resolution regional maps. The clear advantage of the proposed method is that it is a tailor-made approach adapted for basin scale applications in data-sparse regions using the maximum data available and aiming at producing inundation maps that can perform better than regional maps. The method allows modelling with reduced uncertainty particular flood events in terms of estimation of the flood hydrographs, flood water levels and mapping the inundated area. It has the potential to enable crowdsourcing of information for flood events in the form of spatial post event measurements, social media

information, local witnesses, and pictures and videos. Such crowdsourced information is now gaining favor in data-sparse regions as a way to compensate the weaknesses in the traditional measurement networks. Moreover, the method has the potential to include high resolution digital elevation models that are now evolving at an unprecedented pace. The coupled hydrologic/hydraulic model is constrained by past storm events and post events measurements and the results are estimations of the flood water levels along the floodplain with accuracy less than 1 m. The interesting results reveal that good spatial measurements of one event, even of very short time series, are significant in supporting the hydrological/hydraulic modeling. These sparse spatial data at one date may be used in the lack of classical temporal data at the gauge stations.

Comparing the approach with other flood modeling approaches, specifically model coupling approaches, reveals a good cost-performance level. The fine resolution DEM elevated a little the modeling cost but at the same time highly improved the modeling performance.

The approach can serve as a tool for damage assessment of flood events, it supports urban planning and structural design of flood protection measures on a local scale. The approach when combined with organized real time crowdsourcing can serve as a part of a flood forecasting system. Finally, when classical data are lacking, the use of sparse data in a classical modelling approach is encouraging and the proposed framework can be applied to other data-sparse regions facing the same problems.

GENERAL CONCLUSIONS AND PERSPRCTIVES

General conclusions

In this work we developed a framework for flood modeling in data-sparse regions based on analyzing different flood modeling approaches in a cost-performance approach. The study is applied in Lebanon, a data-sparse country of the Eastern Mediterranean. The work begins by analyzing available sparse data on flood events in the country and then reviews and evaluates historical flood events extracted from newspaper archives to evaluate the intensity and spatial occurrence of floods in Lebanon. We discuss the opportunities and limitations of such data sources and then extend to perform a hydrological/hydraulic modeling approach to a selected study site. The detailed modeling was preceded by developing a new cost-performance grid to allow the proper selection of a suitable a cost-effective modeling approach that balances model complexity with the available sparse data condition. Later our approach further extends to assess whether there is an opportunity to constrain the hydrological-hydraulic models by sparse data to simulate extreme floods and establish water levels that can be useful for flood assessment and mitigation and whether this approach remains cost-effective based on the poor condition of data availability. The last step involved developing a flood modelling framework from a coupled hydrological-hydraulic model constrained by past storm events and post-event measurements.

An intensive history scan of newspaper archives and previous reports allows us to extract 196 records extending between 1293 and 2013 out of which we could distinguish 711 flood events in 86 villages in Lebanon. The monthly frequency of occurrence was analyzed, and the spatial occurrence of these events was mapped on a district (caza) scale in five levels. The five northern coastal catchments; el Kabir, Ostouane, Arka, Bared, and Abu Ali (in its low main part in Tripoli), record the highest number of events along with the central catchments of Beirut river and urban Beirut, all at level 5 frequency of occurrence. The Assi, Litani, Hasbani, Awali and Damour catchments come in the second position with level 4 frequency of occurrence of flood events. Generally, the elevated number of floods in these locations could not be linked to a single factor, but to a combination of morphological, hydrological, and vulnerability characteristics. The developed spatial flood occurrence map shows a combination of the flood hazard and the vulnerability to flooding and would be treated as a flood risk map in the absence of detailed studies. The extracted events from newspapers are promising in retrieving information on previous flood events in the absence of data measurements. Such information allows for the first time analyzing the frequency of occurrence of flood events along with mapping their spatial occurrence over the whole country. Although results may not be clear but there is an opportunity to understand the floods and the changes in their regimes. However, for detailed studies, these records remain descriptive focusing on the event's damages (flood risk) more than its characteristics (flood hazard). The map is developed on a large scale (district scale), which does not allow the detailed analysis to obtain information on the flood flows, water levels and extent and hence cannot replace the need for a detailed hydrological-hydraulic modeling. In this regard, we selected the Awali River

Basin, a study site to perform detailed analysis and modeling because it was among the major basins recording high frequency of occurrence of flood events and because of the availability of post-event measurements of an extreme event that occurred in the basin.

For the cost-performance analysis, we propose a new cost-performance grid to evaluate flood modeling approaches in terms of modeling costs and modeling performance. The grid is based on defining metrics to evaluate the three axes of a modeling problem: data availability, model complexity, and modeling performance. As an application on the grid ten arbitrability selected study cases were evaluated and plotted on a cost-performance diagram. The average total cost level was 0.36 and the average performance level was 0.59. The average data cost was 0.23 and the average model cost was 0.47. Lowest modeling costs were associated with empirical approaches but however associated with lower performances. Modelling approaches based on open source data were associated with lower costs but high performances especially in well-gauged basins applications. Plotting the study cases on the cost-performance diagram allows us to highlight 4 modeling zones corresponding to 4 modeling categories (empirical (1), hydraulic (2), hydrological (4), and coupling (5)). The zones of the hydraulic modeling and coupling are associated with good performances and are located above the cost-performance curve. The hydraulic modeling zone is associated with lower costs. The zones of the empirical and the hydrological approaches are located below the cost performance curve and are associated with less performance levels because the outcomes of these approaches do not fulfil the objective of flood inundation mapping. The sensitivity analysis of the grid to the scores and weights shows that the grid is very sensitive to the selected scores scale but less sensitive to the weights' selection. A linear scale of scores of five levels gives better results compared to a logarithmic scale level of scores. The grid is also sensitive to the point of view of the author; the cost levels are mostly sensitive to the year and country of application and the performance levels are mostly sensitive to the objective of the modeling approach.

Last, we develop a framework for flood modeling in data-sparse regions, based on a coupled hydrological-hydraulic model constrained by past storm events and post-event measurements. The approach is tested to the Awali river basin (301 km^2), in Lebanon, particularly to simulate the investigated early January 2013 extreme flood event. The hydrological model was calibrated with 12 past storm events aiming at defining narrow hydrological parameter ranges. The uncertainty in the model parameters was assessed by performing Monte Carlo simulation for the estimated parameter ranges. The uncertainty simulation gave satisfactory results. It was found that the uncertainty in the resulting outflow values is reduced when compared with running simulations based on arbitrarily chosen wide parameter ranges. Social media information on the event characteristics especially on the duration of maximum rainfall was an added value to constrain the hydrological model simulations. Post-event measurements of high-water marks were promising in validating the flood map in space. The interesting results reveal that good spatial measurements of one event, even of very short time series, are significant in supporting the hydrological/hydraulic modeling. These sparse spatial data at one date may be used in the lack of classical temporal data at the gauge stations.

In conclusion, in data-sparse regions where information on flood events are lacking extracted events from newspapers and previous reports are promising in mapping the spatial occurrence of flood events and in highlighting high risk areas. However, these events remain descriptive information, mainly an indication of flood risk, and do not allow the detailed understanding of flood events in terms of hydrological characteristics, peak flows, water levels and inundation extent. Similarly, recently applied geomorphic approaches have also proved to be efficient for flood inundation mapping in data-sparse regions, but these approaches are mainly effective in large scale applications and the resultant maps can only be used for regional flood hazard studies and cannot do the favor in small scale applications. Therefore, when detailed information of flood flows and water levels are required in small basin-scale applications (small to medium sized basins < 1000 km^2) the use of hydrological-hydraulic models is inevitable.

Despite the higher complexities associated with such type of modeling, especially in the lack of sufficient observational data to calibrate and validate the models, it is of our challenge to better exploit data and models available in a way based on reduced modeling costs and improved modeling performance. The proposed cost-performance grid in this study can be a tool to support the comparison, classification, and selection of the modeling procedures by balancing modeling costs with modeling performance. Based on the cost-performance grid, the proposed framework for flood modeling proved to be a cost-effective approach. Comparing the approach with other flood modeling approaches, specifically model coupling approaches, reveals a good cost-performance level. The presented application is not much complicated but rather an intermediate position between complex and simple approaches. Indeed, several simplifications of the process's representation were applied to reduce model requirements and number of parameters. This can be illustrated for example by using the SCS Curve Number approach for runoff computation, which is empirical in origin, along with the SCS-unit hydrograph routing method. 1D HEC-RAS model can be considered as simple by comparison to 2D or 3D hydraulic models. Model complexity depends on how we define it, on the site of application and on the time of application; what was considered complex several years ago is now simpler with the rapid evolution of computational power, development of very high resolution DEM's, and the widespread of geographic information systems (GIS). Despite the slight increase in data costs, seeking higher accuracy in certain measurement fields, such as obtaining high resolution DEM's, can help improve the modeling performance and is recommended to support the classical hydrological-hydraulic modeling in data-sparse regions.

Finally, the presented thesis work opens the door to several applications. For operational purposes the proposed framework is not limited to the selected study site, it can be applied to the other Lebanese catchments to model flood inundation and can be part of a national flood forecasting system. Moreover, the proposed framework can be extended to other data-sparse regions facing the same problems. The clear advantage of the proposed approach is that it is a tailor-made approach adapted for basin scale applications in data-sparse regions using the maximum data available and aiming at producing inundation maps that can perform better than regional maps. The method allows modelling with reduced uncertainty particular flood events in terms of estimation of

the flood hydrographs, flood water levels and mapping the inundated area. It has the potential to enable crowdsourcing of information for flood events in the form of spatial post event measurements, social media information, local witnesses, and pictures and videos. Such crowdsourced information is now gaining favor in data-sparse regions as a way to compensate the weaknesses in the traditional measurement networks. Moreover, the method has the potential to include high resolution digital elevation models that are now evolving at an unprecedented pace. Additionally, the cost-performance grid allows to compare different approaches on a unified scale , classify approaches based on cost and performance levels, and choose the best flood modeling approaches for future applications based on defined objectives and available data and models. Perhaps this grid would be a tool that supports the future selection of cost-efficient modeling approaches. From a philosophical point of view, the grid supports research evolution studies. It allows to study the historical evolution of modeling costs and modeling performances. The grid is flexible and can be tuned to adapt with different modeling objectives and can be periodically updated to follow the recent advances in data measurements and model capabilities. The research is still open, and many other applications are expected to be presented in the future.

Perspectives

This study has highlighted the major challenges and limitations of modeling floods in data-sparse regions based on classical modeling approaches. The study also identified research challenges and gaps that need to be addressed in future works. Below are the main gaps and related requirements to support flood modeling applications.

Improve the existing monitoring river gauge network by replacing the existing traditional river gauge meters with highly automated gauge meters including telemetry transmitting capability. These should be capable to measure every 15 minutes water velocity, water depth, plot flow hydrographs and transmit them automatically. All gauges should have a proper concrete cross sections with a constant wet perimeter. Moreover, there is a need to Increase the number of gauges for each watershed, especially in sub-basins were flash floods take place (North Bekaa basins and sub-basins). The relevant authorities should facilitate recording of the water level during flood events at different locations along the river for further calibrations, which is not the current case due to logistic obstacles. Future works should also include an in depth study of the locations of flow change (extraction from the river and its rate, loss from the river to ground water, springs discharging into the river and their rate…).

Support upgrading/replacing all available rain gauge stations with the capability to measure rainfall intensities at 5min, 15 min, and 1hour intervals, this will allow the construction of the rainfall hyetographs. The installation of a rainfall radar is highly recommended to enable the spatial estimation of rainfall intensity especially taking into consideration the complex morphology of Lebanon. The relevant authorities should facilitate the access to Real time measurements of rainfall intensity and depth to support

current studies and to serve as part of the established early warning system in Lebanon at the Remote Sensing Center (SUNAR). Future work should also include extending the available network of meteorological stations to systematically cover all micro climatic zones taking into consideration the elevation aspect, this will support the correction of the satellite rainfall measurements. Moreover, there is an urgent need for QA/QC on a daily basis for all gauge records released by the various monitoring networks (LNMS, LARI, LRA…)

Support the ongoing work at the Remote Sensing Center to record flood events reported in newspapers and social media on a daily basis. This work is the first step towards developing a national flood database to support future studies and modeling, particularly those dealing with flood risk and damage assessment.

The proposed framework shall be extended to all Lebanese catchments and shall be part of the early warning system operated by the Remote Sensing Center. On a regional scale, the future plan should include supporting field UAV drone surveys to the river channels and flood plains to develop a high resolution DEM's that details the terrain morphology. Drone surveys shall be also performed after big flood events to capture pictures for the flooded areas and support the flood extent mapping. Post-event field surveys shall be periodically performed covering all main rivers after any recorded flood event. Relevant authorities, including the RSC, shall support and encourage any type of crowdsourcing of information from local authorities, residents and field witnesses. This work was initiated by the RSC center as part of the CNRS strategy for Early Warning System (SUNAR). Mobile and tab application were developed by the RSC that allow recording and sharing information on flood events locations and characteristics. Radar images shall also be purchased after each big flood event. This will help in delineating precisely the floodplains and calibrate and validate the hydrological-hydraulic models. In parallel, Land use and cover maps shall be detailed and updated regularly to support in updating catchments' characteristic parameters. Institutional capacity building, legal reforms and law enforcement for strengthening prevention, greater role for public/community engagement with Governmental Institutions (planning schemes, emergency action during floods, raising and maintaining awareness) all are best practices for flood warning and emergency action planning.

Future work shall also support the initiated cost-performance survey. More flood modeling approaches from different categories shall be obtained and analyzed to help in the enhancement of the grid and to further validate our outcomes. Authors, colleagues and experts in the field of flood modeling shall be contacted to obtain their input on their own study cases and receive their feedback on the proposed cost-performance grid. The research is still open, and many other applications are expected to be presented in the future. The grid supports research evolution studies. It allows studying the historical evolution of flood modeling procedures and study the corresponding evolution of the modeling costs in terms of data costs and model complexities. It also supports statistical studies that aim to evaluate the major types of data utilized for modeling, the average model complexities, and the mostly applied modeling procedures, etc. Moreover, the grid

is flexible and can be tuned to adapt with different modeling objectives. The grid shall be updated with time to follow the recent advances in data measurements and model capabilities. The grid is preliminarily customized to fit to flood modeling approaches, but the same methodology can be employed in many other modeling fields.

REFERENCES

Abd-el-Al, I.: Ibrahim Aed-El-Al Oeuvres Completes/ Association des Amis de Ibrahim ABD-El-Al., 1996.

Abdallah, C.: Hydrology & Watersheds., 2010.

Abdallah, C.: Assessment of erosion, mass movements and flood risk in Lebanon, in Review and Perspective of Environmental Studies in Lebanon, Chapter X., edited by H. Kouyoumjian and M. Hamze, pp. 225–246, INCAM-EU/CNRS Lebanon., 2012.

Abdallah, C. and Hdeib, R.: Flood Risk Assessment and Mapping for Lebanon- UNDP/CNRS, 93 P.+ANNEX, Lebanon., 2015.

Abdallah, C. and Hdeib, R.: تقييم مفصل حول مخاطر السيول في رأس بعلبك, National Council for Scientific Research, Lebanon., 2018.

Abdallah, C., Chorowicz, J., Bou Kheir, R. and Khawlie, M.: Detecting major terrain parameters relating to mass movements' occurrence using GIS, remote sensing and statistical correlations, case study Lebanon, Remote Sens. Environ., 99(4), 448–461, doi:10.1016/j.rse.2005.09.014, 2005.

Abdallah, C., Hdeib, R., Hijaz, S., Darwish, T. and Merheb, M.: Flood Hazard Mapping Assessment for Lebanon- UNDP/CNRS-2382, 110pp.+ANNEX, Lebanon., 2013.

Abu Al Anin, H.: Essays on the Geomorphology of Lebanon, Beirut Arab University, Beirut., 1973.

Amengual, A., Romero, R., Gómez, M., Martín, A. and Alonso, S.: A Hydrometeorological Modeling Study of a Flash-Flood Event over Catalonia, Spain, J. Hydrometeorol., 8(3), 282–303, doi:10.1175/JHM577.1, 2007.

Apel, H., Thieken, A. H., Merz, B. and Blöschl, G.: A probabilistic modelling system for assessing flood risks, Nat. Hazards, 38(1–2), 79–100, doi:10.1007/s11069-005-8603-7, 2006.

Apel, H., Merz, B. and Thieken, A. H.: Quantification of uncertainties in flood risk assessments, Int. J. River Basin Manag., 6(2), 149–162, doi:10.1080/15715124.2008.9635344, 2008.

Arnold, J. G., Srinivasan, R., Muttiah, R. S. and Williams, J. R.: Large Area Hydrologic Modeling and Assessment Part I: Model Development, J. Am. Water Resour. Assoc., 34(1), 73–89, 1998.

Aronica, G. T., Bates, P. D. and Horritt, M. S.: Assessing the uncertainty in distributed model predictions using observed binary pattern information within GLUE, Hydrol. Process., 16(10), 2001–2016, doi:10.1002/hyp.398, 2002.

Aronica, G. T., Franza, F., Bates, P. D. and Neal, J. C.: Probabilistic evaluation of flood hazard in urban areas using Monte Carlo simulation, Hydrol. Process., 26(26), 3962–3972, doi:10.1002/hyp.8370, 2012.

ASPRS: Manual of photogrammetry / editor, J. Chris McGlone; associate editors, Edward M. Mikhail, James Bethel, 5th ed., edited by E. M. Mikhail, J. S. (James S. Bethel, and J. C. McGlone, American Society of Photogrammetry and Remote Sensing, Bethesda, Md., 2004.

Di Baldassarre, G. and Montanari, A.: Uncertainty in river discharge observations: a quantitative analysis, Hydrol. Earth Syst. Sci., 13, 913–921, doi:10.5194/hessd-6-39-2009, 2009.

Barnolas, M. and Llasat, M. C.: A flood geodatabase and its climatological applications: the case of Catalonia for the last century, Nat. Hazards Earth Syst. Sci., 7(2), 271–281, doi:10.5194/nhess-7-271-2007, 2007.

Barredo, J. I.: Major flood disasters in Europe: 1950-2005, Nat. Hazards, 42(1), 125–148, doi:10.1007/s11069-006-9065-2, 2007.

Bates, P. D.: Remote sensing and flood inundation modelling, Hydrol. Process., 18(13), 2593–2597, doi:10.1002/hyp.5649, 2004.

Bates, P. D.: Integrating remote sensing data with flood inundation models: How far have we got?, Hydrol. Process., 26(16), 2515–2521, doi:10.1002/hyp.9374, 2012.

Bathurst, J. C. and O'Connell, P. E.: Future of distributed modelling: The Systeme Hydrologique Europeen, Hydrol. Process., 6(3), 265–277, doi:10.1002/hyp.3360060304, 1992.

Bergstrm, S., Lindstrm, G. and Pettersson, A.: Multi-variable parameter estimation to increase confidence in hydrological modelling, Hydrol. Process., 16(2), 413–421, doi:10.1002/hyp.332, 2002.

Bernier, M., Fortin, J.-P., Gauthier, Y., Carbane, C., Somma, J. and Dedieu, J. P.: Intégration de données satellitaires à la modélisation hydrologique du Mont Liban, Hydrol. Sci., 48(6), 999–1112, doi:10.1623/hysj.48.6.999.51428, 2003.

Beven, K.: Facets of uncertainty: Epistemic uncertainty, non-stationarity, likelihood, hypothesis testing, and communication, Hydrol. Sci. J., 61(9), 1652–1665, doi:10.1080/02626667.2015.1031761, 2016.

Beven, K. and Binley, A.: The future of distributed models: Model calibration and uncertainty prediction, Hydrol. Process., 6(3), 279–298, doi:10.1002/hyp.3360060305, 1992.

Beydoun, Z. R.: Observations on geomorphology, transportation and distribution of sediments in western Lebanon and its continental shelf and slope regions, Mar. Geol., 21(4), 311–324, doi:10.1016/0025-3227(76)90013-X, 1976.

Biancamaria, S., Bates, P. D., Boone, A. and Mognard, N. M.: Large-scale coupled hydrologic and hydraulic modelling of the Ob river in Siberia, J. Hydrol., 379(1–2), 136–150, doi:10.1016/j.jhydrol.2009.09.054, 2009.

Bleichrodt, H. and Quiggin, J.: Life-cycle preferences over consumption and health: When is cost-effectiveness analysis equivalent to cost-benefit analysis?, J. Health Econ., 18(6), 681–708, doi:10.1016/S0167-6296(99)00014-4, 1999.

Bonnifait, L., Delrieu, G., Lay, M. Le, Boudevillain, B., Masson, A., Belleudy, P., Gaume, E. and Saulnier, G. M.: Distributed hydrologic and hydraulic modelling with radar rainfall input: Reconstruction of the 8-9 September 2002 catastrophic flood event in the Gard region, France, Adv. Water Resour., 32(7), 1077–1089, doi:10.1016/j.advwatres.2009.03.007, 2009.

Borga, M., Gaume, E., Creutin, J. D. and Marchi, L.: Surveying flash floods: gauging the ungauged extremes, Hydrol. Process., 22(18), 3883–3885., doi:10.1002/hyp.7111, 2008.

Le Boursicaud, R., Pénard, L., Hauet, A., Thollet, F. and Le Coz, J.: Gauging extreme floods on YouTube: Application of LSPIV to home movies for the post-event determination of stream discharges, Hydrol. Process., 30(1), 90–105, doi:10.1002/hyp.10532, 2016.

Brandt, S. A.: Modeling and visualizing uncertainties of flood boundary delineation: algorithm for slope and DEM resolution dependencies of 1D hydraulic models, Stoch. Environ. Res. Risk Assess., 30(6), 1677–1690, doi:10.1007/s00477-016-1212-z, 2016.

Brauch, H. G.: Urbanization and Natural Disasters in the Mediterranean : Population Growth and Climate Change in the 21st Century, 2015.

Brázdil, R., Kundzewicz, Z. W. and Benito, G.: Historical hydrology for studying flood risk in Europe, Hydrol. Sci. J., 51(5), 739–764, doi:10.1623/hysj.51.5.739, 2006.

Brocca, L., Melone, F. and Moramarco, T.: Distributed rainfall-runoff modelling for flood frequency estimation and flood forecasting, Hydrol. Process., 25(18), 2801–2813, doi:10.1002/hyp.8042, 2011.

Casas, A., Benito, G., Thorndycraft, V. R. and Rico, M.: The topographic data source of digital terrain models as a key element in the accuracy of hydraulic flood modelling, Earth Surf. Process. Landforms, 31(4), 444–456, doi:10.1002/esp.1278, 2006.

Castellarin, A.: Probabilistic envelope curves for design flood estimation at ungauged sites, Water Resour. Res., 43(4), 1–12, doi:10.1029/2005WR004384, 2007.

Castellarin, A., Merz, R. and Blöschl, G.: Probabilistic envelope curves for extreme rainfall events, J. Hydrol., 378(3–4), 263–271, doi:10.1016/j.jhydrol.2009.09.030, 2009.

CDR: Schéma d'Aménagement du Territoire Libanais - Rapport Final, , 39–74, 2004.

Chahinian, N., Moussa, R., Andrieux, P. and Voltz, M.: Comparison of infiltration models to simulate flood events at the field scale, J. Hydrol., 306(1–4), 191–214, doi:10.1016/j.jhydrol.2004.09.009, 2005.

Chatterjee, C., Forster, S. and Bronstert, A.: Comparison of hydrodynamic models of different complexities to model floods with emergency storage areas, Hydrol. Process., 22, 4695–4709, doi:10.1002/hyp.7079, 2008.

Cheviron, B. and Moussa, R.: Determinants of modelling choices for 1-D free-surface flow and erosion issues in hydrology: a review, Hydrol. Earth Syst. Sci. Discuss., 12(9), 9091–9155, doi:10.5194/hessd-12-9091-2015, 2015.

Choudhari, K., Panigrahi, B. and Paul, J. C.: Simulation of rainfall-runoff process using HEC-HMS model for Balijore, Int. J. Geomatics Geosci., 5(2), 253–265, doi:Code : EIJGGS5021, 2014.

Cook, A. and Merwade, V.: Effect of topographic data, geometric configuration and modeling approach on flood inundation mapping, J. Hydrol., 377(1–2), 131–142, doi:10.1016/j.jhydrol.2009.08.015, 2009.

Coustau, M., Bouvier, C., Borrell-Estupina, V. and Jourde, H.: Flood modelling with a distributed event-based parsimonious rainfall-runoff model: Case of the karstic Lez river catchment, Nat. Hazards Earth Syst. Sci., 12(4), 1119–1133, doi:10.5194/nhess-12-1119-2012, 2012.

CRED: The human cost of natural disasters, a global perspective. [online] Available from: http://cred.be/sites/default/files/The_Human_Cost_of_Natural_Disasters_CRED.pdf, 2015.

D'Asaro, F. and Grillone, G.: Runoff Curve Number Method in Sicily: CN determination and analysis of the initial abstraction ratio, 4th Fed. Interag. Conf. Las Vegas, NV, June 27 - July 1, 2010, 1–12, 2010.

Dankers, R. and Feyen, L.: Flood hazard in Europe in an ensemble of regional climate scenarios, J. Geophys. Res. Atmos., 114(16), 1–16, doi:10.1029/2008JD011523, 2009.

Darwish, T., Khawlie, M., Jomaa, I., Abou Daher, M., Awad, M., Masri, M., Shaban, A., Faour, G., Bou Kheir, R., Abdallah, C. and Haddad, T.: Digital Soil Map of Lebanon 1 /50, 000. Monograph Series 4. CNRSLebanon, 2006.

Dimitriadis, P., Tegos, A., Oikonomou, A., Pagana, V., Koukouvinos, A., Mamassis, N., Koutsoyiannis, D. and Efstratiadis, A.: Comparative evaluation of 1D and quasi-2D hydraulic models based on benchmark and real-world applications for uncertainty assessment in flood mapping, J. Hydrol., 534, 478–492, doi:10.1016/j.jhydrol.2016.01.020, 2016.

Dogulu, N., López López, P., Solomatine, D. P., Weerts, A. H. and Shrestha, D. L.: Estimation of predictive hydrologic uncertainty using the quantile regression and UNEEC methods and their comparison on contrasting catchments, Hydrol. Earth Syst. Sci., 19(7), 3181–3201, doi:10.5194/hess-19-3181-2015, 2015.

Domeneghetti, A.: On the use of SRTM and altimetry data for flood modeling in data-sparse regions, Water Resour. Res., 52(4), 2901–2918, doi:10.1002/2015WR017967, 2016.

Domeneghetti, A., Vorogushyn, S., Castellarin, A., Merz, B. and Brath, A.: Probabilistic flood hazard mapping: Effects of uncertain boundary conditions, Hydrol. Earth Syst. Sci., 17(8), 3127–3140, doi:10.5194/hess-17-3127-2013, 2013.

Dooge, J. C. .: IIASA Proceedings Series: Logistics and Benefits of Using Methematical Models of Hydrologic and Water Resource Systems (1978, Pisa) General Report on Model Structure and Classification, edited by A. J. Askew, F. Greco, and J. Kindler, International Institute for Applied Systems Analysis, PERGAMON PRESS., 1981.

Dubertret, L.: Cartes geologiques du Liban a l'echelle de 1 /50 000., 1945.

Dutta, D., Herath, S. and Musiake, K.: Flood inundation simulation in a river basin using a physically based distributed hydrologic model, Hydrol. Process., 14(3), 497–519, doi:10.1002/(SICI)1099-1085(20000228)14:3<497::AID-HYP951>3.0.CO;2-U, 2000.

Efstratiadis, A., Koussis, A. D., Koutsoyiannis, D. and Mamassis, N.: Flood design recipes vs. reality: Can predictions for ungauged basins be trusted?, Nat. Hazards Earth Syst. Sci., 14(6), 1417–1428, doi:10.5194/nhess-14-1417-2014, 2014.

El-Fadel, M., Zeinati, M. and Jamali, D.: Water Resources in Lebanon: Characterization, Water Balance, and Constraints, Water Resour. Dev., 16(4), 615–638, doi:10.1080/713672540, 2000.

El-Qareh, R.: The submarine springs of Chekka: exploitation of a confined aquifer discharging in the sea. Unpublished M.Sc. Thesis, American University of Beirut, Geology Department, 80p., 1967.

ELARD: FLOOD RISK MANAGEMENT AND PREVENTION IN BAALBACK – HERMEL / Assessment report prepared by Earth Link and Advanced Resources Development S.A.R.L. (ELARD), Beirut, Lebanon., 2010.

Ewen, J. and Parkin, G.: Validation of catchment models for predicting land-use and climate change impacts. 1. Method, J. Hydrol., 175(1), 583–594, doi:10.1016/S0022-1694(96)80026-6, 1996.

Faour, G.: Evaluating urban expansion using remotely-sensed data in Lebanon., Leban. Sci. J., 16(1), 23–32, 2015.

Faour, G. and Mhawej, M.: Mapping Urban Transitions in the Greater Beirut Area Using Different Space Platforms, Land, 3(3), 941–956, doi:10.3390/land3030941, 2014.

Feldman, A.: Hydrologic Modeling System, , (March), 158 [online] Available from: http://www.hec.usace.army.mil/software/hec-hms/documentation.aspx, 2000.

Freer, J., Beven, K. and Ambroise, B.: Bayesian estimation of uncertainty in runoff prediction and the value of data: An application of the GLUE approach, Water Resour. Res., 32(7), 2161–2173, doi:10.1029/96WR03723, 1996.

Fuentes-Andino, D., Beven, K., Halldin, S., Xu, C.-Y., Reynolds, J.-E. and Di Baldassarre, G.: Reproducing an extreme flood with uncertain post-event information, Hydrol. Earth Syst. Sci. Discuss., 21(July), 3597–3618, doi:10.5194/hess-21-3597-2017, 2017.

Fukami, K., Yamaguchi, T., Imamura, H. and Tashiro, Y.: Current status of river discharge observation using non-contact current meter for operational use in Japan, World Environ. Water Resour. Congr., 2008.

Garambois, P. A., Roux, H., Larnier, K., Castaings, W. and Dartus, D.: Characterization of process-oriented hydrologic model behavior with temporal sensitivity analysis for flash floods in Mediterranean catchments, Hydrol. Earth Syst. Sci., 17(6), 2305–2322, doi:10.5194/hess-17-2305-2013, 2013.

Gaume, E.: Post Flash-flood Investigations-Methodological Note. Floodsite European Research Project, Report D23.2. 62pp., 2006.

Gaume, E. and Borga, M.: Post-flood field investigations in upland catchments after major flash floods: proposal of a methodology and illustrations, J. Flood Risk Manag., 1(4), 175–189, doi:10.1111/j.1753-318X.2008.00023.x, 2008.

Gaume, E., Bain, V., Bernardara, P., Newinger, O., Barbuc, M., Bateman, A., Blaškovicová, L., Blöschl, G., Borga, M., Dumitrescu, A., Daliakopoulos, I., Garcia, J., Irimescu, A., Kohnova, S., Koutroulis, A., Marchi, L., Matreata, S., Medina, V., Preciso, E., Sempere-Torres, D., Stancalie, G., Szolgay, J., Tsanis, I., Velasco, D. and Viglione, A.: A compilation of data on European flash floods, J. Hydrol., 367(1–2), 70–78, doi:10.1016/j.jhydrol.2008.12.028, 2009.

Ghattas, I.: The geology and hydrology of the western flexure of Mount Lebanon between Dbaiyeh and Jdaide. Unpublished M.Sc. Thesis, American University of Beirut, Geology Department, 99p., 1975.

Grayson, R. and Blöschl, G.: Spatial Patterns in Catchment Hydrology, Cambridge University Press. [online] Available from: http://www.cup.cam.ac.uk, 2001.

Grayson, R. B., Moore, I. and Mcmahon, T. A.: Physically based hydrologic modeling 2. Is the concept, Water Resour Res, 26(10), 2659–66, 1992.

Gumbel, E. J.: The return period of order statistics, Ann. Inst. Stat. Math, 12(3), 249–256, doi:10.1007/BF01728934, 1961.

Hakim, B.: Recherches hydrologiques et hydrochimiques sur quelques karsts méditerranéens au Liban, en Syrie et au Maroc, Publications de l'Université Libanaise. Section des études géographiques, tome II, 701p., 1985.

Hall, J., Arheimer, B., Borga, M., Brázdil, R., Claps, P., Kiss, A., Kjeldsen, T. R., Kriauciuniene, J., Kundzewicz, Z. W., Lang, M., Llasat, M. C., Macdonald, N., McIntyre, N., Mediero, L., Merz, B., Merz, R., Molnar, P., Montanari, A., Neuhold, C., Parajka, J., Perdigão, R. A. P., Plavcová, L., Rogger, M., Salinas, J. L., Sauquet, E., Schär, C., Szolgay, J., Viglione, A. and Blöschl, G.: Understanding flood regime changes in Europe: A state-of-the-art assessment, Hydrol. Earth Syst. Sci., 18(7), 2735–2772, doi:10.5194/hess-18-2735-2014, 2014.

Halwatura, D. and Najim, M. M. M.: Application of the HEC-HMS model for runoff simulation in a tropical catchment, Environ. Model. Softw., 46, 155–162, doi:10.1016/j.envsoft.2013.03.006, 2013.

Hdeib, R., Abdallah, C., Colin, F., Brocca, L. and Moussa, R.: Constraining coupled hydrological-hydraulic flood model by past storm events and post-event measurements in data-sparse regions, J. Hydrol., 565, 160–176, doi:10.1016/j.jhydrol.2018.08.008, 2018.

Hervouet, J. M.: A high resolution 2-D dam-break model using parallelization, Hydrol. Process., 14(13), 2211–2230, doi:10.1002/1099-1085(200009)14:13<2211::AID-HYP24>3.0.CO;2-8, 2000.

Horritt, M. S. and Bates, P. D.: Evaluation of 1D and 2D numerical models for predicting river flood inundation, J. Hydrol., 268(1–4), 87–99, doi:10.1016/S0022-1694(02)00121-X, 2002.

Horritt, M. S., Mason, D. C. and Luckman, A. J.: Flood boundary delineation from synthetic aperture radar imagery using a statistical active contour model, Int. J. Remote Sens., 22(13), 2489–2507, doi:10.1080/01431160116902, 2001.

Horritt, M. S., Bates, P. D., Fewtrell, T. J., Mason, D. C. and Wilson, M. D.: Modelling the hydraulics of the Carlisle 2005 flood event, Proc. Inst. Civ. Eng. - Water Manag., 163(6), 273–281, doi:10.1680/wama.2010.163.6.273, 2010.

Hreiche, A.: Modélisation conceptuelle de la transformation pluie-débit dans le contexte méditerranéen, Universite Montpellier II et Universite Saint-Joseph., 2003.

Huang, M. and Liang, X.: On the assessment of the impact of reducing parameters and identification of parameter uncertainties for a hydrologic model with applications to ungauged basins, J. Hydrol., 320(1–2), 37–61, doi:10.1016/j.jhydrol.2005.07.010, 2006.

Hughes, M. L., McDowell, P. F. and Marcus, W. A.: Accuracy assessment of georectified aerial photographs: Implications for measuring lateral channel movement in a GIS, Geomorphology, 74(1–4), 1–16, doi:10.1016/j.geomorph.2005.07.001, 2006.

Hunter, N. M., Bates, P. D., Horritt, M. S., De Roo, a. P. J. and Werner, M. G. F.: Utility of different data types for calibrating flood inundation models within a GLUE framework, Hydrol. Earth Syst. Sci., 9(4), 412–430, doi:10.5194/hess-9-412-2005, 2005.

Jaber, F. H. and Mohtar, R. H.: Stability and accuracy of two-dimensional kinematic wave overland flow modeling, Adv. Water Resour., 26(11), 1189–1198, doi:10.1016/S0309-1708(03)00102-7, 2003.

Jarihani, A. A., Callow, J. N., McVicar, T. R., Van Niel, T. G. and Larsen, J. R.: Satellite-derived Digital Elevation Model (DEM) selection, preparation and correction for hydrodynamic modelling in large, low-gradient and data-sparse catchments, J. Hydrol., 524, 489–506, doi:10.1016/j.jhydrol.2015.02.049, 2015.

Kabout, K.: Master Thesis: Flood Risk Management in Semi-Arid Areas., Lebanese University, Ecole, Doctoral des Sciences et Technologie. Beirut, Lebanon., 2011.

Kampf, S. K. and Burges, S. J.: A framework for classifying and comparing distributed hillslope and catchment hydrologic models, Water Resour. Res., 43(W05423), doi:10.1029/2006WR005370, 2007.

Khan, S. I., Hong, Y., Wang, J., Yilmaz, K. K., Gourley, J. J., Adler, R. F., Brakenridge, R. G., Policelli, F., Habib, S. and Irwin, D.: Satellite Remote Sensing and Hydrological Modeling for Flood Inundation Mapping in Lake Victoria Basin : Implications for Hydrologic Prediction in Ungauged Basins, IEEE Trans. Geosci. Remote Sens., 49(1), 1–23, doi:10.1109/TGRS.2010.2057513, 2009.

Khawlie, M.: Hazard mapping: The Abou A'li river flood, Tripoli – Lebanon, In R. Oliveira, L.F. Rodrigues, A.G. Coelho, and A.P. Cunha, (eds.). Proceedings of the Seventh International Congress, 2049-2057. Lisbona, Portugal, 5-9 September., 1994.

Kim, J., Warnock, A., Ivanov, V. Y. and Katopodes, N. D.: Coupled modeling of hydrologic and hydrodynamic processes including overland and channel flow, Adv. Water Resour., 37, 104–126, doi:10.1016/j.advwatres.2011.11.009, 2012.

Knebl, M. R., Yang, Z. L., Hutchison, K. and Maidment, D. R.: Regional scale flood modeling using NEXRAD rainfall, GIS, and HEC-HMS/ RAS: A case study for the San Antonio River Basin Summer 2002 storm event, J. Environ. Manage., 75(4 SPEC. ISS.), 325–336, doi:10.1016/j.jenvman.2004.11.024, 2005.

Koenig, T. A., Bruce, J. L., O'Connor, J. E., McGee, B. D., Holmes, R.R., J., Hollins, R., Forbes, B. T., Kohn, M. S., Schellekens, M. F., Martin, Z. W. and Peppler, M. C.: Identifying and preserving high-water mark data: U.S. Geological Survey Techniques and Methods, book 3, chap. A24., 2016.

Komi, K., Neal, J., Trigg, M. A. and Diekkrüger, B.: Modelling of flood hazard extent in data sparse areas: a case study of the Oti River basin, West Africa, J. Hydrol. Reg. Stud., 10, 122–132, doi:10.1016/j.ejrh.2017.03.001, 2017.

Kömüşcü, A. Ü. and Çelik, S.: Analysis of the Marmara flood in Turkey, 7-10 September 2009: An assessment from hydrometeorological perspective, Nat. Hazards, 66(2), 781–808, doi:10.1007/s11069-012-0521-x, 2013.

Koutroulis, A. G. and Tsanis, I. K.: A method for estimating flash flood peak discharge in a poorly gauged basin: Case study for the 13-14 January 1994 flood, Giofiros basin, Crete, Greece, J. Hydrol., 385(1–4), 150–164, doi:10.1016/j.jhydrol.2010.02.012, 2010.

Kvočka, D., Falconer, R. A. and Bray, M.: Flood hazard assessment for extreme flood events, Nat. Hazards, doi:10.1007/s11069-016-2501-z, 2016.

Laganier, O., Ayral, P. A., Salze, D. and Sauvagnargues, S.: A coupling of hydrologic and hydraulic models appropriate for the fast floods of the Gardon River basin (France), Nat. Hazards Earth Syst. Sci., 14(11), 2899–2920, doi:10.5194/nhess-14-2899-2014, 2014.

Lastoria, B., Simonetti, M. R., Casaioli, M., Mariani, S. and Monacelli, G.: Socio-economic impacts of major floods in Italy from 1951 to 2003, Adv. Geosci., 7, 223–229, doi:10.5194/adgeo-7-223-2006, 2006.

Leitão, J. P. and de Sousa, L. M.: Towards the optimal fusion of high-resolution Digital Elevation Models for detailed urban flood assessment, J. Hydrol., 561(December 2017), 651–661, doi:10.1016/j.jhydrol.2018.04.043, 2018.

Lerat, J.: Quels apports hydrologiques pour les modèles hydrauliques ? Vers un modèle intégré de simulation des crues, , 190 + annexes, 2009.

Lerat, J., Perrin, C., Andréassian, V., Loumagne, C. and Ribstein, P.: Towards robust methods to couple lumped rainfall-runoff models and hydraulic models: A sensitivity analysis on the Illinois River, J. Hydrol., 418–419, 123–135, doi:10.1016/j.jhydrol.2009.09.019, 2012.

Lhomme, J., Sayers, P., Gouldby, B., Samuels, P., Wills, M. and Mulet-marti, J.: Recent development and application of a rapid flood spreading method, Flood Risk Manag. Res.

Pract., i(October), 15–24, doi:10.1201/9780203883020.ch2, 2009.

Lian, Y., Chan, I. C., Singh, J., Demissie, M., Knapp, V. and Xie, H.: Coupling of hydrologic and hydraulic models for the Illinois River Basin, J. Hydrol., 344(3–4), 210–222, doi:10.1016/j.jhydrol.2007.08.004, 2007.

Liu, Z., Martina, M. L. V and Todini, E.: Flood forecasting using a fully distributed model: application of the TOPKAPI model to the Upper Xixian Catchment, Hydrol. Earth Syst. Sci., 9(4), 347–364 [online] Available from: http://www.hydrol-earth-syst-sci.net/9/347/2005/%5Cnhttp://www.hydrol-earth-syst-sci.net/9/347/2005/hess-9-347-2005.pdf, 2005.

Liu, Z., Merwade, V. and Jafarzadegan, K.: Investigating the role of model structure and surface roughness in generating flood inundation extents using one- and two-dimensional hydraulic models, J. Flood Risk Manag., (June), doi:10.1111/jfr3.12347, 2018.

Llasat, M. C., Llasat-Botija, M., Barnolas, M., López, L. and Altava-Ortiz, V.: An analysis of the evolution of hydrometeorological extremes in newspapers: the case of Catalonia, 1982–2006, Nat. Hazards Earth Syst. Sci., 9(4), 1201–1212, doi:10.5194/nhess-9-1201-2009, 2009.

Llasat, M. C., Llasat-Botija, M., Prat, M. a., Porcú, F., Price, C., Mugnai, a., Lagouvardos, K., Kotroni, V., Katsanos, D., Michaelides, S., Yair, Y., Savvidou, K. and Nicolaides, K.: High-impact floods and flash floods in Mediterranean countries: the FLASH preliminary database, Adv. Geosci., 23, 47–55, doi:10.5194/adgeo-23-47-2010, 2010.

LNCSR-LMoA: Land cover/use map of Lebanon at 1:20,000 scale. National Council for Scientific Research (NCSR) and Ministry of Agriculture (MOA), Lebanon, 2010.

Lowry, C. S. and Fienen, M. N.: CrowdHydrology: Crowdsourcing hydrologic data and engaging citizen scientists, GroundWater, 51(1), 151–156, doi:10.1111/j.1745-6584.2012.00956.x, 2013.

Lumbroso, D. and Gaume, E.: Reducing the uncertainty in indirect estimates of extreme flash flood discharges, J. Hydrol., 414–415, 16–30, doi:10.1016/j.jhydrol.2011.08.048, 2012.

Manfreda, S., Nardi, F., Samela, C., Grimaldi, S., Taramasso, A. C., Roth, G. and Sole, A.: Investigation on the use of geomorphic approaches for the delineation of flood prone areas, J. Hydrol., 517, 863–876, doi:10.1016/j.jhydrol.2014.06.009, 2014.

Mascaro, G., Piras, M., Deidda, R. and Vivoni, E. R.: Distributed hydrologic modeling of a sparsely monitored basin in Sardinia, Italy, through hydrometeorological downscaling, Hydrol. Earth Syst. Sci., 17(10), 4143–4158, doi:10.5194/hess-17-4143-2013, 2013.

Mason, D. C., Schumann, G. J. P. and Bates, P. D.: Data Utilization in Flood Inundation Modelling, in Flood Risk Science and Management, edited by G. Pender and H. Faulkner, pp. 209–233, Blackwell Publishing Ltd., 2010.

Massari, C., Brocca, L., Barbetta, S., Papathanasiou, C., Mimikou, M. and Moramarco,

T.: Using globally available soil moisture indicators for flood modelling in Mediterranean catchments, Hydrol. Earth Syst. Sci., 18(2), 839–853, doi:10.5194/hess-18-839-2014, 2014.

Mazzoleni, M., Juliette, V., Arevalo, C., Wehn, U., Alfonso, L., Monego, M., Ferri, M. and Solomatine, D. P.: Towards assimilation of crowdsourced observations for different levels of citizen engagement : the flood event of 2013 in the Bacchiglione catchment, , (February), 1–40, doi:10.5194/hess-2017-59, 2017.

McCabe, M. F., Rodell, M., Alsdorf, D. E., Miralles, D. G., Uijlenhoet, R., Wagner, W., Lucieer, A., Houborg, R., Verhoest, N. E. C., Franz, T. E., Shi, J., Gao, H. and Wood, E. F.: The Future of Earth Observation in Hydrology, Hydrol. Earth Syst. Sci. Discuss., (February), 1–55, doi:10.5194/hess-2017-54, 2017.

Mejia, A. I. and Reed, S. M.: Evaluating the effects of parameterized cross section shapes and simplified routing with a coupled distributed hydrologic and hydraulic model, J. Hydrol., 409(1–2), 512–524, doi:10.1016/j.jhydrol.2011.08.050, 2011.

Merheb, M., Moussa, R., Abdallah, C., Colin, F., Perrin, C. and Baghdadi, N.: Hydrological response characteristics of Mediterranean catchments at different time scales: a meta-analysis, Hydrol. Sci. J., 61(14), 2520–2539, doi:10.1080/02626667.2016.1140174, 2016.

Merwade, V., Olivera, F., Arabi, M. and Edleman, S.: Uncertainty in flood inundation Mapping: Current Issues and Future Directions, J. Hydrol. Eng., 13(7), 608–620, doi:10.1061/(ASCE)1084-0699(2008)13:7(608), 2008.

Merz, B., Kreibich, H. and Apel, H.: Flood risk analysis: Uncertainties and validation, Osterr. Wasser- und Abfallwirtschaft, 60(5–6), 89–94, doi:10.1007/s00506-008-0001-4, 2008.

Merz, B., Kreibich, H., Schwarze, R. and Thieken, A.: Review article “assessment of economic flood damage,” Nat. Hazards Earth Syst. Sci., 10(8), 1697–1724, doi:10.5194/nhess-10-1697-2010, 2010.

Metni, M., El-Fadel, M., Sadek, S., Kayal, R. and El Khoury, D. L.: Groundwater resources in Lebanon: A vulnerability assessment, Int. J. Water Resour. Dev., 20(4), 475–491, doi:10.1080/07900620412331319135, 2004.

Montanari, A., Young, G., Savenije, H. H. G., Hughes, D., Wagener, T., Ren, L. L., Koutsoyiannis, D., Cudennec, C., Toth, E., Grimaldi, S., Blöschl, G., Sivapalan, M., Beven, K., Gupta, H., Hipsey, M., Schaefli, B., Arheimer, B., Boegh, E., Schymanski, S. J., Di Baldassarre, G., Yu, B., Hubert, P., Huang, Y., Schumann, A., Post, D. a., Srinivasan, V., Harman, C., Thompson, S., Rogger, M., Viglione, A., McMillan, H., Characklis, G., Pang, Z. and Belyaev, V.: “Panta Rhei—Everything Flows”: Change in hydrology and society—The IAHS Scientific Decade 2013–2022, Hydrol. Sci. J., 58(6), 1256–1275, doi:10.1080/02626667.2013.809088, 2013.

Montanari, M., Hostache, R., Matgen, P., Schumann, G., Pfister, L. and Hoffmann, L.: Calibration and sequential updating of a coupled hydrologic-hydraulic model using remote sensing-derived water stages, Hydrol. Earth Syst. Sci., 13(3), 367–380, doi:10.5194/hess-13-367-2009, 2009.

Moriasi, D. N., Arnold, J. G., Van Liew, M. W., Binger, R. L., Harmel, R. D. and Veith, T. L.: Model evaluation guidelines for systematic quantification of accuracy in watershed simulations, Trans. ASABE, 50(3), 885–900, doi:10.13031/2013.23153, 2007.

Morita, M. and Yen, B. C.: Modeling of Conjunctive Two-Dimensional Surface-Three-Dimensional Subsurface Flows, J. Hydraul. Eng., 128, 184–200, doi:10.1061/(ASCE)0733-9429(2002)128:2(184), 2002.

Moussa, R.: Variabilité spatio-temporelle et modélisation hydrologique : application au bassin du Gardon d'Anduze. Thèse de Doctorat, Montpellier 2., 1991.

Moussa, R.: Geomorphological transfer function calculated from digital elevation models for distributed hydrological modelling, Hydrol. Process., 11(5), 429–449, doi:10.1002/(SICI)1099-1085(199704)11:5<429::AID-HYP471>3.0.CO;2-J, 1997.

Moussa, R.: When monstrosity can be beautiful while normality can be ugly: assessing the performance of event-based flood models, Hydrol. Sci. J., 55(6), 1074–1084, doi:10.1080/02626667.2010.505893, 2010.

Moussa, R. and Bocquillon, C.: On the use of the diffusive wave for modelling extreme flood events with overbank flow in the floodplain, J. Hydrol., 374(1–2), 116–135, doi:10.1016/j.jhydrol.2009.06.006, 2009.

Moussa, R. and Chahinian, N.: Comparison of different multi-objective calibration criteria using a conceptual rainfall-runoff model of flood events, Hydrol. Earth Syst. Sci., 519–535, doi:Hydrol. Earth Syst. Sci., 13, 519–535, 2009, 2009.

Moussa, R. and Cheviron, B.: Modeling of Floods—State of the Art and Research Challenges. Chapter 7, 2015a.

Moussa, R. and Cheviron, B.: Rivers – Physical, Fluvial and Environmental Processes, , doi:10.1007/978-3-319-17719-9, 2015b.

Nash, J. E. and Sutcliffe, J. V.: River flow forecasting through conceptual models part I - A discussion of principles, J. Hydrol., 10(3), 282–290, doi:10.1016/0022-1694(70)90255-6, 1970.

Neal, J., Schumann, G. and Bates, P.: A subgrid channel model for simulating river hydraulics and floodplain inundation over large and data sparse areas, Water Resour. Res., 48(11), 1–16, doi:10.1029/2012WR012514, 2012a.

Neal, J., Villanueva, I., Wright, N., Willis, T., Fewtrell, T. and Bates, P.: How much physical complexity is needed to model flood inundation?, Hydrol. Process., 26(15), 2264–2282, doi:10.1002/hyp.8339, 2012b.

NOAA: National Centers for Environmental Information, State of the Climate: Global Hazards for January 2013, published online February 2013, retrieved on February 27, 2017 from http://www.ncdc.noaa.gov/sotc/hazards/201301., 2013.

Noman, N. S., Nelson, E. J., Zundel, A. K. and ASCE, M.: Review of automated floodplain delineation from digital terrain models, J. Water Resour. Plann. Manag., 127(December), 394–402, 2001.

Norbiato, D., Borga, M., Sangati, M. and Zanon, F.: Regional frequency analysis of extreme precipitation in the eastern Italian Alps and the August 29, 2003 flash flood, J. Hydrol., 345(3–4), 149–166, doi:10.1016/j.jhydrol.2007.07.009, 2007.

Oleyiblo, J. O. and Li, Z.: Application of HEC-HMS for flood forecasting in Misai and Wan'an catchments in China, Water Sci. Eng., 3(1), 14–22, doi:http://dx.doi.org/10.3882/j.issn.1674-2370.2010.01.002, 2010.

Panneton, F., L'ecuyer, P. and Matsumoto, M.: Improved long-period generators based on linear recurrences modulo 2, ACM Trans. Math. Softw., 32(1), 1–16, doi:10.1145/1132973.1132974, 2006.

Papaioannou, G., Loukas, A., Vasiliades, L. and Aronica, G. T.: Flood inundation mapping sensitivity to riverine spatial resolution and modelling approach, Nat. Hazards, doi:10.1007/s11069-016-2382-1, 2016.

Papaioannou, G., Vasiliades, L., Loukas, A. and Aronica, G. T.: Probabilistic flood inundation mapping at ungauged streams due to roughness coefficient uncertainty in hydraulic modelling, Adv. Geosci., 44, 23–34, doi:10.5194/adgeo-44-23-2017, 2017.

Pappenberger, F., Beven, K. J., Hunter, N. M., Bates, P. D., Gouweleeuw, B. T., Thielen, J. and Roo, A. P. J. De: Cascading model uncertainty from medium range weather forecasts (10 days) through a rainfall-runoff model to flood inundation predictions within the European Flood Forecasting System (EFFS), Hydrol. Earth Syst. Sci. Discuss., 9(4), 381–393, doi:10.5194/hess-9-381-2005, 2005.

Pappenberger, F., Beven, K. J., Ratto, M. and Matgen, P.: Multi-method global sensitivity analysis of flood inundation models, Adv. Water Resour., 31(1), 1–14, doi:10.1016/j.advwatres.2007.04.009, 2008.

Plassard, J.: Pluviometric map of Lebanon at a scale of 1:200,000. Republic of Lebanon. Ministry of Public Affairs. General Direction of Civil Aviation., 1972.

Raclot, D. and Albergel, J.: Runoff and water erosion modelling using WEPP on a Mediterranean cultivated catchment, Phys. Chem. Earth, 31(17), 1038–1047, doi:10.1016/j.pce.2006.07.002, 2006.

Refsgaard, J. C.: Terminology, Modelling Protocol And Classification of Hydrological Model Codes, in Distributed hydrological modelling, edited by M. B. Abbot and J. C. Refsgaard, pp. 17–39, kluwer academic publishers., 1996.

Robert, C. P. and Casella, G.: Monte Carlo statistical methods, 2nd ed., New York: Springer., 2004.

Robinson, J. S. and Sivapalan, M.: Catchment-scale runoff generation model by aggregation and similarity analyses, Hydrol. Process., 9(5–6), 555–574, doi:10.1002/hyp.3360090507, 1995.

Romanowicz, R. and Beven, K.: Estimation of flood inundation probabilities as conditioned on event inundation maps, Water Resour. Res., 39(3), 12 PP., doi:10.1029/2001wr001056, 2003.

Roux, H., Labat, D., Garambois, P. A., Maubourguet, M. M., Chorda, J. and Dartus, D.:

A physically-based parsimonious hydrological model for flash floods in Mediterranean catchments, Nat. Hazards Earth Syst. Sci., 11(9), 2567–2582, doi:10.5194/nhess-11-2567-2011, 2011.

Salajegheh, A. and Dastorani, J.: Determining of Regional Coefficients of Fuller's Empirical Formula to Estimate Maximum Instantaneous Discharges in Dasht Kavir Basin, Kalshour Sabzevar , Iran, BIABAN J., 11(1), 53–59, 2006.

Saleh, F., Ducharne, A., Flipo, N., Oudin, L. and Ledoux, E.: Impact of river bed morphology on discharge and water levels simulated by a 1D Saint-Venant hydraulic model at regional scale, J. Hydrol., 476, 169–177, doi:10.1016/j.jhydrol.2012.10.027, 2013.

Samaniego, L., Kumar, R. and Jackisch, C.: Predictions in a data-sparse region using a regionalized grid-based hydrologic model driven by remotely sensed data, Hydrol. Res., 42(5), 338–355, doi:10.2166/nh.2011.156, 2011.

Samela, C., Troy, T. J. and Manfreda, S.: Geomorphic classifiers for flood-prone areas delineation for data-scarce environments, Adv. Water Resour., 102, 13–28, doi:10.1016/j.advwatres.2017.01.007, 2017.

Sangati, M., Borga, M., Rabuffetti, D. and Bechini, R.: Influence of rainfall and soil properties spatial aggregation on extreme flash flood response modelling: An evaluation based on the Sesia river basin, North Western Italy, Adv. Water Resour., 32(7), 1090–1106, doi:10.1016/j.advwatres.2008.12.007, 2009.

Der Sarkissian, R.: Master thesis: Watershed management for the AWALI Basin, Faculty of Sciences of the Lebanese University., 2015.

Satyanarayana, P. and Srinivas, V. V.: Regionalization of precipitation in data sparse areas using large scale atmospheric variables - A fuzzy clustering approach, J. Hydrol., 405(3–4), 462–473, doi:10.1016/j.jhydrol.2011.05.044, 2011.

Savage, J. T. S., Bates, P., Freer, J., Neal, J. and Aronica, G.: When does spatial resolution become spurious in probabilistic flood inundation predictions?, Hydrol. Process., 30(13), 2014–2032, doi:10.1002/hyp.10749, 2016.

Schumann, G., Bates, P. D., Horritt, M. S., Matgen, P. and Pappenberger, F.: Progress in intergration of remote sensing derived flood extent and stage data and hydraulic models, Rev. Geophys., 47(2008), 1–20, doi:10.1029/2008RG000274.1.INTRODUCTION, 2009.

Schumann, G. J. P., Neal, J. C., Voisin, N., Andreadis, K. M., Pappenberger, F., Phanthuwongpakdee, N., Hall, A. C. and Bates, P. D.: A first large-scale flood inundation forecasting model, Water Resour. Res., 49(10), 6248–6257, doi:10.1002/wrcr.20521, 2013.

SCS: Soil Conservation Service-Section 4: Hydrology, in National Engineering Handbook, Department of Agriculture, available from US Government Printing Office, Washington, DC., 1972.

Sene, K. J., Marsh, T. J. and Hachache, a.: An assessment of the difficulties in

quantifying the surface water resources of Lebanon, Hydrol. Sci. J., 44(1), 79–96, doi:10.1080/02626669909492204, 1999.

Sene, K. J., Houghton-Carr, H. A. and Hachache, A.: Preliminary flood frequency estimates for Lebanon, , 46(5), 37–41, doi:10.1080/02626660109492863, 2001.

Shamsudin, S., Dan, S. and Rahman, A. A.: Uncertainty Analysis of Hec-Hms Model Parameters Using Monte Carlo Simulation, Int. J. Model. Simul., 31(4), doi:10.2316/Journal.20, 2011.

Sharif, H. O., Sparks, L., Hassan, A. a., Zeitler, J. and Xie, H.: Application of a Distributed Hydrologic Model to the November 17, 2004, Flood of Bull Creek Watershed, Austin, Texas, J. Hydrol. Eng., 15(8), 651–657, doi:10.1061/(ASCE)HE.1943-5584.0000228, 2010.

Singh, V. P. and Woolhiser, D. A.: Mathematical Modeling of Watershed Hydrology, J. Hydrol. Eng., 7(4), 270–292, doi:10.1061/(ASCE)1084-0699(2002)7:4(270), 2002.

Sivapalan, M., Takeuchi, K., Franks, S. W., Gupta, V. K., Karambiri, H., Lakshmi, V., Liang, X., McDonnell, J. J., Mendiondo, E. M., O'Conell, P. E., Oki, T., Pomeroy, J. W., Schertzer, D., Uhlenbrook, S. and Zehe, E.: IAHS Decade on Predictions in Ungauged Basins (PUB), 2003–2012: Shaping an exciting future for the hydrological sciences, Hydrol. Sci. J., 48(6), 857–880, doi:10.1623/hysj.48.6.857.51421, 2003.

Smith, M. J., Edwards, E. P., Priestnall, G. and Bates, P. D.: Exploitation of new data types to create digital surface models for flood inundation modelling., 2006.

Switzman, H., Coulibaly, P. and Adeel, Z.: Modeling the impacts of dryland agricultural reclamation on groundwater resources in Northern Egypt using sparse data, J. Hydrol., 520, 420–438, doi:10.1016/j.jhydrol.2014.10.064, 2015.

Teng, J., Jakeman, A. J., Vaze, J., Croke, B. F. W., Dutta, D. and Kim, S.: Flood inundation modelling: A review of methods, recent advances and uncertainty analysis, Environ. Model. Softw., 90, 201–216, doi:10.1016/j.envsoft.2017.01.006, 2017.

Todini, E. and Ciarapica, L.: The Topkapi Model, Math. Model. large watershed Hydrol., (November), 471–506, doi:10.1006/hmat.1999.2234, 2002.

Tsubaki, R. and Fujita, I.: Unstructured grid generation using LiDAR data for urban flood inundation modelling, Hydrol. Process., 24(11), 1404–1420, doi:10.1002/hyp.7608, 2010.

UNDP: Assessment of Groundwater Resources of Lebanon, Beirut, Lebanon., 2014.

UNISDR: Guidelines for Reducing Flood Losses., 2002.

UNISDR and CRED: The Human Cost of Weather Related Disasters, 1995-2015., 2015.

USACE: Hydrologic Modeling System HEC-HMS:Technical Referance Manual, US Army Corps of Engineers Hydrologic Engineering Center, 609 Second Street Davis, CA 95616-4687 USA., 2000.

USACE: HEC-RAS River Analysis System - Hydraulic Reference Manual, Version 5.0, US Army Corps of Engineers Hydrologic Engineering Center (HEC), 609 Second Street

Davis, CA 95616-4687 USA. [online] Available from: http://www.hec.usace.army.mil/software/hec-ras/documentation.aspx, 2016a.

USACE: Hydrologic Modeling System User's Manual, U.S. Army Corps of Engineers Institute for Water Resources Hydrologic Engineering Center (CEIWR-HEC), 609 Second Street Davis, CA 95616-4687., 2016b.

Du Vaumas, E.: Le Liban (montagne libanaise, Bekka, Anti-Liban, Hermon, Haute Galilee libannaise) : etude de geographie physique., Firmin-Didot, Paris., 1954.

Vozinaki, A. K., Morianou, G. G., Alexakis, D. D. and Tsanis, K.: Comparing 1D- and combined 1D / 2D hydraulic simulations using high resolution topographic data , the case study of the Koiliaris basin , Greece, Hydrol. Sci. J., 0(0), doi:10.1080/02626667.2016.1255746, 2016.

Walley, C. D.: Some outstanding issues in the geology of Lebanon and their importance in the tectonic evolution of the Levantine region, Tectonophysics, 298(1–3), 37–62, doi:10.1016/S0040-1951(98)00177-2, 1998.

Walley, C. D.: The Geology of Lebanon, A summary, , 23–40, 2009.

Whiteaker, T. L., Robayo, O., Maidment, D. R. and Obenour, D.: From a NEXRAD Rainfall Map to a Flood Inundation Map, J. Hydrol. Eng., 11(1), 37, doi:10.1061/(ASCE)1084-0699(2006)11:1(37), 2006.

Wilby, R. L. and Yu, D.: Rainfall and temperature estimation for a data sparse region, Hydrol. Earth Syst. Sci., 17(10), 3937–3955, doi:10.5194/hess-17-3937-2013, 2013.

WMO: Manual on flood forecasting and warning, WMO-No. 10., World Meteorological Organization, Geneva., 2011.

Woodward, D., Hawkins, R., Jiang, R., Hjelmfelt, J., Van Mullem, J. A. and Quan, Q.: Runoff Curve Number Method: Examination of the Initial Abstraction Ratio, World Water Environ. Resour. Congr. 2003, 1–10, doi:doi:10.1061/40685(2003)308, 2003.

Woolhiser, D. A., Smith, R. E. and Goodrich, D. C.: A Kinematic Runoff and Erosion Model, , (March), 1990.

World Bank: World Development Indicators, World Bank, Washington, DC., 2010.

Yamout, G. and El-Fadel, M.: An optimization approach for multi-sectoral water supply management in the Greater Beirut Area, Water Resour. Manag., 19(6), 791–812, doi:10.1007/s11269-005-3280-6, 2005.

Zilberberg, M. D. and Shorr, A. F.: Understanding cost-effectiveness, Clin. Microbiol. Infect., 16(12), 1707–1712, doi:10.1111/j.1469-0691.2010.03331.x, 2010.

ANNEXES

Annex A.
Articles

Journal of Hydrology 565 (2018) 160–176

Contents lists available at ScienceDirect

Journal of Hydrology

journal homepage: www.elsevier.com/locate/jhydrol

Research papers

Constraining coupled hydrological-hydraulic flood model by past storm events and post-event measurements in data-sparse regions

Rouya Hdeib[a], Chadi Abdallah[a,*], François Colin[b], Luca Brocca[c], Roger Moussa[d]

[a] CNRS-RS, National Council for Scientific Research, Remote Sensing Center, Beirut, Lebanon
[b] UMR LISAH, Univ. Montpellier, Montpellier SupAgro, Montpellier, France
[c] Research Institute for Geo-Hydrological Protection, National Research Council, Perugia, Italy
[d] UMR LISAH, Univ. Montpellier, INRA, Montpellier, France

ARTICLE INFO

This manuscript was handled by Marco Borga, Editor-in-Chief, with the assistance of Eylon Shamir, Associate Editor

Keywords:
Sparse data
Flood maps
Post-event measurements
Uncertainty
Lebanon
Mediterranean

ABSTRACT

Flood modelling in data-sparse regions have been always limited to empirical, statistical or geomorphic approaches that are suitable to produce regional hazard maps. Such coarse resolution maps are not adapted for basin-scale applications, small to medium sized basins (< 1000 km²), especially when detailed estimates of flows and water levels of a particular event is required and hence cannot replace the hydrological/hydraulic modelling. The latter is a challenging task in data-sparse regions characterized by floods of typical duration times of a few hours which offer little opportunity for real-time recording by traditional rain-gauge networks, remote sensing or satellite imaging. Such data sparseness is not always compatible with the resolution, in both space and time, of the hydrological and hydraulic models. We propose a framework for flood modelling using sparse data from a coupled hydrological-hydraulic model constrained by past storm events and post-event measurements in space. The approach is applied to the Awali river basin (301 km²), in Lebanon, particularly to simulate the investigated early January 2013 extreme flood event, which is considered one of the largest events in the last three decades. The hydrological model was calibrated and evaluated with 12 past storm events aiming at defining narrow parameter ranges and uncertainty was performed with Monte Carlo simulations for these parameter ranges. The hydraulic model, based on a fine resolution DEM, was simulated using hydrological outflows and validated with 27 post-event measurements in space of high water marks. The resulting outflow values were satisfactory, and uncertainty was reduced when compared with arbitrarily wide parameter ranges. The hydrological model performance was highly variable but for the hydraulic model, 93% of the observed water levels fall within the simulated uncertainty bounds with an RMSE error of 0.26 m. The proposed framework allows mapping the possible inundation and can be compared to other approaches dealing with model complexity and associated performances.

1. Introduction

Recent years floods have become the major natural disaster worldwide accounting for 47% of all other natural disasters (UNISDR, CRED, 2015). With the climate change (WHO, 2002; Jonkman, 2005), urbanization growth, and land use change, especially in flood-prone areas, the frequency and severity of floods is increasing at an alarming rate (UNISDR, 2002). Hence developing more accurate flood modelling tools to better understand and mitigate floods has become a global endeavour. Flood modelling applications in data-sparse regions were always limited to uncertain probabilistic estimates of rainfall, flood flows and water levels based on empirical (e.g. Koutroulis and Tsanis, 2010), statistical (e.g. Castellarin, 2007; Castellarin et al., 2009) or geomorphic approaches (e.g. Manfreda et al., 2014). Such applications are useful for regional flood analysis such as national hazard maps that are mainly of coarse resolution and are not adapted for small to medium size basins (< 1000 km²). Generally, for basin-scale applications and when more detailed understanding of a particular flood event is required and when the study area is relatively small, such regional maps cannot do the favour especially when detailed estimates of flows and water levels are required and hence cannot replace the hydrological/hydraulic modelling.

Reliable information on the flood peak discharge (Gaume et al., 2009), water levels (Saleh et al., 2013; Domeneghetti, 2016) and the flood inundation extent (Merwade et al., 2008), are among the major parameters required in any flood problem and flood modelling

* Corresponding author.
E-mail address: chadi@cnrs.edu.lb (C. Abdallah).

https://doi.org/10.1016/j.jhydrol.2018.08.008
Received 4 January 2018; Received in revised form 20 July 2018; Accepted 4 August 2018
Available online 07 August 2018

Nomenclature

CN	curve number
D	event duration, h
DEM	digital elevation model, 10 m and 10 cm resolution
HSG	hydrological soil groups
Ia	Initial abstraction, mm
LNMS	Lebanese National Meteorological Service
LRA	Litani River Authority
MAE	mean absolute error, m^3/s
n	Manning's coefficient
N	number of observations
NSE	Nash-Sutcliffe efficiency
P_{av}	average rainfall depth over the whole basin
PE	phase error, h
PFE	peak flow error, %
Q_{obs}	observed peak flow, m^3/s
Q_{peak}	peak flow, m^3/s
Q_{sim}	simulated peak flow, m^3/s
r	coefficient of correlation
RMSE	root mean square error, m^3/s or m
T_{lag}	Lag time, min
VE	volume error, %
V_{obs}	observed total runoff volume for a storm event, mm
V_{sim}	simulated total runoff volume for a storm event, mm

represents a way to obtain such information (Bates, 2004; Moussa and Bocquillon, 2009). It classically requires a coupling between a hydrologic model to simulate the rainfall-runoff transformation along hill shades and estimate peak flood flows, and a hydraulic model to simulate the propagation of flood wave along the river channel and establish the corresponding water levels, along with terrain analysis to extract the flood inundation area (Dimitriadis et al., 2016). Model coupling has been applied by several authors in literature on relatively well gauged basins (see for example Knebl et al., 2005; Montanari et al., 2009; Lerat et al., 2012). However, when data are uncertain and too sparse to meet model requirements, and when model coupling is required, the question arises as to whether there is an opportunity to constrain the hydrological-hydraulic model to simulate extreme floods and establish water levels that can be useful for flood assessment and mitigation.

Worldwide, the majority of river basins are either ungauged or poorly gauged and in some cases facing deterioration of the available measurement networks (Sivapalan et al., 2003; Efstratiadis et al., 2014). In a broader classification, most of the basins in the world and especially in developing countries, are denoted as data-sparse basins where reliable information on the characteristics and on the spatial and temporal coverage of extreme flood events are rare or inexistent (see for example Wilby and Yu, 2013; Jarihani et al., 2015; Komi et al., 2017). Classical and sparse data are differentiated in Table 1. Data sparseness is often referred to measurements of limited spatiotemporal resolution; point measurements of coarse time step, and series with gaps, or parameters that have not been collected during simultaneous periods (Samaniego et al., 2011; Mascaro et al., 2013). Some also add that such data may not be available in the period of interest, or are of poor quality or unknown accuracy, and the hydro-meteorological network is of very low density that makes interpolation procedures or filling methods impossible (Satyanarayana and Srinivas, 2011; Switzman et al., 2015). In addition, others point out to when detailed channel bed and topography information are coarse or unavailable (Neal et al., 2012).

In the Mediterranean region, data requirement is particularly acute because most floods occur on a short duration, typically a portion of the day, and are mainly generated by high-intensity, short duration, localized rainfall events (Moussa and Chahinian, 2009). These floods, characterized by response times often less than 2 h and typically occurring in catchments of drainage area not exceeding 1000 km^2 (Borga et al., 2008), can difficultly be captured even by the traditional rain gauge networks (Norbiato et al., 2007; Lumbroso and Gaume, 2012). In addition, impossible direct current meter measurements of the flood peak discharge (Fukami et al., 2008), coarse time step of measurements often skipping the peak conditions, common failure of river stage gauge, flood water exceeding the gauge measurement level resulting in underestimation of the peak discharge (Koutroulis and Tsanis, 2010) are common weaknesses that lead to poorly defined rating curves during floods. Maybe more than in other regions, the specific rainfall and discharge data requirements result in classifying the Mediterranean region as "data-sparse region".

When information on the flood event characteristics, catchment hydrological characteristics and river channel characteristics are sparse or lacking, interesting information can be inferred from recorded past storm events, post-event field investigations, newspapers and social media reports, and from crowdsourcing of information from local citizens on flood events characteristics whenever available.

From the hydrological modelling perspective, past storm events can be extracted from the available simultaneous rainfall and flow data measurements. These are often used in literature to estimate and calibrate the unknown model parameters (see for example Sangati et al., 2009; Massari et al., 2014). However, when past storm events data used for calibration are uncertain or does not meet model requirements, bias and uncertainty arise in model predictions (Pappenberger et al., 2008). Additionally, the calibration procedure may induce equifinality when input data and calibration equally fit the sparse validation data. The latter can be raised through analysing the uncertainty propagation (Aronica et al., 2002). A good understanding of the uncertainty associated with various parameters inherent in modelling is a critical requirement (Merwade et al., 2008). Accordingly, when all relevant uncertainties are taken into consideration, optimal decisions are to be expected (Apel et al., 2008; Domeneghetti et al., 2013).

From the hydraulic modelling perspective, detailed post-event surveys in space, based on traces left by water and sediments, provide a good opportunity when systematic water level and flow measurements are lacking (Horritt and Bates, 2002; Borga et al., 2008). Surveyed channel cross sections and flood marks can be used in estimating the peak flood discharge (Gaume, 2006). Pictures and videos taken by witnesses during the flood event are interesting in highlighting affected areas and in understanding the events characteristics such as the flood duration, flow type and velocity at the time of capturing (Le Boursicaud et al., 2016; Fuentes-Andino et al., 2017). Field surveys and witnesses interviews can provide additional information such as the time of peak, water levels, and flood extent (Gaume and Borga, 2008). Post-event measurements have been used to validate the results of the hydraulic models several times in literature (see for example Hervouet, 2000; Romanowicz and Beven, 2003; Horritt et al., 2010).

Newspaper and social media information on storm events and floods is an interesting well available data source providing an opportunity to

Table 1
Sparse data versus classical data.

Type	Sparse Data	Classical Data
Hydrology	Series with gaps	Long term series
	Coarse time step	Fine time step
	Point measurements	Spatial measurements (ex: radar rainfall)
	Water levels with pour rating curves	Advanced flow measurement techniques
Hydraulics	Post-event measurements	Time series of water level variation

understand some of the events' characteristics. Such information has been used several times in literature to search for historical flood events (Barredo, 2007), develop a flood database and inventories (Barnolas and Llasat, 2007; Llasat et al., 2009), understand the flood regime changes (Hall et al., 2014), support the hydrologic and hydraulic modelling of the flood events (Papaioannou et al., 2016), evaluate flood risk (Llasat et al., 2010; Abdallah and Hdeib, 2015), and understand the socio-economic impacts of floods (Lastoria et al., 2006). Moreover, crowdsourced information from local citizens on flood events is now gaining favour and is facilitated by the wide spread of low-cost monitoring technology and communication systems (Lowry and Fienen, 2013; Montanari et al., 2013; Mazzoleni et al., 2017). All these data sources can give information on the flood characteristics such as the affected areas, the rainfall event characteristics (depth, intensity, and duration), timing of the flood event (duration and time of peak), possible flood depth and inundation area extent, severity, and recorded damages.

In this article, we hypothesise that there is an opportunity to model flood events based on constraining a hydrological-hydraulic model with sparse data, discontinuous in space and time. The focal point is the proposed modelling framework that involves the hydrologic model HEC-HMS (USACE, 2000), combined with the 1-D hydraulic model HEC-RAS (USACE, 2016), along with models' calibration and evaluation with past-storm events, and flood post-event measurements, including uncertainty calculation based on Monte Carlo simulation. The framework is tested and discussed through its application on a challenging study site of the Eastern Mediterranean; "Awali catchment" in Lebanon.

The structure of the paper is as follows: The first section describes the geographical and hydrological characteristics of the study site along with the sparse collected datasets. The second section presents the proposed modelling framework, with the hydrologic, the hydraulic models, outlines the parameterization strategy and the corresponding evaluation procedures. Finally, the major results of the models' processing and calibration are given and discussed through several challenges including the model coupling approach, the reliability of the observational data and uncertainty propagation, the post-event measurements and their use in constraining the model.

2. Study site

2.1. Geographical dataset

The Awali River basin is one of the coastal Eastern Mediterranean catchments, located in Southern Lebanon covering an area of 301 km^2. The river is one of the major Lebanese perennial rivers witnessing floods every other year (Abdallah et al., 2013). It is 48 km long originating from the Barouk mountain at an altitude reaching 1,492 m, and eventually flowing through the western face of Mount Lebanon and into the Mediterranean Sea. The study area of the hydrological model was the whole catchment area, divided into nine sub-catchments. Whereas, it was the lower main course of the river, approximately 5 km of river length, for the hydraulic model which is experiencing flooding after heavy rainfall events (Fig. 1).

The catchment has a rapidly varied topography ranging from elevated areas of Mount Lebanon (1950 m asl), running parallel to the coast and characterized by a continuous snow cover during winter, to flat plains along the low coastal area primarily utilized for agricultural purposes. It is characterized by steep slopes, which converge towards a valley where the Awali River flows. The lithology of the catchment

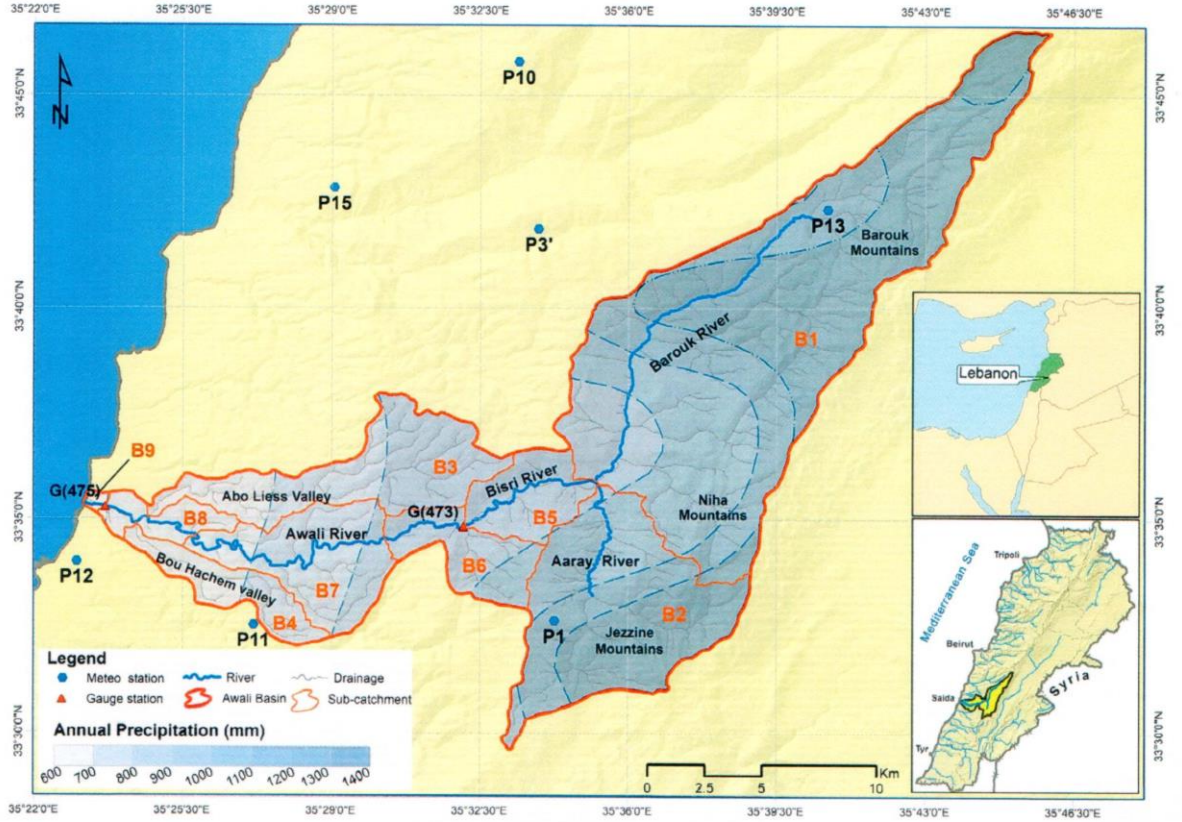

Fig. 1. The Awali River Catchment; site location, available hydrometeorological stations, and the delineated sub-catchments for the hydrological model (HEC-HMS).

covers a sequence from the middle Jurassic rocks to the recent quaternary deposits. The surface is mainly composed of the Cenomanian Sannine limestone formation (C4) which consists of well stratified, fractured, interbedded limestones, dolomites and marls (Dubertret, 1945). The watershed underlies several aquifer formations including the High Central Lebanon Cretaceous, the Kesrouan Jurassic and the Batroun-Jounieh Cretaceous. These aquifers are separated by unproductive formations. Leptosols is the dominant soil class in the catchment covering almost 64% of the total area. The recent soil map of Lebanon classified per the FAO-UNESCO legend, World Reference Base for Soil Resources and the American Soil Taxonomy (Darwish et al., 2006) was used to generate the hydrological soil groups (HSG) (Abdallah et al., 2013). The catchment has a varied land use; wooded lands and grasslands are dominant, covering 46.5 and 26.8% of the total area respectively, whereas, agricultural areas and artificial/urban areas cover 18.2 and 7.2% respectively (LNCSR-LMoA, 2010). The average basin slope in the B1, B2, B3 and B4 sub-catchments is 33.6, 33.3, 29.9, 29.3% respectively (Fig. 2). Detailed river and floodplain geometry was extracted from a fine resolution digital elevation model of 10-cm resolution generated for the purpose of this work. Several drone photography surveys covering the whole floodplain were performed to capture around 5000 raw images acquired in strips with adjacent photographs having an overlap of 80% in the flight direction and 70% between parallel flight tracks. These images were then processed using the Pix4DMapper software to generate the high-resolution DEM based on the criteria described by the American Society of Photogrammetry and Remote Sensing (ASPRS, 2004). The criteria involved identifying and filtering all above ground features to remove false blockages to flow such as bridges. Critical features influencing the flow of water such as walls and building were retained. Additionally, the topography of the entire basin was available from a 10-m digital elevation model (DEM) developed by the Lebanese National Center for Remote Sensing (CNRS-RS). The latter was used to delineate the boundaries of the Awali basin, extract the corresponding stream network, and estimate the basin's hydrological characteristics for the hydrological modelling part.

Table 2
Meteorological stations covering the study site.

Station	Operator	Station Name	Altitude [m]	Data Series	Mean Annual Rainfall [mm]
P1	LNMS	Jezzine	1070	2001–2016	1102
P3'	LNMS	Deir el Kamar	794	2005–2015	1052
P12	LNMS	Saida	14	2001–2014	692
P10	LNMS	Bayssour	940	2000–2016	1201
P11	LNMS	Lebaa	331	2000–2015	870
P15	LNMS	el Meshref	395	2002–2016	890
P13	LNMS	Barouk Fraidis	1114	2000–2011	Not available

2.2. Hydrological dataset

2.2.1. Rainfall

The catchment has a Mediterranean climate; it receives its majority of mean annual rainfall of 1067 mm during the wet fall-winter period extending from November to April, with little or no rain between June and August. The mean annual precipitation ranges between 600 and

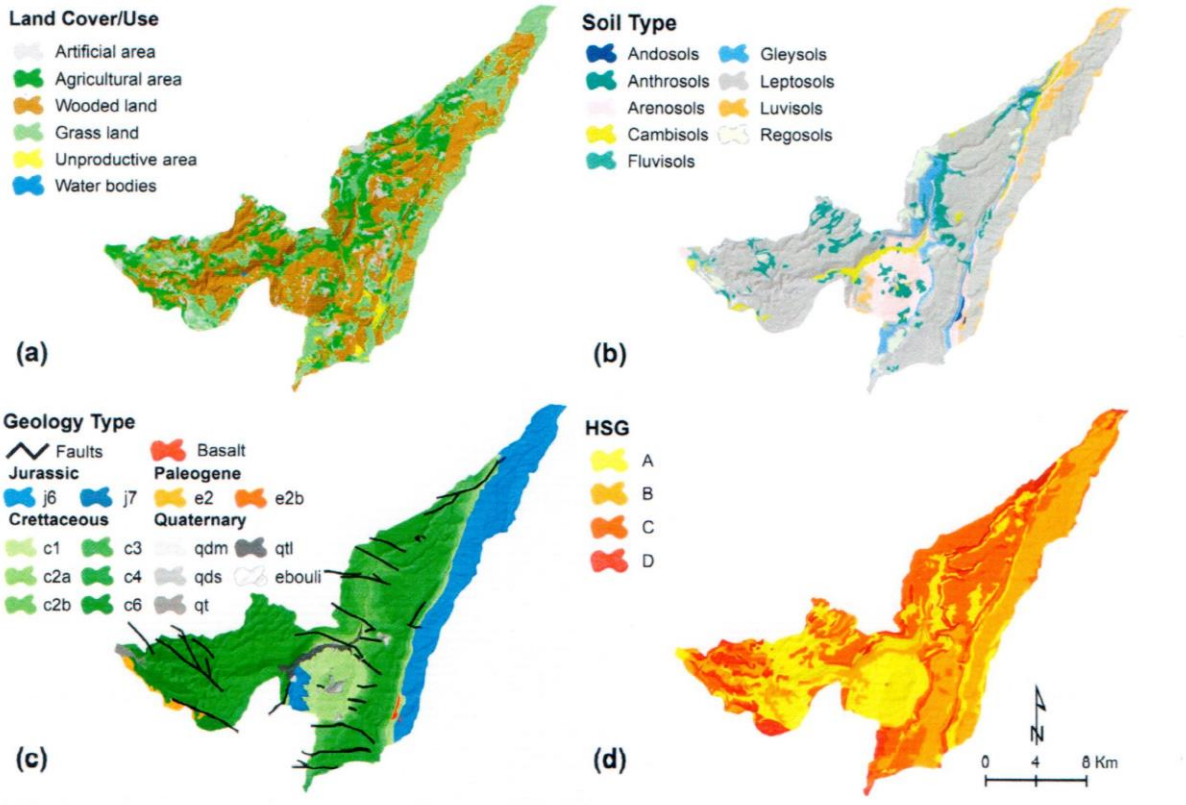

Fig. 2. Study site cartographic data. (a) Land use map (LNCSR-LMoA, 2010), (b) Soil map (Darwish et al., 2006), (c) Geology map (Dubertret, 1945), (d) developed HSG map (Abdallah et al., 2013; SCS, 1972).

700 mm along the coast and 1300–1400 mm over the mountains (Plassard, 1972).

Daily rainfall measurements were obtained from seven meteorological stations operated by the Lebanese National Meteorological Services (LNMS) (Table 2; Fig. 1). These stations were recently established after the Lebanese civil war (1975–1990), during which most of the stations ceased their operation, and have however started recording since 1996. The number and distribution of rainfall stations of density around 130 km^2 per rain gauge is considered satisfactory for the basin area following the WMO requirements of recommended minimum densities of stations.

Early January 2013 a harsh winter storm lashed the eastern Mediterranean coast with snow, high winds, and heavy rains. Flooding caused by torrential rains was recorded in several parts of the region including Turkey, Syria, Lebanon and Jordan (NOAA, 2013). In Lebanon, the storm lasted for 6 days (5th–10th January) and 277 mm total rainfall of 50 years return period was recorded, leaving behind one of the largest floods in the last 25 years. Hourly rainfall records for the Jan2013 storm are available from Baysour meteo station (P_{10}).

2.2.2. Discharge

Two permanent limnigraphic gauge stations, operated by the Lebanese Litani River Authority (LRA), take continuous hourly (or 15 min) measurements of surface water levels. The Marj Bisri gauge station G(473) monitors the flow upstream along the Bisri River and the Saida gauge G(475) monitors the flow at 800 m upstream of the catchment's outlet on the Mediterranean Sea (see Fig. 2). The average annual yield for the basin, at G(475), is approximately 347 Mm^3, out of which 85% occurring during the winter. Stream flow is normally highest in February and lowest in September with an average daily flow of 11 m^3/s (Table 3).

Flow data are also obtained through periodical field point flow measurements that are used to obtain a rough estimate of the monthly river flow volumes and calibrate the river rating curves. Due to the limited resources of the LRA, the shortage in the frequency of the direct field measurement leads to mis-calibration of the rating curves.

2.2.3. Past storm events

Twelve past-storm events, occurring before the Jan2013 flood event, of simultaneous daily rainfall measurements and hourly water levels are used for model calibration. Hourly (or 15 min) water level records were transferred into flow hydrographs for the selected storm events based on the established rating curves. Among the selected events three have information on both gauges in Saida and Marj Bisri, and the rest nine events have only information on downstream Saida gauge. These events were derived from the period extending from 2000 till 2012 in which we consider no major changes on the characteristic of the river have occurred and the hydrometeorological network is the same one operating at the time of the flood. These events vary in intensity of daily rainfall varying between 24 and 199 mm, peak flow varying between 15 and 247 m^3/s, and duration varying between 1 and 7 days. The selected events are the only clearly gauged and consistent for simulation events (Table 4).

2.3. The January 2013 flood dataset

The event of 07 January 2013 is one of the largest floods occurring in the last 25 years. The post-event measurements, pictures, videos, and local witnesses makes this event interesting to assess the robustness of the proposed framework in reproducing flood events of no hydrometric measurements. The presence of both hourly and daily rainfall measurements in addition to social media information on the duration of the storm event is also an added value.

2.3.1. The flood magnitude

On 6th of January 2013 at around 13:00, the intensity of light precipitation that lasted for several hours on the previous day, started to increase reaching a maximum of 17.3 mm/h at around 20:00. On the second day, 7th of January, at around 05:00–06:00 the Awali river level rose and flooded in several locations along the coastal plains and in the middle Marj Bisri plain. The downstream river gauge G(475) was subjected to failure by flood waters. The flood left behind great damages to agricultural lands and green houses. Several cars and roadside walls were damaged causing massive traffic jams. Schools were obliged to close for three days (8th–10th January), (Abdallah et al., 2013).

2.3.2. Post-event measurements

Field investigations of the Jan2013 flood marks were performed two months after the flood event, after which newspaper information, local witnesses' declarations and social media reports were analyzed at the time of the flood. The post-event field surveys were carried out to collect ground control and survey river cross sections, measure water level traces that were still identified and estimate the peak discharge values, identify hotspots and measure extent of floodplains, interview locals who have witnessed the flood event and could support the authors not only by information but in many instances by photos and recorded videos. Collected photos and videos enabled to highlight some flood-prone areas that were further investigated through field surveys to measure water levels. A total of 57 post-event points scattered in space were surveyed out of which 27 are measurements of high water marks (Fig. 3).

2.4. The sparse dataset

In conclusion, our data-sparse region is a region characterised by data summarized in Table 5 in the following form:

1. Past recorded storm events of daily rainfall measurements from ground rainfall gauges incapable of reflecting the rainfall intensity and spatial variability during the storm event, hourly (or 15 min) water level measurements by two traditional river stage gauges mostly non-functional during flood events, and hourly (or 15 min) flow hydrographs extracted based on poorly defined rating curves.
2. Descriptive social media information on the past storm events

Table 3
Characteristics of the permanent gauge stations along the Awali River.

Gauge Station	Name	Altitude [m]	Gauged area [km^2]	Data type	Time step	Period of Record	Average annual flow [m^3/s]	Average annual yield [$M.m^3$]
G (475)	Awali at Saida	6	300	water level & discharge	hour	98–99 till 08–09	11	347
				water level & discharge	15 min	09–10 till 11–12		
G (473)	Awali at Marj Bisri	398	222	water level & discharge	hour	01–02 till 08–09	4	131
				water level & discharge	15 min	09–10 till 11–12		

Table 4
Summary of selected past storm events at the Awali watershed. Three highest rain depths and three highest flows at Saida G(475) are indicated by *.

Event number	Strom event	Duration [h]	Average Rain depth [mm]	Gauge	Average flow [m^3/s]	Peak flow [m^3/s]	Time of peak flow	Observed Stage [m]	Total Runoff volume [mm]
1	19–24 Jan 2000	144	199*	475	82.0*	145.7	19 Jan 2000, 04:00; & 20 Jan 00, 14:00	2.27	117.6
2	15 Dec 2001	24	24	475	7.2	17.4	15 Dec 2001, 08:00	0.83	4.8
				473	2.9	15.3	15 Dec 2001, 01:00	0.36	5.5
3	19–20 Dec 2001	48	43	475	13.9	19.1	20 Dec 2001, 09:00	0.89	13.4
				473	6.4	54.1	20 Dec 2001, 01:00	0.56	15.6
4	6–11 Jan 2002	144	79	475	18.4	28.9	07 Jan 2002, 10:00	1.10	32.0
5	20–22 Jan 2002	72	66	475	29.0	68.0	22 Jan 2002, 24:00	2.21	35.1
6	18–21 Dec 2002	55	120	475	51*	163.0	20 Dec 2002, 17:00	2.84	51.6
7	3–7 Jan 2007	96	81	475	18.7	22.6	07 Jan 2007, 03:00	1.10	25.0
8	19–20 Jan 2007	24	59	475	17.7	27.3	21 Jan 2007, 10:00	1.21	13.7
9	1–7 Feb 2007	144	150*	475	35.0	85.9	06 Feb 2007, 15:00	2.06	65.5
10	24–26 Feb 2007	48	75	475	38.3	69.9	26 Feb 2007, 17:00	1.88	41.7
11	14–19 Feb 2012	120	120	475	84.8*	118.7	18 Feb 2012, 08:15	1.60	108.3
				473	22.6	246.5	17 Feb 2012, 22:30	1.27	66.0
12	28 Feb-3 Mar 2012	168	125*	473	17.8, 22.4	69.0	28 Feb 2012, 22:45 & 3 Mar 2012, 17:00	0.81, 0.76	57.2

related to the duration and spatial variability of the rainfall during the storm.

3. A recent extreme flood event but destructed river stage gauge with daily and hourly rainfall measurements in one nearby rainfall station and post-event measurements of peak flood discharge and high water marks.
4. Descriptive information from newspapers, social media, and field investigations on the extreme flood event related to the inundated areas, time of flood peak, duration of the storm and its spatial variability.

3. The modelling framework

3.1. Hydrological model

Hydrological rainfall-runoff models vary in their complexity from simple lumped models to semi-distributed and fully distributed models. Regardless that fully distributed models are capable of better representing the hydrological processes, several difficulties arise when applying them in data-sparse regions because of their complexity, data requirements and parameter identifiability which may limit their efficiency and adequacy (Lerat et al., 2012). However, when sparse data is available semi-distributed rainfall-runoff models are still efficient alternatives. Thereof, a semi-distributed model based on the SCS-CN method for computing losses, along with Muskingum-Cunge and SCS-unit hydrograph methods for routing flow along channels and hillslopes

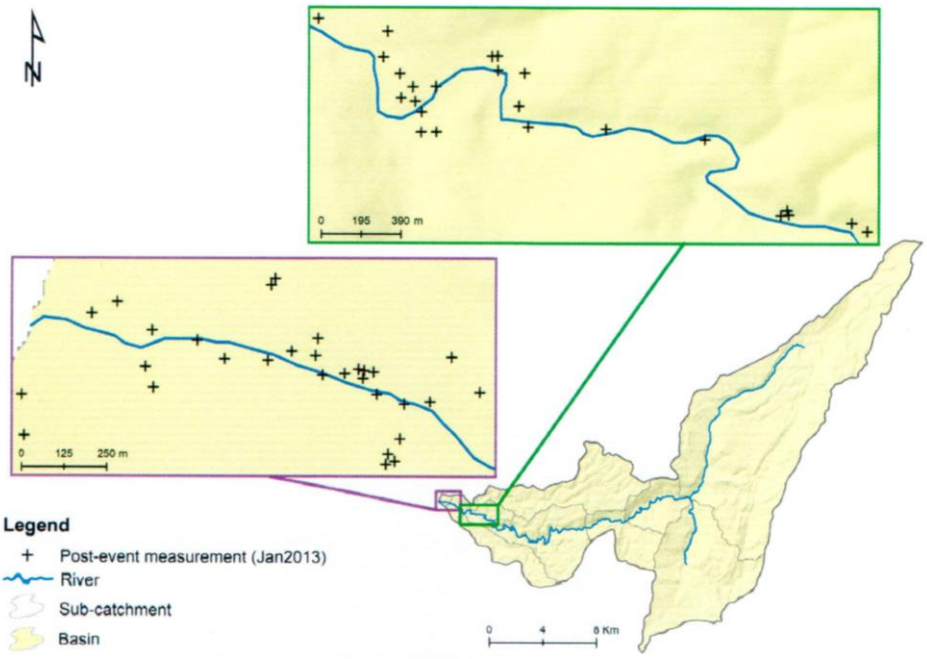

Fig. 3. Hydraulic model study site and post-event measurement locations.

Table 5
Summary of the observational data types available for this study.

Event	Rainfall Data	Flow Data
n past storm events	- daily rainfall data - social media information on the duration of the rain event	- hourly and 15 min water level measurements - hourly and 15 min flow hydrograph extracted based on established rating curves
1 extreme event	- daily and hourly rainfall data	- post-event high water marks measurements and peak flood discharge estimation - social media information and local witnesses on the time of peak flow and flood inundation depth and area

were respectively selected. The model was integrated within the HEC-HMS software. The modelling time step was equal to 30 min, smaller than the sub-basins' estimated time of concentration, to ensure that the flood peak is well captured by the model. Evapotranspiration losses were neglected based on the assumption that the evapotranspiration volume generated during a winter storm event is negligible compared to the runoff volume generated, as demonstrated by Knebl et al. (2005). The baseflow in the model was estimated from the available water level records, the induced flow by the hydropower production plants was estimated based on collected schedules of average monthly water flow in the facilities (1994–2015). Rainfall–runoff simulation of several events was then conducted for the whole catchment (301 km^2) in a semi-distributed approach over sub-catchment units.

The simple SCS curve number loss model (SCS, 1972) was applied because it allows the estimation of direct surface runoff volume for given rainstorms based on a single parameter, curve number which represents the basin's infiltration storage (D'Asaro and Grillone, 2010). Initial, rough CN ranges are assigned for each sub-catchment based on the knowledge of the land use and HSG combinations extracted from available information. Rainfall amounts calculated 5 days before each storm event reflect moderate soil moisture conditions of typical winter days in Lebanon. Accordingly, CN values fall within the average soil moisture conditions (AMCII).

3.2. Hydraulic model

The 1D HEC-RAS model was used to establish the water-surface profiles. This model was selected because it is a well-known open software widely applied for hydraulic modelling, it is usually combined with the HEC-HMS and known for its low computational costs. The hydraulic model is applied to the low main part of the river, approximately 5 km of river length, mostly subjected to flooding. Cross sections are performed at the gauge locations, at locations of considerable changes in flow, morphology, slope, geometry, and roughness, and at representative locations such as sub-basins' outlet of the hydrological model that serve as boundary conditions for the hydraulic model.

The centreline was traced together with the river banks based on the captured high-resolution drone images. The geometry of the river and floodplain is extracted from the fine resolution DEM. The results of the hydrological model are imported into the hydraulic model. Roughness values are initially estimated based on expert knowledge of channel properties. These values are later manually calibrated by a trial and error approach to maximize the fit between the simulated water levels and the observed ones at arbitrarily selected post-event locations on the river channel.

3.3. Modelling framework

The modelling framework is divided into three major steps (Fig. 4):

- Step (1) involves performing the rainfall-runoff modelling through HEC-HMS software for selected past storm events. Parameters to be calibrated are selected based on the model sensitivity analysis. Model calibration and evaluation is performed aiming at defining a narrow range of model parameters, which is taken equal to the estimated range from the calibration.
- Step (2) involves an uncertainty analysis based on the Monte Carlo Sampling of model parameters within the narrow ranges estimated in step (1). The hydrological model is then run to simulate the hydrograph set of the Jan2013 extreme event.
- Step (3) involves the hydraulic model simulation (HEC-RAS) for the Jan2013 flood event based on the hydrograph set obtained in step (2) to generate the respective water surface profiles, post-processing and terrain analysis to interpolate the water levels and extract the inundation area and flood map validation by the post-event measurements.

A preliminary analysis was performed. This includes the catchment and sub-catchment delineation, extraction of their characteristics and parameters, and defining rough initial values of model parameters based on our knowledge of the basin's characteristics.

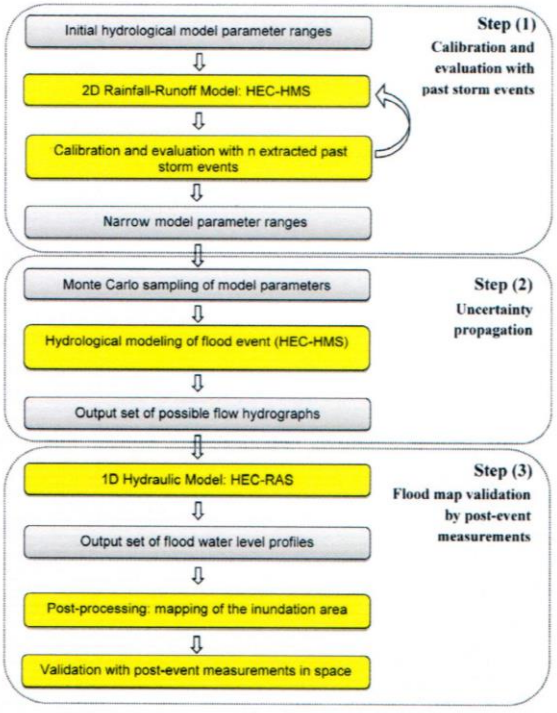

Fig. 4. Detailed scheme of the proposed modelling framework used to produce flood maps using sparse data and a coupled hydrological-hydraulic model constrained by past storm events and post-event measurements in space. Blocks in yellow present the major computational parts of the modelling framework, whereas, blocks in grey present the input/output of the computational parts. (For interpretation of the references to colour in this figure legend, the reader is referred to the web version of this article.)

3.3.1. Hydrological model calibration and evaluation

Unlike classical calibration approaches that end up in a deterministic set of model parameters, the calibration procedure herein is applied aiming at defining a narrow range of model parameters for uncertainty sampling, this range is taken equal to the estimated range from the calibration. The estimated parameter ranges are quite narrower than the wide feasible parameter ranges often defined in classical uncertainty analysis studies (e.g. Freer et al., 1996; Huang and Liang, 2006) which are often chosen, arbitrarily or on a basis of physical argument, to be wider than those expected for the catchment under study.

Available and simultaneous rainfall and water level measurements are analysed to extract past storm events of reliable information. It is preferable to select storm events of variable intensity and duration and occurring in different time of the year. Daily rainfall measurements were discretized uniformly into hourly measurements, however this mostly applicable for floods of long duration and not flash floods. Indeed, several other possible rainfall distributions can be applied and analyzed and may yield more accurate estimates of hourly rainfall depths. In this study we choose the simplest approach (uniform rainfall) as a preliminary analysis. In some cases, additional information was obtained from social media reports and newspapers on the time period of occurrence of the maximum rainfall which is mainly a portion of the day. In these cases, recorded rainfall measurements at that day are discretized into hourly measurements uniformly over the period of occurrence of the maximum rainfall; e.g. if we found information that the storm event was localized within the first quarter of the day; daily rainfall is discretized over the first six hours of the day only. This is mainly because there might not be any rain at all for several hours of the day and discretizing over the whole day may show values even for non-rainy hours.

The calibration involves a combination of both manual and automated calibrations. The manual calibration precedes the optimization to ensure that a physically-meaningful set of initial parameters is used in the model based on initial conditions and on expert knowledge of the basin's physical properties. The automated optimization is then applied to optimize the model parameters. The resulting minimum and maximum values of each optimized parameter define an interval of narrow parameter ranges. Perhaps the more past events evaluated the better results are expected. However, there should be a certain number of events that ensures convergence in the calibration. The convergence in calibration is obtained when calibrating on additional past events do not considerably change the estimated parameter ranges.

Two main categories of evaluation indices were applied for model calibration. The first category of indices is used to evaluate the model for the entire rainfall event:

$$\text{Peakflowerror}(\%)\text{: PFE} = \frac{Q_{obs_{peak}} - Q_{sim_{peak}}}{Q_{obs_{peak}}} \times 100 \quad (1)$$

$$\text{Phaseerror(h): PE} = \tau_{obs} - \tau_{sim} \quad (2)$$

$$\text{Volumeerror}(\%)\text{: VE} = \frac{|V_{obs} - V_{sim}|}{V_{obs}} \times 100 \quad (3)$$

Where $Q_{obs_{peak}}$ and $Q_{sim_{peak}}$ are, the peak observed and simulated flow values for each rainfall-runoff event, τ_{obs} and τ_{sim} are the peak times for the observed and simulated event, V_{obs} and V_{sim} are the total runoff volume for the observed and simulated event, respectively.

The second category is related to the evaluation of the time series of the rainfall-runoff simulation. Most research projects involving watershed modelling utilize some type of predefined model evaluation techniques to compare simulated output with observed data. A combination of graphical techniques, dimensionless, and error index statistics is used for model evaluation (Moriasi et al., 2007):

Coefficient of correlation (standard regression):

$$r = \frac{\sum_{i=1}^{n} [(Q_{obs(i)} - \bar{Q}_{obs})(Q_{sim(i)} - \bar{Q}_{sim})]}{\sqrt{\sum_{i=1}^{n} (Q_{obs(i)} - \bar{Q}_{obs})^2} \sqrt{\sum_{i=1}^{n} (Q_{sim(i)} - \bar{Q}_{sim})^2}} \quad (4)$$

Nash-Sutcliffe efficiency (Nash and Sutcliffe, 1970):

$$\text{NSE} = 1 - \frac{\sum_{i=1}^{n} (Q_{obs(i)} - Q_{sim(i)})^2}{\sum_{i=1}^{n} (Q_{obs(i)} - \bar{Q}_{obs})^2} \quad (5)$$

Error Index; Root mean square error:

$$\text{RMSE} = \sqrt{\frac{\sum_{i=1}^{n} (Q_{obs(i)} - Q_{sim(i)})^2}{N}} \quad (6)$$

Error Index; Mean absolute error:

$$\text{MAE} = \frac{\sum_{i=1}^{n} |Q_{obs(i)} - Q_{sim(i)}|}{N} \quad (7)$$

Where $Q_{obs(i)}$ and $Q_{sim(i)}$ are, the observed and simulated flow values for time step i, $\bar{Q}_{obs}$ and $\bar{Q}_{sim}$ are the mean observed and simulated flow values for each event and N is the number of observations.

3.3.2. Uncertainty in the hydrological modelling

The uncertainty propagation in this approach can be understood by analysing the uncertainty on the hydrological model parameters based on two approaches. The first approach involves a sensitivity analysis for the hydrological model to select the key parameters mainly controlling and forcing the model results. The second approach involves a fuzzy combination based on Monte Carlo simulation for the selected parameters (Robert and Casella, 2004). The selected parameters of minimized ranges in the previous step (1) are statistically sampled based on a uniformly distributed probability density function. Uniform distributions are considered to avoid any prior assumption on the parameters' distribution other than their feasible ranges as discussed by Freer et al. (1996). Random numbers are generated using the Well19937c generator within HEC-HMS (Panneton et al., 2006).

3.3.3. Hydraulic model validation

Hydraulic models have been typically validated using water level or discharge values obtained from the hydrometric network available on the river. However, this is a major challenge when hydrometric measurements are lacking and when remote sensing products are not able to capture the flood event. In this approach we choose to validate the model with the post-event measurements of high water marks. This step is preceded by a terrain analysis to extract the inundation area using the high-resolution terrain model. The simulated maximum water level bounds are matched with the observed water levels. The root mean square error (RMSE) objective function is used to evaluate the fit between the simulated uncertainty bounds of the water levels and the observed ones at the post-event measurement locations:

$$\text{RMSE} = \sqrt{\frac{\sum_{i=1}^{n} (H_{max_{obs}} - H_{max_{sim}})^2}{N'}} \quad (8)$$

$H_{max_{obs}}$ and $H_{max_{sim}}$ are the maximum observed and simulated water levels respectively, and N' is the number of post-event maximum water level measurement points. The RMSE is zero if the observed and simulated water levels fit perfectly; higher RMSE error reflects more divergent values.

4. Results

4.1. Step (1): Hydrological model calibration and evaluation by past storm events

4.1.1. Sensitivity analysis

The sensitivity of the model was first assessed based on the 14–19 February 2012 storm event (event 11), the event was selected because it

is the closest to the Jan2013 flood event. The sensitivity analysis was performed at the river stage Saida (475) and was based on the variation of the curve number parameter, Initial abstraction parameter, percent impervious parameter and the lag time. The reference parameter values are 50.4 for the CN, 12.7 mm for the Ia, 7.7 hr for the lag time, and 0.75% for the percent impervious. The results of the sensitivity analysis are presented in Table 6, based on evaluating the total runoff volume, the peak flow, and the time of peak discharge at Saida (475) gauge. The curve number parameter was found to be the parameter that could mostly affect the calculation results. The initial abstraction affects the runoff volume and peak flow, whereas, the impervious percent mainly affects the runoff volume. The lag time mainly affects the time of peak runoff.

4.1.2. Calibration by past storm events to estimate parameter ranges

Following the sensitivity analysis, the selected key parameters for calibration are the Curve number, the initial abstraction, the lag time, and the Manning's coefficient. Model calibration and evaluation were carried out at two points corresponding to the positions of the gauge stations Saida (475) and Marj Bisri (473). Model calibration was performed on three steps; the number of events is increased in each step and the parameter ranges are compared to the preceding ones, allowing to search for the suitable number of events that ensures a convergence in the calibration. The first step involves calibrating the model with 3 events arbitrarily chosen (events 2, 4, and 12), the second step involves calibrating with 6 events (events 2, 4, 5, 6, 8, and 12), and the last step involves calibrating with the whole 12 events. The parameter ranges for the different sub-basin are taken equal to those obtained by the calibration in each step. Calibration with 3 events resulted in parameter ranges quite narrower than those obtained by calibrating with 6 events. Whereas, calibrating with 6 and 12 events resulted in similar parameter ranges, which means that our approach works well with 12 events. Calibrating with 3 events was not sufficient, because analysing additional storm events further increases the parameter ranges, this is because the additional events are more variable in terms of intensity allowing to obtain a wider parameter range. In our case, the similar parameter ranges obtained by 6 and 12 events indicates a convergence in calibration and allows us to say that we are stabilized with 12 events. Indeed, this approach should be should be further assessed in additional applications because the selected number of past storm events impacts the resulting parameter ranges. The different sub-basin characteristics, their arbitrarily estimated wide parameter ranges, and the estimated ranges by calibrating with 12 events are presented in Table 7. The calibration with 12 events resulted in the estimation of narrow ranges of the characteristic parameters of the different sub-basins, these ranges are narrower than the arbitrarily chosen wide parameter ranges.

The model was relatively more sensitive to the characteristic parameters of sub-basin B1 and B2 which form around 60% of the total area and together contribute to over 31% of the total runoff. For the selected storm events, the CN of sub-basin B1 found to vary from 50 to 62, the lag time varies from 232 to 248 min, and the initial abstraction varies from 7 to 21 mm. Table 8 summarizes the model performance for the selected storm events in terms of the parameters described in Eqs. (1)–(7).

The simulation of the 12 events resulted in an average volume error of 10.7%, average peak flow error of 26.3%, and an average phase error of −3.6 h. The performance of the model was highly variable among the storm events, the evaluation analysis resulted in an NSE ranging between 0.84 and 0.06, R ranging between 0.93 and 0.58, RMSE ranging between 1.46 and 19.7 m^3/s, and MAE ranging between 0.62 and 8.7 m^3/s. The low NSE values for events 2, 3, 9, and 10 are mainly because the observed water levels at Saida gauge (475) presented large fluctuations that may not be related to the runoff generated by rainfall events, but may be related to the sensitivity of the river stage gauge to any perturbation in the water flow that for example may be resulting from the floating objects carried by the river. The low NSE value for event 3 and 11 at Marj Bisri gauge (473) is mainly because the observed hydrograph presented a relatively high peak discharge which might be overestimated by the rating curve. The good NSE value for event 6 is related to discretising rainfall over the storm period of occurrence (first quarter of the day) which reduced the error in the time series and gave better peak flow value.

4.2. Step (2): Uncertainty propagation; flood event of 07 January 2013

The Jan2013 storm event rainfall amounts recorded at the time of flood by the daily rainfall stations P_1, P_3, P_{11}, P_{12}, and P_{15}, and the hourly rainfall station P_{10} are analogous with slightly lower values along the coastal area, indicating no major spatial variation in rainfall. The little difference in rainfall among stations is considered by assigning its relative weight preserving the same hyetograph distribution.

The uncertainty analysis involved the hydrological model parameters CN, Ia, Lag time, and the Manning's roughness. Based on the criteria illustrated by Dimitriadis et al. (2016), testing several parameter samples ranging from 100 to 5000 showed that the convergence in the resulting mean discharge and volume was achieved for sample size starting from 1000 parameters and that increasing the number of samples does not result in a noticeable change in the computed mean discharge and volume. We choose to perform 2000 simulations which is equivalent to more than twelve values per model parameters for an adequate quantitative analysis of acceptable computational cost. The parameters are statistically sampled following a uniformly distributed probability density function within their estimated ranges in step (1). To study the implication of the estimated parameter ranges on the model results, four model simulations were performed, these correspond to the wide parameter ranges defined in Table 7 and the estimated parameter ranges by calibrating on 3, 6 and 12 events. The model simulated hydrographs at all sub-catchments' outlets. The results of the four model simulations are presented in Fig. 5 at Saida G(475) gauge. The simulation based on the wide parameter ranges resulted in numerous possible model realisations of peak flow value ranging between 100 m^3/s and 550 m^3/s with a mean value of 260 m^3/s. In this case, the results of the hydrological modelling are no more representative and may be replaced by empirical or lumped modelling approaches. The simulation based on the estimated parameter ranges by 3 events resulted in few model realisations of peak flow value ranging between 276 m^3/s and 364 m^3/s with a mean value of 339 m^3/s. As expected, this simulation ("3-events") is thought to be underestimating the possible peak flow values because it was based on unstable calibration. Simulations based on estimated parameter ranges by 6 and 12 events resulted in similar model realizations of peak flow values ranging between 324 m^3/s and 429 m^3/s with a mean value of 377 m^3/s observed at 05:00 of 07 January 2013, given that the maximum rainfall intensity of 17.3 mm/hr was observed at 20:00 the day before. For these two simulations ("6-events" and "12-events") the simulated total water volume ranges between 67.44 Mm^3 and 75.05 Mm^3 with a mean value of 71.49 Mm^3. The last two simulations reduce uncertainty in the peak flow values and seem to be satisfactory because of the stable model calibration.

Table 6
Step (1): Sensitivity analysis results on the 14–19 February 2012 rainfall-runoff event with average total rainfall of 120 mm.

Parameter	Curve number	% impervious	Initial abstraction [mm]	Lag time [h]
Range	[10; 90]	[0; 10]	[0; 50]	[0.5; 30]
Volume error [%]	[−16; 41]	[3; 7]	[1; 22]	[1; 9]
Peak flow error [%]	[−37; 56]	[−6; 0]	[−9; 24]	[−67; 8]
Phase error [h]	[−1; 3]	[−1; 0]	[−4; 2]	[−4; 9]

Table 7
Step (1): Sub-basins' characteristics, the arbitrarily estimated wide parameter ranges, and the estimated narrower parameter ranges for different sub-basins obtained from the maximization of the Nash-Sutcliffe efficiency of the 12 selected past storm events.

Element	Area (km^2)	Av. Slope (m/m)	Watershed length (km)	Parameter	Wide feasible parameter ranges	Estimated parameter ranges based on 12 events
Sub-basin B1	141	0.0492	27.80	CN	[20; 80]	[50; 62]
				Ia	[1; 100]	[7; 21]
				T_{lag}	[100; 600]	[232; 248]
Sub-basin B2	51	0.0677	14.46	CN	[20; 80]	[45; 49]
				Ia	[1; 100]	[3; 27]
				T_{lag}	[100; 600]	[111; 167]
Sub-basin B3	31	0.0472	18.01	CN	[20; 80]	[49; 58]
				Ia	[1; 100]	[6; 47]
				T_{lag}	[100; 600]	[129; 299]
Sub-basin B4	11	0.0444	11.23	CN	[20; 80]	[34; 66]
				Ia	[1; 100]	[11; 19]
				T_{lag}	[10; 300]	[76; 174]
Sub-basin B5	13	0.0684	7.62	CN	[20; 80]	[37; 57]
				Ia	[1; 100]	[18; 46]
				T_{lag}	[10; 300]	[120; 123]
Sub-basin B6	13	0.0976	8.67	CN	[20; 80]	[36; 58]
				Ia	[1; 100]	[13; 31]
				T_{lag}	[10; 300]	[133; 202]
Sub-basin B7	24	0.0399	13.66	CN	[20; 80]	[34; 38]
				Ia	[1; 100]	[12; 42]
				T_{lag}	[10; 300]	[57; 194]
Sub-basin B8	6	0.0583	6.52	CN	[20; 80]	[57; 69]
				Ia	[1; 100]	[13; 30]
				T_{lag}	[10; 300]	[70; 74]
All model reaches				n	[0.01; 0.1]	[0.03; 0.07]

4.3. Step (3): Hydraulic modelling and flood map validation by post-event measurements

The HEC-RAS model was applied to the low coastal area that corresponds to the channel running in sub-basins B8 and B9, the channel is bounded upstream by Joun hydropower plant and downstream by the gauge station G(475) and the sea mouth. The resulting hydrographs of the hydrological model corresponding to the "12-events" simulation were then assigned as upstream and downstream boundary conditions and input lateral inflows at junctions for the hydraulic model. The propagation of uncertainty through the hydraulic model was examined using the previously established bounds; maximum, mean, and minimum flow hydrographs providing three realizations of the flood extent. The hydraulic model results are presented in Fig. 6. The resultant flood map is presented in Fig. 7. 93% of the observed water levels fell within the simulated uncertainty bounds and found to be closer to the mean with RMSE error of 0.26 m. The RMSE error was found to be 0.7 m and 0.6 m for the maximum and minimum uncertainty bounds respectively. With an RMSE error in the range of the DEM resolution (10 cm), the results of the hydraulic modelling are found to be very promising.

5. Discussion

5.1. Opportunities in the model coupling approach

A wide range of hydrological and hydraulic models is nowadays available, out of which many are open software and easy to use by the scientific community. The coupling between these models has been also widely discussed in literature. The HEC-HMS and the HEC-RAS models are among these models. These open software have been successfully used in many case studies. Examples include the HEC-HMS model on the Llobregat River in Catalonia (Amengual et al., 2007), the Misai and Wan'an Catchments in China (Oleyiblo and Li, 2010), Sixteen subcatchments in Johor, Malaysia (Shamsudin et al., 2011), and the Balijore Nala watershed in India (Choudhari et al., 2014). Examples on the

Table 8
Step (1): Results of the hydrological model evaluation for the 12 selected past storm events in terms of the parameters presented in equations Eq. (1) till Eq. (7) at locations: Saida gauge (475) and Marj Bisri gauge (473). Q_{peak} refers to observed peak flow estimated from the measured stage with the established rating curves.

Event	Storm Event	D [h]	P_{av} [mm]	Gauge	Q_{peak} [m^3/s]	V_{obs} [mm]	Q_{sim} [m^3/s]	V_{sim} [mm]	PFE [%]	VE [%]	PE [h]	r	NSE	RMSE [m^3/s]	MAE [m^3/s]
1	19–24 Jan 2000	144	199	475	145.7	117.6	99.6	100.8	31.6	14.3	−11	–	–	–	–
2	15 Dec 2001	24	24	475	17.4	4.8	15.4	5.5	11.5	7.2	−0.5	0.68	0.19	2.66	1.78
				473	15.3	5.9	13.6	6.0	11.1	−2.4	−5	0.92	0.84	1.46	0.62
3	19–20 Dec2001	48	43	475	19.1	13.4	20.1	12.4	−5.2	7.2	−0.5	0.58	0.09	4.26	2.51
				473	54.1	15.6	18.6	11.2	65.6	33.5	−5	0.73	0.45	6.89	4.08
4	6–11 Jan 2002	144	79	475	28.9	32.0	24.7	30.7	14.5	3.9	0.5	–	–	–	–
5	20–22 Jan 2002	72	66	475	68.0	35.1	40.7	31.3	40.1	11.1	−2	0.83	0.66	6.03	3.75
6	18–21 Dec 2002	55	120	475	163.0	51.6	164.9	52.3	−1.2	−1.5	−2	0.93	0.80	12.19	6.69
7	3–7 Jan 2007	96	81	475	22.6	25.0	29.4	19.8	−30.1	20.9	0	–	–	–	–
8	19–20 Jan 2007	24	59	475	27.3	13.7	35.4	13.0	−29.7	5.6	−1	0.84	0.56	3.85	1.90
9	1–7 Feb 2007	144	150	475	85.9	65.5	84.7	69.2	1.4	−5.5	7	0.73	0.06	13.61	8.60
10	24–26 Feb 2007	48	75	475	69.9	41.7	58.3	33.4	16.6	19.9	7.5	0.58	0.12	10.83	7.02
11	14–19 Feb 2012	120	120	475	118.7	108.3	117.2	128.6	1.3	−18.7	1	–	–	–	–
				473	246.5	66.0	79.4	66.4	67.8	5.5	−5	0.70	0.40	19.7	8.70
12	28 Feb–3 Mar 2012	168	125	473	69.0	57.2	29.5	57.3	57.2	−0.3	−6	0.65	0.39	7.25	4.59
Average values									26.3	10.7	−3.6	0.74	0.53	7.87	4.67

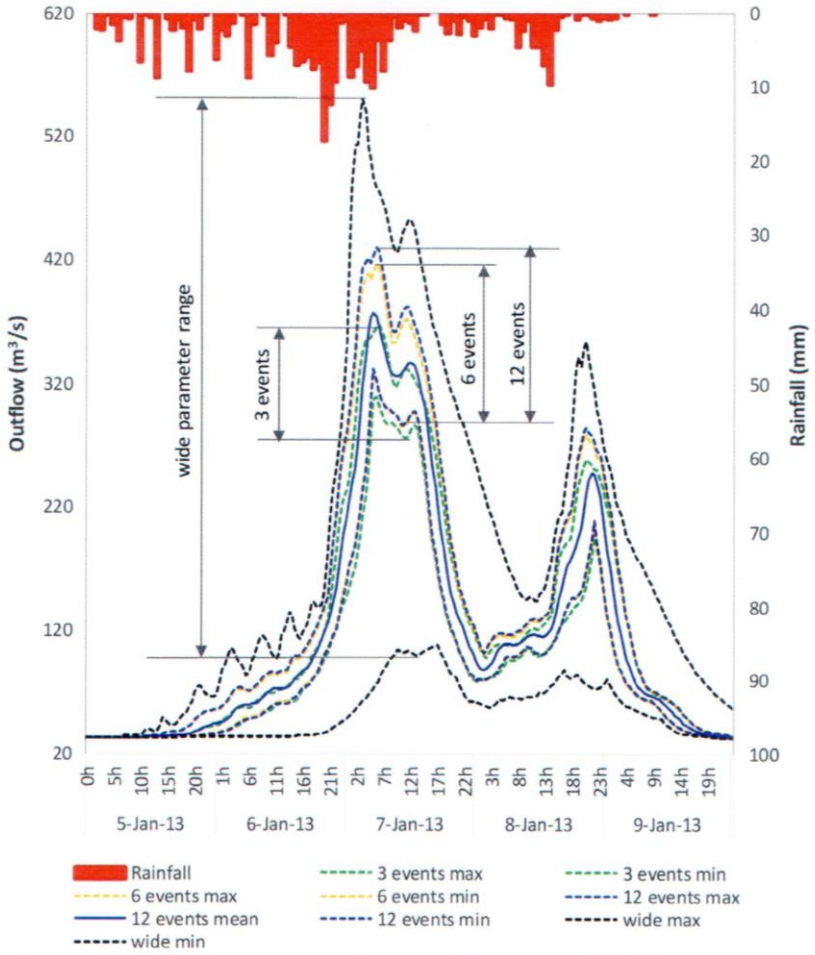

Fig. 5. Step (2): Simulation of the early January 2013 flood hydrograph at Saida gauge (475) location by HEC-HMS with the corresponding uncertainty boundaries based on the arbitrary wide parameter ranges (in black), ranges obtained by the "3-events" calibration (in green), ranges obtained by the "6-events" calibration (in orange), and ranges obtained by the "12-events" calibration (in purple). (For interpretation of the references to colour in this figure legend, the reader is referred to the web version of this article.)

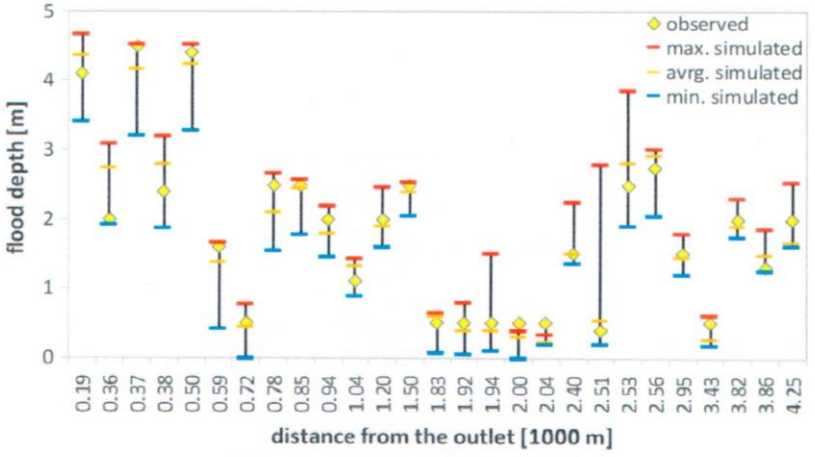

Fig. 6. Step (3): observed post-event maximum water levels versus simulated maximum water levels by the hydraulic model for three selected bounding scenarios, maximum, minimum and average flood flow hydrographs for the early January 2013 extreme event.

Fig. 7. Resultant maximum flood inundation extent for the Jan2013 flood event.

HEC-RAS model include the Severn River in UK (Horritt and Bates, 2002), the Eno River Strouds Creek in North Carolina and Brazos river in Texas (Cook and Merwade, 2009), the Po River in Italy (Di Baldassarre and Montanari, 2009), and the Xerias river in Greece (Papaioannou et al., 2017). The HEC-HMS and the HEC-RAS models have been successfully coupled in different study cases, examples include the San Antonio River basin in Texas (Knebl et al., 2005) and the Giofiros basin in Greece (Koutroulis and Tsanis, 2010). Sufficient discussions have been presented in literature to assess the use of many of these models and evaluate their coupling performance. These models have been tested against classical data in well gauged basins and found to be successful. In this project we do not aim to assess the performance of the model structure; the performance of the model structure can be tested with classical data, to be valid for application with sparse data. Based on what we have mentioned before that most of the river basins are data-sparse basins, we aim to discuss the opportunity of applying these hydrological-hydraulic models using sparse-data.

Unlike classical approaches that involve calibrating the model with one past storm event, the robustness of the applied approach is related to the evaluation of the model with several past storm events of variable intensities. The proper number of past events is selected when calibration based on additional past events do not considerably change the estimated parameter ranges. However, this is not straightforward, this number may vary from one application to another depending on the variability of the events in terms of intensity, period of occurrence of the events; how close are the events to the particular event under study and whether there was evolution in the landuse or modification to the river channel, and number of parameters to evaluate. Perhaps the proper number of past events necessary for the hydrological/hydraulic modelling has always been an open question in hydrology, Koutroulis and Tsanis (2010) calibrated their model based on 8 events, Garambois et al. (2013) evaluated their study based on 10 events, and Massari et al. (2014) calibrated and validated their model based on 16 events. Given the scarcity of data about floods in the area, 12 events of variable intensity is an acceptable number in hydrology and was found to be sufficient to ensure convergence in the calibration; this is clear from the results of calibration of the model by 6 and 12 events where the parameter ranges do not change considerably and the model is quite stable around this parameter range.

The selected events are of variable intensities, involving low flow as well as high flow events allowing to obtain sufficient ranges of variation of the hydrological parameters. Out of the 12 events, 5 are considered low flow events (events 2, 3, 4 7, and 8; peak flow ranging between 17 and 29 m^3/s), 4 are moderate flow events (events 5, 9, 10, and 12; peak flow ranging between 68 and 86 m^3/s), and 3 are high flow events (events 1, 6, and 11; peak flow ranging between 119 and 163 m^3/s). The events were selected for the period between January 2000 and March 2012. For the studied period, no major changes to the landuse and the river network were observed, and the same hydro-meteorological network was operating. Moreover, the study is limited to evaluating only 4 parameters that are thought to mostly impact the results of modelling.

The parameter ranges obtained after evaluating the model with the past events can define narrower parameter ranges for uncertainty evaluation. Perhaps the more past events evaluated the better results are expected. The approach is not suitable for evaluating a big number of parameters, because it is economically unfeasible to evaluate a large number of past events that might not be available in data-sparse

regions. The approach might not be suitable when considerable changes in the flow regime or in the basin's characteristics are noticed.

With an NSE ranging from 0.06 to 0.84, the model performance is highly variable. Low NSE values are obtained for minor as well as major events. Therefore, model performance cannot be clearly related to the event type. However, low NSE when modelling flood events doesn't mean necessary a bad simulation. It can be due to a simple translation of the hyetograph (Moussa, 2010) or data quality issues. For high magnitude events (events 1 and 12), the model tends to underestimate the peak flow, mainly because the discretisation of the daily rainfall measurements into hourly rainfall measurements does not reflect the actual rainfall intensity, which is expected to be higher. Moreover, the low reliability of the estimated rating curves might produce higher observed peak flow values for events exceeding the maximum stage by the rating curve, see for example event 11; the peak flow estimated by the upstream gauge G(473) by 246.5 m^3/s far exceeds the peak flow estimated by the downstream gauge G(475) by 118.7 m^3/s. In some cases (events 2, 3, 9, and 10), the flow hydrographs exhibited large fluctuations that affected the performance of the model. These fluctuations are not linked to precipitation patterns, because the majority are observed when no rainfall is recorded. The mismatch between the precipitations and observed water levels can be linked to either an error in rainfall measurementor to a malfunctioning of the river stage gauge that is highly sensitive to any disturbance induced into the river flow. At this stage and considering the low reliability of the rating curves and the lack of hourly rainfall estimates, these should be considered satisfactory results.

5.2. Uncertainty propagation

The uncertainty in the model results is a propagation of several uncertainties inherent mainly in the input data, model parameters, and model structure. In data-sparse regions, the uncertainty inherent in the hydrological model input and model parameters may be the major sources of uncertainty compared to the hydrological model structure. This is because the selected hydrological model structure is widely accepted and have been verified before on several properly gauged basins worldwide and the uncertainties inherent in its structure are negligible compared to the poor uncertain data available. This might be a difference between hydrological and hydraulic models in which the uncertainty inherent in the hydraulic model structure might outperform the one emerged from the hydraulic model parameters as demonstrated by Dimitriadis et al. (2016). However, additional hydrological model structures, through other software, should be tested in future research to further test this statement. The lack of sufficient observational data necessary to parameterize the model is the major source of uncertainty in the model parameters which is propagated to the output variables. Classical hydrological modelling techniques in well gauged basins involve calibrating the model with a set of past observation data. The result is a defined set of parameters capable to a certain extent of well reproducing the hydrological rainfall-runoff transformations within the basins in a deterministic way. On the other side, if no model calibration is performed, analysing the uncertainty propagation through modelling based on a wide range of feasible parameter ranges will result in numerous possible model realisations. Sometimes, when the uncertainty bounds are too wide, the results of the modelling are no more representative and can be substituted by other empirical or simplified methods. Based on what have been discussed, the calibration approach applied in this study aims to define the hydrological model parameters ranges to reduce uncertainty in the output flows. The "12-events" model simulation resulted in a peak flow difference of around 105 m^3/s between the maximum and minimum uncertainty bounds. This is much better than solely performing the uncertainty analysis based on the arbitrarily chosen wide parameter ranges that resulted in a peak flow difference of around 450 m^3/s. The future work involves testing this approach on other study sites to assess the effect of variable number of past storm events chosen for calibration.

Rainfall is the major input data to the model of major uncertainty inherent in the time step of measurement, especially in regions characterized by flash floods of response times in the order of hours. Discretizing the daily rainfall measurements into hourly measurements over the period of occurrence of maximum rainfall was found to be encouraging. This interprets the relatively good NSE value obtained for event 6 for which rainfall was discretised over the first quarter of the day only; the time period of occurrence of maximum rainfall. Further analysis is to be performed to compare different rainfall discretization methods, to analyse the uncertainty induced by the time step of measurement, especially when no information on the time of occurrence of the rain event is available. Other sources of rainfall data uncertainties are inherent in its spatial variability and measurement method. Such uncertainties can be ignored compared to the uncertainties inherent in the time step of measurement because the Jan2013 storm event was widely spread over the whole country with no major spatial variation in the rainfall intensity observed over the relatively small basin's area. The analogous records of six daily rainfall stations, well distributed over the area, also support our observation and reduces the uncertainty inherent in the spatial variability of rainfall and in its measured values.

5.3. Opportunities in post-event measurements

The spatial water level measurements based on high water marks such as fragments in trees, traces left by water along the river section and floodplain, and water lines on building walls were acknowledged by several scientists in literature (e.g. Horritt and Bates, 2002; Borga et al., 2008; Fuentes-Andino et al., 2017). Indeed, these measurements are biased by river modification over time and a greater uncertainty is associated with rapid flow conditions. Despite this uncertainty, those measurements may represent the best available evidence for flood events. The uncertainty in measurements can be assessed by the field surveyors themselves considering the conditions that formed the high-water marks. In rapid flow conditions and if good care was taken when measuring the water peaks, uncertainty in measurements may not exceed the 0.15 m as suggested by the USGS (Koenig et al., 2016).

In this study, no major modification to the river channel was observed. Maximum water level measurements were carefully chosen with proper awareness. Unreliable or confusing points with variable or unclear high-water marks were avoided, allowing to keep only the clear and best quality points. This evaluation criteria limited the number of post-event measurements to 27 measurements. In some cases, an average of two or three water marks was estimated to improve confidence in the measurement. Sometimes, viewing the complete set of points of a water line on one side of the bank and comparing it to the opposite bank allows estimating the best water line. Moreover, information on water levels obtained from local witnesses was considered reliable because the field survey was performed in two months after the flood event and the local witnesses' memory about the event was still fresh.

In this study and based on our observation, the uncertainty in the post-event measurements may not exceed the 0.5 m. Despite this uncertainty most of the observed water levels fall within the uncertainty bounds and are very close to the mean simulation of the hydraulic model. In the lack of hydrometric measurements, the results indicate the robustness of the applied approach in modelling flood levels and the capability of validating the results on different locations scattered in space.

The resolution of the topographic data is a key element in the accuracy of the hydraulic model (Casas et al., 2006; Cook and Merwade, 2009). Several studies in literature have pointed out to the sensitivity of the hydraulic models to the resolution of digital elevation models (Tsubaki and Fujita, 2010; Papaioannou et al., 2016; Savage et al., 2016). Many have acknowledged the use of high resolution DEM's for hydraulic modelling and flood mapping specially with basins of rapidly

varied topography and steep river slopes (Schumann et al., 2009; Bates, 2012; Brandt, 2016).

In this approach, validation of the hydraulic model with post-event measurements in space is encouraging when based on a fine resolution DEM. A prior simulation for the hydraulic model was performed based on the available 10 m resolution DEM. The hydraulic model experienced a lot of numerical instabilities. The resulting water levels were far beyond the real observed water levels, and in some locations, were more than triple the observed ones. This is primarily because the geometry and slopes of the river channel and the floodplain are not well represented in the coarse DEM; i.e. a river channel of width in the order of 5–10 m and a flood plain in the order of 30–50 m are unrealistically presented by 3–5 cells only in the coarse DEM. In hydraulic models, errors induced by poor terrain and slopes representation are much higher than those induced by poor estimation of the Manning's coefficient (see for example Jaber and Mohtar, 2003). With the advancement of the remote sensing and drone photography techniques, fine resolution DEM's are expected to be widely spread in the future. These techniques, mainly the drone photography, are being favourable because of their ease of use, high accuracy, and wide applicability (McCabe et al., 2017; Leitão and de Sousa, 2018). Accordingly, the availability of the fine resolutions DEM's should not be an issue in data-sparse regions in the coming years.

5.4. What if sparse spatial data are better than classical temporal data?

Calibration and evaluation of the hydrological model with several past storm events increased the results robustness. Unlike classical uncertainty analysis techniques in ungauged basins involving wide parameter ranges, the results robustness is obtained by evaluating the model with several storm events of variable intensities that allowed the estimation of possible parameter ranges of the hydrological model that are narrow enough to reduce the uncertainty in the model predictions. Moreover, the presented results have to be compared with the classical calibration approach that results in a set of deterministic model parameters and do not allow easily for the uncertainty propagation through the model.

Classically, hydraulic models are calibrated and validated based on "classical temporal data at one point", these are measured water levels or flow values at the gauge stations. However, several potential errors arise when using this type of observational data related to the accuracy of measurement and its spatial resolution. For large flood events and when river stage gauges are not damaged by the flood, water level measurements may exceed the maximum gauge measurement levels or exceed the maximum value used in the derivation of the rating curves that are unable to reflect the hydraulic behaviour of the rated section (Horritt et al., 2010). Even though the river stage accurately measures the water levels that are within the range of the rating curves, it is still required to obtain information on other cross sections based on field investigation of flood marks. Those levels often exceed the range of stage-discharge relationships that may exist on site (Gaume and Borga, 2008). Despite the narrow temporal sampling of the water levels at the river stage, there is lack of spatial data that do not allow the verification of the distributed model predictions, whereas, the use of finer resolution DEM increases the confidence in the distributed model predictions (Moussa and Cheviron, 2015). The use of "sparse spatial data at one date" in the form of post-event measurements of water levels scattered in space alone supports the spatial validation of the flood inundation model. Such spatial sparse information of non-binary nature may be used in the lack of short time step temporal hydrograph on a given point, especially in time periods of approximately steady flow conditions. Whereas, the "classical temporal data at one point" of too sparse spatial resolution should always be accompanied with other diverse sources such as the aerial photos, remote sensing or post-event measurements of flood marks to allow the spatial validation of the model predictions. On the other hand, the broader distribution and the greater number of post-event measurements, the better validation is achieved, because this type of data is subjected to several limitations (Hunter et al., 2005). For example, in the case of unsteady flow conditions the flood inundation could behave differently in the upstream and downstream areas and the post-event measurements might not reflect the flood dynamics.

5.5. Model complexity vs performance for a given condition of data availability

The more complex the flood model is, the greater is the risk of the uncertainty inherent in the required input data, model parameters, and in the model structure. Applying complex models in a data-sparse basin cannot be easy verified.

Several studies on DEM-based Geomorphic approaches have been performed in literature to delineate flood prone areas. These simplified methods that rely on basin geomorphologic feature characterization revealed to be an efficient low-cost strategy (e.g. Moussa, 1997; Noman et al., 2001; Manfreda et al., 2014; Samela et al., 2017). The geomorphic approaches allow highlighting preliminarily the locations of flooded areas and give rough estimation on the extent and depth of flood inundation. Such approaches proved to be efficient in large scale applications (Samela et al., 2017) and the outcomes are relatively sufficient to inform decision makers on the range of variability of the flood hazard for general planning purposes. However, general geomorphic approaches may not be very efficient when detailed information on the inundation levels and extent is required especially in small scale applications and therefore cannot easily replace the hydrological-hydraulic approaches (Manfreda et al., 2014).

Moreover, most geomorphic approaches require probabilistic information on rainfall (e.g. design rainfalls of 50 years, 100 years, etc.) obtained from statistical analysis of rainfall series and make use of the hydraulic scaling functions based on contributing areas to estimate water levels. These estimations based on probabilistic input do not always allow the detailed understanding of particular events of unknown severity level, such as the Jan2013 flood event. Working with particular event is not like working with statistical approaches.

Although complex models require an increasing number of data to reach adequate reliability and it is preferable to be avoided. But for practical problems the use of complex distributed models is inevitable (Grayson and Blöschl, 2001). It is of a challenge to better use the available information and to seek additional information to increase the confidence in model simulations. Model complexity depends on how we define it, on the site of application and on the time of application; what was considered complex several years ago is now simpler with the rapid evolution of computational power, development of very high resolution DEM's, and the widespread of geographic information systems (GIS).

The presented application is not much complicated but rather an intermediate position between complex and simple approaches. Indeed, several simplifications of the processes representation were applied to reduce model requirements and number of parameters. This can be illustrated for example by using the SCS Curve Number approach for runoff computation, which is empirical in origin, along with the SCS-unit hydrograph routing method. 1D HEC-RAS model can be considered as simple by comparison to 2D or 3D hydraulic models.

Added value information from social media, post-event surveys and past storm events helped constrain the model and improve the quality of results. The availability of a high-resolution DEM encouraged the application of the 1D hydraulic model (HEC-RAS) which proved to give reasonably promising results. The error in the simulated water levels is in the order of 20–30 cm which might not be achieved when applying simplified geomorphic approaches. However, this doesn't prove our approach will be efficient in all circumstances, but at least it strengthens our confidence in its value.

6. Conclusions

The objective of this paper was to assess whether there is opportunity to constrain hydrological-hydraulic models with sparse data to simulate extreme floods and establish water levels that can be useful for flood maps adapted for basin scale applications. For this purpose, we develop a framework based on a coupled hydrological-hydraulic model constrained by past storm events and post-event measurements. The approach is applied to the Awali river basin (301 km^2), in Lebanon, particularly to simulate the investigated early January 2013 extreme flood event. The hydrological model was calibrated with 12 past storm events aiming at defining narrow hydrological parameter ranges. The uncertainty in the model parameters was assessed by performing Monte Carlo simulation for the estimated parameter ranges. The uncertainty simulation gave satisfactory results. It was found that the uncertainty in the resulting outflow values is reduced when compared with running simulations based on arbitrarily chosen wide parameter ranges. Social media information on the event characteristics especially on the duration of maximum rainfall was an added value to constrain the hydrological model simulations. Post-event measurements of high-water marks were promising in validating the flood map in space.

The results show the potentials and the limitations of applying hydrological-hydraulic models using sparse data and the challenge of producing flood maps that can replace the coarse resolution regional maps. The clear advantage of the proposed method is that it is a tailor-made approach adapted for basin scale applications in data-sparse regions using the maximum data available and aiming at producing inundation maps that can perform better than regional maps. The method allows modelling with reduced uncertainty particular flood events in terms of estimation of the flood hydrographs, flood water levels and mapping the inundated area. It has the potential to enable crowdsourcing of information for flood events in the form of spatial post event measurements, social media information, local witnesses, along with pictures and videos. Such crowdsourced information are now gaining favor in data-sparse regions as a way to compensate the weaknesses in the traditional measurement networks. Moreover, the method has the potential to include high resolution digital elevation models that are now evolving at an unprecedented pace. The coupled hydrologic/hydraulic model is constrained by past storm events and post events measurements and the results are estimations of the flood water levels along the floodplain with accuracy less than 1 m. The interesting results reveal that good spatial measurements of one event, even of very short time series, are significant in supporting the hydrological/hydraulic modeling. These sparse spatial data at one date may be used in the lack of classical temporal data at the gauge stations. The approach can serve as a tool for damage assessment of flood events, it supports urban planning and structural design of flood protection measures on a local scale. The approach when combined with organized real time crowdsourcing can serve as a part of a flood forecasting system. Finally, when classical data are lacking, the use of sparse data in a classical modelling approach is encouraging and the proposed framework can be applied to other data-sparse regions facing the same problems.

Acknowledgements

This research is part of a PhD thesis of the first author funded by the National Council for Scientific Research-Lebanon (CNRS-L) with the cooperation of the Laboratory for the study of Soil-Agrosystem-Hydrosystem interactions at the French National Institute for Agricultural Research (INRA-LISAH) and the Montpellier National Superior School of Agronomy (Montpellier-SupAgro). The project was partially funded by the Italian National Research Council (CNR) project (Third Call for Proposals for joint research projects 2015-2016 CNR-CNRS-L) entitled "Hydrological modelling optimization in poorly gauged and small sized basins – Lebanon as a case study". The Authors thank the reviewers for their constructive comments, they also thank the authorities of the CNRS and CNR for their continuous support.

Appendix A. Supplementary data

Supplementary data associated with this article can be found, in the online version, at https://doi.org/10.1016/j.jhydrol.2018.08.008.

References

Abdallah, C., Hdeib, R., 2015. Flood Risk Assessment and Mapping for Lebanon-UNDP/CNRS, 93. P. + ANNEX, Lebanon.
Abdallah, C., Hdeib, R., Hijazi, S., Darwich, T., Merheb, M., Karam, F., 2013. Flood Hazard Mapping Assessment for Lebanon-UNDP/CNRS-2382, 110pp. Lebanon.
Amengual, A., Romero, R., Gómez, M., Martín, A., Alonso, S., 2007. A hydrometeorological modeling study of a flash-flood event over Catalonia. Spain. J. Hydrometeorol. 8, 282–303. https://doi.org/10.1175/JHM577.1.
Apel, H., Merz, B., Thieken, A.H., 2008. Quantification of uncertainties in flood risk assessments. Int. J. River Basin Manag. 6, 149–162. https://doi.org/10.1080/15715124.2008.9635344.
Aronica, G.T., Bates, P.D., Horritt, M.S., 2002. Assessing the uncertainty in distributed model predictions using observed binary pattern information within GLUE. Hydrol. Process. 16, 2001–2016. https://doi.org/10.1002/hyp.398.
ASPRS, 2004. Manual of photogrammetry/editor, J. Chris McGlone; associate editors, Edward M. Mikhail, James Bethel, fifth ed. American Society of Photogrammetry and Remote Sensing, Bethesda, Md.
Barnolas, M., Llasat, M.C., 2007. A flood geodatabase and its climatological applications: the case of Catalonia for the last century. Nat. Hazards Earth Syst. Sci. 7, 271–281. https://doi.org/10.5194/nhess-7-271-2007.
Barredo, J.I., 2007. Major flood disasters in Europe: 1950–2005. Nat. Hazards 42, 125–148. https://doi.org/10.1007/s11069-006-9065-2.
Bates, P.D., 2012. Integrating remote sensing data with flood inundation models: how far have we got? Hydrol. Process. 26, 2515–2521. https://doi.org/10.1002/hyp.9374.
Bates, P.D., 2004. Remote sensing and flood inundation modelling. Hydrol. Process. 18, 2593–2597. https://doi.org/10.1002/hyp.5649.
Borga, M., Gaume, E., Creutin, J.D., Marchi, L., 2008. Surveying flash floods: gauging the ungauged extremes. Hydrol. Process. 22, 3883–3885. https://doi.org/10.1002/hyp.7111.
Brandt, S.A., 2016. Modeling and visualizing uncertainties of flood boundary delineation: algorithm for slope and DEM resolution dependencies of 1D hydraulic models. Stoch. Environ. Res. Risk Assess. 30, 1677–1690. https://doi.org/10.1007/s00477-016-1212-z.
Casas, A., Benito, G., Thorndycraft, V.R., Rico, M., 2006. The topographic data source of digital terrain models as a key element in the accuracy of hydraulic flood modelling. Earth Surf. Process. Landforms 31, 444–456. https://doi.org/10.1002/esp.1278.
Castellarin, A., 2007. Probabilistic envelope curves for design flood estimation at ungauged sites. Water Resour. Res. 43, 1–12. https://doi.org/10.1029/2005WR004384.
Castellarin, A., Merz, R., Blöschl, G., 2009. Probabilistic envelope curves for extreme rainfall events. J. Hydrol. 378, 263–271. https://doi.org/10.1016/j.jhydrol.2009.09.030.
Choudhari, K., Panigrahi, B., Paul, J.C., 2014. Simulation of rainfall-runoff process using HEC-HMS model for Balijore. Int. J. Geomatics Geosci. 5, 253–265 doi: Code: ELJGGS5021.
Cook, A., Merwade, V., 2009. Effect of topographic data, geometric configuration and modeling approach on flood inundation mapping. J. Hydrol. 377, 131–142. https://doi.org/10.1016/j.jhydrol.2009.08.015.
D'Asaro, F., Grillone, G., 2010. Runoff Curve Number Method in Sicily: CN determination and analysis of the initial abstraction ratio. 4th Fed. Interag. Conf. Las Vegas, NV, June 27–July 1, 2010, pp. 1–12.
Darwish, T., Khawlie, M., Jomaa, I., Abou Daher, M., Awad, M., Masri, M., Shaban, A., Faour, G., Bou Kheir, R., Abdallah, C., Haddad, T., 2006. Digital Soil Map of Lebanon 1/50,000. Monograph Series 4. CNRS Lebanon.
Di Baldassarre, G., Montanari, A., 2009. Uncertainty in river discharge observations: a quantitative analysis. Hydrol. Earth Syst. Sci. 13, 913–921. https://doi.org/10.5194/hessd-6-39-2009.
Dimitriadis, P., Tegos, A., Oikonomou, A., Pagana, V., Koukouvinos, A., Mamassis, N., Koutsoyiannis, D., Efstratiadis, A., 2016. Comparative evaluation of 1D and quasi-2D hydraulic models based on benchmark and real-world applications for uncertainty assessment in flood mapping. J. Hydrol. 534, 478–492. https://doi.org/10.1016/j.jhydrol.2016.01.020.
Domeneghetti, A., 2016. On the use of SRTM and altimetry data for flood modeling in data-sparse regions. Water Resour. Res. 52, 2901–2918. https://doi.org/10.1002/2015WR017967.
Domeneghetti, A., Vorogushyn, S., Castellarin, A., Merz, B., Brath, A., 2013. Probabilistic flood hazard mapping: effects of uncertain boundary conditions. Hydrol. Earth Syst. Sci. 17, 3127–3140. https://doi.org/10.5194/hess-17-3127-2013.
Dubertret, L., 1945. Cartes geologiques du Liban a l'echelle de 1/50000.
Efstratiadis, A., Koussis, A.D., Koutsoyiannis, D., Mamassis, N., 2014. Flood design recipes vs. reality: Can predictions for ungauged basins be trusted? Nat. Hazards Earth Syst. Sci. 14, 1417–1428. https://doi.org/10.5194/nhess-14-1417-2014.
Freer, J., Beven, K., Ambroise, B., 1996. Bayesian estimation of uncertainty in runoff prediction and the value of data: an application of the GLUE approach. Water Resour. Res. 32, 2161–2173. https://doi.org/10.1029/96WR03723.
Fuentes-Andino, D., Beven, K., Halldin, S., Xu, C.-Y., Reynolds, J.-E., Di Baldassarre, G.,

2017. Reproducing an extreme flood with uncertain post-event information. Hydrol. Earth Syst. Sci. Discuss. 21, 3597–3618. https://doi.org/10.5194/hess-21-3597-2017.

Fukami, K., Yamaguchi, T., Imamura, H., Tashiro, Y., 2008. Current status of river discharge observation using non-contact current meter for operational use in Japan. World Environ. Water Resour. Congr.

Garambois, P.A., Roux, H., Larnier, K., Castaings, W., Dartus, D., 2013. Characterization of process-oriented hydrologic model behavior with temporal sensitivity analysis for flash floods in Mediterranean catchments. Hydrol. Earth Syst. Sci. 17, 2305–2322. https://doi.org/10.5194/hess-17-2305-2013.

Gaume, E., 2006. Post Flash-flood Investigations-Methodological Note. Floodsite European Research Project, Report D23.2. 62pp.

Gaume, E., Bain, V., Bernardara, P., Newinger, O., Barbuc, M., Bateman, A., Blaškovicová, L., Blöschl, G., Borga, M., Dumitrescu, A., Daliakopoulos, I., Garcia, J., Irimescu, A., Kohnova, S., Koutroulis, A., Marchi, L., Matreata, S., Medina, V., Preciso, E., Sempere-Torres, D., Stancalie, G., Szolgay, J., Tsanis, I., Velasco, D., Viglione, A., 2009. A compilation of data on European flash floods. J. Hydrol. 367, 70–78. https://doi.org/10.1016/j.jhydrol.2008.12.028.

Gaume, E., Borga, M., 2008. Post-flood field investigations in upland catchments after major flash floods: proposal of a methodology and illustrations. J. Flood Risk Manag. 1, 175–189. https://doi.org/10.1111/j.1753-318X.2008.00023.x.

Grayson, R., Blöschl, G., 2001. Spatial Patterns in Catchment Hydrology, Spatial Patterns in Catchment Hydrology: Observations and Modelling. Cambridge University Press.

Hall, J., Arheimer, B., Borga, M., Brázdil, R., Claps, P., Kiss, A., Kjeldsen, T.R., Kriauciuniene, J., Kundzewicz, Z.W., Lang, M., Llasat, M.C., Macdonald, N., McIntyre, N., Mediero, L., Merz, B., Merz, R., Molnar, P., Montanari, A., Neuhold, C., Parajka, J., Perdigão, R.A.P., Plavcová, L., Rogger, M., Salinas, J.L., Sauquet, E., Schär, C., Szolgay, J., Viglione, A., Blöschl, G., 2014. Understanding flood regime changes in Europe: a state-of-the-art assessment. Hydrol. Earth Syst. Sci. 18, 2735–2772. https://doi.org/10.5194/hess-18-2735-2014.

Hervouet, J.M., 2000. A high resolution 2-D dam-break model using parallelization. Hydrol. Process. 14, 2211–2230. https://doi.org/10.1002/1099-1085(200009)14:13<2211::AID-HYP24>3.0.CO;2-8.

Horritt, M.S., Bates, P.D., 2002. Evaluation of 1D and 2D numerical models for predicting river flood inundation. J. Hydrol. 268, 87–99. https://doi.org/10.1016/S0022-1694(02)00121-X.

Horritt, M.S., Bates, P.D., Fewtrell, T.J., Mason, D.C., Wilson, M.D., 2010. Modelling the hydraulics of the Carlisle 2005 flood event. Proc. Inst. Civ. Eng. Water Manag. 163, 273–281. https://doi.org/10.1680/wama.2010.163.6.273.

Huang, M., Liang, X., 2006. On the assessment of the impact of reducing parameters and identification of parameter uncertainties for a hydrologic model with applications to ungauged basins. J. Hydrol. 320, 37–61. https://doi.org/10.1016/j.jhydrol.2005.07.010.

Hunter, N.M., Bates, P.D., Horritt, M.S., De Roo, A.P.J., Werner, M.G.F., 2005. Utility of different data types for calibrating flood inundation models within a GLUE framework. Hydrol. Earth Syst. Sci. 9, 412–430. https://doi.org/10.5194/hess-9-412-2005.

Jaber, F.H., Mohtar, R.H., 2003. Stability and accuracy of two-dimensional kinematic wave overland flow modeling. Adv. Water Resour. 26, 1189–1198. https://doi.org/10.1016/S0309-1708(03)00102-7.

Jarihani, A.A., Callow, J.N., McVicar, T.R., Van Niel, T.G., Larsen, J.R., 2015. Satellite-derived digital elevation model (DEM) selection, preparation and correction for hydrodynamic modelling in large, low-gradient and data-sparse catchments. J. Hydrol. 524, 489–506. https://doi.org/10.1016/j.jhydrol.2015.02.049.

Jonkman, S.N., 2005. Global perspectives on loss of human life caused by floods. Nat. Hazards 34, 151–175. https://doi.org/10.1007/s11069-004-8891-3.

Knebl, M.R., Yang, Z.L., Hutchison, K., Maidment, D.R., 2005. Regional scale flood modeling using NEXRAD rainfall, GIS, and HEC-HMS/ RAS: a case study for the San Antonio River Basin Summer 2002 storm event. J. Environ. Manage. 75, 325–336. https://doi.org/10.1016/j.jenvman.2004.11.024.

Koenig, T.A., Bruce, J.L., O'Connor, J.E., McGee, B.D., Holmes, R.R., J., Hollins, R., Forbes, B.T., Kohn, M.S., Schellekens, M.F., Martin, Z.W., Peppler, M.C., 2016. Identifying and preserving high-water mark data: U.S. Geological Survey Techniques and Methods, book 3, chap. A24, Applications of Hydraulics, doi: 10.3133/tm3A24.

Komi, K., Neal, J., Trigg, M.A., Diekkrüger, B., 2017. Modelling of flood hazard extent in data sparse areas: a case study of the Oti River basin, West Africa. J. Hydrol. Reg. Stud. 10, 122–132. https://doi.org/10.1016/j.ejrh.2017.03.001.

Koutroulis, A.G., Tsanis, I.K., 2010. A method for estimating flash flood peak discharge in a poorly gauged basin: case study for the 13–14 January 1994 flood, Giofiros basin, Crete, Greece. J. Hydrol. 385, 150–164. https://doi.org/10.1016/j.jhydrol.2010.02.012.

Lastoria, B., Simonetti, M.R., Casaioli, M., Mariani, S., Monacelli, G., 2006. Socio-economic impacts of major floods in Italy from 1951 to 2003. Adv. Geosci. 7, 223–229. https://doi.org/10.5194/adgeo-7-223-2006.

Le Boursicaud, R., Pénard, L., Hauet, A., Thollet, F., Le Coz, J., 2016. Gauging extreme floods on YouTube: application of LSPIV to home movies for the post-event determination of stream discharges. Hydrol. Process. 30, 90–105. https://doi.org/10.1002/hyp.10532.

Leitão, J.P., de Sousa, L.M., 2018. Towards the optimal fusion of high-resolution digital elevation models for detailed urban flood assessment. J. Hydrol. 561, 651–661. https://doi.org/10.1016/j.jhydrol.2018.04.043.

Lerat, J., Perrin, C., Andréassian, V., Loumagne, C., Ribstein, P., 2012. Towards robust methods to couple lumped rainfall-runoff models and hydraulic models: a sensitivity analysis on the Illinois River. J. Hydrol. 418–419, 123–135. https://doi.org/10.1016/j.jhydrol.2009.09.019.

Llasat, M.C., Llasat-Botija, M., Barnolas, M., López, L., Altava-Ortiz, V., 2009. An analysis of the evolution of hydrometeorological extremes in newspapers: the case of Catalonia, 1982–2006. Nat. Hazards Earth Syst. Sci. 9, 1201–1212. https://doi.org/10.5194/nhess-9-1201-2009.

Llasat, M.C., Llasat-Botija, M., Prat, M.A., Porcú, F., Price, C., Mugnai, A., Lagouvardos, K., Kotroni, V., Katsanos, D., Michaelides, S., Yair, Y., Savvidou, K., Nicolaides, K., 2010. High-impact floods and flash floods in Mediterranean countries: the FLASH preliminary database. Adv. Geosci. 23, 47–55. https://doi.org/10.5194/adgeo-23-47-2010.

LNCSR-LMoA, 2010. Land cover/Use Map of Lebanon at 1:20,000 Scale. National Council for Scientific Research (NCSR) and Ministry of Agriculture (MOA), Lebanon.

Lowry, C.S., Fienen, M.N., 2013. Crowd hydrology: crowdsourcing hydrologic data and engaging citizen scientists. Ground Water 51, 151–156. https://doi.org/10.1111/j.1745-6584.2012.00956.x.

Lumbroso, D., Gaume, E., 2012. Reducing the uncertainty in indirect estimates of extreme flash flood discharges. J. Hydrol. 414–415, 16–30. https://doi.org/10.1016/j.jhydrol.2011.08.048.

Manfreda, S., Nardi, F., Samela, C., Grimaldi, S., Taramasso, A.C., Roth, G., Sole, A., 2014. Investigation on the use of geomorphic approaches for the delineation of flood prone areas. J. Hydrol. 517, 863–876. https://doi.org/10.1016/j.jhydrol.2014.06.009.

Mascaro, G., Piras, M., Deidda, R., Vivoni, E.R., 2013. Distributed hydrologic modeling of a sparsely monitored basin in Sardinia, Italy, through hydrometeorological downscaling. Hydrol. Earth Syst. Sci. 17, 4143–4158. https://doi.org/10.5194/hess-17-4143-2013.

Massari, C., Brocca, L., Barbetta, S., Papathanasiou, C., Mimikou, M., Moramarco, T., 2014. Using globally available soil moisture indicators for flood modelling in Mediterranean catchments. Hydrol. Earth Syst. Sci. 18, 839–853. https://doi.org/10.5194/hess-18-839-2014.

Mazzoleni, M., Juliette, V., Arevalo, C., Wehn, U., Alfonso, L., Monego, M., Ferri, M., Solomatine, D.P., 2017. Towards assimilation of crowdsourced observations for different levels of citizen engagement: the flood event of 2013 in the Bacchiglione catchment. Hydrol. Earth Syst. Sci. Discuss. 1–40. https://doi.org/10.5194/hess-2017-59.

McCabe, M.F., Rodell, M., Alsdorf, D.E., Miralles, D.G., Uijlenhoet, R., Wagner, W., Lucieer, A., Houborg, R., Verhoest, N.E.C., Franz, T.E., Shi, J., Gao, H., Wood, E.F., 2017. The future of earth observation in hydrology. Hydrol. Earth Syst. Sci. Discuss. 1–55. https://doi.org/10.5194/hess-2017-54.

Merwade, V., Olivera, F., Arabi, M., Edleman, S., 2008. Uncertainty in flood inundation mapping: current issues and future directions. J. Hydrol. Eng. 13, 608–620. https://doi.org/10.1061/(ASCE)1084-0699(2008) 13:7(608).

Montanari, A., Young, G., Savenije, H.H.G., Hughes, D., Wagener, T., Ren, L.L., Koutsoyiannis, D., Cudennec, C., Toth, E., Grimaldi, S., Blöschl, G., Sivapalan, M., Beven, K., Gupta, H., Hipsey, M., Schaefli, B., Arheimer, B., Boegh, E., Schymanski, S.J., Di Baldassarre, G., Yu, B., Hubert, P., Huang, Y., Schumann, A., Post, D.A., Srinivasan, V., Harman, C., Thompson, S., Rogger, M., Viglione, A., McMillan, H., Characklis, G., Pang, Z., Belyaev, V., 2013. "Panta Rhei—Everything Flows": change in hydrology and society—the IAHS scientific decade 2013–2022. Hydrol. Sci. J. 58, 1256–1275. https://doi.org/10.1080/02626667.2013.809088.

Montanari, M., Hostache, R., Matgen, P., Schumann, G., Pfister, L., Hoffmann, L., 2009. Calibration and sequential updating of a coupled hydrologic-hydraulic model using remote sensing-derived water stages. Hydrol. Earth Syst. Sci. 13, 367–380. https://doi.org/10.5194/hess-13-367-2009.

Moriasi, D.N., Arnold, J.G., Van Liew, M.W., Binger, R.L., Harmel, R.D., Veith, T.L., 2007. Model evaluation guidelines for systematic quantification of accuracy in watershed simulations. Trans. ASABE 50, 885–900. https://doi.org/10.13031/2013.23153.

Moussa, R., 2010. When monstrosity can be beautiful while normality can be ugly: assessing the performance of event-based flood models. Hydrol. Sci. J. 55, 1074–1084. https://doi.org/10.1080/02626667.2010.505893.

Moussa, R., 1997. Geomorphological transfer function calculated from digital elevation models for distributed hydrological modelling. Hydrol. Process. 11, 429–449. https://doi.org/10.1002/(SICI)1099-1085(199704)11:5<429::AID-HYP471>3.0.CO;2-J.

Moussa, R., Bocquillon, C., 2009. On the use of the diffusive wave for modelling extreme flood events with overbank flow in the floodplain. J. Hydrol. 374, 116–135. https://doi.org/10.1016/j.jhydrol.2009.06.006.

Moussa, R., Chahinian, N., 2009. Comparison of different multi-objective calibration criteria using a conceptual rainfall-runoff model of flood events. Hydrol. Earth Syst. Sci. 519–535.

Moussa, R., Cheviron, B., 2015. Rivers – Physical, Fluvial and Environmental Processes. doi: 10.1007/978-3-319-17719-9.

Nash, J.E., Sutcliffe, J.V., 1970. River flow forecasting through conceptual models part I – a discussion of principles. J. Hydrol. 10, 282–290. https://doi.org/10.1016/0022-1694(70)90255-6.

Neal, J., Schumann, G., Bates, P., 2012. A subgrid channel model for simulating river hydraulics and floodplain inundation over large and data sparse areas. Water Resour. Res. 48, 1–16. https://doi.org/10.1029/2012WR012514.

NOAA, 2013. National Centers for Environmental Information, State of the Climate: Global Hazards for January 2013, published online February 2013, retrieved on February 27, 2017 from http://www.ncdc.noaa.gov/sotc/hazards/201301.

Noman, N.S., Nelson, E.J., Zundel, A.K., ASCE, M., 2001. Review of automated floodplain delineation from digital terrain models. J. Water Resour. Plann. Manag. 127, 394–402.

Norbiato, D., Borga, M., Sangati, M., Zanon, F., 2007. Regional frequency analysis of extreme precipitation in the eastern Italian Alps and the August 29, 2003 flash flood. J. Hydrol. 345, 149–166. https://doi.org/10.1016/j.jhydrol.2007.07.009.

Oleyiblo, J.O., Li, Z., 2010. Application of HEC-HMS for flood forecasting in Misai and Wan'an catchments in China. Water Sci. Eng. 3, 14–22. https://doi.org/10.3882/j.issn.1674-2370.2010.01.002.

Panneton, F., L'ecuyer, P., Matsumoto, M., 2006. Improved long-period generators based on linear recurrences modulo 2. ACM Trans. Math. Softw. 32, 1–16. https://doi.org/10.1145/1132973.1132974.

Papaioannou, G., Loukas, A., Vasiliades, L., Aronica, G.T., 2016. Flood inundation mapping sensitivity to riverine spatial resolution and modelling approach. Nat. Hazards. https://doi.org/10.1007/s11069-016-2382-1.

Papaioannou, G., Vasiliades, L., Loukas, A., Aronica, G.T., 2017. Probabilistic flood inundation mapping at ungauged streams due to roughness coefficient uncertainty in hydraulic modelling. Adv. Geosci. 44, 23–34. https://doi.org/10.5194/adgeo-44-23-2017.

Pappenberger, F., Beven, K.J., Ratto, M., Matgen, P., 2008. Multi-method global sensitivity analysis of flood inundation models. Adv. Water Resour. 31, 1–14. https://doi.org/10.1016/j.advwatres.2007.04.009.

Plassard, J., 1972. Pluviometric Map of Lebanon at a Scale of 1:200,000. Republic of Lebanon. Ministry of Public Affairs. General Direction of Civil Aviation.

Robert, C.P., Casella, G., 2004. Monte Carlo Statistical Methods, second ed. Springer, New York.

Romanowicz, R., Beven, K., 2003. Estimation of flood inundation probabilities as conditioned on event inundation maps. Water Resour. Res. 39. https://doi.org/10.1029/2001wr001056.

Saleh, F., Ducharne, A., Flipo, N., Oudin, L., Ledoux, E., 2013. Impact of river bed morphology on discharge and water levels simulated by a 1D Saint-Venant hydraulic model at regional scale. J. Hydrol. 476, 169–177. https://doi.org/10.1016/j.jhydrol.2012.10.027.

Samaniego, L., Kumar, R., Jackisch, C., 2011. Predictions in a data-sparse region using a regionalized grid-based hydrologic model driven by remotely sensed data. Hydrol. Res. 42, 338–355. https://doi.org/10.2166/nh.2011.156.

Samela, C., Troy, T.J., Manfreda, S., 2017. Geomorphic classifiers for flood-prone areas delineation for data-scarce environments. Adv. Water Resour. 102, 13–28. https://doi.org/10.1016/j.advwatres.2017.01.007.

Sangati, M., Borga, M., Rabuffetti, D., Bechini, R., 2009. Influence of rainfall and soil properties spatial aggregation on extreme flash flood response modelling: an evaluation based on the Sesia river basin, North Western Italy. Adv. Water Resour. 32, 1090–1106. https://doi.org/10.1016/j.advwatres.2008.12.007.

Satyanarayana, P., Srinivas, V.V., 2011. Regionalization of precipitation in data sparse areas using large scale atmospheric variables – a fuzzy clustering approach. J. Hydrol. 405, 462–473. https://doi.org/10.1016/j.jhydrol.2011.05.044.

Savage, J.T.S., Bates, P., Freer, J., Neal, J., Aronica, G., 2016. When does spatial resolution become spurious in probabilistic flood inundation predictions? Hydrol. Process. 30, 2014–2032. https://doi.org/10.1002/hyp.10749.

Schumann, G., Bates, P.D., Horritt, M.S., Matgen, P., Pappenberger, F., 2009. Progress in intergration of remote sensing derived flood extent and stage data and hydraulic models. Rev. Geophys. 47, 1–20. https://doi.org/10.1029/2008RG000274.1. INTRODUCTION.

SCS, 1972. Soil Conservation Service-Section 4: Hydrology. National Engineering Handbook. Department of Agriculture, available from US Government Printing Office, Washington, DC.

Shamsudin, S., Dan, S., Rahman, A.A., 2011. Uncertainty analysis of Hec-Hms model parameters using Monte Carlo simulation. Int. J. Model. Simul. 31. https://doi.org/10.2316/Journal.20.

Sivapalan, M., Takeuchi, K., Franks, S.W., Gupta, V.K., Karambiri, H., Lakshmi, V., Liang, X., McDonnell, J.J., Mendiondo, E.M., O'Conell, P.E., Oki, T., Pomeroy, J.W., Schertzer, D., Uhlenbrook, S., Zehe, E., 2003. IAHS decade on predictions in ungauged basins (PUB), 2003–2012: shaping an exciting future for the hydrological sciences. Hydrol. Sci. J. 48, 857–880. https://doi.org/10.1623/hysj.48.6.857.51421.

Switzman, H., Coulibaly, P., Adeel, Z., 2015. Modeling the impacts of dryland agricultural reclamation on groundwater resources in Northern Egypt using sparse data. J. Hydrol. 520, 420–438. https://doi.org/10.1016/j.jhydrol.2014.10.064.

Tsubaki, R., Fujita, I., 2010. Unstructured grid generation using LiDAR data for urban flood inundation modelling. Hydrol. Process. 24, 1404–1420. https://doi.org/10.1002/hyp.7608.

UNISDR, 2002. Guidelines for Reducing Flood Losses, United Nations – Headquarters (UN), available on-line at: https://www.unisdr.org/we/inform/publications/558.

UNISDR, CRED, 2015. The Human Cost of Weather Related Disasters, 1995–2015, The United Nations Office for Diaster Risk Reduction, available online at: https://www.unisdr.org/archive/46793.

USACE, 2016. HEC-RAS River Analysis System – Hydraulic Reference Manual, Version 5.0. US Army Corps of Engineers Hydrologic Engineering Center (HEC), 609 Second Street Davis, CA 95616-4687, USA.

USACE, 2000. Hydrologic Modeling System HEC-HMS:Technical Referance Manual. US Army Corps of Engineers Hydrologic Engineering Center, 609 Second Street Davis, CA 95616-4687, USA.

WHO, 2002. Floods: Climate Change and Adaptation Strategies for Human Health. World Health Organization Regional Office for Europe, Copenhagen Available online at: http://www.euro.who.int/_data/assets/pdf_file/0007/74734/E77096.pdf.

Wilby, R.L., Yu, D., 2013. Rainfall and temperature estimation for a data sparse region. Hydrol. Earth Syst. Sci. 17, 3937–3955. https://doi.org/10.5194/hess-17-3937-2013.

A cost-performance grid to compare different flood modelling approaches

Rouya Hdeib[1] et al.

[1]CNRS-RS, National Council for Scientific Research, Remote Sensing Center, Beirut, Lebanon
[2]Laboratory example, city, postal code, country

Correspondence to: Rouya Hdeib (rouya.hdeib@gmail.com)

Abstract.

Flood inundation models have gained favor as a tool for understanding the flood dynamics and impacts, evaluate flood risk and implement mitigation measures. Numerous models are now available in both fields of hydrology and hydraulics aiming at understanding the flood processes ranging from simpler ones, with a limited number of parameters, to highly complex ones, with many parameters. Therefore, the choice of selection of an effective and economic model is not an easy exercise as it is dependent on a number of factors: the cost of data and models, the performance of the models, and the benefits behind applying the selected modelling approach. In this study, the structure of a cost-performance analysis grid designed for flood inundation modelling is presented. Most notably, the methodology employed for the evaluation of the cost of modelling and the performance of the selected approach is developed. For this purpose, we define metrics in order to characterize and quantify the three axes of a flood modelling problem: data availability, model complexity and prediction performance. An online survey has been developed and is made public to collect information from different colleagues and centers. As a first application on the grid, 10 different flood modelling approaches of variable complexity presented in literature were arbitrarily selected and analyzed to provide guidance on the implementation of the proposed grid. Results show that lowest modeling costs were associated with empirical approaches but however associated with lower performances. Modelling approaches based on open source data were associated with lower costs but high performances especially in well-gauged basins applications. Hydraulic and coupling approaches are associated with good performances and are located above the cost-performance curve, whereas, empirical and hydrological approaches are located below and are associated with less performance levels. The developed cost-performance grid is a tailor-made application. From an operational point of view the grid can be a tool to support the comparison, classification, and future selection of cost-effective modeling approaches. From a philosophical point of view the grid supports research evolution studies, it can be tuned to adapt with different modeling objectives and can be periodically updated to follow the recent advances in data measurements and model

capabilities. The research is still open, and other applications are expected to be presented in the future.

Keywords: cost-performance, data availability, model complexity, flood modeling, inundation maps, simple model

1 INTRODUCTION

Since 1970's, advances in watershed mathematical modeling occurred at an unprecedented pace and were triggered by the digital revolution in both fields of numerical and statistical analysis (Singh and Woolhiser, 2002). Following the rapid growth in computational power, systematic efforts within the research community have largely improved the capability of mathematical models and paved the way to their use in most water resources and engineering applications, also, more specifically in flood modelling applications (Teng et al., 2017). Nowadays, a plethora of mathematical models, namely, rainfall-runoff and hydraulic models, are now available that vary in complexity from simple empirical or black box models with few parameters to complex physically based, distributed models with many parameters. Although physically based distributed models are gaining favor to better represent the physical processes within the catchment, their practical application depends on addressing their specific weaknesses, which include heavy computational requirements, large number of parameters to evaluate, and lengthy training periods (Bathurst and O'Connell, 1992). Hence, the discussion on the wise selection of the modelling approach which balances modelling objectives with model complexity and data availability has become a topic of an increasing scientific interest (Bergstrm et al., 2002; Grayson and Blöschl, 2001; Neal et al., 2012b).

Till now there is no common base for comparing different modelling approaches based on measuring or quantifying model complexity, data availability and performance. Many studies compared and benchmarked various models and algorithms, but most were based on comparing models based on their structure or their representation of processes. Also, developers compared their models with one or few other popular models in literature (Singh and Woolhiser, 2002). Grayson and Blöschl (2001) described the trade-off between model complexity and the prediction performance for given conditions of data availability (Figure 1). The authors show that for a given condition of data availability there is an optimum model complexity that corresponds to the highest model performance beyond which additional complexity induces identifiability problems and reduces the performance. In this case complex models require an increasing number of data to reach adequate reliability. Perhaps, these illustrated conceptual relations between data, models, and performance can form the basis for

assessing or comparing different modelling approaches of variable complexities, however, there arises a need to develop metrics that are able to quantify these three components of the modelling problem. In this paper we define metrics in order to characterize and quantify the three axes data availability, model complexity and prediction performance. Quantifying the three axis allows assessing the cost-effectiveness of the approach

In this context, and in response to the significant number of reported flood events that is increasing at an alarming rate, development and application of flood inundation models has become a major challenge in hydrologic and hydraulic studies over the last years. Flood inundation models have become a prerequisite for various applications, these include but not limited to, real-time flood forecasting (e.g. Liu et al., 2005; Schumann et al., 2013), flood damage assessment and risk mapping (Abdallah and Hdeib, 2015; Apel et al., 2006; Merz et al., 2008, 2010), flood hazard mapping (Aronica et al., 2012; Kvočka et al., 2016), along with other applications related to catchment hydrology, river bank erosion, sediment transport, and contaminant transport.

The scientific literature is replete with various modelling approaches applied for flood inundation modelling that vary in complexity and in concept these include: 1. application of different empirical methods such as measurements, surveys and remote sensing or statistical approaches (Gaume and Borga, 2008; Horritt et al., 2001; Schumann et al., 2009). 2. single application of a hydraulic model to simulate flood propagation by solving physical equations of flow dynamics of variable complexity, i.e. in a one-dimensional (1D), two-dimensional (2D) or three-dimensional (3D) approach (Dimitriadis et al., 2016; Neal et al., 2012a). 3. application of simplified conceptual models that do not solve the physical equations of flow dynamics but are based on simplified hydraulic concepts (Lhomme et al., 2009). An overview of the first three approaches is provided by Teng et al. (2017). 4. applications limited to hydrologic models, mostly rainfall-runoff, to estimate rainfall excess, overland flows and river flood discharges (Coustau et al., 2012; Dutta et al., 2000; Khan et al., 2009; Sharif et al., 2010), these models vary in complexity from empirical and lumped conceptual models to fully distributed physically based models that simulate surface, sub-surface and groundwater flow processes. 5. applications that involve coupling hydrologic and hydraulic models , that is mainly applied to estimate flood flows in different locations specially when information on the flood characteristics are lacking (Bonnifait et al., 2009; Hdeib et al., 2018; Lerat et al., 2012), or as part of a flood forecast system where rainfall-runoff models are fed by rainfall forecasts to obtain different realizations of runoff (Pappenberger et al., 2005). Finally, 6. Applications based on geomorphic approaches to delineate flood prone areas by using simplified methods that rely on basin geomorphologic feature characterization (Manfreda et al., 2014; Samela et al., 2017), such applications were found to be successful in large-scale applications of data-sparse regions. These applications largely differ in terms of type of input data required,

computational efficiency and the nature of output variables, their resolution and accuracy. For practical applications, the major challenge that awaits the modeler is the proper selection of the most efficient low-cost flood modelling approach that balances the data available with model complexity based on defined modelling objective.

One possible method for comparing different modelling approaches is a cost analysis approach. This approach is a form of economic analysis that compares the relative costs and outcomes of different courses of action and help decide if an application is worth the costs by understanding the benefits or effects of pursuing it. One common form of such approaches is the “cost-effectiveness analysis”. The concept is used in many fields, such as pharmacoeconomics and energy efficiency investments, and refers to analyses that examine the ratio of the cost of a particular intervention to a chosen unit of effectiveness of non-monetary value (Zilberberg and Shorr, 2010). Unlike cost-benefit analysis where costs and outcomes are presented in monetary values (Bleichrodt and Quiggin, 1999).

In this paper we present the proposed cost-performance grid in part two and describe the criteria selected for the costs and performance evaluation. In part three we present an application on the proposed grid to demonstrate the methodology employed to apply the grid. Part four presents the results and then follows a discussion on the opportunities and the limitations of the proposed grid in part five. The paper ends with a general conclusion and opens the door for future research applications of the grid.

2 METHODOLOGY

The choice of the modeling approach is largely governed by three main factors: the nature of the prototype system or study site, the objective of modeling, and the nature of input and output data. The adequate definition of the problem, modelling objective, is the primary step towards the successful application of the modeling approach (Dooge, 1981). Once the modelling objective is defined, numerous combinations of data, models and performance criteria are possible. Other factors may also affect the choice of the modeling approach these include the type and quality of available observational data, country of application, modeler capabilities and experience, type of the flood event (low or extreme event), size/scale of the study site, year of application, etc. Based on the wide variety of models available, many model configurations are possible. Therefore, we introduce a cost-performance grid for comparing flood modelling approaches, we define several categories for defining the modelling costs and assessing their performance.

We define a “simple model” by the model that is able to meet the objective of modeling by reproducing the system behavior efficiently with minimal level of complexity; i.e. based on a

low cost and giving high performance. The choice of selection of this “simple model” depends on balancing the modeling costs with the modeling performance.

The “modelling cost” is a measure of the “data availability” which is the amount and quality of the data used for model simulation, calibration, and validation, and the “model complexity” which is the detail of process representation by the model. In this regard, we hypothesize that the “cost of data” is directly proportional to data availability, and the “cost of models” is directly proportional to model complexity. The more data is available in terms of quantity and quality, the higher is the cost of data. Similarly, the more complex the model is the higher is the cost of the model. The total cost of a modeling approach is therefore a function of the cost of data and the cost of models. The general relationship can be illustrated as follows in Eq. 1 to 3:

$$\text{Cost of data} \propto \text{Data availability} \quad (1)$$

$$\text{Cost of models} \propto \text{Model complexity} \quad (2)$$

$$\text{Cost of modeling} = \mathbf{f}(\text{cost of data, cost of models}) \quad (3)$$

In economics, the total cost of any project or plan is the summation of all costs paid in every stage of the project; the total cost you pay to realize a project is the sum of every penny you pay during the project. The addition of costs here is associative and commutative; the order of paying money in every stage does not change the total cost you pay. In this regard, we suggest that the total cost of a modeling approach is a sum function; it is the direct sum of the cost of data and the cost of models.

We define the measure of data availability as “cost of data”, denoted as $\boldsymbol{C_D}$, and the measure of model complexity as “cost of model”, denoted as $\boldsymbol{C_M}$. The modeling cost denoted as $\boldsymbol{C_T}$ is the sum of the cost of data and cost of models and is a measure of the overall complexity of the modeling approach. The more data is required and the more complex the model is, the higher is the modeling cost. The general relation between the cost of data and cost of models is presented in Eq. 4.

$$C_T = C_D + C_M \quad (4)$$

The “modelling performance”, denoted as $\boldsymbol{P_M}$, is a measure of how well the model is able to reproduce the system behavior, and how much the modeling outcomes fit to observations and satisfy our understanding of the hydrological processes under study.

Figure 2 illustrates the conceptual relationship between the three components of a modelling problem: data availability (X-axis), model complexity (Y-axis) and the prediction performance (Z-axis). Figures 2a and 2b are the projections of Figure in the (X-Z) plane and (Y-Z) plane respectively. In the (X-Z) plane (Fig. 2a), and for a given model complexity, adding more data

increases the model predictive performance up to a level where additional data does not improve the performance of the model because the model is no more able to exploit all the information in the data. This is the best performance a model can give based on its complexity level, adding more complexity to the model can exploit more information in the data and improve performance. Similarly, in the (Y-Z) plane (Fig. 2b), and for a given condition of data availability, additional model complexities lead to better model performance reaching an optimum complexity beyond which identifiability problems arise and reduce the model performance. This is because the more complex model has many parameters but not enough data to be verified and tested for reliability. Perhaps this is the most common problem in modelling exercises where too complex models are being used with limited data availability. Either such too complex models should be avoided and replaced with simpler ones or an increasing number of data is required to reach adequate reliability (Grayson and Blöschl, 2001).

Figure 4 illustrates our suggestion of the conceptual relationship between modeling costs and modeling performance. The performance of the modelling approach increases with the cost of modelling up to a point where the ratio of the performance to costs, performance-cost ratio denoted as ***PC***, is the highest (Eq. 5). Beyond this point adding modelling cost increases the performance at lower rates, up to a level where higher modelling costs does not add any considerable performance and may reduce the prediction performance. In practical applications there is a minimum mandatory cost that should be paid which represents the basic data required to run the model and the minimal model complexity at which a representative model can be developed.

$$PC = \frac{P_M}{C_T} \qquad (5)$$

2.1 The cost of modelling

We define the cost of modeling as the relative cost that encompasses all data utilized (in terms of amount and quality) and resources/models expended (in terms of complexity) to perform the modeling approach. One should distinguish between the relative cost defined here and the actual cost defined in economy as the net amount of money paid to perform the approach. The actual cost (value) is highly variable from one case to another depending on the country of application, availability of data, expertise, and models. It may also differ from one application to another; for example, research centers tend to use their own models that they are familiar with which might be more complex but cheaper if compared to purchasing new modeling software of lower complexity. Whereas, the relative cost is a qualitative measure of the modeling approach that depends on the type, amount and significance of data used and on the complexity of model applied despite the real amount of money paid.

To evaluate the total cost of modeling, we define certain metrics to evaluate the cost of data and cost of models. Figure 4 presents a schematic diagram developed to evaluate such values.

Data and models are categorized into main categories and subcategories based on data types and model representations. Quantitative or qualitative evaluation criteria are defined for each subcategory to calculate its cost. For the cost evaluation we suggest incorporating a “weighted sum model”. The weighted sum model is the best known and simplest multi-criteria decision model often used for multicriteria decision making projects. i.e. for evaluating a number of alternatives in terms of a number of decision criteria that may influence the choice or decision. The reason for selecting this model is primarily because the total cost is a sum function, as demonstrated before, and secondly to give some elements more "weight" or influence on the result than other elements in the same category or subcategory. This is because some evaluation criteria are more significant than the others and are thought to more impact the quality of data or complexity of models. Say for example, for an event-based flood modeling approach, the spatial or temporal scale of the hydrometeorological data are more significant than the duration of data available, and hence those evaluation criteria (spatial and temporal scale) should be associated with higher weights compared to the other evaluation criterion (duration).

For this reason and to emphasize on the significance of some evaluation criteria with respect to the others, weights, denoted as ***w***, are given to each evaluation criteria. Higher weights imply more significant evaluation criteria. Similarly, within the same category, some subcategories are more significant than the others, and accordingly global weights, denoted as ***gw***, are given to each subcategory.

Indeed, the cost of modeling cannot be presented in monetary values, because some of the cost evaluation criteria are qualitative measures that cannot be compared or summed up together. For this reason, we choose to calculate the cost of each evaluation criteria based on a scoring system, i.e. the cost of the evaluation criteria is defined on a scale of scores, denoted as ***f***, higher score refers to a more expensive measure which is mostly a more complex measure. This is similar to the grading system used in universities and schools to evaluate the total mark of a student. In a subject exam (here a sub-category), each question (here evaluation criterion) is given a certain grade (here score), and the total mark in an exam (here cost of sub-category) is the sum of grades of all questions. Also, the total mark of a student (here total cost of modeling) is the weighted sum of all grades given for each subject. The weighted sum is applied to emphasize on the importance of one subject with respect to the others.

Moreover, one should mention that the grading system is variable from one country to another or from an institution to another. This is because each country has its own grading strategy. Say for example the French system suggests a 20-point grading scale. With a grade from 16 to 20 is given an honor “very good” (très bien: TB), and a grade from 0 to 9.9 is considered a “fail” (insuffisant). The American grading system suggests a numerical grading scale from 0 to 100 which is broken down into a letter grade of five levels as well (A, B, C, D and F), with A considered the highest grade and F considered a fail grade.

In our approach several scoring scales would be suggested to evaluate the cost of an evaluation criterion. We propose to calculate the score ***f*** of an evaluation criterion based on a scale of five levels, an approach similar to the US 5 levels grading system. The values of ***f*** range from “Very Low” (VL) indicating the lowest score which corresponds to the lowest cost/quality/quantity to “Very High” (VH) indicating the highest score which corresponds to the highest cost/quality/quantity. “Low” (L) indicates a low score, “Medium” (M) indicates a medium score, and “High” (H) indicates a high score. Similarly, and for simplification, the weights are evaluated in three influence levels: low influence (L), medium influence (M), and high influence (H).

Let ***S*** denote the total cost of a sub-category ***j***, hence the cost S_j of a sub-category ***j*** can be evaluated following Eq. (6):

$$S_j = \sum f_i . w_i \qquad (6)$$

For a given sub-category ***j***, f_i is the score of evaluation criterion ***i*** rated on a scale of five levels {(VL), (L), (M), (H), and (VH)}, ***f*** is zero if the criterion is not applied. w_i is the weight of evaluation criterion ***i*** of value (L), (M), or (H).

Let ***C*** denote the total cost of a category, hence the total cost C_k of a category ***k*** can then be evaluated following Eq. (7):

$$C_k = \sum S_j . gw_j \qquad (7)$$

For a given category ***k***, gw_j is the global weight of sub-category ***j*** of value (L), (M), or (H).

In typical flood modeling approaches we distinguish four main categories, the first category corresponds to the cost of data for hydrological model (C_{D1}), the second category corresponds to the cost of data for hydraulic model (C_{D2}), the third category corresponds to the cost of the hydrological model (C_{M1}), and the fourth category corresponds to the cost of the hydraulic model (C_{M2}). Flood modeling approaches do not necessarily cover the four categories but may for example cover the C_{D1} and C_{M1} categories if the application is solely a hydrological modeling approach. In this case, the cost of the other categories (C_{D2} and C_{M2}) will be zero. In

what follows the hydrological and hydraulic models will be denoted as model 1 and model 2 respectively.

2.1.2 The cost of data

The choice of selection of the models is dictated by the nature and quality of data available and data requirements for modeling. Hydrological and hydraulic models differ largely in terms of data requirements.

In flood inundation modeling approaches that involve a hydrological model, either alone or coupled with a hydraulic model, the most common practice is the application of a rainfall-runoff model to simulate flood producing rainfall events and estimate the flood discharge. Overland flow and channel flow are the major processes simulated by these models. Classically, rainfall is the major input data and runoff is the basic observational data for calibrating and validating the model. With the advance of physically based distributed models, more processes are being represented such as evapotranspiration, sub-surface flow, and ground water flow that require extensive data such as high-resolution digital elevation models, discretization into saturated and unsaturated zones, vegetation cover, soil profiles, etc. The more processes are represented by the model the more are their data requirements.

Data requirements for watershed hydrology modeling were distinguished by Singh and Woolhiser (2002) in six categories: hydrologic data, hydrometeorologic data, geomorphologic data, agricultural data, pedologic data, and geologic data. Hydrologic data includes all hydrological variables such as flow depth, discharge, and base flow. Hydrometeorologic data includes all meteorological variables such as rainfall, snow, humidity and temperature. Geomorphic data represents the topography of the study site in the form of topographic maps or digital elevation models (DEM's). Agricultural (land use and vegetation cover), pedologic (soil information), and geologic (stratigraphy and lithology) data can be grouped in one category named "geographical and background data".

The first two subcategories, hydrologic and hydrometeorologic data, are evaluated following Table 1. Four evaluation criteria are assigned to these two subcategories those include: duration of the dataset, spatial resolution of the data (point gauge data versus spatial measurement), temporal resolution of the data (monthly and daily time step of measurement versus hourly or less time steps), and the completeness or continuity of the dataset (gaped data versus time series).

In the presented evaluation table, we present our suggestion on how to evaluate the scores for each evaluation criteria. For example, for the temporal resolution evaluation criterion, higher scores are associated with finer time steps; a score of (VL) is given for a temporal resolution equal or exceeding a monthly time step, a score of (M) is given to daily time steps, and a

score of (VH) is given to hourly time steps or less. We suggested the daily time step to be in the middle (score “M”) because this is a common case in most countries. Nowadays, daily rainfall measurements are typically recorded by using simple traditional rain gauges and are often available in most countries equipped with monitoring networks.

Moreover, the tables also present our suggestion of the weights associated with each evaluation criterion. For simplification, we choose to present the weights in three levels low (L), medium (M), and high (H). These weights can be understood as the relative influence of each evaluation criterion on the cost with respect to other evaluation criteria in the same sub-category. i.e. evaluation criteria that are thought to have more influence on the cost of a sub-category are given higher weights with respect to the others.

Geomorphic data are evaluated following Table 2. For this sub-category three evaluation criteria were assigned those include: the type of the geomorphic information obtained (topographical maps versus gridded elevation data such as DEM’s), the scale or resolution of the data (coarse resolution in the order of hundreds of meters versus fine resolution in the order of 10 meters), and the availability of the data (whether available, developed, or purchased). The resolution of geomorphic data is associated with the highest weight and the availability of such data is associated with the lowest.

Geographical and background data are evaluated following Table 1S. For this sub-category three evaluation criteria were assigned those include: the number of maps required to build the model (land use map, soil map, geology map, vegetation cover map, etc.), the scale or resolution of the data (large scale versus small scale), and the availability of the data (whether available, developed, or purchased).

From a hydraulic modeling perspective, data requirements for flood inundation modeling have been summarized and discussed several times in literature (Bates, 2004; Mason et al., 2010; Smith et al., 2006), these can be divided into four major sub-categories: topographic data to construct the model grid, time series of bulk flow rates and stage data to provide model inflow and outflow boundary conditions, roughness coefficients of channel and floodplain, and data for model calibration, validation, and assimilation.

Topographic data are evaluated following Table 2S. High accuracy digital elevation models are the major topographic data requirement by hydraulic models to represent the ground surface and overland flow controlling structures. Classically topographic data was obtained either through expensive and time-consuming field surveys in the form of cross sections perpendicular to the channel or by using the available national topographic maps which are often of low accuracy and poor spatial resolution. Nowadays, with the evolution of the remote sensing techniques digital elevation models are obtained for wider areas with higher accuracy compared to national topographic maps. Topographic data is evaluated based on three

criteria: the type of topographic data, the scale or resolution of the data, and the availability of the data. This similar to the geomorphic data of the hydrological model, the only difference is that higher scores are given to the resolution of the data, because hydraulic models require more accurate topographic data than hydrologic models. Hydraulic modeling in rural areas require a DEM accuracy of at least 10 m (Mason et al., 2010), whereas modeling in urban areas require a spatial resolution of 0.5 m to resolve gaps between buildings (Smith et al., 2006).

Roughness data are evaluated following Table 3S. In general, roughness values are preliminarily assigned based on expert knowledge using two separate global coefficients, one for the channel and the other for the floodplain and then it is usually estimated by calibration. However, such calibration results in a compensation for model structural and input flow errors and it is often difficult to disentangle the contribution due to friction from that attributable to compensation (Mason et al., 2010) . Ideally roughness data has to be calculated based on the physical and biological variables of the channel and the floodplain and should reflect the actual spatial variability of friction.

Information on the flood extent and the water levels are important for the calibration and validation of the hydraulic models. Traditionally, mapping the flood extent was done through intensive field surveys directly after the flood event. However, these surveys remain very time consuming and relatively expensive especially for large inundation areas. Nowadays, with the advancement of the remote sensing techniques, flood extent mapping can be obtained from relevant satellite images or through drone/aerial photography surveys, both thought to be cheaper than heavy ground surveys. Classically information on water levels was obtained from stage gauge records or through post-events measurements. Both measurements do not allow to study the spatial variability of water levels and hence may impact the efficiency of the model in reproducing the flood event and flood plains. Today, spatial measurements of water stage can be obtained from satellite images or altimeters. (refer to Table 4S).

2.1.2 The cost of models

The scientific literature agreed on the difficulty of providing a common classification scheme for hydrologic models. Several authors proposed different model classification schemes (Dooge, 1981; Kampf and Burges, 2007; Refsgaard, 1996; Singh and Woolhiser, 2002). Dooge (1981) proposed several classification criteria for mathematical models for 34 papers presented at a previous symposium, Singh and Woolhiser (2002) provided a comprehensive compendium of available catchment models and discussed some data and modeling requirements. Kampf and Burges (2007) reviewed and compared different spatially distributed models and proposed criteria for model comparison based on the model representation of flow processes in time and space. The latter is among the best classification schemes proposed for

hydrological models. We therefore suggest to develop our cost evaluation criteria following the classification proposed by Kampf and Burges (2007) with minor modifications and eliminations for simplification.

Our methodology for cost evaluation of the hydrological model is suggested as follows: The cost is evaluated based on two main sub-categories; model type and model code (procedural model). The model calibration, and uncertainty analysis methods are also thought to impact the complexity of the modeling approach. Although the latter maybe considered as part of the model type, we suggest keeping it in a separate sub-category.

The hydrological model type subcategory is evaluated based on the model representation of water flow pathways in space and time in seven evaluation criteria: spatial scale (single hillslopes versus continental scale), temporal scale (event-based or continuous), number of events (if event-based) or duration (if continuous), nature of basic algorithm (empirical, conceptual, or physically based), spatial representation (lumped, semi-distributed, or distributed), computational time step (time step of model runs, monthly, daily or hourly…), and flow processes represented (overland flow, channel flow, subsurface flow, other processes…). Indeed, several other evaluation criteria may exist such as those related the model parametrization and computational schemes, the user interfaces and the sensitivity analysis packages, but these model features remain peripheral to the core structure configuration. Also having to mention, that for typical flood modeling approaches, hydrological models are mainly meant to reproduce the rainfall-runoff processes and hence do not requires extra complexity. Perhaps these are the major evaluation criteria that may impact the model type and its complexity (Refer to table 3).

There are several studies in literature that compare and benchmark different hydraulic models of variable complexities aiming at the selection of the best model structure for flood inundation modeling (Chatterjee et al., 2008; Dimitriadis et al., 2016; Horritt and Bates, 2002; Liu et al., 2018; Neal et al., 2012b). most studies agree that the nature of flow equations and the spatial representation of the hydraulic model are the basic characteristics that impact the complexity of a hydraulic model. In what follows, the cost/complexity evaluation of the hydraulic model type is based on five evaluation criteria: spatial scale (global versus reach scale), temporal scale (event-based or continuous), number of events (if event-based) or duration (if continuous), flow equations (empirical vs complete Saint-Venant equation), and the model spatial representation (1D, 2D, Quasi 2D, or 3D), with the last two criteria being the key evaluation criteria and hence given the highest weights. Table 4 presents the evaluation criteria for the hydraulic model type.

Another factor that can impact the model cost and complexity is the model code. For instance, building a new model code is much expensive (in terms of time consumed and expertise

employed) than using available and developed model codes. Moreover, purchasing a new modeling software rather than using available freeware would also add costs to the modeling approach. Similarly, the code length may also be an indication of the model complexity. Models of short codes are generally less complex than models of very long codes and algorithms. Hence, the code development and the code length are the two evaluation criteria suggested for the evaluation of the model code for both hydrologic and hydraulic models. Refer to Table 5S for the representation of the evaluation criteria and corresponding scores of cost evaluation.

The model calibration and uncertainty evaluation strategy can also impact the modeling cost and complexity. Although these may be indirectly related to the model type, but we choose to keep them in a separate sub-category because the calibration and uncertainty evaluation strategy can highly influence the model performance. Many authors in literature have pointed at the importance of model calibration and uncertainty evaluation in the model predictions (Aronica et al., 2002; Papaioannou et al., 2017). For simplification, we choose to evaluate the cost of calibration based on the “number of parameters to calibrate”; the more parameters selected for calibration the higher is the modeling cost. For instance, applying an uncalibrated model may be cheaper than applying a simpler model with many parameters and rounds of calibration. Similarly, we choose to reflect the uncertainty evaluation criteria by the “type of input and parameter specification”. Models that do not involve uncertainty evaluation are said to be deterministic models. Some applications involve a stochastic input, others involve stochastic parameters, some are more complex and involve both stochastic input and parameters, and few approaches are performed in an uncertainty evaluation framework. Table 6S presents the evaluation criteria suggested for calculating the calibration and uncertainty analysis costs.

2.2 The performance of modelling

The value and reliability of models affect their performance and efficiency. This is dependent on different factors including the parameter identifiability (uncertainty), the physical process description, and the applicability domain (Brocca et al., 2011) Moreover, the number and type of criteria functions used to evaluate the model are an indication of the performance of the model. Many efforts have been made to compare model outputs with another but model structures differ a lot so that it’s difficult to predict the reason for difference in model performance (Kampf and Burges, 2007).

For model performance evaluation, we suggest that the best model performance is understood in how well the model is able to meet the modeling objective with minimal level of error. i.e. how well the model outputs answer the model problem and fit the real or observed values. In a

typical flood modeling approach, we are concerned in four levels of output: the peak flood discharge value, the flood flow hydrograph, the flood water stages, and the flood inundation extent. The model's performance is measured in what type of output it gives and how efficient is the model in predicting the flows, water levels and extent with minimum error levels. For instance, and when the objective of the modeling is flood inundation mapping, models that can only predict flood peak discharge and hydrographs are considered unsatisfactory and hence are rated less in terms of efficiency. Moreover, in any modeling approach the more the criteria functions utilized to evaluate and validate the model the better are the expected results.

In this approach we choose to evaluate the modeling performance based on a fixed objective; flood inundation map. Hence, the modelling performance can be evaluated following Table 5 based on six evaluation criteria: the type of output obtained, criteria functions used, and the error value for each level of output. i.e. value of the criteria functions to evaluate the peek flow and volume error, hydrograph error, water level error, and flood extent error. The highest weight is given to the type of output, because this plays a big role in assessing the suitability of the applied modeling approach. The method of evaluation of the modeling performance (criteria functions used) is given a moderate weight, and the error levels are given a low weight compared to the previous two evaluation criteria.

3 APPLICATION: DATASETS

We present an application on the proposed cost-performance grid based on ten selected study cases in literature, to demonstrate the methodology employed to calculate the different sections of the grid and to test the efficiency of the proposed grid. Furthermore, we suggest some domains of application of the grid and discuss its opportunities and limitations. In this application we do not intend to evaluate or assess the validity of any modeling approach, we basically aim to demonstrate an application on the proposed grid only. These approaches were analyzed to extract all the data sets used, models applied, and performance levels evaluated. These data and models were then evaluated based on the evaluation criteria presented in the methodology part and the corresponding scores and weights were calculated based on tables 1 to 5 and tables 1S to 6S.

All scores and rates relative to each selected study case were assigned based on our own understanding of the approach, and thus reflect our own point of view and not the main authors' point of view. In our approach several scoring scales would be suggested to evaluate the cost of an evaluation criterion. We propose to calculate the score ***f*** of an evaluation criterion based on a linear scale of five levels, varying from 1 to 5. 1 indicates the lowest cost/quality/quantity (VL) and 5 indicates the highest cost/quality/quantity (VH). Low (L) is 2, medium (M) is 3, and high (H) is 4. Similarly, and for simplification, we propose to assign

weights and global weights values ranging from 1 to 3. 1 indicates low influence (L), 2 indicates medium influence (M), and 3 indicates highest influence (H).

For each evaluation criterion we also calculate the maximum cost which corresponds to the highest possible score **f(max)**. The maximum possible cost for each sub-category denoted as $\mathbf{C_k(max)}$ is then the weighted sum of all maximum costs of evaluation criteria. A dimensionless cost denoted as $\mathbf{C_{k[1]}}$ can then be evaluated following Eq. 8.

$$C_{k[1]} = \frac{C_k}{C_k(\max)}, \qquad 0 < C_{k[1]} \leq 1 \qquad (8)$$

Similarly, the dimensionless cost of data $\mathbf{C_{D[1]}}$, models $\mathbf{C_{M[1]}}$ and the total dimensionless cost $\mathbf{C_{T[1]}}$ can be calculated following Eq. 9 to 11.

$$C_{D[1]} = \frac{C_D}{C_D(\max)}, \qquad 0 < C_{D[1]} \leq 1 \qquad (9)$$

$$C_{M[1]} = \frac{C_M}{C_M(\max)}, \qquad 0 < C_{M[1]} \leq 1 \qquad (10)$$

$$C_{T[1]} = \frac{C_T}{C_T(\max)}, \qquad 0 < C_{T[1]} \leq 1 \qquad (11)$$

Where $\mathbf{C_D(max)}$, $\mathbf{C_M(max)}$, and $\mathbf{C_T(max)}$ are the maximum costs of data, models, and the total maximum cost of modeling.

A maximum performance value, denoted as $\mathbf{P_M(max)}$, is also calculated by assigning the maximum possible score for each evaluation criterion. And the dimensionless performance value, denoted as $\mathbf{P_{M[1]}}$ can be calculated following Eq. 12.

$$P_{M[1]} = \frac{P_M}{P_M(\max)}, \qquad 0 < P_{M[1]} \leq 1 \qquad (12)$$

The reason behind evaluating these dimensionless values, is to simplify the comparison between different study cases and to interpret the cost levels and performance values obtained.

The selected cases belong to the flood modeling categories 1, 2, 4 and 5. There is no main reason for this selection but because our first intention was to choose flood modeling categories that apply models similar to our approach suggested in (Hdeib et al., 2018). The study is primarily limited to 10 study cases to test the applicability of the proposed grid. However, an online survey is designed and shared with colleagues working in the same field

aiming at collecting information on their modelling approaches. The survey is just launched and will remain open to obtain a sufficient number of study cases for future assessments.

The selected study cases for analysis are presented in Table 6. Five study cases are model coupling approaches (study cases 1, 3, 7, 8, and 9) that belong to category 5. Three are hydrological modeling approaches that belong to category 4 (study cases 5, 6, and 10), one is a hydraulic modeling approach that belong to category 2 (study case 4), and the last is an empirical approach that belong to category 1 (study case 2). Among these study cases three are our own studies (Study case 1, 2, and 5) and hence we are familiar with all the data and models employed. Study case 1 (Hdeib et al., 2018) involves developing a framework for modeling in data-sparse regions. The Study is applied on the Awali river basin in Lebanon (301 km^2), it involves a coupling between a semi-distributed conceptual hydrological model (HEC-HMS) and a 1D hydraulic model (HEC-RAS) to model extreme flood events (category 5). The hydrological model is constrained by 12 past storm events and the hydraulic model is simulated based on different realizations of flood flow hydrographs established based on Monte Carlo uncertainty analysis for the hydrological part. The basic data available are daily rainfall at seven ground gauges, hourly water level measurements at two river gauges, and a fine resolution DEM (10 cm) for the river channel and flood plain based on UAV drone surveys.

Study case 2 (Abdallah et al., 2013) is also applied in the Awali River basin in Lebanon, it involves an empirical approach (category 1) to estimate the flood discharge based on Fuller empirical formula (Salajegheh and Dastorani, 2006) and a 1D hydraulic model (HEC-RAS) to estimate water levels. The approach is deterministic, and the basic available data are daily flow values and post-event measurements at gauge location.

Study case 5 (Moussa, 1991) is a hydrological modeling approach (category 4) applied on the Gardon River in France (542 km^2). It involves developing a new distributed event-based hydrological model based on simplified physical concepts to simulate river flow and establish flow hydrographs. The approach is deterministic, and the model is calibrated based on 30 past storm events. Basic data available are hourly rainfall at seven ground gauges and hourly discharge measurements at two river gauges.

Study case 3 (Knebl et al., 2005) is a flood modeling approach applied on the San Antonio River Basin in Central Texas (10,000 km^2). It involves coupling (category 5) an event-based distributed conceptual hydrological model (HEC-HMS, SCS-CN +Modclark) with a 1D hydraulic model (HEC-RAS) to establish flood inundation maps. The approach is deterministic, and watershed parameters are calibrated manually to produce a good simulation of discharge at 12 sub-basins. The basic data available are NEXRAD Level III radar rainfall (4x4km), hourly

stream flow and water level measurements at 12 USGS river gauges, and Landsat TM images for flood extent evaluation.

Study case 4 (Neal et al., 2012a) is a hydraulic modeling approach (category 2) for simulating the spatially distributed dynamics of water surface elevation, wave speed, and inundation extent over large data sparse domains. The approach is applied on the Niger River in Mali (210,389 km^2). The numerical scheme is based on an extension of the distributed hydraulic model LISFLOOD-FP to include a subgrid-scale representation of channelized flows (2D/1D model), which allows river channels with any width below that of the grid resolution to be simulated. The approach is deterministic, and the model is continuous simulated for 8 years. Basic data available are an SRTM 90m DEM modified to a 905 m DEM and daily discharge values for 8 years. The model is calibrated based on open source 24 Landsat TM5 images for flood extent mapping, and 127 observations of water level from ICESat laser altimeter at 18 locations.

Study case 6 (Coustau et al., 2012) is a hydrological modeling approach (category 4) to establish flood flow hydrographs applied on the Lez River catchment in Montpellier, France (114 km^2). It involves applying an event-based distributed conceptual hydrological model available within the ATHYS modeling platform (modified SCS + linear lag and route). The approach is deterministic, and the model is calibrated based on 21 past-storm events and water levels from 12 piezometers at hourly time step (2000,2008). The basic data available are hourly radar rainfall (1 km^2).

Study case 7 (Koutroulis and Tsanis, 2010) is a flood modeling approach for poorly gauged basins applied on the Giofiros basin in Greece (158 km^2). The approach involves coupling an event-based semi-distributed conceptual hydrological model (HEC-HMS) and a 1D hydraulic model (HEC-RAS) to model flood events (category 5). The hydrological model is calibrated based on 8 past storm events and uncertainty analysis was performed on the input rainfall and on the hydrologic parameters by adding a percent of variation +/- 10%. The hydraulic model is simulated based on different realizations of the flow hydrograph obtained from the hydrological model. The basic data available are daily rainfall measurements from 4 ground gauges, hourly flow measurements at one river stage, available DTM (1/10,000), and post-event field measurements at river gauge location.

Study case 8 (Fuentes-Andino et al., 2017) is a flood modeling approach for ungauged basins with uncertainty analysis within a GLUE framework applied on the floodplain of Tegucigalpa in Honduras (811 km^2). The approach involves coupling (category 5) an event-based distributed physically based hydrological model (TOPMODEL + Muskingum–Cunge–Todini routing) with a 2D/1D hydraulic model (LISFLOOD-FP with subgrid scale). The basic data available are hourly rainfall records for two days from two ground gauges assumed uniformly distributed

over the whole area, a LIDAR DTM (15 cm), and around 100 post-event measurements of high water marks along the river channel at 100m spacing.

Study case 9 (Montanari et al., 2009) is a model coupling approach for flood modeling (category 5) basically performed for the objective of estimation of antecedent moisture condition from volume of runoff, applied on the Alzette River in the Grand Duchy of Luxembourg (356 km^2). The approach involves coupling an event-based lumped conceptual hydrological model Nash IUH (model developed by Nash (1960); n linear reservoirs of K storage + IUH routing) with a 1D hydraulic model (HEC-RAS). Basic data available are water level values (15 min time step) from 6 stream gauges, rainfall records (15 min time step) from one ground gauge, a LIDAR DEM (2m) with 200 bathymetric cross sections. Model calibration was performed based on Monte Carlo sampling of parameters within intervals of plausible values. The results are evaluated with 84 flood extent marks by GPS, maximum water level measurements at 7 points using a theodolite, and two SAR images (ERS-2 & ENVISAT).

Study case 10 (Liu et al., 2005) is a hydrological modeling approach (category 4) for the purpose of flood forecasting applied to Upper Xixian catchment in Huaihe River, China (10,000 km^2). The approach involves applying a new version of a continuous fully distributed physically based hydrological model (TOPKAPI) that evaluates the runoff depth in each model cell. The approach is deterministic, and the basic data available are rainfall and evapotranspiration records for 1.5 years from 24 rain gauges and 1 evaporation station (6 hr. time step), open source USGS DEM (GTOPO30, 1000m), open source soil texture data (global soils dataset of Reynolds et al. (1999), 10km), and landuse (UMD land cover map of the world, 1 km). the model has around 27 parameters to calibrate, calibration was performed for the first six months period and was chiefly based upon moderate variations of parameter values from those estimated on physical grounds, as in common traditional calibration. The author later assesses four parameter uncertainties by estimating a posterior parameter probability density via Bayesian inference. But here we only choose the first approach for our analysis because we find it more significant.

4 RESULTS

All costs of data and models and performance levels corresponding to the different study cases were evaluated. Detailed results of the cost-performance analysis for the selected study cases are presented in Table 7. Performance levels ranged between 0.33 and 0.82 (dimensionless, 1 indicates maximum possible performance) with study case 9 recording the highest performance level and study case 2 recording the lowest. The total cost of modelling levels ranged between 0.19 and 0.46 (similarly dimensionless, 1 indicates the maximum possible cost) with study case 3 recording the highest modeling cost and study case 2

recording the lowest. The performance-cost ratio ranged between 0.9 and 3.01 with study case 5 recording the lowest performance-cost ratio and study case 4 recording the highest. For the selected ten events, the average total cost of modeling was 0.36 and the average performance level was 0.59. The average cost of data was around 0.23 and the average cost of models was 0.47.

Figure presents the distribution of costs of data and models and the corresponding performances for different categories of modeling. Study case 2 which is an empirical approach is associated with the lowest cost of modelling and the lowest performance ($C_{T[1]}$ and $P_{M[1]}$ are 0.19 and 0.33 respectively), this is not surprising because this is an empirical approach and the only data required are average flow values, estimation of global manning's coefficients, and simple post-event measurements at the river gauge location for validation which minimizes the costs of data and models. Similarly, the low performance value is because the approach only allows the estimation of the flood discharge and water levels at one location (river gauge) and do not allow the spatial validation of the flood inundation.

Study case 8 which is a model coupling approach is associated with the highest cost of models ($C_{M[1]}$ is 0.69), this is because the approach couples two relatively complex models; a distributed physically based hydrological model and a 2D/1D hydraulic model. The whole modeling approach is performed in an uncertainty analysis framework which increases the computational costs. The uncertainty analysis was performed to compensate the lack of observational data to calibrate and validate the models.

Generally, the model coupling approaches (study cases 1, 3, 7, 8 and 9) record the highest cost of models, this is not surprising because compared to other approaches, the model coupling uses two models instead of one, which elevates the model cost. However, study case 5 which is a hydrologic modeling approach also record a high cost of models, this is because the approach uses a new tailor-made hydrological model which elevates the cost of models compared to using available open source models.

The results of the cost-performance analysis are further presented on the graphs below. The total cost of modelling ($\mathbf{C_{T\,[1]}}$) versus the performance of the modelling approach ($\mathbf{P_{M\,[1]}}$) is plotted in Figure 6, the cost of data ($\mathbf{C_{D\,[1]}}$) versus the performance of modelling ($\mathbf{P_{M\,[1]}}$) is plotted in Figure 1S, the cost of models ($\mathbf{C_{M\,[1]}}$) versus the performance of modelling ($\mathbf{P_{M\,[1]}}$) is plotted in Figure 2S, the cost of models ($\mathbf{C_{M\,[1]}}$) versus the cost of data ($\mathbf{C_{D\,[1]}}$) is plotted in Figure 3S.

The graph of Figure 6 presents the general relation between the modeling costs and the modeling performance. The general trend of the presented study cases (dotted blue line), in what follows is called cost-performance curve, is consistent with the suggested conceptual relationship between modelling cost and modelling performance presented in Figure 3. Six

study cases are situated above the cost-performance curve with performance levels ranging between 0.6 and 0.82, and modeling cost levels ranging between 0.27 and 0.46. These correspond to the five model coupling approaches and to the hydraulic (2D/1D) modeling approach. The rest four study cases are hydrologic modeling approaches and empirical approaches, these are situated below the trend line with performance levels ranging between 0.33 and 0.51, and cost levels ranging between 0.19 and 0.42.

The general plot of the modeling costs versus the modeling performance for the selected events allows us to distinguish four major zones presented in Figure 7, these are a preliminary proposition for the localization of different modeling approaches on the cost-performance diagram based on the evaluated study cases.

The first zone comprises the model coupling approaches (category 5) and located on the top right corner of the cost-performance diagram. The zone is located above the falling lump of the cost-performance curve. For this zone modeling cost levels approximately range between 0.35 and 0.5, and modeling performance levels approximately range between 0.55 and 0.85. Higher performance levels are associated with lower modeling costs and vice-versa.

The second zone comprises the hydrologic modeling approaches (category 4) and located on the lower right corner of the cost-performance diagram. The zone is located below the falling lump of the cost-performance curve. For this zone modeling cost levels approximately range between 0.3 and 0.5, and modeling performance levels approximately range between 0.3 and 0.55. Higher performance levels are associated with lower modeling costs and vice-versa.

The third zone comprises the hydraulic modeling approaches (category 2) and located on the upper left corner of the cost-performance diagram. The zone is located above the rising lump of the cost-performance curve. For this zone modeling cost levels approximately range between 0.2 and 0.35, and modeling performance levels approximately range between 0.6 and 0.85. Higher performance levels are associated with higher modeling costs and vice-versa.

The fourth zone comprises the empirical or statistical modeling approaches (category 1) and located on the lower left corner of the cost-performance diagram. The zone is located below the rising lump of the cost-performance curve. For this zone modeling cost levels approximately range between 0.17 and 0.3, and modeling performance levels approximately range between 0.2 and 0.5. Higher performance levels are associated with higher modeling costs and vice-versa.

The proposed zones are not fixed and may be modified based on further analysis based on additional study cases. These are preliminarily marked based on the selected study cases but

are thought to be beneficial in highlighting the general localization of different modeling approaches.

4.1 Sensitivity of the grid to the selection of weights

We have proposed the weight levels for different evaluation criteria and for different sub-categories based on three influence levels (high, medium and low). However, these weights are assigned based on our own expert knowledge and may be variable from one author to another based on his point of view and his own understanding of the approach. In this part we present a sensitivity analysis on the proposed weights and global weights for the cost-performance analysis. In this application we suppose that no weights are associated with the different evaluation criteria and subcategories, and hence all evaluation criteria and subcategories have the same weights or influence levels. i.e. all weights and global weights are considered 1.

The results of the cost-performance application are presented in Table 7S. The total cost of modeling varies from 0.23 to 0.48, and the performance varies from 0.2 to 0.77. the major observation is that the cost and performance levels are now much closer to each other, but the cost and performance level distribution is still proportional. i.e. study cases recording highest performance did not change, similarly those recording highest cost, lowest cost and lowest performance did not change as well.

The total cost of modeling $C_{T[1]}$ is plotted versus the performance of the modeling $P_{M[1]}$ are plotted in Figure 8. The study cases distribution over the cost-performance diagram is still similar to the previous diagram of Figure 7 with slight modification in the cost and performance levels. The cost-performance curve is more convex, i.e. the slope of the rising and falling lumps is higher. The same four zoning can be delineated; the right two zones corresponding to the coupling and hydrologic approaches are slightly more inclined, whereas the left two zones corresponding to hydraulic and empirical approaches are still maintained. Study case 3 is now localized below the cost-performance curve whereas it was above before.

4.2 Sensitivity of the grid to the selection of scores

In this application we propose to calculate the score ***f*** of an evaluation criterion based on a linear scale of five levels, varying from 1 to 5. 1 indicates the lowest cost/quality/quantity (VL) and 5 indicates the highest cost/quality/quantity (VH). However, different scoring scales might be proposed. To analyze the sensitivity of the cost-performance grid to the selection of the scoring scale, we perform a sensitivity analysis by proposing a logarithmic scale (non-linear scale) based on five levels ranging from 1 to 10,000 (***f*** values are 1, 10, 100, 1000, and

10,000). 1 indicates the lowest cost/quality/quantity (VL) and 10,000 indicates the highest cost/quality/quantity (VH).

The results of the sensitivity analysis are presented in Table 8S. The total cost of modeling varies from 0.23 to 0.48, and the performance varies from 0.2 to 0.77. The major observation here is that the cost and performance levels are now much dispersed, i.e. study cases recording highest and lowest performance levels are now very far from other study cases. What was high is now much higher, what was low is now much lower, and everything else is in the middle. The cost-performance curve is not well defined, looking flat a little bit. Zoning cannot be performed because most of the study cases are in the middle. Moreover, the selection of the scores was not flexible, i.e. a score between 100 and 1000 (which is considered 3.5 in the linear scale application) was not easily assigned.

Generally, the logarithmic scale level of scores is not applicable in the cost-performance analysis, because it gives more importance to study cases recording higher scores, and neglects those of lower scores. Which does not allow the proper comparison between study cases. The linear scale is more representative.

5 DISCUSSION

5.1 Sensitivity of the grid to the point of view of the author

Regardless of the scoring scale applied, although we propose to be a linear 5 levels scale, variable scores maybe assigned to the same datasets or models based on the user's/author's point of view. In the presented application we assign scores based on our understanding of the approach and on our personal point of view, however, the study cases may be evaluated differently by the original authors. This is because several factors may affect the scoring process; these may include the year of application, country of application, size/scale of the study site, level of expertise employed, and type of the flood event (low vs extreme event or flash flood vs overbank flooding).

For example, in developing countries where the monitoring networks are still limited to traditional rain gauges and river stages, the "daily" measurement time step is the most common measurement time step and would be given a moderate score ("M", here 3). In more developed countries where the monitoring networks are based on the recent advances of technology (e.g. radar measurements), the "hourly" measurement time step is very common and would be given a moderate score ("M", here 3) whereas the "daily" time step would be given a low or very low score ("VL", here 1). For this reason, in our approach we choose an intermediate scoring level that can fit industrialized countries as well as the very developing

countries. In general, this does not contradict with the freedom to adjust the scoring if the grid is to be applied for example solely in an industrialized country.

The same applies for the year of application; modeling approaches that were performed in the 80's and 90's would be associated with low data costs but in fact they would have had higher data costs, because the spatio-temporal scale of data measurements was coarser in the past. For example, data measurements of "daily" time step would have been given higher scores in the past compared to the current application. Similarly models that were considered complex in the past would be now considered less complex. For example, semi-distributed models would have been given higher scores in the past when compared to current application. For this purpose, we consider the grid applicable based on the current conditions of data availability and current model complexities. Therefore, the grid should be updated in future to incorporate new advances in data measurements and model capabilities and hence scores are updated accordingly.

The size or scale of the study site plays a role in the score selection. For example, a DEM of 100 m resolution would be scored higher when applied in a large study area (say for example 10,000 km^2) than in a small study area (say for example 100 km^2). In the proposed grid the scoring of the DEM resolution is selected based on the average required DEM resolution for hydrological modeling and hydraulic modeling separately regardless of the scale of the study site.

The approach is also sensitive to the level of expertise of the modeler himself. A modeler expert in a certain model would consider it less complex even when compared with a really less complex model but of no experience with. The proposed grid evaluates the cost of models (model complexity) regardless of the level of expertise of the modeler but based on the basic model features (spatial representation, temporal representation, flow equations…). Perhaps, the availability of the model (open source vs developed or purchased) would be the most sensitive evaluation criterion.

The selection of scores may differ based on the type of the flood event. For example, in flash flood events finer spatio-temporal scales are required. Hence an "hourly" time step of measurement in flash flood modeling may be assigned less score if compared to an overbank flood event where higher scores are assigned to hourly time step of measurement. In general, scores are assigned in a way acceptable for different types of flood events, but the score values can be tuned to fit the type of flood event under study.

5.2 Sensitivity of the grid to the objective of the modeling approach

The objective of the modeling approach highly impacts the categorization of data and models, and accordingly impacts the selection of the criteria functions for cost and performance evaluation. Similarly, the objective of modeling also impacts the selection of the scores and weights for cost and performance evaluation.

For the proposed grid, data and models are categorized based on the flood modeling objective. If the grid is to be applied for other modeling objectives (say for example water budget evaluation) the data and model categorization would differ. The cost of data for hydraulic modeling would be eliminated, similarly the hydraulic model evaluation will also be eliminated. More attention will be paid to the hydrological model evaluation, probably hydrological and hydrometeorological data will be further subdivided (evaporation, snow melt, infiltration, ground water…). Similarly, more evaluation criteria will be added to the hydrological model costing (e.g. number of model layers, the simulation of the water movement through the subsurface, etc.).

For the purpose of flood modeling, the modeling objective may also differ. Some approaches intend to estimate the peak flood discharge only, others intend to estimate the flood flow hydrograph, others are performed for the objective of estimation of water levels, and some are performed for the objective of full flood inundation mapping. The performance evaluation is highly sensitive to the above mentioned objectives. If the objective is the flood flow hydrograph simulation, several study cases would have obtained higher performance levels, particularly the hydrological modeling approaches (study cases 5, 6, and 10). Having to mention that these objectives are nested; if a modeling approach evaluates the flood flow hydrograph it definitely evaluates the peak flood discharge. Therefore, the smaller the objective of the modeling (say for example estimation of the peak flood discharge) the more study cases obtain high performance levels. In the proposed cost-performance grid we choose to fix the objective of modelling to mapping the flood inundation area. This is because mapping the inundation area is the most complicated objective among the other objectives and it’s the current goal of most flood modeling approaches. However, the grid is flexible to be adjusted for another modeling objectives, this can be done simply by adjusting the scores of the modeling outcomes and the error levels.

The objective of modeling may also change with time and hence performance levels would also differ. Modeling approaches that were performed in the past, for example in the 80’s and 90’s, would be associated with higher performance levels if the grid was applied in the past. For example, if the grid was applied in the 90’s, study case 5 would have obtained higher performance level compared to the current application. In the past obtaining a flood flow hydrograph with good performance level was considered satisfactory in flood modeling

applications, whereas nowadays models are expected to efficiently delineate the whole floodplain extent. Similarly, with the advances of the flood modeling techniques more modeling objectives would be possible and hence the grid should be adjusted to cover any new objective.

5.3 The use of the grid from an operational point of view

After presenting the cost-performance methodology and after giving an application to illustrate the methodology employed to apply the grid. The question arises on the real benefit of applying such grid from an operational point of view. i.e. what is the scientific use of this grid and what is the interest behind applying such methodology?

The proposed grid is a new tailor-made cost-performance grid. We are not aware of any similar grid before. The grid allows for the same time plotting different flood modeling approaches on one graph based on a unified scale. It also allows for the first time comparing different modeling approaches in terms of modeling costs and modeling performance. Evaluating the relative position of different modeling approaches on the cost-performance diagram allows us to classify the approaches into categories based on their cost and performance levels. Perhaps comparing and classifying modeling approaches is the first step towards the proper selection of the best modeling methodology for a defined modeling objective and based on available data and models. Hence, the proposed grid can be a tool that supports the future selection of modeling approaches.

Moreover, plotting any new modeling approach on the cost-performance diagram gives an insight on the relative position of this approach with respect to the others, and may improve our understanding in the applicability or the validity of the proposed approach. Also comparing the relative position of the modeling approaches on the cost-performance diagram allows us to extract any outlier approach (say for example approach of very high cost or very high performance and vice-versa) and analyze the reasons behind this difference in position.

5.4 The use of the grid from a philosophical point of view

From a philosophical point of view, the grid has many applications. The grid supports research evolution studies. It allows studying the historical evolution of flood modeling procedures and study the corresponding evolution of the modeling costs in terms of data costs and model complexities. It also supports statistical studies that aim to evaluate the major types of data utilized for modeling, the average model complexities, and the mostly applied modeling procedures, etc.

The grid is flexible and can be tuned to adapt with different modeling objectives. The grid can be updated with time to follow the recent advances in data measurements and model capabilities. The grid is preliminarily customized to fit to flood modeling approaches, but the same methodology can be employed in many other modeling fields. Hence, the research is still open, and many other applications are expected to be presented in the future. Moreover, additional study cases are expected to be employed to help in the enhancement of the grid.

6 CONCLUSION

In this paper we have presented an application on the proposed cost-performance analysis grid. Ten arbitrability selected study cases were evaluated and plotted on a cost-performance diagram. The average total cost level was 0.36 and the average performance level was 0.59. The average data cost was 0.23 and the average model cost was 0.47. Lowest modeling costs were associated with empirical approaches but however associated with lower performances. Modelling approaches based on open source data were associated with lower costs but high performances especially in well-gauged basins applications. Plotting the study cases on the cost-performance diagram allows us to highlight 4 modeling zones corresponding to 4 modeling categories (empirical (1), hydraulic (2), hydrological (4), and coupling (5)). The zones of the hydraulic modeling and coupling are associated with good performances and are located above the cost-performance curve. The hydraulic modeling zone is associated with lower costs. The zones of the empirical and the hydrological approaches are located below the cost performance curve and are associated with less performance levels because the outcomes of these approaches do not fulfil the objective of flood inundation mapping.

A sensitivity analysis of the grid to the scores and weights shows that the grid is very sensitive to the selected scores scale but less sensitive to the weights' selection. A linear scale of scores of five levels gives better results compared to a logarithmic scale level of scores. The grid is also sensitive to the point of view of the author; the cost levels are mostly sensitive to the year and country of application and the performance levels are mostly sensitive to the objective of the modeling approach.

From an operational point of view, the grid allows to compare different approaches on a unified scale , classify approaches based on cost and performance levels, and choose the best flood modeling approaches for future applications based on defined objectives and available data and models. From a philosophical point of view the grid supports research evolution studies. It allows to study the historical evolution of modeling costs and modeling performances. The grid is flexible and can be tuned to adapt with different modeling objectives and can be periodically updated to follow the recent advances in data measurements and

model capabilities. The research is still open, and many other applications are expected to be presented in the future.

REFERENCES

Abd-el-Al, I.: Ibrahim Aed-El-Al Oeuvres Completes/ Association des Amis de Ibrahim ABD-El-Al., 1996.

Abdallah, C.: Hydrology & Watersheds., 2010.

Abdallah, C.: Assessment of erosion, mass movements and flood risk in Lebanon, in Review and Perspective of Environmental Studies in Lebanon, Chapter X., edited by H. Kouyoumjian and M. Hamze, pp. 225–246, INCAM-EU/CNRS Lebanon., 2012.

Abdallah, C. and Hdeib, R.: Flood Risk Assessment and Mapping for Lebanon-UNDP/CNRS, 93 P.+ANNEX, Lebanon., 2015.

Abdallah, C. and Hdeib, R.: تقييم مفصل حول مخاطر السيول في رأس بعلبك, National Council for Scientific Research, Lebanon., 2018.

Abdallah, C., Chorowicz, J., Bou Kheir, R. and Khawlie, M.: Detecting major terrain parameters relating to mass movements' occurrence using GIS, remote sensing and statistical correlations, case study Lebanon, Remote Sens. Environ., 99(4), 448–461, doi:10.1016/j.rse.2005.09.014, 2005.

Abdallah, C., Hdeib, R., Hijaz, S., Darwish, T. and Merheb, M.: Flood Hazard Mapping Assessment for Lebanon- UNDP/CNRS-2382, 110pp.+ANNEX, Lebanon., 2013.

Abu Al Anin, H.: Essays on the Geomorphology of Lebanon, Beirut Arab University, Beirut., 1973.

Amengual, A., Romero, R., Gómez, M., Martín, A. and Alonso, S.: A Hydrometeorological Modeling Study of a Flash-Flood Event over Catalonia, Spain, J. Hydrometeorol., 8(3), 282–303, doi:10.1175/JHM577.1, 2007.

Apel, H., Thieken, A. H., Merz, B. and Blöschl, G.: A probabilistic modelling system for assessing flood risks, Nat. Hazards, 38(1–2), 79–100, doi:10.1007/s11069-005-8603-7, 2006.

Apel, H., Merz, B. and Thieken, A. H.: Quantification of uncertainties in flood risk assessments, Int. J. River Basin Manag., 6(2), 149–162, doi:10.1080/15715124.2008.9635344, 2008.

Arnold, J. G., Srinivasan, R., Muttiah, R. S. and Williams, J. R.: Large Area Hydrologic Modeling and Assessment Part I: Model Development, J. Am. Water Resour. Assoc., 34(1), 73–89, 1998.

Aronica, G. T., Bates, P. D. and Horritt, M. S.: Assessing the uncertainty in distributed model predictions using observed binary pattern information within GLUE, Hydrol. Process., 16(10), 2001–2016, doi:10.1002/hyp.398, 2002.

Aronica, G. T., Franza, F., Bates, P. D. and Neal, J. C.: Probabilistic evaluation of flood hazard in urban areas using Monte Carlo simulation, Hydrol. Process., 26(26), 3962–3972, doi:10.1002/hyp.8370, 2012.

ASPRS: Manual of photogrammetry / editor, J. Chris McGlone; associate editors, Edward M. Mikhail, James Bethel, 5th ed., edited by E. M. Mikhail, J. S. (James S. Bethel, and J. C. McGlone, American Society of Photogrammetry and Remote Sensing, Bethesda, Md., 2004.

Di Baldassarre, G. and Montanari, A.: Uncertainty in river discharge observations: a quantitative analysis, Hydrol. Earth Syst. Sci., 13, 913–921, doi:10.5194/hessd-6-39-2009, 2009.

Barnolas, M. and Llasat, M. C.: A flood geodatabase and its climatological applications: the case of Catalonia for the last century, Nat. Hazards Earth Syst. Sci., 7(2), 271–281, doi:10.5194/nhess-7-271-2007, 2007.

Barredo, J. I.: Major flood disasters in Europe: 1950-2005, Nat. Hazards, 42(1), 125–148, doi:10.1007/s11069-006-9065-2, 2007.

Bates, P. D.: Remote sensing and flood inundation modelling, Hydrol. Process., 18(13), 2593–2597, doi:10.1002/hyp.5649, 2004.

Bates, P. D.: Integrating remote sensing data with flood inundation models: How far have we got?, Hydrol. Process., 26(16), 2515–2521, doi:10.1002/hyp.9374, 2012.

Bathurst, J. C. and O'Connell, P. E.: Future of distributed modelling: The Systeme Hydrologique Europeen, Hydrol. Process., 6(3), 265–277, doi:10.1002/hyp.3360060304, 1992.

Bergstrm, S., Lindstrm, G. and Pettersson, A.: Multi-variable parameter estimation to increase confidence in hydrological modelling, Hydrol. Process., 16(2), 413–421, doi:10.1002/hyp.332, 2002.

Bernier, M., Fortin, J.-P., Gauthier, Y., Carbane, C., Somma, J. and Dedieu, J. P.: Intégration de données satellitaires à la modélisation hydrologique du Mont Liban, Hydrol. Sci., 48(6), 999–1112, doi:10.1623/hysj.48.6.999.51428, 2003.

Beven, K.: Facets of uncertainty: Epistemic uncertainty, non-stationarity, likelihood, hypothesis testing, and communication, Hydrol. Sci. J., 61(9), 1652–1665, doi:10.1080/02626667.2015.1031761, 2016.

Beven, K. and Binley, A.: The future of distributed models: Model calibration and uncertainty prediction, Hydrol. Process., 6(3), 279–298, doi:10.1002/hyp.3360060305, 1992.

Beydoun, Z. R.: Observations on geomorphology, transportation and distribution of sediments in western Lebanon and its continental shelf and slope regions, Mar. Geol., 21(4), 311–324, doi:10.1016/0025-3227(76)90013-X, 1976.

Biancamaria, S., Bates, P. D., Boone, A. and Mognard, N. M.: Large-scale coupled hydrologic and hydraulic modelling of the Ob river in Siberia, J. Hydrol., 379(1–2), 136–150, doi:10.1016/j.jhydrol.2009.09.054, 2009.

Bleichrodt, H. and Quiggin, J.: Life-cycle preferences over consumption and health: When is cost-effectiveness analysis equivalent to cost-benefit analysis?, J. Health Econ., 18(6), 681–708, doi:10.1016/S0167-6296(99)00014-4, 1999.

Bonnifait, L., Delrieu, G., Lay, M. Le, Boudevillain, B., Masson, A., Belleudy, P., Gaume, E. and Saulnier, G. M.: Distributed hydrologic and hydraulic modelling with radar rainfall input: Reconstruction of the 8-9 September 2002 catastrophic flood event in the Gard region, France, Adv. Water Resour., 32(7), 1077–1089, doi:10.1016/j.advwatres.2009.03.007, 2009.

Borga, M., Gaume, E., Creutin, J. D. and Marchi, L.: Surveying flash floods: gauging the ungauged extremes, Hydrol. Process., 22(18), 3883–3885., doi:10.1002/hyp.7111, 2008.

Le Boursicaud, R., Pénard, L., Hauet, A., Thollet, F. and Le Coz, J.: Gauging extreme floods on YouTube: Application of LSPIV to home movies for the post-event determination of stream discharges, Hydrol. Process., 30(1), 90–105, doi:10.1002/hyp.10532, 2016.

Brandt, S. A.: Modeling and visualizing uncertainties of flood boundary delineation: algorithm for slope and DEM resolution dependencies of 1D hydraulic models, Stoch. Environ. Res. Risk Assess., 30(6), 1677–1690, doi:10.1007/s00477-016-1212-z, 2016.

Brauch, H. G.: Urbanization and Natural Disasters in the Mediterranean : Population Growth and Climate Change in the 21st Century, 2015.

Brázdil, R., Kundzewicz, Z. W. and Benito, G.: Historical hydrology for studying flood risk in Europe, Hydrol. Sci. J., 51(5), 739–764, doi:10.1623/hysj.51.5.739, 2006.

Brocca, L., Melone, F. and Moramarco, T.: Distributed rainfall-runoff modelling for flood frequency estimation and flood forecasting, Hydrol. Process., 25(18), 2801–2813,

doi:10.1002/hyp.8042, 2011.

Casas, A., Benito, G., Thorndycraft, V. R. and Rico, M.: The topographic data source of digital terrain models as a key element in the accuracy of hydraulic flood modelling, Earth Surf. Process. Landforms, 31(4), 444–456, doi:10.1002/esp.1278, 2006.

Castellarin, A.: Probabilistic envelope curves for design flood estimation at ungauged sites, Water Resour. Res., 43(4), 1–12, doi:10.1029/2005WR004384, 2007.

Castellarin, A., Merz, R. and Blöschl, G.: Probabilistic envelope curves for extreme rainfall events, J. Hydrol., 378(3–4), 263–271, doi:10.1016/j.jhydrol.2009.09.030, 2009.

CDR: Schéma d'Aménagement du Territoire Libanais - Rapport Final, , 39–74, 2004.

Chahinian, N., Moussa, R., Andrieux, P. and Voltz, M.: Comparison of infiltration models to simulate flood events at the field scale, J. Hydrol., 306(1–4), 191–214, doi:10.1016/j.jhydrol.2004.09.009, 2005.

Chatterjee, C., Forster, S. and Bronstert, A.: Comparison of hydrodynamic models of different complexities to model floods with emergency storage areas, Hydrol. Process., 22, 4695–4709, doi:10.1002/hyp.7079, 2008.

Cheviron, B. and Moussa, R.: Determinants of modelling choices for 1-D free-surface flow and erosion issues in hydrology: a review, Hydrol. Earth Syst. Sci. Discuss., 12(9), 9091–9155, doi:10.5194/hessd-12-9091-2015, 2015.

Choudhari, K., Panigrahi, B. and Paul, J. C.: Simulation of rainfall-runoff process using HEC-HMS model for Balijore, Int. J. Geomatics Geosci., 5(2), 253–265, doi:Code : EIJGGS5021, 2014.

Cook, A. and Merwade, V.: Effect of topographic data, geometric configuration and modeling approach on flood inundation mapping, J. Hydrol., 377(1–2), 131–142, doi:10.1016/j.jhydrol.2009.08.015, 2009.

Coustau, M., Bouvier, C., Borrell-Estupina, V. and Jourde, H.: Flood modelling with a distributed event-based parsimonious rainfall-runoff model: Case of the karstic Lez river catchment, Nat. Hazards Earth Syst. Sci., 12(4), 1119–1133, doi:10.5194/nhess-12-1119-2012, 2012.

CRED: The human cost of natural disasters, a global perspective. [online] Available from: http://cred.be/sites/default/files/The_Human_Cost_of_Natural_Disasters_CRED.pdf, 2015.

D'Asaro, F. and Grillone, G.: Runoff Curve Number Method in Sicily: CN determination and

analysis of the initial abstraction ratio, 4th Fed. Interag. Conf. Las Vegas, NV, June 27 - July 1, 2010, 1–12, 2010.

Dankers, R. and Feyen, L.: Flood hazard in Europe in an ensemble of regional climate scenarios, J. Geophys. Res. Atmos., 114(16), 1–16, doi:10.1029/2008JD011523, 2009.

Darwish, T., Khawlie, M., Jomaa, I., Abou Daher, M., Awad, M., Masri, M., Shaban, A., Faour, G., Bou Kheir, R., Abdallah, C. and Haddad, T.: Digital Soil Map of Lebanon 1 /50, 000. Monograph Series 4. CNRSLebanon, 2006.

Dimitriadis, P., Tegos, A., Oikonomou, A., Pagana, V., Koukouvinos, A., Mamassis, N., Koutsoyiannis, D. and Efstratiadis, A.: Comparative evaluation of 1D and quasi-2D hydraulic models based on benchmark and real-world applications for uncertainty assessment in flood mapping, J. Hydrol., 534, 478–492, doi:10.1016/j.jhydrol.2016.01.020, 2016.

Dogulu, N., López López, P., Solomatine, D. P., Weerts, A. H. and Shrestha, D. L.: Estimation of predictive hydrologic uncertainty using the quantile regression and UNEEC methods and their comparison on contrasting catchments, Hydrol. Earth Syst. Sci., 19(7), 3181–3201, doi:10.5194/hess-19-3181-2015, 2015.

Domeneghetti, A.: On the use of SRTM and altimetry data for flood modeling in data-sparse regions, Water Resour. Res., 52(4), 2901–2918, doi:10.1002/2015WR017967, 2016.

Domeneghetti, A., Vorogushyn, S., Castellarin, A., Merz, B. and Brath, A.: Probabilistic flood hazard mapping: Effects of uncertain boundary conditions, Hydrol. Earth Syst. Sci., 17(8), 3127–3140, doi:10.5194/hess-17-3127-2013, 2013.

Dooge, J. C. .: IIASA Proceedings Series: Logistics and Benefits of Using Methematical Models of Hydrologic and Water Resource Systems (1978, Pisa) General Report on Model Structure and Classification, edited by A. J. Askew, F. Greco, and J. Kindler, International Institute for Applied Systems Analysis, PERGAMON PRESS., 1981.

Dubertret, L.: Cartes geologiques du Liban a l’echelle de 1 /50 000., 1945.

Dutta, D., Herath, S. and Musiake, K.: Flood inundation simulation in a river basin using a physically based distributed hydrologic model, Hydrol. Process., 14(3), 497–519, doi:10.1002/(SICI)1099-1085(20000228)14:3<497::AID-HYP951>3.0.CO;2-U, 2000.

Efstratiadis, A., Koussis, A. D., Koutsoyiannis, D. and Mamassis, N.: Flood design recipes vs. reality: Can predictions for ungauged basins be trusted?, Nat. Hazards Earth Syst. Sci., 14(6), 1417–1428, doi:10.5194/nhess-14-1417-2014, 2014.

El-Fadel, M., Zeinati, M. and Jamali, D.: Water Resources in Lebanon: Characterization,

Water Balance, and Constraints, Water Resour. Dev., 16(4), 615–638, doi:10.1080/713672540, 2000.

El-Qareh, R.: The submarine springs of Chekka: exploitation of a confined aquifer discharging in the sea. Unpublished M.Sc. Thesis, American University of Beirut, Geology Department, 80p., 1967.

ELARD: FLOOD RISK MANAGEMENT AND PREVENTION IN BAALBACK – HERMEL / Assessment report prepared by Earth Link and Advanced Resources Development S.A.R.L. (ELARD), Beirut, Lebanon., 2010.

Ewen, J. and Parkin, G.: Validation of catchment models for predicting land-use and climate change impacts. 1. Method, J. Hydrol., 175(1), 583–594, doi:10.1016/S0022-1694(96)80026-6, 1996.

Faour, G.: Evaluating urban expansion using remotely-sensed data in Lebanon., Leban. Sci. J., 16(1), 23–32, 2015.

Faour, G. and Mhawej, M.: Mapping Urban Transitions in the Greater Beirut Area Using Different Space Platforms, Land, 3(3), 941–956, doi:10.3390/land3030941, 2014.

Feldman, A.: Hydrologic Modeling System, , (March), 158 [online] Available from: http://www.hec.usace.army.mil/software/hec-hms/documentation.aspx, 2000.

Freer, J., Beven, K. and Ambroise, B.: Bayesian estimation of uncertainty in runoff prediction and the value of data: An application of the GLUE approach, Water Resour. Res., 32(7), 2161–2173, doi:10.1029/96WR03723, 1996.

Fuentes-Andino, D., Beven, K., Halldin, S., Xu, C.-Y., Reynolds, J.-E. and Di Baldassarre, G.: Reproducing an extreme flood with uncertain post-event information, Hydrol. Earth Syst. Sci. Discuss., 21(July), 3597–3618, doi:10.5194/hess-21-3597-2017, 2017.

Fukami, K., Yamaguchi, T., Imamura, H. and Tashiro, Y.: Current status of river discharge observation using non-contact current meter for operational use in Japan, World Environ. Water Resour. Congr., 2008.

Garambois, P. A., Roux, H., Larnier, K., Castaings, W. and Dartus, D.: Characterization of process-oriented hydrologic model behavior with temporal sensitivity analysis for flash floods in Mediterranean catchments, Hydrol. Earth Syst. Sci., 17(6), 2305–2322, doi:10.5194/hess-17-2305-2013, 2013.

Gaume, E.: Post Flash-flood Investigations-Methodological Note. Floodsite European Research Project, Report D23.2. 62pp., 2006.

Gaume, E. and Borga, M.: Post-flood field investigations in upland catchments after major flash floods: proposal of a methodology and illustrations, J. Flood Risk Manag., 1(4), 175–189, doi:10.1111/j.1753-318X.2008.00023.x, 2008.

Gaume, E., Bain, V., Bernardara, P., Newinger, O., Barbuc, M., Bateman, A., Blaškovicová, L., Blöschl, G., Borga, M., Dumitrescu, A., Daliakopoulos, I., Garcia, J., Irimescu, A., Kohnova, S., Koutroulis, A., Marchi, L., Matreata, S., Medina, V., Preciso, E., Sempere-Torres, D., Stancalie, G., Szolgay, J., Tsanis, I., Velasco, D. and Viglione, A.: A compilation of data on European flash floods, J. Hydrol., 367(1–2), 70–78, doi:10.1016/j.jhydrol.2008.12.028, 2009.

Ghattas, I.: The geology and hydrology of the western flexure of Mount Lebanon between Dbaiyeh and Jdaide. Unpublished M.Sc. Thesis, American University of Beirut, Geology Department, 99p., 1975.

Grayson, R. and Blöschl, G.: Spatial Patterns in Catchment Hydrology, Cambridge University Press. [online] Available from: http://www.cup.cam.ac.uk, 2001.

Grayson, R. B., Moore, I. and Mcmahon, T. A.: Physically based hydrologic modeling 2. Is the concept, Water Resour Res, 26(10), 2659–66, 1992.

Gumbel, E. J.: The return period of order statistics, Ann. Inst. Stat. Math, 12(3), 249–256, doi:10.1007/BF01728934, 1961.

Hakim, B.: Recherches hydrologiques et hydrochimiques sur quelques karsts méditerranéens au Liban, en Syrie et au Maroc, Publications de l'Université Libanaise. Section des études géographiques, tome II, 701p., 1985.

Hall, J., Arheimer, B., Borga, M., Brázdil, R., Claps, P., Kiss, A., Kjeldsen, T. R., Kriauciuniene, J., Kundzewicz, Z. W., Lang, M., Llasat, M. C., Macdonald, N., McIntyre, N., Mediero, L., Merz, B., Merz, R., Molnar, P., Montanari, A., Neuhold, C., Parajka, J., Perdigão, R. A. P., Plavcová, L., Rogger, M., Salinas, J. L., Sauquet, E., Schär, C., Szolgay, J., Viglione, A. and Blöschl, G.: Understanding flood regime changes in Europe: A state-of-the-art assessment, Hydrol. Earth Syst. Sci., 18(7), 2735–2772, doi:10.5194/hess-18-2735-2014, 2014.

Halwatura, D. and Najim, M. M. M.: Application of the HEC-HMS model for runoff simulation in a tropical catchment, Environ. Model. Softw., 46, 155–162, doi:10.1016/j.envsoft.2013.03.006, 2013.

Hdeib, R., Abdallah, C., Colin, F., Brocca, L. and Moussa, R.: Constraining coupled hydrological-hydraulic flood model by past storm events and post-event measurements in data-sparse regions, J. Hydrol., 565, 160–176, doi:10.1016/j.jhydrol.2018.08.008, 2018.

Hervouet, J. M.: A high resolution 2-D dam-break model using parallelization, Hydrol.

Process., 14(13), 2211–2230, doi:10.1002/1099-1085(200009)14:13<2211::AID-HYP24>3.0.CO;2-8, 2000.

Horritt, M. S. and Bates, P. D.: Evaluation of 1D and 2D numerical models for predicting river flood inundation, J. Hydrol., 268(1–4), 87–99, doi:10.1016/S0022-1694(02)00121-X, 2002.

Horritt, M. S., Mason, D. C. and Luckman, A. J.: Flood boundary delineation from synthetic aperture radar imagery using a statistical active contour model, Int. J. Remote Sens., 22(13), 2489–2507, doi:10.1080/01431160116902, 2001.

Horritt, M. S., Bates, P. D., Fewtrell, T. J., Mason, D. C. and Wilson, M. D.: Modelling the hydraulics of the Carlisle 2005 flood event, Proc. Inst. Civ. Eng. - Water Manag., 163(6), 273–281, doi:10.1680/wama.2010.163.6.273, 2010.

Hreiche, A.: Modélisation conceptuelle de la transformation pluie-débit dans le contexte méditerranéen, Universite Montpellier II et Universite Saint-Joseph., 2003.

Huang, M. and Liang, X.: On the assessment of the impact of reducing parameters and identification of parameter uncertainties for a hydrologic model with applications to ungauged basins, J. Hydrol., 320(1–2), 37–61, doi:10.1016/j.jhydrol.2005.07.010, 2006.

Hughes, M. L., McDowell, P. F. and Marcus, W. A.: Accuracy assessment of georectified aerial photographs: Implications for measuring lateral channel movement in a GIS, Geomorphology, 74(1–4), 1–16, doi:10.1016/j.geomorph.2005.07.001, 2006.

Hunter, N. M., Bates, P. D., Horritt, M. S., De Roo, a. P. J. and Werner, M. G. F.: Utility of different data types for calibrating flood inundation models within a GLUE framework, Hydrol. Earth Syst. Sci., 9(4), 412–430, doi:10.5194/hess-9-412-2005, 2005.

Jaber, F. H. and Mohtar, R. H.: Stability and accuracy of two-dimensional kinematic wave overland flow modeling, Adv. Water Resour., 26(11), 1189–1198, doi:10.1016/S0309-1708(03)00102-7, 2003.

Jarihani, A. A., Callow, J. N., McVicar, T. R., Van Niel, T. G. and Larsen, J. R.: Satellite-derived Digital Elevation Model (DEM) selection, preparation and correction for hydrodynamic modelling in large, low-gradient and data-sparse catchments, J. Hydrol., 524, 489–506, doi:10.1016/j.jhydrol.2015.02.049, 2015.

Kabout, K.: Master Thesis: Flood Risk Management in Semi-Arid Areas., Lebanese University, Ecole, Doctoral des Sciences et Technologie. Beirut, Lebanon., 2011.

Kampf, S. K. and Burges, S. J.: A framework for classifying and comparing distributed hillslope and catchment hydrologic models, Water Resour. Res., 43(W05423),

doi:10.1029/2006WR005370, 2007.

Khan, S. I., Hong, Y., Wang, J., Yilmaz, K. K., Gourley, J. J., Adler, R. F., Brakenridge, R. G., Policelli, F., Habib, S. and Irwin, D.: Satellite Remote Sensing and Hydrological Modeling for Flood Inundation Mapping in Lake Victoria Basin : Implications for Hydrologic Prediction in Ungauged Basins, IEEE Trans. Geosci. Remote Sens., 49(1), 1–23, doi:10.1109/TGRS.2010.2057513, 2009.

Khawlie, M.: Hazard mapping: The Abou A'li river flood, Tripoli – Lebanon, In R. Oliveira, L.F. Rodrigues, A.G. Coelho, and A.P. Cunha, (eds.). Proceedings of the Seventh International Congress, 2049-2057. Lisbona, Portugal, 5-9 September., 1994.

Kim, J., Warnock, A., Ivanov, V. Y. and Katopodes, N. D.: Coupled modeling of hydrologic and hydrodynamic processes including overland and channel flow, Adv. Water Resour., 37, 104–126, doi:10.1016/j.advwatres.2011.11.009, 2012.

Knebl, M. R., Yang, Z. L., Hutchison, K. and Maidment, D. R.: Regional scale flood modeling using NEXRAD rainfall, GIS, and HEC-HMS/ RAS: A case study for the San Antonio River Basin Summer 2002 storm event, J. Environ. Manage., 75(4 SPEC. ISS.), 325–336, doi:10.1016/j.jenvman.2004.11.024, 2005.

Koenig, T. A., Bruce, J. L., O'Connor, J. E., McGee, B. D., Holmes, R.R., J., Hollins, R., Forbes, B. T., Kohn, M. S., Schellekens, M. F., Martin, Z. W. and Peppler, M. C.: Identifying and preserving high-water mark data: U.S. Geological Survey Techniques and Methods, book 3, chap. A24., 2016.

Komi, K., Neal, J., Trigg, M. A. and Diekkrüger, B.: Modelling of flood hazard extent in data sparse areas: a case study of the Oti River basin, West Africa, J. Hydrol. Reg. Stud., 10, 122–132, doi:10.1016/j.ejrh.2017.03.001, 2017.

Kömüşcü, A. Ü. and Çelik, S.: Analysis of the Marmara flood in Turkey, 7-10 September 2009: An assessment from hydrometeorological perspective, Nat. Hazards, 66(2), 781–808, doi:10.1007/s11069-012-0521-x, 2013.

Koutroulis, A. G. and Tsanis, I. K.: A method for estimating flash flood peak discharge in a poorly gauged basin: Case study for the 13-14 January 1994 flood, Giofiros basin, Crete, Greece, J. Hydrol., 385(1–4), 150–164, doi:10.1016/j.jhydrol.2010.02.012, 2010.

Kvočka, D., Falconer, R. A. and Bray, M.: Flood hazard assessment for extreme flood events, Nat. Hazards, doi:10.1007/s11069-016-2501-z, 2016.

Laganier, O., Ayral, P. A., Salze, D. and Sauvagnargues, S.: A coupling of hydrologic and hydraulic models appropriate for the fast floods of the Gardon River basin (France), Nat.

Hazards Earth Syst. Sci., 14(11), 2899–2920, doi:10.5194/nhess-14-2899-2014, 2014.

Lastoria, B., Simonetti, M. R., Casaioli, M., Mariani, S. and Monacelli, G.: Socio-economic impacts of major floods in Italy from 1951 to 2003, Adv. Geosci., 7, 223–229, doi:10.5194/adgeo-7-223-2006, 2006.

Leitão, J. P. and de Sousa, L. M.: Towards the optimal fusion of high-resolution Digital Elevation Models for detailed urban flood assessment, J. Hydrol., 561(December 2017), 651–661, doi:10.1016/j.jhydrol.2018.04.043, 2018.

Lerat, J.: Quels apports hydrologiques pour les modèles hydrauliques ? Vers un modèle intégré de simulation des crues, , 190 + annexes, 2009.

Lerat, J., Perrin, C., Andréassian, V., Loumagne, C. and Ribstein, P.: Towards robust methods to couple lumped rainfall-runoff models and hydraulic models: A sensitivity analysis on the Illinois River, J. Hydrol., 418–419, 123–135, doi:10.1016/j.jhydrol.2009.09.019, 2012.

Lhomme, J., Sayers, P., Gouldby, B., Samuels, P., Wills, M. and Mulet-marti, J.: Recent development and application of a rapid flood spreading method, Flood Risk Manag. Res. Pract., i(October), 15–24, doi:10.1201/9780203883020.ch2, 2009.

Lian, Y., Chan, I. C., Singh, J., Demissie, M., Knapp, V. and Xie, H.: Coupling of hydrologic and hydraulic models for the Illinois River Basin, J. Hydrol., 344(3–4), 210–222, doi:10.1016/j.jhydrol.2007.08.004, 2007.

Liu, Z., Martina, M. L. V and Todini, E.: Flood forecasting using a fully distributed model: application of the TOPKAPI model to the Upper Xixian Catchment, Hydrol. Earth Syst. Sci., 9(4), 347–364 [online] Available from: http://www.hydrol-earth-syst-sci.net/9/347/2005/%5Cnhttp://www.hydrol-earth-syst-sci.net/9/347/2005/hess-9-347-2005.pdf, 2005.

Liu, Z., Merwade, V. and Jafarzadegan, K.: Investigating the role of model structure and surface roughness in generating flood inundation extents using one- and two-dimensional hydraulic models, J. Flood Risk Manag., (June), doi:10.1111/jfr3.12347, 2018.

Llasat, M. C., Llasat-Botija, M., Barnolas, M., López, L. and Altava-Ortiz, V.: An analysis of the evolution of hydrometeorological extremes in newspapers: the case of Catalonia, 1982–2006, Nat. Hazards Earth Syst. Sci., 9(4), 1201–1212, doi:10.5194/nhess-9-1201-2009, 2009.

Llasat, M. C., Llasat-Botija, M., Prat, M. a., Porcú, F., Price, C., Mugnai, a., Lagouvardos, K., Kotroni, V., Katsanos, D., Michaelides, S., Yair, Y., Savvidou, K. and Nicolaides, K.: High-impact floods and flash floods in Mediterranean countries: the FLASH preliminary database,

Adv. Geosci., 23, 47–55, doi:10.5194/adgeo-23-47-2010, 2010.

LNCSR-LMoA: Land cover/use map of Lebanon at 1:20,000 scale. National Council for Scientific Research (NCSR) and Ministry of Agriculture (MOA), Lebanon, 2010.

Lowry, C. S. and Fienen, M. N.: CrowdHydrology: Crowdsourcing hydrologic data and engaging citizen scientists, GroundWater, 51(1), 151–156, doi:10.1111/j.1745-6584.2012.00956.x, 2013.

Lumbroso, D. and Gaume, E.: Reducing the uncertainty in indirect estimates of extreme flash flood discharges, J. Hydrol., 414–415, 16–30, doi:10.1016/j.jhydrol.2011.08.048, 2012.

Manfreda, S., Nardi, F., Samela, C., Grimaldi, S., Taramasso, A. C., Roth, G. and Sole, A.: Investigation on the use of geomorphic approaches for the delineation of flood prone areas, J. Hydrol., 517, 863–876, doi:10.1016/j.jhydrol.2014.06.009, 2014.

Mascaro, G., Piras, M., Deidda, R. and Vivoni, E. R.: Distributed hydrologic modeling of a sparsely monitored basin in Sardinia, Italy, through hydrometeorological downscaling, Hydrol. Earth Syst. Sci., 17(10), 4143–4158, doi:10.5194/hess-17-4143-2013, 2013.

Mason, D. C., Schumann, G. J. P. and Bates, P. D.: Data Utilization in Flood Inundation Modelling, in Flood Risk Science and Management, edited by G. Pender and H. Faulkner, pp. 209–233, Blackwell Publishing Ltd., 2010.

Massari, C., Brocca, L., Barbetta, S., Papathanasiou, C., Mimikou, M. and Moramarco, T.: Using globally available soil moisture indicators for flood modelling in Mediterranean catchments, Hydrol. Earth Syst. Sci., 18(2), 839–853, doi:10.5194/hess-18-839-2014, 2014.

Mazzoleni, M., Juliette, V., Arevalo, C., Wehn, U., Alfonso, L., Monego, M., Ferri, M. and Solomatine, D. P.: Towards assimilation of crowdsourced observations for different levels of citizen engagement : the flood event of 2013 in the Bacchiglione catchment, , (February), 1–40, doi:10.5194/hess-2017-59, 2017.

McCabe, M. F., Rodell, M., Alsdorf, D. E., Miralles, D. G., Uijlenhoet, R., Wagner, W., Lucieer, A., Houborg, R., Verhoest, N. E. C., Franz, T. E., Shi, J., Gao, H. and Wood, E. F.: The Future of Earth Observation in Hydrology, Hydrol. Earth Syst. Sci. Discuss., (February), 1–55, doi:10.5194/hess-2017-54, 2017.

Mejia, A. I. and Reed, S. M.: Evaluating the effects of parameterized cross section shapes and simplified routing with a coupled distributed hydrologic and hydraulic model, J. Hydrol., 409(1–2), 512–524, doi:10.1016/j.jhydrol.2011.08.050, 2011.

Merheb, M., Moussa, R., Abdallah, C., Colin, F., Perrin, C. and Baghdadi, N.: Hydrological

response characteristics of Mediterranean catchments at different time scales: a meta-analysis, Hydrol. Sci. J., 61(14), 2520–2539, doi:10.1080/02626667.2016.1140174, 2016.

Merwade, V., Olivera, F., Arabi, M. and Edleman, S.: Uncertainty in flood inundation Mapping: Current Issues and Future Directions, J. Hydrol. Eng., 13(7), 608–620, doi:10.1061/(ASCE)1084-0699(2008)13:7(608), 2008.

Merz, B., Kreibich, H. and Apel, H.: Flood risk analysis: Uncertainties and validation, Osterr. Wasser- und Abfallwirtschaft, 60(5–6), 89–94, doi:10.1007/s00506-008-0001-4, 2008.

Merz, B., Kreibich, H., Schwarze, R. and Thieken, A.: Review article “assessment of economic flood damage,” Nat. Hazards Earth Syst. Sci., 10(8), 1697–1724, doi:10.5194/nhess-10-1697-2010, 2010.

Metni, M., El-Fadel, M., Sadek, S., Kayal, R. and El Khoury, D. L.: Groundwater resources in Lebanon: A vulnerability assessment, Int. J. Water Resour. Dev., 20(4), 475–491, doi:10.1080/07900620412331319135, 2004.

Montanari, A., Young, G., Savenije, H. H. G., Hughes, D., Wagener, T., Ren, L. L., Koutsoyiannis, D., Cudennec, C., Toth, E., Grimaldi, S., Blöschl, G., Sivapalan, M., Beven, K., Gupta, H., Hipsey, M., Schaefli, B., Arheimer, B., Boegh, E., Schymanski, S. J., Di Baldassarre, G., Yu, B., Hubert, P., Huang, Y., Schumann, A., Post, D. a., Srinivasan, V., Harman, C., Thompson, S., Rogger, M., Viglione, A., McMillan, H., Characklis, G., Pang, Z. and Belyaev, V.: “Panta Rhei—Everything Flows”: Change in hydrology and society—The IAHS Scientific Decade 2013–2022, Hydrol. Sci. J., 58(6), 1256–1275, doi:10.1080/02626667.2013.809088, 2013.

Montanari, M., Hostache, R., Matgen, P., Schumann, G., Pfister, L. and Hoffmann, L.: Calibration and sequential updating of a coupled hydrologic-hydraulic model using remote sensing-derived water stages, Hydrol. Earth Syst. Sci., 13(3), 367–380, doi:10.5194/hess-13-367-2009, 2009.

Moriasi, D. N., Arnold, J. G., Van Liew, M. W., Binger, R. L., Harmel, R. D. and Veith, T. L.: Model evaluation guidelines for systematic quantification of accuracy in watershed simulations, Trans. ASABE, 50(3), 885–900, doi:10.13031/2013.23153, 2007.

Morita, M. and Yen, B. C.: Modeling of Conjunctive Two-Dimensional Surface-Three-Dimensional Subsurface Flows, J. Hydraul. Eng., 128, 184–200, doi:10.1061/(ASCE)0733-9429(2002)128:2(184), 2002.

Moussa, R.: Variabilité spatio-temporelle et modélisation hydrologique : application au bassin du Gardon d’Anduze. Thèse de Doctorat, Montpellier 2., 1991.

Moussa, R.: Geomorphological transfer function calculated from digital elevation models for distributed hydrological modelling, Hydrol. Process., 11(5), 429–449, doi:10.1002/(SICI)1099-1085(199704)11:5<429::AID-HYP471>3.0.CO;2-J, 1997.

Moussa, R.: When monstrosity can be beautiful while normality can be ugly: assessing the performance of event-based flood models, Hydrol. Sci. J., 55(6), 1074–1084, doi:10.1080/02626667.2010.505893, 2010.

Moussa, R. and Bocquillon, C.: On the use of the diffusive wave for modelling extreme flood events with overbank flow in the floodplain, J. Hydrol., 374(1–2), 116–135, doi:10.1016/j.jhydrol.2009.06.006, 2009.

Moussa, R. and Chahinian, N.: Comparison of different multi-objective calibration criteria using a conceptual rainfall-runoff model of flood events, Hydrol. Earth Syst. Sci., 519–535, doi:Hydrol. Earth Syst. Sci., 13, 519–535, 2009, 2009.

Moussa, R. and Cheviron, B.: Modeling of Floods—State of the Art and Research Challenges. Chapter 7, 2015a.

Moussa, R. and Cheviron, B.: Rivers – Physical, Fluvial and Environmental Processes, , doi:10.1007/978-3-319-17719-9, 2015b.

Nash, J. E. and Sutcliffe, J. V.: River flow forecasting through conceptual models part I - A discussion of principles, J. Hydrol., 10(3), 282–290, doi:10.1016/0022-1694(70)90255-6, 1970.

Neal, J., Schumann, G. and Bates, P.: A subgrid channel model for simulating river hydraulics and floodplain inundation over large and data sparse areas, Water Resour. Res., 48(11), 1–16, doi:10.1029/2012WR012514, 2012a.

Neal, J., Villanueva, I., Wright, N., Willis, T., Fewtrell, T. and Bates, P.: How much physical complexity is needed to model flood inundation?, Hydrol. Process., 26(15), 2264–2282, doi:10.1002/hyp.8339, 2012b.

NOAA: National Centers for Environmental Information, State of the Climate: Global Hazards for January 2013, published online February 2013, retrieved on February 27, 2017 from http://www.ncdc.noaa.gov/sotc/hazards/201301., 2013.

Noman, N. S., Nelson, E. J., Zundel, A. K. and ASCE, M.: Review of automated floodplain delineation from digital terrain models, J. Water Resour. Plann. Manag., 127(December), 394–402, 2001.

Norbiato, D., Borga, M., Sangati, M. and Zanon, F.: Regional frequency analysis of extreme precipitation in the eastern Italian Alps and the August 29, 2003 flash flood, J. Hydrol., 345(3–

4), 149–166, doi:10.1016/j.jhydrol.2007.07.009, 2007.

Oleyiblo, J. O. and Li, Z.: Application of HEC-HMS for flood forecasting in Misai and Wan'an catchments in China, Water Sci. Eng., 3(1), 14–22, doi:http://dx.doi.org/10.3882/j.issn.1674-2370.2010.01.002, 2010.

Panneton, F., L'ecuyer, P. and Matsumoto, M.: Improved long-period generators based on linear recurrences modulo 2, ACM Trans. Math. Softw., 32(1), 1–16, doi:10.1145/1132973.1132974, 2006.

Papaioannou, G., Loukas, A., Vasiliades, L. and Aronica, G. T.: Flood inundation mapping sensitivity to riverine spatial resolution and modelling approach, Nat. Hazards, doi:10.1007/s11069-016-2382-1, 2016.

Papaioannou, G., Vasiliades, L., Loukas, A. and Aronica, G. T.: Probabilistic flood inundation mapping at ungauged streams due to roughness coefficient uncertainty in hydraulic modelling, Adv. Geosci., 44, 23–34, doi:10.5194/adgeo-44-23-2017, 2017.

Pappenberger, F., Beven, K. J., Hunter, N. M., Bates, P. D., Gouweleeuw, B. T., Thielen, J. and Roo, A. P. J. De: Cascading model uncertainty from medium range weather forecasts (10 days) through a rainfall-runoff model to flood inundation predictions within the European Flood Forecasting System (EFFS), Hydrol. Earth Syst. Sci. Discuss., 9(4), 381–393, doi:10.5194/hess-9-381-2005, 2005.

Pappenberger, F., Beven, K. J., Ratto, M. and Matgen, P.: Multi-method global sensitivity analysis of flood inundation models, Adv. Water Resour., 31(1), 1–14, doi:10.1016/j.advwatres.2007.04.009, 2008.

Plassard, J.: Pluviometric map of Lebanon at a scale of 1:200,000. Republic of Lebanon. Ministry of Public Affairs. General Direction of Civil Aviation., 1972.

Raclot, D. and Albergel, J.: Runoff and water erosion modelling using WEPP on a Mediterranean cultivated catchment, Phys. Chem. Earth, 31(17), 1038–1047, doi:10.1016/j.pce.2006.07.002, 2006.

Refsgaard, J. C.: Terminology, Modelling Protocol And Classification of Hydrological Model Codes, in Distributed hydrological modelling, edited by M. B. Abbot and J. C. Refsgaard, pp. 17–39, kluwer academic publishers., 1996.

Robert, C. P. and Casella, G.: Monte Carlo statistical methods, 2nd ed., New York: Springer., 2004.

Robinson, J. S. and Sivapalan, M.: Catchment-scale runoff generation model by aggregation

and similarity analyses, Hydrol. Process., 9(5–6), 555–574, doi:10.1002/hyp.3360090507, 1995.

Romanowicz, R. and Beven, K.: Estimation of flood inundation probabilities as conditioned on event inundation maps, Water Resour. Res., 39(3), 12 PP., doi:10.1029/2001wr001056, 2003.

Roux, H., Labat, D., Garambois, P. A., Maubourguet, M. M., Chorda, J. and Dartus, D.: A physically-based parsimonious hydrological model for flash floods in Mediterranean catchments, Nat. Hazards Earth Syst. Sci., 11(9), 2567–2582, doi:10.5194/nhess-11-2567-2011, 2011.

Salajegheh, A. and Dastorani, J.: Determining of Regional Coefficients of Fuller's Empirical Formula to Estimate Maximum Instantaneous Discharges in Dasht Kavir Basin, Kalshour Sabzevar , Iran, BIABAN J., 11(1), 53–59, 2006.

Saleh, F., Ducharne, A., Flipo, N., Oudin, L. and Ledoux, E.: Impact of river bed morphology on discharge and water levels simulated by a 1D Saint-Venant hydraulic model at regional scale, J. Hydrol., 476, 169–177, doi:10.1016/j.jhydrol.2012.10.027, 2013.

Samaniego, L., Kumar, R. and Jackisch, C.: Predictions in a data-sparse region using a regionalized grid-based hydrologic model driven by remotely sensed data, Hydrol. Res., 42(5), 338–355, doi:10.2166/nh.2011.156, 2011.

Samela, C., Troy, T. J. and Manfreda, S.: Geomorphic classifiers for flood-prone areas delineation for data-scarce environments, Adv. Water Resour., 102, 13–28, doi:10.1016/j.advwatres.2017.01.007, 2017.

Sangati, M., Borga, M., Rabuffetti, D. and Bechini, R.: Influence of rainfall and soil properties spatial aggregation on extreme flash flood response modelling: An evaluation based on the Sesia river basin, North Western Italy, Adv. Water Resour., 32(7), 1090–1106, doi:10.1016/j.advwatres.2008.12.007, 2009.

Der Sarkissian, R.: Master thesis: Watershed management for the AWALI Basin, Faculty of Sciences of the Lebanese University., 2015.

Satyanarayana, P. and Srinivas, V. V.: Regionalization of precipitation in data sparse areas using large scale atmospheric variables - A fuzzy clustering approach, J. Hydrol., 405(3–4), 462–473, doi:10.1016/j.jhydrol.2011.05.044, 2011.

Savage, J. T. S., Bates, P., Freer, J., Neal, J. and Aronica, G.: When does spatial resolution become spurious in probabilistic flood inundation predictions?, Hydrol. Process., 30(13), 2014–2032, doi:10.1002/hyp.10749, 2016.

Schumann, G., Bates, P. D., Horritt, M. S., Matgen, P. and Pappenberger, F.: Progress in intergration of remote sensing derived flood extent and stage data and hydraulic models, Rev. Geophys., 47(2008), 1–20, doi:10.1029/2008RG000274.1.INTRODUCTION, 2009.

Schumann, G. J. P., Neal, J. C., Voisin, N., Andreadis, K. M., Pappenberger, F., Phanthuwongpakdee, N., Hall, A. C. and Bates, P. D.: A first large-scale flood inundation forecasting model, Water Resour. Res., 49(10), 6248–6257, doi:10.1002/wrcr.20521, 2013.

SCS: Soil Conservation Service-Section 4: Hydrology, in National Engineering Handbook, Department of Agriculture, available from US Government Printing Office, Washington, DC., 1972.

Sene, K. J., Marsh, T. J. and Hachache, a.: An assessment of the difficulties in quantifying the surface water resources of Lebanon, Hydrol. Sci. J., 44(1), 79–96, doi:10.1080/02626669909492204, 1999.

Sene, K. J., Houghton-Carr, H. A. and Hachache, A.: Preliminary flood frequency estimates for Lebanon, , 46(5), 37–41, doi:10.1080/02626660109492863, 2001.

Shamsudin, S., Dan, S. and Rahman, A. A.: Uncertainty Analysis of Hec-Hms Model Parameters Using Monte Carlo Simulation, Int. J. Model. Simul., 31(4), doi:10.2316/Journal.20, 2011.

Sharif, H. O., Sparks, L., Hassan, A. a., Zeitler, J. and Xie, H.: Application of a Distributed Hydrologic Model to the November 17, 2004, Flood of Bull Creek Watershed, Austin, Texas, J. Hydrol. Eng., 15(8), 651–657, doi:10.1061/(ASCE)HE.1943-5584.0000228, 2010.

Singh, V. P. and Woolhiser, D. A.: Mathematical Modeling of Watershed Hydrology, J. Hydrol. Eng., 7(4), 270–292, doi:10.1061/(ASCE)1084-0699(2002)7:4(270), 2002.

Sivapalan, M., Takeuchi, K., Franks, S. W., Gupta, V. K., Karambiri, H., Lakshmi, V., Liang, X., McDonnell, J. J., Mendiondo, E. M., O'Conell, P. E., Oki, T., Pomeroy, J. W., Schertzer, D., Uhlenbrook, S. and Zehe, E.: IAHS Decade on Predictions in Ungauged Basins (PUB), 2003–2012: Shaping an exciting future for the hydrological sciences, Hydrol. Sci. J., 48(6), 857–880, doi:10.1623/hysj.48.6.857.51421, 2003.

Smith, M. J., Edwards, E. P., Priestnall, G. and Bates, P. D.: Exploitation of new data types to create digital surface models for flood inundation modelling., 2006.

Switzman, H., Coulibaly, P. and Adeel, Z.: Modeling the impacts of dryland agricultural reclamation on groundwater resources in Northern Egypt using sparse data, J. Hydrol., 520, 420–438, doi:10.1016/j.jhydrol.2014.10.064, 2015.

Teng, J., Jakeman, A. J., Vaze, J., Croke, B. F. W., Dutta, D. and Kim, S.: Flood inundation modelling: A review of methods, recent advances and uncertainty analysis, Environ. Model. Softw., 90, 201–216, doi:10.1016/j.envsoft.2017.01.006, 2017.

Todini, E. and Ciarapica, L.: The Topkapi Model, Math. Model. large watershed Hydrol., (November), 471–506, doi:10.1006/hmat.1999.2234, 2002.

Tsubaki, R. and Fujita, I.: Unstructured grid generation using LiDAR data for urban flood inundation modelling, Hydrol. Process., 24(11), 1404–1420, doi:10.1002/hyp.7608, 2010.

UNDP: Assessment of Groundwater Resources of Lebanon, Beirut, Lebanon., 2014.

UNISDR: Guidelines for Reducing Flood Losses., 2002.

UNISDR and CRED: The Human Cost of Weather Related Disasters, 1995-2015., 2015.

USACE: Hydrologic Modeling System HEC-HMS:Technical Referance Manual, US Army Corps of Engineers Hydrologic Engineering Center, 609 Second Street Davis, CA 95616-4687 USA., 2000.

USACE: HEC-RAS River Analysis System - Hydraulic Reference Manual, Version 5.0, US Army Corps of Engineers Hydrologic Engineering Center (HEC), 609 Second Street Davis, CA 95616-4687 USA. [online] Available from: http://www.hec.usace.army.mil/software/hec-ras/documentation.aspx, 2016a.

USACE: Hydrologic Modeling System User's Manual, U.S. Army Corps of Engineers Institute for Water Resources Hydrologic Engineering Center (CEIWR-HEC), 609 Second Street Davis, CA 95616-4687., 2016b.

Du Vaumas, E.: Le Liban (montagne libanaise, Bekka, Anti-Liban, Hermon, Haute Galilee libannaise) : etude de geographie physique., Firmin-Didot, Paris., 1954.

Vozinaki, A. K., Morianou, G. G., Alexakis, D. D. and Tsanis, K.: Comparing 1D- and combined 1D / 2D hydraulic simulations using high resolution topographic data , the case study of the Koiliaris basin , Greece, Hydrol. Sci. J., 0(0), doi:10.1080/02626667.2016.1255746, 2016.

Walley, C. D.: Some outstanding issues in the geology of Lebanon and their importance in the tectonic evolution of the Levantine region, Tectonophysics, 298(1–3), 37–62, doi:10.1016/S0040-1951(98)00177-2, 1998.

Walley, C. D.: The Geology of Lebanon, A summary, , 23–40, 2009.

Whiteaker, T. L., Robayo, O., Maidment, D. R. and Obenour, D.: From a NEXRAD Rainfall Map to a Flood Inundation Map, J. Hydrol. Eng., 11(1), 37, doi:10.1061/(ASCE)1084-0699(2006)11:1(37), 2006.

Wilby, R. L. and Yu, D.: Rainfall and temperature estimation for a data sparse region, Hydrol. Earth Syst. Sci., 17(10), 3937–3955, doi:10.5194/hess-17-3937-2013, 2013.

WMO: Manual on flood forecasting and warning, WMO-No. 10., World Meteorological Organization, Geneva., 2011.

Woodward, D., Hawkins, R., Jiang, R., Hjelmfelt, J., Van Mullem, J. A. and Quan, Q.: Runoff Curve Number Method: Examination of the Initial Abstraction Ratio, World Water Environ. Resour. Congr. 2003, 1–10, doi:doi:10.1061/40685(2003)308, 2003.

Woolhiser, D. A., Smith, R. E. and Goodrich, D. C.: A Kinematic Runoff and Erosion Model, , (March), 1990.

World Bank: World Development Indicators, World Bank, Washington, DC., 2010.

Yamout, G. and El-Fadel, M.: An optimization approach for multi-sectoral water supply management in the Greater Beirut Area, Water Resour. Manag., 19(6), 791–812, doi:10.1007/s11269-005-3280-6, 2005.

Zilberberg, M. D. and Shorr, A. F.: Understanding cost-effectiveness, Clin. Microbiol. Infect., 16(12), 1707–1712, doi:10.1111/j.1469-0691.2010.03331.x, 2010.

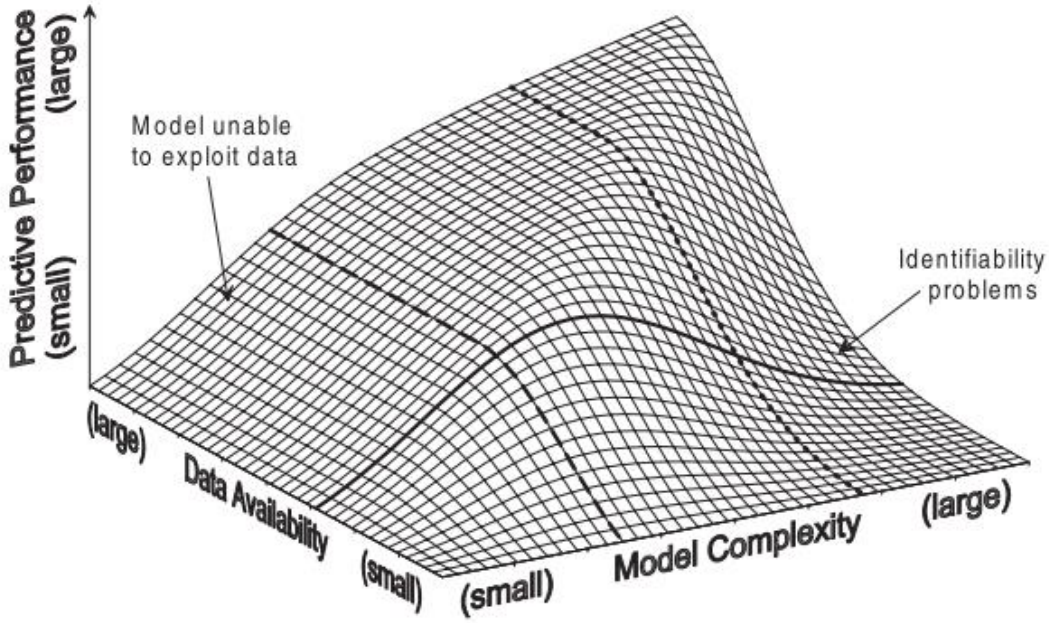

Figure 1 The conceptual relationship between model complexity, data availability and predictive performance (Grayson and Blöschl, 2001)

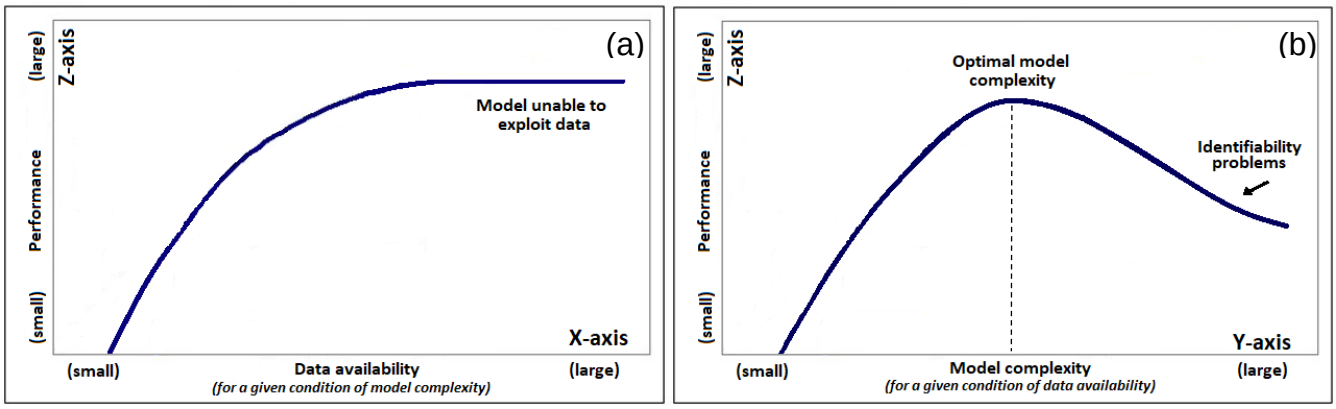

Figure 2(a) The conceptual relationship between data availability and model performance for a given condition of model complexity (X-Z plane), (b) the conceptual relationship between model complexity and prediction performance for a given condition of data availability (Y-Z plane).

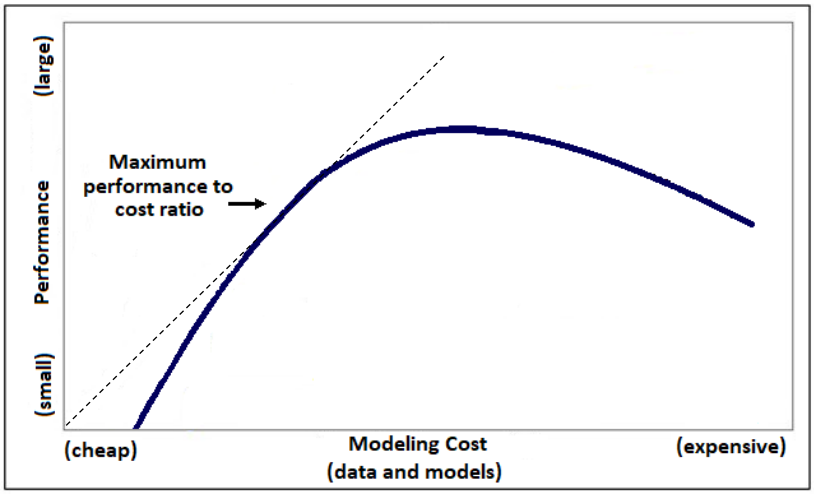

Figure 3 The conceptual relationship between modelling cost and modelling performance.

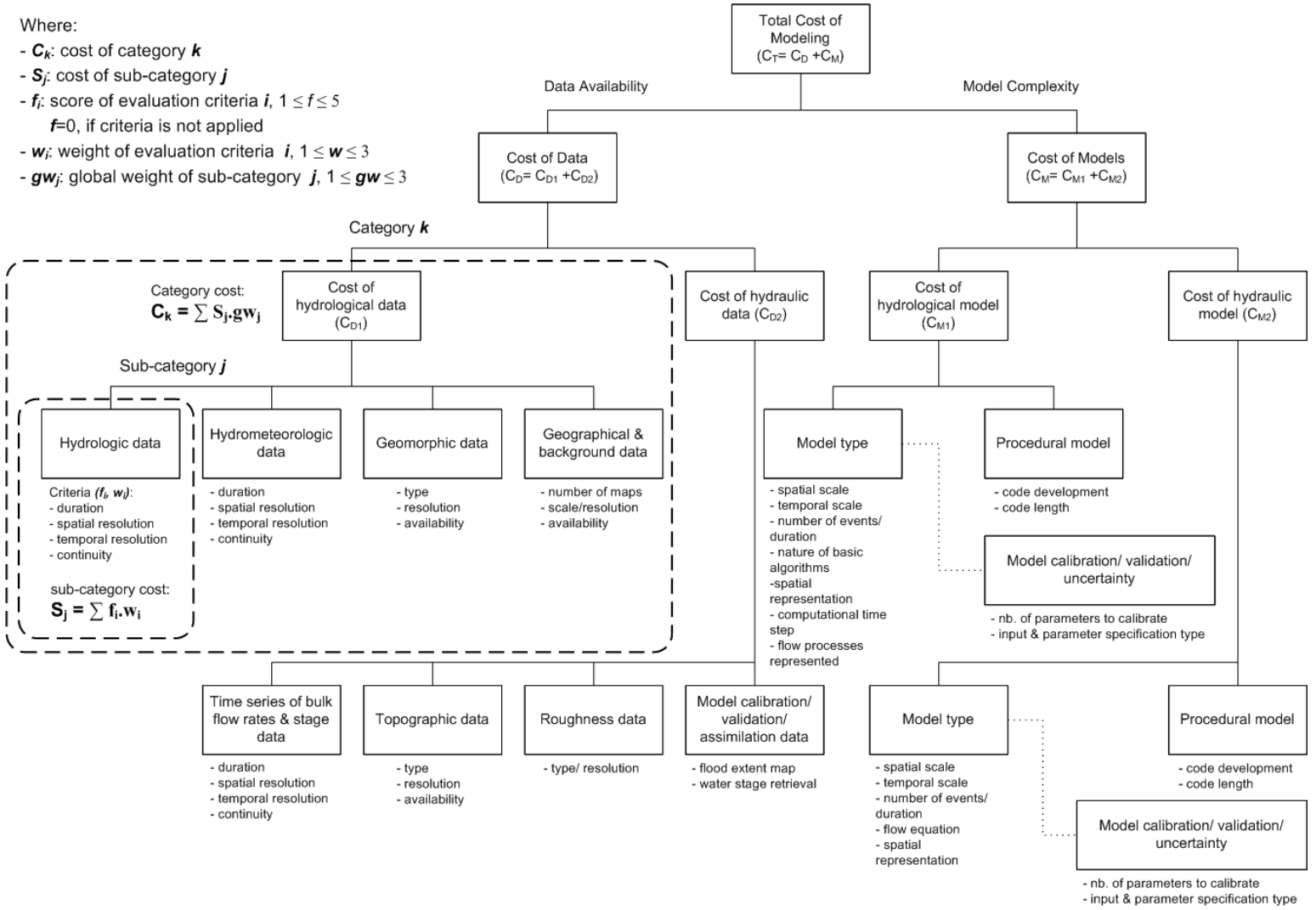

Figure 4 Schematic diagram presenting the cost evaluation criteria for data and models

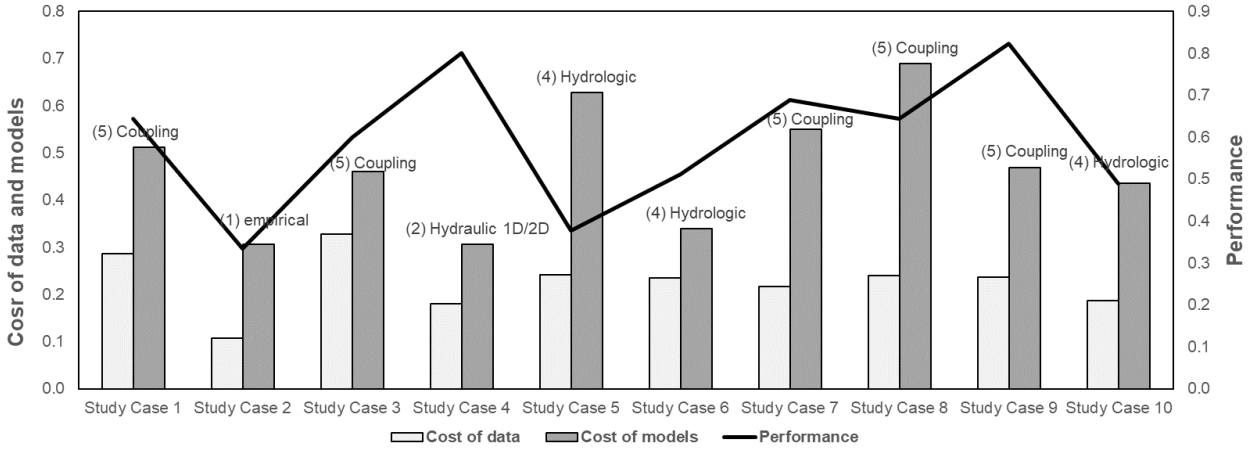

Figure 5 Results of the costs and performance evaluation for different study cases.

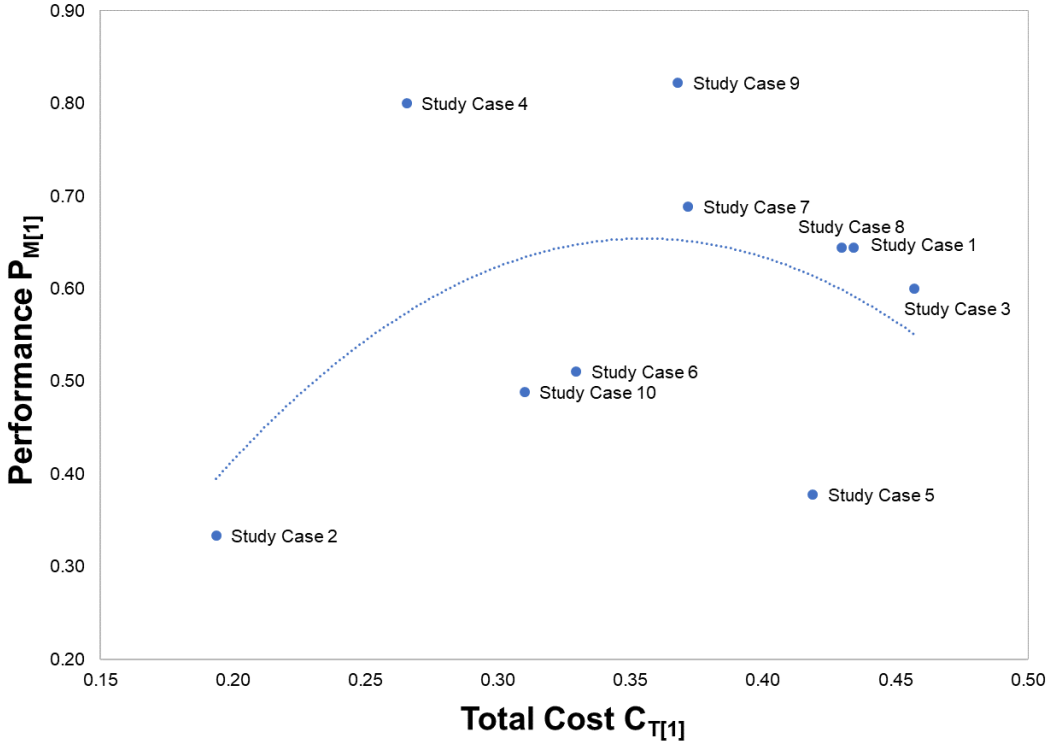

Figure 6 Results of the cost-performance analysis for ten selected study cases, the total cost of modelling versus the performance of the modelling approach.

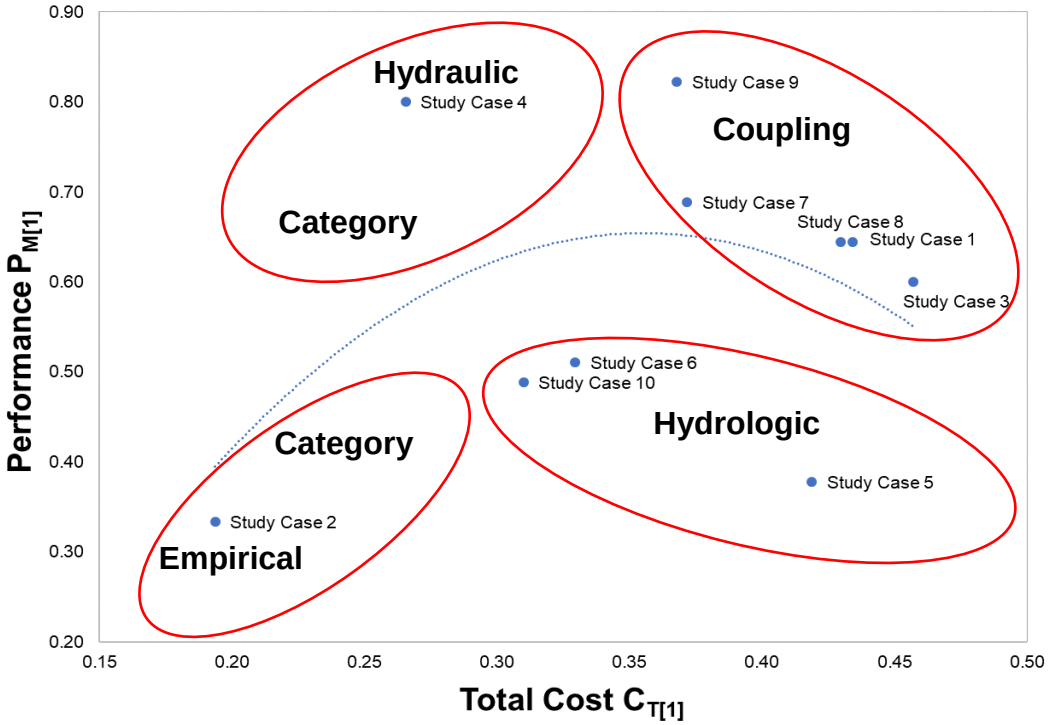

Figure 7 Proposed zoning of four modelling categories (empirical (1), hydraulic (2), hydrologic (4), and coupling (5)) based on the cost-performance grid.

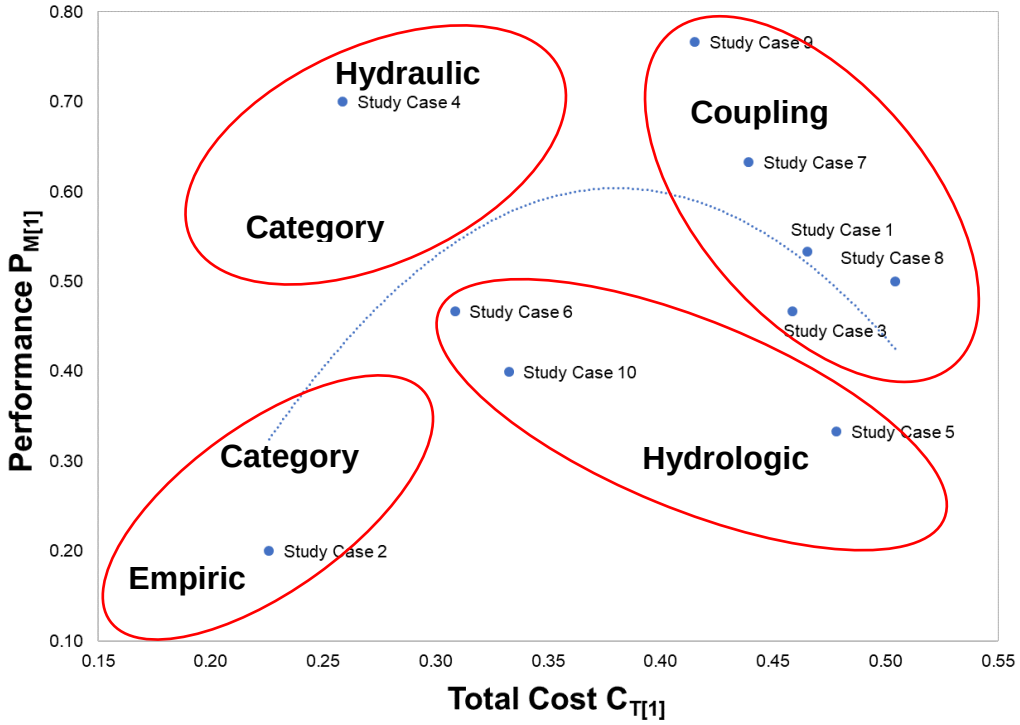

Figure 8 Results of the sensitivity analysis on the weights of the cost-performance grid; all weights are considered 1. The total cost of modelling versus the performance of the modelling approach. The proposed zoning of the four modelling categories (empirical (1), hydraulic (2), hydrologic (4), and coupling (5)) are presented in red.

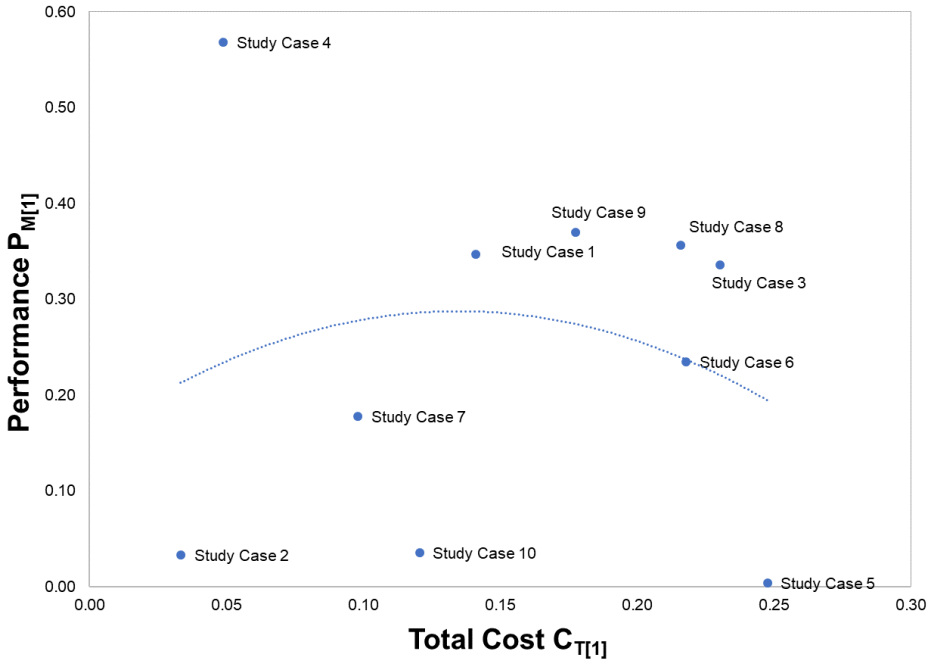

Figure 9 Results of the sensitivity analysis on the scores of the cost-performance grid; scores are evaluated based on a log scale of five levels from 1 to 10,000.

Table 1 Evaluation criteria for hydrologic and hydrometeorologic data of the hydrological model.

Hydrologic and Hydrometeorologic data	**Scores**					**Weight**
Evaluation criteria	**VL**	**L**	**M**	**H**	**VH**	
Duration	≤ 1 M	1Y	10 Y	50 Y	≥ 100 Y	M
Spatial resolution	point data/ ground gauge		remote sensing		spatial measurement	H
Temporal resolution	≥ monthly		daily		≤ hourly	H
Continuity/ completeness	many gaps		some gaps		time series	L

Table 2 Evaluation criteria for geomorphic data of the hydrological model.

Geomorphic data	**Scores**					**Weight**
Evaluation criteria	**VL**	**L**	**M**	**H**	**VH**	
Type	cartographic	Remote sensing (ex: SRTM)	aerial photogrammetry, LIDAR	+ sonar bathymetry	Ground surveying	M
Scale/resolution	low resolution ≥100 m	90 m	60 m	30 m	high resolution ≤ 10 m	H
Availability	Open source/ available		developed		purchased	L

Table 3 Evaluation criteria for hydrological model type.

Hydrological model type	**Scores**					**Weight**
Evaluation criteria	**VL**	**L**	**M**	**H**	**VH**	
Spatial scale	global	continental	regional	basin	parcel	L
Temporal scale	event-based				continuous	M
Number of events (if event-based)	1	5	10	15	≥ 20	L
Duration (if continuous)	≤ 1 M	1Y	10 Y	50 Y	≥ 100 Y	L
Nature of basic algorithm	empirical/ black box	regression	conceptual		physically based	H
Spatial representation	lumped		semi-distributed		distributed	H
Computational time step	coarse fixed time step (> day)				fine adaptive time step (< hour)	L
Flow processes presented	overland flow		+channel flow	+sub-surface flow	+other processes	L

Table 4 Evaluation criteria for hydraulic model type.

Hydraulic model type	**Scores**					**Weight**
Evaluation criteria	**VL**	**L**	**M**	**H**	**VH**	
Spatial scale	global		regional		reach scale	L
Temporal scale	event-based				continuous	M
Number of events (if event-based)	1	5	10	15	≥ 20	L
Duration (if continuous)	≤ 1 M	1Y	10 Y	50 Y	≥ 100 Y	L
Flow equations	empirical/ black box	uniform flow formula	Kinematic wave	Diffusive wave	Complete SV	H
Spatial representation	1D		2D	Quasi 2D/ subgrid	3D	H

Table 5 Evaluation criteria for model performance.

Performance	**Scores**					**Weight**
Evaluation criteria	**VL**	**L**	**M**	**H**	**VH**	
Type of output	Peak flood discharge/ flood volume	Flood flow hydrograph at outlet	Flood flow hydrograph at different locations	Flood water levels	Flood inundation map	H
Criteria function	single variable/ single criteria				Multi-variable/ multi-criteria/ multi-site	M
Peak flow and volume error (% error)	≤ 50%	30%	10%	5%	0%	L
Hydrograph error (ex: Nash)	≤ 0.5	0.6	0.7	0.8	1	L
water level error (ex: RMSE)	> 200 cm	150 cm	100 cm	50 cm	≤ 10cm	L
flood extent error (ex: skill of mapping)	0	0.4	0.6	0.8	1	L

Table 6 Description of the ten arbitrarily selected flood modeling study cases for cost-performance analysis.

Study case ID	Study case	Study Site/ Country	Area [km^2]	Modeling approach	Objective function
Study Case 1	Hdeib et al. (2018)	Awali River Basin, Lebanon	301	(5) Coupling	Flood inundation map
Study Case 2	Abdallah et al. (2013)	Awali River Basin, Lebanon	301	(1) Empirical	Flood inundation map
Study Case 3	Knebl et al. (2005)	San Antonio River Basin, Central Texas, USA	10,000	(5) Coupling	Flood inundation map
Study Case 4	Neal et al. (2012a)	Niger river, Mali.	210,389	(2) Hydraulic 1D/2D	Flood inundation map
Study Case 5	Moussa (1991)	Gardon Basin, France	542	(4) Hydrologic	Flow hydrograph
Study Case 6	Coustau et al. (2012)	Lez catchment, France	114	(4) Hydrologic	Flow hydrograph
Study Case 7	Koutroulis and Tsanis (2010)	Giofiros basin, Greece	158	(5) Coupling	Flow hydrograph
Study Case 8	Fuentes-Andino et al. (2017)	Floodplain of Tegucigalpa, Honduras	811	(5) Coupling	Flood inundation map
Study Case 9	Montanari et al. (2009)	Alzette River (Grand Duchy of Luxembourg)	356	(5) Coupling	Flood inundation, estimation of antecedent moisture condition from volume of runoff
Study Case 10	Liu et al. (2005)	Upper Xixian catchment in Huaihe River, China	10,000	(4) Hydrologic	Flood forecasting

Table 7 Results of the cost-performance calculation for ten selected study cases in literature based on the proposed cost-performance grid. Scores are evaluated based on a linear scale of five levels from 1 to 5. Weights and global weights are evaluated based on three levels 1, 2, and 3. The different parameters are calculated following equations Eqs. 4 to 12. Refer to supplementary material for detailed calculation results, and to the table of abbreviations for parameter description.

Study case ID	C_D (max)	C_M (max)	C_T (max)	C_D	$C_{D\,[1]}$	C_M	$C_{M\,[1]}$	C_T	$C_{T\,[1]}$	P_M (max)	P_M	$P_{M\,[1]}$	PC = $P_{M\,[1]}/ C_{T\,[1]}$
Study Case 1	460	180	640	183	**0.29**	92	**0.51**	275	**0.43**	45	29	**0.64**	**1.50**
Study Case 2	460	180	640	69	**0.11**	55	**0.31**	124	**0.19**	45	15	**0.33**	**1.72**
Study Case 3	460	180	640	210	**0.33**	83	**0.46**	293	**0.46**	45	27	**0.60**	**1.31**
Study Case 4	460	180	640	115	**0.18**	55	**0.31**	170	**0.27**	45	36	**0.80**	**3.01**
Study Case 5	460	180	640	155	**0.24**	113	**0.63**	268	**0.42**	45	17	**0.38**	**0.90**
Study Case 6	460	180	640	150	**0.23**	61	**0.34**	211	**0.33**	45	23	**0.51**	**1.55**
Study Case 7	460	180	640	139	**0.22**	99	**0.55**	238	**0.37**	45	31	**0.69**	**1.85**
Study Case 8	460	180	640	154	**0.24**	124	**0.69**	278	**0.43**	45	29	**0.64**	**1.48**
Study Case 9	460	180	640	151	**0.24**	85	**0.47**	236	**0.37**	45	37	**0.82**	**2.23**
Study Case 10	460	180	640	120	**0.19**	79	**0.44**	199	**0.31**	45	22	**0.49**	**1.58**

Table of abbreviation

C_D	Cost of data, unit of score	***j***	A sub-category for data or models
$C_{D\,[1]}$	Cost of data, dimensionless	***k***	A main category for modelling (hydrological/hydraulic models or data)
C_k	Cost of category *k,* unit of score	NSE	Nash-Sutcliffe efficiency
$C_{k\,[1]}$	Cost of category *k,* dimensionless	PE	Phase error, h
C_M	Cost of models, unit of score	PFE	Peak flow error, %
$C_{M\,[1]}$	Cost of models, dimensionless	P_M	Performance of the modelling approach, dimensionless
C_T	Total cost of a modelling approach, unit of score	r	Coefficient of correlation
$C_{T\,[1]}$	Total cost of a modelling approach, dimensionless	RMSE	Root mean square error, m^3/s or m
f_i	Score of evaluation criteria *i*, $1 \leq f \leq 5$; f=0, if criteria is not applied	S_j	Cost of sub-category *j*
gw_j	Global weight of sub-category j, $1 \leq gw \leq 3$	VE	Volume error, %
i	Cost evaluation criteria	w_i	Weight of evaluation criteria *i*, $1 \leq w \leq 3$

Annex B.
Extracted historical flood events

Table B.1 List of the extracted flood events from newspapers and previous reports.

Source	Year	Month	Weather Extreme	Location or Area Affected	Damage (estimated losses; million $)
An-Nahar	1293	Jun	Flood	Baalbek	100,000 people deceased
An-Nahar	1317	May	Flood	Baalbek	500 houses ruined,131 stores,17 bakery, 11 mills, 1 school,40 corn field, 140 or more people deceased
An-Nahar	1345	Jan	Flood	Tripoli	people killed, great agricultural losses
An-Nahar	1345	Apr	Flood	Tripoli	ditto
An-Nahar	1408	Jan	Flood	Tripoli	hundreds of houses collapsed
An-Nahar	1503	Summer	Assi, Litani, Fraidis, El-Safa, Kalb, Rivers flood	All Lebanon	Damages in houses, bridges, roads, agricultural lands
An-Nahar	1507	6 Jul	Flood	El Chouf	Agricultural land around Nahr ElSafa flooded
An-Nahar	1557	-	Kadicha river Flood	Bcherri	Bridges collapse, tens of mills and trees destroyed
An-Nahar	1612	-	Abo Ali Flood	Tripoli	Destruction of Mamluk monuments, Many people dead.
An-Nahar	1674	Nov	-	Tripoli	-
An-Nahar	1677	Mar	-	Tripoli	-

An-Nahar	1749	Mar	-	Tripoli	More than 500 people dead
An-Nahar	1776	Nov	Nahr Bcherri Flooded	Bcherri	not recorded
An-Nahar	1780	May	Flood	Keserouan, Nahr elKalb	Nahr elkalb bridge collapsed
An-Nahar	1787	Nov	Flood	Beskenta	12 persons dead
An-Nahar	1799	Dec	Flood	Mount Lebanon	Vast area of olives trees destroyed
An-Nahar	1804	Sep	Nahr el Kalb Flood	Keserouan	Nahr elkalb bridge collapsed
An-Nahar	1853	12 Nov	Flood	Keserouan	-
An-Nahar	1854	2 Dec	Flood	Keserouan	houses destroyed, 1 person deceased
An-Nahar	1874		Flood	Keserouan	-
An-Nahar	1876	Jan	Flood	Jbeil, Batroun	Agricultural land damaged, mills destroyed.

An-Nahar	1878	25 Dec	Nahr el Kalb and Nahr Ashkout Flood	Keserouan	Jisr der Shamra collapse
(Khawlie, 1994)	1955	-	Flood	Tripoli	440 people died, 2000 families displaced, thousands of acres of citrus plantations destroyed, 4 bridges collapsed, landslides…
An-Nahar	1971	1 Dec	Torrential rain	Ehmej, Kfar Selwan	Road failure, agricultural damage
An-Nahar	1972	2 Jan	ditto	same area	ditto
An-Nahar	1975	3 Feb	torrents, floods, tempest, avalanche	Beirut, Zahle, Faraya	structural failure, ships, damage, water pollution, electricity and phones out, agriculture-4 people deceased
An-Nahar	1976	4 Feb	snow (at 400m elevation)	Bint Jbeil	ditto
An-Nahar	1977	5 Feb	torrent, floods & snow accumulation	Akkar, Beqaa, Dbaye, Beirut, Tripoli	ditto, cattle
An-Nahar	1977	6 Mar	ditto	ditto	ditto
An-Nahar	1978	7 Jan	torrent, floods	Dbaye	ditto & trains derailed
An-Nahar	1978	8 Mar	hailstorms, floods	Bhamdoun, Aley, Akkar, Zghorta, Koura, Batroun	huge soil erosion
An-Nahar	1979	9-Jan	ditto; floods in: Al-Kabir river, El-Mot river, sea storm	Cheikh Zennad, Machta Hassan & Machta Hammoud, Bekai'a, Beirut, Tripoli	ditto
An-Nahar	1980	10 Jan	torrents	Akkar, Chekka	roads & tunnel failure, landslides
An-Nahar	1980	11 Feb	flood in Antelias river	Antelias	agricultural destruction, cattle
An-Nahar	1981	12 Mar	hail storm, sea storm	mountains Chouf, coastal stretch, IPC refinery	communications, structural failure, roads, agriculture, electricity & phone, seaports
An-Nahar	1982	13 Feb	wind storm	Chouf	agriculture
An-Nahar	1983	14 Feb	rain storm, hail storm, avalanches	all coastal cities, Beqaa, El-Baidar, Batroun, Michmich, Fnaidek, Bcharri, A'qoura	huge damage in many sectors cattle

An-Nahar	1983	15 Mar	torrents and floods in rivers: Kfarchima, Hauch Harimi (Litani), EL Awali, Barghouth, sea storm, hail storm & avalanches	South Lebanon, Hasbaya, Bekai'a, Chouf, Beqaa, Akkar, Broummana, Bar Elias, Niha, EL-Ballout, EL-Kharroub, Rihan, Choueifat, Bcharri, Sir, Fakra, O'iun siman, Ainata, Cedars, all coastal cities	landslides, bridges, canals, roads, houses, ships, agriculture, forest, 90 people deceased, 3000 cattle heads
An-Nahar	1984	16 Jan	rain storm, flood in Bisri river	Bisri, Sour	agriculture, soil erosion
An-Nahar	1984	17 Nov	hailstorm	Bcharri, Ainata, Cedars	roads, forest
An-Nahar	1984	18 Dec	torrents, avalanches	Baalbek, D. Choueir, Hezzerta, Qbayat, O'iun Siman	ditto, agriculture, cattle
An-Nahar	1986	19 Jan	wind storm, torrents, avalanches	all mountains	roads, agriculture
An-Nahar	1986	20 Feb	ditto & sea storm with huge waves	all coastal cities, Mairouba	ditto, ports, ships
An-Nahar	1986	21 Nov	torrents, flood in Kalb river	Zouk, Dbaye	roads, agriculture
An-Nahar	1986	22 Dec	ditto, floods in Berdawni & Hasbani rivers	Beirut & suburb, Sour, Zahle, Hasbaya, Rachaya, Sir	landslides, huge destruction in structures, roads, ports, public services, agriculture, isolating communities, cattle
An-Nahar	1987	23 Mar	storm & torrents	all coastal stretch, Akkar	landslides, communications
An-Nahar	1987	24 Oct	torrents, flood in Assi river	Baalbek, Hermel, Rachaya, Younine, Fakra, Zahle	huge destruction, 1 person deceased
An-Nahar	1987	25 Dec	ditto & sea storm with huge waves, flood in Ibrahim river & Beirut river	Saida, Ankoun, Kfar Hetta, Chouf, Ras Bayyada, Zouk, Yahchouch, Beirut, Jbeil & surrounding	ditto, 4 persons deceased
Net	1987	-	Flood	-	-

Arab Center for Information/ Al-Safir	1987	17 Oct- 19 Oct	Heavy and Huge Torrents (Cause: hail fall then heavy rainfall in great volume and short time + flow on steep and arid slopes)	El-Fakha, Jdeidet El-Fakha, El-Assi valley, Kaa, Ras Baalbek	Water level reached about 10 m of width reaching 200 m, 13 hours of flow with high speed reaching 10 m^3/s filling a reservoir of 3 Mm^3 volume, recurrence about 150 years. Water level reached more than 80 cm on average. Great structural, agricultural and animal losses, Landslides, soil erosion, roads cut, flood lasted 3 days, 10 persons deceased, 200 people displaced, Severity level 2, affected area about 12690 sq. Km, Magnitude 4.9
An-Nahar	1988	26 Feb	ditto, flood in Awali river, Kasimieh river, Ghadir river torrents	Saida, Choueifat	landslides, roads, agriculture
An-Nahar	1988	27 Mar	torrents	Tripoli, Dbaye	ditto, building failure 4 persons deceased (Tripoli
An-Nahar	1991	28 Mar	ditto, flood in Bared river	Beqaa, Baalbek, Hermel, Akkar, coastal cities	ditto, huge destruction
CNRS	1991	21 Dec/ 23 Dec-28 Dec	Floods, Heavy rainfall of severity class 1; recurrence 4 years	Central Bekaa valley	duration 6 days, 1 person deceased, 2000 people displaced, Magnitude:4.8
An-Nahar	1992	21 Jan	torrential rain, floods in rivers of: Al-Awali, Kasimieh, Ezzahrani, El-Kabir& Hasbani river, water level rise, snow melting	Bcharri, Sour, Akkar, Tell Hmierh, Samakieh	road damage, landslide, soil drifting
An-Nahar	1992	6 Feb	floods in EL-Kabir river, torrents, snow melting	Beirut, Akkar, Nabatiye, Sour	road damage, agriculture, huge destruction, soil drifting
An-Nahar	1992	12 Feb	torrential rain, rain storm, avalanche, floods in rivers of Kasimieh & Sinique	Akkar, Chouf, Hasbaya, Sour, Nabatiye	overflow in Qaraoun lake, agriculture, soil drift, 5 persons deceased

An-Nahar	1993	1 Jan	torrents, snow storms, flood in Kasimieh river	Sour	flood in Litani river, agriculture
An-Nahar	1993	10 Mar	flood in Hasbani river, snow storms	Baalbek, Bcharri, Ia'at, Shlifa, Deir el-Ahmar	agriculture, road damage, closing major roads
An-Nahar	1993	16 Nov	hailstorm, torrents, snow storm	Bcharri, Amioun, Tripoli, Baalbek, EL Qmameen	landslide, agriculture, road damage, soil & rock drifting, isolation of 1500 persons, ships
An-Nahar	1994	1 Jan	Torrents	all coastal cities, Hasbaya, Chouf, Sour	roads cutting, landslides, communications, huge damages
An-Nahar	1994	7 Nov	hailstorm, tempest, rain	all coastal cities, Akkar, Qalamoun, Aridah, Beirut region, Bekaa region	roads destruction, 1 person deceased, soil drift
An-Nahar	1994	3 Nov	torrential rain, floods in Asroun river in Akkar	Beirut, Sour, Bcharri	destruction, soil drift, building failure
An-Nahar	1994	5 Dec	rain storm, torrents, floods in EL-Kabir river & Ostouan river	Akkar, Chouf, Baalbek	roads damage collapsing, soil drift
Arab Center for Information/ Al-Safir	1994	3 Oct	Heavy torrents (Cause: Clouds, lightning and thunders, rapid & heavy hail fall covering almost all mountains in the eastern flange, hail melt due to high temperature)	Nahle, Shaghoor, El-Jmalah valley, Baalbek (Ain Bourday, Aamishky, El-Ta'adod neighborhood, El-wad neighborhood, Baalbek main entrance)	soil & rock drifting, roads cut, trees took off
An-Nahar	1995	8 Feb	torrential rain	Beirut	soil & rock drifting, roads cut
An-Nahar	1995	3 Dec	floods. Torrents	Jeita, Aintoura, Ain Rihaneh, Saqiet el Ouadi	road destruction in Jeita, floods in Aintoura, damages
An-Nahar	1996	24 Jan	hailstorm, heavy rain, avalanche	Elmdeirj, Dahr El-Baydar, Bourj	road damages, rock collapse

An-Nahar	1996	28 Feb	hailstorm, torrential rain, floods in Abou Ali river	Hasbaya, Chouf, Zahle, D. Choueir, Ehden, Bcharri	electricity, construction, damage, agriculture
An-Nahar	1996	10 Dec	snow, torrents	Jbeil, Bcharri	road damage, landslide, 1 person wounded
An-Nahar	1997	27 Feb	hailstorm, torrents	Jbeil, Bcharri, Cedars, Ehden	rock failure, landslides, soil erosion, isolating villages, construction damage
An-Nahar	1997	10 Dec	torrential rain	Beirut	road damages & cut
An-Nahar	1997	17 Dec	hailstorm, floods of rivers of EL-Kabir, Hasbani, Istouan, Arka	Halba	water intrusion into houses, traffic problems, soil erosion, (100 mm ppt in 1 day)
An-Nahar	1998	9 Feb	torrential rains	Beirut, Zahle, Chouf, Nahr Jalala	water intrusion into houses, soil erosion, sea wag overflow, communications
An-Nahar	1998	28 Mar	heavy wind storm	all the Lebanese regions (Mediterranean area)	huge damage in all vital projects & construction, i.e. electricity, communications...
An-Nahar	1999	27 Oct	Heavy torrents	Ras Baalbek, Qaa	In Ras Baalbek water level reached about 3m high in narrow places and its width increased from 10-14m to 60-70m near post, In Qaa water level reached 2 m
Arab Center for Information/ An-Nahar	2000	20 Jan	Heavy rainfall, Torrents	Aley, Saida, Nabatiye	Water level in El-Awali river increased to reach the bridge and covered most of the eastern lands
Arab Center for Information/ An-Nahar	2000	28 Jan	Flood	Istouan river & El-Bared river	Water level increased in both rivers to cover surrounding agricultural lands and houses
Arab Center for Information/ An-Nahar	2001	3 May	Wind storm, Heavy rainfall, Torrents, Hails	Baalbek, Northern Bekaa, Ain, Ras Baalbek, El-Fakha, Aersal, Qaa	In Ras Baalbek water level reached about 3m and in Qaa about 6 m

flood events	2002	20-22 Dec	Heavy rainfall, Floods in Sayneeq river, Litani river, Wazzani river, Hasbani river, El-Kabir river, Al-ostuwan river, Ibrahim river	Sidon, Sour, Akkar, Kesrouan, Eastern Bekaa valley, Hasbaya, Beirut, Nabatiye.	Severity level 1, 300 persons displaced, Magnitude 4.1, Rain and floods in the "past few days" have caused severe damage. The entire Bekaa valley area affected - flooded mountain villages, lots of cattle swept away, and 80% of crops ruined.
تقرير الهيئة العليا للإغاثة	2003	-	torrents	A'arqa, Jannit A'arqa	-
تقرير الهيئة العليا للإغاثة	2003	-	torrents	Tripoli	Destruction of Tripoli citadel
تقرير الهيئة العليا للإغاثة	2003	-	torrents	Diba'al	Destruction of Diba'al mosque
تقرير الهيئة العليا للإغاثة	2003	-	torrents	Bekaa-Mashghara	Destruction of Mashghara-Bekaa road
An-Nahar	2003	5 Jan	floods & snow accumulation	Taanayel, Jlala, Kobb Elias,Elchouf	water intrusion into houses, economical losses in stores and houses, roads blockage
An-Nahar	2003	6 Jan	wind storm, El-Kabir, Estwan and Hasbani rivers flood,	Tripoli, Ehden, Bcharri, Saida, Hasbaya	agricultural damage, landslides, retaining walls collapse, Shakaa bridge collapse,
An-Nahar	2003	16 Jan	Torrential rainfall	Batroun, Bcharri, Matn elAala	Landslides, roads blockage
An-Nahar	2003	22 Jan	Torrential rainfall	Beirut, Wata el-Msaitbe, Kola	water flooding roads,
An-Nahar	2003	29 Jan	Snow accumulation, Torrential rainfall	Dahr elbaidar, Ayoun elSiman, Tripoli, Akkar, Sir elDiniye, Elchouf, Hasbaya	Water flooded agricultural lands, roads blockage, landslides and rock failure
An-Nahar	2003	5 Feb	Wind storm, Snow Storm, Litani and el Kabir river floods	All Lebanon	Agricultural lands destruction, ships, 5 persons injured, landslides, Floods in Litani river, Lake of Rmeish flooded and entered houses and stores,

Arab Center for Information/ An-Nahar	2003	14-21 Feb	Heavy rainfall, Torrents, floods in Litani river, Ghzayil river, El kabir river, Istoaun river, Rasha'ain river	EL-Marj, Hawsh EL-Harimeh, El-Rawda, Ghazeh, El-Mansourah, Bar Elias, Aanjar, Kob Elias, Akkar, Hikr El-Dahri, EL-Simakiyeh, El-Aarida, El-Knayseh, Talbireh, Zghorta (EL-A'akabeh, El-Mkhadah, EL-Merdashiyeh), EL-Diman, Wadi Kannoubin, Barghoon, Upper Maten (Bitbeyet, El-Krayyeh, Kabia'a, Kernayil, Der El-Harf), Aley, Rishmayyah, Sharoon, Aaramta, El-Rihan	In El-Marj flood from Litani & Ghzayel river covers wide areas, roads cut, houses flooded with water, villages isolated, water flooded from El-Kabir & Ostouan river covers wide agricultural areas, soil erosion, landslides, Structural losses, In El-Rihan water level reached 80 cm and more than 500 houses isolated; estimated economical losses 1 milliard L. L
An-Nahar	2003	25-26 Feb	Snow accumulation, Litani, Hasbani, Bou Ali, Rasheein, Joiaat and Kadisha rivers flooded	All Lebanon	snow at 600 m, water flooded lands and houses, structural damage, road failures landslides and villages and family's isolation,
An-Nahar	2003	2 Mar	Snow accumulation, wind storm	Cedres, Litoral zone, Bekaa, Bcharri	roads blockage, avalanche, 1 person deceased, 2 injured, villages isolated, electricity off, phones off in Kanoubin, destruction threatened many buildings
An-Nahar	2003	10 Mar	torrents,	Ehden, Bcharri	Landslides, roads blockage
An-Nahar	2003	19 Mar	sandy wind storms, and rain storm	Littoral zone	electrical current off, trees and panels taken off
An-Nahar	2003	20-25 Mar	Torrential rainfall	Batroun, Chouf, Tripoli, Bcharri	waves cover harbor in Batroun, ships and nests destroyed, landslides in Bcharri -Diman, roads and field filled with mud, trees taken off, (No Suggestions) river flooded, retaining walls destroyed
An-Nahar	2003	27-29Mar	torrents	Bekaa, Chouf	floods in roads and field, water intrusion into houses, agricultural damage, landslides, structural damages in houses and stores
An-Nahar	2003	8 Apr	Springs up	Baalbek	Nahr Sbat flooded off its course, water entered houses,
As- Safir	2003	16-17Dec	Snow storm	Bekaa, Chouf, Bcharri, dahr elBaidar, Mount Lebanon, Tripoli, Hasbaya, Rachaya	snow at 700 m, electricity off, retaining walls destruction in Hasbani, Landslides in Diman, roads blockage, port out of service

As-Safir	2003	3-4. Oct	Torrents, rainfall, Assi river flooded	Bekaa, Akkar, Tripoli, Saida	losses in houses, crops, restaurants, fish, cattle, water pipes blocked in Akkar, electricity and phones damages, trees torn off,
As-Safir	2003	30 Oct	Torrential rainfall, El Kabir and Arka rivers flood	West Bekaa, Rachaya, Akkar, Tripoli, Bcherri	electrical current off, landslides, agricultural lands damaged, houses isolated, retaining walls collapse
As-Safir	2003	10 Nov	Torrential rainfall	Saida, Zgharta	Roads flooded, crops on the banks of Rasheein river damaged, great economical losses
As-Safir	2003	11 Nov	Torrential rainfall	Beirut, Bekaa	mad sea, 2 persons deceased and 5 injured, port off.
An-Nahar	2004	08.Jan (07. Jan till 10. Jan)	Heavy rainfall, Snow storm, Hail fall, Wind storms and Thunder storms, Flood in Ostouan river, water level rises in Joaait river in Zgharta, Abo Ali river, El-Bared river, El-Kabir river and Arka river	All Lebanon	car losses, soil and rock erosion, landslides(along Bayssour-Majdelya road, along several roads in El-Chouf) structural losses, electricity lines cut, roads cut, villages isolated by snow, schools off in mountains, agricultural lands flooded with rain water, agricultural losses, palm trees cut along Saida shoreline, ships stood away from the port, trees cut in high mountains, Boat losses
An-Nahar	2004	24.Jan	Wind storm (heavy wind saturated with sand) and High Waves, Snow Storm in high mountains, Heavy rainfall	All Lebanon	Waves height reached meters and hit houses, structural losses, trees cut, roads flooded with water, electricity off, soil and rock erosion, Airplanes affected by strong winds and obliged to land in Kobros, Damascus and Oman, Agricultural losses and Greenhouses destruction, Work stopped in Ports and high waves flooded most roads and houses, car losses, roads cut by snow in mountains, schools off, landslides along Choueifat-Damour road

An-Nahar	2004	16.Feb (14. Feb till 16. Feb)	Snow storm (400m and above), Hail fall, Avalanche, Flood in Ostouan river and El-Kabir river in villages: Hikr El-Dahry, EL-Simakiyyeh,El-aarida, Telbibeh, Sheikh Zned.	All Lebanon	Roads cut, landslides and rock failure (along Zgharta-Ehden road, in Eyto, Ijbea'a, along Bcharreh-Hadath El-Jobeh road, El-Kaytea'a-Eljord road between Hrar and Kaba'ait), electricity and phone lines cut and out of service, people trapped by snow, trees losses, destruction of water pipes, water leakage into houses, villages isolated, agricultural losses
An-Nahar	2004	23.Feb	Snow Storm (600m and above), Frost	Northern Jurds, Bekaa, Akar, Tripoli, Ehden, Bcharre, Hasroun, Cedres, Zghorta, Korah, Batroun, Baalbeck, Zahle, Dahr El-Baydar, El-Shouf	Water freeze in pipes, roads cut by snow, Damage of electricity lines, villages isolated, landslide along Kannoubin Valley road, car accidents, trees cut
An-Nahar	2004	25.Nov (23-24. Feb)	Snow Storm	All Lebanon, mainly: Caza of Bcharre, Caza El-jobeh, Cedres, Kannoubin Valley, Tannourine,	Roads cut, villages isolated, electricity off, trees losses, schools off, frozen roads, people and cars trapped by snow, agricultural losses, green house destructions, over 1000 banana tree took off,

An-Nahar	2004	27.Nov (26. Nov)	Heavy rainfall, Wind Storm, Hail fall, Snow in Mountains, torrents, Flood in: Kfar Halda river, Kfar Halda falls, El-Jouz river, Rachaine river in Zghorta; El-Merdashiyyeh, El-Asfour river, Flood in Hab Valley flow path, High waves exceeding 4 m (mainly in Kfar Abida), water level in Habouch river reached the bridge and Flood in Kashish spring in Zibdine,	All Lebanon	Buildings flooded with water, Reception halls in Beirut Airport flooded with water, mud, soil, and rocks erosions, car losses, agricultural losses, roads cut by torrents, landslides (Kfar Halda, Tannourine, Kfour El-Arabi, Hadath El-Jobeh, El-Diman, Ras El-Nabea'a Road in Hasroun, Bekaa Kafra, Bcharre,Hadchit, Zgharta Ehden Roads mainly near Sarkis Yamin Farm, El-Mokhtara-Khraybe road), Retaining walls destruction, Car accidents, 1 person injured, great losses due to heavy torrents in El-kaa, Ras Baalbek, El-Fakha, and due to snow melt in Bcharre, Fish losses, schools off in mountains
As-Safir	2005	3 Jan	Torrents, rainfall, landslides	Chouf	Landslide at Chouf-Niha road,
As-Safir	2005	6 Jan	Snow storm	Baalbek, Taanayel	Flooding of some minor water courses into agricultural lands and roads, roads blockage
As-Safir	2005	24 Jan	Snow storm, and heavy rainfall	All Lebanon	Snow at 800 m, trees and panels taken off, phones off, agricultural lands and greenhouses damaged
As- Safir	2005	5-9. Feb	Torrential rainfall, El Kabir, Estwan, Arka Ghzayel, Litani rivers flood	Akkar, South Lebanon, Bekaa	Snow at 800 m, destruction of retaining walls, land failure, water in lakes and rivers flooded into houses, electricity damages
As-Safir	2005	22.Feb	Torrents	Bcharre,	Landslides, electricity off, Pine trees fell, damages in fruit trees
As-Safir	2005	5 Apr	Torrential rainfall	Bhamdoon, Akkar, Bekaa	Mainly agricultural damage

An-Nahar	2005	6.Jan	Torrential rainfall, Increased levels in Al Kabir, Ostuan, Bared, and Arka rivers	Akkar, Tripoli, Sour	1 Ship crashed, landslides in Akkar
An-Nahar	2005	21.Nov	Torrential Rainfall	Saida, Chouf	Torrents on Saida roads, Landslides in Chouf
تقرير الهيئة العليا للإغاثة	2005	12.Dec	torrents	Batroun, El-Koura, EL-Minieh, Jbeil, Jnah	-
An-Nahar	2005	18.Dec	Heavy rainfall, torrents	Bcharri, Midan, Wadi Kanoubin, Baalbek, Batroun	Landslides, Torrents holding soils and rocks, Trees taken off, agricultural losses, electrical malfunctions, frost on roads
An-Nahar	2005	24.Dec	Wind Storm	Baalbek, Chouf, Bcharre	greenhouses damaged, roads blocked with snow, phone and electricity malfunctions
An-Nahar	2006	9.Jan to 13. Jan	Snow storm, and heavy rainfall	All Lebanon, Snow starting at 1200 m	Level rising of Elkabir, Ostouan, Arka and Bared with no losses, roads blocked in Qoubayat, Fnaidek.
An-Nahar	2006	21.Jan	Rain storm, Wind Storm	All Lebanon	roads cut, sea waves exceeding normal height
An-Nahar	2006	27.Jan	Snow storm, Torrential rainfalls	Nabatiye, Bebnin, Bhamdoun, Eklim elToufah,	Floods in roads and field in Nabatiye,Rise in level of Zahrani and Litani rivers, Collapse of part of Mina Sour pavement, agricultural damage especially in Bebnine and Ouadi Jamous
An-Nahar	2006	13.Feb	Snow Storm	Qoubayat, Hermel, Marjeoun, El Abde, Sawfar	Flood in Marjeouyoun valley caused the damage of agricultural crops, roads blocked, 2 injuries
As-Safir	2006	10.Mar	Snow Storm,	All Lebanon	Roads blocked with snow, Major agricultural damage, Land Slides in Aley and Maten,
As-Safir	2006	16.Mar	Snow storm and Torrents	All Lebanon	Floods in Batroun, landslides in dahr elBaidar, electricity and phones damages in some regions, 2 injuries in a car accident

As-Safir	2006	3 to 6. Apr	Rain storm with mud, Floods in Abou Ali river, Bouhayrat Ayoun ElSamak, Nahr elBared,	Bekaa, Maten, Akkar, Saida, Batroun, Bent Jbail, Sour	Rise in Abou Ali 1m above level, torrents and water intrusion into houses, landslides, torrents on roads, fields filled with mud, water into basements in Saida, Fields surrounding Zahrani flooded, collapse in river bridges, 5 injuries in Akkar,
A-Safir	2006	26.Apr	Rainstorm	All Lebanon	Landslides, water flooded roads and fields in Saida, Batroun, bent Jbeil, Nabatiye, water intrusion into houses in Ebba, Adshit and surroundings, Electricity Damages, Torrents and Landslides in Akkar
تقرير الهيئة العليا للاغاثة	2006	-	torrents	Hrajel & Mairouba	
As-Safir	2006	16.Oct	Heavy Rainfall and Torrents	Wata EL-Msaitbeh, Jnah, Ouzaui, Hersh Elkatil,Nabatiye, Tripoli	Roads, stores and houses filled with water, trees grasped, roads blocked, Landslides in Chekka, 2 persons deceased, 3 injured
Arab Center for Information/ An-Nahar/As-Safir	2006	29.Oct	Rain storm, Torrents	Akkar, Bint Jbeil, Sour, Nabatiye, Tripoli, Bekaa, Rachaya	roads cutting, agricultural losses, fields flooded with water, water intrusion to houses and stores, Landslides,10 injuries, 2 deceased, 125 cattle deceased,
As-Safir	2006	6.Nov	Heavy Rainfall, Floods in El-Kabir river, Al-Ostuwan river, Arka river	North Lebanon	torrents caused damages in cattle and crops in Jabal elBeddawi, water entered houses and cut roads
As-Safir	2006	28.Dec	Snow Storm	All Lebanon, Snow starting at 800 m	Roads blocked in Mountains, In south roads filled with water, and snow covered countries at 700 m.
An-Nahar	2007	7.Jan	Snow storm	Akkar, Dahr elBaidar, Tripoli, Chouf	Mountainous roads are blocked, phone breakage.
An-Nahar	2007	22.Jan	Snow Storm, Torrential rainfall, Hasbani river flooded	Chouf,Sour,Saida	agricultural crops damaged, roads flooded, strong winds, avalanches, ports off.

An-Nahar	2007	17.Feb	Torrential Rainfall, Landslide in Falougha	Falougha, Hasbaya	Great Landslide in Falougha blocked road and threatened houses.
An-Nahar	2007	26.Feb	Heavy rainfall	Nabatiye, Chouf, Jezzine	Torrents in roads holding soils and rocks, landslides in Chouf, failure in some roads
An-Nahar	2007	25.Mar	Snow Storm	All Lebanon	roads and fields flooded in Akkar,
An-Nahar	2007	28.Mar	Heavy Rainfall	Akkar	Bebnine road blocked due to rockslide
An-Nahar	2007	2.Apr	Heavy rainfall, Hail fall	Hasbaya, Beirut, Bhamdoun, Aley	Torrents holding soils and rocks, hail fell and affected crops, springs burst
AL-Safir	2007	27.July	Heavy Torrents	El-Fakha, Labweh, Ras Baalbek & along Assi river	
An-Nahar	2007	24.Oct	Heavy Rainfall	Akkar	flooded roads and fields
An-Nahar	2007	21 to 23. Nov	Heavy Rainfall, El-Kabir river flood	Beirut, South Lebanon, Aley, Hasbaya, Chouf, Ehden, Bcharre, Hasroun, Saida, Akkar	roads turned into lakes, landslides, hails damaged crops, springs electricity breakdowns, burst out,
An-Nahar	2007	7.Dec	Heavy Rainfall	North	Roads flooded, landslides, ceiling collapsed in Rawdat ElFaihaa, agricultural damage
An-Nahar	2007	17.Dec	Heavy rainfall	Tripoli, Chouf, Rmeileh, Saida	Landslides on Chouf roads, torrents blocked roads
An-Nahar	2008	9.Jan to 15. Jan	Frost	Bekaa,North Lebanon, South Lebanon	agriculture, life losses, schools and work closed.
An-Nahar	2008	31.Jan	Frost	All Lebanon	agriculture, life losses, schools and work closed, snow reached littorals, Borj elBarajne Palestinian camp flooded.
An-Nahar	2008	13.Feb	Snow Storm, Heavy Rainfall, El Joz River Flooded	Akkar, Batroun	Torrents on roads detained cars and people, Landslides, mud and rocks held with torrents
An-Nahar	2008	20.Feb	Snow Storm	All Lebanon, Snow at 600 m	agriculture losses, road blockage, torrents in Sahl Jdeideh (Zgharta), electricity poles and trees taken off

An-Nahar	2008	16.Oct	Heavy rainfall, torrents	All Lebanon,	Floods in roads in Akkar, Ayn elMrayse, Sabra…
An-Nahar	2008	23.Oct	Heavy Rainfall	Akkart, Wata elMsaitbe, Kola, Barbir, Kornish elMazraa	Torrents and Lakes in roads, water intrusion into houses
An-Nahar	2008	25.Oct	Heavy Rainfall, floods in Bekaa valley	Aersal, Ras Baalbek, Kaa,	Floods in Oronte valley, Road Baalbek-Homs blocked.
Al-Akhbar /An-Nahar	2008	30.Oct	Heavy Rainfall	Aersal, Ras Baalbek, Kaa, El-Shawaghir village, Wadi ElTaim	Destruction of the anti-smuggling measures along the Syrian-Lebanese Border border, agriculture, destruction of fish breeding basins
An-Nahar	2008	21.Nov	Heavy Rainfall	Akkar, Bekaa	Torrent in Baalbek, 2 people deceased
Al-Kods	2008	25.Nov	Heavy torrents, Heavy rainfall	Northern Bekaa: EL-Assi valley, Aersal, Ras Baalbek, Kaa, EL-Fakha	International road Baalbek-Homs was cut at El-Fakha bridge
An-Nahar	2008	25.Dec	Heavy Rainfall and Snow	Nabatiye, Chouf, Saida, Batroun, Akkar	Roads turned to lakes in Nabatiye, and Wadi elTaim, roads blocked
تقرير الهيئة العليا للاغاثة	2008	-	torrents	Wata EL-Msaitbeh	-
An-Nahar	2009	30.Jan	Heavy Rainfall	Beirut, Saida, Sour, Jnah, Bekaa	Torrents, water intrusion into houses, landslides and car accidents
An-Nahar	2009	13.Feb	Heavy Rainfall	All Lebanon	Landslides in Aazour, and Jroud ElDeneye
An-Nahar	2009	23.Feb	Al Kabir River Flooded	Akkar, Tripoli	Water level raised more than 8m, roads blocked. Landslides,
An-Nahar	2009	2.Mar	Snow Storm, Litani and Hasbani rivers flooded	All Lebanon	Roads blocked, landslides in Kaa el Rim, Roads and fields flooded in Marjeyon, water entered houses, retaining walls collapsed in Manasef, Litani River Flooded

An-Nahar	2009	11.Mar	Torrential Rainfall, Berdawni river Flooded	Jezzine, Zahle, Baalbek	Water flooded agricultural lands and restaurants, roads blockage, landslides and rock failure
An-Nahar	2009	8.Apr	Heavy Rainfall Younine River Flooded	Baalbek, Sahl Shaath	Damages in plastic houses, Torrents in Baalbek and Shaath valley
As-Safir	2009	23.Sep	Torrential Rainfall	Batroun, Bekaa	Torrents flooded houses and destructed walls and bridges, landslides, agricultural and cattle and poultry losses
As-Safir	2009	2 to 3 Nov	Heavy Rainfall, Snow Storm,	All Lebanon	Floods in Bir Hasan, Bent Jbeil, Sour, Baalbek, Akkar, High sea waves, Ports closed, landslides, torrents holding soils and rocks, great agricultural losses.
Al-Akhbar/As-Safir	2009	18.Dec (15. Dec till 20. Dec)	Heavy rainfall, Snow storm, Thunder storms, Wind storms, Hail fall in high area, Swamps in plains, Heavy Torrents, Floods in: El-Zahrani river, Berdawni river, El-Kabir river, Litani river & small rivers like: Zraykoon river, Shhim river, Abo Dajejeh, El-Deleb, El-Hosh, EL-Madfoon river, and flood in Bshamzin valley near Amyoon and El-Koura	All Lebanon (storm coming from Greece)	Great losses, landslides, rock rupture, roads cut, muddy torrents, traffic jams, car losses, car accidents, structural damage, cattle losses, houses flood with water, boats damaged, Ghaziyyeh bridge cut by torrents, beshmizine roads collapses, telephone(cell) lines out of service, electricity, trees damaged, agricultural lands flooded and crops damaged, schools flooded and closed, torrents level exceeded 2 m, and snow thickness exceeded 1 m in high mountains as in Cedres, seasonal springs early active,

As-Safir	2009	23.Dec	Torrential Rainfalls, ElBared Canal collapsed	North Lebanon	Water of Bared Canal flooded houses and crops in Bebnine,
As-Safir	2010	15.Jan	Torrential rainfall	Akkar	Water Canal exploded leaving a great hole that hindered traffic,
As-Safir	2010	19 to 26Jan	Rain Storm, Hasbani, Zahrani, Litani, Zyrakoon, Baraghith, Berdawni and Gzayel rivers Flooded, ElKabir river flooded	Nabatiye, Bekaa, Sour, Saida, Akkar, Tripoli, Batroun, Taanayel, Marj,	Torrents, water intrusion into houses, landslides and car accidents, roads collapsed in Ehden and Jbeil, Bridge collapsed on Hasbani river, electricity damages.
As-Safir	2010	4.Feb	Heavy Rainfall, Floods in Litani and Berdawni rivers	Nabatiye, Marj, Taanayel, Chouf, Ehden Zgharta	Landslides in Ehden, Agricultural losses in Bekaa, roads blocked, accidents,30 cattle deceased in Ter Debba due to flood in water canal in Hadaya valley
As-Safir	2010	1.Mar	Heavy Rainfall, Hails, Zahrani, Hasbani river flooded, Tasse Spring flooded	All Lebanon	roads blockage, avalanche, electricity and phones off, fields flooded and taken by torrents,75 cattle deceased
As-Safir	2010	9.Oct	Heavy Rainfall	Beirut	Torrents and Lakes in roads causing traffic
As-Safir	2010	30.Oct	Heavy Rainfall	Tripoli	Floods in roads
As-Safir	2010	7.Dec	Heavy Rainfall, Snow Storm	Akkar, Ehden, Zgharta, Ryak, Tripoli	Roads flooded, river in Merdashiye flooded, torrents slide soils and rocks to roads, rockslide btw Kfarhouna and Jezzine and in Ehden, great economical losses

As-Safir	2010	13 to 18. Dec	Snow Storm, Rain and Wind Storm, Litani, Zayrakoun and Hasbani river flooded	All Lebanon	Roads blocked and filled with water in Akkar and Beirut, trees and Panels taken off, water entered houses, numerous electrical malfunctions, countries in Bekaa and Rachaya isolated with snow, Port in Jiyye destructed, Sea waves flooded roads and reached house, 1 person deceased, more than 200 cattle dead
An-Nahar	2011	31.Jan to 2. Feb	Snow Storm, ElKabir river flooded	All Lebanon	Increased level in Elkabir river, avalanches in Akkar, floods in water canals in Bekaa, agricultural losses, 6 injuries
An-Nahar	2011	5.Feb	Snow Storm, torrential rainfall, Hasbani river flooded	West Bekaa, Rachaya, Bekfaya, Akkar, Tripoli, Hasbaya, Arkoub, Nabatiye	floods in water canals entered houses in west Bekaa, retaining walls collapsed in Rachaya and Akkar, panels and trees taken off, agricultural crops damaged,
As-Safir/Daily Star	2011	17&19to21. Feb	Heavy rainfall, Hasbani River overflowed	All Lebanon	ports of Sour and Sidon were closed to maritime activities, the heavy rain caused flooding in areas near the coast, compounded by sewage networks that were overflowing. People were trapped in their homes, heavy damage to greenhouse agriculture in Hasbani, villages isolated due to roads collapse,2 injuries,20 cattle heads dead.
As-Safir	2011	28.Feb	Rain Storm, Litani, Abou Djaji, Delb, Hasbani rivers flooded	Zahle, Ryak, West Bekaa, Akkar, Rachaya, Hasbaya	Landslides, Water floods fields and entered houses, agricultural crops damaged, plastic houses destructed…
As-Safir	2011	1.Mar	Rain Storm, Litani, Ghzayel, Abou Djaji, Delb, Hasbani rivers flooded	Rachaya, West Bekaa, Ehden, Sour, Akkar, Hasbaya	Torrents, landslides in Ehden and Hasbaya, water bridge collapsed in Hasbani, agricultural crops damaged (wheat in Ayha field)
As-Safir	2011	10.Mar	Snow and hail Storms, El Kabir, Hasbani, Wazzani, Litani rivers flooded	All Lebanon	closed roads and schools in mountainous areas, wind blew over electricity poles along Sidon's corniche, and uprooted trees, 3 Syrians swept away by El-Kabir river, storm damaged agricultural crops and greenhouses in the Zahrani and Sour districts

Daily Star	2011	14.May	Windstorm, Rainfall	West Bekaa	Fisher lost in Qaraoun Lake due to strong waves
Daily Star	2011	4 to 5. Nov	Torrential rainfall	Bcharre, Ehden,	flooded roads caused damage to property and stores, large support wall in Jounieh collapsed,50 people injured, power outages
Future/Daily Star	2011	19.Nov	Heavy Rainfall, (Wind storm, Thunder storm, Hail fall and Torrents in Bekaa), Refreshing (Litani river, Qaraoun and Tea'aneyil Lakes, A'amik Swamps)	Beirut and Suburbs, Bekaa (Job Jennine, Ghazeh, Bar Elias, Hosh EL Harimeh, El-Marj, Industrial City Zahle), Sennine, Barouk, Toumat Niha	Great traffic jams, water level reached 80 cm to 1 m and flooded into houses and stores, roads cut, Car slides and accidents. Note: precipitation reached (145.8mm) more than twice the average yearly rainfall till this date (66.7mm) in the airport, i.e. precipitation reached 10 mm in 8 hours, similarly in Tripoli and Hoch El-Omara precipitation reached 185mm and 80mm respectively whereas it was 125mm and 63mm respectively as a yearly average
Daily Star	2012	12.Jan	Torrential rainfall	Chouf, Akkar,	roads were transformed into artificial lakes, trapping vehicles
Daily Star	2012	20.Feb	Torrential Rainfall	Bekaa, Akkar,Tripoli, Saida, Zahrani, Bcharre, Tanourine,	major roadways cutoff and infrastructure damaged, roads and houses flooded, panels and trees uprooted, powerlines down, high waves in Saida kept marine road closed,
Al-Akhbar/ Daily Star	2012	02.Mar (28. Feb till 03. Mar)	Rain Storm, Snow Storm (snow starting from 300m elevation), Flood in El-Hasbani river, threat of flood in El-Kabir river	All Lebanon	structural failure, roads cut by snow reaching 2 m in some regions, landslides, trees, boats damage, agriculture and greenhouses destruction, villages isolated, electricity out, schools off, houses flooded with water, sewage networks failure
An-Nahar	2012	30.Jul	Flood	Aarsal, Zamrane	-
An-Nahar	2012	07.Oct	Heavy Hail fall, Rainfall	Ehden (EL-Baoul, EL-Motel, Ijbea'a, Beslokit, EL-Bohayrah…), Keserouan, Aely, Akkar (Hrar, Mishmish, Beit you, Beit Youngest, Fnaidek)	Large hails (ping-pong size) covering almost all Akkar, North and Ehden, Glass crushed, Cars damaged, agriculture losses (fruits mainly apples and Vegetables), Rain floods on roads eroding all garbage containers, sand, stones and leaves

Daily Star	2012	21.Dec	Torrential Rainfall	Beirut, Zahrani Saida, Tyre, Tripoli, Akkar, bcharre, West Bekaa, Rachaya, Chouf	power line knocked down in the south, damages in greenhouses, In mountainous areas, heavy snowfall blocked roads, landslides in Chouf
As-Safir /Daily Star	2012	13.Nov and 12. Nov (10. Nov till 12. Nov)	Heavy Rainfall, Thunder storms, Hail fall, Moderate speed Winds, Torrents, floods in tributaries of West Bekaa (Kawkaba, Jib Farah, Aakaba, Kafarqouq, Rachaya, El Mhaydthe, El Rafid mainly along Kawkaba-El Mhaydthe road, Khirbit roha, Dahr El Ahmar, El Marj, Ghazeh, Kamed El Lawz), Southern Highway in Saida;Sainik flooded with water and near garbage recycling factory	All Lebanon mainly: Rachaya and Western Bekaa, Saida, Zahrani, Eklim ELTofah.	Roads cut, water accumulation in valleys and depressions due to torrents, soil-stone and pebbles erosion, sewage networks flooded with water, landslides and failure in RW (Bekaa-Tal Amara, Eklim El Tofah, Saida, Shibaa-Hasbaya), car accidents, roads destruction, houses flooded with water in flooded villages, Electricity off, Saida Harbour stopped working, Agricultural losses, greenhouses losses,1 death, 1 injured
As-Safir	2012	05.Dec	Heavy Rainfall, Heavy Winds, Torrents	Central Bekaa	Heavy torrents along Dahr El Baidar International road and along Firzel road with stones and soil erosion, traffic jams, roads cut with heavy accumulated water
As-Safir	2012	12.Dec	Snow fall starting from 1250m	Central Bekaa (Dhour Zahle, Hizzerta, Dahr El Baidar,Dhour El Chwair-Tarchich Road,	
As-Safir	2012	12.Dec	Snow fall starting from 1600m, Heavy Winds, Hail Fall	Akkar (Kammouaa, Kalaait Aarouba, Wata Michmich, Jroud Fneidik	Agricultural and Green Houses Losses (Bibnine, Wadi El Jamous, El Abde, Berkayil, El Mhamra), Work stopped in El Abde Harbour

As-Safir/Daily Star	2012	21.Dec and 22. Dec (19. Dec evening till 22. Dec morning)	Heavy Rainfall, thunder storms, snow above 1200m, torrents, Flood in Hasbani River, flood of spring in Deir El Mkhallis in Mazboud El Mghayriyyeh	All Lebanon	//On 21.Dec// RWs failure in some regions(Ain Arab-Bakka and in Rachaya-Aiha), Stores and houses flooded with water in Rachaya due to torrents and in Tyr, Harbor closed in Saida with some losses, fire in 2 stores in Nabatiyeh along Habboush-ArabSalim Road, Maaser El Chouf-Arz-Kifraya road cut by snow.//On 22.Dec// Agricultural Losses, road destruction, soil erosion, Rw failure, car losses, roads cut by snow,8 people stuck in 3 cars by snow in region between tallet El Salib and Korna El Sawda-Jroud Ehden, Some people stuck in their cars by torrents in Tyr(Ras El Ain-El Aabbara), destruction of some Electric poles, Electricity and Telephone and Internet OFF, water level in Hasbani river exceeded 2m which flooded on both sides leaving great agricultural losses+ destruction of irrigation canals failure of RW+rock and soil erosion over roads. In Ain Arab and Wadi Khansa plains about 750 acres of agricultural lands flooded by torrents, water from Deir Mkallis spring along with torrents flooded over the bridge, cattle losses while crossing the water course.
As-Safir	2013	7to 9 Jan	Snow Storm, Torrential Rainfalls, Floods in Beirut river,Ghadir, Litani, ElKabir,Bared,ElKalb,Joiaat and Ostouan rivers	All Lebanon, Snow at 300 m,	villages isolated,5 people deceased, 45 injured, roads turned into lakes covering cars and entering houses, landslides, ghadir bridge collapsed, roads cut, schools off for 3 days.

Annex C.
Sample of the developed online survey

Analysis Grid for Different Flood Modeling Approaches

Section A: General Information

Flood modelling has gained favour as a tool for flood assessment and mitigation. Numerous models are now available in both fields of hydrology and hydraulics ranging from simpler ones, with a limited number of parameters, to highly complex ones, with many parameters. Therefore, the choice of selection of the efficient low-cost model by balancing between model complexity and data availability is not an easy exercise. In this context, we are developing an analysis grid to develop a state of the art of different flood modelling approaches of riverine floods (surface water only). The grid is structured in five parts:

Section A: General Information
Section B: Data Availability
Section C: Model Complexity
Section D: Modeling Performance
Section E: Summary

This work is part of the Ph.D. thesis of **Rouya HDEIB** with the **CNRS-Lebanon** and **UMR LISAH Montpellier, France.** The survey is designed to collect information on different flood modeling approaches of variable complexity; the **study case should be a known reference (journal article, thesis, or available & citable report).**

There are two categories of questions in the survey:
Objective questions: involve collecting real data about the study case (data, models...)
Subjective questions, marked by (*): represent the author's point of view, and the author is free to answer or disregard.

The survey will take around **23 minutes** and it is specified for each study case\report.

There are no obligatory questions, so please continue the survey to the end. We, therefore, appreciate your participation to support this project.

1. Please provide your contact information

Name	
Affiliation	
City/Town	
Country	
Email Address	

2. Please provide information on the study case.

Title	
Year	
Study site	
Country & City	
Reference/ citation/ doi	

3. Objective/output required from the modeling approach.
Please select all that applies.

note: some objectives may be nested (ex: obtaining a flow hydrograph involves obtaining the flood peak flow)

- [ ] flood peak discharge
- [ ] flood water levels
- [ ] flood flow hydrograph at one location/outlet
- [ ] flood inundation map
- [ ] flood flow hydrograph at different locations
- [ ] Other (please specify)

4. Level of data acquisition

- ( ) ungauged
- ( ) research basin
- ( ) poorly-guaged
- ( ) new acquisitions
- ( ) classical
- ( ) Other (please specify)

5. Scale of the study site

- ( ) parcel/field
- ( ) continental
- ( ) basin
- ( ) global
- ( ) regional
- ( ) Other (please specify)

6. Study site area range

- ◯ [0; 100] Sqkm
- ◯ [101; 1000] Sqkm
- ◯ [1001; 10,000] Sqkm
- ◯ [10,001; 100,000] Sqkm
- ◯ more than 100,000 Sqkm

Please specify the study site area

7. * Why did you choose this study site?

8. Please select to which category does your flood modelling approach belong

- ◯ Category 1: Empirical, statistical, regionalization, etc...
- ◯ Category 2: Single application of a hydraulic model 1D, 2D, or 3D
- ◯ Category 3: Simplified hydraulic conceptual model
- ◯ Other (please specify)
- ◯ Category 4: Single application of a hydrological model
- ◯ Category 5: Coupled hydrological-hydraulic model
- ◯ Category 6: Geomorphic approach

Next

Section B: Data Availability

9. **Hydrological Data** (water levels, flow, etc...)

Please provide the requested information on the basic hydrological data in your study. It is required to mention the type & duration, spatial & temporal resolution, and the continuity of the data measurements.

(Please scroll right if the whole matrix is not fully presented)

	data set	data type	duration	spatial resolution/ nb of gauges or measurement points	temporal resolution	continuity
Data set 1						
Data set 2						
Data set 3						
Data set 4						

- "Other", please specify the data type by mentioning the dataset number (ex: data set 3 is piezometric levels)
- provide any additional information you find helpful in describing your dataset

10. * **Hydrological Data** (water levels, flow, etc...)

Several evaluation criteria are selected for each data type to evaluate its cost. In what follows, a rate on a scale of five is given for each evaluation criterion. The rate varies from "Very Low" indicating a low data cost, quality, or quantity, to "Very High" indicating a very high data cost, quality, or quantity. This rate represents the cost of data based on its quality, quantity, and cost of production.

In general, and from your point of view, how do you rate the cost of your hydrological data based on the evaluation criteria described below?

*For example, discharge data from a **single gauge for 10 years on hourly time step with some gaps** would be rated **"High"** in terms of data type, **"Very Low"** in terms of spatial resolution, **"Moderate"** in terms of duration, **"Very High"** in terms of temporal resolution, and **"Low"** in terms of continuity. The rate should be compromised between cost, quality and quantity.*

	Very Low	Low	Moderate	High	Very High	Not applicable
data type	○	○	○	○	○	○
duration	○	○	○	○	○	○
spatial resolution	○	○	○	○	○	○
temporal resolution	○	○	○	○	○	○
continuity	○	○	○	○	○	○

Please provide any additional information you find helpful in rating your data set

11. **Hydrometeorological Data** (rainfall, evapotranspiration, etc.)

Please provide the requested information on the **basic** hydrometeorological data in your study. It is required to mention the type & duration, spatial & temporal resolution, and the continuity of the data measurements.

(please scroll right if the matrix is not fully presented)

	data set	data type	duration	spatial resolution/ nb of gauges or measurement points	temporal resolution	continuity
Data set 1						
Data set 2						
Data set 3						
Data set 4						
Data set 5						

- "Other", please specify the data type and mention dataset number (ex: data set 3 is wind speed)
- provide any additional information you find helpful in describing your dataset

12. ***Hydrometeorological Data** (rainfall, evapotranspiration, etc.)
Similarly, and from your point of view, how do you rate the cost of your hydrometeorological data based on the criteria described below?

	Very Low	Low	Moderate	High	Very High	Not applicable
data type	○	○	○	○	○	○
duration	○	○	○	○	○	○
spatial resolution	○	○	○	○	○	○
temporal resolution	○	○	○	○	○	○
continuity	○	○	○	○	○	○

Please provide any additional information you find helpful in rating your data.

13. **Topographical Data** (DEM, river cross sections, cartographic maps...)
Please specify the **basic** topographic data used and provide the requested information. Please specify below any additional information not presented in the drop-down list.
(Please scroll right if the whole matrix is not fully presented)

	data set	data type	scale/resolution	availabilty
Topo Data 1				
Topo Data 2				
Topo Data 3				
Topo Data 4				

Other (please specify)

14. ***Topographical Data** (DEM, river cross sections, cartographic maps...)
Similarly, and from your point of view, how do you rate the cost of your topographical data based on the criteria described below?

	Very Low	Low	Moderate	High	Very High	Not applicable
data type	○	○	○	○	○	○
scale/resolution	○	○	○	○	○	○
availabilty	○	○	○	○	○	○

Please provide any additional information you find helpful in rating your data

15. **Geographical and Background Data (land use, soil, geology...)**

Please specify the **basic** geographical and background data required for your study. Please mention in the comment box below data types not available in the drop-down list.

(Please scroll right if the whole matrix is not fully presented)

	type	scale/resolution	availability
data set 1			
data set 2			
data set 3			
data set 4			
data set 5			
data set 6			
data set 7			

If your data type does not appear in the drop-down list above and you choose "other", please specify below the type of data by mentioning its data set number.

16. **Data for model Calibration/validation**

If relevant to your study case, please provide the requested information on the data sets required for model calibration & validation, and rate these data accordingly. Please disregard those not included in the study.

(Please scroll right if the whole matrix is not fully presented)

	Data type	*Rate (cost/quality/quantity)
Flood extent mapping		
Water stage retrieval		
data set 3		
data set 4		
data set 5		

- Other (please specify)
- specify data sets that were not mentioned above.

17. * Why did you choose these types of data? *(select all that applies)*

- [ ] No other option, these are the only available data
- [ ] These are high quality data
- [ ] Available data
- [ ] These data are required by the models
- [ ] These are low cost data
- [ ] Other (please specify)

Prev Next

Section C: Model Complexity

18. **Hydrological Model**

If your approach involves applying a hydrological model, please specify the model name or any other relevant information for describing your model. *(in case of a new or unknown model specify type, equations or reference..)*

19. **Hydrological Model Type**

If your approach involves applying a hydrological model, please specify the required information.

(Please scroll right if the whole matrix is not fully presented)

	Spatial scale	Temporal scale	No. events/ Duration	Basic algorithm	Spatial presentation	Time step	Flow processes
Type							

Other (please specify)

20. ***Hydrological Model:**

In general, and from your point of view, please give a rate for each criterion mentioned below. the rate should reflect the level of complexity of the model.

For example, if you apply a conceptual semi-distributed event-based basin scale model for 5 events on an hourly time step simulating overland and channel flow. the rate of the following would be:

Conceptual: "moderate" or "low" for basic algorithm

semi-distributed: "moderate" or "high" for spatial presentation

event-based: "Very low" or "low" for temporal scale

basin: "high" for spatial scale

5 events: "low" for the number of events

hourly: "high" for time step

overland and channel flow: "moderate" for processes presented

Note: you may choose the rate that you feel relevant to your application, regardless of the rates given in the previous example which is presented for clarification purpose.

	Very Low	Low	Moderate	High	Very High	Not applicable
Spatial scale	◯	◯	◯	◯	◯	◯
Temporal scale	◯	◯	◯	◯	◯	◯
No. events/ Duration	◯	◯	◯	◯	◯	◯
Basic algorithm	◯	◯	◯	◯	◯	◯
Spatial presentation	◯	◯	◯	◯	◯	◯
Time step	◯	◯	◯	◯	◯	◯
Flow processes presented	◯	◯	◯	◯	◯	◯

Other (please specify)

21. **Hydraulic Model:**

If your approach involves applying a hydraulic model, please specify the model name or any other relevant information for describing your model. *(in case of a new or unknown model specify type, equations or reference..)*

22. **Hydraulic Model Type:**

If your approach involves applying a hydraulic model, please specify the required information.

(please scroll right if the whole matrix is not fully presented)

	Spatial scale	Temporal scale	No. events/ Duration	Flow equations	Spatial representation
Hydraulic model	⇕	⇕	⇕	⇕	⇕

Other (please specify)

23. ***Hydraulic Model**

In general, and from your point of view, please give a rate for each criterion mentioned below. the rate should reflect the level of complexity of the model.

	Very Low	Low	Moderate	High	Very High	Not applicable
Spatial scale	○	○	○	○	○	○
Temporal scale	○	○	○	○	○	○
No. events/ Duration	○	○	○	○	○	○
Flow equation	○	○	○	○	○	○
Spatial representation	○	○	○	○	○	○

Other (please specify)

24. **Code development**

Please specify the code characteristics for the models applied in your approach.

	code development	*code length
model 1 (hydrologic)		
model 2 (hydraulic)		

Other (please specify)

25. **Model calibration/validation/uncertainty evaluation**

Please specify the type of input and parameter specification along with the number of parameters to calibrate for models applied in your approach.

	Number of parameters to calibrate	Type of input & parameter specification
model 1 (hydrologic)		
model 2 (hydraulic)		

Other (please specify)

26. * What were the reasons for choosing this model(s)? *(select all that applies)*

- [ ] Arbitrary selection
- [ ] Available model
- [ ] Open source model
- [ ] Our own model
- [ ] Low cost model
- [ ] I am expert in this model
- [ ] Other (please specify)
- [ ] The model is simple
- [ ] The model is efficient
- [ ] I believe the model is based on valid assumptions
- [ ] The model fits the data available
- [ ] The model is very advanced and can present all possible processes

Prev Next

Section D: Modeling Performance

27. Type of output obtained.
(select all that applies)

- [ ] Peak flood discharge/flood volume
- [ ] flood flow hydrograph at outlet
- [ ] flood flow hydrograph at different locations
- [ ] Other (please specify)
- [ ] flood water levels
- [ ] flood inundation map

28. *In general, how would you rate your model performance evaluation method?

Single variable/ Single criteria (1)	(2)	(3)	(4)	Multi variable/ Multi criteria/ Multi site (5)
☆	☆	☆	☆	☆

Other (please specify)

29. Did you evaluate the peak flow and volume error? (select YES/NO)
If yes, please mention the criteria functions used and the average error value (or its range of variation).
(ex: average peak flow error = 8%; average volume error = 3%)

Please mention the criteria functions used

30. Did you evaluate the flow hydrograph error? (select YES/NO)

If yes, please mention the criteria functions used and the average error value (or its range of variation) in SI units.

Example:

Nash Sutcliffe efficiency; average Nash = 0.87,

Coefficient of correlation; average r = 0.91,

Mean absolute error; average MAE = 3 CMS

Please mention the criteria functions used and the corresponding average error values

31. Did you evaluate the water level error? (select YES/NO)

If yes, please mention the criteria functions used and the average error value (or its range of variation) in SI units.

Example:

Root mean square error; 0.2<RMSE<0.6 m.

Please mention the criteria functions used and the average error values

32. Did you evaluate the flood extent error? (select YES/NO)

If yes, please mention the criteria functions used and the average error value (or its range of variation) in SI units.

Example:

A spatial performance measure proposed by Aronica et al. [2002] (where 1 is perfect agreement and zero is no skill); Skill of mapping: 0.7

Please mention the criteria functions used and the average error values

33. Did you use another evaluation criteria? (select YES/NO)
If yes, please describe the evaluation criteria and mention the average error value (or its range of variation) in SI units.

Please mention the criteria functions used and the average error values

34. *In general, how would you rate the overall model performance in reproducing the peak flood discharge, flood flow hydrograph, water levels, and flood inundation extent

	Poor	Fair	Good	Very Good	Excellent	N/A
Peak flood discharge and volume	○	○	○	○	○	○
flood flow hydrograph	○	○	○	○	○	○
flood water levels	○	○	○	○	○	○
flood inundation extent	○	○	○	○	○	○

Other (please specify)

Prev Next

Section E: Summary

35. *In general, how would you rate your level of data availability in terms of quality, and quantity?

- ◯ Excellent
- ◯ Very good
- ◯ Good
- ◯ Fair
- ◯ Poor

36. *In general, how would you rate your level of model complexity?

- ◯ Very complex
- ◯ Complex
- ◯ Moderate
- ◯ Simple
- ◯ Very Simple

37. *In general, how would you rate the cost of your data and models?

	Very Low	Low	Moderate	High	Very High
Cost of data	◯	◯	◯	◯	◯
Cost of models	◯	◯	◯	◯	◯

38. *In general, how would you rate your flood modelling approach when comparing modelling performance to the cost of data and models?

- ◯ Excellent
- ◯ Very good
- ◯ Good
- ◯ Fair
- ◯ Poor

This work is a first step towards developing an analysis grid for different flood modeling approaches. We are happy to receive any comments or suggestions from your side to help improve the work.

Prev Done

Sample of The Survey Response (Study Case 1)

Collector:	Web Link 1 (Web Link)
Started:	Monday, November 12, 2018 10:17:44 am
Last Modified:	Monday, November 12, 2018 10:37:56 am
Time Spent:	00:20:12
IP Address	85.112.78.34

Page 1: Section A: General Information

Q1 Please provide your contact information

Name	**Rouya Hdeib**
Affiliation	**CNRS**
City/Town	**Beirut**
Country	**Lebanon**
Email Address	**rouya.hdeib@gmail.com**

Q2 Please provide information on the study case.

Title	**Constraining coupled hydrological-hydraulic flood model by past storm events and post-event measurements in data-sparse regions**
Year	**2018**
Study site	**Awali river Basin**
Country & City	**Lebanon**
Reference/ citation/ doi	**10.1016/j.jhydrol.2018.08.008**

Q3 Objective/output required from the modeling approach. Please select all that applies. Note: some objectives may be nested (ex: obtaining a flow hydrograph involves obtaining the flood peak flow)	**flood inundation map**
Q4 Level of data acquisition	**poorly-gauged**
Q5 Scale of the study site	**basin**
Q6 Study site area range	**[101; 1000] Sqkm**

Q7 * Why did you choose this study site?

Site of available post-event measurements

Q8 Please select to which category does your flood modelling approach belong

Category 5: Coupled hydrological-hydraulic model

Page 2: Section B: Data Availability

Q9 Hydrological Data (water levels, flow, etc...) Please provide the requested information on the basic hydrological data in your study. It is required to mention the type & duration, spatial & temporal resolution, and the continuity of the data measurements. (Please scroll right if the whole matrix is not fully presented)

	data set	data type	duration	spatial resolution/ nb of gauges or measurement points	temporal resolution	continuity
Data set 1	**Water level**	**Gauge data**	**up to 10 year**	**up to 3 gauges**	**hourly**	**many gaps**
Data set 2						
Data set 3						
Data set 4						

Q10* Hydrological Data (water levels, flow, etc...) Several evaluation criteria are selected for each data type to evaluate its cost. In what follows, a rate on a scale of five is given for each evaluation criterion. The rate varies from "Very Low" indicating a low data cost, quality, or quantity, to "Very High" indicating a very high data cost, quality, or quantity. This rate represents the cost of data based on its quality, quantity, and cost of production. In general, and from your point of view, how do you rate the cost of your hydrological data based on the evaluation criteria described below?

For example, discharge data from a single gauge for 10 years on hourly time step with some gaps would be rated “High" in terms of data type, "Very Low" in terms of spatial resolution, "Moderate" in terms of duration, "Very High" in terms of temporal resolution, and "Low" in terms of continuity. The rate should be compromised between cost, quality and quantity.

data type	**Low**
duration	**Moderate**
spatial resolution	**Low**
temporal resolution	**High**
continuity	**Low**

Q11 Hydrometeorological Data (rainfall, evapotranspiration, etc.) Please provide the requested information on the basic hydrometeorological data in your study. It is required to mention the type & duration, spatial & temporal resolution, and the continuity of the data measurements. (please scroll right if the matrix is not fully presented)

	data set	data type	duration	spatial resolution/ nb of gauges or measurement points	temporal resolution	continuity
Data set 1	**Rainfall**	**Gauge data**	**up to 10 years**	**up to 7 gauges**	**daily**	**many gaps**
Data set 2						
Data set 3						
Data set 4						
Data set 5						

Q12* Hydrometeorological Data (rainfall, evapotranspiration, etc.) Similarly, and from your point of view, how do you rate the cost of your hydrometeorological data based on the criteria described below?

data type	**Low**
duration	**Moderate**
spatial resolution	**Low**
temporal resolution	**Very Low**
continuity	**Low**

Q13 Topographical Data (DEM, river cross sections, cartographic maps...)

Please specify the basic topographic data used and provide the requested information. Please specify below any additional information not presented in the drop-down list. (Please scroll right if the whole matrix is not fully presented)

	data set	data type	scale/resolution	availability
Topo Data 1	**DEM**	**Cartographic**	**between 11 & 30 m**	**Available**
Topo Data 2	**DEM**	**Drone (UAV) survey**	**< 1 m**	**Developed**
Topo Data 3				
Topo Data 4				

Q14* Topographical Data (DEM, river cross sections, cartographic maps...)

Similarly, and from your point of view, how do you rate the cost of your topographical data based on the criteria described below?

data type	**Moderate**
scale/resolution	**Very High**
availability	**High**

Q15 Geographical and Background Data (land use, soil, geology...)

Please specify the basic geographical and background data required for your study. Please mention in the comment box below data types not available in the drop-down list. (Please scroll right if the whole matrix is not fully presented)

	type	scale/resolution	availability
data set 1	**Land use**	**medium resolution/scale**	**available**
data set 2	**geology**	**medium resolution/scale**	**available**
data set 3	**soil**	**medium resolution/scale**	**available**
data set 4	**roughness**	**low resolution/large scale**	**available**
data set 5			
data set 6			
data set 7			

Q16 Data for model Calibration/validation.

If relevant to your study case, please provide the requested information on the data sets required for model calibration & validation and rate these data accordingly. Please disregard those not included in the study. (Please scroll right if the whole matrix is not fully presented)

	Data type	*Rate (cost/quality/quantity)
Flood extent mapping	**field investigation/descriptive/pictures/witnesses**	**Moderate**
Water stage retrieval	**post-event measurements of watermarks**	**High**
data set 3		
data set 4		

Q17* Why did you choose these types of data? (select all that applies)

Available data,

These are low cost data,

These data are required by the mode

Page 3: Section C: Model Complexity

Q18 Hydrological Model

If your approach involves applying a hydrological model, please specify the model name or any other relevant information for describing your model. (in case of a new or unknown model specify type, equations or reference...)

HEC-HMS

Q19 Hydrological Model Type

If your approach involves applying a hydrological model, please specify the required information.

(Please scroll right if the whole matrix is not fully presented)

	Spatial scale	Temporal scale	No. events/ Duration	Basic algorithm	Spatial presentation	Time step	Flow processes
Type	**basin**	**event-based**	**<= 15event**	**conceptual**	**semi distributed**	**30 min**	**O + channel flow (C)**

Q20* Hydrological Model:

In general, and from your point of view, please give a rate for each criterion mentioned below. the rate should reflect the level of complexity of the model. For example, if you apply a conceptual semi distributed event-based basin scale model for 5 events on an hourly time step simulating overland and channel flow. the rate of the following would be: Conceptual: "moderate" or "low" for basic algorithm semi-distributed: "moderate" or "high" for spatial presentation: event-based: "Very

low" or "low" for temporal scale basin: "high" for spatial scale5 events: "low" for the number of events hourly: "high" for time step overland and channel flow: "moderate" for processes presented Note: you may choose the rate that you feel relevant to your application, regardless of the rates given in the previous example which is presented for clarification purpose.

Spatial scale	**Moderate**
Temporal scale	**Low**
No. events/ Duration	**Moderate**
Basic algorithm	**Low**
Spatial presentation	**Moderate**
Time step	**Very High**
Flow processes presented	**Moderate**

Q21 Hydraulic Model:

If your approach involves applying a hydraulic model, please specify the model name or any other relevant information for describing your model. (in case of a new or unknown model specify type, equations or reference...)

HEC-RAS

Q22 Hydraulic Model Type:

If your approach involves applying a hydraulic model, please specify the required information. (please scroll right if the whole matrix is not fully presented)

	Spatial scale	Temporal scale	No. events/ Duration	Flow equations	Spatial representation
Hydraulic model	**reach scale**	**event-based**	**1 event**	**Saint Venant**	**1D**

Q23* Hydraulic Modeling general, and from your point of view, please give a rate for each criterion mentioned below. the rate should reflect the level of complexity of the model.

Spatial scale	**Low**
Temporal scale	**Low**
No. events/ Duration	**Very Low**
Flow equation	**High**
Spatial representation	**Moderate**

Q24 Code development

Please specify the code characteristics for the models applied in your approach.

	code development	*code length
model 1 (hydrologic)	**open source**	**moderate code**
model 2 (hydraulic)	**available**	**moderate code**

Q25 Model calibration/validation/uncertainty evaluation

Please specify the type of input and parameter specification along with the number of parameters to calibrate for models applied in your approach.

	Number of parameters to calibrate	Type of input & parameter specification
model 1 (hydrologic)	**5 parameters**	**stochastic parameters**
model 2 (hydraulic)	**1 parameter**	**stochastic input**

Q26* What were the reasons for choosing this model(s)? (select all that applies)

Open source , model

Low cost , model

I am expert in this , model

The model fits the data available

Page 4: Section D: Modeling Performance

Q27 Type of output obtained. (select all that applies)

flood inundation map/

Q28* In general, how would you rate your model performance evaluation method? **(3)**

Q29 Did you evaluate the peak flow and volume error? **YES,**

(select YES/NO)
If yes, please mention the criteria functions used and the average error value (or its range of variation). (ex: average peak flow error = 8%); **% peak flow= 20% % volume error = 15%**

Q30 Did you evaluate the flow hydrograph error? (select YES/NO) If yes, please mention the criteria functions used and the average error value (or its range of variation) in SI units. Example: Nash Sutcliffe efficiency; average Nash = 0.87, Coefficient of correlation; average r = 0.91, Mean absolute error; average MAE = 3 CMS	**YES, Nash= 0.6**
Q31 Did you evaluate the water level error? (select YES/NO) If yes, please mention the criteria functions used and the average error value (or its range of variation) in SI units. Example: Root mean square error; 0.2<RMSE<0.6 m.	**YES, RMSE=0.26m**
Q32 Did you evaluate the flood extent error? (select YES/NO) If yes, please mention the criteria functions used and the average error value (or its range of variation) in SI units. Example: A spatial performance measure proposed by Aronica et al. [2002] (where 1 is perfect agreement and zero is no skill); Skill of mapping; 0.7	**NO**
Q33 Did you use another evaluation criterion? (select YES/NO) If yes, please describe the evaluation criteria and mention the average error value (or its range of variation) in SI units.	**NO**

Q34* In general, how would you rate the overall model performance in reproducing the peak flood discharge, flood flow hydrograph, water levels, and flood inundation extent

Peak flood discharge and volume	**Good**
flood flow hydrograph	**Fair**
flood water levels	**Very Good**
flood inundation extent	**Very Good**

Page 5: Section E: Summary

Q35* In general, how would you rate your level of data availability in terms of quality, and quantity?

Fair

Q36* In general, how would you rate your level of model complexity?

Moderate

Q37* In general, how would you rate the cost of your data and models?

Cost of data	**Moderate**
Cost of models	**Very Low**

Q38* In general, how would you rate your flood modelling approach when comparing modelling performance to the cost of data and models?

Good

Annex D.
Results of the cost-performance analysis

Study case ID	Study case	Study Site/ Country	Journal	Area (km^2)	Modeling approach	Objective function	Data acquisition	Number of sites
Study Case 1	Hdeib et al., 2018	Awali River Basin, Lebanon	Journal of Hydrology	301	(5) Coupling	Flood inundation map	poorly gauged	1
Study Case 2	Abdallah et al., 2013	Awali River Basin, Lebanon	CNRS Report	301	(1) empirical	Flood inundation map	poorly gauged	1
Study Case 3	Knebl et al., 2005	San Antonio River Basin, Central Texas, USA	Journal of Environmental management	10,000	(5) Coupling	Flood inundation map	classical	1
Study Case 4	Neal et al., 2012	Niger river, Mali.	Water resources research	210,389	(2) Hydraulic 1D/2D	Flood inundation map	classical	1
Study Case 5	Moussa (1991)	Gardon river, France	PhD Thesis	542	(4) Hydrologic	Flow hydrograph	classical	2
Study Case 6	Coustau et al., 2012	Lez catchment, France	Natural Hazards and Earth System Sciences	114	(4) Hydrologic	Flow hydrograph	classical	1
Study Case 7	Koutroulis and Tsanis, 2010	Giofiros basin, Greece	Journal of Hydrology	158	(5) Coupling	Flow hydrograph	poorly gauged/classical	1
Study Case 8	Fuentes-Andino et al., 2017	Floodplain of Tegucigalpa, Honduras	Hydrology and Earth System Sciences	811	(5) Coupling	Flood inundation map	poorly gauged	1
Study Case 9	Montanari et al., 2009	Alzette River (Grand Duchy of Luxembourg)	Hydrology and Earth System Sciences	356	(5) Coupling	flood inundation, estimation of antecedent moisture condition from volume of runoff	poorly gauged	1
Study Case 10	Liu et al. 2005	Upper Xixian catchment in Huaihe River, China	Hydrology and Earth System Sciences	10,000	(4) Hydrologic	Flood forecasting	classical	1

Hydrological Model Dataset																
Hydrologic Data (water level, flow…)															Cost of hydrologic data	Max. Cost
Study case ID	Type	No. of variables	Duration			Spatial resolution			Temporal resolution			Continuity				
			Des.	S	W	Des.	S	W	Des.	S	W	Des.	S	W	category weight	Total	Total
Study Case 1	water levels	1	10Y	3	2	point data/ two gauges	1	3	hourly	5	3	many gaps	1	1	2	50.00	90.00
Study Case 2	Discharge	1	10Y	3	2	point data/ one gauge	1	3	Daily	3	3	many gaps	1	1	2	38.00	90.00
Study Case 3	stream flow and water level	1	1M	1	2	12 USGS gauges	3	3	hourly	5	3	time series	5	1	2	62.00	90.00
Study Case 4	Not applicable	-	-	-	2	-	-	3	-	-	3	-	-	1	2	0.00	90.00
Study Case 5	discharge	1	10 Y	3	2	2 gauge stations	2	3	hourly	5	3	time series	5	1	2	64.00	90.00
Study Case 6	discharge	1	20 Y	4	2	one gauge	1	3	hourly	5	3	time series	5	1	2	62.00	90.00
Study Case 7	discharge	1	10 Y	3	2	one gauge	1	3	hourly	5	3	some gaps	4	1	2	56.00	90.00
Study Case 8	peak flow or time of peak estimation	1	1 day	1	2	@ 7 locations	2	3	one estimation	1	3	many gaps	1	1	2	24.00	90.00
Study Case 9	water level/flow	1	1M	1	2	6 stream gauges		3	15 min	5	3	few gaps	4	1	2	42.00	90.00
Study Case 10	No data	-	-	-	2	-	-	3	-	-	3	-	-	1	2	0.00	90.00

Hydrological Model Dataset

Hydrometeorologic data (rainfall, snow, temp…)															Cost of hydrometeorologic data		Max. Cost
Study case ID	Type	No. of variables	Duration			Spatial resolution			Temporal resolution			Continuity					
			Des.	S	W	Des.	S	W	Des.	S	W	Des.	S	W	category weight	Total	Total
Study Case 1	Rainfall	1	10Y	3	2	multiple points low density (7 gauges by Theisen)	2	3	daily	3	3	some gaps	3	1	2	48.00	90.00
Study Case 2	No rainfall	1			2			3			3			1	2	0.00	90.00
Study Case 3	Rainfall	1	June 30–July 9, 2002 (10 days)	1	2	Radar (NEXRAD) 4x4 km	5	3	hourly	5	3	continuous series	5	1	2	74.00	90.00
Study Case 4	Rainfall ignored	1			2			3			3			1	2	0.00	90.00
Study Case 5	Rainfall	1	10 Y	3	2	7 gauges	3	3	hourly	5	3	time series	5	1	2	70.00	90.00
Study Case 6	Rainfall	1	14 Y	3	2	4 gauges/ Radar 1 km2	5	3	hourly	5	3	time series	5	1	2	82.00	90.00
Study Case 7	Rainfall	1	10 Y	3	2	3 to 4 gauges by Theisen	2	3	daily/hourly	3.5	3	some gaps	4	1	2	53.00	90.00
Study Case 8	rainfall	1	2 days	1	2	2 gauges (average assumed uniformly distributed)	2	3	hourly	5	3	time series	5	1	2	56.00	90.00
Study Case 9	rainfall	1	1M	1	2	1 gauge (assumed uniformly distributed)	1	3	15 min	5	3	time series	5	1	2	50.00	90.00
Study Case 10	rainfall + evaporation	2	1 year and 6 months	2	2	24 rain gauges + 1 evaporation station	2	3	6-hour	4	3	time series	5	1	2	108.00	90.00

Hydrological Model Dataset												
Geomorphic Data										Cost of geomorphic data		Max. Cost
Study case ID	Type			Resolution			Availability					
	Des.	S	W	Des.	S	W	Des.	S	W	category weight	Total	Total
Study Case 1	DEM, cartographic	1	2	10	4	3	available @ CNRS	1	1	1	15.00	30.00
Study Case 2	No DEM		2			3			1	1	0.00	30.00
Study Case 3	USGS NED online DEM's	3	2	30 m (tuned with 10 m)	4.5	3	open source	1	1	1	20.50	30.00
Study Case 4	Not applicable		2			3			1	1	0.00	30.00
Study Case 5	DEM, cartographic	1	2	250m	1	3	developed	3	1	1	8.00	30.00
Study Case 6	not applicable		2			3			1	1	0.00	30.00
Study Case 7	available DTM	1	2	1/10,000	2	3	available	1	1	1	9.00	30.00
Study Case 8	SRTM DEM	2	2	90 m	2	3	open source	1	1	1	11.00	30.00
Study Case 9	no geomorphic data required		2			3			1	1	0.00	30.00
Study Case 10	GTOPO30 public domain DEM, USGS	1	2	1000 m	1	3	open source	1	1	1	6.00	30.00

Hydrological Model Dataset															
Geographical and background data											Cost of geographical data		Max. Cost	Total cost of Hydrological Data	Max. cost of Hydrological Data
Study case ID	Type	Number			Scale/Resolution			Availability							
	Des.	Des.	S	W	Des.	S	W	Des.	S	W	category weight	Total	Total		
Study Case 1	LUC, soil, geology	3	2	3	Moderate scale (1:20,000)	3	2	developed/ available	1	1	1	13.00	30.00	126.00	240.00
Study Case 2	No LUC			3			2			1	1	0.00	30.00	38.00	240.00
Study Case 3	LUC (NLCD92), soil (STATSGO)	2	2	3	30m; 1/250,000;	4	2	available open source	1	1	1	15.00	30.00	171.50	240.00
Study Case 4	Not applicable			3			2			1	1	0.00	30.00	0.00	240.00
Study Case 5	LUC, soil, Geo	3	2	3	approximations	3	2	available	1	1	1	13.00	30.00	155.00	240.00
Study Case 6	not applicable			3			2			1	1	0.00	30.00	144.00	240.00
Study Case 7	LUC, soil, geology	3	2	3	no information	3	2	provided by authority	1	1	1	13.00	30.00	131.00	240.00
Study Case 8	Uniform LUC and Geology	2	1	3	uniform	1	2	available	1	1	1	6.00	30.00	97.00	240.00
Study Case 9	lumped 3 parameters model (no geographical data required)			3			2			1	1	0.00	30.00	92.00	240.00
Study Case 10	Soil texture data (global soils dataset of Reynolds et al. (1999)), landuse (UMD land cover map of the world)	2	1	3	10 km, 1km	1	2	available open source	1	1	1	6.00	30.00	120.00	240.00

Hydraulic Model Dataset												
Topographic Data										Cost of topographic data		Max. Cost
Study case ID	Type			Resolution			Availability					
	Des.	S	W	Des.	S	W	Des.	S	W	category weight	Total	Total
Study Case 1	DEM, drone	3	2	10 cm	5	3	developed	3	1	2	48.00	60.00
Study Case 2	DEM available @ CNRS	1	2	10m	3	3	available @ CNRS	1	1	2	24.00	60.00
Study Case 3	same available DEM + cross section surveys	4	2	few cross sections >100m spacing	1	3	developed	3	1	2	28.00	60.00
Study Case 4	DEM, SRTM	3	2	905 m	1	3	open source	1	1	2	20.00	60.00
Study Case 5	no hydraulic model		2			3			1	2	0.00	60.00
Study Case 6	no hydraulic model		2			3			1	2	0.00	60.00
Study Case 7	no information/ same available DTM		2			3			1	2	0.00	60.00
Study Case 8	LIDAR survey DTM, vertical accuracy 0.14m + cross section surveys	4	2	15 cm	5	3	available	1	1	2	48.00	60.00
Study Case 9	LIDAR DEM + 200 bathymetric cross sections	4	2	2m	4	3	available	1	1	2	42.00	60.00
Study Case 10	no hydraulic model		2			3			1	2	0.00	60.00

Hydraulic Model Dataset																
Time series of bulk flow rates & stage data														Cost of flow and stage data		Max. Cost
Study case ID	Type	Duration			Spatial resolution			Temporal resolution			Continuity					
	Des.	Des.	S	W	Des.	S	W	Des.	S	W	Des.	S	W	category weight	Total	Total
Study Case 1	Input from hydrological model			2			3			3			1	3	0.00	135.00
Study Case 2	Input from hydrological model			2			3			3			1	3	0.00	135.00
Study Case 3	Input from hydrological model			2			3			3			1	3	0.00	135.00
Study Case 4	Discharge	2002-2009	3	2	3 gauge stations	2	3	daily	3	3	time series	5	1	3	78.00	135.00
Study Case 5	no hydraulic model			2			3			3			1	3	0.00	135.00
Study Case 6	no hydraulic model			2			3			3			1	3	0.00	135.00
Study Case 7	input form hydrological model			2			3			3			1	3	0.00	135.00
Study Case 8	Input from hydrological model			2			3			3			1	3	0.00	135.00
Study Case 9	Input from hydrological model			2			3			3			1	3	0.00	135.00
Study Case 10	no hydraulic model			2			3			3			1	3	0.00	135.00

Hydraulic Model Dataset							
Roughness data					Cost of roughness		Max. Cost
Study case ID	Type	Type/ Resolution					
	Des.	Des.	S	W	category weight	Total	Total
Study Case 1	based on LUC	spatial 1/20,000	3	1	1	3	5
Study Case 2	based on LUC	spatial 1/20,000	3	1	1	3	5
Study Case 3	based on LUC	30 m	4	1	1	4	5
Study Case 4	estimated based on LUC	spatial	3	1	1	3	5
Study Case 5	not applicable			1	1	0	5
Study Case 6	not applicable			1	1	0	5
Study Case 7	no information	estimated	3	1	1	3	5
Study Case 8	uniform for reach and floodplain along all reaches	estimated	1	1	1	1	5
Study Case 9	uniform for reach and floodplain	estimated	1	1	1	1	5
Study Case 10				1	1	0	5

Hydraulic Model Dataset											
Data for model calibration/validation							Cost of calibration/ validation data		Max. cost	Total cost of hydraulic data	Max. cost of hydraulic data
Study case ID	flood extent mapping			water stage retrieval							
	Des.	S	W	Des.	S	W	category weight	Total	Total		
Study Case 1	+ social media inf., pictures/ witnesses	1	1	27 post-events of max. water marks	2	1	2	6	20	57.00	220.00
Study Case 2	+ social media inf., pictures/ witnesses	1	1	post-event at gauge	1	1	2	4	20	31.00	220.00
Study Case 3	Landsat TM images	3	1	no information	0	1	2	6	20	38.00	220.00
Study Case 4	24 Landsat TM5 images (free images)	3	1	ICESat laser altimeter 127 obs. @ 18 locations (free images)	4	1	2	14	20	115.00	220.00
Study Case 5			1			1	2	0	20	0.00	220.00
Study Case 6	not applicable	0	1	12 piezometers at hourly step (2000,2008)	3	1	2	6	20	6.00	220.00
Study Case 7	+ cross section and local witnesses	1	1	filed measurements @ gauge	1.5	1	2	5	20	8.00	220.00
Study Case 8	field witnesses + previous deterministic rainfall-runoff and hydraulic modeling	2	1	around 100 post event measurements @100m spacing	2	1	2	8	20	57.00	220.00
Study Case 9	84 flood extent marks by GPS + 2 SAR images	4	1	max water level at 7 points by theodolite + 2 SAR images (ERS-2 & ENVISAT)	4	1	2	16	20	59.00	220.00
Study Case 10			1			1	2	0	20	0.00	220.00

Hydrological model

Type of hydrological model

ID	Type	Spatial scale			Temporal scale			Nb. of events/ Duration			Nature of basic algorithms			Spatial representation			Computational time step			flow processes represented			Cost of hydrological model type		Max. Cost
	Des.	Des.	S	W	Des.	S	W	Des.	S	W	Des.	S	W	Des.	S	W	Des.	S	W	Des.	S	W	category weight	Total	Total
1	HEC-HMS (SCS-CN +SCS-UH)	Basin	4	1	event-based	1	2	12	3	1	conceptual	4	3	semi-distributed	3	3	30 min	5	1	overland & channel flow	3	1	1	38.00	60.00
2	empirical	Basin	4	1	event-based	1	2	1	1	1	empirical	1	3	lumped	1	3	coarse	1	1	overland flow	1	1	1	15.00	60.00
3	HEC-HMS (SCS-CN +Modclark)	Regional	3	1	event-based	1	2	1	1	1	conceptual	4	3	distributed (gridded)	5	3	not provided	3	1	overland flow	1	1	1	37.00	60.00
4	no model		0	1		0	2		0	1		0	3		0	3		0	1		0	1	1	0.00	60.00
5	?	basin	4	1	event-based	1	2	30	5	1	conceptual physically based	4.5	3	distributed	5	3	1 hr to 15 min	5	1	overland & channel flow	3	1	1	47.50	60.00
6	modified SCS + linear lag & route	basin	4	1	event-based	1	2	21	5	1	conceptual	4	3	distributed	5	3	1hr	5	1	overland flow	1	1	1	44.00	60.00
7	HEC-HMS	basin	4	1	event-based	1	2	8	3	1	conceptual	4	3	semi-distributed	4	3	1hr	5	1	overland & channel flow	3	1	1	41.00	60.00
8	TOPMODEL + Muskingum–Cunge–Todini	Basin	4	1	event-based	1	2	1	1	1	physically based	5	3	distributed	5	3	5 min	5	1	overland, channel & sub-surface flow	4	1	1	46.00	60.00
9	Nash IUH	basin	4	1	event-based	1	2	2 + 5	2.5	1	conceptual	3	3	lumped	1	3	hourly	5	1	overland flow	1	1	1	26.50	60.00
10	TOPKAPI	basin	4	1	continuous	5	2	6 M + 1Y	2.5	1	physically based	5	3	distributed	5	3	6-hour	4	1	overland, channel, inter flow, ground water…	5	1	1	55.50	60.00

Hydrological model								
Procedural model						Cost of code		Max. cost
code development			code length					
Des.	S	W	Des.	S	W	category weight	Total	Total
ready to wear	1	2	moderate	3	1	1	5.00	15.00
ready to wear	1	2	simple	1	1	1	3.00	15.00
ready to wear	1	2	moderate	3	1	1	5.00	15.00
no hydrological model	0	2		0	1	1	0.00	15.00
tailor-made	5	2	complex	4.5	1	1	14.50	15.00
modify existing code	3	2	moderate	3	1	1	9.00	15.00
ready to wear	1	2	moderate	3	1	1	5.00	15.00
ready to wear	1	2	moderate to complex	4	1	1	6.00	15.00
ready to wear	1	2	simple	1	1	1	3.00	15.00
modify existing code	3	2	complex	5	1	1	11.00	15.00

Hydrological model								
model calibration/ validation/ uncertainty analysis						Cost of calibration/ uncertainty…		Max. cost
Nb. of parameters to calibrate			type of input and parameter specification					
Des.	S	W	Des.	S	W	category weight	Total	Total
3	2	1	stochastic: Unct. on parameters	3	1	2	10.00	20.00
no calibration	0	1	deterministic	1	1	2	2.00	20.00
4	3	1	deterministic	1	1	2	8.00	20.00
not applicable	0	1		0	1	2	0.00	20.00
4 to 6	3	1	deterministic	1	1	2	8.00	20.00
5	3	1	deterministic	1	1	2	8.00	20.00
5	3	1	stochastic: Unct. on parameters & input rainfall	4	1	2	14.00	20.00
6	4	1	stochastic: Unct. on parameters & input rainfall	5	1	2	18.00	20.00
3	2	1	stochastic: Unct. on parameters	3	1	2	10.00	20.00
around 27	5	1	deterministic	1	1	2	12.00	20.00

Total cost of Hydrologic model	Max. cost of Hydrologic model
53.00	95.00
20.00	95.00
50.00	95.00
0.00	95.00
70.00	95.00
61.00	95.00
60.00	95.00
70.00	95.00
39.50	95.00
78.50	95.00

Hydraulic model																		
Type of hydraulic model																	Cost of hydraulic model type	Max. cost
Study case ID	Type	Spatial scale			Temporal scale			Nb. of events/ Duration			Flow equations			Spatial representation				
	Des.	Des.	S	W	Des.	S	W	Des.	S	W	Des.	S	W	Des.	S	W	category weight	Total	Total
Study Case 1	HEC-RAS	downstream reach (5 km)	5	1	event-based	1	2	1	1	1	1D SV	5	3	1D	1	3	1	26.00	50.00
Study Case 2	HEC-RAS	downstream reach (5 km)	5	1	event-based	1	2	1	1	1	1D SV	5	3	1D	1	3	1	26.00	50.00
Study Case 3	HEC-RAS	regional (6 major streams)	3	1	event-based	1	2	1	1	1	1D SV	5	3	1D	1	3	1	24.00	50.00
Study Case 4	Sub-Grid LISFLOOD-FP	regional (9500 km of river network)	3	1	Continuous	4.5	2	8 Y	3	1	KW/DW	4	3	1D/2D	4	3	1	39.00	50.00
Study Case 5	?	one reach?	5	1	event-based	1	2	?	5	1	DW	4	3	1D	1	3	1	27.00	50.00
Study Case 6	no hydraulic model		0	1		0	2		0	1		0	3		0	3	1	0.00	50.00
Study Case 7	HEC-RAS	downstream reach (6 km)	5	1	event-based	1	2	1	1	1	1D SV	5	3	1D	1	3	1	26.00	50.00
Study Case 8	Sub-Grid LISFLOOD-FP	downstream floodplain (13 km)	5	1	event-based	1	2	1	1	1	KW/DW	4	3	1D/2D	4	3	1	32.00	50.00
Study Case 9	HEC-RAS	19 km river reach	5	1	event-based	1	2	2	1	1	1D SV	5	3	1D	1	3	1	26.00	50.00
Study Case 10	-			1			2			1			3			3	1	0.00	50.00

Hydraulic model									
Procedural model							Cost of code		Max. cost of code
Study case ID	code development			code length					
	Des.	S	W	Des.	S	W	category weight	Total	Total
Study Case 1	ready to wear	1	2	moderate	3	1	1	5.00	15.00
Study Case 2	ready to wear	1	2	moderate	3	1	1	5.00	15.00
Study Case 3	ready to wear	1	2	moderate	3	1	1	5.00	15.00
Study Case 4	modify existing code	3	2	complex	4	1	1	10.00	15.00
Study Case 5	tailor-made	5	2	complex	4	1	1	14.00	15.00
Study Case 6	no		2			1	1	0.00	15.00
Study Case 7	ready to wear	1	2	moderate	3	1	1	5.00	15.00
Study Case 8	ready to wear	1	2	complex	4	1	1	6.00	15.00
Study Case 9	ready to wear	1	2	moderate	3	1	1	5.00	15.00
Study Case 10	-		2			1	1	0.00	15.00

Hydraulic model										
model calibration/ validation/ uncertainty analysis							Cost of calibration/ validation/ uncertainty evaluation		Max. cost	Total cost of Hydraulic model	Max. cost of Hydraulic model
Study case ID	number of parameters to calibrate			type of input and parameter specification							
	Des.	S	W	Des.	S	W	category weight	Total	Total		
Study Case 1	1	1	1	stochastic: input	3	1	2	8.00	20.00	39.00	85.00
Study Case 2	1	1	1	deterministic	1	1	2	4.00	20.00	35.00	85.00
Study Case 3	1	1	1	deterministic	1	1	2	4.00	20.00	33.00	85.00
Study Case 4	3	2	1	deterministic	1	1	2	6.00	20.00	55.00	85.00
Study Case 5	?		1	deterministic	1	1	2	2.00	20.00	43.00	85.00
Study Case 6	not applicable	0	1		0	1	2	0.00	20.00	0.00	85.00
Study Case 7	1	1	1	stochastic: input	3	1	2	8.00	20.00	39.00	85.00
Study Case 8	3 (6 boundary conditions)	3	1	stochastic parameter and input	5	1	2	16.00	20.00	54.00	85.00
Study Case 9	2 parameters (channel and floodplain roughness), 1 downstream boundary condition, 1 upstream boundary condition	2	1	stochastic parameter and input	5	1	2	14.00	20.00	45.00	85.00
Study Case 10			1			1	2	0.00	20.00	0.00	85.00

Performance of modelling																	Performance of models		Max. Perf.
Type of output			Criteria function			Peak flow and volume error			hydrograph error			water level error			flood extent error					
Des.	S	W	Des.	S	W	Des.	S	W	Des.	S	W	Des.	S	W	Des.	S	W	category weight	Total	Total
flood inundation map	5	3	multi variable/nash optimization	3	2	Peak error, 20%	2	1	Nash, 0.6	2	1	RMSE, 0.26 m	4	1	not available	0	1	1	29.00	45.00
water levels	4	3	single variable/ single criteria	1	2	peak flow error 50%	1	1	no	0	1	no	0	1	no	0	1	1	15.00	45.00
flood inundation map	5	3	multi variable/ multicriteria	3	2	not calculated, around 30%	2	1	avrg. MAE, 66%; R, 0.78	2	1	not calculated	0	1	compared with Landsat, around 0.45 match	2	1	1	27.00	45.00
Flood inundation map	5	3	multi variable/ multicriteria	5	2	not calculated	2	1	Nash, 0.91	4	1	RMSE, 1.26	2	1	between 0.4 and 0.7	3	1	1	36.00	45.00
Flow hydrograph @ outlet	2	3	single variable/ multicriteria	3	2	peak flow error 30%	2	1	Nash, 0.3 to 0.8	3	1	no	0	1	no	0	1	1	17.00	45.00
Flow hydrograph @ outlet	2	3	multi variable/ multicriteria	5	2	peak flow error 15 %	3	1	Nash, 0.69 to 0.75	4	1	no	0	1	no	0	1	1	23.00	45.00
water levels	4	3	multi variable/ multicriteria	4	2	peak flow error 0.2%	5	1	Nash, 0.78	4	1	@1section, 0.4%	2	1	no	0	1	1	31.00	45.00
flood inundation map	5	3	likelihood measure of individual simulations by using the degree of belief of a trapezoidal fuzzy membership function	4	2	peak flow uncertainty range 50%	1	1	peak flow and phase uncertainty range 20% to 50% and 0.5 to 2.5 hrs respectively	2	1	between 0.5 and 1.8 m error	3	1	not evaluated, comparison based on previous study, (around 60% match)	0	1	1	29.00	45.00
flood inundation map	5	3	multi variable/ multicriteria	4	2	not calculated, around 13%	3	1	Nash, 0.95	4.5	1	match score of 0.84	3	1	92% of surveyed flood marks lie within confidence bounds of the SAR-derived flood boundary.	3.5	1	1	37.00	45.00
runoff at each cell	4	3	parameter adjustment by trial and error	2	2	calibration period: -10.5% validation period: 4.4%	3	1	R 0.844	3	1	not evaluated	0	1	not evaluated	0	1	1	22.00	45.00